11th AIVC Conference
Ventilation System Performance

(held at Hotel Villa Carlotta, Belgirate, Lake Maggiore,
Italy 18-21 September 1990)

Proceedings

Volume 1

© Copyright Oscar Faber PLC 1991

All property rights, including copyright are vested in the Operating Agent (Oscar Faber Consulting Engineers) on behalf of the International Energy Agency.

In particular, no part of this publication may be reproduced, stored in a retrieval system or transmitted in any form or by any means, electronic, mechanical, photocopying, recording or otherwise, without the prior written permission of the Operating Agent.

CONTENTS (i)

Volume 1

Preface (iii)

Papers:

Keynote Speech - Mr Alessandro Sandelewski, TEKNE Spa, Gruppo Finitecnica, Milano, Italy 1

1. Intelligent Buildings: Innovative Techniques for the Environment
R Seyer and L Trepte. 15

2. Indoor Air Quality in "Buildings of the Year" Max Productivity - Minimum of Complaints.
G Flatheim 27

3. Indoor Air Quality Guide for Property Managers in Office Buildings.
C Y Shaw, F Vaculik, D W Patton, G M Comeau 41

4. Demand Controlled Systems for Dwelling-houses of the Future.
R Kohonen 55

5. Indoor Air Flow & Pollutant Removal in a Room with Task Ventilation.
W J Fisk, D Faulkner, F S Bauman, E A Arens 79

6. Tests of Localized Ventilation Systems in a New Controlled Environment Chamber.
E A Arens, F S Bauman, L P Johnston, H Zhang 99

7. The Man-Machine-Interface for the Air Exchange Measurement System Multi-Cat.
R Rabenstein, F D Heidt 131

8. Experimental Evaluation of a Hygroregulating Natural Ventilation System.
P Wouters, L Vandaele 149

9. An Automated Apparatus for Air Infiltration Measurements with Tracer Gases
R Borchiellini, M Cali 157

10. Comparison of Tracer-Gas Methods for Measuring Air Flows in Two-Zone Buildings.
F D Heidt, R Rabenstein, G Schepers 171

11.	Measurement of Airflow in HVAC Systems Using Tracer Gas Techniques. S B Riffat, M Holmes	195
12.	Ventilation Efficiency Assessment in Residential Buildings. D Bienfait	215
13.	Structure of Models for the Prediction of Airflow and Contaminant Dispersal in Buildings R A Grot, J A Axley	223
14.	Effect of Wind Pressure Fluctuations on Air Movements Inside Buildings. J Riberon, D Bienfait, G Barnaud, J Villain	267
15.	Interaction between Air Infiltration and Combustion Appliances- Validation of a Numerical Model. G V Fracastoro, M Masoero, E Mazza	283
16.	Air Curtains for Infiltration Control - A Computational Fluid Dynamics Analysis. J K W Lam, K G Ruddick, G E Whittle	301
17.	Calculation of the Air Flow Pattern in A Proposed New European Test Chamber for Radiators. A Huber, A Moser, Q Chen	325
18.	The Ventilation Chamber of the University of Basilicata. G V Fracastoro, E Nino, G Coretti	343
19.	Ventilation Systems and Removal of Particles. R Schwab, E Mayer	361
20.	Building Performance and Ventilation System. W Braun	367
21.	Two Directional Air Movements in Stairwells. R Edwards, C Irwin	379
22.	Air Flow Through Building Slits and Components. B A Fleury	389
23.	Sensor for Continuous Ventilating Rate Measurement in Livestock Buildings. D Berckmans, Ph. Vandenbroeck, V.Goedseels	401
24.	Ventilation System Performance of Vertical Exhaust Common-Duct in a Multi-Story House. S Murakami, H Yoshino, K Mizutani, S Akabayashi, K Hasegawa	421

Preface

International Energy Agency

The International Energy Agency (IEA) was established in 1974 within the framework of the Organisation for Economic Co-operation and Development (OECD) to implement an International Energy Programme. A basic aim of the IEA is to foster co-operation among the twenty-one IEA Participating Countries to increase energy security through energy conservation, development of alternative energy sources and energy research development and demonstration (RD&D). This is achieved in part through a programme of collaborative RD&D consisting of forty-two Implementing Agreements, containing a total of over eighty separate energy RD&D projects. This publication forms one element of this programme.

Energy Conservation in Buildings and Community Systems

The IEA sponsors research and development in a number of areas related to energy. In one of these areas, energy conservation in buildings, the IEA is sponsoring various exercises to predict more accurately the energy use of buildings, including comparison of existing computer programs, building monitoring, comparison of calculation methods, as well as air quality and studies of occupancy. Seventeen countries have elected to participate in this area and have designated contracting parties to the Implementing Agreement covering collaborative research in this area. The designation by governments of a number of private organisations, as well as universities and government laboratories, as contracting parties, has provided a broader range of expertise to tackle the projects in the different technology areas than would have been the case if participation was restricted to governments. The importance of associating industry with government sponsored energy research and development is recognized in the IEA, and every effort is made to encourage this trend.

The Executive Committee

Overall control of the programme is maintained by an Executive Committee, which not only monitors existing projects but identifies new areas where collaborative effort may be beneficial. The Executive Committee ensures that all projects fit into a pre-determined strategy, without unnecessary overlap or duplication but with effective liaison and communication. The Executive Committee has initiated the following projects to date (completed projects are identified by *):

I Load Energy Determination of Buildings*
II Ekistics and Advanced Community Energy Systems*
III Energy Conservation in Residential Buildings*

IV Glasgow Commercial Building Monitoring*
V Air Infiltration and Ventilation Centre
VI Energy Systems and Design of Communities*
VII Local Government Energy Planning*
VIII Inhabitant Behaviour with Regard to Ventilation*
IX Minimum Ventilation Rates*
X Building HVAC Systems Simulation*
XI Energy Auditing*
XII Windows and Fenestration*
XIII Energy Management in Hospitals*
XIV Condensation*
XV Energy Efficiency in Schools
XVI BEMS - 1: Energy Management Procedures
XVII BEMS - 2: Evaluation and Emulation Techniques
XVIII Demand Controlled Ventilating Systems
XIX Low Slope Roof Systems
XX Air Flow Patterns within Buildings
XXI Thermal Modelling
XXII Energy Efficient Communities
XXIII Multizone Air Flow Modelling

Annex V Air Infiltration and Ventilation Centre

The IEA Executive Committee (Building and Community Systems) has highlighted areas where the level of knowledge is unsatisfactory and there was unanimous aggreement that infiltration was the area about which least was known. An infiltration group was formed drawing experts from most progressive countries, their long term aim to encourage joint international research and increase the world pool of knowledge on infiltration and ventilation. Much valuable but sporadic and uncoordinated research was already taking place and after some initial groundwork the experts group recommended to their executive the formation of an Air Infiltration and Ventilation Centre. This recommendation was accepted and proposals for its establishment were invited internationally.

The aims of the Centre are the standardisation of techniques, the validation of models, the catalogue and transfer of information, and the encouragement of research. It is intended to be a review body for current world research, to ensure full dissemination of this research and based on a knowledge of work already done to give direction and firm basis for future research in the Participating Countries.

The Participants in this task are Belgium, Canada, Denmark, Germany, Finland, Italy, Netherlands, New Zealand, Norway, Sweden, Switzerland, United Kingdom and the United States of America.

VENTILATION SYSTEM PERFORMANCE

11th AIVC Conference, Belgirate, Italy
18-21 September, 1990

KEYNOTE SPEECH

Alessandro Sandelewski

TEKNE SPA
Gruppo Finitecnica
Sede Legalee Uffici
20124 Milano
V.Le Restelli 3
ITALY

VENTILATION AND INDOOR AIR QUALITY - A DESIGN ENGINEER'S POINT OF VIEW

1. Introduction

Mr. Chairman, ladies and gentlemen

I consider it a great honour to have been asked to participate to this meeting as keynote speaker. I am neither an indoor air quality specialist nor a ventilation expert: I am an engineer, responsible for design and commissioning of civil and industrial HVAC systems for TEKNE SpA, a leading consulting engineering firm based in Milan.

I think you will agree with me that designing air-conditioning systems for humans (as opposed to cattle, poultry or industrial products) can be stimulating and challenging at times, but also frustrating and infuriating.
This is because HVAC impinges on human comfort which, as everybody knows, is a highly subjective notion.

An electrical engineer's life is much easier: his systems either work or don't, and if they don't the cause is usually straightforward and fairly easy to find. But the air-conditioning expert isn't so lucky; he is beset with objective technical problems (nothing works as intended, at least in the beginning), and harassed by complaints from the tenants and users who are either too hot, or too cold, or complain of draughts ... and so on, ad infinitum.

But I do not want to bore you with my lamentations: I think I had better mention the points one ought to bear in mind when designing for satisfactory indoor air quality, outline the consequences which can befall when one does not, and finally try and define the information which design engineers need and expect from specialists such as you, in order to avoid the most obvious pitfalls and satisfy the highest possible percentage of clients.

2. Design fundamentals for satisfactory indoor air quality

Textbooks say that, in order to minimize indoor air quality problems, the HVAC design engineer must take at least the following parameters into account:

- indoor air temperature and relative humidity;
- ventilation rates;
- air circulation;
- air filtration.

About the first two parameters a lot has been said and written, and there is very little to add to the comfort range diagram published e.g. in the ASHRAE Handbook of Fundamentals (Fig. 1). It is just worth mentioning that relative humidity, which according to the above mentioned chart can be allowed to swing in a rather broad range (30 -70%), should really be controlled more closely because of its impact on IAQ parameters, and should be limited to the 40 - 60% range (fig. 2).

As for ventilation rates, there is no clear cut rule in Italy; the UNI standards recommend a minimum outdoor air flow rate of 15 m3/h (4.17 L/s), to be increased to 20 - 25 m3/h (5.5 - 6.95 L/s) if smoking is allowed. Local health authorities may enforce higher values, and they usually do for specific applications such as classrooms, theatres or hospitals.

In my professional practice, if no local standard or regulation specifies otherwise, I use the ventilation rates laid out in ASHRAE 62-1989 standard.

Air circulation (intending as such the total air flow rate in a room with its associated terminal velocity) is seldom a problem in Italy, given the widespread popularity of 2 - and 4 - pipe fan-coil systems with or without primary air. I do not have great sympathy for fan-coil units; they are noisy, take up floor space, are useless against indoor air contaminants, and their filters just act as dirt collectors, not to mention the fact that they require maintenance, at least for filter cleaning/changing. It is a fact, however, that they are very popular with tenants because they feel they are in control.

UNI standards recommend that terminal velocities be kept lower than 0.15 m/s. Since all-air systems are not very common outside the industrial environment or special applications (auditoria, theaters etc.), and VAV systems in particular are few and far between, the problems about ventilation effectiveness as outlined in ASHRAE 62 (fig. 3) are no great source of concern.

Outdoor and return air must of course be filtered; the former to reduce the amount of contaminants present in a city environment, the latter to control the indoor pollutants. Except when a higher efficiency is required (such as in hospitals or clean rooms) we specify a filtration system with an efficiency of 95% N.B.S. dust spot methods on all air handling units: and this even though it is known that this is not sufficient to remove typical indoor contaminants such as bacteria, tobacco smoke and fungi. More efficient filtration systems however are too expensive to install and maintain in an office environment; an acceptable compromise can thus be reached by associating a medium efficiency filter with adequate outdoor air dilution as required by ASHRAE 62 - 1989.

I think that it is only natural for the HVAC engineer to expect that there will hardly be any complaints if he designs his system according to these guidelines; but unfortunately it is not always so.

3. Case histories

The parameters influencing human comfort and indoor are quality are many, and the designer must be aware of them all. If he misses out just one, he is bound to have complaints; but if he tries to account for all of them, he may still have problems.

In a revamped office building in Northern Italy the designer had specified an all-air constant volume HVAC system with terminal reheat (provided, as it should always be done, by heat recovery condensers in the air-cooled chillers).

Indoor air conditions specified were within the comfort diagram, and in particular the design relative humidity in winter was 40%. Specifications for outdoor air called for 50 m3/h (13.6 L/s) per person, or 1.5 air changes/h, whichever the greater. Outdoor air was fed to the air-handling units, located one on each floor, via an air handler equipped with a coarse filter having an efficiency of 88% according to ASHRAE 52/76; each floor unit, which handled both outdoor and return air, was provided with a bag filter, efficiency 95% N.B.S.

During commissioning outdoor and total air volumes, as well as ambient temperatures and humidities, were determined; all values conformed to Specifications within the permitted ranges. In theory, then, everything was fine: the tenants, however, did not agree.

The most frequent complaint was of "air draughts", and was interesting enough to notice that they occurred more often in winter and in the intermediate seasons than in summer.
Two types of air outlets had been envisaged for air diffusion: one was a conventional linear grille, and the other a perforated type diffuser, which was integrated in the false ceiling structure.

Because of architectural reasons, the linear grilles were used in some rooms which had a large window area and a shallow depth: the resulting cooling load was so large that 10 - 12 air changes were required to offset it. Even so, the measurements showed terminal velocities at the workplaces below 0.15 m/s; but the billowing of the curtains due to the large amount of supply air was very impressive, and upset and frightened the tenants.

With the perforated diffusers, complaints came mainly from those who sat immediately below the air outlet: in some cases terminal velocities of 0.3 - 0.5 m/s were detected in spot measurements. However, this velocity depended to a very large extent on the temperature of supply air; if the reheat coil was working, and supply air temperature was at 23 - 25°C, there was no problem: but if someone was hot and suddenly decreased the room thermostat set point, he would experience an immediate shower of cold air at 16° C as the valve on the reheat coil closed immediately.

Eventually a solution was worked out by resetting room and supply air temperature upward in those rooms where cooling was required in intermediate seasons: in other cases the solution had to be more drastic, and involved either relocating the diffusers or spreading the air flow over a greater number of supply outlets.

In another building a complaint was registered immediately after system start-up ; many of the tenants complained of itches and skin and nose irritations. A specialized organization was called upon to analyse room air; as well as a total dust content variable from 0.3 and 2.3 mg/m3, chiefly due to site dirt, a concentration of 1 to 7 fibers/liter of fiberglass was found. This insulating material had been specified chiefly for acoustic purposes as duct liner downstream of the VAV boxes; obviously, wherever the installation had been incorrectly applied, it had become loose and detached itself, being carried into the rooms by the air stream.

After a few days, the complaints ceased and did not occur again: obviously all the material which could become loose had done so.

4. Consequences

The above examples show that textbook knowledge and experience sometimes are not sufficient to prevent a building from being defined "sick" (i.e. such that more than 20% of the tenants experience various illnesses which cease upon leaving the building). Design may be done "by the book", and yet the client is dissatisfied. Some obvious down-to-earth consequences which can be drawn are:

- do not use internal duct lining if at all possible;
- even though there is no way to anticipate the actual behaviour of air outlets in a given environment until the system is started, select them with great care. Check terminal velocities for many ranges of room and air temperatures (there are now computer programs which allow the designer to "see" the effect on his video);

- in VAV systems, always use outlets which can vary their area according to their flow rate, so that throw and air movement is not impaired; at the air handling unit, provide controls to maintain constant outdoor air flow rate at part load;
- if a final room layout is not available, build some leeway into the diffusers; use flexible duct connections, and leave some blanked-off duct runouts;
- either do not allow the tenant to fiddle with the room thermostat, or else explain in simple terms how the system works, what it can do and what cannot be expected to do;
- recognize that the best design is no guarantee against faulty installation and sloppy execution, and monitor contractors very closely;
- finally, design for maintenance. Filter cleaning must be easy, or it will never get done. Oppose the architects in their attempts to cut technical room space and height.

5. What the engineer needs from ventilation and IAQ specialists

Basically, what is needed is not a collection of papers full of graphs and formulae, but some design guidelines. For instance:

a) More data about he best pattern for air distribution. I have read that at the latest ASHRAE meeting it was maintained that the maximum ventilation effectiveness (as defined by ASHRAE 62-1989) is achieved by introducing air at floor level and returning and exhausting it from the ceiling. If so, which floor outlets should be used and how should they be spaced? What is the minimum supply air temperature and the maximum outlet air velocity available? Is this solution applicable with VAV systems? What happens in the heating season?

b) ASHRAE 62 states that there is an Indoor Air Quality procedure which can be used to achieve acceptable IAQ in lieu of the Ventilation Rate procedure. How does one apply it in practice? Which instrumentation should the HVAC consultant acquire?

c) How does one calculate or determine the stratification factor S defined in Appendix F of ASHRAE 62?

These are just a few questions, and the list can probably be much longer. I am convinced that the answers to these questions can be easily supplied by many in the audience, and I apologize to those for my ignorance. What I have tried to convey in these few minutes is the concern, which is probably shared by many colleagues of the design community, for the IAQ problem, and the desire to find help and advise. Like Socrates of old, I "know that I do not know", and this, hopefully, is the basis of real knowledge.

Mr. Chairman, ladies and gentlemen, thank you very much for your attention

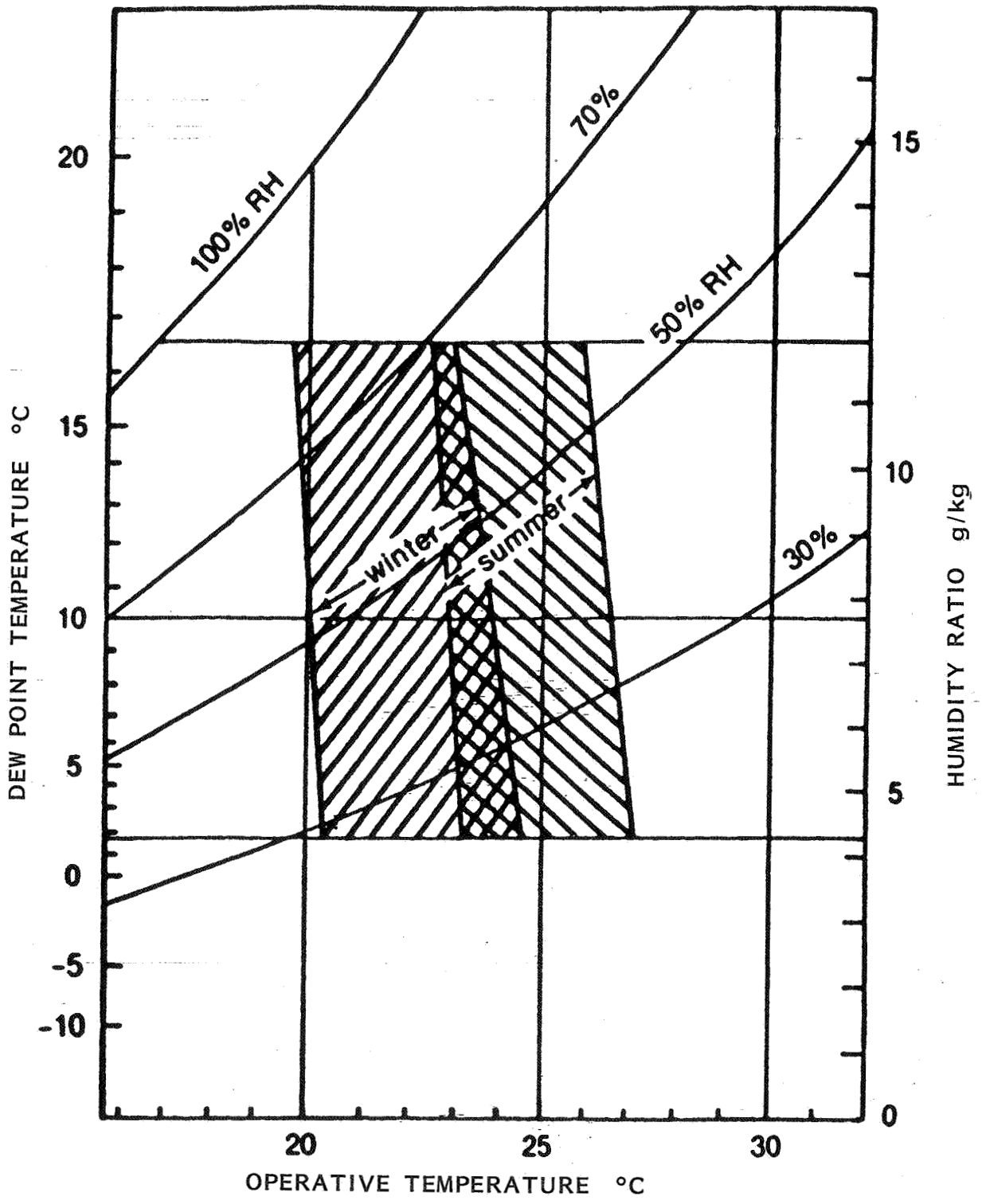

Figure 1. Acceptable ranges of operative temperature and humidity for persons clothed in typical summer and winter clothing, at light, mainly sedentary, activity (⩽1.2 met)

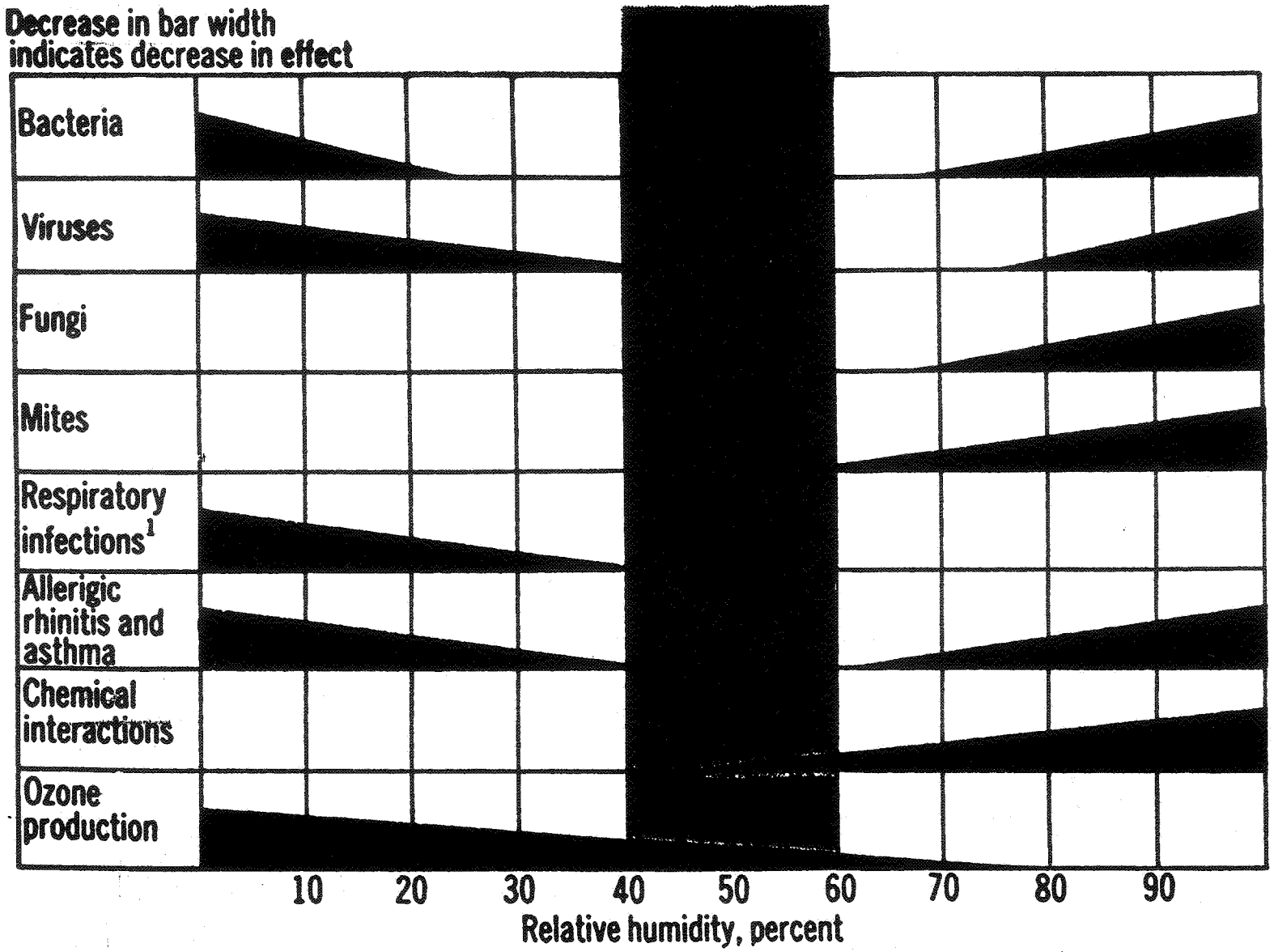

Figure 2. Optimum relative humidity ranges for health

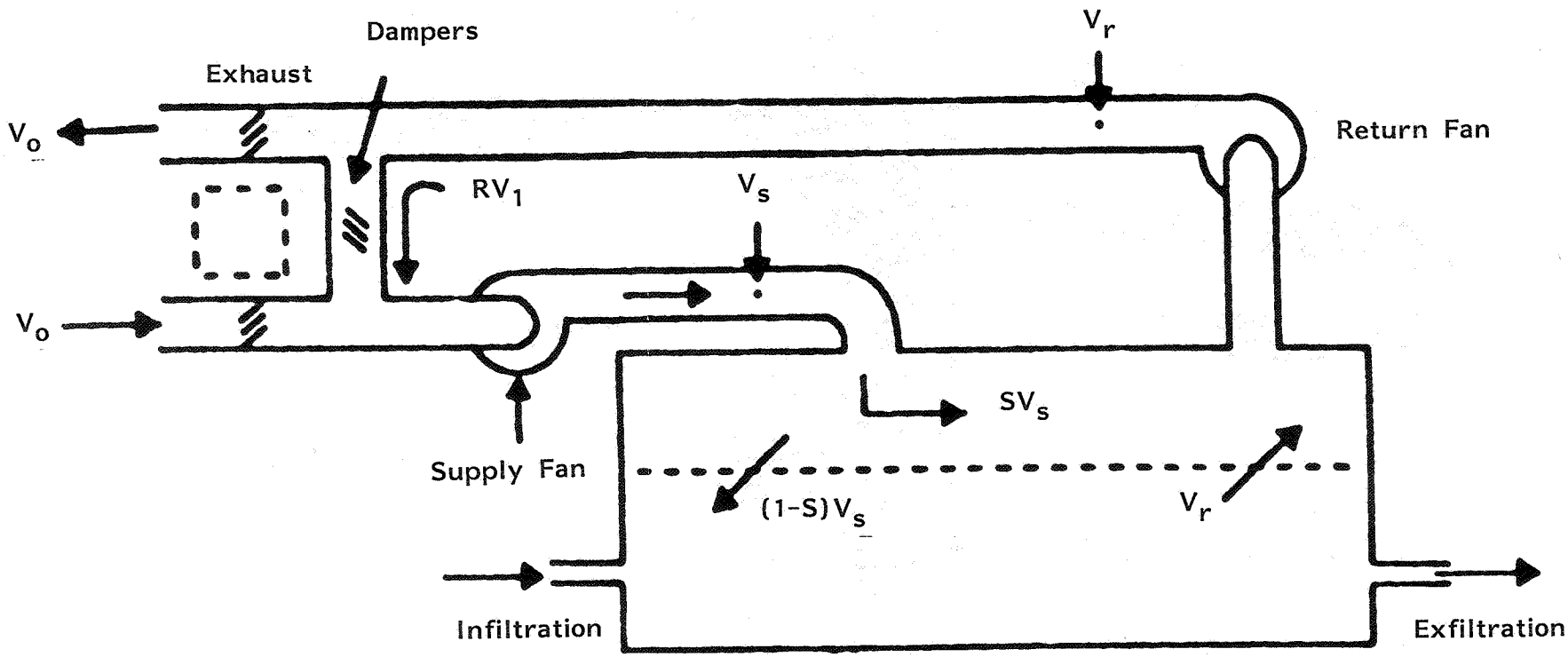

Figure 3. Typical air distribution system

Discussion

Keynote Speech

M J Holmes (Arup R & D, UK)

You have requested that good design guidance is required not calculation methods. Your example of a linear diffiner with 12 air changes and room velocities of 0.1 m/s resulting in discomfort is in conflict with a UK design guide. Could you elaborate and explain why conventional guidance was not satisfactory?

A Sandelewski (Techne, Italy)

The result is not in conflict with the guide you mention. Terminal air velocity measurements at the workplace were consistently lower than 0.1 m/s. However, the shallowness of the room made the air flow very evident at the window. Curtains billowed alarmingly, and this was worrying for the room tenant. Moreover, in the room there was an objective operating problem because of the large window area. However, purely from air diffusion standpoint everything was ok.

VENTILATION SYSTEM PERFORMANCE

11th AIVC Conference, Belgirate, Italy
18-21 September, 1990

Paper 1

INTELLIGENT BUILDINGS - INNOVATIVE TECHNIQUES FOR THE ENVIRONMENT

REINHARD SEYER* AND LUTZ TREPTE**

* Daimler Benz AG, Research Institute, D-6000 Frankfurt/M.,
Federal Republic of Germany

** Dornier GmbH, D-7990 Friedrichshafen,
Federal Republic of Germany

SYNOPSIS

All around the world the quality of the air is steadily decreasing on account of the strong nuisance caused by combustion deposits. This process is accompanied by a distribution of pollutants occuring even in the highest atmospheric layers due to air traffic. Additionally, the amount of chlorofluorohydrocarbons increases, ozone is produced by photochemical oxidants, and the dust load is growing on account of traffic, industry and domestic heating.

Caused by the relatively high concentration of carbondioxide in the atmosphere, the greenhouse effect leads to climatic changes. Acid rain is produced on account of the increasing exhaust of noxious gases, such as SO_2 and NO_x, which additionally are under founded suspicion of being responsible for the dying of the forests. Causing a strong nuisance to the respiratory air, unburnt hydrocarbons are carcinogenic and lead to allergies.

Independent of this situation, people are more and more aware of the restrictedness of fossil fuels and realize that the conservation of natural resources by comprehensive energy savings will represent one of the essential and most challenging tasks of the future.

The pressure generated by this development is currently leading to fundamental reorientation in all areas which contribute to the strong environmental impact described above. Besides industry and traffic, the domestic area plays a role in this process which should not be underestimated. The end use of energy for heating and hot water amounts to approximately 22% of the overall energy consumption. This value is applicable in the Federal Republic of Germany where heating consumes an important part of the domestic energy supply. In our latitudes, the portion of the energy required for domestic heating amounts to 80% of the energy totally supplied to the average home. In Southern European countries like Italy, Greece, or Spain, these values are certainly different.

With respect to architecture and building materials, this reorientation process has led to advanced technological developments designed to achieve a reduction in the consumption of resources for heating purposes. There is a general trend to reduce the heat loss caused by a transmission through walls and windows. Today, triple glazing and well-insulated walls are used to cut the heating energy demand. On a medium-term basis, the transmission loss might be reduced by approx. 70% so that an average energy consumption of 50 kWh per m^2 and year might possibly be attained in the future. Compared to the present situation in Germany with average values of about 150 kWh for the existing building stock, a reduction by the factor three seems to be achievable within a few years, from technical as well as from economic aspects.

If we assume the ventilation loss to remain stable, its portion in the overall heat consumption would rise from about 20% today to 50% or more, depending on the air exchange rate, in the future [1]. This clearly indicates that ventilation in general, as well as the ventilation loss, will be of increasing significance with respect to domestic heating and the enrgy balance of buildings. Therefore, special emphasis must be placed to this development even now.

Parallel to this tendency in the field of heat supply which also concerns building materials and their architectural application, various developments in the electronics sector currently being performed will definitely lead to an extensive use of information technology and communications in building design and construction. The performance capacity of modern communications structures is steadily increasing whereas their costs are going down. On account of this process, automation systems which have already been applied to building automation will improve with respect to their level of utilization and, thus, gain acceptance in the private sector on account of the favourable cost development. On the basis of these systems several areas, such as heating, ventilation, lighting, communications, safety and security, will be demand-optimized within the scope of different partial processes. Responsible for the individual areas, the integrated computer intelligence ensures that the supply is optimally adapted to the actual demand. Additionally, considerable advantages result from synergetic effects and the possibility of easily installing the communications medium.

1. INNOVATIVE TECHNOLOGY

New approaches show that future processor systems will be cost-effective and highly efficient. Being already utilized in automated commercial buildings, such systems will soon be modified in order to be suitable for residential buildings or even apartments. In this case, the benefits of such systems would also become effective in the private sector.

Today, even small and inexpensive microprocessor systems are capable of planning and processing demand-oriented automation strategies. The basis of this development is a communications system technologically accomplished in the form of a bus system. Moreover, 'intelligent systems' have to be developed, controlled by microprocessors and capable of being mutually connected via the communications system. Then, the first connections between such systems will be established to achieve automation of partial areas. The final objective consists in the optimization of heat and fresh-air supply in this area according to the principle of supply and demand.

With respect to ventilation, this means that the air exchange rate has to correspond with the actual demand of the inhabitants. The air quality is controlled by means of sensors. Ventilation systems ensure that polluted air from kitchen and bathroom is extracted and, simultaneously, fresh air is led into areas where the nuisance is relatively low - bedroom, living room and hall. Similar optimization strategies can be accomplished for heating, water, lighting, and the like. In addition to the automation of individual partial areas, however, the technical system of a bus structure offers another decisive advantage: On account of the given structure, the different partial areas can be interconnected without any additional effort. This offers the opportunity to consider a house or building as an overall system and, thus, to achieve overall optimization throughout all partial areas. Synergetic effects result from an elaborate coordination of individual processes. Ventilation is a main link between energy conservation and indoor air quality and, thus, will play a major role in buildings installation (s. fig. 1). This paper is intended to explain this type of common utilization of information in the areas heating, ventilation, and safety and security, as well as to present its advantages.

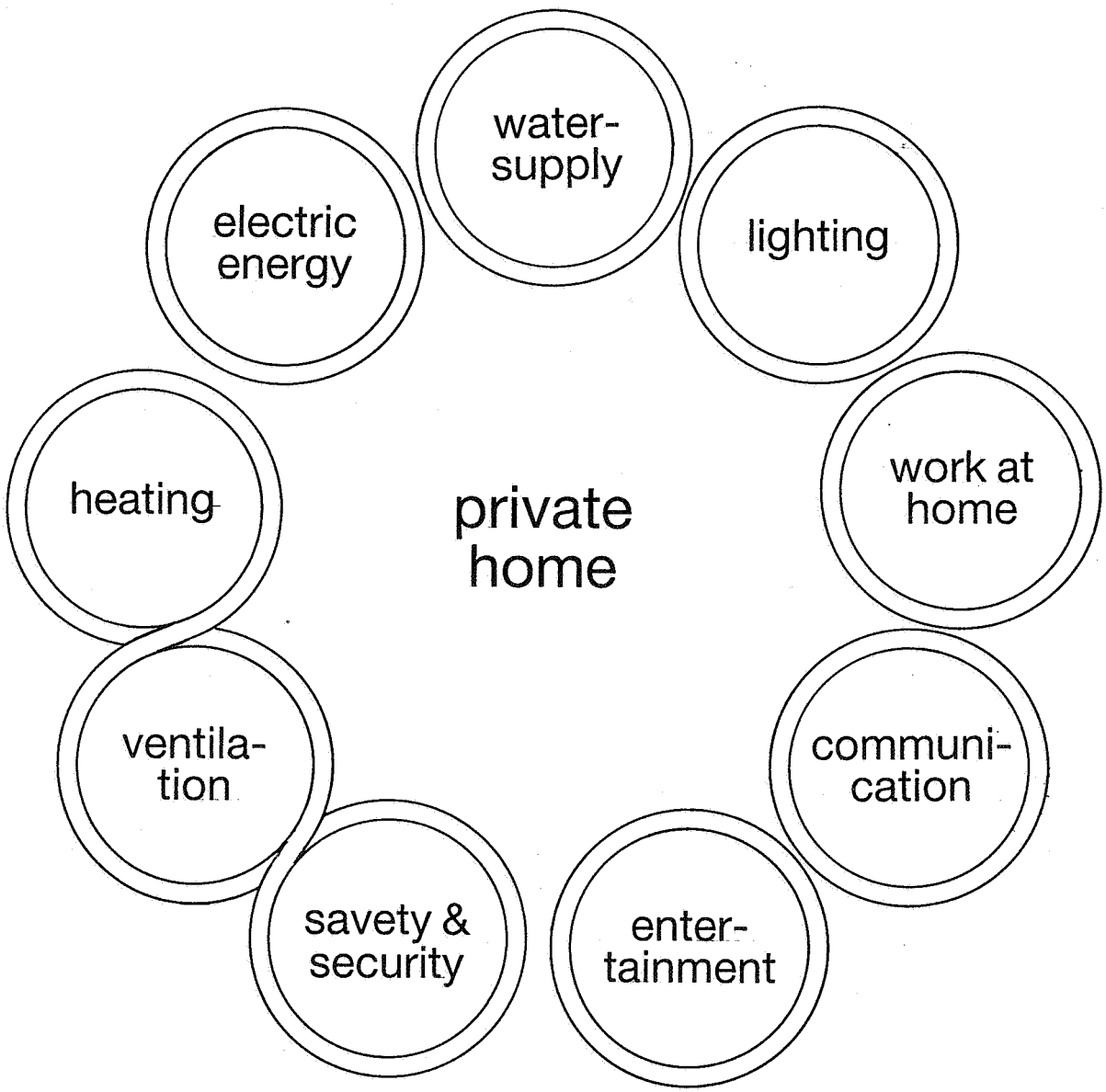

Ventilation as a main subsystem of an integrated interactive home

figure 1

This means that the heating system is provided with information on the number of persons present supplied by the safety and security system. Regulation of the heating system is no longer time-controlled only, but the presence of persons can also be taken into consideration and included in the automation strategy. The basic prerequisite, however, is a building with absolutely separate heating areas.

The same applies to ventilation. If no persons are present, the air exchange rate can be considerably reduced. This would automatically be made by means of a sensor-controlled system, the information that no person is in the house or apartment, however, is especially advantageous with regard to the optimization of the control parameters [2]. In this case, a much faster reaction is possible. In turn, however, a sensor-controlled ventilation system can supply information to a safety and security system. Sensors for indicator gases to regulate the air exchange can easily be complemented to sensor systems which do not only detect CO_2 but also concentrations of other gas components. In the future scenario of a fully automated building absolutely new and useful cross links can result from the interconnection of different partial areas. If the building has a gas port and gas is used in the domestic area, detection of the methane concentration will be extremely appropriate. Even small leaks can be early recognized, the inhabitants alerted, and the gas supply automatically cut off. In coordination with the cut-off, the air exchange rate are increased to the maximum value, and all gas appliances, like heatings, stoves, or flow heaters, turned off. All electrical loads are switched off and the electrical supply is interrupted. If no persons are present in the building, the alarm message is automatically transmitted to an external unit, such as the gas supply company. Different actions to be taken in different areas are coordinated and appropriately harmonized with each other.

In almost the same way a fire detection system can be accomplished. Fire usually starts with smouldering producing CO. If a second element measuring the CO concentration in the air is combined with the sensor, fire detection is possible on the basis of the signals transmitted by this measuring element. In this case, the cross link to the safety and security system is also evident.

Furthermore, sensors monitoring the position of windows and doors can also be appplied in various ways. Their monitoring data are of special significance for the ventilation, as well as for the safety and security system. With respect to multiple application, actuators can also play an important role. If a future system possesses window and door actuators, they can obviously be used by both systems.

Interaction can also be found between heating and ventilation, especially if a reduction of the consumption of heating energy can be accomplished to such an extent that the air in the room can significantly act as a heat transfer medium. In this context, significance means that an important part of the heat transfer is performed via air without increasing the air exchange rate, producing disturbing noise, or causing unpleasant drafts. Under average conditions insulation should be so good that the normal air exchange rate of 0.8 per hour is sufficient to ensure the necessary indoor air quality. It remains to be seen, however, whether this objective can be attained in the future - in any case, it is absolutely worth striving for.

2. IMPROVEMENT POTENTIAL

As already described above, advanced insulation materials and new processing techniques offer a considerable improvement potential in the building area. The potential to be depicted here results from the selected example of an interactive connection between heating, ventilation, and safety and security systems, principally based on the improvement effect caused by new materials. In other words, it represents the 'finishing touch'. If all possibilities of insulation improvement have been exhausted and corresponding tightness of the building has been achieved, the benefit of an intelligent interactive system will reach its maximum.

This benefit can be derived on account of the demand-oriented working principle of the system. It only provides as little system performance in the form of heating energy and fresh-air supply as required under the given circumstances. Thus, it adapts itself perfectly to user behaviour and environmental changes. It offers comprehensive services accomplished with minimum effort independent of the respective circumstances.

This implies saving of energy and, thus, considerable cost reduction. Ventilation regulation ensures constantly high air quality and a healthy room climate. It prevents condensation and removes odour, dust, and pollen. Additionally, uniform heat distribution is sustained.

The integrated safety and security system recognizes hazards, transmits corresponding messages, and eliminates the risk. For the user, such system acts as an attentive butler who assists and relieves him in necessary activities with respect to heat and fresh-air supply and, thus, improves comfort and snugness.

With regard to the environment, two decisive aspects result from the reduction of heating and ventilation efforts. On the one hand the reduced consumption of energy helps to conserve the natural resources, and on the other hand the amount of combustion deposits produced with the supply of heating energy is decreased.

The effect of resource conservation - particularly concerning fossil fuels - can even be intensified, if regenerative energies are integrated and appropriately utilized in the energy supply process. This would result in a reduction of the exhaust of CO and noxious gases, such as SO_2 and NO_x.

3. TECHNICAL REALIZATION

Technical realization of an integrated system is performed in three steps. First, a communications system is required, capable of ensuring the necessary exchange of information independent of the respective application. Such system must be easy to install and adaptable to specific company requirements.

A proposal for standardization of a corresponding system is currently being prepared within the scope of the ESPRIT project 2431 "Home Systems" by 10 of the major electrical manufacturers. The participants comprise ABB, BT, DB/AEG, GEC, LEGRAND, PHILIPS, SIEMENS, THOMSON, THORN, ZELTRON/ZANUSSI. Independent of this project several renowned European companies - under the leadership of SIEMENS - are developing an

installation bus system which will be put on the market under the designation European Installation Bus (EIBus). A third system is currently being announced by MERLAN GERAND under the name 'BATIBUS'. In the USA, corresponding activities are performed to introduce a similar system called 'CEBus' (Consumer Electronics Bus). The most advanced development, however, can be found in Japan where first applications of the so-called 'HBS' (Home Bus System) have already been sold. The large variety of these activities gives an indication of the importance attached to this technology and its marketing expectations in the most important industrial regions of the world. It would exceed the scope of the present contribution to discuss the individual specifications, advantages and disadvantages of the different systems. For this reason, only some general remarks shall be made.

Each of these communications systems is based on a bus structure. This means in principle that the entire information exchange is performed via one common information channel so that all information are available to every participant. In some cases, however, this fundamental principle is broken by the application of cluster and sub-bus systems. Certain systems contain different communications media and possess self-organization as well as self-configuration features. Figure 2 depicts the structure and configuration of a general integrated system based on a bus structure.

In addition to a bus system, intelligent components are required in order to ensure information exchange via bus. Concerning our example described above, these components include heating controllers, pumps, valves, fans, vent doors, and various sensors. These sensors mainly perform monitoring of room temperature, air quality, air humidity, and flow velocity. Furthermore, window and door, as well as access control sensors are required. Sensors for air quality monitoring comprise several detectors which determine the concentration of different gas components, such as CO_2, methane, and hydrocarbons in general. CO sensors are important for fire detection while NO_x sensors are required for the elimination of nitrogen oxides produced under smog conditions. In addition to these complex sensors for gas concentration determination, simple temperature and humidity sensors are required. Some of these sensors and detectors can be combined to multisensors - a step which considerably reduces the overall design and integration effort, since evaluation software, as well as a bus system interface, is only required once.

All components, sensors, and actuators are interconnected by means of a bus system requiring little cabling effort. This bvus system includes different communications media, such as twisted pair, coax, radio frequency, diffused infrared, mains communications, and plastic optical fibres. According to the respective application and system environment, appropriate systems can be selected and mutually combined. For retrofit purposes mains signalling is suitable, whereas in new buildings twisted pair seems to be appropriate for heating, ventilation, and safety and security. IR and RF, however, will only be used for portable systems, such as remote control devices for audio and video systems or portable telephones.

Every component of the communications system has to possess its own information interface for reception and transmission. This is also applicable to the simplest components, like switches, valves, pumps, and sensors.

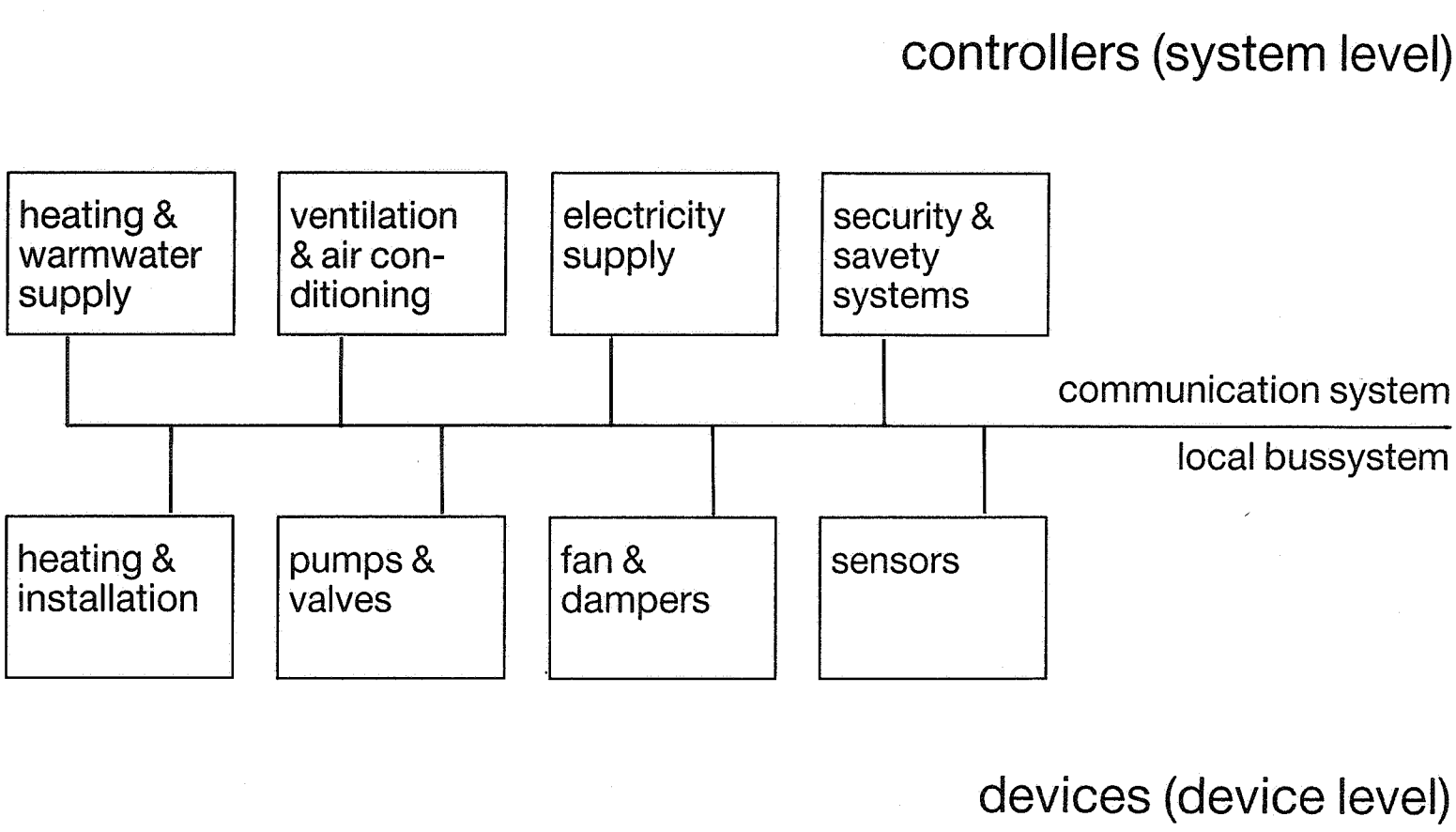

Configuration of an integrated system

figure 2

Logical interconnection of these elements is performed by means of control units equipped with a more complicated software. Such a control unit is capable of combining the different components installed in an area to a small but complete automation system. It contains the entire strategy according to which a coordinated, fully automatic process can be controlled or, in many cases, even regulated.

Each system possesses a user interface. Even if the systems are considered to be fully automatic, the user often wants to interact for information and data retrieval purposes.

The system has a hierarchical structure which also provides redundancies. This increases system safety in case of failure which will never lead to total system failure, since all partial systems are capable of working independently. In case of a failure of the main control unit, the partial systems work on a lower organization level. In case of failure of a partial system, either a redundant system assumes its task or an emergency program is executed. In no case another partial system is impaired. Particularly these considerations concerning system reliability are of special significance in the private sector, since a commercial service infrastructure does not exist. This is at least applicable to the introduction phase.

4. PROSPECTS

It is astonishing to see how the technical capability of processing silicon allows to develop a wide range of new technological systems. Traditional fields, like heating and ventilation, come closer together. And other areas, such as safety and security, entertainment, and communications, which have always been absolutely separate are also combined with the traditional ones. In a continuous evolution, small units grow to modular systems which offer completely new properies. Information availability, free and independent of local circumstances, forms the basis for the accomplishment of these properties. Complex intelligent systems can be accomplished and will replace conventional equipment.

The factor which is decisive for the development of completely new characteristics is the possibility of executing processes in a demand-oriented way due to the increased utilization of information. Another important feature is represented by the anticipation of low costs which are the prerequisite for the required technical basis and the penetration of technology into all social areas. In the future information systems will be an integral part of standard house and apartment equipment. This in turn offers everyone the possibility of contributing decisively to environmental protection. In the first place, the reduction in heating energy consumption will be achieved on account of new building and insulation materials and amount to approx. 60%. All savings going beyond this value, however, will result from intelligent energy consumption supported by advanced information systems. If this process helped to cut the consumption again by half, only 20% of today's heating energy consumption would remain. And eventually, if it were possible to integrate solar energy to a considerable extent into heating energy supply, there would be justified hope that a reduction to even 10% of the present consumption could finally be achieved.

This means that the consumption in the private sector could drastically be reduced. Parallel to such reduction in consumption the atmospheric pollution caused by CO_2 and noxious combustion deposits would be decreased. Additionally, however, another improvement potential can be found in this area, based on continuous optimization of the combustion process by intelligent process control combined with advanced catalytic converters and filtering techniques. If a reduction potential of 90% is assumed for the exhaust of noxious gases, the pollutant emissions in the domestic area will even decrease to 1% compared to the currently applicable values.

Other reduction potentials, though not in the same order, exist in the areas of electrical energy and water supply. Here, damand-oriented systems will also contribute to an increase in the utilization ratio by integrating regenerative resources in the form of solar energy and rainwater. Demand-controlled ventilation only represents a first step in the right direction. In the future, energy and air quality management will find their way to the market in order to meet the complex requirements for the protection of indoor and outdoor environment.

REFERENCES

1. HENSELER, H.-J. and TREPTE, L.
"Energiesparende Lüftungsmaßnahmen in Wohngebäuden" (in German language), Ki Klima Kälte Heizung, pp 275-278 (1982)

2. RAATSCHEN, W. (Ed.)
"Demand Controlled Ventilating System", State of the Art Review of Annex 18 of the Programme 'Energy Conservation in Buildings and Community Systems', Swedish Council for Building Research, 1990

Discussion

Paper 1

H Hens (Leuven, Belgium)

Be careful with automatising in the private sphere! First: analysis of what people accept, then: automatising the "Autonomous Neutral System" of the building not the private sphere of the user/inhabitant/employee?

R Seyer (Daimler Benz AG, Germany)

Agree.

VENTILATION SYSTEM PERFORMANCE

11th AIVC Conference, Belgirate, Italy
18-21 September, 1990

Paper 2

INDOOR AIR QUALITY IN "BUILDINGS OF THE YEAR". MAX PRODUCTIVITY - MINIMUM OF COMPLAINTS

GAUTE FLATHEIM M.sc.NTH
INDOOR AIR QUALITY CONSULTANT (MEMBER FIDIC)
MEMBER OF THE COMMITTEE FOR HEALTH AND
INDOOR ENVIRONMENT
NORWEGIAN ASSOCIATION OF CHARTERED ENGINEERS
STAVANGER
NORWAY

ABSTRACT

Sustained efforts to conserve energy during the last 15 years have taken place at the expense of the indoor environmental quality. Ventilation air volume has been reduced to a minimum. The use of new materials, substances and equipment which emit gases, vapours, fibres and other pollutants into indoor air are an additional reason for the increasing frequency of complaints about the indoor environment.

If air quality is improved by increasing air volume, the energy demand will increase - and extended initial costs will rise.

Adverse effects on health, caused by poor air quality, have been recorded. These include irritation of the skin and mucuous membranes, fatigue and headaches. Such conditions are also of significance for ill-health which is related to allergy and respiratory disorders. Evidence available from research and official statistics indicate that complaints about the indoor climate are clearly related to well-being and productivity in our places of work (1).

1. Introduction.

For more than 25 years air consultancy has been focused on low investment cost in addition to the question of energy consumption. After the oil embargo in the mid 1970's, several energy conservation efforts have had a negative impact on the indoor air quality (IAQ). This very unfortunate situation is about to be changed.

Major companies take a different attitude regarding employees, and have become more concerned about their comfort, productivity and health. These companies ask what we - as planners - can do to provide a new building, with a secure indoor environment, a minimum of contaminants, and sufficient amount of well filtered outdoor air.

One of these companies is Norsk Hydro who decided to build a 22000 sq. meter building in Bergen for the administration of the Oseberg oilfield in the North sea. They started in 1985 with an evaluation of architects and ended up with a paid

competition between five very qualified architectural companies in Norway.

As HVAC-consultants for Hydro, our company was responsible primarily for capital costs and minimizing energy consumption. We made the complete specifications for technical installations (HVAC) and supervised detail engineering done by the winning contractor based on the winning architect's sketches. This approach was completely new in Norway, and the result as far as indoor environment was very good.

Even during the construction of the Norsk Hydro Administration Building in the mid-eighties, new technology in the field of indoor environment was widely expanded. This new technology will enable the next two buildings that Norsk Hydro has scheduled for construction to be built in an even more cost effective manner regarding total costs over the lifetime of the building than the first building. This will result in substantial savings when one considers that personnel costs represent close to 90 percent of the total costs.

2. Indoor Climate

The consequences of energy technology for indoor climate have not received much attention. New developments in energy technology and the use of new materials in buildings have, to a greater extent than previously, created buildings with indoor climate problems (SBS). Simultaneously, health, comfort and productivity have become factors to which greater attention is attached during debates about developments in society. When calculating the annual costs of a building it is therefore not only economy that counts, but also the value of health, comfort, and productivity of employees.*

The problems around indoor climate can now be documented by means of questionnaires in which people give their opinion about their situation. Common complaints are:

- *Draughts.*
- *Dust or dry air.*
- *Humming and noise from ventilators, etc.*

** SBS - Sick Building Syndrome*

- *Heavy air, headaches, nausea, dry throats, fatigue and smarting eyes.*
- *Too cold or too warm.*

Many individual cases also point towards conditions being worse in buildings having lower ventilation rates than in others. The minimum requirements of the Building Codes today do not contain adequate consideration of:

- *Processes in the building (the work function itself).*
- *Cleaning (including cleaning agents).*
- *Copying equipment.*
- *Computers, terminals and printers.*
- *Degassing from furniture and fittings.*
- *Textile fibres.*
- *Floor adhesives.*
- *Other "hairy" surfaces.*
- *Rock-wool fibres (MMMF).*
- *Fall-out from panelled ceilings (MMMF) & dust.*
- *Textile fibres from clothing.*
- *Dust in the duct network.*
- *Etc.*

These factors represent pollution in excess of that which people themselves produce. Importance must be attached to the sum of the pollution when the ventilation volume and the principles concerning ventilation are being determined.

3. Energy requirements in office buildings.

The energy required for heating modern office buildings has been reduced in recent years. This is because the need for energy conservation has resulted in buildings with improved insulation, triple glazing, improved air infiltration, and reduced ventilation volumes. A new office building for Statoil in Stavanger (330.000 sq.feet) has only used energy for NOK 100.000,- during the first year of operation.

Despite this, we often see that modern office buildings have large total energy requirements, perhaps just as large as previously. We also see that energy requirements, to a greater extent than previously, must be met by electricity. The explanation for this is that buildings are now filled with equipment needing to be powered by electricity, such as computer equipment, printing and copying, and general office equipment. Large

data processing centres and communication centres are also common. All these produce excess heat which needs cooling through the air conditioning system - which also requires electricity.

It seems that the reduced energy requirement per device is insufficient to outweigh the great increase in the number of devices being installed in our buildings. Additionally, improvement in the efficiency of light fixtures seems to be proceeding much more slowly than expected.

Low energy consumption in modern office buildings is therefore only possible if the air conditioning system is designed in such a way that transferred heat can be exploited to cover heat losses (2). Figure 1 shows the energy flow in a modern building. Heat loss, ventilation loss and domestic hot water requirements determine the thermal energy requirement. At the same time, we have, as just mentioned, a great need for electric power to run equipment - including fans and pumps.

Fig. 1

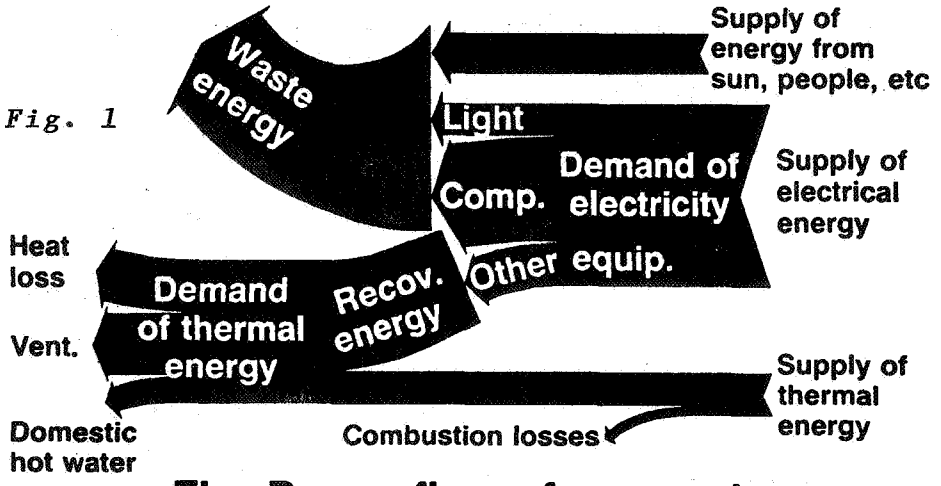

Fig: Power flow of energy in an office building

If the excess heat from operating equipment, the sun, and human beings can be recovered and used to meet the thermal energy requirements, then the necessary input of thermal energy will be merely a balancing item. This superfluity of thermal energy in our office buildings offers us possibilities for upgrading the indoor climate without

specially significant consequences for energy consumption (1).

To put this into a more tangible form, we have looked at a building planned for Statoil in Trondheim, Norway. This building has a gross floor space of approximately 25000 sq. meter and will meet the needs of approximately 750 people. We will assume that the building has a present day standard regarding choice of materials, and that smoking is permitted. A separate EDP department requires 300 kW of energy to operate the data processing equipment.

The building will be equipped with combined cooling units which cools EDP machines, cools ceilings in the offices, and ventilation air in the summer. The excess heat is transferred to a water based heating system. This energy can thereby be exploited to meet a substantial portion of the thermal requirements.

Figure 2 shows the energy requirements per square meter of this building, with the three different demands on air quality (3).

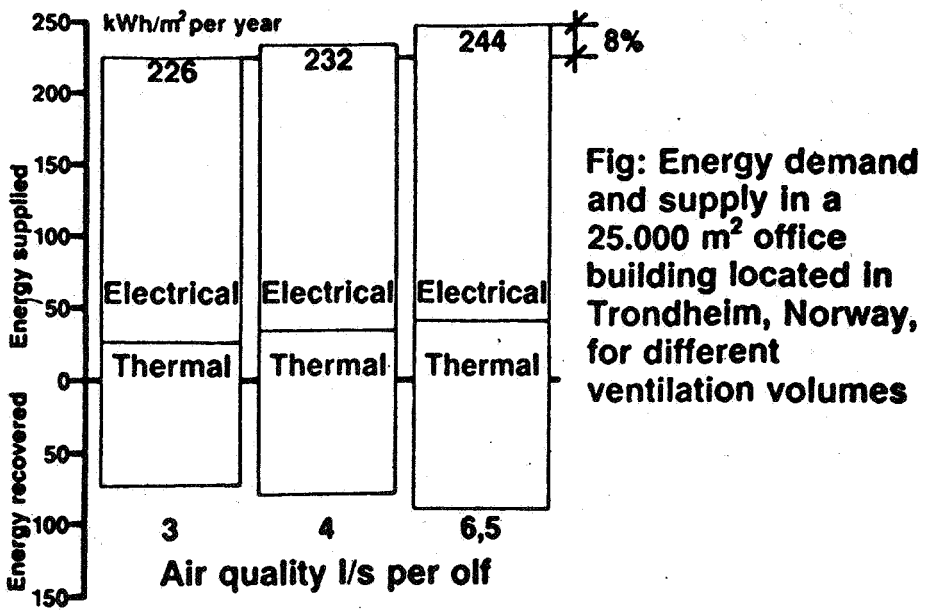

Fig: Energy demand and supply in a 25.000 m² office building located in Trondheim, Norway, for different ventilation volumes

We see that the need for electric power for lighting, operating equipment, etc., is greater than the need for thermal energy for air conditioning. Furthermore, exploiting possibilities

for recovering heat from electrical equipment, the sun, etc., will significantly reduce the actual demand for thermal energy.

If we want to improve the air quality in this building by increasing the air flow from approximately 7.2 up to 15.6 cubic meters per square meter per hour, we see that it results in only marginal increases in total energy consumption. To reduce the expected number of complaints from 35% to 20% requires an increase from 226 to 244 kilowatt hours per square meter per year, or about 8%. (Professor P.O. Fanger) (3).

This calculation confirms that there is excess energy present in modern office buildings. When we have an increase in energy consumption with an increase in air flow, this is largely related to increased energy for operating fans.

An 8% increase in energy consumption means in this case that operating costs will increase by approximately 315 Norwegian kroner (48 US$) per year for each employee - which is negligible.

4. *Performance and Well-being.*

As regards environmental questions, pollution of the external environment is the theme that politicans and the media are preoccupied with. The fact that people are mostly indoors is rarely pointed out. The reason seems to be that we have not considered it a health hazard to be indoors in homes and places of work, except for a few industrial work-places (4).

At present time there seems to be a change in attitude towards this in Scandinavia. More and more people make the point that the indoor environment is also important for public health. Professional building owners have long since realized that investment in a good indoor climate is an investment in the well-being of employees and in increased productivity (5). In October this year FIABCI Common Market Committee will arrange their study days in Stavanger, and the main topics are energy consumption and indoor air quality and their inpact on the value of real estate.*

** FIABCI - FEDERATION INTERNATIONALE DES PROFESSIONS IMMOBILIERS*

Our Statoil project does not attempt to carry out a broad investigation of the relationship between air quality and productivity. Such a study would demand too many resources. We nevertheless believe that the information available from official statistics and related research projects can prove such a connection (6).

5. What are total costs?

The annual costs of a building consist of depreciation on invested capital costs plus operational costs (Fig. 3). When a new building is being planned, it has become more and more common to use annual costs as a decision making tool. The reason for this is that the costs during the operating phase increase relatively; particularly labour and power costs.

The annual costs are often evaluated per square meter floor space. Obviously the costs should be kept as low as possible.

Annual costs are then related to the building instead of to the employees working in the building.

Costs like these are related to the building itself and running the building. But why do we put up an office building in the first place? Of course it is because we have work to be done, and this can be done in a less expensive way if the temperature feels comfortable and the productivity is high. A good indoor environment is one of the most important factors to improve the efficiency of any staff. This is elementary - but do we act like this in our building industry? Do the building owners act like this? I am afraid not, and therefore I have started to bring up an extended expression for total cost. Total cost must be related to the sum of wage-related and building costs. This is shown in the Oseberg complex in Bergen (Norsk Hydro) where personnel related costs per square meter is NOK 14.882,- in the left columns (Fig. 3).

The total costs for what I call Indoor Air Quality Standard (IAQ Std) 7.5 cubic meters per square meter per hour, is NOK 16.555,-. If we raise the standard to 15 cubic meter per square meter per hour and take precautions with selec-

tion of materials, building procedures, cleaning procedures etc., the costs will rise to NOK 16.667,- and the difference is mainly in investment costs: 9.4 - 8.8 = 6%. The personnel related costs dominate totally.

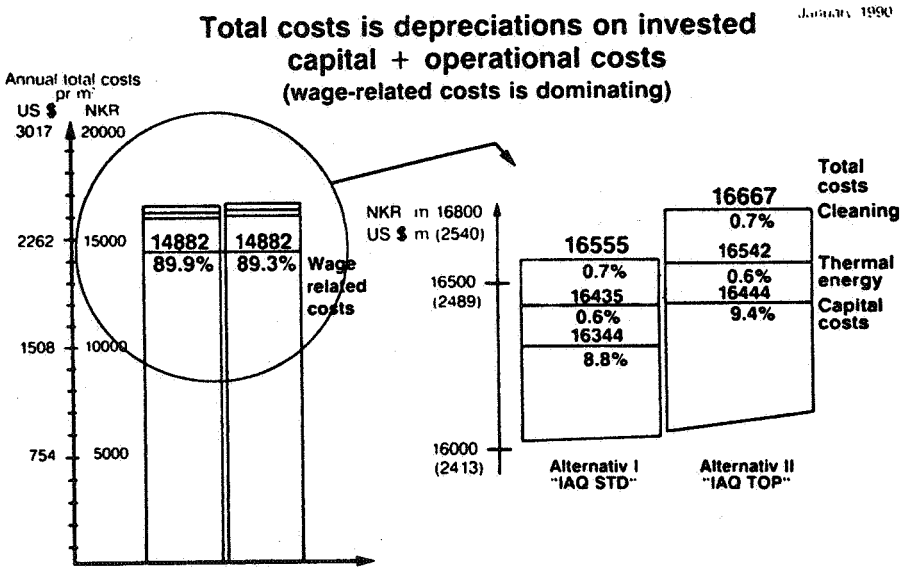

6. *Are the buildings for the owner or for the tenants?*

When we receive a commission as consulting engineers, the main task normally is to provide buildings with low total costs for planning, construction and maintenance of the building, which are primariely:

- *Investment costs.*
- *Energy costs.*
- *Maintenance of buildings (MOB).*
- *Cleaning.*

The above costs are just about 10% of the total picture because wage-related costs dominate after the building is occupied. Total cost is depreciation on invested capital plus operational costs. Instead of talking about the building itself, we should concentrate on the tenants which should have as close to an optimal indoor environment as possible. This environment is a multiple of the

following factors ("Seven Sisters") which overlap each other:

- *Thermal environment (humens heat balance).*
- *Atmospheric environment (contaminants and VOC's).*
- *Acoustic environment (hearing, sound, noise).*
- *Actinic environment (lightning, radon and electromagnetic radiation).*
- *Mechanical environment (feeling, pain, accidents etc.).*
- *Psychosocial environment (relationships between people).*
- *Aesthetics (what's good for our senses- eyes, smell, ears, taste, feeling and balance).*

In "buildings of the year" - three office buildings under construction - we have made specifications and drawings especially for the tenants - and the owners have accepted all new information we have provided for the combination of the "Seven Sisters" above:

- *Choice of materials with low emissions in any part of the buildings.*
- *Air condition systems of the very best design.*
- *Specifications for full temperature control year around (20 - 24oC)*
- *15 m3 filtered air per square meter per hour in offices.*
- *Displacement ventilation in some offices and dilution in others - max. air velocity 12 cm per second.*
- *The best filtration (EU7 or 8) of outside air.*
- *High quality cleaning.*
    - *After the building is tightened.*
    - *Before laying carpets.*
    - *Before closing suspended ceilings.*
    - *Before moving into the buildings.*
    - *Good cleaning procedures during the buildings lifetime.*
    - *High quality carpets, curtains and furniture.*
    - *Central vacuum cleaning systems.*

Qualified personnel are contracted to overlook building procedures under the construction period, and in addition to be consultants for HVAC installations, have a special responsibility for the total indoor environment.

7. Conclusions.

- All substances, materials, fixtures and equipment must, in addition to the individual, be looked upon as sources of pollution.

- Architects and planners must be made conscious of the need to minimize the pollution load indoors.

- All offices and EDP equipment in our buildings produce a heat surplus which can be exploited for heating. The air conditioning systems must be designed in such a way that heat recovery is possible. This, however, leads to a move towards using more electricity and less thermal energy for meeting the energy requirements in such buildings.

- To be able to upgrade the air quality we can hardly avoid increasing the air volume compared with the small volumes that have been made desirable due to the energy conservation drive. IAQ top means about 15 cubic meter filtered air per sq. meter per hour.

- An optimal air quality is believed to be a factor in increasing productivity. Regarding the thermal indoor climate, a 5-10% reduction in productivity has been shown to occur with only small variations from the optimal climate. Moreover, we know that of the registered cases of illness, 25% are related to eyes, nose and the respiratory system. We believe that productivity can be readily increased by up to 3% by improving the air quality.

- Even a productivity improvement of only 1% would more than cover the increased costs including energy costs and capital costs.

- Increased energy consumption as a result of upgrading the air quality may be up to 8%. This has little financial significance for the individual employer or owner/builder.

- *Any increase in energy consumption is undesirable from the viewpoint of society in general. A marginal increase for upgrading the air quality must, nevertheless, be looked upon from the viewpoint that demands for energy conservation have for a long time taken place at the expense of air quality*

- *Total cost is dominated by wage-related costs, and investments and energy costs are negligible compared to that.*

- *It is always cheaper in the long run to make the right decisions before making any drawing.*

Stavanger, Norway
May, 1990

Gaute Flatheim

Bibliography

(1) FLATHEIM G. & ROEDSETH A.: "Energy consequences of upgrading indoor air quality". ENERGY for TOMORROW, Division 2 Energy and the Environment, World Energy Conference 14'th Congress, Montreal '89.

(2) ROEDSETH A.: "Effect - and energy consumption in modern office buildings". (In Norwegian, English summary.) Siv.ing. Gaute Flatheim A/S, June '89, Norway.

(3) FANGER P.O.: "A solution to the sick building mystery". Proceedings of the 4th International Conference on Indoor Air Quality and Climate. Berlin (Vest), 17.-21. Aug. 1987.

(4) "AFTER INDOOR AIR '87". Publication no. 4. The Committee for Health, and Indoor Environment (HK-HTI), 1988 (In Norwegian, English summary). Oslo, Norway.

(5) HAUKENES J.P.: "Annual costs. Investments-operating costS - productivity". Annual refresher-course days at the Technical University of Norway, Trondheim, 4.-6. Jan. 1989 (In Norwegian, English summary).

(6) "Indoor Climate and Energy Saving". Publication no. 5. The Committee for Health and Indoor Environment. 1988 (In Norwegian, English summary).

(7) SKOV P., VALBJOERN O. & GYNTELBERG F.: Rådhusundersøgelsen, Copenhagen, Arbejdsmiljøfondet 1989, Denmark. (The town Hall study). English summary.

(8) ALLERGIUTREDNINGEN. (Att förebygga ALLERGI/-överkanslighet) Statens offentliga utredningar 1989:76 Socialdepartementet, Sweden.

(9) WYON D.: "Indoor Climate and Productivity". Annual refresher-course days at the Technical University of Norway, Trondheim, 1985.

(10) FLATHEIM G.: "Quality improvements with displacement ventilation", VVS & Energi nr. 5/86, Stockholm, Sweden (Reprint in English)

VENTILATION SYSTEM PERFORMANCE

11th AIVC Conference, Belgirate, Italy
18-21 September, 1990

Paper 3

Indoor Air Quality Guide for Property Managers in Office Buildings

C.Y. Shaw, F. Vaculik, D.W. Patton and G.M. Comeau

Institute for Research in Construction
National Research Council,

Realty Services, Public Works Canada,

G.K. Yuill & Associates Ltd

Management for acceptable indoor air quality in office buildings requires that the buildings are properly designed, operated and maintained, and that property managers have the knowledge necessary to respond to changes in building operation and use. Although most property managers are non-technical people, with clearly defined guidelines they are capable of achieving this objective.

This paper presents an IAQ guide for such a purpose. The guide has been tested by four property managers for accuracy in detecting potential problems and ease of use. Four office buildings were used for this purpose. The results are discussed.

INTRODUCTION

The indoor air quality (IAQ) issue has come to the fore, in part, because of an increase in environmental awareness and general expectations of today's building occupant. Employee representative associations have also helped increase the focus on all aspects of the working environment, including air quality.

At the same time, the property manager's and building operator's task of providing a productive working environment has become increasingly complex due to greater use of synthetic materials in construction and furnishings; tighter building construction; and more sophisticated heating, ventilation, cooling and control systems. Ironically, the very complexity of the environmental control system often results in a diminished ability of occupants to directly control the environment which surrounds them. In some cases this can contribute to the occupants' frustration and perhaps even suspicion regarding environmental quality.

Managing buildings for good air quality requires a well coordinated effort by the building management team - operators, maintenance support and technical staff - spearheaded by the property manager. Although most property managers are non-technical people, with clear guidelines they are capable of handling this complex task. This paper describes one such guide. The proposed guide has been tested in four high-rise, air-conditioned office buildings by each building's property manager. The test results are discussed.

THE GUIDE

The primary focus of this guide is on indoor air quality and the directly related issues of ventilation, temperature and humidity[1]. Other environmental factors such as noise, lighting and space layout are covered briefly. The Guide can be divided into two parts: Part I, basic information and Part II, checklists for conducting walk-through inspections. Details are discussed below.

PART I - BASIC INFORMATION

Part I of the guide presents all the information and the action plans required by property managers to effectively manage their buildings for acceptable IAQ. It also includes the definition of IAQ used in the guide and describes the role of property managers to help them understand their responsibilities in dealing with IAQ related issues.

Definition of Indoor Air Quality Levels Used in This Guide

The levels of indoor air quality can be classified into three categories: unhealthy and unsafe, healthy and safe, and comfortable and productive (Figure 1). The first two are defined strictly from a health and safety viewpoint, based on various health and safety standards established mainly for industrial workers. The US Occupational Safety and Health Association (OSHA) and the American Conference of Governmental Industrial Hygienists (ACGIH) have published two such standards[2,3]. The third category is introduced to reflect the fact that under certain conditions, many office workers in a healthy and safe environment may still experience various symptoms of discomfort, such as mucous membrane irritations, headaches and fatigue. As these symptoms can adversely affect employees' well-being and productivity, for office buildings it is more appropriate to look beyond basic health and safety to employee comfort and productivity.

Two standards have been developed by the American Society of Heating, Refrigerating, and Air-Conditioning Engineers (ASHRAE) for this purpose. Standard 62-1989[4] prescribes a maximum CO_2 concentration of 1000 ppm and a minimum outdoor air supply rate per person of 10 L/s to provide an acceptable air quality in normal office buildings. Standard 55-81[5] sets the conditions for an acceptable thermal environment by specifying air temperature, air velocity, relative humidity and mean radiant temperature. Given the differences in seasonal clothing, the ASHRAE Standard 55-81 defines two thermal comfort zones - one for winter and the other for summer. The recommended temperature and relative humidity ranges satisfying the majority (80%) of healthy people are 20-27 C with 20-70% R.H. Guidelines are given in the Standard for determining if specific combinations of temperature, relative humidity, air velocity, and mean radiant temperature lie within the seasonal comfort zone.

With the current level of knowledge for detecting, controlling and assessing health impacts of various indoor air contaminants, both individually and in combination, ASHRAE[4,5] recognizes that it may not always be possible to satisfy everyone. The above standards are intended to result in 80% or more of a building's occupants being satisfied with their environment.

Role of Property Managers

The fundamental responsibility of property managers with respect to indoor air quality is to ensure their buildings are operated to meet established environmental standards. To fulfill this role, they must be knowledgeable about indoor environmental standards, indoor air quality issues,

potential air contaminant sources, and the environmental control systems in their building. They should also understand the roles and interrelationships of the various parties involved in the indoor air quality issue - the building owner/operator, health authorities, regulatory agencies, and the occupants - to be able to handle occupants' complaints about indoor air quality, investigate the causes, and coordinate any corrective action.

It should be stressed that property managers are not health professionals, and should therefore avoid becoming involved in assessing and analyzing suspected health problems. These should be referred, in consultation with the employee, to the responsible health authority. The property manager should work hand in hand with the responsible health official to seek a successful solution.

Action Plan for Prevention of IAQ Problems

The most effective way to maintain an acceptable indoor air quality in buildings is to adopt a preventive approach by regularly conducting a walk-through investigation together with an assessment of the building systems and its operating activities (such as the inventory of chemicals used for cleaning, plant maintenance, etc.). Such walk-through inspections allow potential environmental problems to be identified and corrective actions taken before they become real problems. A five-step plan, as shown in Figure 2, has been developed for this purpose. Step 1 is to recognize the importance of such a proactive management program and to know what is involved in implementing such a plan. The effort and time required to properly implement such a program is significant; the property manager has to be totally committed to the program to ensure its success. Once the property manager is committed to such a program, Step 2 is to become knowledgeable about the elements of the IAQ issue, such as the basic concepts of the operation of the building's HVAC systems, the definition of indoor air quality, and the common causes and solutions to indoor air quality problems. Such information enables the property manager to professionally address environmental problems and intelligently discuss these matters with specialists, occupants and union representatives.

The next step is to prevent environmental problems by regularly inspecting the building's systems and assessing operational activities which can affect the indoor air quality. Frequent building walk-through inspections will help ensure potential problems are identified promptly. They also provide an opportunity for property managers to encourage occupants to participate in a program to improve the air quality in their work place, for example, by not blocking ventilation outlets. Ideally, a walk-through inspection should be conducted every three months (one

inspection per season). At a minimum, a walk-through inspection should be conducted once a year. It can be combined with other visits or inspections such as overall building condition or building performance reviews.

The fourth step is to address and correct any deficiencies found during the preventive inspection. Experience has shown that communication between inspection personnel and building occupants is something that cannot and should not be avoided. Occupants should be made aware that the inspection is preventive in nature and that any necessary corrective measures will be undertaken without delay. Guidelines for communication with occupants are included.

Action Plan for Management of IAQ Complaints and Problems

Figure 3 outlines the steps required to handle occupant's complaints. Upon receiving an IAQ related complaint, the first step is to document and analyze the nature of the complaint. This will usually help the property manager to distinguish between minor local incidents and significant general complaints, and to take the appropriate actions.

Three levels of investigation are recommended for handling occupants' complaints. Level 1 investigation should be carried out by the property manager in consultation with the building operator. There is often not one single cause but rather a combination of causes, so the property manager should not arbitrarily discontinue the investigation when one deficiency is found.

If the results of the Level 1 investigation are inconclusive, the next step is to initiate follow-up IAQ investigations by technical specialists, at a progressively increasing level of expertise as required (i.e., Level 2 and 3 investigations). As most IAQ problems will likely be identified with a Level 1 investigation, the property manager should not normally launch a Level 2 or 3 investigation without first having undertaken a Level 1 investigation. Guidelines for initiating Level 2 and 3 technical investigations are included.

The three levels of investigation are intended to address complaints related to building occupants' comfort and productivity. For health and safety related concerns, the appropriate health and safety authority should be contacted for advice. At the same time, the property manager should initiate a Level 1 and subsequently, if necessary, Level 2 and 3 investigations, to confirm whether or not the building or its ventilation systems may be contributing to the health complaints. The property manager should establish a close liaison with the health authority during a health and safety investigation.

The next two steps involve taking remedial actions to correct problems identified during IAQ investigations and then verifying their effectiveness. Again, dialogue with all parties involved should take place throughout all the stages described above.

PART II - INDOOR AIR QUALITY INSPECTION CHECKLISTS

Two checklists are included: one is very detailed and one is simplified. The detailed checklist includes the kind of information related to the building and its use that does not require frequent updating. Also included are the necessary forms for recording information related to the building, its HVAC systems and maintenance procedures, major renovations, and the nature of occupants' complaints. This checklist is, therefore, intended to be used for the first preventive inspection and for Level 1 investigations of occupant complaints. The simplified checklist is used for regular follow-up inspections. It has been derived from the detailed one by removing those questions related to the building characteristics that have been recorded in the first walk-through inspection, and that will not usually change.

The first walk-through inspection will be the most time consuming. The detailed checklist provides a guide for the walk-through inspection, identifies where special attention is required and the degree of urgency to be given for each corrective action. Each question on the checklist is to be answered by a "tick" in the **"Yes"** or **"No"** columns. Action symbols are used throughout the checklist to indicate the urgency of action to be taken. When the answer to the question is **"No"** this indicates that a satisfactory condition exists and no remedial action is required at the time. Precautionary measures may, however, be indicated for follow-up consideration. When the answer to the question is **"Yes"** some form of remedial action is likely needed. The urgency is indicated by "x" for immediate attention and "o" for precautionary action. Questions that do not have indicator symbols are included in the checklist to provide information that may be useful in troubleshooting potential problems.

In addition, some of the questions are marked with a symbol 'z' to indicate that they are applied to individual ventilation zones. In cases where occupant complaints are limited to one ventilation zone, the inspection should initially focus on these questions.

VALIDATION

The proposed guide was applied to four high-rise, air-conditioned office buildings to check its accuracy and ease of use in detecting potential indoor air quality problems. Each building was inspected by its respective property manager using the detailed checklist only. None of the property managers were involved in the development of the guide; nor were they given any extra instructions on how to use it.

The participating property managers all found that the guide and the checklist were useful and easy to follow. As all these buildings had been checked independently by the building specialists of Public Works Canada prior to the property managers' inspections, the specialists' results were used to evaluate the accuracy of the property managers' inspection results. Because of the greater number and more general nature of the findings in the property managers' reports compared to a lesser number of more specific observations in the specialists' reports, only 56 answers could be selected for comparison (11 to 17 answers were selected for each building). Of the 56 answers compared, 39 or 70% were in agreement. Some of the disagreements were due to the fact that some of the deficiencies identified by the building specialists had already been corrected before the inspections by the property managers. One example was that the air filters in the HVAC systems had been replaced between the two inspections.

The results suggest that non-technical property managers can use the guide and obtain IAQ inspection results that are comparable to that conducted by building specialists.

SUMMARY

A guide has been developed for assisting non-technical property managers in conducting walk-through building inspections for preventing and solving problems related to indoor air quality in office buildings. The proposed guide was tested by the property managers of four high-rise, air-conditioned office buildings. The results indicated that the proposed guide was easy to use. The property managers' inspection results agreed well with those obtained by building specialists who had conducted similar inspections on the four buildings independently.

ACKNOWLEDGEMENT

This guide was prepared by an interdisciplinary team from Public Works Canada and the National Research Council.

Synthesis of the overall framework for Property Managers to manage indoor air quality was led by D.W. Patton, Director, Property Management Policies, Public Works Canada. Development of the comprehensive Indoor Air Quality Inspection protocol and technical descriptions in the manual was spearheaded jointly by F. Vaculik, Senior Maintenance Engineer (Mechanical), Public Works Canada and by C.Y. Shaw, Senior Research Officer, National Research Council, in consultation with G.K. Yuill, Consultant. The inspection protocol was validated by the property managers of four office buildings operated by Public Works Canada.

Finally, the draft manuscript was reviewed and revised by H.F. Hull, former Property Management executive, and edited by Corporate Communications Branch, Public Works Canada.

REFERENCES

1. PWC/NRC. 1990, "Managing Indoor Air Quality - Manual for Property Managers", Public Works Canada and Institute for Research in Construction, National Research Council, Canada.

2. ACGIH. 1983, "Threshold Limit Values for Chemical Substances in Workroom Air", ACGIH, Cincinnati, Ohio.

3. OSHA. 1981, "OSHA General Industry Safety and Health Regulation, US Code of Federal Regulations", OSHA, USA.

4. ASHRAE. 1989, "ASHRAE Standard 62-1989, Ventilation for Acceptable Indoor Air Quality", The American Society of Heating, Refrigerating, and Air-Conditioning Engineers, Inc.

5. ASHRAE. 1981, "ASHRAE Standard, 55-81, Thermal Environmental Conditions for Human Occupancy", The American Society of Heating, Refrigerating, and Air-Conditioning Engineers, Inc.

Figure 1

Conceptual Relationship Between Health and Safety, Comfort and Productivity Standards for Indoor

Air Quality & Client Satisfaction

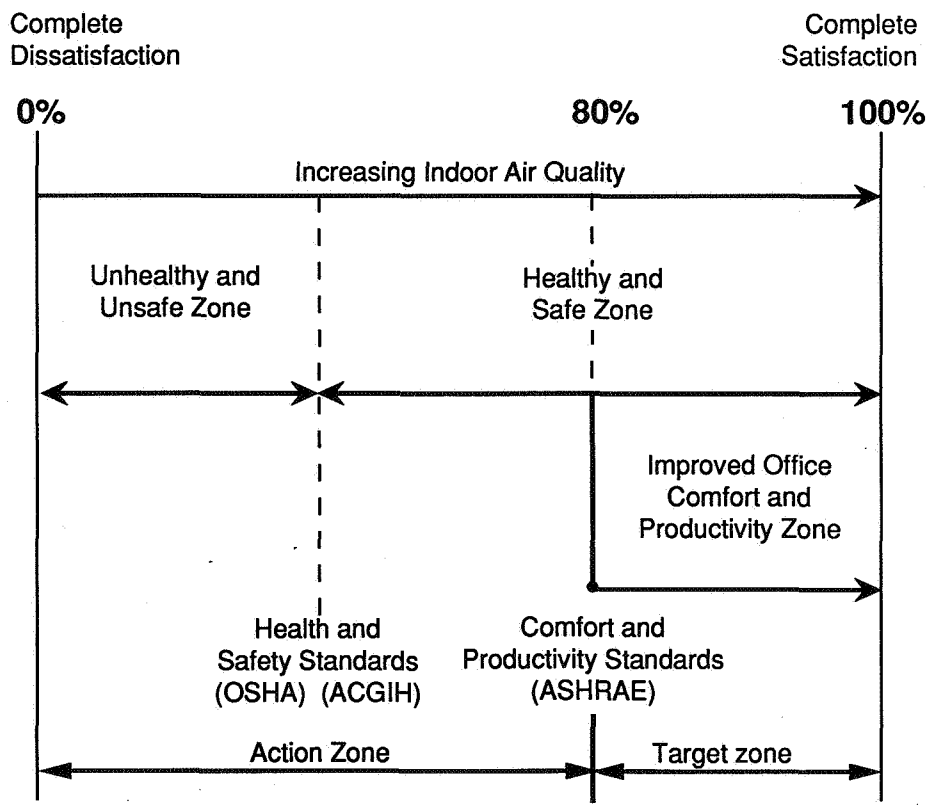

Figure 2

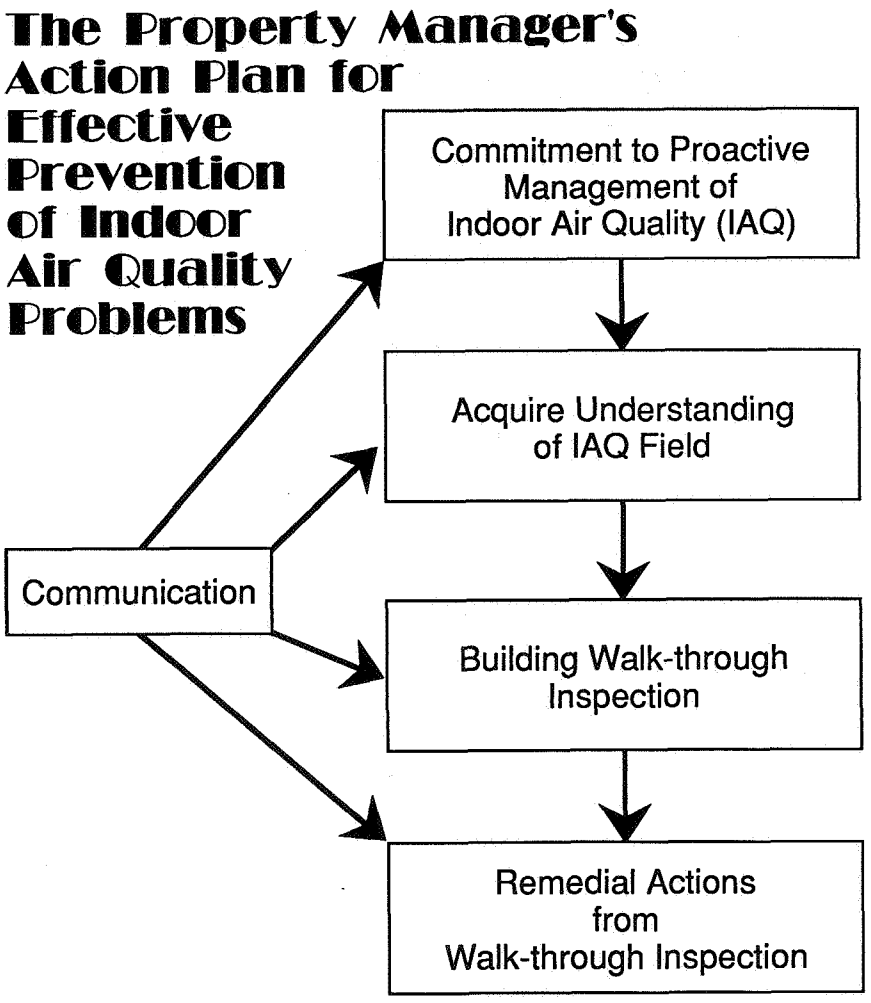
The Property Manager's Action Plan for Effective Prevention of Indoor Air Quality Problems
Commitment to Proactive Management of Indoor Air Quality (IAQ)
Acquire Understanding of IAQ Field
Communication
Building Walk-through Inspection
Remedial Actions from Walk-through Inspection

Figure 3

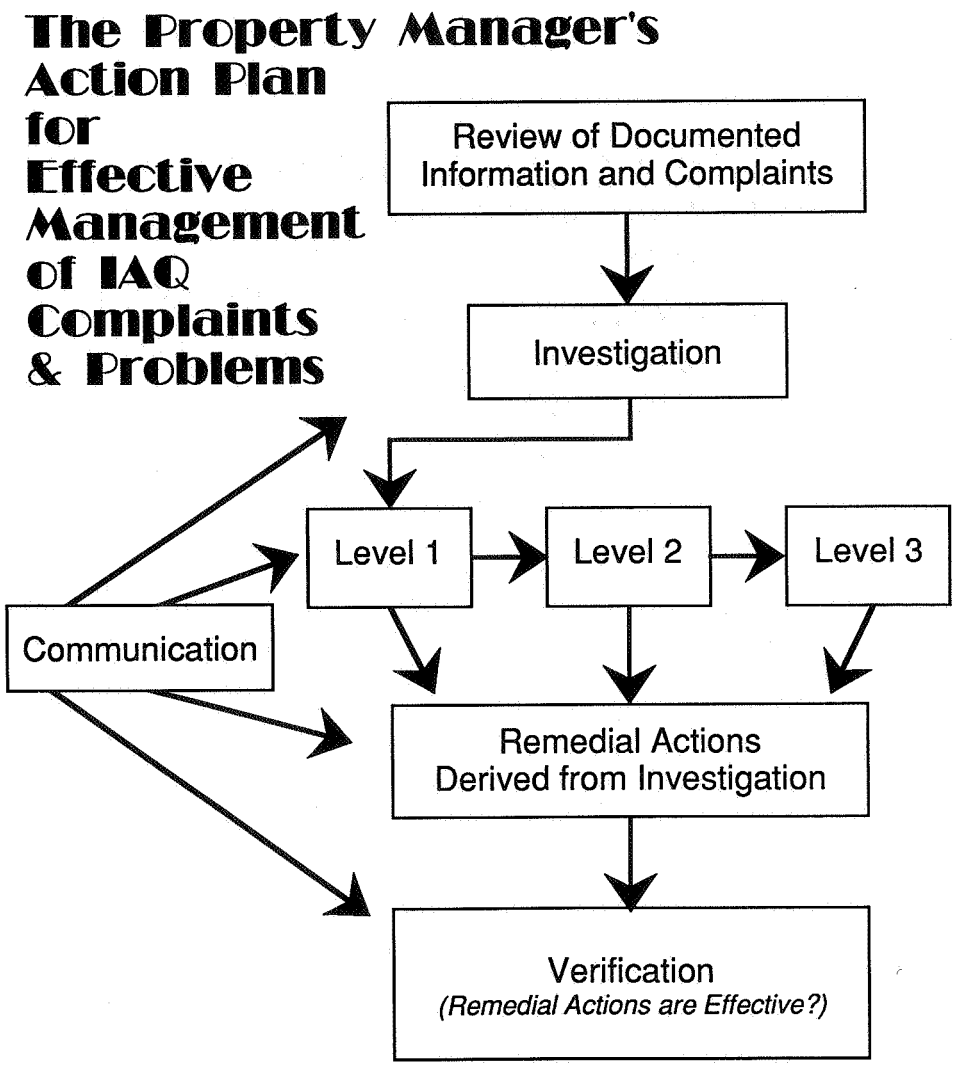
The Property Manager's Action Plan for Effective Management of IAQ Complaints & Problems
Review of Documented Information and Complaints
Investigation
Level 1
Level 2
Level 3
Communication
Remedial Actions Derived from Investigation
Verification
(Remedial Actions are Effective?)

Discussion

Paper 3

M.Masoero (Politecnico di Torino, Italy)

In developing your checklists for property managers, have you made any use of the work on Energy Auditing of buildings that was completed by IEA a few years ago?

D.Patton (Public Works Canada)

The checklist was developed by the National Research Council in conjunction with G K Yuill Consultants, who I am sure would be aware of the information available from the Energy Auditing work.

A.Sandelewski (Tekne SpA, Italy)

Did you notice any difference in the various kinds of HVAC systems (CAV,VAV, fan-cooled) as far as IAQ problems are concerned? Was there any type which consistently drew complaints?

D.Patton (Public Works Canada)

No. We have noticed no particular trends. However, when VAV systems were first introduced in Canada there were some features which caused problems, e.g. diffusers could close completely when temperature conditions were satisfied, stopping air flow altogether. These features have been corrected in current VAV systems. Free cooling is a very desirable feature in Canada.

J.Satish (Zurich, Switzerland)

Are there any regulations in Canada which require the maintenance of ventilation systems? This is mandatory for heating systems in Switzerland for example. People are more likely to do something either if they have to or if they get return on investment.

D.Patton (Public Works Canada)

No. Not in the same sense that regulations call for maintenance and testing of certain safety building components such as elevators, fire alarms and emergency generators. In Federal buildings the Department of Labour Regulations do, however, require that building environments meet certain performance standards.

E.Arens (Univ of California, USA)

Could the inspection/monitoring of the air quality in the building be assigned to the worker/occupants rather than (or in conjunction with) the property managers?

D.Patton (Public Works, Canada)

In practice one of the indicators of air quality is feedback/complaints from building occupants. In that sense occupants are continuously monitoring the quality of air. In the event of an investigation of an IAQ problem, it is important to keep occupants fully informed and to involve them if possible. This builds a relationship of trust. Accordingly I would not rule out tenant participation on an IAQ inspection with the property manager.

VENTILATION SYSTEM PERFORMANCE

11th AIVC Conference, Belgirate, Italy
18-21 September, 1990

Paper 4

DEMAND CONTROLLED VENTILATION SYSTEMS FOR DWELLING HOUSES OF THE FUTURE

Reijo Kohonen

TECHNICAL RESEARCH CENTRE OF FINLAND
Laboratory of Heating and Ventilation
Lämpömiehenkuja 3, 02150 Espoo, FINLAND

1. INTRODUCTION

Many deficiencies have been observed in the functionality of ventilation in experimental building sites. In the case of ventilation systems with mechanical air extraction, the most typical of these shortcomings have been draughts, stuffiness, the diffusion of odours both from one dwelling to another and within individual dwellings, and condensation problems in the structures. Mechanical extraction ventilation systems are quite common in Finnish houses, being found in some 60 per cent of multi-storey dwelling houses. In experimental buildings equipped with mechanical air supply and extraction as well as warm air heating, the complaints are mainly concerned with noise, draughts, the diffusion of odours from one dwelling to another and problems related to the use and maintenance of the systems. Less than 10 per cent of the Finnish housing stock is equipped with both mechanical air supply and extraction.

An extensive field study on the operation of ventilation in domestic dwellings and its requirements in terms of health and comfort (Ruotsalainen et al. 1990), which included 251 buildings. The sample consisted of both detached or semi-detached houses and blocks of flats. Three different types of ventilation systems were included.

The mean ventilation rates measured during a two-week period varied remarkably from 0.1 to 1.5 ach across the sample. The average was 0.52 ach including also the ventilation caused by the airing. The differences between the ventilation systems were small. However, the ventilation rates were on average smaller in houses than in apartments. Especially stuffyness and dryness of the bedroom air were problems in the residences. Almost half of the occupants felt the bedroom air in the mornings to be at least sometimes stuffy. 40 % of the occupants felt the bedroom air to be usually too dry. Humidifiers were used in over one third of the risidences. The dissatisfaction with the humidity increased considerably, when the relative humidity was below 40 %.

The occupants of the apartments reported systematically more symptoms and environmental complaints than the occupants of the houses. In the houses the symptoms and environmental complaints were more common among the occupants with natural ventilation than with balanced ventilation. In the apartments with balanced ventilation the occupants reported more symptoms and complaints than those with natural ventilation.

In experimental buildings it has also been observed, for instance, that the dual-speed systems typical of multi-storey buildings do not correspond to people's living habits, and that it must be possible to exercise both temporal and spatial control over the ventilation system. At the very least, occupants must be able to increase (accelerate) the rate of extraction or fresh air in spaces exhibiting a large variation in the production of air-borne impurities. Such premises are the kitchen, the bathroom and the WC.

Housing and ventilation have also been examined theoretically from the social psychological standpoints (Anttila 1990). In an analysis of the comfort of the occupants, a principle of minimum functionality for ventilation was outlined.

The principle is based on the requirement that ventilation should function satisfactorily even if the occupants themselves do not actively be engaged in the control of the ventilation. The occupants would nevertheless be able to regulate the ventilation themselves. The minimum functionality principle also won favour among the residents of the Turku housing-exhibition estate.

The functional and technical requirements which have been set for ventilation systems in dwelling houses of the future will result in ventilation systems featuring trouble-free and demand-controlled operation (Luoma, Kohonen 1988). This paper discussed the functional requirements and technical solutions of such ventilation systems.

2. FUNCTIONAL REQUIREMENTS

The most important functional requirements for ventilation systems in dwelling houses of the future are that:

- an occupant should have the ability to operate the ventilation according to his/her needs
- the ventilation system should not be sensitive to external disturbances
- the efficiency of the ventilation in living spaces should be high
- the ventilation system should be economical in terms of energy consumption and should also be reliable
- subsequent modification of the quality standard should be possible.

Demand controlled operation and accelerating of ventilation

With airflows complying with Finnish Building Code, the ventilation of small dwellings in particular may be unnecessarily great. Conversely, the ventilation in some of the rooms of large dwellings may occasionally be inadequate. In spaces where ventilation-loading factors vary a great deal (such as in the kitchen and the bathroom), the ventilation may be unnecessarily great most of the time and yet inadequate on the occasions when the load level is high. The problem applies to systems in which the airflows are constant. At the present time there are no clear principles on which to base the airflow ranges of demand controlled ventilation. Generally speaking, demand controlled ventilation rate may be greater or smaller than that prescribed in the regulations.

The necessary level of ventilation is determined according to the factors that load the ventilation. On the basis of load data and criteria from the literature, Saari (1990) has used the Monte-Carlo simulation to determine numerically the airflow ranges suitable for various rooms and various load situations in living spaces (Table 1).

The basic requirement for ventilation is that it should be sufficient to remove the impurities emitted by the materials of the building structures. Moreover, the ventilation of an unloaded room must not fall below the values of the basic norm even in the event of air extraction being increased in some other room space.

It should be possible to control the accelerating of ventilation both temporally and spatially. In such circumstances it must be possible to increase the air extraction so that a marked effect will be achieved.

It should also be possible to increase an air vent's airflow from the basic level by at least 50 per cent. There should not be unequal effects among the various dwellings, which should experience an approximately even increase in the airflow. When the extract airflows are increased, it is also necessary to ensure that there will be an adequate supply of outdoor air. The pressure difference over the external walls may not exceed 30 Pa, which tends to limit the magnitude of the increased extract airflow.

In addition to air vent-specific accelerating, there may also be a need to increase the airflows in individual dwellings, e.g. when cooling with outdoor air. In advanced systems there must also be the facility to accelerate the air extraction in more than one room, not only in "dirty" spaces but also in bedrooms and living rooms.

Controlling thermal forces and the effects of wind

The ventilation system should function well in all weather conditions. The most important disturbance factors are wind and boyance effects arising from temperature differences. The control of thermal forces can be influenced by selection of the air pressure in the ducts, the airtightness of the building envelope and the operating pressure difference of the fans. The criterion is that the uppermost floors of a multi-storey building should have a negative pressure even in conditions of severe frost (-20 ... -30°C).

Correspondingly, the criterion for the effects of the wind is that there should be no air infiltration into a dwelling even in a high wind (10 m/s). The airtightness of the external walls is of critical significance to the air infiltration. The airtightness of the external walls should be at least $n_{50} = 0.5$ dm³/s. By contrast, the effect of the airtightness characteristics of other structural components and of the pressure difference of the air vents on air infiltration is minimal. A suitable ratio of supply to extract airflow rates is about 0.8.

The internal airtightness of the building is also of considerable importance as far as the control of ventilation is concerned. The airtightness of ducts and the walls between individual dwellings and between the dwellings and the staircases should be specifically ensured. The system should also be insensitive to the opening of windows and doors.

The calculated values for the airtightness characteristics of structures necessary in order to control pressure conditions are (Karvonen, Luoma 1990):

- a pressure head of 50-100 Pa should be available for the air vents
- air leakage through external walls at a pressure difference of 50 Pa should be less than 0.5 dm^3/s
- air leakage through intermediate floors at a pressure difference of 50 Pa should be less than 0.1 dm^3/sm^2
- air leakage through a closed dwelling door at a pressure difference of 50 Pa should be less than 2 dm^3/s.

Modification and improvement of the quality level

Modifications are generally a question of improving the level of quality at a later date. The following improvements may come into question: provision of mechanical air supply, filtering of supply air, provision or expansion of the facility to accelerate air extraction, heat recovery, reduction of the noise level and measures concerned with aesthetic aspects.

Various design solutions can be employed to allow for future improvement of quality level. Wide dimensioning of the ductwork will make it possible to increase the airflows. Extract ducts for individual dwellings will allow the use of dwelling-specific units and thus the control of dwelling-specific airflows. Ducting supply air into the building facilitates centralized filtering and mechanical blowing. Figure 1 shows an example of an air conditioning system, whose quality can be improved.

Thermal comfort and energy economy

It has been observed in experimental buildings that draughts generally occur in constant airflow systems based on air extraction when there is no control exercised over the supply air. Moreover, the supply air inlets easily cause draughts in the wintertime.

The ASHRAE standard 55-1981 defines the limits for the maximum rate of operative temperature change, for the steady drift rate and for the maximum amplitude during rapid temperature fluctuation. According to the standard, the operative temperature may drift if the rate of change is less than 0.6°C/h. The temperature may vary with an amplitude of less than 1.1°C, but if the amplitude exceeds 1.1°C, the rate of change must not be greater than 2.2°C/h. The standard can be applied to a rising temperature trend. There is no equivalent standard for a declining trend. The effects of falling temperature on comfort have also been investigated, but the results of the various studies are contradictory.

In a dwelling house a temperature of +18°C may be regarded as the minimum acceptable room temperature. In order to ensure that the temperature does not fall below +18°C in the accelerated ventilation mode during the heating period, e.g. increasing of the airflows in a bedroom at night, the higher heating load must be taken into account in the design of the heating system.

When the air inlets are installed above the radiator, the cold air will not flow to the floor level immediately. On the other hand, to prevent through-flow, it would be better to try and use only one wall for the positioning of the outdoor air inlets.

In supply and extraction ventilation systems the distribution of the air in the room can be designed to prevent draughts even when the ventilation rate is high. The maximum is about 4.0 dm^3/s, which is based on a study by Sandberg (1987).

Although the priority of energy cost is not very high at the moment, energy economy is also a goal when systems are being developed. The object is that a variable airflow system must not consume more energy than any system designed in accordance with the present building regulations. That is no problem, since the energy consumption of demand controlled systems is lower than that of conventional systems.

Operational availability

The availability of a system is described using the following criteria:

1. Usability expresses the ability of the system to function without downtime or breakdowns.

2. Operational reliability expresses the ability of the equipment to function without the occurrence of a defect for a required period of time.

3. Ease of maintenance expresses the facility for returning defective equipment to serviceable condition as a consequence of maintenance measures. In many cases ease of maintenance is more important than operational reliability from the standpoint of its availability. It would seem reasonable that a defect might occur in a system once a year but, if it were to take 11 months to repair the fault, its availability (in this case the ease of servicing) could hardly be considered satisfactory.

4. Maintenance reliability expresses the ability and readiness of the maintenance organization (spare parts, tools, personnel, documents, etc.) to repair and maintain the system or a component device.

In availability analyses the biggest problem with extraction ventilation systems proved to be how to take outdoor air without causing draughts. In the case of outdoor air vents, there are significant shortcomings in production, design, installation and operation. The task of replacing the filters in outdoor air vents is generally left to the occupants themselves. This calls for operating and maintenance instructions clearly explaining the need to change the filter. If the air vent has various control settings, it must be possible to lock them in place, and while the filter is being replaced, they must not deviate from the previously selected settings. It must also be possible to lock the control

settings of extract air vents, so that they cannot be intentionally or unintentionally changed.

In supply and extraction ventilation systems there is an obvious need for greater automation in both the ventilation unit and the flow controllers for dwellings. Measuring and alarm points will be necessary, especially in the case of volume flow, freezing and melting. The opportunities for versatile operation emphasize the need for clear instructions concerning use and maintenance.

Compatibility with the component system building technique

The future way of construction will feature the characteristics of low density housing, with the emphasis in multi-storey buildings placed on good sound proofing between dwellings, ventilation control for individual dwellings, and low-rise construction. The TAT (Totally Adaptable Technology) component building system (Sarja 1990), which emerged as a result of a development project for office and residential buildings, is a hierarchical, module-based, open system for the design and construction of residential and office buildings. The system comprises architectural principles, a space system, compatible and integratable technical subsystems, and a dimensional and tolerance system. The TAT building system is based on the industrial production of building parts and components. The assembly of the buildings and the systems takes place at the work site.

The ventilation system is one of the technical subsystems of a building, and its construction has been adapted to the concept of industrial construction. In practice, this means that there must be a certain range of compatible, industrially manufactured components from which the desired ventilation system can be assembled.

The hierarchical levels of the TAT system are the building, the sub-building, the module and the component.

The technical components of the ventilation subsystem are the air-handling unit, the duct, the flow controller, the terminal unit and the control unit. Depending on standard of quality, the components include various functions. Air-conditioning systems can be divided into four different categories on the basis of the decentralizing principle.

3. DESIGN PRINCIPLES

In the LVIS-2000 research program's project "Ventilation systems for dwelling houses of the future", only three types of system were examined:

- (centralized) air supply and extraction system for individual sub-buildings
- air input and extraction system for individual dwellings

- air supply systems for individual dwellings and air extraction systems for individual sub-buildings (centralized air extraction systems).

The most important technical criteria in the design of ventilation systems are:

1. A basic ventilation rate of 0.35 dm^3/sm^2 is implemented in all room spaces in all circumstances

2. The airflow of an air vent in the accelerated mode should be 50 per cent greater than that of the normal operation mode

3. 25 dm^3/s is the greatest airflow through any single air vent (because of the noise)

4. The pressure difference across the air vent must not be greater than 100 Pa (because of the noise)

5. Increased airflows must not raise the pressure difference across an outside wall above 30 Pa

6. The building must not have a positive pressure difference

7. In order to avoid excessive energy consumption, the overall airflow in the dwelling may be raised by a factor of two at the most

8. Energy consumption may not be greater than would be the case if a system made in accordance with the Finnish Building Code were to be used.

The slower the airflow velocity in the ducts and the more airtight they are, the better is the functioning of ductwork. Numerical flow and noise models have been combined with actual measurements to determine the maximum permissible airflow velocity in the ductwork and its maximum permissible noise levels on the basis of the highest noise level in the room (Laine 1989). By also taking account of the pressure losses permissible in the ductwork in order to achieve an adequate level of controllability, the set of dimensioning curves for ductwork shown in Figure 2 is obtained.

Without noise nuisance, a pressure level of 100-150 Pa can be achieved using good modern control and terminal equipment. In that case the highest permissible pressure loss of the ductwork would be 50-75 Pa. One could then "standardize" the operationally optimal total pressure loss of the ductwork at 200 Pa. In order to be able to implement temporal and spatial control of the ductwork, the pressure level of the control and terminal equipment should be about 100 Pa. In addition, fans should be controlled separately because it is impossible to influence the total airflow of the air-conditioning unit without noise nuisance by using the control and terminal equipment of branch ducts.

The air-conditioning plant's airflows, pressures and noise levels cannot be controlled unless the ductwork is airtight. Good ductwork should always

meet the Building Code's air tightness class C, i.e. 0.1 m^3/sm^2 at 250 Pa pressure difference.

When using a fan with a slightly sloping curve, the required pressure difference above the flow controllers is small or pressure controllers are entirely unnecessary. Ductwork control based on a slightly sloping fan curve is highly suitable in situations where the total airflow control range is 50-100% of the maximum airflow.

The technical prerequisites for accelerating the total airflow using various fan control methods have been examined numerically (Haikarainen 1990), (Table 2).

We can see from the table that, using the constant pressure control, the total airflow can be tripled without raising the pressure level of the ductwork. At the same time it is estimated that if dwellings increasing the airflows make up 30% of the total number of dwellings, then one dwelling's supply and extract airflows can be raised to more than 7 times the basic operation mode. Increasing the airflow sevenfold will not succeed unless the ductwork within the dwelling is made very wide and the room air vents are allowed a sufficient pressure difference. Correspondingly, if the ductwork is dimensioned such that the basic airflow has a friction pressure loss of less than 0,5 Pa/m and the room air vent pressure loss is at least 75% of the usable pressure loss for the dwelling, then one room's airflow can be quadrupled.

Room temperature behaviour during accelerated ventilation

Room temperature behaviour during accelerated ventilation mode has been examined using dynamic system simulation (Haikarainen 1990). The systems under examination featured extraction ventilation with heating from radiators of varying output capacity. Another heat distribution method which was examined was combined radiator and floor heating. Figure 3 gives an example of the results of the simulation.

The results of the calculation show that radiator size does not affect temperature control speed when using a thermostatic radiator valve. Using radiators of varying output capacity, the drop in room temperature after the accelerated ventilation had been started was just as much during the first ten minutes. A decrease in room temperature nevertheless causes an increase in radiator output about one hour after the accelerating has begun, at which time radiator output and room temperature are, practically speaking, in a steady-state condition.

If ventilation is accelerated for a longer period of time, then the radiator should be dimensioned on the basis of the maximum airflow so that the room temperature remains at its set value. In circumstances of short-term ventilation increase, an over-sized radiator will not produce the maximum output if a thermostatic radiator valve is used. On the other hand, ventilation increase is generally accompanied by internal heat loads which compensate for the increased output requirement.

The maximum ventilation rate presented by Haikarainen is based on maintaining the room's thermal comfort during accelerated ventilation such that the number of those dissatisfied with the temperature conditions in the space rises to no more than 20% with the PPD at a basic level of 10%. In such circumstances the room temperature may drop by no more than 2.5°C and the average radiation temperature should remain almost constant. Airflows are determined on the basis of an outside design temperature of -27°C.

In a dwelling-specific system it is difficult to assess the draught because, when the extract airflow is increased during accelerated operation, a greater flow of outdoor air enters the room, to some extent uncontrollably, in the form of air leakage.

If a dwelling-specific ventilation unit were to be equipped with an adjustable heater and the supply airflow were to be increased at the same time as the extract airflow, then it would be possible to increase the airflows in the same way as in a supply and extraction ventilation system.

For instance in room space with a volume of 50 m^3 calculated in accordance with a specific ventilation rate of 0.5 dm^3/s is:

$$q_{i0,h} = 0.5 \times 50/3.6 \text{ dm}^3/\text{s} = 6.9 \text{ dm}^3/\text{s}$$

Based on the studies by Haikarainen the basic airflow, the maximum airflow at an outdoor temperature of -27°C is obtained:

- on the basis of the ductwork of the supply and extraction ventilation system

  $4 \times q_{i0,h} = 27.8 \text{ dm}^3/\text{s}$

- on the basis of thermal comfort in the extraction ventilation system

  $0.5 + 1.0 \text{ dm}^3 \rightarrow 20.7 \text{ dm}^3/\text{s}$

- on the basis of the ductwork in a dwelling-specific ventilation system

  $4 \times q_{i0,h} = 27.8 \text{ dm}^3/\text{s}$

In an extraction ventilation system, a prerequisite for a fresh airflow of 20.7 dm^3/s is that there are at least 4 outdoor air vents in the room, because modern outdoor air vents enable a draughtfree airflow into the room space of no more than 6 dm^3/s per air vent when the outside air temperature is at or below 0°C. In a dwelling-specific system an airflow of 27.8 dm^3/s is too great if the temperature of the supply air is permitted to be below +16°C.

4. SYSTEM DESCRIPTIONS

4.1 CENTRALIZED SUPPLY AND EXTRACTION VENTILATION SYSTEM

Operating principle

A centralized air supply and extraction ventilation system (Figure 4) serves dwellings situated no higher than on the sixth floor. The size of the ventilation unit then remains reasonable and pressure differences in the building and the ventilation ductwork are controllable.

The ventilation system can be employed in three different ways. During a long period of absence, the ventilation of the dwelling can be centrally switched to the reduced level, which is lower than that of normal use.

In normal use, room-specific ventilation is accelerated through the supply and extract air vents. Thus the occupant can handle the accelerating on a demand controlled basis.

The airflow is doubled or trebled by readjusting just one air vent at a time. The extract airflow can be accelerated in the kitchen, washroom and WC as well as in the living room and bedroom. The supply airflow can be accelerated in the living room and bedroom. A readjusted air vent reverts to the basic setting in "dirty" spaces but not in living rooms and bedrooms. More over, the total airflow of the dwelling can be raised to the ventilation rate necessary to achieve a marked cooling effect.

The hallway's supply airflow corresponds to the extract airflow from "dirty" spaces. There are coupled supply and extract air terminal units in living rooms and bedrooms, so that an increase in the supply airflow also raises the extract airflow at the same time.

Ductwork and terminal unit

Within the dwelling, the extracts from different rooms are connected to the same duct. Each dwelling is fitted with one supply and one extract duct, so that the dwelling's total airflows can be controlled. The dwelling's air supply and extract ducts are fitted with closeable fire screens. The dwellings' air supply and extraction ducts are connected to sub-building-specific supply ducts. The ductwork is widely dimensioned.

Air-handling unit

The air-conditioning unit is designed so that dwelling-specific flow controllers and air vents can use a pressure difference of 100 Pa. The air-conditioning unit operates on a constant pressure principle. Basic and cooling situations are achieved by the use of dwelling-specific flow controllers.

Operation during accelerated ventilation mode

The system can be dimensioned so that when the ventilation is being accelerated, the dwelling's total airflow either increases at almost the same rate as that of the readjusted air vent (additional principle), increases to some degree, or does not increase significantly at all (borrowing principle). Different alternatives are implemented through the dimensioning of the dwelling-specific flow control device.

Calculations indicate that it is advantageous if the pressure loss of the air vent is at least half that of the available pressure loss (Table 4). In high-rise residential buildings, drawbacks arising from thermal forces can be diminished by controlling the air inlet devices on lower floors on the basis of the outside temperature.

4.2 DWELLING-SPECIFIC SUPPLY AND SUB-BUILDING-SPECIFIC EXTRACTION VENTILATION SYSTEM

Operating principle

A mechanical extraction ventilation system, which makes use of a common extract duct system, serves dwellings located on six successive floors, and a mechanical extraction ventilation system, in which there is dwelling-specific ducting, correspondingly serves dwellings located on four floors. The extraction unit then remains reasonably sized and the pressure differences in the building and in the ventilation ducts are controllable.

In an air extraction system, the ratio of supply to extract airflows in individual dwellings does not need to be kept so precisely constant as in a centralized supply and extraction ventilation system. Consequently, there are a number of different ducting principles (Figure 5).

The occupant can accelerate the extract airflow as the need arises. A readjusted air vent should return automatically to the normal setting, but it can also be locked on the accelerated setting.

Terminal units

The extract airflows of individual terminal units are given in Table 5. The kitchen airflow in the accelerated mode is a minimum of 20 dm^3/s and a maximum of 42 dm^3/s.

Noise insulation between dwellings is handled by noise dampers in either the terminal unit or the rising ducts.

Ductwork

In a building-specific extraction system, the rising ducts of the kitchens and those of the bathrooms and clothes closets are connected to a connection box

before the extract fan. In dwelling-specific extract ductwork, the dwellings have their own rising ducts which are similarly connected to a connection box before the extraction fan. The connection box is dimensioned so that the flow rate is less than 4 m/s. In the normal operation mode the terminal unit's pressure head is 80-120 Pa.

Extract unit

The extract unit consists of noise damper, extract fans and a pressure controller. The static pressure produced in the duct by the extract unit is no more than 1.5 times the air vent's pressure loss in the normal situation. The sound level caused by the extract fan in the duct should not exceed the values given in Table 6, if there is no damper in the terminal unit. The fan always requires separate noise damper.

An extract fan having a slightly sloping fan curve is selected so that the pressure difference in the duct falls by no more than 10% from value of the normal mode when accelerating is in progress. Pressure control based on a slightly sloping fan curve is highly appropriate when the total airflow increase is not very great (e.g. less than 100%).

In two-step pressure control, a pressure switch increases or decreases the speed of rotation on the basis of a pressure sensor reading. Each control phase operates for at least half an hour. Two-step pressure control is suitable in a situation where one wants, for example, to double or treble the airflow. The change in the fan rotation speed should be quite small (e.g. less than 30%).

In constant pressure control, a separate arrangement is required to maintain constant pressure (a setting of 100 Pa, for instance) in the duct. Constant pressure control is suitable for a large range of ventilation rates.

4.3 DWELLING-SPECIFIC SUPPLY AND EXTRACT VENTILATION SYSTEM

Operating principle

A dwelling-specific ventilation system is particularly well suited both to low and high-rise residential buildings. The use of dwelling-specific ventilation and separate stairwells makes it possible to avoid the spread of smells and dampness from lower to higher floors, which is a problem especially in high-rise buildings. There are various alternatives for ventilation units and extract ducting.

The occupant can increase the total extract airflow of a dwelling as the need arises. When the total airflow is being increased, the fan switches to a faster rotation speed. The airflow can also be increased in individual rooms, e.g. in the kitchen and bathroom. In such circumstances the ventilation system operates on the borrowing principle. The dwelling has a heat recovery unit which is always equipped with a supply fan. The extract fan can be located in the dwelling or on the roof of the building.

Conveying extract air out of the building

The ducting of extract air is an important aspect in the case of an apartment building equipped with dwelling-specific ventilation.

Table 6 shows the problems associated with various alternatives and ways in which they may be solved technically. Smells can spread into the dwellings from positive-pressure duct in structural cavities. Noise as well as condensation problems are also associated with several alternatives.

After heat recovery it is not economic to convey extract air inside structural cavities because the extract air then heats up again. If cold extract air is conveyed outside structural cavities, there is then the danger of condensation and freezing. These difficulties can be avoided by blowing the extract air straight out through the wall.

When expelling extract air directly, its initial velocity should be high (e.g. 10 m/s) so that the wind and the temperature difference between the extract and outdoor air does not divert the jet back onto the building envelope. The outdoor air intake and the air expulsion unit are positioned on different walls.

Terminal units and airflows

Extract airflows per air vent are given in Table 7. The smaller airflow range applies to the normal situation and the larger to accelerated operation.

In a mechanical supply and extraction system, the intake of outdoor air is planned according to Part D2 of the Finnish Building Code in order to ensure that supply airflows are adequate. In the normal situation the supply airflow is 80% of the extract airflow.

The handling of the noise insulation between dwellings depends on the extract ducting solution employed. If a common extract duct is used, the noise insulation is achieved either by using a noise damper located in a terminal device or by adhering to Part C6 of the Building Code.

Ductwork

The airflow velocity in a dwelling duct should be less than 3 m/s. In the normal situation, the average pressure loss of the terminal unit is 50 Pa. The outdoor air duct is insulated against heat (100 mm) and dampness if the duct is located in a warmer space.

6. DISCUSSION

In the LVIS-2000 research programme, alternative system solutions are sought for the control of energy use and indoor climate conditions in buildings of the future. The starting point for the development project concerned with ventilation systems in residential buildings was that the occupant is regarded as the ventilation system user. In a study which approaches occupant activity from a socio-psychological standpoint, dwelling ventilation developed on the minimum functionality principle functions satisfactorily without the occupant playing any active role. On the other hand, the occupant is in a position to regulate the ventilation if he so desires. The occupant is indifferent as to what kind of ventilation system is used to produce a good indoor climate.

The minimum functionality principle can be technically implemented using a variable airflow ventilation system. Other objectives were set for the variable airflow system besides the facility of accelerating the ventilation. The system should not be susceptible to external interference factors. Ventilation efficiency should be good, especially in living spaces. The system should be economically efficient with regard to energy. It should be possible to modify the system at a later date.

In the development project associated with industrial component construction, the ventilation systems have been classified according to the decentralization principle and operational functions. From this extensive classification, three system types were selected for examination and they are the centralized supply and extraction system, the centralized extraction system and the dwelling-specific ventilation system. Natural ventilation systems were not examined.

At present the most important component used for accelerating a dwelling ventilation system is the cooker hood. The cooker hood should satisfy the following operating requirements: in the basic situation the airflow should be small and pressure difference great (e.g. 6 dm^3/s and 80 Pa). During accelerated operation mode the airflow should be greater and pressure difference smaller (20 dm^3/s and 40 Pa).

On the basis of a price comparison of ventilation systems, a mechanical supply and extraction system or a dwelling-specific system is 100-300 FIM/m^2 more expensive than a mechanical extraction system. The dwelling-specific system has the lowest annual energy and operational costs.

In this project it has been assumed that variable airflow ventilation systems will be controlled manually. Automatic control can also be arranged. At present it seems that CO_2-, moisture and air-quality sensors will be used. It is difficult to justify the need for a CO_2-sensor to the occupant as moisture removal is generally not a problem in Finland's climate, and air-quality sensors are, for the time being, unreliable.

The ventilation concepts introduced in this paper have already found their applications in practice. Three demonstration dwelling-houses are under construction and a product development has just started (Luoma, Laine, Kohonen 1990 and Luoma 1990).

BIBLIOGRAPHY

1. Saari, M., Determination of air exchange rates for demand controlled ventilation. Poster paper submitted to the 11th AIVC Conference, to be held in Italy, 18-21.9.1990.

2. Haikarainen, J., Room air temperature control in demand controlled ventilation. Poster paper submitted to the 11th AIVC Conference, in Italy, 18-21.9.1990.

3. Luoma, M., Kohonen, R., A ventilation concept for future dwelling houses. 9th AIVC Conference, Belgium, 12-15.9.1988. Proceedings, Vol. 1, pp. 329-342.

4. Laine, J., Demand controlled ductwork. 10th AIVC Conference, Finland, 25-28.9.1989, Preprints, Vol. 2, pp. 333-347.

5. Demand controlled ventilation, State-of-the-Art-Review, June 1989. International Energy Agency, Energy Conservation in Buildings and Community Systems Programme, Annex XVIII Demand controlled Ventilating Systems.

6. Anttila, U., Ilmanvaihto, asukkaiden viihtyvyys ja energiansäästö (Ventilation, habitant and energy conservation). Ministry of Trade and Industry, Energy Department, Series D:181 (in Finnish). Helsinki 1990. 74 p.

7. Luoma, M., Demand controlled ventilation systems for dwelling houses, Indoor Air '90, Toronto, Canada.

8. Luoma, M., Laine, J., Kohonen, R., Demand controlled ventilation in three Finnish demonstration dwelling houses. International CIB W67 Symposium on Energy, Moisture and Climate in Buildings, 3-6.9.1990, Rotterdam.

9. Karvonen, M-L., Luoma, M., Asuntoilmanvaihtojärjestelmien laskennallinen tarkastelu (Numerical Simulation Study on the Performance of Residential Ventilation System). Technical Research Centre of Finland, Research Reports to be published 1990 (in Finnish).

10. Sandberg,M., System med radiatoruppvärmning. Luftutbytseffektivitet, ventilationseffektivitet, temperatur och hastighetsfördelning i cellkontor. Gävle 1987. Statens institut för byggnadsforskning. 90 p.

11. Sarja, A., Principles and solutions of the new system building technology (TAT). Technical Research Centre of Finland, Research Reports No. 662. Espoo 1989. 61 p.

12. Ruotsalainen, R., et al. Symptoms and environmental complaints in occupants of houses and apartments with different ventilation systems. Indoor Air '90, the 5th international conference on indoor air quality and climate, Toronto, Canada 29.7.-3.8.1990.

TABLES

MEAN AIR EXCHANGE RATES FOR APARTMENT	
- material emission loads	0.1 - 0.5 1/h
- humidity loads	0.1 - 0.4 1/h
- heat load (in summer)	1.0 - 3.0 1/h
AIR FLOW RATES FOR DIFFERENT LOADS	
Sleeping rooms	
- human based odours,	
• at night	4 dm^3/s, person
• daytime	8 dm^3/s, person
Living rooms	
- human based odours,	
• normally	4-8 dm^3/s, person
• visitors	8 dm^3/s, person
Kitchen	
- humidity loads,	
• during use	15-40 dm^3/s
Bathroom	
- humidity loads,	
• during shower	50-100 dm^3/s
• bath	20-30 dm^3/s
• washed clothes drying	10-20 dm^3/s
Sauna	
- humidity loads,	
• during use	4 dm^3/s, person (≈5-10 1/h)
Toilet	
- removal of odours in 10 minutes	20 dm^3/s
Clothes closet	
- material emission loads	0.5 - 1.5 1/h
Smoking	
- odours of smoking	20-40 dm^3/s, smoker

Table 1. Demand controlled ventilation rates for various room spaces (Saari 1990)

CRITICAL FACTOR / SYSTEM	FAN 1= constant pressure control 2= two-steps fan control 3= slightly sloping fan curve	Ductwork R<0,5 Pa/m	Control of supply air coil	Thermal comfort	Draught
Supply and extract	1 : 9 x $q_{i0,h}$	4 x $q_{i0,h}$	12 x $q_{i0,h}$	No limitations if $T_{supply} \geq +16°C$	n_{max} 4,0 1/h
Extract - water radiator heating - water radiator and floor heating	2 : 7 x $q_{i0,h}$ 3 : 4 x $q_{i0,h}$	4 x $q_{i0,h}$		$n_{max} = n_0 +$ 1,0 1/h 1,2 1/h	maximum fresh air flow rate 6 dm^3/s per air vent
Dwelling-specific	3 : 2-10 x $q_{i0,h}$	4 x $q_{i0,h}$		like above	

Table 2. Greatest allowed total airflow acceleration based on different criteria.

Mode	Flow rate
Standby	< 0,35 dm^3/sm^2
Normal	0,35-1,0 dm^3/sm^2
Cooling	0,50-1,5 dm^3/sm^2

Space	Air flow, dm3/s	
	Supply	Extract
Bedroom	5	6
Livingroom	6	8
Kitchen		8
Bathroom		8
Toilet		5
Clothes closet		3
Hall	(K + BaR + WC) x 0,8	

Table 3. The modes of use and airflow ranges (dm^3/sm^2) of the centralized supply and extraction ventilation system.

Pressure diff.		Air vent position	Increase in the total air flow
Air vent Pa	Flow controller Pa		%
75	25	1 → 2	62
75	25	1 → 3	82
50	50	1 → 2	32
50	50	1 → 3	38
25	75	1 → 2	13
25	75	1 → 3	15

Table 4. Dependency of total and air vent-specific airflows on the usable pressure head between the terminal unit and flow control device.

	Common ducting	Individual ducting
Space	Flowrate dm^3/s	Flowrate dm^3/s
Kitchen	13 - 20	6 - 20
Bathroom	15	15
Toilet	10	10
Clothes closet	3	3

Table 5. Air vent-specific airflows.

Space	Flowrate dm^3/s
Kitchen	6...8 - 20...30
Bathroom	5...8 - 15...20
Toilet	10...12
Clothes closet	3...5

Table 6. Extract airflows per air vent.

FIGURES

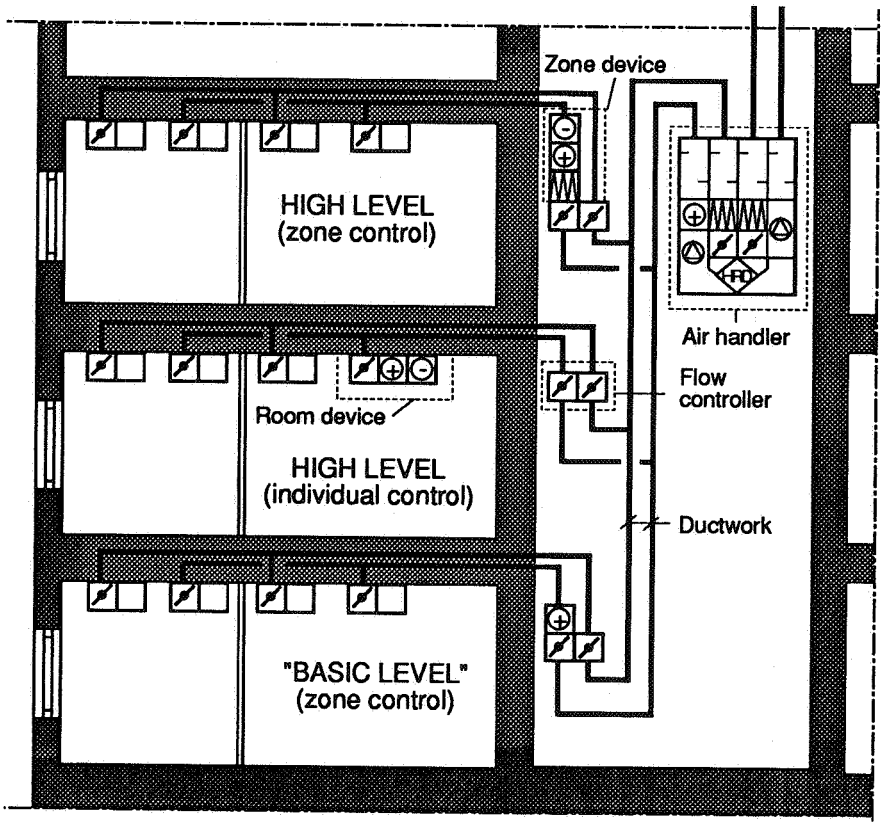

Figure 1. Air conditioning system, whose quality can easily be improved.

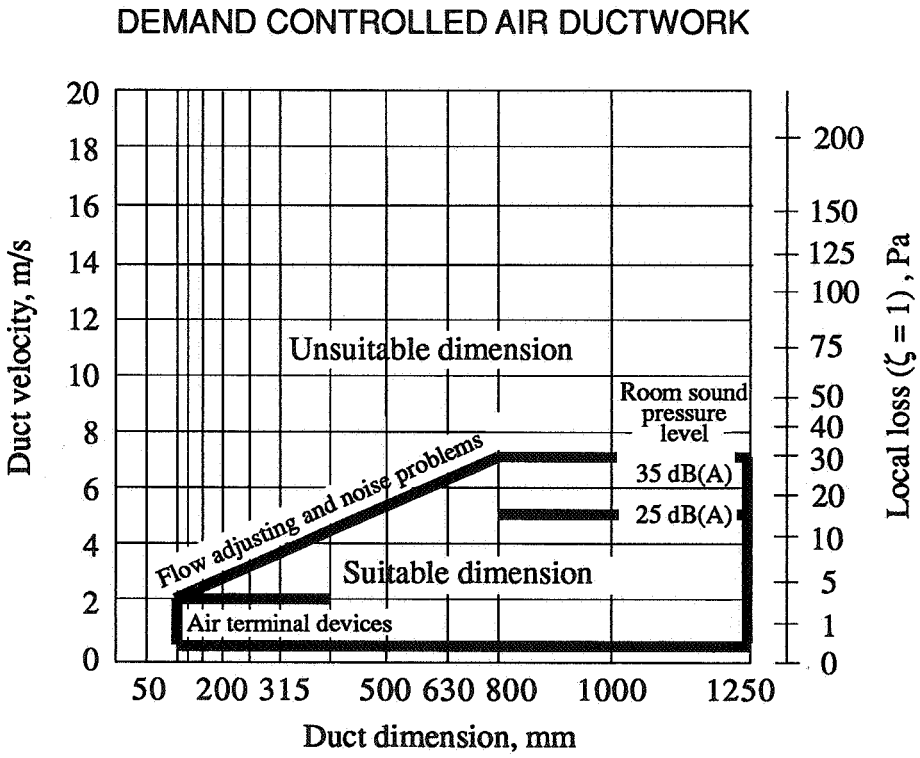

Figure 2. Set of dimensioning curves for ductwork.

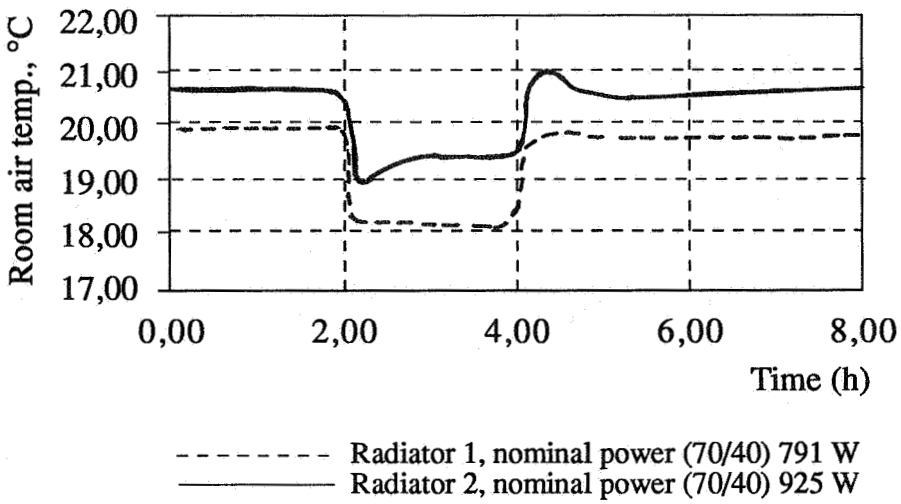

Figure 3. Room temperature when the space is equipped with one water radiator. The extract airflow in the space changes to 6.6 dm^3/s at moment 2:00 and then reverts to the original value at moment 4:00. The outside temperature os -27°C and the return water temperature is +70°C.

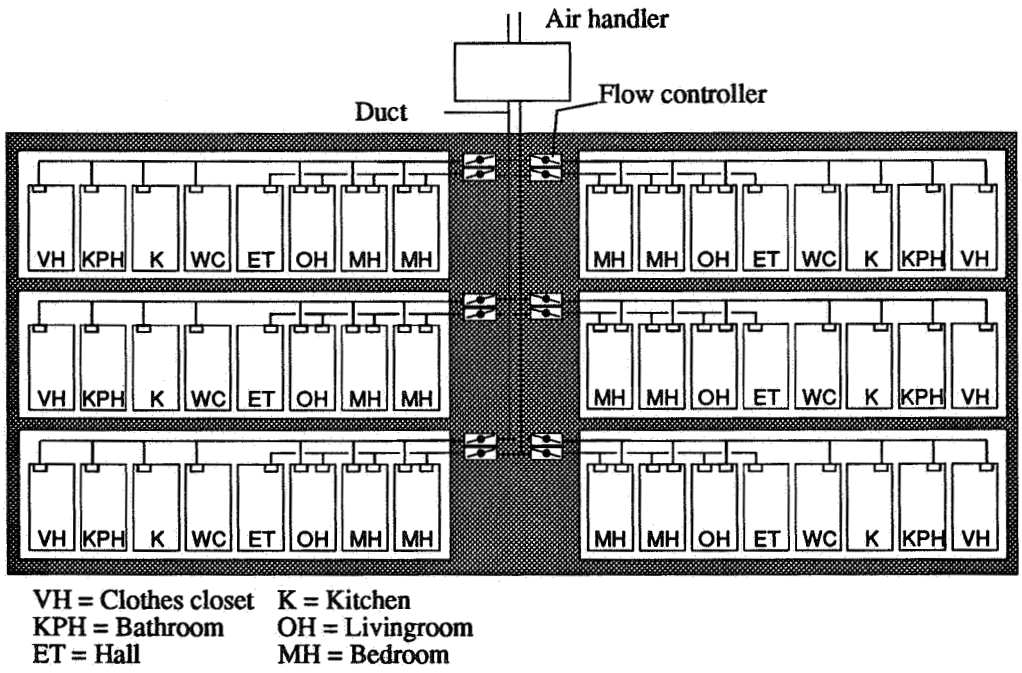

Figure 4. A centralized supply and extraction ventilation system.

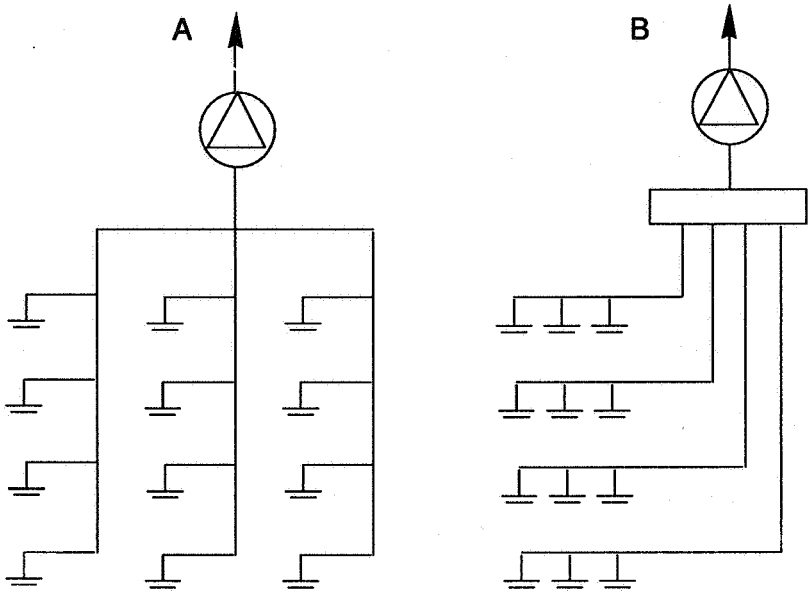

Figure 5. Ducting principles for the dwelling-specific supply sub-building-specific extraction ventilation system.
A Dwelling-specific vertical extract ducts
B Separate vertical ducts in kitchens, bathrooms etc.

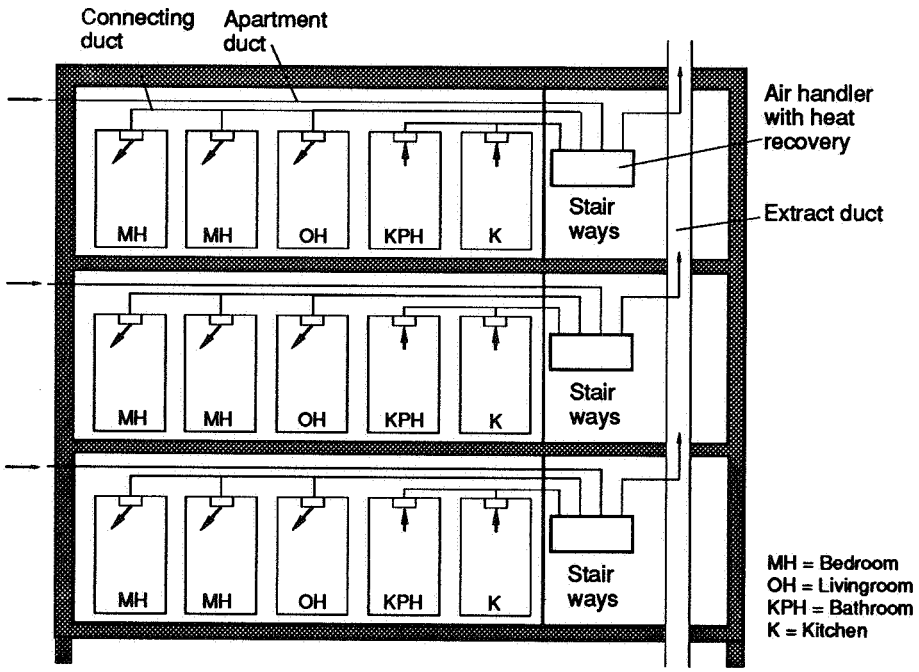

Figure 6. A dwelling-specific supply and extract ventilation system.

Discussion

Paper 4

W.Raatschen (Dornier GmbH, Germany)

a) How do you achieve a low cost DCV system? You said you need bigger duct work, variable fan speed sensors, dampers etc., all things which cost much money. b) You said every occupant should use the ventilation system as he wants. Could you point out what interferences and ways to operate the system a user should have?

R.Kohonen (VTT, Finland)

First I would like to remark that the costs of ventilation systems cannot be considered separately from the other systems. But to answer your question. We made parallel designs for a house of dwellings. We found that the investment costs of HVAC systems with DCV are 30-50% higher than those of our reference system (common vertical duct exhaust system). But if we take into account the operational cost the difference of annual costs are not much different. I am sorry if you got the impression that occupants should use the ventilation system as they want. My remark was that occupants should be able to use ventilation according to their needs. In our paper we give the system descriptions that give us the limitations to the demand-based use

J.Van Der Maas (LESO, EPFL, Switzerland)

Demand controlled ventilation systems require a knowledge of the room temperature behaviour during accelerated ventilation in order to access the comfort level during ventilation. Do you include thermal air stratification in your modelling? Indeed this can have much influence on the comfort.

R.Kohonen (VTT, Finland)

Thermal stratification was not included in our thermal modelling but surface and air temperatures were used to circulate PPD-indices. But in the table giving recommendations for the range of ventilation acceleration we take into account some practical limitations like the maximum fresh air intake airflow per airvent (6 dm3/s) in order to not cause draught or thermal discomfort.

VENTILATION SYSTEM PERFORMANCE

11th AIVC Conference, Belgirate, Italy
18-21 September, 1990

Paper 5

INDOOR AIR FLOW AND POLLUTANT REMOVAL IN A ROOM WITH TASK VENTILATION

W.J. FISK, D. FAULKNER, F.S. BAUMAN,[1] E.A. ARENS,[1]
D. PIH, AND P.J. MCNEEL

Indoor Environment Program
Applied Science Division
Lawrence Berkeley Laboratory
Berkeley, CA 94720 USA

[1]Center for Environmental Design Research
University of California, Berkeley
Berkeley, CA 94720 USA

Abstract

In an experimental facility, we studied the performance of a task ventilation system designed for use in office buildings. With this system, occupants can adjust the flow rate and direction of air supplied to their work space through four floor-mounted supply grills. Air typically exits the ventilated space through ceiling-mounted return grills. To study indoor air flow patterns, we measured the age of air at multiple indoor locations using the tracer gas stepup procedure. To study the intra-room transport of tobacco smoke particles, cigarettes were smoked mechanically in one workstation and particle concentrations were measured at multiple indoor locations. Test variables included the furnishing of the chamber, the location(s) of air supply, supply flow rates, temperatures, and directions, and internal heat loads. Our major findings were as follows: (1) In most tests, deviations from a uniform age of air, and a uniform particle concentration, were less than 30 percent. (2) Some supply air short circuits to the return grill when the air is directed toward the return grill with a high velocity. (3) Low supply velocities resulted in a floor-to-ceiling displacement ventilation flow pattern. (4) Directing the supply air toward the occupant, or away from the center of the four supply grills, typically yielded an age of air at the occupant's breathing level that was 15 to 25 percent lower than the age at other breathing-level locations. (5) With low supply velocities and air directed toward the occupants, tobacco smoke particle concentrations in a ventilated non-smoking workstation were 50 percent of the chamber-average concentration.

1.0 RESEARCH OBJECTIVES

The primary objectives of the research described in this paper were to determine the spatial variability in ventilation and pollutant removal efficiency in a room ventilated with a floor-based task ventilation system under a variety of operating conditions. More specifically, we desired to compare the rate of ventilation (as indicated by an age of air) at the position of the occupant to the rate of ventilation elsewhere in the room; to determine if the system resulted in a displacement flow pattern; and to determine the efficiency of removing tobacco smoke particles with a task ventilation system.

2.0 INTRODUCTION

We define "task ventilation" as a method of ventilation that provides for individual control of some local air supply parameters such as flow rate, temperature, or direction. Two task ventilation (T.V.) systems are being introduced in the U.S. The Task Air™ system, manufactured by Tate Architectural Products, Inc., has occupant-adjustable, floor-level air supply modules, has been installed in all or part of approximately twelve North American buildings,[1] and is used extensively in South Africa. This system, hereinafter called the "Tate System," is the object of the investigation reported in this paper and is described in detail in a later section. Johnson Controls, Inc., has recently introduced their Personal Environments® system that allows occupants to adjust the flow rate, temperature, and direction of air supplied through desk-mounted supply diffusers. In West Germany, the Krantz Company markets T.V. systems with air supplies at floor level and, in some cases, at the desk top.[2]

The potential for improved thermal comfort, because occupants can (to some extent) adjust their local thermal environment, is a major impetus for the use of task ventilation. Improved indoor air quality is another potential benefit

because the freshest (least polluted) air can be supplied more directly to the region around the occupant. T.V. systems may also, in some situations, result in a displacement (piston-like) air flow pattern in the floor-to-ceiling direction because slightly cool air, more dense than room air, is supplied at floor or desk level and air is typically removed from the room at or near the ceiling. Displacement flow often results in lower pollutant concentrations at the breathing level and higher concentrations in the ceiling-level exhaust air. However, the typically high air supply velocities of T.V. systems may inhibit displacement flow because of air mixing caused by entrainment of room air in the supply-air jets.

T.V. systems could potentially use less or more energy than conventional heating, ventilating, and air conditioning (HVAC) systems (i.e., systems with ceiling-level air supply diffusers and no provisions for occupant control) as discussed by Heinemeier.[3] Fan energy use and energy required for cooling or heating could differ between task and conventional systems due to: different supply temperatures (typically higher during cooling with T.V. systems); the large numbers of small supply fans and reduced supply-air ductwork in some T.V. systems; different indoor temperature profiles; different outside air requirements due to different efficiencies in pollutant removal; and the occupant use pattern of T.V. systems.

3.0 TATE SYSTEM

With the Tate System, air is supplied by a conventional air-handling unit (AHU) to a sub-floor supply plenum maintained at approximately room air pressure. The AHU may supply some recirculated indoor air but, according to the manufacturer, often supplies 100% outside air. In regions of the building with high heat loads, fan-coil units may be installed in the floor plenum to further cool the plenum air. Alternately, fan-coil units may be installed throughout the floor plenum and the central AHU used only for precooling and dehumidification. The supply plenum is the space beneath a raised access floor, i.e., a system of carpet-covered, removable floor panels suspended on a metal framework approximately 0.3 to 0.6 m above the permanent floor. Air supply modules, called task air modules (or TAMs), can be installed in place of any floor panel and easily moved to new positions. A TAM, depicted in Figure 1, contains a fan that draws air from the supply plenum and discharges air into the room through the slots (inclined 40° from vertical) in four plastic grills each 0.13 m in diameter. Using a recessed thumb wheel, the fan speed and, thus, air flow rate can be adjusted between approximately 40 L/s and 90 L/s resulting in maximum air supply velocities of 2 to 6 m/s (or the fan may be turned off). The direction of air supply can be changed by rotating any or all of the four grills. Occupants cannot control the supply air temperature which, to reduce the potential for cold drafts, is typically about 18 °C or 5 °C higher than the supply temperature of many conventional U.S. HVAC systems. Based on our experiments, the air supplied to the floor plenum may have a significantly lower temperature -- heat transfer through the floor will remove some space heat and increase the temperature of air supplied through TAMs. The Tate System may include some floor-mounted supply-air modules that are not subject to occupant control but instead are controlled by thermostats and some supply modules may contain electric-resistance heating elements. Air is typically withdrawn from the occupied spaces through ceiling-level return grills connected to return-air ducts or a return-air plenum located above a suspended ceiling.

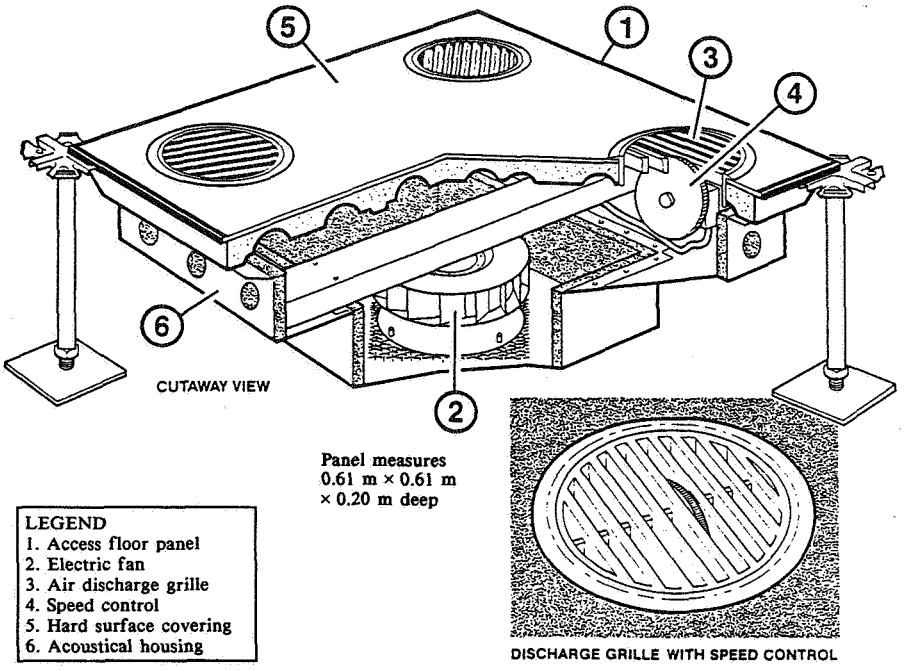

Figure 1. Cutaway diagram of a task air module (TAM).

Three recent papers provide information on the Tate System. Bauman et al.[4] and Arens et al.[5] report on an experimental investigation of thermal comfort conditions (velocities and temperatures) in a chamber with the Tate System. Their investigations of thermal comfort complement the research described in this paper and were performed coincident to the research in the same experimental facility. Major findings are: (1) the Tate System permits substantial adjustment of thermal comfort parameters at the occupant's location; (2) the system results in air velocities that often exceed the velocity limits of thermal comfort standards (however, the traditional limits on air velocity may be inappropriate for a situation with occupant control); and (3) with minimum air supply rates, the indoor temperature profiles resembled those obtained with displacement ventilation systems (i.e., substantial increases in temperature with height above floor). These papers also provide a brief review of available published information on task ventilation. Spoormaker[6] describes the use of the Tate System in 400,000 m^2 of office space within South Africa, describes the recommended system configuration, and presents indoor temperature and velocity data. Hedge[7] describes the results of a survey of six managers and 151 occupants of U.S. buildings with the Tate System. Building managers were very satisfied with the Tate System and indicated that occupants had fewer complaints about thermal comfort and ventilation compared to occupants of buildings with ceiling-level air supplies. Two thirds of the occupants indicated that the Tate System resulted in better temperature and ventilation conditions than the system with a ceiling-level air supply in their previous building.

4.0 EXPERIMENTAL FACILITY, INSTRUMENTATION AND PROCEDURES

4.1 Facility

All experiments were performed in a controlled environment chamber (CEC) with a 5.5 m by 5.5 m floor and a 2.5 m high ceiling. The CEC resembles a modern office space and has provisions for a high degree of control over the method of ventilation and indoor thermal environment.[8] The floor is covered with carpet tiles, finished gypboard walls are heavily insulated and painted white, windows in the two exterior walls provide a view to outside, the suspended ceiling contains patterned acoustical tile, and six recessed dimmable lighting fixtures are mounted in the ceiling. As shown in Figure 2, a raised access floor results in a 0.6 m high sub-floor plenum and the suspended ceiling provides a 0.5 m high ceiling plenum. A reconfigurable air distribution system permits air supply to and removal from any combination of ceiling and floor locations using ductwork and/or the plenums. Figure 2 illustrates the air flow configuration for the majority of experiments described in this paper. Supply air was directed into the sub-floor plenum and delivered to the room via TAMs installed in the access floor. In tests with the CEC unfurnished, return air passed through slots in the ceiling tiles, into the ceiling plenum, and then into the HVAC system. During the majority of tests, the CEC contained three workstations with furnishings typical of those in offices as shown in Figure 3, the slots in the ceiling tiles were sealed, and a duct connected a ceiling-level return grill (located in place of a ceiling tile) to the HVAC system.

The furnished chamber contained sources of heat and air motion typical of real offices including: overhead lights (with a total power of 500W of which roughly 100 W directly entered the chamber); 75 W task lights in each workstation; and a personal computer containing a small cooling fan and a monitor in each workstation (90 W each). Only one of the three workstations was occupied by a seated mannequin. Electric resistance heating elements wrapped around the mannequin released 75 W (a typical rate of release of sensible heat by an office worker). During a few tests, internal loads were increased by combinations of the following: operation of extra task lights; operation of a 200 W radiant heater beneath a desk; operation of mixing fans within the chamber; and operation of particle sampling and counting instrumentation within the chamber. In one test, the computers were turned off (to eliminate operation of the small cooling fans) and a small heater was operated to release approximately the same amount of heat.

The CEC's HVAC system provides a separate stream of conditioned air that is directed through plenums in the two exterior walls and between the inner two window panes called the annular space. During most tests, this system maintained the temperature of the interior window pane at approximately the average indoor temperature. Consequently, the exterior walls and windows were not a source of strong natural-convection airflow, but affected indoor airflow much like interior walls. During tests with heating of the chamber, cooled air was passed between the windows.

The CEC's HVAC system has a personal-computer-based direct digital control system. This system controlled and monitored various temperatures and air flow rates during the tests. For increased accuracy, supply and return air flow rates were generally also measured using pitot-static tubes centered in sections of plastic pipe. At the start and end of some tests, the rate of air supply through TAMs was measured with a flow hood.

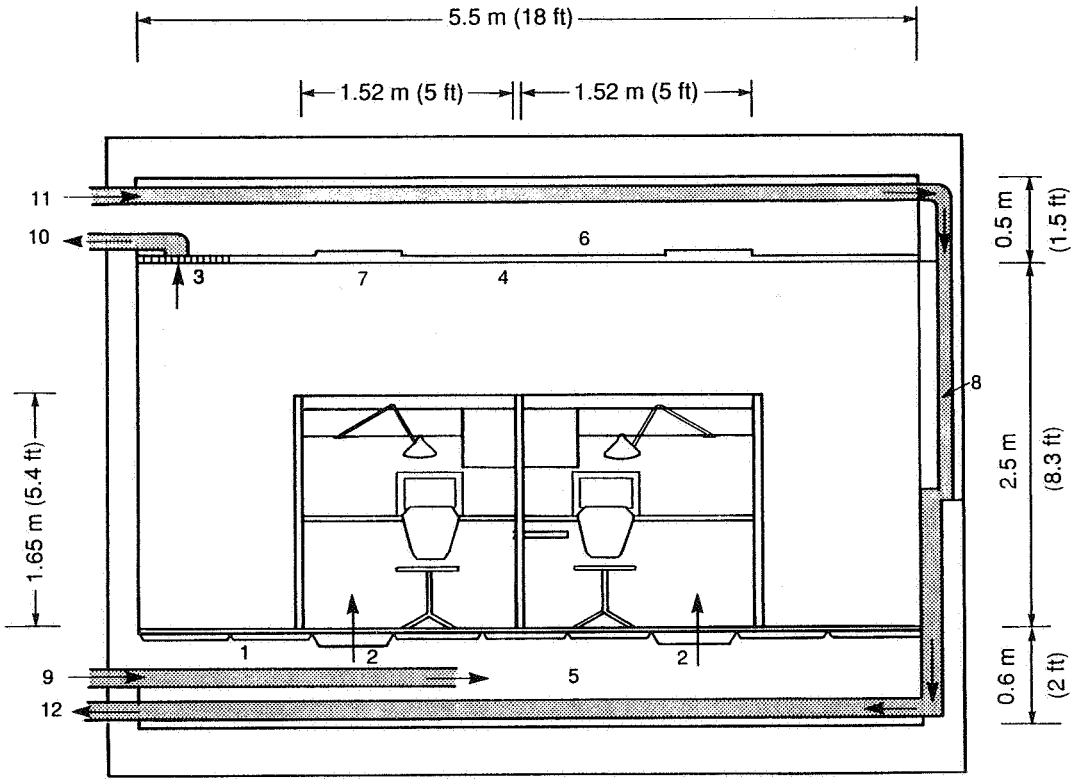

Figure 2. Cross section of CEC. Numbered items are: 1 = floor panel; 2 = TAM; 3 = return grill; 4 = suspended ceiling; 5 = subfloor plenum; 6 = ceiling plenum; 7 = light fixture; 8 = annular space between windows; 9 = air supply to subfloor plenum; 10 = air return to HVAC system; 11 = conditioned air supply to annular space; 12 = air return from annular space to HVAC system. The return-air grill is centered between the front and back walls.

4.2 Tracer Gas Measurements

The tracer gas stepup procedure [9,10,11] was used to study indoor airflow patterns and the spatial variability of ventilation. In this procedure, the supply air was labeled with a tracer gas and the rate of increase of tracer gas concentrations at a location indicated how rapidly the indoor air was replaced with "new" air that entered the building since the start of tracer gas injection. During the stepups, a mixture of 1% sulfur hexafluoride SF_6 in air was injected at a constant rate into the supply airstream. A peristaltic pump drew the tracer/air mixture from a storage bag and directed the mixture through a flow meter and tubing and into the supply duct. Injection rate was monitored using rotometers calibrated with a bubble flow meter and was generally stable within 2%. To ensure thorough mixing of the SF_6 in the supply airstream, an array of small propeller fans was installed downstream of the injection point. These fans were oriented to cause air flow perpendicular to the general direction of flow in the duct. Mixing was confirmed by collection and analysis of air/tracer samples. During the tests, air samples were drawn continuously through copper tubes from nine total locations to three gas chromatographs (GCs) equipped with electron capture detectors. Five of these samples originated from within the chamber at a subset of the locations illustrated in Figure 3 and four samples originated within the HVAC system. The GCs were capable of analyzing a sample within 1 minute using: a 0.38 m long molecular sieve main column; a backflush column with two sections (0.08 m of 5% phosphoric acid on Chromosorb GAW followed by 0.38 m of

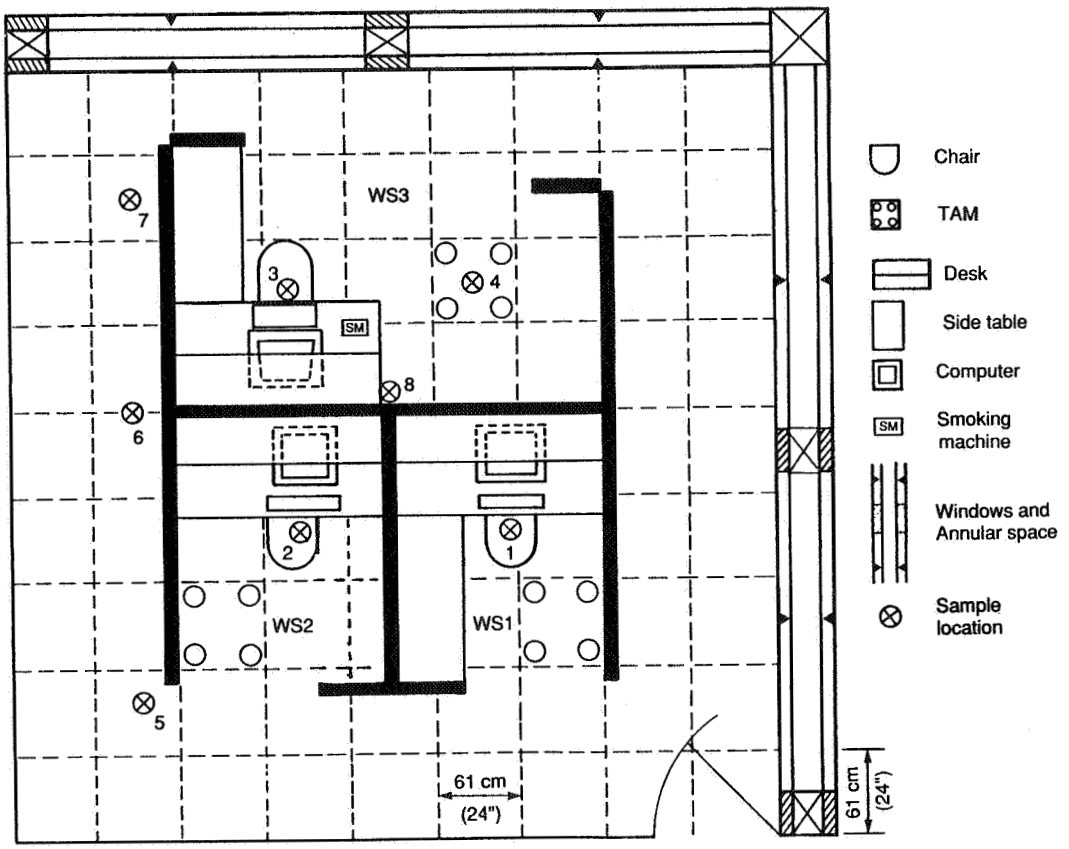

Figure 3. Plan view of CEC with workstations denoted WS1, WS2, and WS3. Tracer gas was sampled at points 1-4 (0.4 m, 1.1 m and 2.1 m above floor), at points 5 & 7 (1.1 m above floor), at point 6 (1.1 m and 2.1 m above floor), and at point 8 (2.1 m above floor). Particles were sampled at points 1-4 and 6 at heights indicated in Table 4.

molecular sieve); carrier gas (5% methane, 95% argon) flow rates of approximately 40 cc/min, and approximately a 12 s backflush time. (This measurement procedure was recommended by D. Harjje of Princeton University.) Therefore, at each sample location the tracer gas concentration was measured every three minutes. During the tests, bag samplers also directed air/tracer samples at a constant rate into 0.5 L sample bags. Bag sampling commenced at the start of tracer gas injection and continued until tracer gas concentrations were stable at which time syringe samples were collected manually from the same locations. The fourteen bag samplers collected samples from the locations within the chamber depicted in Figure 3. (Sample locations were slightly different during tests with an unfurnished chamber.) Air samples were directed to both a sample bag and a GC from two locations, thus, samples were collected and analyzed from 17 unique locations within the CEC. Bag and syringe samples were analyzed using the GCs immediately after completion of the tests. Equipment and procedures are similar to those used previously and described by Fisk et al.[10,11,12].

The GCs were calibrated prior to each test using nine total calibration gases with SF_6 concentrations of 0 ppb to 185 ppb. Measurements of tracer gas concentrations were generally repeatable within a couple ppb.

4.3 Tobacco Smoke Particle Measurements

The efficiency of removing tobacco smoke particles, and intra-room particle transport, were investigated during some of the tests. A cigarette was smoked by a cigarette-smoking machine located on the desk in workstation number 3 and particle concentrations were measured as a function of time during and after the period of smoking at four locations within the CEC identified in Figure 3 and Table 4 and also in the supply duct and at the return grill. An optical particle counter (OPC), calibrated by the manufacturer immediately before the first test, measured particle number concentrations in 15 size bins ranging from 0.09 μm to 3.00 μm. Air samples were drawn (at a rate of 5 L/min) to the optical particle counter through lengths of 1.3 cm diameter copper tubing connected to electrically actuated ball valves mounted on a copper manifold. The OPC drew an air sample from this manifold at a rate of 3 cc/min.

5.0 TEST CONDITIONS

Table 1 lists the test conditions. Gaps in the sequence of test numbers are due to unsuccessful tests or tests with air supplied through a conventional ceiling-level supply diffuser which are not discussed in this paper. The initial tests were conducted with an unfurnished chamber and a single TAM installed near the center of the floor. An electric resistance heating film was placed over the surrounding floor. Power to the heating film was controlled by a proportional controller to maintain a temperature of 24 °C at a location 1.4 m above the floor and away from the direct influence of the supply jet. The supply air temperature was maintained at 18.3 °C, except during Test 8 when the CEC was heated. Based on the manufacturer's recommended operating procedure, the four supply grills were oriented so that air was directed inward toward a line perpendicular to the center of the TAM and also upward at an angle of 60° from horizontal. (This supply direction is designated "inward" in Table 2 and in subsequent text and figures.) At maximum air delivery, the four jets converge at a height of 0.20 to 0.25 m.

During the majority of tests (CEC listed as furnished in Table 1), the CEC was subdivided into three workstations by 1.65 m tall partitions with no gaps between the partitions and the floor. TAMs were installed in each workstation at the locations indicated on Figure 3 and the workstations were furnished as described previously. During most of these tests, only one TAM operated and the outlet grills of the other TAMs were sealed with plastic. Test variables included the supply flow rate, internal heat load, direction of air supply, the location of the operating TAM, and the percent of outside air in the supply airstream (generally 100%). Air supply directions include "inward," as described in the previous paragraph, and also "outward" and "toward." An outward supply direction refers to air supply away from the center of the TAM (toward the four corners of the TAM) and at an angle of 60° from the horizontal. "Toward" refers to air supply from all four supply grills directed toward the mannequin and at an angle of 60° from horizontal. The heated mannequin was always seated in a workstation with an operating TAM. In most tests, the CEC was cooled by air supplied through the TAM. During Tests 8 and 34, the windows were cooled, internal heat generation was reduced, and the supply air was used to heat the chamber. During Tests 20 33, and 38, designed to determine measurement precision by comparing the results of measurements at different locations, the air within the chamber was mixed vigorously with fans. Tests 20D and 38D were tracer gas decays (instead of stepups) with the tracer gas concentration uniform at the start of the decay and no tracer injection during the decay.

Table 1. Test Conditions

Test #, Type*	CEC Furnished	Internal Load W/m^2	TAM Location†	Supply Flow L/S	Supply Temp. °C	TAM Supply Direction‡	CEC Temp. °C	Window Temp. °C #	Comments
3,T	N	NA	Central	101	NA	Inward	24	18	
7,T	N	NA	Central	80	18	Inward	24	24	
8,T	N	NA	Central	84	25	Inward	21	13	Heating test
9,T	N	NA	Central	57**	18	Inward	24	24	
10,T	Y	19	WS1	95	NA	Inward	24	24	Unsealed TAMS in WS 1&2
12,T	Y	19	WS3	98	20	Inward	24	24	
13,T	Y	19	WS3	98	22	Inward	26	26	
14,T	Y	19	WS3	94	23	Inward	26	26	
15,T	Y	19	WS3	97	23	Inward	26	26	
16,T	Y	19	WS1	97	19	Inward	24	21	
17,T	Y	19	WS1	98	25	Inward	28	29	
18,T	Y	19	WS2	96	17	Inward	24	24	
19,T	Y	19	WS2	98	22	Inward	28	28	
20,T	Y	30	WS3	95	17	Inward	24	24	Mixing fans in CEC
20D,T	Y	19	WS3	97	19	Inward	24	24	Tracer decay
26,T	Y	23	WS2	95	19	Inward	24	24	Computers off
27,T	Y	26	WS3	94	18	Toward	24	23	
29, T&P	Y	63	WS3	90	16	Inward	26	24	High internal load
30,T	Y	35	WS1	90	17	Inward	24	24	Unsealed TAMS in WS 2 & 3
31, T&P	Y	35	WS3	105	17	Outward	24	24	
32, T&P	Y	35	WS1&3	73	16	Toward	25	24	Low-supply velocity
33,T&P	Y	43	WS3	105	15	Toward	24	24	Mixing fans in CEC
34,T&P	Y	16	WS3	103	NA	Toward	24	13	Heating test
35,T&P	Y	35	WS3	108	17	Outward	24	24	20% Outside air
36,T&P	Y	35	WS3	111	17	Outward	24	24	
37,T&P	Y	35	WS3	101	16	Inward	24	24	
38,T&P	Y	43	WS3	107	16	Toward	24	24	Mixing fans in CEC
38D, T&P	Y	35	WS3	107	17	Toward	25	24	Tracer decay

* D = Tracer decay, all other tests are tracer stepups, T = tracer gas test, P = tobacco smoke particle removal test

† WS1 = work station #1, WS2 = work station #2, WS3 = work station #3

‡ Inward = four grills direct air inward and upward; Outward = four grills direct air outward and upward; Toward = four grills direct air toward mannequin

\# Temperature of air passed through annular space between window panes

** To obtain low-supply flows, floor plenum was depressurized relative to interior of CEC

6.0 DATA ANALYSIS METHODS

6.1 Tracer Gas Data

Equations based on age distribution theory[9] were used to calculate the ages of air. We present only the equations for a tracer gas stepup, similar equations for data from tracer gas decays are presented elsewhere.[9] Using tracer gas concentrations as a function of time, the following equation was employed

$$A = \int_0^{t_{ss}} [1 - C(t)/C(t_{ss})]dt \qquad (1)$$

where: A is the age of air; t is the time variable set equal to zero at the start of tracer gas injection; C(t) is the tracer gas concentration at time t, and t_{ss} is the time when concentrations have stabilized. The integral is evaluated numerically. Using the tracer gas concentrations in bag and syringe samples, C_{bag} and C_{syr}, respectively, age of air was determined using the equation

$$A = t_{syr}[1 - C_{bag}/C_{syr}] \qquad (2)$$

where t_{syr} is the time when the syringe sample is collected.

To indicate the spatial variability in age of air, we use various ratios based on the ages. For example, the age of air in the return duct divided by the age at breathing level in the "occupied" workstation (with mannequin and operating TAM) is an indicator of ventilation efficiency -- higher values of this ratio indicate more efficient air flow patterns with increased ventilation (lower ages) at the location of the occupant. When ratios contain an average of the age measured at several locations, we use volume-weighted averages assuming that each measurement is representative of a volume that extends half way to adjacent measurement points and/or to the edge of the workstation.

6.2 Particle Data

To evaluate the particle data collected at the different sample locations, we compute total particle number concentrations (for all size bins) minus the "background" particle concentration (i.e., the concentration before the cigarette is smoked and after an extended period of ventilation). To indicate the spatial variability of particle concentration and the efficiency of particle removal, we compare time-average values of these background-corrected particle concentrations measured at different indoor locations. Concentrations are averaged over the time period between the start of smoking and the time when particle concentrations have returned to the background concentration (i.e., over the period of tobacco smoke exposure).

7.0 RESULTS

7.1 Test with Mixing Fans in CEC

If the air in the CEC was perfectly mixed and measurement precision was perfect, ages of air (and particle concentrations) measured at each location within the CEC, and in the return duct, would be identical and all ratios based

on these measurements would equal unity. The age-of-air ratios from tests with mixing fans within the CEC (23,33,38) are always within 0.11 of unity (see Table 3), with two exceptions. The exceptions, ratios of 1.13 and 1.15, are based on measurements of age in the jet of air exiting the TAM where imperfect mixing is definitly expected despite the use of mixing fans. Hence, we neglect these two ratios, and assume that an age-of-air ratio greater than 0.11 from unity is significant from the measurement-precision perspective.

We believe that at least three factors cause imprecision in the multiple (multi-point) measurements of age of air. First, there is a small bias between ages determined from: (a) numerical integration of real-time data, and (b) the bag and syringe samples. (We are investigating the cause of this bias.) Second, the air in the CEC was probably not perfectly mixed due to the internal partitions. Third, there is undoubtably some random error in the measured ages due to such factors as instrument imprecision. When we gain more experience and data, a statistical evaluation of measurement precision may become appropriate.

7.2 Unfurnished CEC

Age-of-air ratios from tests with no furnishings in the CEC are provided in Table 2. All ratios for tests with a high supply velocity (Tests 3, 7, and 8) are within 0.3 of unity; therefore, the deviation from uniform ventilation (actually, uniform age of air) during these tests is not large.

In Tests 3 and 7 (with CEC cooled, high supply flow rates, and air directed inward and upward), the age of air in the CEC return duct is lower than ages within the chamber, hence, there is some short circuiting of air from the TAM to the return. Surprisingly, the results indicate negligible short-circuiting in Test 8 which is similar except that the supply air is warmer than the CEC air (chamber is heated). Possibly, the indoor air is more completely mixed in Test 8 due to increased natural convection caused by the cold windows.

Table 2. Age-of-air ratios from tests with unfurnished CEC. Ratios in bold print are considered significantly different from unity from a perspective of measurement precision.

	Test #			
Ratio	3*	7	8	9
Return Duct / All B.L. Points	**0.84**	**0.87**	0.94	**1.30**
Return Duct / All CEC Points	**0.85**	0.92	0.97	**1.33**
A.L. of Central Ring / A.L. above TAM	1.11	**1.24**	**1.20**	**2.18**
B.L. of Outer Ring / B.L. of Central Ring	0.98	**1.30**	1.04	0.99

KEY: B.L. = Breathing Level (0.4 m above floor)
A.L. = All Levels (0.4 m, 1.3 m, and 2.1 m above floor)
Central Ring = 4 points, 1.2 m to 2.4.m from TAM
Outer Ring = 4 points, 2.2 m to 3.0 m from TAM
* missing data could have significantly affected ratios

In the single test with a low supply velocity (Test 9 with chamber cooled and air directed inward and upward), the ratios indicate a displacement flow pattern between TAM and return (i.e., a significantly higher age in the return). Ages also increase with height above floor. Evidently, there is less mixing of the indoor air during this test due to the low supply velocity. The measurements by Bauman et al.[4] and Arens et al. [5] are consistent -- they found considerable thermal stratification in tests with low supply velocities.

The third row of ratios in Table 2 indicate that the average age of air at locations above the TAM (in line with the jet of supply air) is significantly lower than the average age in a ring of points located 1.2 m to 2.4 m away from the TAM. These findings are consistent with expectations.

7.3 Age-of-Air Measurements in Furnished CEC

Table 3 provides age-of-air ratios from tests with the CEC furnished. A large majority of the ratios are within 0.2 of unity; therefore, in most tests, the deviation from uniform ventilation is not large.

During all tests (18, 19, and 26) with air supplied through a TAM located in work station number 2 (WS 2), the age of air in the return duct is significantly lower than the average age at the breathing level of the occupied workstation (WS 2), as illustrated in Figure 4, and also significantly lower than the average age at all levels within all workstations. We suspect that this short circuiting of air to the return is caused by the close proximity of the return grill (closer to WS 2 TAM than to any other TAM) and by the inward and upward direction of air supply.

In several tests, the age at the breathing level of unoccupied workstation(s) is significantly greater than the age at the breathing level of the occupied WS. In other words, the results of these tests indicate a significant, but generally modest, enhancement of ventilation at the occupant (i.e., true "task" ventilation). As illustrated in Figure 5, this efficient pattern of ventilation was evident in all tests with air directed toward the occupant (Tests 27, 32, 34, and 38D) and in two of three tests with air directed outward (35 and 36 but not 31) but in only two of 14 tests with air directed inward and upward (excluding Test 20 with mixing fans in the CEC). Possibly, the higher ages in unoccupied workstations during Tests 35 and 36 is caused by short circuiting of air from the TAM to the return grill. We have no explanation for the enhanced ventilation at the occupant during Test 30.

In several tests, the age of air at knee level in the occupied workstation is significantly greater than the age at breathing level -- with no evident correlation to test conditions. Our only possible explanation is that the knee level sampling point was in a protected location beneath the desk.

Some of the age-of-air ratios from Test 32 deviate very substantially from unity. In this test, there is a very significant enhancement of ventilation (reduced age of air) at the breathing level of the occupied workstations and age of air increases substantially with height, indicating a displacement flow, in both workstations with an operating TAM. The test was unique. Two TAMs were operating, the supply flow from each TAM was as low as possible, and air was directed toward the mannequin in WS3 and the chair to the desk of WS1. The finding of displacement flow when supply velocities are low is consistent with the results of Test 9 and with the results of complementary research on thermal comfort and temperature distributions.[4,5] Additional tests are required to further examine this general mode of operation.

Table 3. Age-of-air ratios from tests with furnished CEC. Ratios that are underlined are considered significantly different from unity from a perspective of measurement precision.

Test #	Return B.L. of OWS	Return B.L. of AWS	Return AWS Loc.	B.L. of UWS B.L. of OWS	C.L. of OWS B.L. of OWS	K.L. of OWS B.L. of OWS	C.L. of AWS B.L. of AWS	K.L. of AWS B.L. of AWS
10	1.03	1.07	1.11	0.90	0.97	1.13	0.97	1.08
12	1.09	1.03	1.11	1.01	1.08	0.98	0.95	0.99
13	NA	NA	NA	NA	NA	NA	0.97	1.11
14	1.09	0.97	1.05	1.06	1.04	1.05	0.96	1.13
15	1.12	1.06	1.07	0.98	1.03	1.07	1.13	1.16
16	1.13	1.10	1.07	1.02	0.86	0.99	1.06	1.11
17	NA	1.06	1.08	NA	NA	NA	0.99	1.02
18	0.87	0.84	0.88	1.05	0.92	1.03	1.01	0.90
19	1.04	0.86	0.83	1.20	1.06	1.29	1.18	1.12
20*	1.06	1.03	1.00	1.05	1.06	1.10	1.05	1.07
20D	1.21	1.10	1.12	1.06	1.02	1.18	1.01	1.08
26	0.96	0.82	0.83	1.15	0.96	1.02	0.98	1.09
27	1.01	0.94	0.85	1.19	1.03	1.23	1.09	1.09
29	1.14	1.00	0.98	1.13	1.01	1.17	1.04	1.11
30	1.23	1.00	0.99	1.22	1.05	1.36	1.03	1.14
31	1.11	1.03	1.01	1.07	1.12	1.02	NA	1.17
32+	1.46	1.06	0.99	1.73	1.76	1.20	1.31	0.93
33*	1.09	1.00	0.92	1.13	1.11	1.15	1.10	1.11
34	1.06	0.89	0.93	1.19	0.90	1.13	0.92	1.06
35	1.07	0.91	0.91	1.17	1.02	1.23	1.07	1.06
36	1.13	1.00	0.89	1.17	1.18	1.24	1.13	1.17
37	1.00	1.00	0.96	0.98	0.93	1.20	1.02	1.18
38*	1.01	1.04	1.00	1.00	1.00	0.90	1.06	1.03
38D	1.17	0.93	0.90	1.33	1.24	1.07	1.07	1.00

KEY: Return = chamber return duct; B.L. = Breathing Level (1.1 m above floor); C.L. = Ceiling Level (2.1 m above floor); K.L. = Knee Level (0.4 m above floor); OWS = occupied work station (with mannequin); AWS = all work stations; UWS = unoccupied work station(s); Loc. = locations

* mixing fans in CEC

+ OWS includes both WS1 and WS3

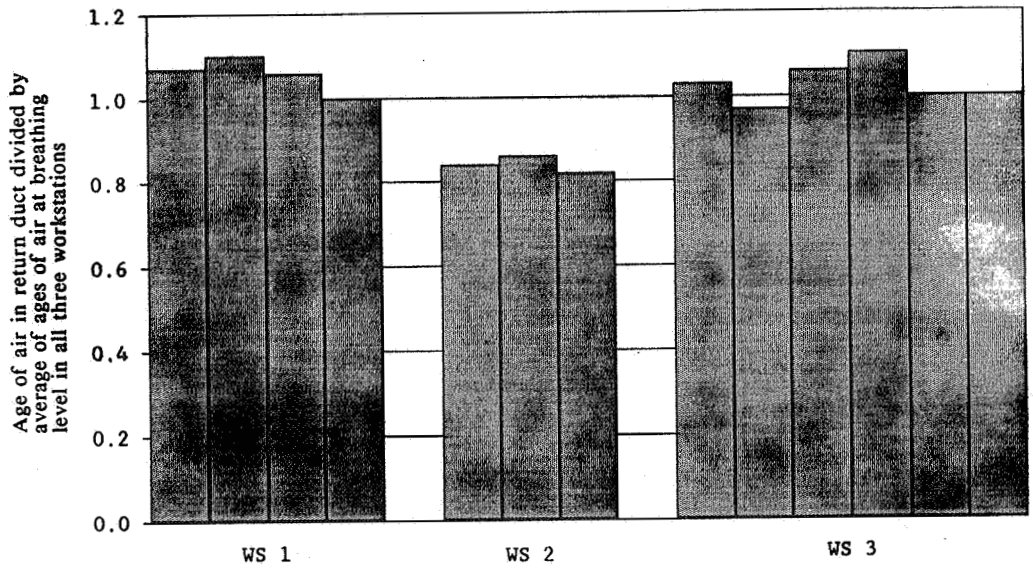

Figure 4. Age of air in return duct divided by average of ages of air at breathing level in all three workstations. Tests are divided into three groups depending on location of the operating TAM (WS1, WS2, or WS3). Tests with mixing fans in the CEC and Test 32 with two TAMS operating are not included.

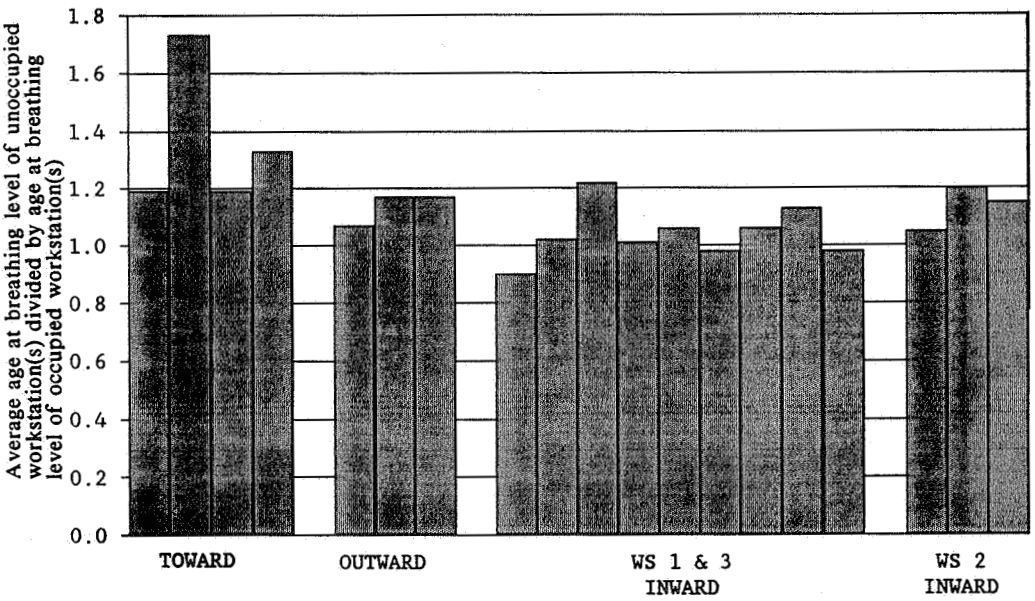

Figure 5. Average age of air at breathing level of unoccupied workstations divided by air of air at breathing level of occupied workstation(s). Only occupied wokrstations have an operating TAM. Tests with mixing fans in the CEC are not included. Tests are divided into groups depending on direction of air exiting TAM (toward occupant, outward, inward and upward). With air directed inward and upward, we separate tests with TAM operation in WS2 which was associated with short circuiting of supply air to the return grill.

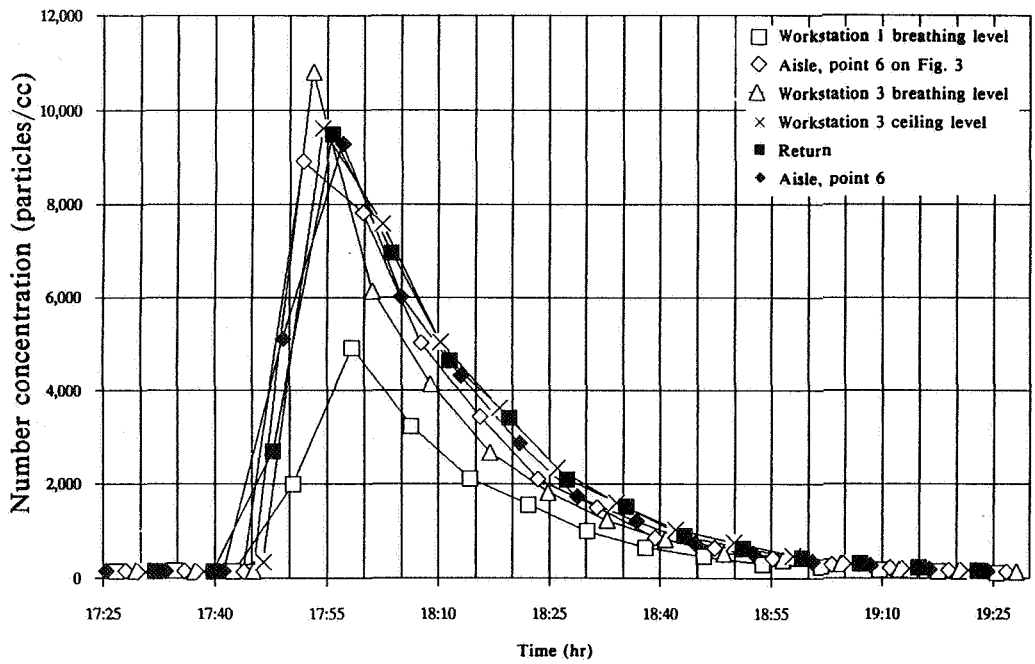

Figure 6. Total (for all size bins) particle number concentration versus time for Test 32. A cigarette was smoked in workstation 3 between 17:45 and 17:55 and TAMs operated in both WS1 and WS3.

Table 4. Total (for all size bins) time-average particle number concentrations (particles/cm^3), minus the background concentrations before and long after cigarette smoking

	Location								
Test #	B.L. of WS1	B.L. of WS2	B.L. of WS3*	B.L.m of WS3+	C.L. of WS2	C.L. of WS3	Return Grill	Supply Duct	Aisle#
31	1099	1116	1331	1265	---	---	1236	62	---
32	986	---	1693	---	---	1926	1939	---	1930
33†	1127	---	1091	---	---	1168	1175	---	1112
34	---	1525	1549	---	1514	1639	1693	208	---
35	---	1718	1496	---	1709	1633	1800	703	---
36	---	1913	1838	---	1944	1964	2047	233	---
37	---	1643	1765	---	1560	1620	1582	292	---
38U†	---	2292	2041	---	2242	2020	1869	333	---
39D	---	1876	1672	---	1902	1934	2071	275	---

Key: B.L. = Breathing Level (1.1 m above floor); C.L. = Ceiling Level (2.1 m above floor); WS1 = Work Station #1; WS2 = Work Station #2; WS3 = Work Station #3

* near mannequin (Point 3 in Figure 3)
\+ second B.L. location in WS3 (Point 4 in Figure 3)
\# point 6 on Figure 3
† mixing fans in CEC

Several test variables did not seem to significantly influence the spatial pattern of age of air. There is only a slight hint of short circuiting of air from supply to return in Test 34 with heating; this is consistent with the results of the Test 8 with heating and an unfurnished CEC. Turning off the computers, which contain small cooling fans, did not noticeably affect results. The magnitude of internal heat load did not seem to influence results for the range of loads studied. Recirculation of air by the air handler (Test 35) also had no apparent effect on results. The insignificant impact of computer fans, increased heat sources, and recirculation is probably a consequence of the relatively thorough mixing within the chamber even without these factors.

7.4 Particle Removal Experiments

Table 4 contains the time-average particle number concentrations from all tests with tobacco smoking and Figure 6 provides an example of concentration versus time for one test. During Tests 33 and 38, the air within the chamber was mixed with fans. The ratio of maximum to minimum measured particle concentration for these two tests was 1.20 and 1.23, respectively, which compares to an ideal ratio of unity in a perfectly mixed chamber if there is no measurement imprecision. Therefore, we assume differences in particle concentrations greater than approximately 20 percent are real, i.e., not caused by measurement imprecision.

In tests without mixing fans, excluding Test 32, there is little spatial variability in the time-average particle concentration based on the limited number of measurement locations. In fact, the ratio of maximum to minimum concentration during these tests is always below 1.25. During Test 32 (with large spatial differences in age of air as noted previously), the particle concentration at one indoor measurement location is approximately 50 percent of the other measured concentrations (see Figure 6). The low concentration was measured at breathing level in WS 1 which has an operating TAM directing air at low velocity toward the occupant. Apparently the partitions separating WS 1 from WS 3 (the cigarette was smoked in WS 3) and the direct supply of air in WS 1, were sufficient to substantially reduce particle transport to the breathing location in WS 1. We would not expect this region of low particle concentration if the ventilation were provided in the typical manner through ceiling-mounted air supply diffusers; however, additional experiments are required to confirm this expectation.

8.0 SUMMARY OF MAJOR FINDINGS

1. Except in tests with the minimum possible rate of air supply through the TAMs, age-of-air ratios were almost always within 0.3 of unity indicating that deviations from uniform ventilation were not large. We hypothesize that entrainment of room air in the high velocity supply jets was a major cause of mixing of the indoor air.

2. With the minimum possible rate of air supplied through TAMs, there was a significant displacement flow pattern in the CEC. More tests with low supply velocities are required.

3. In almost all tests with air directed toward the occupant or in an outward direction, but very few tests with air directed inward, the age of air at breathing level of the occupant was significantly (but, in general, only moderately) lower than the age of air at other indoor locations.

4. Directing air inward and upward toward a return grill was associated with a slight amount of short circuiting between the floor-mounted TAM and the ceiling-mounted return.

5. Increased internal heat load, operation of computers containing small cooling fans, and recirculation of air by the main air-handling unit had no discernible impact on the spatial pattern of age of air, probably due to relatively thorough mixing without these factors.

6. With workstations separated by partitions, using the task ventilation system to directly supply air toward the occupant's breathing location appears to inhibit the transport of tobacco smoke particles to that location from an adjacent workstation.

9.0 ACKNOWLEDGMENTS

This work was supported by the Assistant Secretary for Conservation and Renewable Energy, Office of Building and Community Systems, Building Systems Division of the U.S. Department of Energy (DOE) under Contract No. DE-ACO3-76SF00098. Generous furniture and partition donations from Steelcase, Inc., Grand Rapids, MI, also contributed to the performance of this research. The authors also acknowledge the support and technical assistance of Gene Brager and John Zeren, formerly of Tate Access Floors, Jessup, MD.

10.0 REFERENCES

1. Tate Access Floors, "Tate Task Air™ System, Project Update," Product information supplied by Tate Access Floors, Jessup, Maryland.

2. Sodec, F., "The Underfloor Air Supply System - the European Experience," Paper SL-90-7-4, presented at the June 1990 meeting of the American Society of Heating, Refrigerating, and Air Conditioning Engineers, St. Louis, MO, 1990. To be published in *ASHRAE Transactions*.

3. Heinemeier, K.E., Schiller, G.E., and Benton, C.C., "Task Conditioning for the Workplace: Issues and Challenges," Paper SL-90-7-3, presented at the June 1990 meeting of the American Society of Heating, Refrigerating, and Air Conditioning Engineers, St. Louis, MO, 1990. To be published in *ASHRAE Transactions*.

4. Bauman, F.S., Johnston, L.P., Zhang, H., and Arens, E.A., "Performance Testing of a Floor-Based Occupant-Controlled Office Ventilation System," University of California, Berkeley. Submitted for presentation at the January 1991 meeting of ASHRAE and publication in *ASHRAE Transactions*.

5. Arens, E.A., Bauman, F.S., Johnston, L.P., and Zhang, H., "Testing of Localized Thermal Distribution Systems in a New Controlled Environment Chamber," to be presented at te 11th AIVC Conference "Ventilation System Performance" September 18-21, Belgirate, Italy, and published in conference proceedings by the Air Infiltration and Ventilation Centre, Coventry, Great Britain.

6. Spoormaker, H.J., "Low-Pressure Underfloor HVAC System," Paper SL-90-7-2, presented at the June 1990 meeting of the American Society of Heating, Refrigerating, and Air Conditioning Engineers, St. Louis, MO, 1990. To be published in *ASHRAE Transactions.*

7. Hedge, A., Abi, M., Parmelee, S., "Reactions of Facilities Managers and Office Workers to Underfloor Task Air Ventilation," Cornell University, Ithaca, NY. In press.

8. Bauman, F.S. and Arens, E.A., "The Development of a Controlled Environment Chamber for Physical and Subjective Assessment of Human Comfort in Office Buildings," In: A New Frontier: Environments for Innovation, *Proceedings of the International Symposium on Advanced Comfort Systems for the Work Environment,* Kroner, W. Ed., Troy, NY: Center for Architectural Research, May 1988.

9. Sandberg, M. and Sjoberg, M., "The Use of Moments for Assessing Air Quality in Ventilated Rooms," *Building and Environment* **18**, pp. 181-197, 1983.

10. Fisk, W.J., Prill, R.J., and Seppanen, O., "Commercial Building Ventilation Measurements Using Multiple Tracer Gases," In *Proceedings of the 9th AIVC Conference,* "Effective Ventilation," Vol. 1, pp. 161-182, 1988. Published by the Air Infiltration and Ventilation Centre, Coventry, Great Britain.

11. Fisk, W.J., Prill, R.J., and Seppanen, O., "A Multi-Tracer Technique for Studying Rates of Ventilation, Air Distribution Patterns, and Air Exchange Efficiencies," In *Proceedings* of "Building Systems: Room Air and Air Contaminant Distribution," pp. 237-240. Published by ASHRAE, 1989.

12. Fisk, W.J. et al., "Multi-Tracer System for Measuring Ventilation Rates and Ventilation Efficiencies in Large Mechanically Ventilated Buildings." In *Supplement to Proceedings of the 6th AIVC Conference* "Ventilation Strategies and Measurement Techniques," pp. 69-93, 1985. Published by the Air Infiltration and Ventilation Centre, Coventry, Great Britain.

Discussion

Paper 5

W.Raatschen (Dornier GmbH, Germany)

Is the ratio of the exit age vs. local mean age an appropriate value to characterise a displacement flow system?

W.Fisk (LBL, USA)

An increase in the age of air with height above the floor is a proper indication of displacement flow in the floor-to-ceiling direction. This trend was indicated by measurements at three heights within the chamber plus measurements at the ceiling-level return grille. Comparing the exit age (age at return grille) to a single local age (e.g. at breathing level) is a less certain indication of displacement flow.

M.Masoero (Politecnico di Torino, Italy)

According to some system manufacturers, subfloor air distribution is beneficial to IAQ because the raised floor can be raised and cleaning performed. Other people agree that subfloor space contains plastic electric cables that can themselves be sources of pollution. Can you comment on this? See comment by Mike Holmes.

W.Fisk (LBL, USA)

My response to the question by M J Holmes applies to this question. I also note that many return-air plenums contain electrical cable and that we have many plastics, adhesives, caulks, etc., within the occupied spaces of our buildings. I am not aware of data indicating that electrical cables are an important source of indoor pollutants.

M.J.Holmes (Ove Arup, London)

There are two types of underfloor systems, neutral and pressurized floors. The neutal pressure floor can be achieved by either ducting recirculation air and using fans to overcome the terminal resistance, or a non ducted system with a terminal fan. Floor pollution is obvious in the latter case, in the form debris falling into the system could cause a problem. Pressurized floors also have a contamination problem and they leak. Have you any comments?

W.Fisk (LBL, USA)

Our primary interest is task (i.e. occupant controlled) ventilation which does not necessarily require the use of a subfloor supply air plenum. We have no practical experience with accumulation of dirt in these plenums. However, avoiding a subfloor plenum does not eliminate problems of dirt accumulation on surfaces in contact with air supplied to occupants. Dirt can accumulate inside supply ducts (this problem may be increased when ducts are lined with a porous insulation) and also in return-air plenums.

Bas Knoll (TNO, Netherlands)

How does compartmentation by the separations affect or improve displacement flow?

W. Fisk (LBL, USA)

Displacement flow doesn't seem majorly affected by it.

VENTILATION SYSTEM PERFORMANCE

11th AIVC Conference, Belgirate, Italy
18-21 September, 1990

Paper 6

TESTING OF LOCALIZED THERMAL DISTRIBUTION SYSTEMS IN A NEW CONTROLLED ENVIRONMENT CHAMBER

E.A. ARENS, F.S. BAUMAN, L.P. JOHNSTON, and H. ZHANG

Center for Environmental Design Research
390 Wurster Hall, University of California
Berkeley, California 94720 USA

SYNOPSIS

This paper describes tests of thermal and ventilation performance of two relatively new occupant-controlled localized thermal distribution (also called task ventilation) systems. The first is a raised-floor distribution system providing air through grilles in the floor panels, and the second is a desk-mounted unit supplying conditioned air at desktop level. These systems have been tested in a mockup of a typical partitioned open-plan office, and the resulting temperature and air velocity distributions are reported for a variety of system and locally controlled conditions. Comfort model predictions are presented to describe the degree of control and range of occupant comfort levels produced in the local workstation. The results are also compared to those produced by a conventional ceiling supply system.

The tests were performed in a new controlled environment chamber (CEC) having unique capabilities for detailed studies of space conditioning and thermal comfort in office environments. The CEC closely resembles a contemporary office space 5.5 m x 5.5 m x 2.5 m in size, with exterior windows on two walls and reconfigurable HVAC and lighting systems. Air can be supplied and returned from floor or ceiling levels, the surface temperature of the windows controlled by air circulated through the triple-pane glazing, and two separately controlled air supplies can be provided to the space simultaneously.

The tests investigated the effects of supply volume, supply location, supply vent orientation, supply/return temperature difference, heat load density, and workstation size and layout. Temperature differences in the range of 1-2.5°C were observed between adjacent workstations, and local velocities in the vicinity of outlets could exceed 3 m/s. Such wide-ranging values could violate existing comfort standards, if strictly interpreted. However, since these systems put the local thermal conditions within the workstations under the direct control of their occupants, it is likely that the standards should grant exceptions to such systems.

1. INTRODUCTION

It has become increasingly difficult for conventional centralized HVAC systems to satisfy the environmental preferences of individual office workers. Offices today have large amounts of heat-generating equipment (computers, printers, etc.) whose loads vary considerably from workstation to workstation. The workstations are separated by partitions that divert the flow of air between ceiling-mounted supplies and returns so that the workstations themselves are not well ventilated. The workstations are also increasingly reconfigured to accommodate changing tenant needs, affecting the HVAC system's ability to meet the loads for which they were designed. Compounding this problem, there is a growing awareness of the importance of the comfort, health, and productivity of the individual office workers, giving rise to an increased demand among employers and employees for a high quality work environment.

Localized thermal distribution (LTD) systems distribute conditioned air through vents in the direct vicinity of the occupant. The vents can be located in the floor plane or in the office furniture, such as desks or workstation partitions. Such distribution systems have the potential to improve the ventilation efficiency at the breathing level and at the same time provide individual workers with the ability to adjust their local environments to their individual comfort preferences. They also appear to have energy-saving potential, particularly when occupancy sensors are

fitted to the local supply units to turn them off when their associated workstations are unoccupied. Localized thermal distribution systems are frequently combined with raised access floors installed to facilitate cable management and workstation reconfigurability.

In one of the earlier publications on occupant-controlled thermal distribution, David[1] describes several of the underfloor systems available at that time. The literature reports relatively few experimental studies of how such systems perform. Sodec[2], Barker[3], Barker et al.[4], Tuddenham[5], Rowlinson and Croome[6], and Hanzawa et al.[7] present data from test chamber studies of floor and desk-mounted supply vents. More recently, Spoormaker[8] describes his experiences in South Africa with a floor supply system very similar to the one studied in the present investigation. Sodec and Craig[9] describe the European experience with both floor and desk-level supply systems. Additional references are contained in a discussion by Bauman et al.[10].

Under low supply velocity conditions, the performance of floor-based systems will resemble that of displacement ventilation systems, producing increased stratification while providing relatively uniform conditions at any given height within the occupied space. At higher rates of flow the supply air may form jets and produce nonuniform thermal conditions and localized drafts. Both of these could lead to local thermal discomfort even when whole-body comfort is acceptable. Research during recent years has studied the impact of turbulence intensity on the sensation of draft and concluded that further reductions in velocity limits contained in the present comfort standards may be necessary for airflows having higher levels of turbulence[11]. Even with their present limits, the requirements of ASHRAE Standard 55-81[12] and ISO Standard 7730[13] are probably not met by many LTD's under normal operation because of high velocities in the vicinity of the supply vents and also because of temperature variations that may exist within the occupied zone.

On the other hand, there is some evidence that the variable climate they produce, when occupant controlled, may in fact be desirable for an office ventilation system. A recent survey of three installations of a floor-level LTD system found that two-thirds of the workers felt that an underfloor LTD system provided improved temperature and ventilation conditions compared with the overhead ventilation system in their previous buildings[14]. One might also look at this from the perspective of what appear to be inherent limitations to comfort standards. Both the ASHRAE and ISO comfort standards specify a zone of relatively uniform conditions within which no more than 20% of the occupants are to be dissatisfied. Although 20% is in itself a fairly large number, a recent field study in office buildings suggests that the dissatisfaction level for environments maintained within the comfort zone may in fact be higher[15]. In addition, this study and others[16,17], have found that lack of air movement is one of the most common complaints in office environments, although the low air movement rates are permitted by the standard. Giving workers control over the temperature and ventilation in their local environment might be the only way to satisfy a larger percentage of people than is currently possible with traditional centralized control. If so, existing comfort standards will need to be reevaluated in terms of a broader definition of what are acceptable environmental conditions.

The authors are involved in a multiyear study to examine the performance of LTD systems, both in terms of the physical environments they produce and their effect on worker satisfaction. This paper describes some of the physical tests being made in our laboratory (the Controlled Environment Chamber) on two commercially available LTD systems.

2. DESCRIPTION OF SYSTEMS

2.1 Floor system

The floor system consists of self-powered supply modules that are components of a raised access floor system. Each module, measuring 0.6 m x 0.6 m, can be located at any position by exchanging it with a solid floor panel of equal size. Figure 1 shows a cutaway diagram of the floor supply module. A fan/motor assembly draws air from the sub-floor plenum and supplies it to the room through four 127 mm diameter discharge grilles. The grilles are molded of fire-resistant polycarbonate, and will support foot traffic and furniture. The individual vanes in the grilles are inclined 40° from vertical. A rotary speed control knob is recessed into one grille and each grille can be rotated through 360°, allowing office workers to control both the direction and quantity of air supplied from the module.

When the fan is switched on, the floor supply module can deliver between 40 and 90 L/s from a zero or very low pressure plenum. Over this same range of airflows the maximum outlet velocity measured at the grille varied between 2 and 6 m/s. The manufacturer's recommended operating procedures call for the four grilles to be turned inward toward the center of the module. At maximum air delivery, the four individual air jets converge at a height of 200-250 mm and produce a strong vertical turbulent jet and rapid vertical mixing with the room air. Under typical operation the Archimedes number (Ar) ranges between about 0.001 and 0.004, indicating that the force of inertia from the jet dominates the buoyancy forces in the room. (Ar is defined here as $Ar = g \cdot d_0 \cdot \Delta T_0 / (v_0^2 \cdot T_r)$, where g is the acceleration due to gravity (m/s^2), d_0 is the outlet diameter (m), v_0 is the outlet velocity (m/s), ΔT_0 is the temperature difference at jet entry (K), and T_r is the room temperature (K)).

The largest number of installations of this system occur in South Africa, although there are now nearly a dozen in North America.

2.2 Desk-mounted system

The desk-mounted system uses a self-powered mixing box (559 mm x 381 mm x 241 mm) that is hung in the back or corner of the knee space of the desk, and connected by flexible duct to two supply nozzles on the top of the desk (Figure 2). The supply vents may be rotated 360° in the horizontal plane and contain outlet vanes that are adjustable ±30° in the vertical plane. The mixing box uses a small variable-speed fan to pull supply air from a zero or very low pressure plenum either under the floor (as indicated) or from flexible ducts in the office partitions supplied from the ceiling. A second fan pulls air from the knee space. The unit has a desktop control panel containing sliders controlling: the speed of the air emerging from the vents, its temperature (produced by adjusting the ratio of supply to recirculated air, providing a design range of 10°C), the temperature of a 200 W radiant heating panel located in the knee space, the dimming of the occupant's task light, and a white noise generator in the unit that issues a rushing sound through the supply vents. The control panel also contains an infrared occupancy sensor that shuts the unit off when the workstation has been unoccupied for a few minutes.

Each workstation unit is capable of providing approximately 20-70 L/s of air.

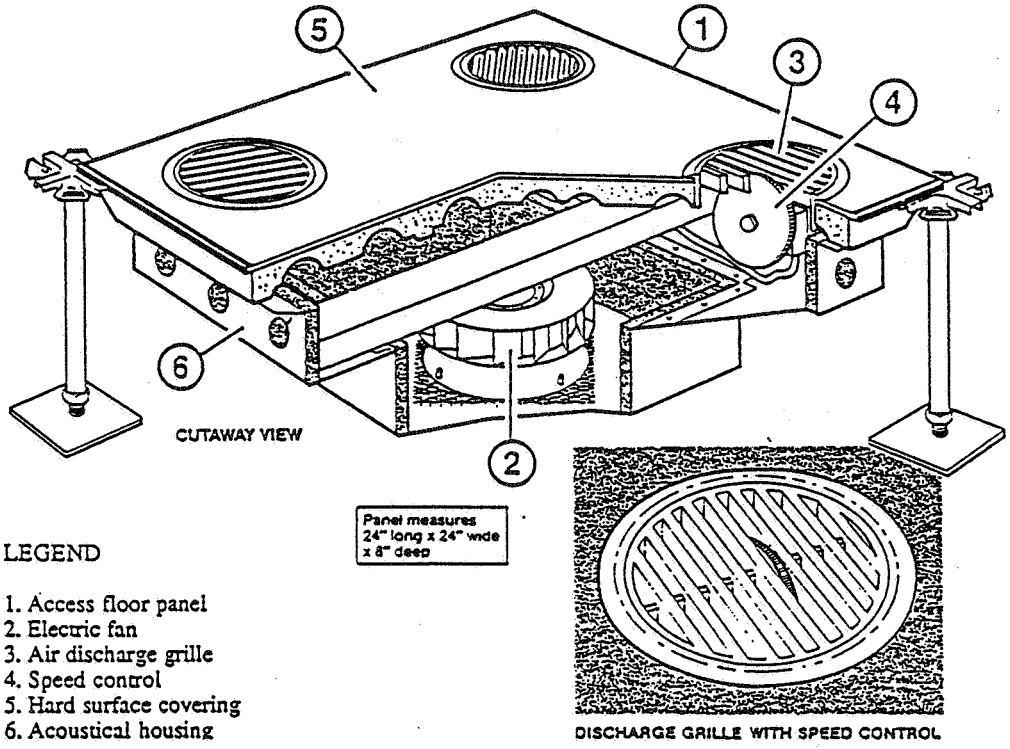

LEGEND

1. Access floor panel
2. Electric fan
3. Air discharge grille
4. Speed control
5. Hard surface covering
6. Acoustical housing

Figure 1. Floor Supply Module

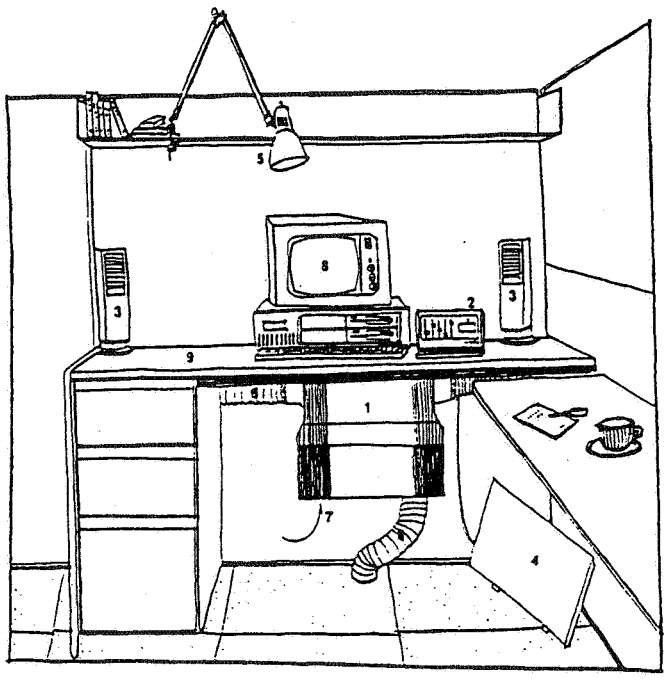

1 desk-level supply module
2 desk-level control panel
3 desk-level supply nozzle
4 radiant heating panel
5 task light
6 flexible supply duct
7 recirculated room air
8 personal computer
9 desk

Figure 2. Desk-Mounted Supply System

Even when its internal fans are turned off, the system is designed to deliver 20 L/s to satisfy minimum ventilation requirements. The maximum outlet velocity measured at the face of the 58 x 100 mm supply vent varied between 2 and 7.5 m/s over the same range of airflows described above. In operation a design supply air temperature of 13°C is provided by a variable air volume HVAC system, with desk-level outlet temperatures in the range of 18°C. Under typical operating conditions, the Archimedes number for each outlet ranges between about 3.5-50 x 10^{-4}, where Ar is defined as above.

3. EXPERIMENTAL METHODS

3.1 Controlled environment chamber

The two LTD systems have been tested in a controlled environment chamber (CEC) measuring 5.5 m x 5.5 m x 2.5 m, and located in a university laboratory. The CEC is designed to resemble a modern office space while still allowing a high degree of control over the test chamber's thermal environment[18]. The floor is fully covered with carpet tiles, finished gypboard walls are heavily insulated and painted white, triple-pane windows in the two exterior walls provide a view to the outside, the suspended ceiling contains acoustical tile with adjustable slots, and six 0.6 m square recessed dimmable lighting fixtures are mounted in the ceiling. As shown in Figure 3A, a raised access floor system provides a 0.6 m high sub-floor plenum, and the suspended ceiling provides a 0.5 m ceiling plenum.

A reconfigurable air distribution system permits ducted or plenum air to be supplied to and returned from the test chamber at any combination of ceiling and floor locations. Figure 3B shows the air flow configurations used during the tests reported here. All tests of the floor system used a sub-floor plenum supply. During these tests, a floor supply module was located within each of three modular workstations, as indicated in Figure 3B. For comparision with the floor system, a limited number of office tests were performed using a conventional ducted ceiling supply and return system. In this case a single perforated ceiling diffuser was used for supply air. To investigate the desk-mounted system, a separate supply line was ducted through the sub-floor plenum to the mixing box under the desk. The ducted ceiling supply diffuser was also used during some tests to control the average room temperature at the desired setpoint, while the supply air conditions at the desk could be varied to control the local workstation environment. During all LTD tests air was returned at the ceiling level through a single ducted perforated return grille (Figure 3A).

The CEC air distribution system also allows a separately controlled supply of air to be provided through the plenum-wall construction of the two exterior chamber walls. Air flow through this annular space was used to control the interior window surface temperature at a level equal to the average room air temperature.

3.2 Instrumentation and equipment

Detailed air velocity and temperature measurements within the test room were accomplished by using a lightweight sensor rig fabricated out of aluminum tubing, that allowed a vertical array of sensors to be positioned at desired measurement heights and moved around the room to map out a grid of selected measurement lo-

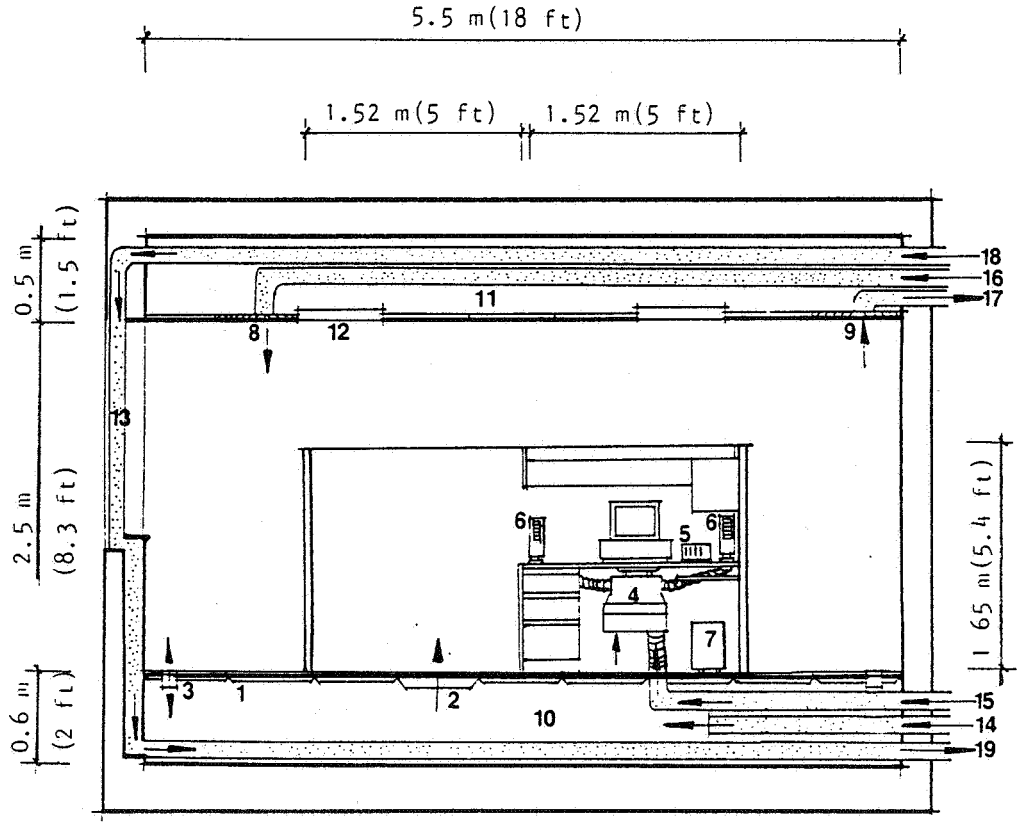

1 access floor system
2 floor supply module
3 floor register
4 desk-level supply module
5 desk-level control panel
6 desk-level supply nozzle
7 radiant heating panel
8 ceiling supply diffuser
9 ceiling return register
10 sub-floor plenum
11 ceiling plenum
12 ceiling luminaire
13 window plenum
14 floor-plenum supply
15 desk-level supply
16 ceiling supply
17 ceiling return
18 annular space supply
19 annular space return

Figure 3A. Section: Controlled Environment Chamber

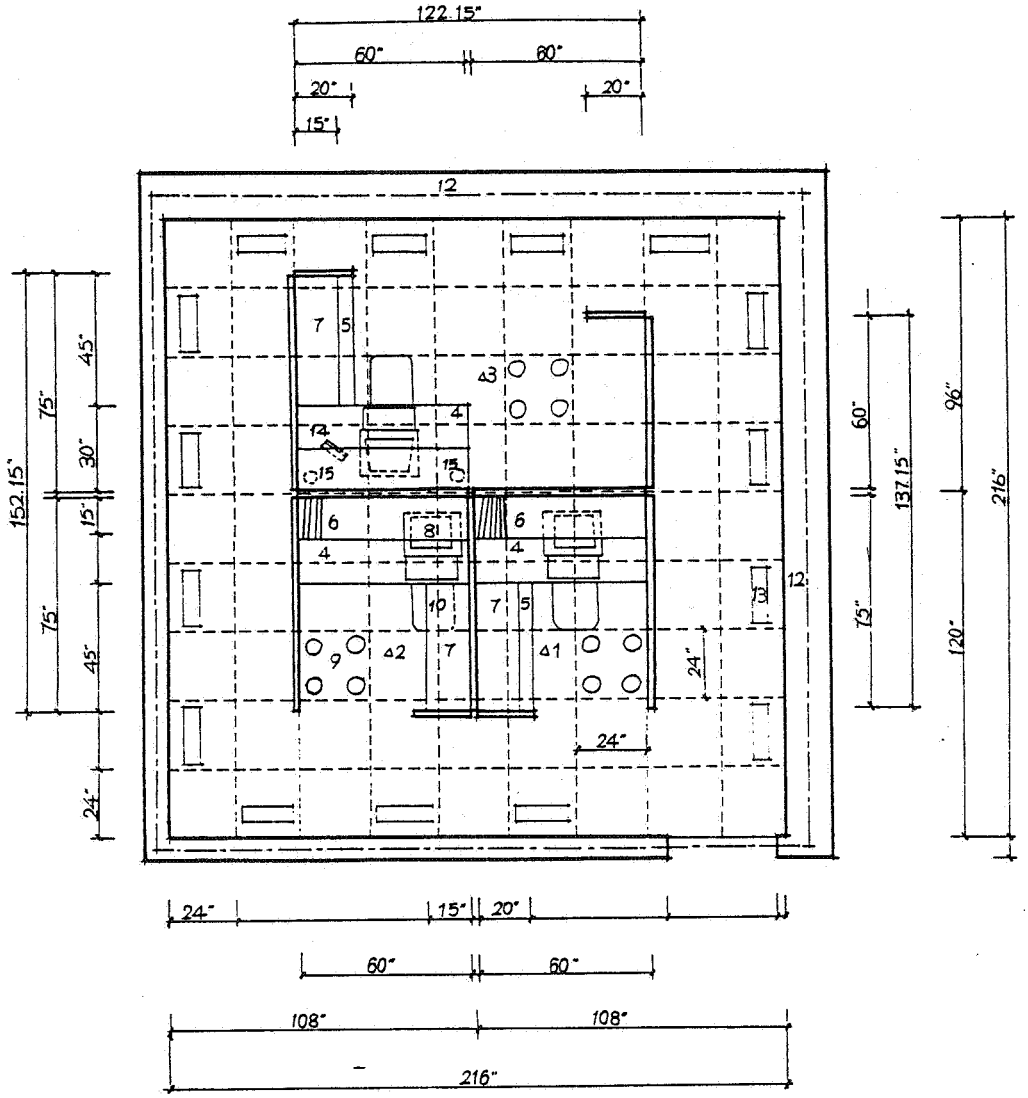

1--workstation #1
2--workstation #2
3--workstation #3
4--desk
5--sidetable
6--bookshelf
7--overhead storage
8--computer
9--floor supply module
10--chair
12--annular space
13--floor register
14--desk-level control panel
15--desk-level supply nozzle

Figure 3B. Chamber Plan 1:50

cations (Figure 4). By positioning the sensors within the space defined by the structural elements of the rig, protection was provided against damage from accidental encounters with office furniture and other obstacles. At each location in the room, air velocity and temperature were generally measured at six heights: 0.1 m, 0.6 m, 1.1 m, 1.7 m, 2.0 m, and 2.35 m. The 0.1 m, 0.6 m, and 1.1 m levels correspond to recommended measurement heights for seated subjects, and the 0.1 m, 1.1 m, and 1.7 m levels correspond to heights recommended for standing subjects, as specified by ASHRAE Standard 55-81. Velocities were measured with spherical-element omnidirectional anemometers having a range of 0-3.5 m/s, and temperatures were measured with shielded thermistor temperature probes. A portable computer-based data acquisition system was used to record the readings from the velocity and temperature sensors mounted on the aluminum sensor rig.

Supply and return air volumes were monitored by running the supply air through straight-lengths of small-diameter pipes with pitot tubes mounted to measure the fully-developed flow. The volume of supply air entering the test room through each floor supply module or ceiling diffuser was checked and balanced with a flowhood. The supply volume from the desk-level nozzles was checked with a precision portable thermal anemometer and revolving vane anemometer. Tests to measure the air velocity and turbulence intensity at a single point in the room were performed with an eliptical-element omnidirectional anemometer. This anemometer was used because of its relatively quick response time (0.2 sec for 90%) and associated signal conditioning and recording unit. Flow visualization of the room airflow patterns was performed with a helium-filled bubble generator.

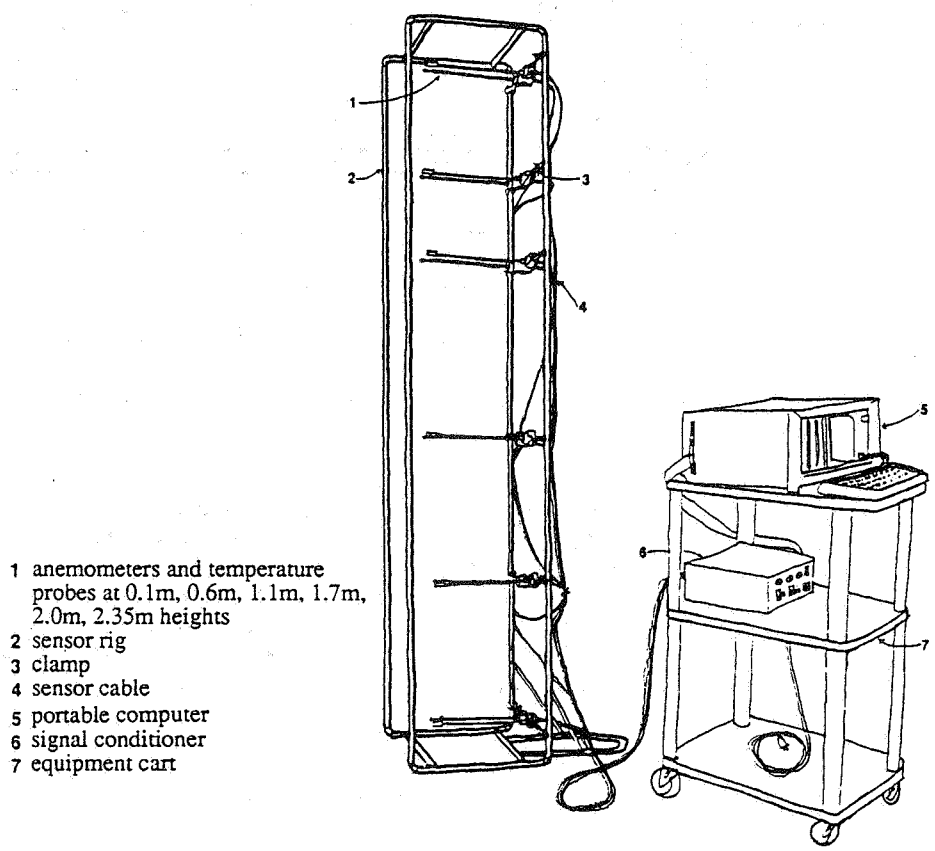

Figure 4. Sensor Rig and Data Acquisition System

Additional temperature measurements in the ducts and room were made with thermistor elements contained in duct immersion or wall-mounted units. These along with other test parameters were monitored and recorded through the direct digital control system for the CEC. Globe temperature was measured with a 38 mm diameter table tennis ball, as described by Benton et al.[19]. Room surface temperatures were checked by scanning with an infrared thermometer.

3.3 Test procedures

3.3.1 Office configuration with floor system

To study the performance of the floor supply module in an office environment, a modular workstation configuration shown in Figure 3B was installed in the test chamber. Solid partitions (1.65 m tall) were set up to produce two small 1.5 m x 1.9 m workstations and one double-sized 3.0 m x 1.9 m workstation. The arrangement of the furniture, including desks, side tables, and overhead storage bins, is also shown in the figure.

Heat loads were provided to simulate typical office load distributions and densities. A personal computer and monitor (≈90 W total) were placed on each of the three desktops. Each workstation had a 75 W task light above the desk. A second 75 W light bulb was located at the 1.1 m level near the edge of the desk to simulate the sensible heat load from a typical office worker. The six overhead lighting fixtures had a total power rating of 600 W. Energy balance tests indicated that only a small fraction of the overhead lighting load contributed to the room load. During the test, the experimenter and computer-based data acquisition system added approximately 150 W to the total load. Two different office heat load densities were studied during the experiments. The heat sources described above generated a load density of approximately 35 W/m^2. A higher load density of 55 W/m^2 was produced by placing a 200 W electric radiant heater on the floor under each desk to represent larger computer processing units.

All experiments were carried out under steady-state conditions chosen to represent an interior zone of an office building. To achieve these conditions the electrical heat sources in the room and the mechanical system were turned on in the morning and allowed to warm up the room until the expected average room temperature for the upcoming experiment was reached (24-28°C during these tests). Figure 5 presents a time plot of temperature control provided by the mechanical system during the warm-up and subsequent steady-state test period for a typical experiment at 130 L/s supply volume. During the warm-up period primary air was provided directly to the test room through flexible ducts pulled up through open floor panels. This avoided heating up the sub-floor plenum and allowed the desired test conditions to be reached much more quickly. After completing the warm-up, the supply ducts were returned to the plenum, the access floor was closed up, the supply air volume and temperature were adjusted to their selected setpoints, and conditions in the room were allowed to further stabilize. Figure 5 shows that as the room temperature balance point is reached the cycling of the chiller is evidenced by the fluctuating temperature of the primary air supplied to the sub-floor plenum. These fluctuations are largely damped out by the time the air passes through the floor supply module. Typical control of the supply air temperature entering the room was 18°C ±0.5°C. Also shown is the return temperature of the annular space airflow, demonstrating how it was controlled to a level close to the average room temperature. Room humidity levels were not controlled during the tests.

FIGURE 5. TEMPERATURE CONTROL

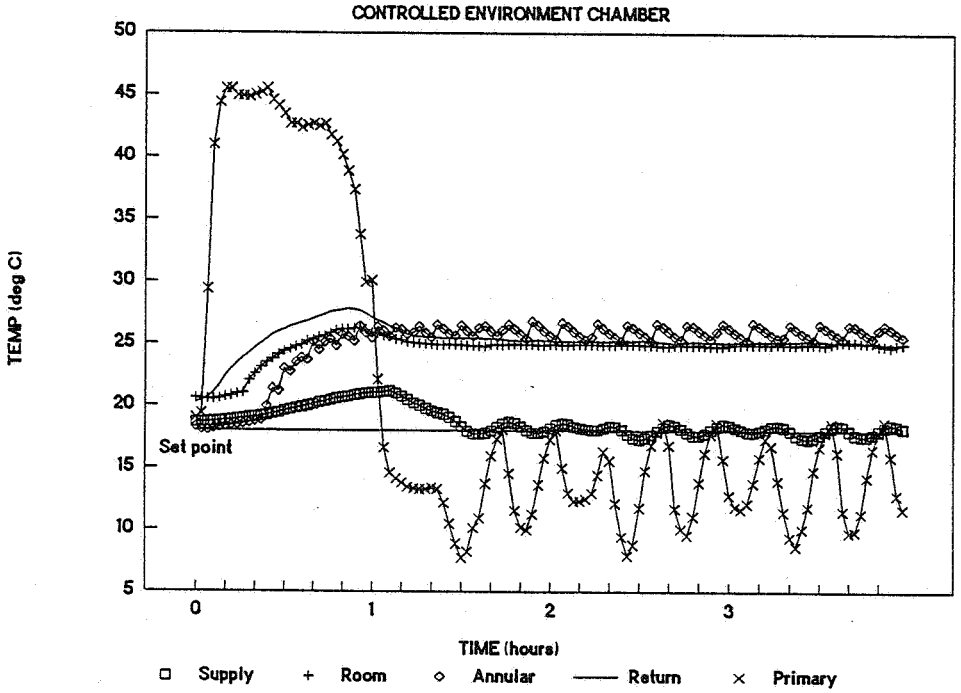

The supply air volume provided to the sub-floor plenum was balanced with the flow requirements of the floor supply modules, thus producing the desired low-pressure plenum. Pressure measurements across the access floor indicated pressure differentials between -0.25 and +0.25 Pa for the range of test conditions investigated. Transient load effects of heat storage in furniture, partitions, and room surfaces were also minimized by running the experiments under steady state conditions. Floor, wall, and ceiling surface temperatures were monitored with an infrared thermometer before and after each test period as a check of these storage effects.

The characteristics of the floor system tests can be seen in Table 1. Combinations of one, two, or three floor supply modules were investigated. The most common total supply air condition was 90 L/s at 18.0°C, supplied through one or split between two floor supply modules. The supply/return air temperature differentials ranged between 6 and 10°C, depending on load and flow conditions. As indicated the effects of grille position were studied for three orientations: (1) grilles turned inward, toward the center of the module; (2) all grilles turned toward the desk in the workstation; and (3) a combination of the above, usually with one or two grilles turned toward the desk and one or two turned inward or away.

Measurements using the sensor rig were made at two-foot intervals, with the vertical array of sensors centered over one of the access floor panels. Figure 6 shows the measurement locations used during most tests, which focussed on the thermal conditions within each of the three workstations. After positioning the sensor rig at the desired measurement location, all sensors were sampled over a one-minute measurement period. Preliminary tests had determined the length of this period as the minimum sampling time that still produced acceptable repeatability between consecutive measurements at the same position.

TABLE 1. FLOOR SYSTEM TEST CONDITIONS

	CHAMBER						WORKSTATIONS								
							#1			#2			#3		
Test Number	Supply Air Volume (L/s)	Heat Load (W/sq.m)	Return Air Volume (L/s)	Supply Air Temp. (deg C)	Room Temp (deg C)	Return Air Temp. (deg C)	Air Volume (L/s)	Temp. (deg C)	Grille Position	Air Volume (L/s)	Temp. (deg C)	Grille Position	Air Volume (L/s)	Temp. (deg C)	Grille Position
1A	92	55	66	17.9	25.7	26.4	0	-	-	0	-	-	92	17.9	Toward
1B	92	55	66	18.0	26.0	25.5	0	-	-	0	-	-	92	18.0	Inward
1C	91	55	66	18.0	26.2	25.9	0	-	-	0	-	-	91	18.0	Comb.
2A	91	55	66	18.1	27.5	27.7	41	18.2	Toward	0	-	-	45	17.9	Toward
2B	91	55	66	18.0	27.7	27.8	41	18.2	Comb.	0	-	-	45	17.9	Comb.
3	90	55	80	18.0	25.9	26.2	46	18.2	Comb.	44	17.7	Comb.	0	-	-
4	133	55	116	17.9	25.1	25.2	46	18.4	Comb.	44	17.8	Comb.	43	17.6	Toward
5A	64	55	49	18.1	27.3	27.6	0	-	-	0	-	-	64	18.0	Toward
5B	67	55	47	18.0	27.8	28.0	0	-	-	0	-	-	67	18.0	Inward
6A	89	35	66	18.0	23.9	23.5	0	-	-	0	-	-	89	18.0	Toward
6B	91	35	65	17.9	24.1	23.8	0	-	-	0	-	-	91	17.9	Inward
6C	91	35	68	18.0	24.6	24.4	0	-	-	0	-	-	91	18.0	Comb.
7	91	35	67	17.9	24.8	25.2	45	18.1	Toward	0	-	-	45	17.7	Toward
8	91	35	67	18.0	24.5	24.6	45	18.2	Comb.	45	17.7	Toward	0	-	-
9	90	35	67	18.0	24.9	24.4	90	18.0	Comb.	0	-	-	0	-	-
10A	65	35	48	18.1	25.1	25.2	0	-	-	0	-	-	65	18.1	Toward
10B	65	35	48	18.1	25.4	25.4	0	-	-	0	-	-	65	18.1	Inward
11A	65	35	48	18.0	25.9	25.8	65	17.9	Inward	0	-	-	0	-	-
11B	65	35	48	18.0	25.7	25.8	65	18.0	Comb.	0	-	-	0	-	-

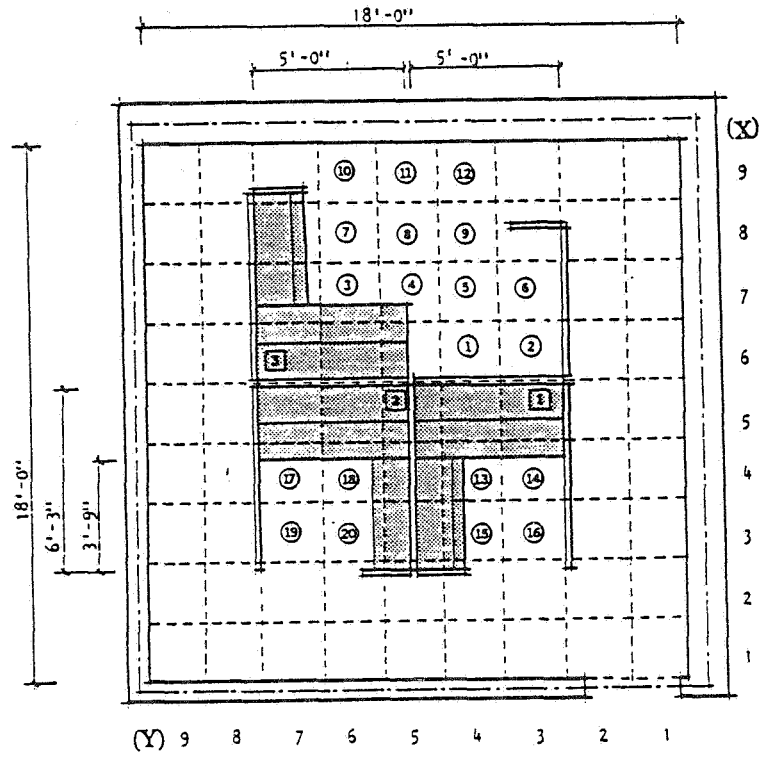

Figure 6. Test Position: Office Configuration

3.3.2 Office configuration with desk-mounted system

The desk-mounted system was installed in the larger Workstation #3, as indicated in Figures 2 and 3. During these tests, Workstations #1 and #2 had no local air supply. During some tests, supplemental space conditioning (beyond that provided by the desk-mounted system) was provided by a ceiling supply diffuser. For this purpose, the diffuser was positioned near one side of the room at (x=5, y=2), as defined by the nine by nine grid of 0.6 m by 0.6 m panels shown in Figure 6. The internal pattern deflectors of the diffuser were adjusted to produce a 3-way airflow pattern, away from the adjacent wall. The ceiling return register was located at (5,9) during all tests.

As with the floor system tests, experiments were performed under steady-state conditions. Testing of the desk-mounted system is still in progress, so only a limited number of preliminary results are presented here. Table 2 lists the conditions of the tests completed to date. All tests were made at the higher heat load density of 55 W/m^2, resulting in relatively high average room temperatures (26-28.5°C). Primary air supplied to the desk module was controlled at 13°C, resulting in desk-level supply air temperatures of 17-19°C. As indicated, different combinations of supply nozzle position and control panel settings for airflow and temperature were investigated. The nozzle positions studied included: (1) both nozzles turned toward the occupant with vanes level; (2) both nozzles turned toward the occupant with vanes up or down; (3) both nozzles turned to the left or right, away from the occupant; and (4) a combination of the above with one nozzle turned toward the occupant and one turned away. Velocity and temperature measurements with the sensor rig were made at the same locations shown in Figure 6.

TABLE 2. DESK-MOUNTED SYSTEM TEST CONDITIONS

Test Number	CHAMBER					
	Ceiling Sup. Air Volume (L/s)	Heat Load (W/sq.m)	Return Air Volume (L/s)	Ceiling Sup. Air Temp. (deg C)	Room Temp. (deg C)	Return Air Temp. (deg C)
1A	37	55	60	14.3	26.8	27.6
1B	37	55	59	14.2	26.9	27.8
2A	52	55	67	12.0	26.2	26.0
2B	52	55	68	11.9	26.3	26.3
3A	0	55	43	-	28.5	29.0
3B	0	55	39	-	28.0	28.4
4A	40	55	67	13.4	26.5	26.9
4B	37	55	58	13.8	26.8	27.5

Test Number	WORKSTATION #3					
	Supply Air Volume (L/s)	Supply Air Temp. (deg C)	Temp. Setting	Air Flow Setting	Nozzle Position	
					Left	Right
1A	23	18.9	Min.	Min.	Toward, Level	Toward, Level
1B	24	18.5	Min.	Min.	Right, Level	Straight, Level
2A	66	17.3	Min.	Max.	Toward, Level	Toward, Level
2B	66	17.5	Min.	Max.	Right, Level	Straight, Level
3A	43	18.0	Min.	Max.	Toward, Down	Toward, Up
3B	48	17.8	Min.	Max.	Toward, Level	Toward, Level
4A	Variable	Variable	Variable	Variable	Variable	Variable
4B	Variable	Variable	Variable	Variable	Variable	Variable

3.3.3 Office configuration with overhead supply system

For comparison with the floor system, a limited number of tests were performed with a conventional overhead ducted supply and return system, positioned at the same ceiling locations as described in 3.3.2. For consistency, the supply air volume was controlled at 90 L/s, equal to the volume used during most of the floor supply tests. For this airflow rate, the throw of the diffuser was slightly below the minimum level recommended by the manufacturer to achieve acceptable room air diffusion. Supply air temperature was controlled at 13°C, a typical value for overhead supply systems. Tests were performed only for the higher heat load density (55 W/m^2).

3.3.4 Tests of controllability and comfort

To investigate the degree of control and range of comfort conditions that an office worker could produce in the local workstation, a series of short-term adjustments were made to the LTD systems installed in Workstation #3, and the resulting thermal conditions were monitored at the nearby desk. Each system was studied separately. The controllability tests studied changes in fan speed and grille position for the floor system, and changes in nozzle position and airflow and temperature settings for the desk-mounted system.

As with previously described test procedures, the room was allowed to warm up and stabilize until the room temperature balance point was reached. For the floor system test, a constant volume of 90 L/s primary air was supplied to the sub-floor plenum throughout the test and its temperature was controlled to maintain an 18.0°C supply air temperature, as averaged between the three floor supply modules. Initially the floor supply module in Workstation #3 was turned off; the 90 L/s supply air volume was split equally between Workstations #1 and #2, by adjusting the fan speed to its minimum flow setting in each of the two floor supply modules. Since floor modules #1 and #2 maintained their constant air volumes throughout the test, when floor module #3 was turned on, a flow imbalance existed between the primary air supply and the three floor modules. In this case, rectangular floor grilles, located around the perimeter of the chamber, were opened to allowed the air supply requirements of the floor modules to be made up with room air (see Figure 2A).

Throughout the desk-mounted system test, a fairly constant supply of air was provided through the ceiling diffuser to maintain the desired average room air temperature (≈27°C). The desk unit was initially turned off, although as previously described, some minimum air supply (≈20 L/s) was still provided under these conditions.

The sensor rig was placed directly in front of the desk at the normal working position (measurement location #3 in Figure 6). Globe temperature was also monitored at the 1.1 m height to allow the calculation of mean radiant temperature. Sensor readings were recorded at exactly two-minute intervals throughout the tests.

After recording the initial conditions, the system was turned on and the airflow and temperature controls, and grilles/nozzles were adjusted to their desired positions. These settings were maintained for 16 minutes, after which a second adjustment was made to the system. This procedure was repeated for a total of eight different control settings for the floor system (see Table 3), and nine settings for the desk-mounted system (see Table 4). The tests were performed at the higher office heat load density of 55 W/m^2.

Table 3. Floor System Controllability Test: Control Settings

No.	Airflow	Grille Position
1	OFF	---
2	maximum	toward
3	maximum	inward
4	minimum	inward
5	minimum	toward
6	50%	toward
7	50%	combination
8	OFF	---

Table 4. Desk-Mounted System Controllability Test: Control Settings

	Control Panel		Nozzle Position	
No.	Airflow	Temperature	Left	Right
1	OFF	---	away	away
2	maximum	minimum	toward, level	toward, level
3	maximum	maximum	toward, level	toward, level
4	maximum	maximum	toward, up	toward, up
5	maximum	minimum	toward, up	toward, up
6	maximum	minimum	left, level	left, level
7	50%	minimum	left, level	toward, level
8	minimum	minimum	toward, level	toward, level
9	OFF	---	away	away

4. RESULTS

4.1 Floor system

4.1.1 Heat load effects

Due to the large amount of experimental data, a limited number of tests have been selected from the lists shown in Tables 1 and 2 for presentation and discussion. A more complete data set is contained in Bauman et al.[20]. The emphasis of the data presented here is on the local thermal conditions within each workstation. Results of concurrent ventilation efficiency experiments performed on the floor system in the same test facility are described by Fisk et al.[21]. For brevity, average conditions at a given height in a workstation are defined below and in subsequent sections of the paper as the velocity or temperature calculated by averaging the measured values obtained from the four locations directly in front of the desk. Referring to Figure 6, average conditions in Workstation #1 (WS#1) are based on points 13, 14, 15, and 16, those in Workstation #2 (WS#2) are based on points 17, 18, 19, and 20, and those in Workstation #3 (WS#3) are based on points 3, 4, 7, and 8.

Figures 7A and 7B present the average velocity and temperature results for Tests 2A and 7. Test conditions are identical for both tests (minimum flow setting in both WS#1 and WS#3), except 2A has the higher heat load. The observations are as follows:

1. The effect of higher heat loads is clearly visible as all temperatures are increased by 2-3°C between tests. The relative shape of the vertical temperature profiles, however, are quite similar.
2. For these conditions, a temperature difference in the range of 1-2.5°C can be maintained at the 0.6 m level between adjacent workstations. As expected, the warmer temperature always occurs in WS#2, where the floor supply module is turned off.
3. Under minimum flow conditions, the supply air jets do not reach the 1.7 m level, as evidenced by the minimal velocities above this height. Instead, the cool supply air remains near the floor, producing conditions similar to displacement ventilation. The vertical temperature profiles indicate that the characteristic stationary front separating the cool lower zone and warm upper zone occurs between the 1.1 m and 1.7 m heights, in agreement with other experimental results[22].
4. The stratification produced in WS#1 and WS#3 exceeds the comfort limits for vertical temperature difference of 3°C between the 0.1 m and 1.7 m levels[12]. In fact, due to the angle of the supply jet, a larger temperature difference exists between the 0.6 m and 1.7 m levels.
5. Under similar supply air conditions, WS#1, the smaller workstation, is always cooler than WS#3. This suggests that floor supply modules should not be located in small workstations, such as WS#1, where the supply jet enters directly into a regularly occupied space. The larger WS#3 allows the module to be positioned further away at a location that is only occasionally occupied.
6. The higher average velocities in the occupied zone of WS#1 and WS#3, compared to WS#2, where no floor supply is provided, is clearly visible in Figure 7B.

FIGURE 7. FLOOR SYSTEM HEAT LOAD EFFECTS

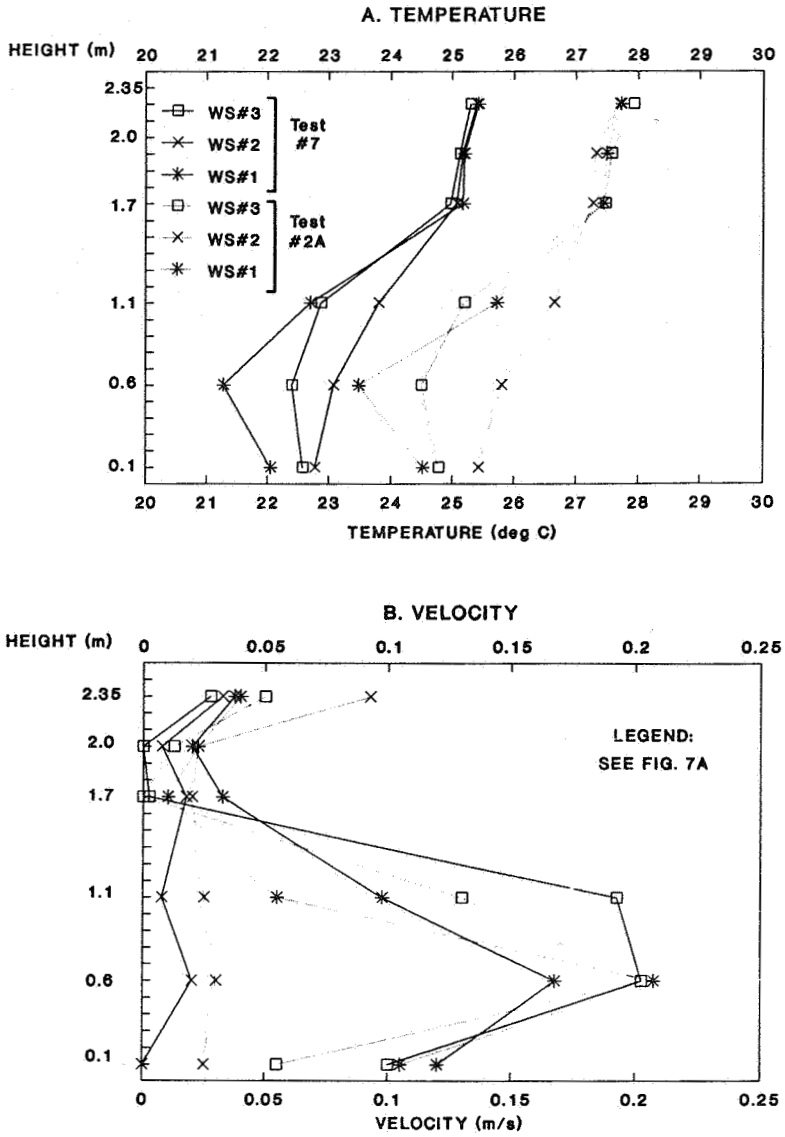

4.1.2 Local supply volume effects

Figures 8A and 8B present the average temperature and velocity results for Tests 8 and 9. In these tests, performed at the lower heat load level, the total supply volume to the chamber remains the same. The local supply characteristics vary, however, as WS#1 and WS#2 are set at minimum flow in Test 8, and in Test 9, the total air volume is supplied in WS#1, set at maximum flow. The observations are as follows:

1. As in Tests 2A and 7, the conditions of Test 8 resemble displacement ventilation performance. Due to the lower heat load level, the 3°C vertical temperature difference limit is not exceeded in any workstation.
2. In Test 9, when the air is supplied in a strong vertical jet, the degree of stratification is reduced at all locations in the room, despite the existence of flow obstacles (partitions and furniture) in the room. This effect is very visible in WS#3, which has no local supply air in either test.
3. Due to the reduced mixing of the low speed supply jets in Test 8, temperatures near the floor are actually cooler than those obtained in Test 9. This occurs in all three workstations.
4. Temperatures profiles above the partition height (1.65 m) are all quite similar, and exhibit only slight stratification, except those above WS#1 in Test 9. At these same levels, velocities are higher in Test 9 compared to the negligible values found in Test 8.

FIGURE 8. FLOOR SYSTEM LOCAL SUPPLY VOLUME EFFECTS

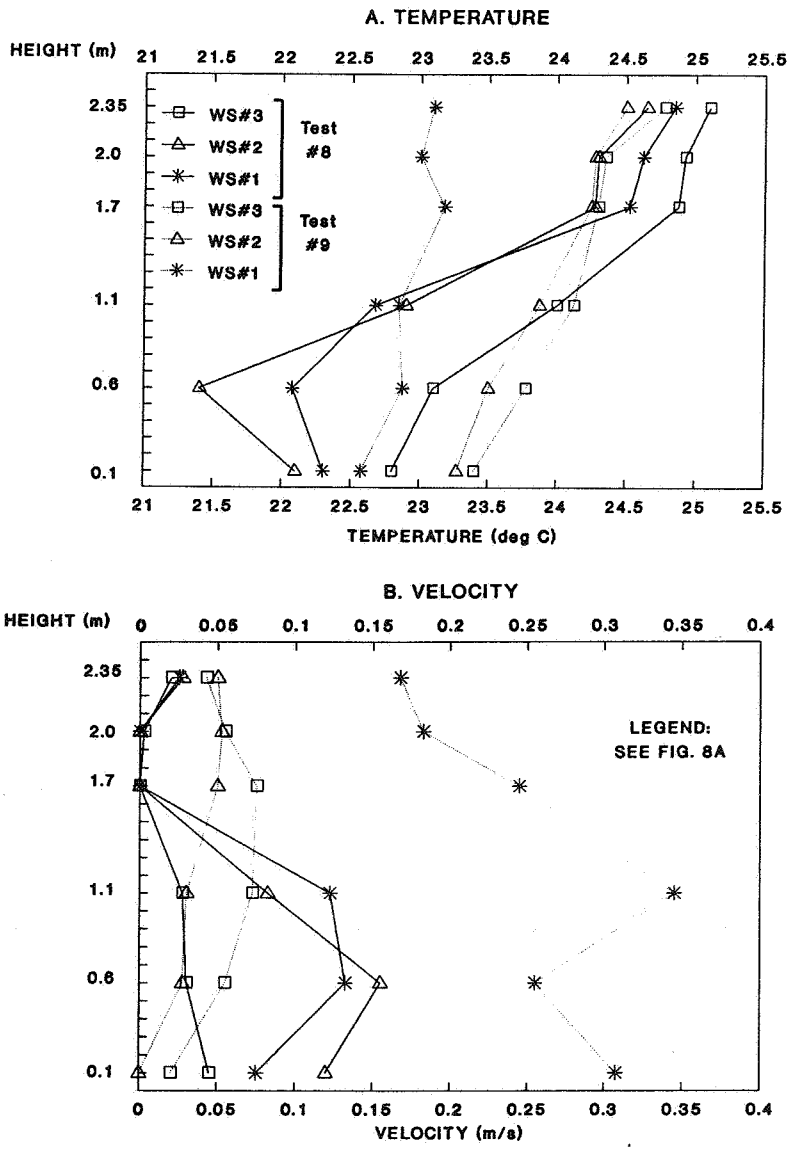

4.1.3 Controllability and comfort

Potentially the most significant performance characteristic of LTD systems are their controllability by individual office workers. A test was performed to determine the range of thermal conditions which could be achieved in a relatively short length of time (16 min) by simply adjusting the fan speed and grille positions of the floor supply module.

Figure 9 presents plots of temperature and velocity versus time for a series of adjustments made to the floor supply module. The circled numbers along the top of each plot refer to the flow control settings listed in Table 3. The observations are as follows:

1. Initially, with the supply turned off, the workstation experiences warm, stratified low-velocity conditions.
2. When the flow is set to 100% and the grilles are turned toward the desk, the stratification disappears and maximum velocities reach 0.6 m/s.
3. When the grilles are turned inward, only small stratification persists and the globe and air temperatures at the 1.1 m level rise because they are no longer in line with the supply jet. Velocities in the occupied zone do not exceed about 0.25 m/s.
4. When the flow is reduced to its minimum level, stratification reappears as the temperatures at the upper levels increase and those near the floor decrease. Velocities in the upper region approach zero.
5. When the grilles are turned towared the desk, the temperatures are reduced and velocities increased at the lower levels.
6. When the flow is increased to 50% of maximum, the conditions are quite similar to those achieved with maximum flow for the same grille position.
7. A combined grille position with two toward and two inward produces an improved temperature distribution with velocities no greater than 0.3 m/s.
8. Finally, conditions return to their initial levels when the floor supply module is turned off.

Three-minute turbulence intensity measurements at the 1.1 m height found a range of 35-45% for the conditions of the above test. All conditions produced a value of 45% except the maximum flow setting with grilles positioned toward the desk. These turbulence levels are in agreement with representative measurements reported by Hanzawa et al.[23]. However, if more restrictive velocity limits are applied in relation to increasing turbulence levels, as suggested by Fanger et al.[11], almost all flow fields in the vicinity of an operating floor supply module would experience some excessive velocities in the occupied zone.

The Fobelets and Gagge[24] two-node comfort model was used to predict the characteristic comfort indices for each of the flow control settings studied. Measurements recorded at the end of each 16-minute test period were used as input to the model along with assumed values of 50% relative humidity, 0.5 clo, and 1.2 met. The model was run for two sets of data for each test condition: (1) data recorded at the 1.1 m level, representing the head/neck region of a seated person, and recognized as the most sensitive area to draft discomfort; and (2) data averaged for the 0.1, 0.6, and 1.1 m levels, representing a whole-body average for a seated person.

The comfort model predictions for ET*, DISC, and PMV are listed in Table 5. The two control settings producing the most comfortable conditions are: (1) minimum flow setting (≈40 L/s) with grilles turned toward the desk, and (2) 50% flow setting (≈65 L/s) with grilles in a combined position. As previously discussed the

FIGURE 9. FLOOR SYSTEM CONTROLLABILITY

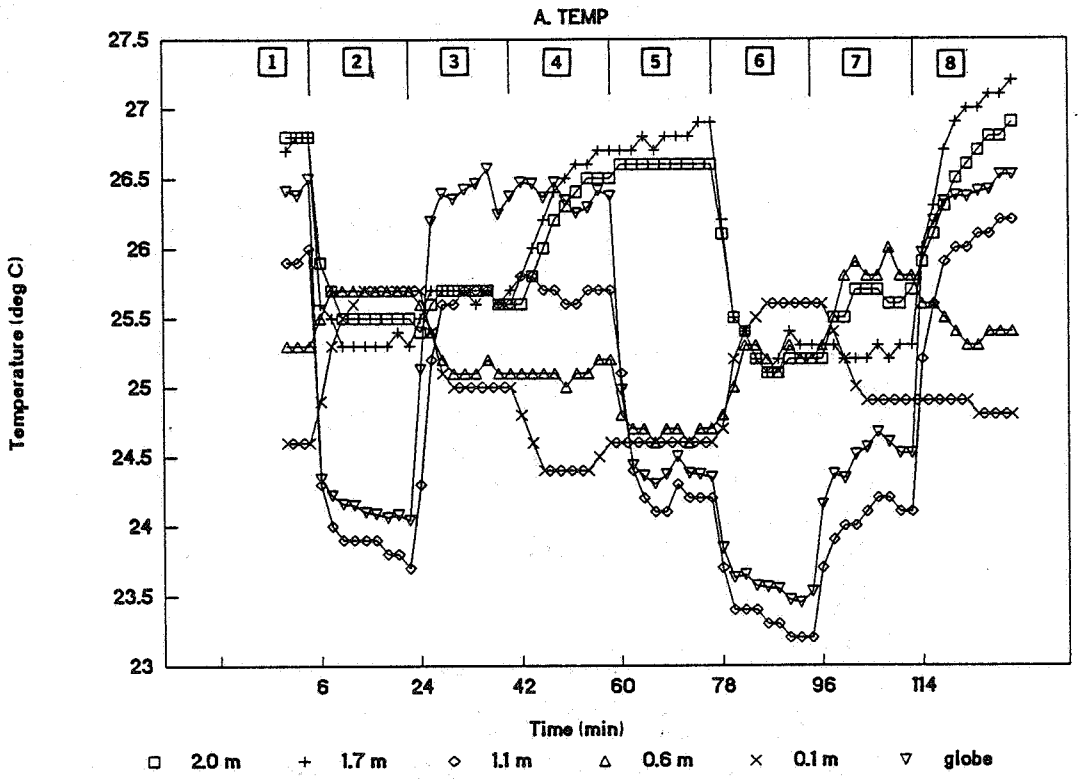

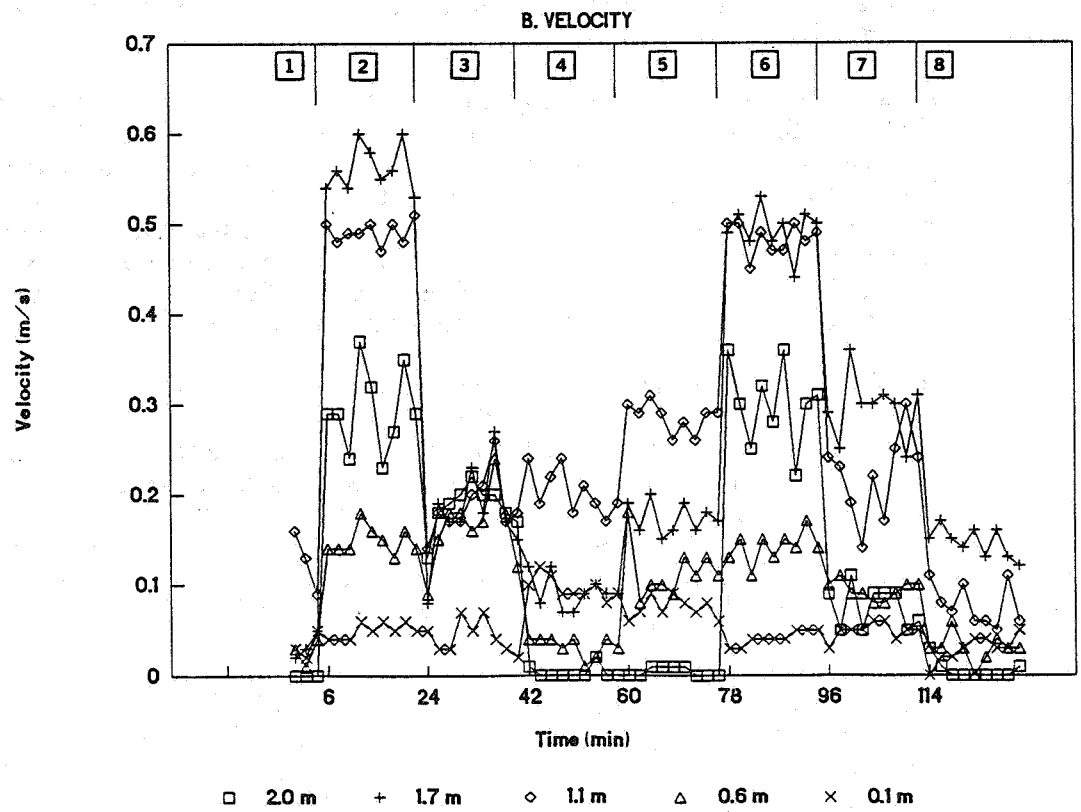

Table 5. **Floor System Controllability Test: Comfort Model Results** (RH = 50%, 0.5 clo, 1.2 met)

Control Setting No.†	Data Set	ET* (°C)	DISC	PMV
1	1.1 m	26.5	0.58	0.59
1	avg	26.4	0.53	0.57
2	1.1 m	24.2	-0.05	-0.28
2	avg	23.6	-0.01	-0.15
3	1.1 m	26.6	0.62	0.61
3	avg	26.5	0.57	0.59
4	1.1 m	26.6	0.63	0.60
4	avg	26.5	0.56	0.58
5	1.1 m	24.4	-0.01	-0.07
5	avg	24.3	0.05	0.05
6	1.1 m	23.7	-0.09	-0.32
6	avg	23.0	-0.03	-0.26
7	1.1 m	24.7	0.08	0.08
7	avg	24.4	0.08	0.08
8	1.1 m	26.5	0.55	0.58
8	avg	26.4	0.52	0.57

† see Table 3

3°C limit for vertical temperature difference is often exceeded under minimum flow conditions. In all probability the second, intermediate setting represents the most comfortable control setting tested.

4.2 Desk-mounted system

4.2.1 Local supply volume effects

Figures 10A and 10B present the average temperature and velocity results for Tests 3A and 3B (Table 2). During these tests air was supplied to the room only through the desk-mounted nozzles at a relatively high airflow rate. Conditions were very similar during both tests with the exception of the nozzle positions. In Test 3A, both nozzles were turned toward the normal working location in front of the desk (measurement point #3) with the left vanes turned down and right vanes turned up. In Test 3B, the vanes of both nozzles were adjusted to a level orientation while still pointing toward the work location. The observations are as follows:

1. The lowest temperatures and highest velocities are obtained in WS#3 with both nozzles level and pointed toward the head level (1.1 m) of the work location (Test 3B). For these test conditions, which were quite warm, a temperature difference in the range of 1-1.5°C could be maintained at all heights up to 1.1 m between WS#3 and both WS#1 and WS#2.
2. As expected, in Test 3B a maximum velocity occurs at the 1.1 m level. The velocity recorded at point #3 was greater than 2 m/s.
3. The horizontal injection of supply air during Test 3B maintains lower temperatures and increased air motion at and below the 1.1 m level over a larger floor area of WS#3.
4. During Test 3A with nozzle vanes turned up and down, temperatures in WS#3 are about 1°C warmer than they were in Test 3B, and velocities are only slightly higher than those found in WS#1 and WS#2.
5. Floor-to-ceiling stratification was no greater than 1.5°C in all workstations except WS #3 during Test 3B. For this ventilation system, air supply at the desk height did not produce the same evidence of displacement ventilation found in the floor system tests.

FIGURE 10. DESK SYSTEM LOCAL SUPPLY VOLUME EFFECTS

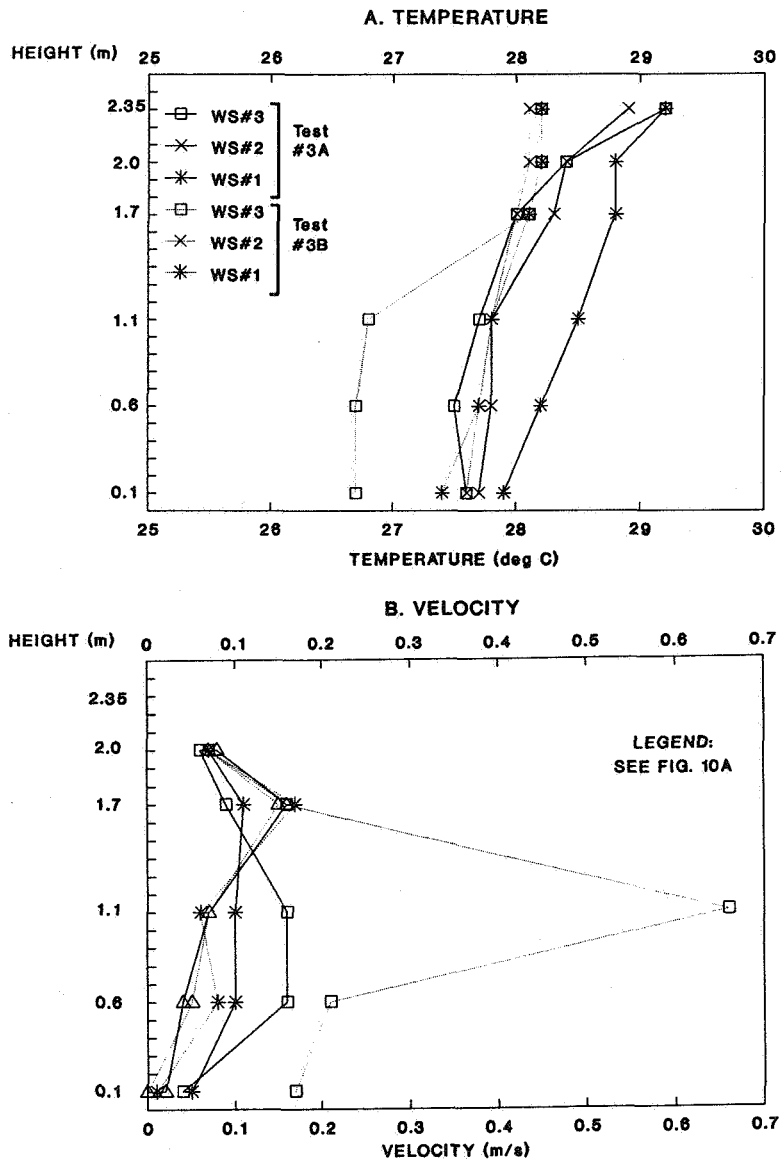

4.2.2 Controllability and comfort

Figure 11 presents plots of temperature and velocity versus time for the series of adjustments made to the desk-mounted system control panel and supply nozzle positions. The circled numbers along the top of each plot refer to the control settings listed in Table 4. Comfort model predictions for ET*, DISC, and PMV for the nine combinations of control settings are listed in Table 6. The model predictions were made using the same methodology described previously for the floor system. The observations are as follows:

1. From the initial warm, stratified and low-velocity conditions, velocities and temperatures below the 1.7 m level change dramatically when the airflow is set to maximum and the nozzles are turned toward the measurement location. At the 1.1 m level a velocity greater than 3 m/s is obtained at a temperature that is 1-2°C cooler than those found at all other heights (for purposes of showing greater detail in the velocity results, only velocities up to 1 m/s are displayed in Figure 11B). Not surprisingly, the greatest degree of cold discomfort is obtained from the comfort model predictions for these conditions.
2. When the control panel setting for temperature is changed from minimum to maximum, about a 1°C increase in air and globe temperature at the 1.1 m level is obtained.
3. When the vanes of both nozzles are turned upward, velocities approaching 2 m/s are found at the 1.7 m level, and greater than 0.5 m/s at the 2.0 m level. These same heights also experience the lowest temperatures as stratification is reversed. Lowering the temperature control setting to a minimum produces only a 0.5°C decrease at these same locations.
4. Turning the nozzles to the left in an attempt to provide a circular air motion within the partitioned workstation produces air velocities in the 0.1-0.2 m/s range within the occupied zone (0.1-1.7 m), but is unable to provide adequate cooling. The comfort model predicted the highest degree of warm discomfort for this control setting.
5. A 50% airflow setting with only one nozzle pointed toward the measurement location provides velocities around 0.5 m/s at the 1.1 m level and improves conditions considerably compared to the previous warm conditions.
6. At the minimum airflow setting with both nozzles level and toward the measurement location, air velocities up to 1 m/s are obtained at the 1.1 m level, and temperatures at the 0.1 and 1.1 m levels decrease significantly. Comfort model runs predict the most comfortable conditions for this test. This demonstrates the large effect of the airflow control when compared to the rather cool conditions that existed for control setting #2, having maximum airflow with both nozzles toward the work location.
7. The results indicate that office workers using the desk-mounted system are capable of controlling their comfort levels over a range of values for ET*, DISC, and PMV corresponding to the full range of the ASHRAE-specified summer comfort zone[12].

FIGURE 11. DESK SYSTEM CONTROLLABILITY

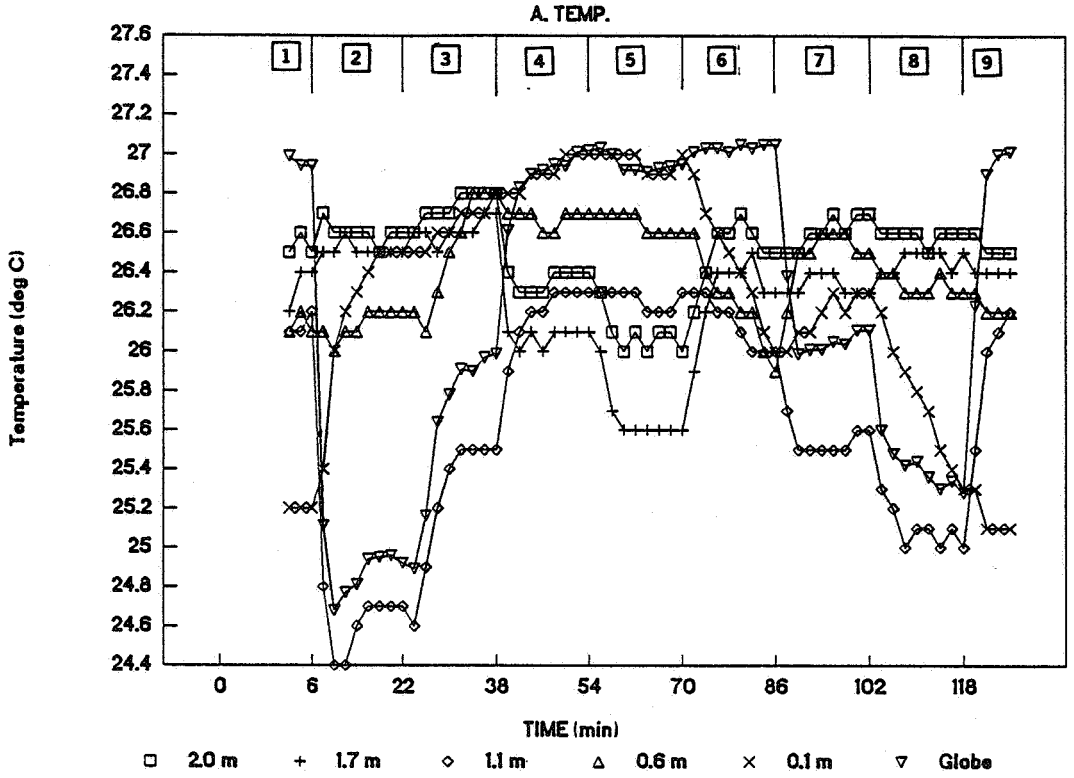

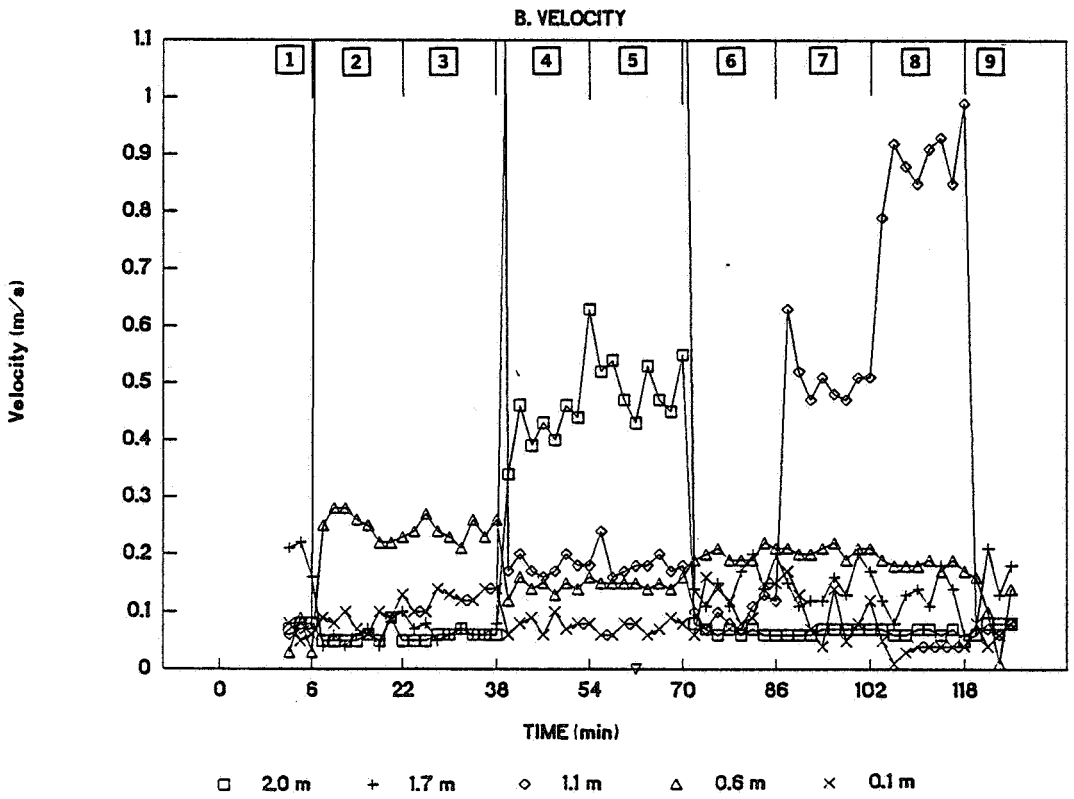

Table 6. Desk-Mounted System Controllability Test: Comfort Model Results (RH = 50%, 0.5 clo, 1.2 met)

Control Setting No.†	Data Set	ET* (°C)	DISC	PMV
1	1.1 m	27.0	0.67	0.70
1	avg	26.9	0.62	0.68
2	1.1 m	25.1	-0.27	-0.46
2	avg	24.3	-0.20	-0.42
3	1.1 m	26.4	-0.13	-0.33
3	avg	25.7	-0.07	-0.29
4	1.1 m	27.3	0.81	0.78
4	avg	27.1	0.75	0.73
5	1.1 m	27.2	0.78	0.76
5	avg	27.0	0.73	0.71
6	1.1 m	27.2	0.77	0.78
6	avg	27.3	0.81	0.80
7	1.1 m	26.4	0.18	0.21
7	avg	26.1	0.38	0.37
8	1.1 m	25.5	-0.04	-0.27
8	avg	25.1	0.00	-0.02
9	1.1 m	27.1	0.70	0.73
9	avg	27.1	0.73	0.75

† see Table 4

4.3 Overhead supply system

Available velocity and temperature data from the overhead supply test were limited to WS#1 and WS#2, plus four points outside of these two workstations. Data collected within the occupied zone (0.1 m - 1.7 m) at these same 12 measurement locations for Test 3 of the floor system were used to make the comparison. The ASHRAE-specified ADPI method[25] was used to evaluate and compare the air diffusion performance of the two systems.

The calculated ADPI for the overhead system was 90% compared to 52% for the floor system. This demonstrates that overhead systems can perform quite adequately in a partitioned office under the right conditions. The rather poor performance of the floor-based system is not surprising since the use of floor supply modules in small workstations is not optimal, as previously noted. ADPI may not be the most appropriate method to evaluate floor-based or desk-mounted system performance, since it does not allow velocities to exceed 0.35 m/s within the occupied zone. This is a very strict requirement for any ventilation system supplying air directly to the occupied zone, except low-velocity displacement systems.

5. CONCLUSIONS

Measurements have been made of the thermal performance of two occupant-controlled localized ventilation systems. The experiments were performed in a controlled environment chamber configured to resemble a modern office space with modular partitioned workstations. Tests were conducted to investigate the effects of supply volume, supply location, supply direction, supply/return temperature difference, heat load density, and workstation size and layout. The major conclusions are as follows:

1. The jet supply characteristics of the floor supply module produced high velocity air in the vicinity of the module. The risk of draft discomfort did exist in this region. However, under certain conditions, within short distances (less than 1 m) of the module, the velocities reduced to more acceptable levels.
2. Under minimum flow conditions from a floor module, significant stratification was produced, which, depending on heat load levels and total supply volume, exceeded the 3°C vertical temperature difference limit specified by ASHRAE Standard 55-81. This stratification in the surrounding office space was greatly reduced at maximum flow conditions. For all tests of the desk-mounted system, no excessive stratification was observed, presumably due to the higher supply location in the room.
3. Under minimum flow from a floor module, the overall ventilation performance of the room resembled that of displacement ventilation systems.
4. The primarily horizontal injection of air from the desk-mounted system distributed supply air to a larger area of the office, providing both cooler temperatures and increased air motion in the occupied zone.
5. Using existing ASHRAE test methods, an overhead supply system received a significantly higher performance rating compared to that of the floor system. However, the ADPI method may not be appropriate for evaluating such occupant-controlled systems.
6. Short-term tests indicated that the LTD systems could be controlled over a wide range, giving workers the opportunity to fine-tune the local environment to their individual preferences.
7. The perceived comfort benefits of having personal control over the local environment are not accounted for in existing comfort and performance standards.

Future work on occupant-controlled ventilation systems is needed to address the following issues.

1. Performance testing of other occupant-controlled ventilation systems.
2. Optimization of comfort control with human subject studies in laboratories.
3. Occupant comfort field surveys of operational systems.
4. Investigation of energy and productivity issues related to these systems.
5. Investigation of mechanical system control requirements for occupant-controlled systems.
6. Evaluation of compatibility of existing comfort and performance standards with occupant-controlled systems.

6. REFERENCES

1. David, J. 1984. "Under Floor Air Conditioning." *Journal of the Chartered Institution of Building Services*, August.

2. Sodec, F. 1984. "Air distribution systems." Krantz-Report, May, pp. 57-68.

3. Barker, C.T. 1985. "Ensuring Insurers Work in Comfort." *Chartered Mechanical Engineer*, November.

4. Barker, C.T.; Anthony, G.; Waters, R.; McGregor, A.; Harrold, M. 1987. "Lloyd's of London." *Air Conditioning: Impact on the Built Environment.* New York: Nichols Publishing Company.

5. Tuddenham, D. 1986. "A Floor-based Approach." *ASHRAE Journal*, July.

6. Rowlinson, D.; Croome, D. J. 1987. "Supply Characteristics of Floor Mounted Diffusers." Proceedings: *ROOMVENT-87, Air Distribution in Ventilated Spaces*, 10-12 June, Stockholm.

7. Hanzawa, H.; Nagasawa, Y.; Nitadori, M. 1989. "Thermal Comfort with Under Floor Air Conditioning System." *Proceedings of The Second World Congress on Heating, Ventilating, Refrigerating and Air Conditioning - CLIMA 2000.* August 1989, Sarajevo.

8. Spoormaker, H.J. 1990. "Low-Pressure Underfloor HVAC System." ASHRAE Transactions, Vol. 96, Part 2.

9. Sodec, F.; Craig, R. 1990. "The Underfloor Air Supply System -- The European Experience." ASHRAE Transactions, Vol. 96, Part 2.

10. Bauman, F.S.; Johnston, L.P.; Zhang, H.; Arens, E.A. 1991. "Performance Testing of a Floor-Based Occupant-Controlled Office Ventilation System." To be published in ASHRAE Transactions, Vol. 97, Part 1.

11. Fanger, P.O.; Melikov, A.K.; Hanzawa, H.; Ring, J. 1988. "Air Turbulence and Sensation of Draught." *Energy and Buildings*, 12.

12. ASHRAE. 1981. *ANSI/ASHRAE Standard 55-1981*, "Thermal Environmental Conditions for Human Occupancy." Atlanta, GA: American Society of Heating, Refrigerating, and Air-Conditioning Engineers.

13. ISO. 1984. *International Standard 7730*, "Moderate Thermal Environments - Determination of the PMV and PPD Indices and Specification of the Conditions for Thermal Comfort." Geneva: International Standards Organization.

14. Hedge, A.; Abi, M.; Parmelee, S. In press. *Reactions of Facilities Managers and Office Workers to Underfloor Task Air Ventilation.* Ithaca, NY: Cornell University.

15. Schiller, G.E.; Arens, E.A.; Bauman, F.S.; Benton, C.C. 1988. "A Field Study of Thermal Environments and Comfort in Office Buildings." *ASHRAE Transactions*, Vol. 94, Part 2.

16. Croome, D.J., Rollason, D. 1988. "Freshness, Ventilation and Temperature in Offices." *Proceedings of CIB Conference Healthy Buildings 88*, 5-8 September, Stockholm.

17. Harris, L., and Associates. 1989. *Office Environment Index 1989.* Grand Rapids, MI: Steelcase, Inc.

18. Bauman, F.S.; Arens, E.A. 1988. "The Development of a Controlled Environment Chamber for the Physical and Subjective Assessment of Human Comfort in Office Buildings." In: *A New Frontier: Environments for Innovation, Proceedings: International Symposium on Advanced Comfort Systems for the Work Environment*, Kroner, W., ed. Troy, NY: Center for Architectural Research, May 1988.

19. Benton, C.C.; Bauman, F.S.; Fountain, M.E. 1990. "A Field Measurement System for the Study of Thermal Comfort." *ASHRAE Transactions*, Vol. 96, Part 1.

20. Bauman, F.; Johnston, L.; Zhang, H.; Arens, E.; Schiller, G. In press. "Individualized Comfort Control in Office Buildings." Center for Environmental Design Research, University of California.

21. Fisk, W.J.; Faulkner, D.; Bauman, F.S.; Arens, E.A.; Pih, D.; McNeel, P.J. 1990. "Indoor Airflow and Pollutant Removal in a Room with Task Ventilation." To be presented at *11th AIVC Conference, Ventilation System Performance*, 18-21 September 1990, Belgirate, Italy. Lawrence Berkeley Laboratory and Center for Environmental Design Research, University of California.

22. Sandberg, M.; Blomqvist, C. 1989. "Displacement Ventilation Systems in Office Rooms." *ASHRAE Transactions*, Vol. 95, Part 2.

23. Hanzawa, H.; Melikov, A.K.; Fanger, P.O. 1987. "Air Flow Characteristics in the Occupied Zone of Ventilated Spaces." *ASHRAE Transactions*, Vol. 93, Part 1.

24. Fobelets, A.P.R.; Gagge, A.P. "Temperature ET*, As a Measure of the Enthalpy of the Human Indoor Environment," *ASHRAE Transactions* 94: 12-31, 1988.

25. ASHRAE. 1990. *ANSI/ASHRAE Standard 113-1990*, "Method of Testing for Room Air Diffusion." Atlanta, GA: American Society of Heating, Refrigerating, and Air-Conditioning Engineers.

7. ACKNOWLEDGMENTS

This project was supported in part by the Universitywide Energy Research Group, University of California, Berkeley. Generous furniture and partition donations from Steelcase, Inc., Grand Rapids, MI, have also contributed to the performance of this research. The authors would like to especially acknowledge the support and technical assistance of Gene Brager and John Zeren, formerly of Tate Access Floors, Jessup, MD; and Peter Brothers of Johnson Controls, Milwaukee, WI. Additional equipment donations were received from Environmental Technologies, Inc., Clearwater, FL, and Flexible Technologies, La Mirada, CA. Marc Fountain, a Ph.D. candidate in the Department of Architecture, University of California, Berkeley, performed the comfort model simulations.

Discussion
Paper 6

W. Raatschen (Dornier GmbH, Germany)

Aren't these systems with a fan in the subfloor or below the desk very noisy?

E Arens (LBL, USA)

No, they seem quite silent. We have not measured sound levels. It does appear to reduce air noise, but I have no experience with this.

VENTILATION SYSTEM PERFORMANCE

11th AIVC Conference, Belgirate, Italy
18-21 September, 1990

Paper 7

THE MAN-MACHINE-INTERFACE FOR THE AIR EXCHANGE MEASUREMENT SYSTEM MULTI-CAT

R. RABENSTEIN, F.D. HEIDT

Dept of Physics
University of Siegen
Adolf-Reichwein-Strabe
D-5900 Siegen
Federal Republic of Germany

ABSTRACT

The use of computers for data acquisition and analysis in air exchange measurements with tracer gases has become state of the art for the researcher.

However, for air exchange measurements in the field, reliable operation of the equipment and the proper reporting of the results are still points of concern. Here, the computer can assist the user in the correct handling of the tracer gas equipment, in dealing with unfavourable measurement conditions, and in the production of a readable report. These features are of special importance if the measurements have to be conducted by non-expert personnel.

This contribution describes the control and evaluation programs of the air exchange measurement system MULTI-CAT[1]. They provide a man-machine-interface, which achieves the mentioned goals by software driven guidance of the user through the whole measurement procedure. Its features include the input of building and measurement data, setup and performance of the measurement, data evaluation, report generation, error messages and help screens on demand.

1. INTRODUCTION

The use of computers for data acquisition and analysis in air exchange measurements with tracer gases has become state of the art for the researcher [1]. In many laboratories exist sophisticated computer controlled tracer gas systems for the measurement of the external infiltration rate of a building, the air change rate of single zones or the interzonal air flows in a multi cell building (see [8] and the literature cited there). A variety of different tracer gas methods is in use or under current development using one or more tracer gasses and various control and evaluation algorithms. Measurements are usually carried out under the supervision of the principal researcher and by staff, who was involved in the construction of the tracer gas system. The persons who conduct the measurements are often directly interested in the results, in order to include them into their own thesis, research report, etc. We can therefore expect reliable results from these often complicated measurement systems, since they are operated by persons who have expertise and motivation alike.

The situation is different for field measurements. Typically, the owner of a building needs some information on the air exchange. Sometimes, he may not even know exactly what he needs to know to answer his questions. He calls a consulting engineer in order to get the desired information at the lowest cost possible. The consulting engineer in turn asks a technician to perform quickly some tracer gas measurements. The technician responds to the best of his abilities and available equipment. The results are included in a report to the owner of the building, who has no other choice than to take these results for granted. A compilation of the problems usually encountered in field measurements is given in [4].

In some countries exist national standards for tracer gas measurements [5,6]. However it is not their intention to be detailed enough to protect the untrained operator from the pitfalls of his measurement device or the building under investigation. Due to this unpleasant situation, practioners in architecture and HVAC equipment often consider tracer gas measurements as an unreliable and uncorrect measurement method. This is a main obstacle to a wide application of air exchange measurements with tracer gas methods.

[1] MULTI-CAT: Multichannel Concentration Analysis of Tracers

A proven way to obtain reliable measurements is to support the operator of a tracer gas equipment with a computer controlled measurement and instrumentation system with integrated user guidance [4]. It is the experience of the authors, that also non-expert operators can conduct successful tracer gas measurements after a moderate training period (e.g. one day).

This contribution describes the control and evaluation programs for the air exchange measurement system MULTI-CAT. They provide a man-machine-interface, which assists the user in

- the preparation of the measurement,
- the correct handling of the tracer gas equipment,
- dealing with unfavourable measurement conditions,
- the evaluation of the collected concentrations profiles and
- the generation of a readable report

by software driven guidance through the whole measurement procedure.

2. GENERAL DESCRIPTION OF THE MULTI-CAT MEASURING SYSTEM

At the University of Siegen a mobile air exchange measuring system MULTI-CAT has been built and carefully examined [2]. It uses N_2O and SF_6 as tracer gasses for initial concentration decay as well as for constant emission measurement methods. This section describes its main components.

2.1 Equipment and Components

The experimental equipment consists of the following main subsystems:

- two gas analyzers (N_2O, SF_6)
- PC with keyboard, screen, printer and data acquisition interfaces
- tracer gas supply
- injection and sampling control unit
- operation mode control unit.

Additional necessary and important components of the system are electric power supplies, interface-adapters between PC and electronic devices, electronic control system, pumps and magnetic valves.

Key components of the measuring system are two IR gas analysers for N_2O and SF_6, which detect low concentrations (1 - 100 ppm) of both gasses with low cross-sensitivities to water

vapor. The PC is able to control all activities needed to perform measurements and data acquisition. Even tracer gas injection and air sampling can be operated and controlled by PC. Because preparation phase and performance of measurements require different flow schemes, an operation mode control is necessary which alters gas flows and tubings according to the required conditions.

The system addresses up to eight different zones or rooms. For common measurements with single zone theory, the eight channels for sampling and injection are interconnected with main headers. Additional sensors for temperatures, indoor-outdoor pressure differences, wind speed and wind direction are available for further analysis and interpretation of air exchange measurements.

2.2 Measuring- and Evaluation Programs

Various programs enable the user to carry out measurements, evaluate and report their results and display them graphically. A detailed description is given in [3].

- The control program MEASURE is the interface between the operator and the hardware of the measurement system. It controls the measurement procedure, records measured data and performs preliminary data analysis with graphic visualization of data and results.

- The evaluation program EVALUATE is intended and suited to perform a detailed analysis of already measured data at any time after measurements. By this way, erroneous measurement data can be omitted or the evaluation procedure can be restricted to a certain time interval without invalid measuring points.

- The program REPORT compiles the input data and the results into a readable report and formats the measurement values (concentration, temperature, pressure difference, wind data) for the output to spread-sheet, statistical and graphic presentation programs.

- The program PLOT uses a commercially available graphic package (NAG PC Graphics Library) to display the recorded time series graphically on various output devices.

Especially the first two programs are characterized by a strong user support via screen driven guidance either directly or by help screens on demand. This guidance is available for all parts of the measurement and evaluation procedure, including control of tracer gas equipment, data acquisition, data analysis and report generation.

MULTI-CAT allows to produce standardized and comparable air exchange measurements under varying conditions. It has been used since the end of 1988 for air exchange measurements in houses with natural ventilation as well as with uncontrolled and demand controlled mechanical ventilation systems [7].

3. MULTI-CAT USER INTERFACE

Although MULTI-CAT has been designed to serve mainly for research purposes, it was our intention to provide a user interface which allows also the operation by non-expert users. Some general concepts for PC-controlled air exchange measurements are outlined in [4]. In this section, we will describe the MULTI-CAT man machine-interface following these guidelines.

The general rule is to restrict the required operator action to a minimum, leaving the rest to a thoroughly tested control program. Thus, a high degree of standardization is automatically achieved, since all measurements follow the same control flow as dictated from the software. It is, of course, not possible to exclude any possible error just by a smart control program. But the restriction of the operator to his actual duties prevents the detrimental effect of unnecessary actions. It also minimizes the required time for the user training.

3.1 Control Program MEASURE

3.1.1 Structure

The control program possesses a linear structure, leading the operator from the beginning to the end of the measurement in a logical step by step procedure. On the software side, the control program is coupled with a data base which provides as much a priori available information as possible and with a set of numerical routines including data evaluation, control algorithms and error analysis. On the hardware side, the control program interfaces to a injection and sampling unit for the control of the air and tracer gas flows and to sensors for tracer gas concentration and environmental data. These relations of the control program to the components of the tracer gas system are shown in Figure 1. Optional help screens are available at each program step. They are self explainatory, so that no manual is required during the measurement.

3.1.2 Data Base

The data base contains four sets of data:

1. data describing the tracer gas system,
2. data describing the building under investigation,
3. data describing the measurement setup on site,
4. results of the measurement and evaluation.

Data, which describe the tracer gas system are the number of available data channels, measurement ranges of the gas analyzer, flow meters, and other sensors, maximum tracer gas injection rates, etc. These informations are write-protected from the operator.

Data, which describe the building under investigation are room designations and volumes according to the building plan, etc. An input menue prompts the user for all necessary inputs. This insures that all required information for the operator is available. This information can be input prior to the measurement and stored in a parameter file. On site, the data of the building under investigation are read from the corresponding parameter file. Figure 3 shows the screen after the input of eight rooms with the designations G-4xx and their respective volumes. Each room is assigned to one of the eight channels of the injection and sampling system.

Data, which describe the measurement setup are the numbering of the sampling and injection channels, date, start time and duration of the measurement, etc. Date and time information are read from the internal clock of the PC, so that the operator is prompted only for a minimal amount of information.

Results of the measurement and evaluation are concentration values, air exchange rates, error bounds, etc. They are stored in the data base by the control program with no user action required.

The advantages of this structured data base are

- all relevant information is available for the measurement itself as well as for the measurement report,
- it is possible at all stages of the input to check the data for the feasability of the experiment.

The last point is extremly important. According to the tracer gas balance there is a close relationship between the room volume, the tracer gas injection rate and the concentration level. A meaningful measurement is only possible if the possible injection rates, the analyzer range and the room volume match. A simple data check after the input of data set 2 (building data) with data set 1 (tracer gas system data) reveals whether the injection rates are sufficient to yield a reasonable concentration in the rooms to investigate. It is thus possible to detect mismatches before the operator goes to the site. It is one of the tasks of the control program to perform such checks.

3.1.3 Injection and Sampling

Gas handling for injection and sampling is especially critical for measurement performance and, at the same time, it usually requires special skillness of the operator.

For the tracer decay method, certain quantities of tracer gas have to be released into different rooms at the beginning of the measurement. The actual values depend on the corresponding volumes and the desired concentration. The control program calculates the required masses of tracer gas for each room or zone if volumes and projected concentrations are given.

Figure 2 illustrates the injection system which is able to supply tracer gas by PC-control. It consists of a supply container, hand valve, pressure vessel with pressure gage and magnetic valves at the interface to various rooms.

For a given volume of the pressure vessel corresponds the amount of tracer gas to the gas pressure. Thus the pressure gage at the vessel indicates the amount of gas which is contained in the vessel. It is the task of the operator to fill the pressure vessel to the pressure calculated

by the control program and to hit a key when the required pressure is reached. Then the control program opens the corresponding magnetic valve to the room and the specified mass of tracer gas is released. This procedure is repeated for all rooms.

A similar structure and procedure has been developed for the sampling system, which draws samples from the different rooms under investigation with the aid of PC-controlled pumps and magnetic valves. The sampling system is fully automated with no user action required.

The advantage of this kind of PC-controlled injection and sampling is that only a minimal amount of operator action is necessary. He can read the required information (pressure) from the PC-screen and does not have to perform mind calculations or organization tasks. Thus, sources for errors are minimized, as the operator cannot confuse room number, tube number, injection and sampling tube, required amount of tracer gas and so on.

Figure 4 shows the PC-screen during the injection into room G-406 (channel 7). The operator is about to input the desired inital concentration. The control program proposes a default value of 100 ppm. Once this value is accepted (or overridden), the required pressure in the vessel will be calculated and shown on the screen (see channels 1-6). If the operator is not shure at this point about the necessary actions on his part, he can obtain support from the help screen shown in Figure 5. Similar help screens exist for all stages of the control program where user action is required.

3.1.4 Data Acquisition

Measuring air exchange means measurement of tracer gas concentration in the course of time. After the injections have been accomplished, the important problems for any operator are:

- When to start with data acquisition of concentration measurements?
- How long data acquisition should continue?

The decision for starting concentration measurements with data acquisition is up to the operator and should be guided by two aspects: One is to meet the measuring range of tracer gas analyzer at its upper part, the second is to achieve uniform mixing in the room under investigation. The control program pauses at this point. The operator watches the analog concentration display at the gas analyzer and starts the data acquisition from keyboard, when the concentration shows a steady decay.

During the data acquisition, the operator can switch arbitrarily between two different screen outputs. A graphic screen shows the development of the concentration profile in real time. A numeric screen gives the current measurement values for concentration, temperature (9 channels), pressure difference (8 channels) and wind speed and direction.

The duration of data acquisition can be influenced by different ways and depends on measurement conditions:

- a priori input by the user/operator (This may be appropriate if a certain measuring plan has to be followed.),
- user/operator decision on site (May be caused by unforeseen events during measurements, requires graphic visualization of the measured values.),
- automatic (PC-controlled) termination of measurements, when concentration has dropped below a certain level.

3.1.5 Evaluation

After the data acquisition has been completed, a preliminary data evaluation is performed in order to inform the operator immediately about the outcomings of his measurement. The control program compiles on a single screen information on the performed parameter estimation, on the resulting air exchange rate including error bounds and on the average values of the measured environmental parameters. For constant injection measurements, the effective room volume is also calculated.

The screen output of a concentration decay measurement is shown in figure 6. The deviation of the measured concentration data from the fitted curve was so small (0.9 ppm) that the parameters of the fitted curve and the air change rate were calulated with very high precision (±1%). The temperatures varied from 4.7 °C (outside) to 20.2 °C (inside). Pressure differences were rather low with one pressure transducer (nr. 8) not connected.

3.2 Evaluation Program EVALUATE

The Control Program MEASURE performs a first stage of data evaluation. It is important to show any errors which may have been happened during the measurements. It gives an indication whether the measurement should be repeated or even omitted.

The second stage of evaluation possibilities is performed by the evaluation programm EVALUATE. It aims at investigations which have to performed any time after the data acquisition. It has access to the existing data bases from previous mesurements. EVALUATE uses the same numerical procedures as the evaluation part of the control program MEASURE. Furthermore it allows to screen the concentration profiles for any events that could make the measurement unreliable, e.g poor mixing or accidental opening of doors and windows. Faulty sections can be excluded from the data analysis. The results of the evaluation program are added to the data base.

3.3 Programs REPORT and PLOT

Generation of a report must be a part of the whole measurement procedure. REPORT uses a standardized reporting format presenting a summary of the measured data. This summary should be given not only as a collection of numbers but as a readable text. Furthermore interfaces the reporting program to a word processor for special editing and report generation purposes. REPORT has access to all data stored in the data base. Data not suitable for being printed in a report (e.g. concentration samples) are stored in separate data files for further processing, like graphical representation with the program PLOT. It is able to display time series data (tracer concentration, environmental parameters) on various output devices.

Figure 7 shows the skeleton of an output of the program REPORT (same measurement as figure 6). It can be used in any word processor to produce a complete report on the measurement. The graphical result of some features of the program EVALUTE are shown in figure 8. Here, a window was opened in the course of a concentration decay measurement. A separate evaluation of the concentration curve before and after the opening reveals the different air change rates.

4. CONCLUSIONS

The contents of this contribution can be summarized in four points:

- Measurements of air change rate are not that easy as methods may suggest, because boundary conditions and information transfer can be a problem.
- There exist general concepts for measurement procedures which avoid or at least reduce the encountered problems by using PC-assistance.
- A measuring system MULTI-CAT for air exchange measurements and belonging environmental data following most of these concepts has been operating since two years.
- Experiences in practice collected from measurements in real houses with trained student helpers and technicians are very positive. Sufficient expertise for performing measurements and evaluation is acquired by the operating personnel after a one day training period only.

Therefore, air exchange measuring systems with PC-controlled instrumentation, measurements and evaluation are strongly recommended. They allow to conduct measurements easier and could lead to more widespread application, thus creating and increasing data bases for air infiltration and exchange research. Moreover, better evaluation techniques including the calculation of error bounds and standardized methods for better comparison of results can be introduced.

5. ACKNOWLEDGEMENTS

This work is associated with a research and development project entitled "Weiterentwicklung und Erprobung von Methoden der Luftwechselmessung in Räumen und Gebäuden (further development and application of air exchange measuring methods for rooms and buildings)". The authors gratefully acknowledge the financial support provided by the BMFT (German Ministry for Research and Technology).

6. REFERENCES

[1] F.D. Heidt, H. Werner: Microcomputer Aided Measurement of Air Change Rates, Energy and Buildings, Vol. 9, 1986, pp. 313 - 320

[2] F.D. Heidt, R. Rabenstein: MULTI-CAT (multichannel concentration analysis of tracers) Dokumentation, Internal Report (in German), Dept. of Physics, University of Siegen, November 1988

[3] R. Rabenstein: Weiterentwicklung und Erprobung von Methoden der Luftwechselmessung in Räumen und Gebäuden (further development and application of air exchange measuring methods for rooms and buildings), Internal Report (in German), Dept. of Physics, University of Siegen, February 1990

[4] R. Rabenstein, F.D. Heidt: Standardized Air Exchange Measurements by Computer-Controlled Instrumentation, submitted to ASHRAE symposium "Field Studies on Ventilation Efficiency", New York, USA, Jan. 1991

[5] American Standard Test Method ASTM E 741, Determining Air Leakage by Tracer Dilution, Annual Book of ASTM Standards, Vol. 04.07

[6] Swedish Standard SS 02 15 56, Buildings - Determination of the total outdoor air flow (in swedish), identical to INSTA 131

[7] H. Werner, W. Fies: Fortschrittliche Systeme für die Wohnungslüftung, Teil B: Lüftungstechnische und energetische Untersuchungen in einem Testgebäude in Einfamilienhausgröße (advanced ventilation systems, part B: ventilation and energetic investigations in a single family house sized test building), report EB-21/1989 (in german), Fraunhofer-Institut für Bauphysik, Holzkirchen, FRG

[8] F.D. Heidt, R. Rabenstein, G. Schepers: Comparison of Tracer Gas Methods for Measuring Air Flows in Two Zone Buildings, these proceedings

FIGURE CAPTIONS

Fig. 1: Control Program for Air Exchange Measurements and its Interfaces.

Fig. 2: Scheme of PC-controlled Injection System.

Fig. 3: PC-screen: interactive input of building data

Fig. 4: PC-screen: interactive tracer gas injection

Fig. 5: PC-screen: help screen for tracer gas injection

Fig. 6: PC-screen: results of data evaluation

Fig. 7: Reporting format

Fig. 8: Example of advanced data evaluation and graphical representation

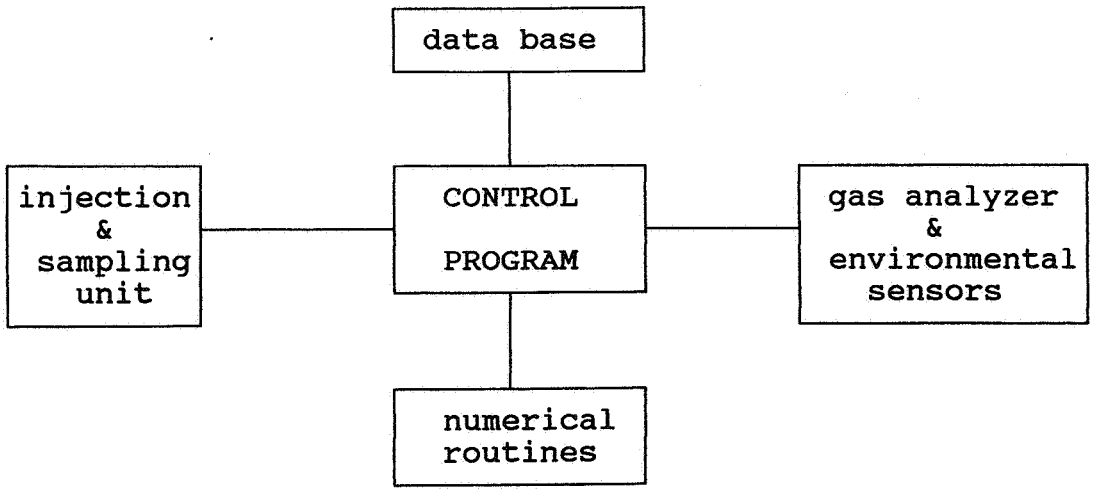

Figure 1: MULTI-CAT Control Program and its Interfaces

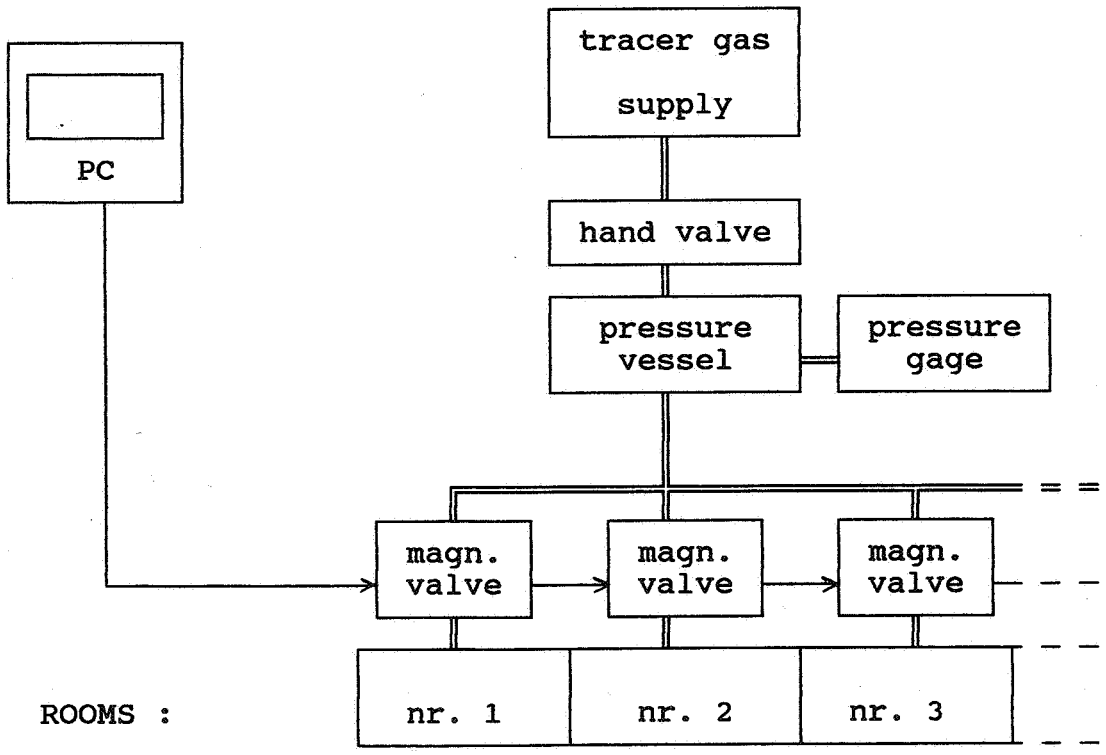

Figure 2: PC-Controlled Injection System

M U L T I - C A T (C) Prof. Heidt 1988

Specification of the rooms to be measured:

name of room	number	volume (cubic meters)
G-409	1	101.00
G-411	2	83.00
G-401	3	64.00
G-402	4	65.00
G-403	5	51.00
G-404	6	88.00
G-406	7	47.00
G-407	8	105.00

Type F1 for help, Bild to proceed

Figure 3: PC-screen: interactive input of building data

M U L T I - C A T (C) Prof. Heidt 1988

Initial tracer gas injection into the specified rooms:

name of room	number	init. concentration	required pressure
G-409	1	100	3.4
G-411	2	100	2.8
G-401	3	100	2.1
G-402	4	100	2.2
G-403	5	100	1.7
G-404	6	100	2.9
G-406	7	100	

Type F1 for help, Bild to proceed

Figure 4: PC-screen: interactive tracer gas injection

M U L T I - C A T (C) Prof. Heidt 1988

Initial Tracer Gas Injection:

Follow these steps for each room:

1. Type in the desired initial concentration (in ppm).
2. Type Bild
3. The program shows you the required pressure (in bar) for the vessel and opens the valve into the current room.
4. Close the hand valve at the pressure vessel.
5. Fill the vessel with tracer gas up to the required pressure.
6. Close the valve at the tracer gas container.
7. Open the valve at the vessel to release the tracer gas into the room.
8. Wait a few seconds.
9. Close hand valve at the vessel and type Bild to proceed.

Type F1 to return

Figure 5: PC-screen: help screen for tracer gas injection

M U L T I - C A T (C) Prof. Heidt 1988

CALCULATION OF THE RESULTS:

curve fitting for concentration data
c(t) = A * exp (B*t) + C

A = 47.5 ± 0.0 ppm
B = -1.0 ± 0.0 1/h
C = 0.0 ppm
std. deviation of data = 0.9 ppm

air change rate:

dyn.: n = 1.0 ± 0.0 1/h (± 1%)

sensor nr.	0	1	2	3	4	5	6	7	8
temperature (°C)	4.7	20.2	19.7	18.0	19.1	19.0	18.9	18.3	17.9
pressure diff. (Pa)		-0.6	0.5	0.6	1.2	0.8	-0.4	1.1	-50.0

wind data: (average values) speed = 1.0 m/s direction = 34°

Type Bild↓ to proceed

Figure 6: PC-screen: results of data evaluation

```
-----------------------------------------------------------------------
                          M U L T I - C A T
-----------------------------------------------------------------------
date : 1-9-1990            begin 11:8:17 h                file: 090190il
-----------------------------------------------------------------------
user input:

measurement procedure:

method                : initial injection
duration              : 1200 s
sample spacing        : 1 s
minimal concentration : 2 ppm

 room nr.          room name            volume/m**3

     1               G-409                101.00
     2               G-411                 83.00
     3               G-401                 64.00
     4               G-402                 65.00
     5               G-403                 51.00
     6               G-404                 88.00
     7               G-406                 47.00
     8               G-407                105.00

total number :   8          total volume : 604.00 m**3
-----------------------------------------------------------------------
description of measurement :

date : 1-9-1990          begin  11:8:17 h        actual duration : 1200 s

                       number of values       min.            max.

concentration [ppm]         1201             34.40           48.60
-----------------------------------------------------------------------
results:

parameter estimation  c(t) = A * exp(B*t) + C       range:    0 to 1200 s
                        A =  47.51 ±  0.00 ppm
                        B =  -0.99 ±  0.01 1/h
                        C =   0.00 ±  0.01 ppm

standard deviation: data from fitted curve 0.92 ppm
                    gas analyser           1.00 ppm
                    flow meter             2.00 1/h

air change rate     dynamic 1.0 ±  0.0 1/h (± 1.0 %)

total volume        nominal  604.00 ±  0.00 m**3

-----------------------------------------------------------------------
                   temperature (°C)                 pressure (Pa)
room             min.     φ      max.             min.     φ      max.

  0              4.57    4.73    4.86
  1             20.10   20.18   20.25            -0.66   -0.58   -0.50
  2             19.62   19.67   19.72             0.43    0.54    0.62
  3             17.84   18.04   18.24             0.48    0.64    0.74
  4             18.91   19.06   19.22             1.15    1.22    1.34
  5             18.92   18.96   19.00             0.65    0.84    1.10
  6             18.89   18.93   18.99           -17.40   -0.35    0.83
  7             18.19   18.31   18.37             1.06    1.15    1.22
  8             17.87   17.90   17.92           ******  *****   *****
```

Figure 7: Reporting Format

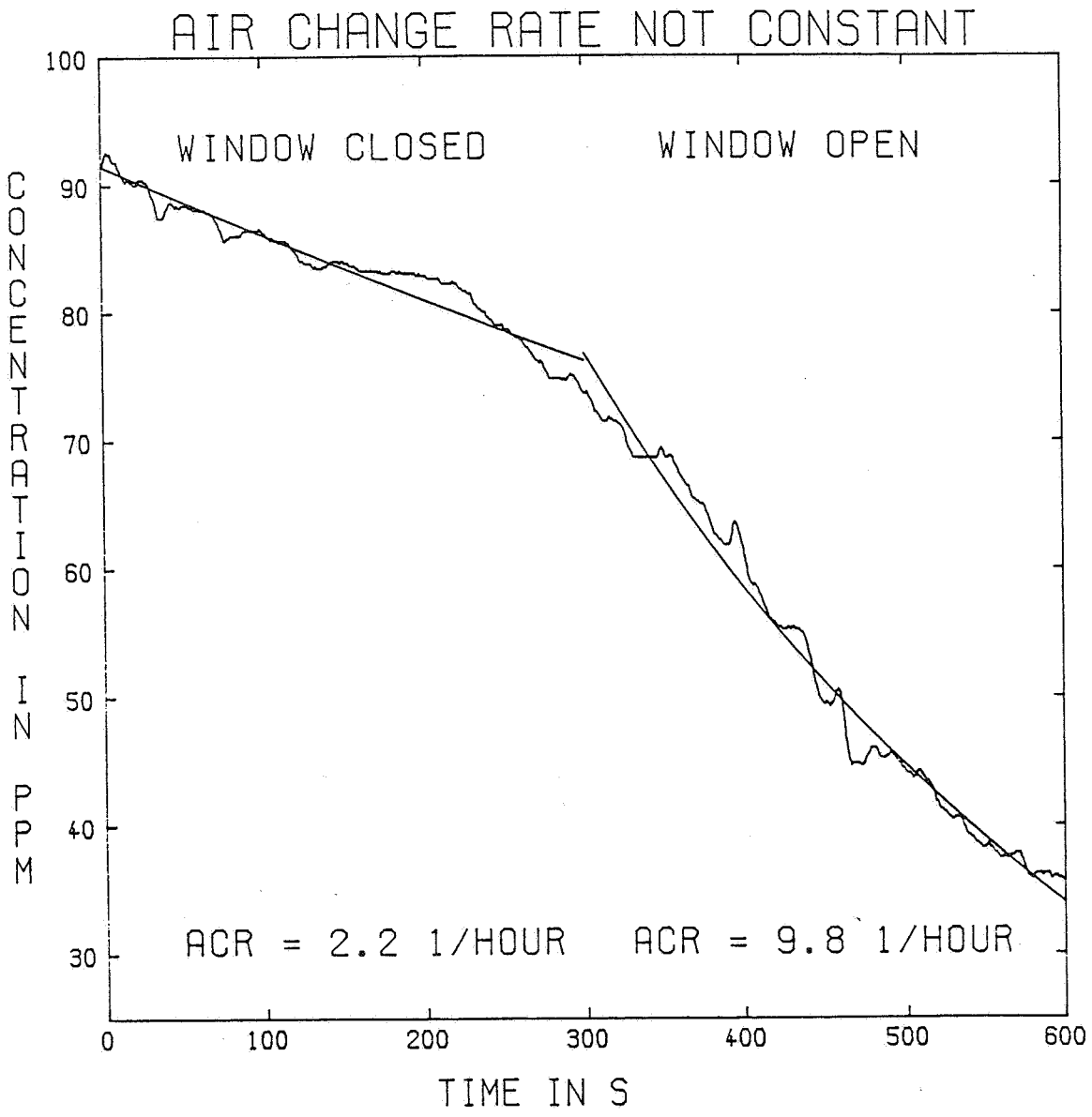

Figure 8: Example of advanced data evaluation and graphical representation

VENTILATION SYSTEM PERFORMANCE

11th AIVC Conference, Belgirate, Italy
18-21 September, 1990

Paper 8

EXPERIMENTAL EVALUATION OF A HYGROREGULATING NATURAL VENTILATION SYSTEM

P. Wouters, L. Vandaele
Belgian Building Research Institute
B-1342 Limelette
Belgium

EXPERIMENTAL EVALUATION OF A HYGROREGULATING NATURAL VENTILATION SYSTEM

P. Wouters, L. Vandaele
Belgian Building Research Institute
B-1342 Limelette, Belgium

ABSTRACT

In the framework of a CEC-DGXVII demonstration project a hygroregulating natural ventilation system is being evaluated in 52 occupied apartments. Therefore a multi purpose automated tracer gas equipment has been developed enabling the detailed monitoring of air flow rates in 60 rooms continuously. In addition the humidity levels, CO_2 levels and air temperatures are measured as well as the outdoor climate. The first measurement campaigns partly used for evaluation of the measurement system are reported and show an impressive amount of data enabling various types of detailed analysis. The ventilation and air quality parameters of the apartments equipped with the humidity controlled ventilation system are compared with those of the reference apartments.

1. INTRODUCTION

The detailed study of the flow rates in natural ventilated apartments, as well as the air quality in these apartments, is carried out in the framework of the CEC-DGXVII demonstration project "Passive humidity controlled ventilation in existing dwellings". The main intention of this project is the study of the possibilities of humidity controlled air inlet and outlet devices in comparison with ordinary inlets and outlets. Therefore, a detailed monitoring programme is running in 3 apartment buildings of which the main features are indicated in table 1.
All apartments have a ventilation duct in the kitchen, WC and bathroom.
A detailed description as well as the theoretically predicted performance of the humidity controlled inlet and outlet devices is given in (1).
This paper gives global results of the first measurement campaigns. More refined results will be published later on.

TABLE 1. Characteristics of the monitored buildings

Location	Year of construction	Number of floors	Number of apartments monitored	
			Reference	Humidity controlled
Namur (Belgium)	1978-1982	9	9	9
Orsay (France)	1969-1973	5	10	10
Schiedam (The Netherlands)	1965	10	7	7

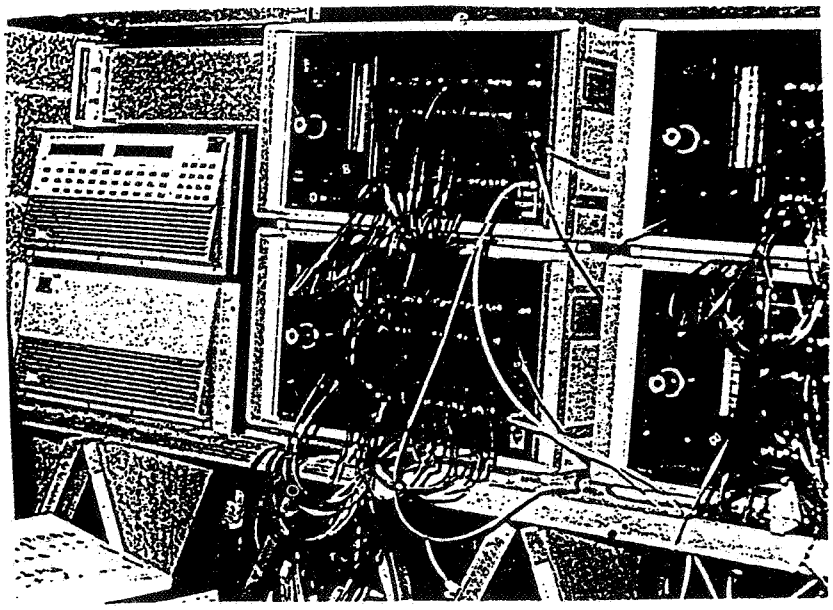

FIGURE 1. The BBRI-MATE System

2. THE MEASUREMENT SYSTEM

The ambition of the project is rather high : a detailed study of the ventilation and air quality in some 20 apartments at the same time. For practical and budgettary reasons, most of the attention is focused on the ventilation ducts. The MATE-system (Multipurpose Automated Tracergas Equipment) allowing to follow 60 channels automatically (fig. 1) was developed for this purpose. The system determines for each duct : the air temperature (°C), the flow rate (m^3/h), the CO_2-level (ppm), the humidity level (Pa, g/kg).
Wind direction and velocity, outdoor air temperature, humidity and CO_2-level are also recorded. One complete cycle of all measurements requires some 20 minutes.
It is planned to have 3 to 4 measurement campaigns in the 3 buildings, each campaign taking some 3 to 4 weeks or between 6 and 12 months of data. The first complete campaign started in October 1989 and the last campaign is planned for the spring of 1991.

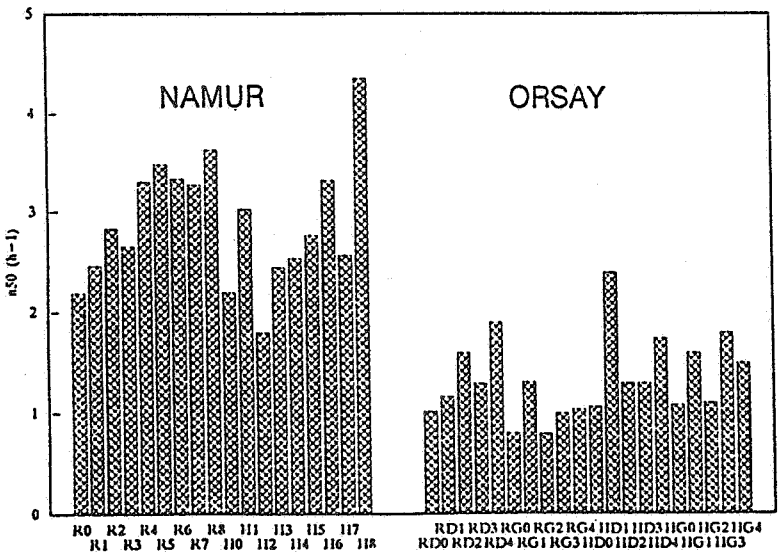

FIGURE 2. Pressurization results Namur and Orsay

The measurement of flow rates, CO_2- and humidity levels is done by one centralised sensor for each variable. Calibration tests indicated an accuracy of better than 10 % in the range 10-80 m^3/h.

3. AIRTIGHTNESS OF THE APARTMENTS

The airtightness of 18 apartments in Namur and 20 apartments in Orsay, as well as the leakage distribution was measured. The results are presented in figure 2.
The apartments in Orsay are very airtight. The air change rate for a pressure difference of 50 Pa is on the average 1.3 h^{-1}.

4. FLOW RATES - AIR QUALITY

4.1. Recorded data

The amount of data collected is impressive, each day some 60 000 observations of flow rates, air temperatures, humidity and CO_2 levels in the kitchen, WC and bathroom of each of the 20 apartments as well as the outdoor temperature, wind speed and direction, humidity and CO_2 levels, various wind pressures on facades are recorded.
An analysis of the measurements in Orsay for the 2 measurement periods 1-19 October 1989 and 6-28 January 1990 is given in 4.2 to 4.5.

4.2. Flow rates

The average daily flow rate for the 20 apartments in Orsay is shown in fig. 4 as a function of time.
The average air change rate for all 20 apartments is 0.62 h^{-1} (0.71 for reference apartments, 0.53 for humidity controlled apartments). The average weather conditions were : θe = 9 °C and v = 3.1 m/s, which are comparable with the average winter conditions in this region.
Fig. 3 shows that the total flow rate is rather stable with the exception of the period 22-28 January, characterised by very high wind speeds.

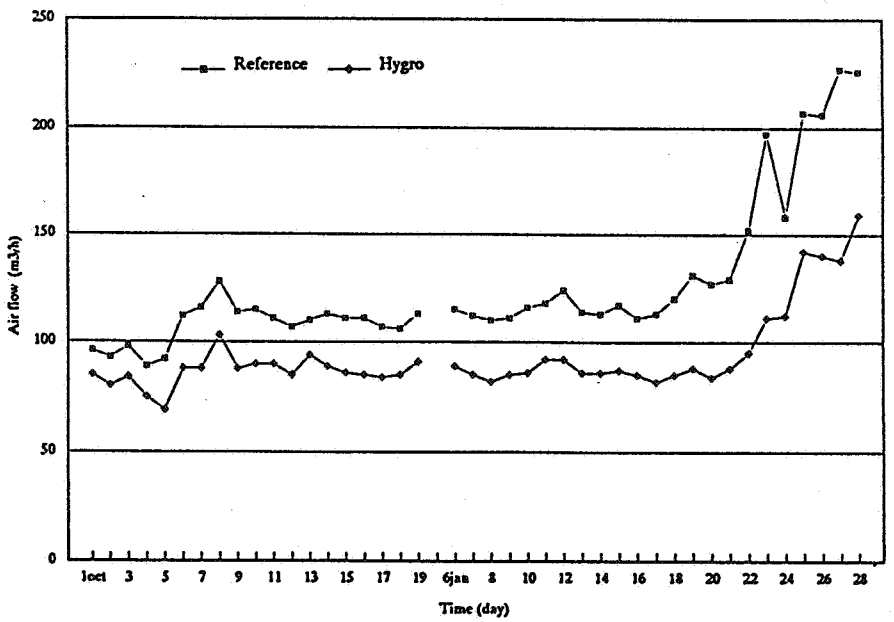

FIGURE 3. Daily average flow rates for the average reference and humidity controlled apartments in Orsay.

TABLE 2. Minimum, average and maximum daily values for the average of the 10 reference apartments and the 10 humidity controlled apartments, respectively, Orsay, 1-19 October 1989 and 6-28 January 1990.

	MINIMUM		AVERAGE		MAXIMUM	
Total air change rate (h^{-1})	0.50	0.39	0.71	0.53	1.28	0.90
x kitchen (m^3/h)	36	30*)	53	49*)	94	87*)
x WC (m^3/h)	23	17	37	21	69	35
x bathroom (m^3/h)	26	16	37	24	65	37
Outside temperature (°C)	0.4		9.1		16.0	
Wind speed (Trappes) (m/s)	1.4		3.1		8.1	

*) Ordinary outlet grilles

According to (2) we propose the following model

$Q = Av^2 + B\Delta T + C$ (m^3/h)

which in our case leads to :

$Q = 69 + 2.1v^2 + 1.9\Delta T$ (m^3/h)

The standard deviations are s_A = 0,22 (F=91), s_B = 0.59 (F=11) and r = 0.86

4.3. CO_2-levels

Fig. 4 shows the average CO_2-levels and extracted CO_2-quantities for the Orsay apartments. Table 3 gives a summary of the results.

There is a significant difference in extracted CO_2-quantities between the reference and the humidity controlled apartments. This is probably due to a difference in occupation pattern. The difference between the highest and lowest average daily values is very large, especially if one knows that the outdoor CO_2-concentration is 400 ppm. The average CO_2-level is - as might be expected - strongly correlated with the total air change rate.

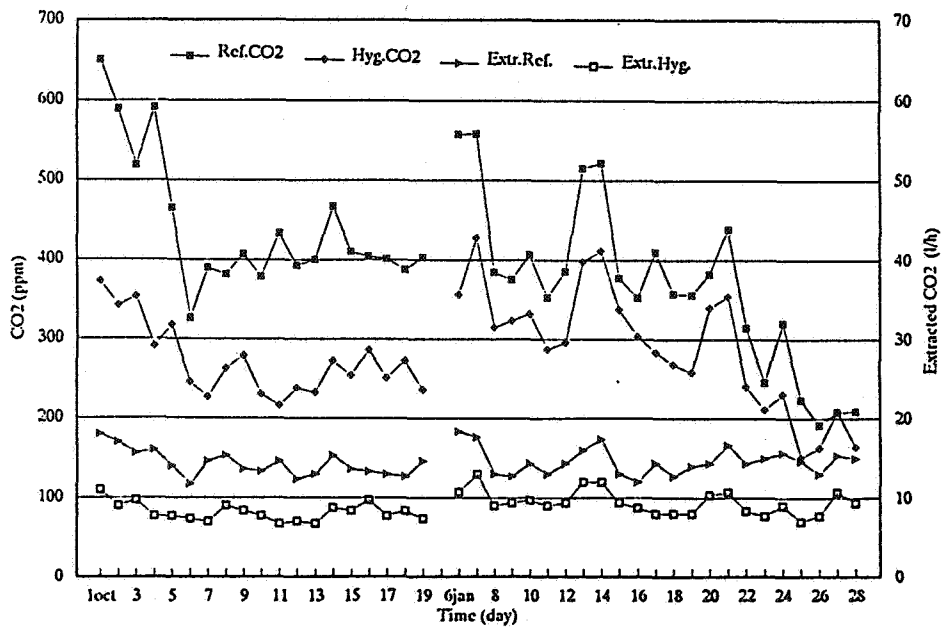

FIGURE 4. Average CO_2-levels and extracted CO_2-quantitites for the Orsay apartments.

TABLE 3. Minimum, average and maximum daily values of CO_2 for the average of the 10 reference apartments and of the 10 humidity controlled apartments; Orsay, 1-19 October 1989 and 6-28 January 1990.

	MINIMA		AVERAGE		MAXIMA	
	REF.	HUMID.	REF.	HUMID.	REF.	HUMID.
CO_2-levels						
* average (ppm)	590	550	800	680	1 050	830
* kitchen (ppm)	630	550	850	710	1 100	880
* WC (ppm)	580	550	700	690	1 060	840
* bathroom (ppm)	560	540	750	650	990	760
CO_2-quantities						
* total (l/h)	35	20	43	27	55	39
* kitchen (l/h)	15	11	20	15	25	23
* WC (l/h)	10	4	12	6	17	9
* bathroom (l/h)	8	4	11	6	19	9

If we assume the formula :

$CO_2 = 400 + A/Q$ (ppm)

we find :

$CO_2 = 400 + 48073/Q$ (ppm)

where the standard deviation is $s_A = 1066$ (F=45) and r = 0.82

The CO_2 quantities extracted give a good picture of the occupancy (since each occupant produces some 15...20 l/h of CO_2) at the condition that there are no other CO_2-sources like gas cookers and that most of the air leaves the apartments through the ducts. A first indication of the importance of air leaving the apartment through the facade openings is obtained by asking the numbers of occupants during the night.

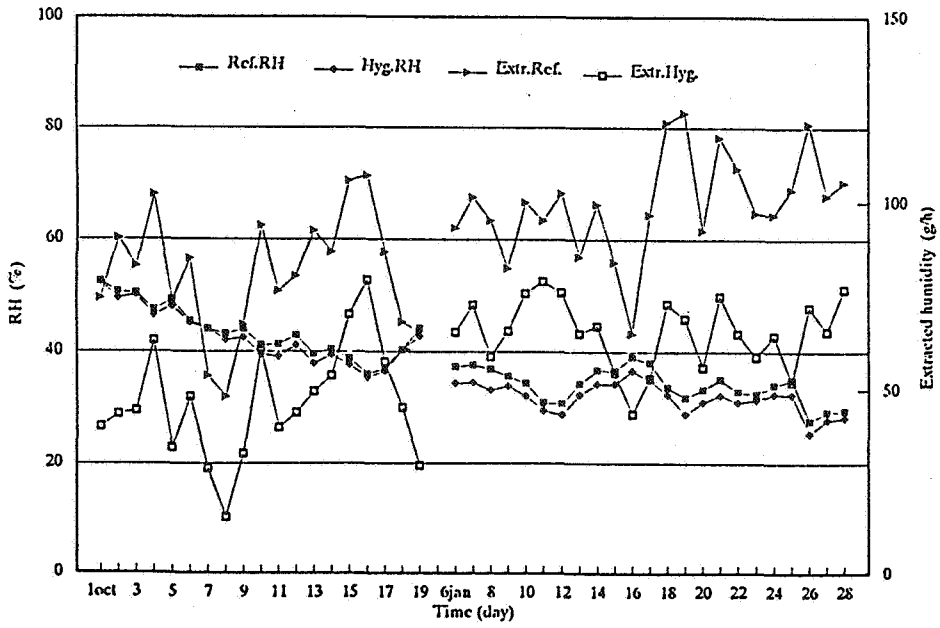

FIGURE 5. Daily average humidity levels and daily extracted quantities of water vapour for the Orsay apartments

TABLE 4 Minimum, average and maximum daily values for the 10 reference apartments and for the 10 humidity controlled apartments in Orsay, 1-19 October 1989 and 6-28 January 1990.

	MINIMA		AVERAGE		MAXIMA	
	REF.	HUMID.	REF.	HUMID.	REF.	HUMID.
Relative humidity						
* average (%)	28	25	38	37	53	52
* kitchen (%)	29	28	39	39	53	54
* WC (%)	26	24	35	34	46	48
* bathroom (%)	28	25	41	37	59	55
Extracted humidity						
* total (g)	144	46	273	170	372	238
* kitchen (g)	50	30	106	86	153	138
* WC (g)	24	-6	62	31	94	49
* bathroom (g)	65	22	105	53	139	77

4.4. Humidity

There are no important problems observed due to mould growth or condensation. Fig. 5 shows the average humidity levels and the water vapour quantities evacuated per day. Table 4 summarizes the results.

5. CONCLUSIONS

Detailed measurements of extraction flow rates and air quality parameters are running in some 52 apartments in France, Belgium and the Netherlands. The results of the first measurement campaign show very interesting results. The first analysis of the measurement data as well as the detailed calibration measurements on the measurement system indicates a very large potential for various types of analysis.

6. ACKNOWLEDGEMENTS

The authors wish to thank the organisations who sponsored this project : The Commission of the European Communities DG XVII, AERECO (France), E.D.F. (France), CETIAT (France), TNO (The Netherlands) and BBRI (Belgium). The following persons contributed to the preparation of this publication :
Messrs. Jardinier and Simonnot (AERECO), Messrs. Nicolas and Niard (EDF), Mr. Gaillard (CETIAT), Messrs. de Gids and Phaff (TNO/MT), Messrs. Bossicard, L'Heureux, Voordecker, Gengoux and Miss De Keyser (BBRI).

7. REFERENCES

(1) Jardinier, P., Simonnot, J., La Ventilation Naturelle Hygroréglable, CIB Energy, Moisture and Climate in Buildings (1990).
(2) Liddament, M., Air Infiltration Calculation Techniques - An Applications Guide, Air Infiltration and Ventilation Centre (1986).

VENTILATION SYSTEM PERFORMANCE

11th AIVC Conference, Belgirate, Italy
18-21 September, 1990

Paper 9

AN AUTOMATED APPARATUS FOR AIR INFILTRATION MEASUREMENTS WITH TRACER GASES
(Researbh activity at Politecnico di Torino)

R. Borchiellini and M. Cali

Dipartimento di Energetica
Politecnico di Torino
Corso Duca degli Abruzzi 24,
Torino
Italy

Synopsis

This paper describes the activity on Air Infiltration and Ventilation of the research group of "Dipartimento di Energetica" in Politecnico of Turin. The group formed in 1988 and only at the beginning of 1990 it began to work on multizone flow analysis.
The aim of the group is to set up an apparatus for air infiltration measurement comparable to those of other countries; up to now only measurements using decay technique were made in laboratory in a scale-model which represents a two-zone system.

1 Introduction

Brief on the previous activity of the research group in the field of AIV

Research in this field started in 1982 during studies on building energy balance in a test room. Particular attention was devoted to the study of heat losses due to mass flow-rates of the air entering and exiting the room. Both pressurisation tests and tracer gas measurements were performed. The gas used was methane; the sampling was carried out by bags whose content was afterward analyzed in laboratory. The results are exposed in [1].

Research went on in the following two years due to a request of measurements of the air changes in the internal volume of a car. In a first step, a test room was built in laboratory to calibrate an apparatus for the measurements of the N_2O concentration by an infrared gas analyzer. At the same time calibration was also made by the pressurisation technique. The calibrated apparatus was used to measure the air flow rate through the internal volume of a car subjected to a high speed external wind; the measurements were performed in a wind tunnel using only the pressurisation technique. The high values (ten or more) of air change rates made it impossible to use the tracer gas method. The results are reported in [2, 3].

Many other measurements have been made in rooms and dwellings by the decay method for some months, with the aim of evaluating the infiltration energy loss in a more complex study of energy balance in buildings.

In 1985 the research group broke up and the activity in this field was suspended. In 1988 some people of the previous group started again to study the air infiltration problem, but many parts of the laboratory needed rebuilding and some instruments had to be replaced with new ones.

This paper refers to this latter activity, which is essentially devoted to building an experimental apparatus that allows us to reach the same level as the one of the other countries [4, 5, 6, 7, 8, 9] in AIVC and, at the same time, to applying the experience developed in the theoretical studies of inverse problems (applied to heat conduction) to air infiltration studies.

Actual activity

Presently, both Italian universities and some public and private laboratories are showing a growing interest in the knowledge of experimental techniques for the measurement of the air exchanged between different zones of buildings. The main reasons for such concern are the introduction of a more severe standards in fire protection, the major attention to air quality problems and the high number of fatal accidents in houses due to bad ventilation of rooms containing combustion equipments.

Consequently, universities and research centres are more and more involved in field measurements and in improving the knowledge in this research area by companies and consultants.

In order to answer to these requests we are trying to develop our activity in two main directions.

The aims of the first one are essentially:

a. That researchers and technicians of our laboratory working in this field can develop an adequate degree of knowledge of the theoretical problems and of apparatus in the market.

b. Designing, constructing and calibrating a laboratory apparatus that can be used as a reference device for portable instrumentation. The characteristics of this apparatus must include flexibility (constant concentration, decay and constant flow-rate methods), high quality of devices and high automatization.

c. Designing, constructing and calibrating a portable apparatus, for field measurements.

The second goal is essentially theoretical. We have some experience in the field of inverse problems applied to the measurement of thermophysical properties, solved with numerical and probabilistic methods. As the measurement of the concentration versus time of one or more tracer gases in one or more interconnected rooms is essentially an inverse problem, we are

studying the application of this theory to the experimental techniques in AIV studies. Other researchers are working successfully in this field (for example see [10]).

Only some of these aims have been presently attained (first half 1990):

1. A laboratory test room, which will be described later on, has been equipped with measurement and control devices. Up to now only single room measurements have been carried out and the data analysis algorithms have been tested [11].
2. An apparatus for measurement in more zones interconnected is being built.

2 Apparatus description

This apparatus was designed for on-site measurements and for laboratory test. It consists of two main sub-sets of components:

- Sub-Set A (SSA): a compact and mobile multi-tracer gas system developed for multizone analysis and for on-site measurements;
- Sub-Set B (SSB): it just includes the components used in laboratory experiments in order to test the calculation technique based on the "Ill - posed problems" theory [12, 13]. Since the conservation equations of the mass of tracer and the mass of air are written for a zero-dimensional model, we have decided to use small boxes, easy to build, to model different zones.

Figure 1 displays schematically SSA. The system consists of:

- two infrared-photometer for the measurements of the nitrogen protoxyde (N_2O) and sulphur hexafluoride (SF_6), Leybold-Heraeus model Binos 1.1 and Binos 3 with the following characteristics:
  - *Measurement accuracy*: ≤ 2% at full-scale
  - *Number of channels*: 1
  - *Zero drift per week*: < 2% at full-scale
  - *Typical temperature effect per K*: ≤ 0.1% at full-scale
  - *Influences of gas or ambient pressure*: 0.1% of measured value per 1 mbar pressure difference
  - T_{90} *time*: 1.8 s ..... 10 s

- *measuring gas flow*: approx. 1 l/min (0,1....2,5 l/min)

- PC computer, laptop model based on Intel 80C286 12 MHz processor; the computer controls the valves position and acquires data (tracer concentration, indoor and outdoor temperature);
- an IBM - compatible multifunction analog and digital I/O board (16 single-ended analog input channels 12 bits resolution, 2 analog output channels 12 bits resolution, 8 digital inputs and 8 digital outputs);

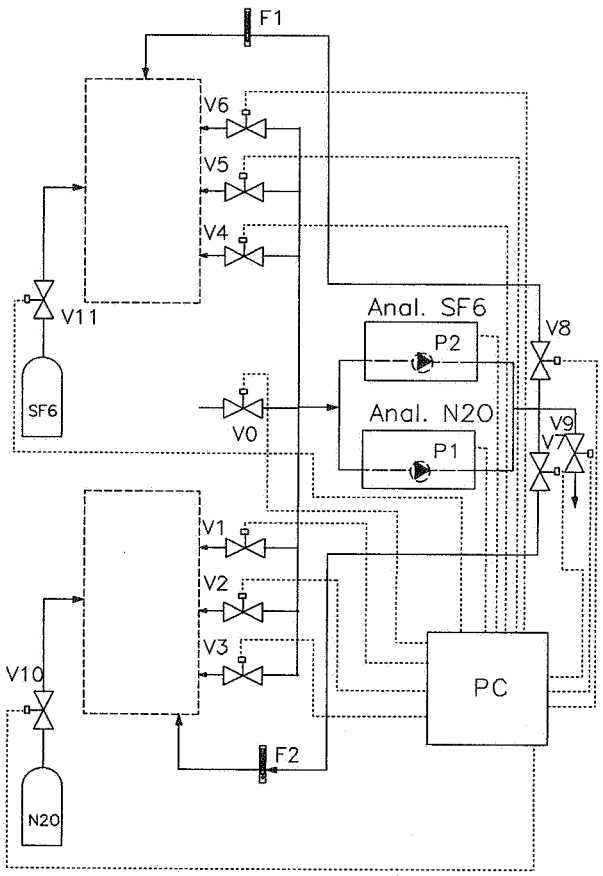

Figure 1 - SSA sub-system

- an IBM - compatible digital I/O board (24 channels of digital I/O, three 8-bit groups independently selectable for I/O, connected to a solid-state relay sub-systems);
- an HP-3497A data acquisition control unit able to replace the two IBM - compatible boards;

- twelve solenoid valves (V0 - V11) to perform the sampling of air and the gas injection; the valves requires 24 V electrical supply.

The sub-system SSB is schematically represented in figure 2; it consists of:

- two small boxes made of wood: the volumes of the first (ZONE 1) and the second (ZONE 2) are respectively 0.0525 m^3 (0.35 x 0.50 x 0.30 m) and 0.1242 m^3 (0.467 x 0.566 x 0.470 m); they are a small scale representation of two different zones connected by a pipe between the points 14 and 15 of figure 2; each zone has three sampling points (points 1 - 2 - 3 for ZONE 1 and 4 - 5 - 6 for ZONE 2) and is connected to the external environment by a pipe equipped with a flow-meter (see points 13 and 14 in figure 2); the injection of the tracer gas and the air supply are accomplished in zone 1 only (points 10 and 12);
- two mixing fans, one for each zone;
- three flow-meters and three pumps to control the air change and verify the mass balance in each zone;
- one electric resistance to vary the air temperature;

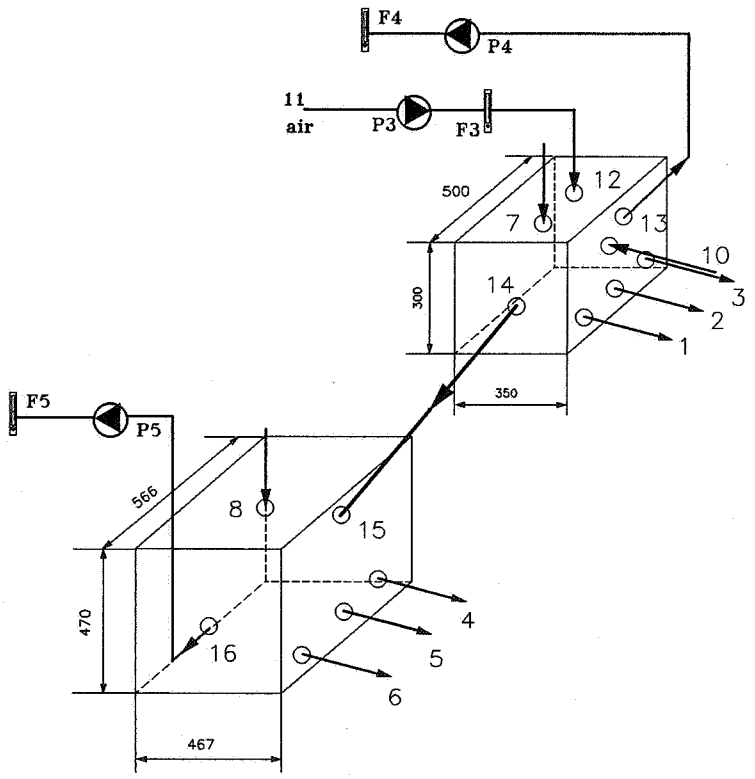

Figure 2 - SSB sub-system

- two platinum resistance thermometers to measure the air temperature in each zone, so that it can be taken into account in the mass balance equations as pointed out by Roulet [14].

The two sub-systems are presently used to perform laboratory tests whose main purposes are improving our experience on tracer gas measurement and obtaining the wide set of experimental results necessary to check the numerical technique chosen to calculate the air flows.

As shown in fig. 3, the complete apparatus is a multizone and single tracer gas system. The zones are represented by the two boxes, which are very tight as indicated by the pressurization test results (see Table I).

Table I - Results of the pressurization tests

Q [l/h]	ΔP[Pa]		
	ZONE 1	ZONE 2	ZONE 1+2
20	460	300	320
30	850	430	600
40	1230	560	920
50	> 1500	690	1100

In the tests without pumps P4 and P5 and with an air flow-rate due to the pump F3 equal to 116 l/h, the pressure drop across the flow-meters F4 and F5 is approximately 200 Pa; hence, the internal pressure in the two zones is very high and Table I shows that the air exfiltration is not negligible; on the other hand all air flows had to be known in our test in order to be able to compare calculated and measured flows. For this reason the two pumps P4 and P5 have been introduced in the system; the difference between the cases with pumps and without pumps are shown in Table II.

Both the constant tracer flow-rate technique and the constant concentration technique requires the control of the tracer gas flow-rate injected. In our apparatus the volumes of the boxes are so small that suitable valves are not only very expensive but also difficult to find on the market. Moreover, this type of valves could be used only in laboratory tests due to their small operating

ranges, which make them unsuitable to field applications. Therefore, keeping in mind our goals, only decay techniques has been developed up to now; an example of measurements results is shown in figure 4.

Table II - Pressure differences between inside zones and outside during measurement		
Q [l/h]	ΔP[Pa]	
	Without pumps P4 and P5	With pumps P4 and P5
100	270	15
125	310	9
150	350	7
175	390	~ 0

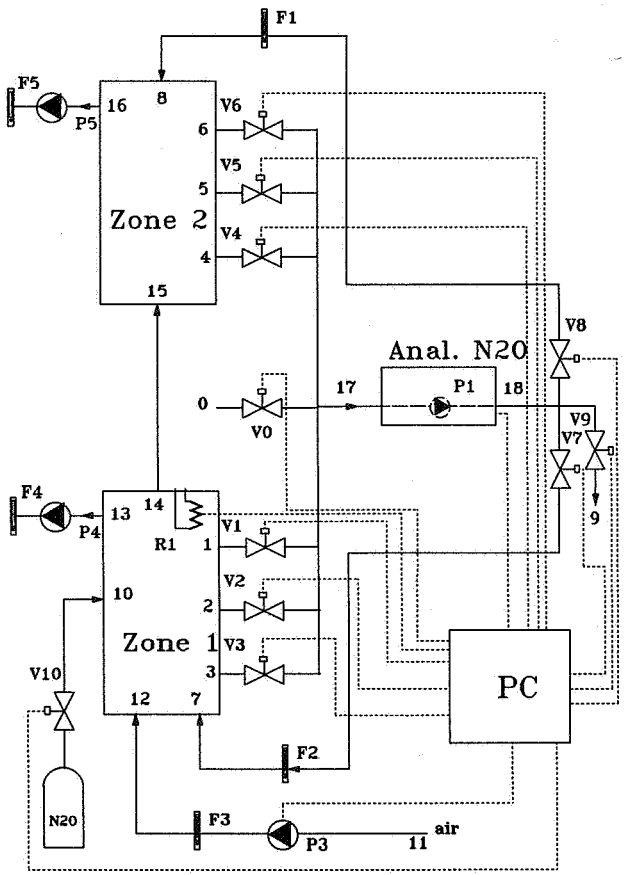

Figure 3 - The complete laboratory apparatus

A computer program interactive with the operator runs on the PC and executes all the different operations required to carry out the measurements; the main steps are (see fig. 3):

a - injection of the tracer gas to reach the defined initial concentration level; closure of all valves;

b - opening of valves V0 to V9 to wash the pipe between the points 0 and 9 with external air (required time: about 29 seconds);

c - closure of valve V0 and opening of the valves for sampling from the defined zone (V1, V2 and V3 or V4, V5 and V6); this step is necessary to avoid that an amount of tracer gas and air mixture of the previous sampling period circulates once more in the zone (required time: about 10 seconds);

d - closure of valve V0 and opening of the valve that circulates again the sampling mixture and wait for stationary condition on the analyzer to be reached (required time: about 19 second);

e - save the measured tracer gas concentration on the hard disk or floppy disk, write and plot this new concentration value on PC monitor;

f - repetition of steps b - e for each zone.

The program includes also utilities to set the zero and full scale points of the analyzer; the on-line calculation of the air change and of the initial tracer concentration are also displayed.

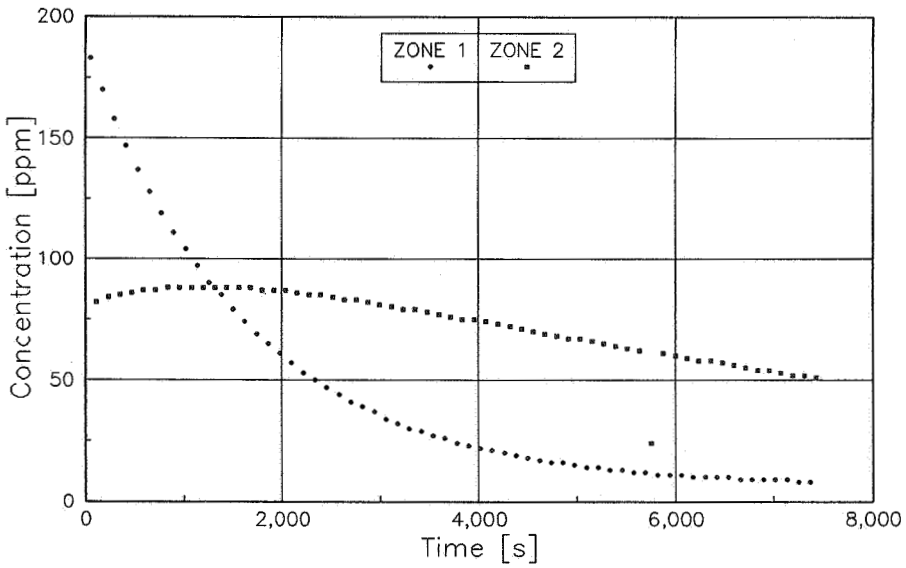

Figure 4 - Example of measurement results

3 Data analysis

A model is the mathematical physical reality representation; it establishes analytical correlations between the physical quantities that properly describe the phenomenon. As to AIV problems, for example, the model consist of the mass conservation equation. The quantities used in the model's equations can be distinguished in measurable quantities (y) and parameters (v). Then the model's equations can be written in the general form:

$$y = f(v) \tag{1}$$

The measurable quantities in our problems are tracer gases concentrations, source flow-rates, temperatures and pressures, while the parameters are volumes of each zone and air flow-rates [10].

Therefore, the estimation of the parameters v made by the measured concentrations c is a typical "inverse problem" which has been widely treated in literature; we chose the calculation strategy exposed in [12, 13, 15] and using statistical considerations [10] it's possible to define the scalar S, which is a quadratic function of the parameters, as follows:

$$S = e^T W e + S^* \tag{2}$$

S^* is a regularization term and e is the error defined by:

$$e = c - y = e(v) \tag{3}$$

The values v which minimize S are an extimation of the model parameter.

We have applied this approach successfully to single-room measurements; the measured data were analyzed after the end of the experiments (whole domain technique); now we are trying to apply this approach to multizone measurements using either whole domain or sequential (on-line) technique.

4 Conclusions

All the aims haven't been presently attained, but we are motivated to continue by our brief experience; as also pointed out by other authors [14, 10], the outcomes of the research work made up till now show that great attention must be paid to:

- the influence of the temperature difference between zones and also to temperature changes during measurements;

- the data covariance matrix, mainly when high speed acquisition system is used.

Therefore next year our efforts will be devote to improving the data analysis technique.

5 Acknowledgements

The authors wish to thank G. Vannelli and V. Regazzoni, who contributed to the construction of the scale-model and the tracer gas system.
This work has been supported by the Italian National Research Centre (C.N.R. - P.F.E.) contract n. 87.02154.59

6 References

1 Borchiellini R.
"Studio analitico sperimentale degli scambi di energia per trasporto di massa negli edifici"
Tesi di laurea in Ingegneria meccanica, Politecnico di Torino, 1983

2 Vacchelli P.
"Studio teorico sperimentale delle tecniche di misura delle infiltrazioni d'aria. Applicazione alla climatizzazione degli autoveicoli"
Tesi di laurea in Ingegneria meccanica, Politecnico di Torino, 1986

3 Calì M., Fracastoro G.V., Vacchelli P.
"Studio con la tecnica dei gas traccianti delle infiltrazioni d'aria in una camera a ventilazione controllata"
Atti del XLI Congresso Nazionale A.T.I., pp. VI-103, VI-117, Napoli, 23-26 settembre 1986.

4 D'Ottavio T.W., Senum G.U., Dietz R.N.
"Error Analysis Techniques for Perfluorocarbon Tracer Derived Multizone Ventilation Rates"
Bldg. Envir., Vol 23, No.3, 1988, pp. 187-194.

5 Bohac D.L., Harrje D., Norford L.K.
"Constant Concentration Infiltration Measurement Technique: an Analysis of its Accuracy and Field Measurements"
Proc. ASHRAE-DOE-BTECC Conference on Thermal Performance of the Exterior Envelopes of Buildings, III, pp. 176-200, Clearwater, FL, Dec. 1985.

6 Roulet C., Scartezzini J.L.
"Measurement of Air Change Rate in an Inahabited Building with a Constant Tracer Gas Concentration Technique"
ASHRAE Trans, Part 2, 1987, pp. 1371-1380.

7 Sandberg M., Stymne H.
"*The Constant Tracer Flow Technique*"
Bldg. Envir., Vol 24, No.3, 1989, pp. 209-219.

8 Sandberg M.G.
"*Predicting a Time-varying Flow Rate using the Constant Concentration and Decay Technique*"
ASHRAE Trans, Part 2, 1987, pp. 1381-1393.

9 Sherman M.H.
"*Uncertainty in Air Flow Calculation Using Tracer Gas Measurements*"
Bldg. Envir., Vol 24, No.4, 1989, pp. 347-354.

10 Sherman M.H.
"*On the Estimation of Multizone Ventilation Rates From Tracer Gas Measurements*"
Bldg. Envir., Vol 24, No.4, pp. 355-362, 1989.

11 Calì M. et al.
"*La misura della portata d'aria di ventilazione in un ambiente confinato con il metodo dei gas traccianti*"
PT-DE 226 Dipartimento di Energetica Politecnico di Torino, 1990.

12 Beck J.V., Arnold K.J.
"*Parameter Estimation in Engineering And Science*"
J.Wiley & S., New York 1977.

13 Beck J.V., Blackwell B., St. Clair C.R. Jr.
"*Inverse Heat Conduction, Ill-posed Problems*"
J.Wiley & S., New York 1985.

14 Roulet C.A., Compagnon R.
"*Multizone Tracer Gas Infiltration Measurement - Interpretation Algorithms for Non-Isothermal*"
Bldg. Envir., Vol.24, No.3, 1989, pp.221-227.

15 Tarantola A.
"*Inverse Problem Theory*"
Elsevier, New York, 1987.

VENTILATION SYSTEM PERFORMANCE

11th AIVC Conference, Belgirate, Italy
18-21 September, 1990

Paper 10

COMPARISON OF TRACER GAS METHODS FOR MEASURING AIR FLOWS IN TWO ZONE BUILDINGS

F.D. HEIDT, R. RABENSTEIN, G. SCHEPERS

Dept of Physics
University of Siegen
Adolf-Reichwein-Strabe
D-5900 Siegen
Germany

ABSTRACT

This paper discusses three methods for measuring interzonal air movements in two zone buildings:

1. initial injection of one tracer into a single room,
2. repeated injection of one tracer in two rooms,
3. initial injection of two tracers in two rooms.

The description of these methods includes an outline of the theoretical background, the presentation of suitable injection strategies and algorithms for the evaluation of the concentration profiles. A detailed error analysis using Monte-Carlo-Simulation shows the accuracy of these methods for a variety of cases, such as different magnitudes of the interzonal air flows and various measurement durations. The numerical results agree with tracer gas measurements conducted at a laboratory-scale physical model with two chambers.

1. INTRODUCTION

The knowledge of the air exchange between the interior and the exterior of a building (external air exchange) as well as between its individual rooms (interzonal air flow) is of great practical importance for its thermal, physical and hygienic characterization. Examples are the energy or the moisture balance of the building or the concentration of air pollutants in the interior. In passive solar buildings, the interzonal air exchange fulfills further important functions, such as convective heat transfer between the locations of solar gain, storage and use.

Unfortunately, air exchange is one of the least understood processes in building physics, since it is determined by a variety of parameters, which are not easily accessible. They include climatic parameters (e.g. wind velocity and temperature), building related parameters (e.g. shape and location of the windows) and behavior of the inhabitants. Theoretical calculations of air exchange rates are therefore difficult and unreliable. Accurate results for the quantity of air flows in a building can only be obtained by measurements. There are two principal measuring methods:

- pressurization methods,
- tracer gas methods.

Pressurization methods are suitable for leakage tests of a whole building or for measuring the external air exchange rate under standardized conditions (i.e. a fixed pressure difference between inside and outside). Tracer gas methods are capable of the determination of the external and the interzonal air flows under natural conditions.

Tracer gas methods for the measurement of the external air change rate are widely used in the field. They have been standardized in several countries [1,2]. Tracer gas methods for the measurement of interzonal air flows are still an area of research. Several laboratories have built multiple tracer gas systems, where a different tracer substance is used for each zone [3,...,9]. Various single tracer gas methods have been proposed [10,...,13] in order to avoid the simultaneous handling of multiple tracer gases. However, these methods are still in an early stage of development.

It is the purpose of this paper to compare several tracer gas methods for the measurement of interzonal airflows. Two single tracer and one multiple tracer gas method will be considered. This comparison is based on

- theoretical investigations,
- Monte Carlo simulation using synthetic data,
- air flow measurements using a small scale two zone building model with adjustable airflows.

The restriction to two zones simplifies the theoretical treatment and the experimental setup. It is adequate for the modelling of single family houses with a ground floor and an upper floor.

2. MEASUREMENT METHODS FOR THE AIR FLOW IN TWO ZONE BUILDINGS

2.1 Basic Equations

In order to measure the air flows between the zones of a building, it is necessary to distinguish at each moment of time between air that enters a certain zone from the outside or from a neighboring zone and air that has already been present in that zone. To this end, one marks the air in the zone under investigation with a tracer gas. The tracer concentration varies with time and tells at each moment the relation of "old air" to "fresh air".

Figure 1 describes this process in detail for a two zone building model. Two zones numbered 1 and 2 are interconnected with each other as well as with the outside air (0). Tracer gas is injected into each zone, resulting in a certain tracer gas concentration. Zones 1 and 2 are characterized by

V_i volume in m^3,

$c_i(t)$ tracer gas concentration (dimensionless),

$Q_i(t)$ tracer gas injection rate in m^3/h,

where i = 1,2. The outside air (zone 0) can be described by

$V_0 \rightarrow \infty$ infinite volume,

$c_0(t) = 0$ zero tracer gas concentration,

$Q_0(t) = 0$ no tracer gas injection.

F_{ij} denotes the air flow from zone i to zone j. Further we assume,

- the air flows do not vary with time: $F_{ij} \neq F_{ij}(t)$
- the total air flow into a zone is equal to the total air flow out of that zone:

  $$\sum_j F_{ij} = \sum_j F_{ji} ,$$

- the temperature (and thus the density of air) does not vary with time,
- the tracer gas concentration is uniform in each zone.

According to these assumptions, we can write the conservation of tracer gas in each zone as a volume balance:

$$V_1 \dot{c}_1(t) = - (F_{10} + F_{12})\, c_1(t) + F_{21}\, c_2(t) + Q_1(t) \qquad (1a)$$

$$V_2 \dot{c}_2(t) = F_{12}\, c_1(t) - (F_{20} + F_{21})\, c_2(t) + Q_2(t) \qquad (1b)$$

or with

$$F_{01} + F_{21} = F_{10} + F_{12} = - F_{11} \qquad (2a)$$

$$F_{02} + F_{12} = F_{20} + F_{21} = - F_{22} \qquad (2b)$$

as

$$V_1 \dot{c}_1(t) = F_{11}\, c_1(t) + F_{21}\, c_2(t) + Q_1(t) \qquad (3a)$$

$$V_2 \dot{c}_2(t) = F_{12}\, c_1(t) + F_{22}\, c_2(t) + Q_2(t) \qquad (3b)$$

Rather than expressing the air and tracer gas flows in absolute quantities, we can relate them to the volume of this zone

$$f_{11} = \frac{F_{11}}{V_1} = - \frac{F_{01} + F_{21}}{V_1} = - \frac{F_{10} + F_{12}}{V_1} , \quad f_{12} = \frac{F_{21}}{V_1} \qquad (4a,b)$$

$$f_{22} = \frac{F_{22}}{V_2} = - \frac{F_{02} + F_{12}}{V_2} = - \frac{F_{20} + F_{21}}{V_2} , \quad f_{21} = \frac{F_{12}}{V_2} \qquad (4c,d)$$

$$q_1(t) = \frac{Q_1(t)}{V_1}, \quad q_2(t) = \frac{Q_2(t)}{V_2} \qquad (5a,b)$$

and obtain

$$\dot{c}_1(t) = f_{11}\, c_1(t) + f_{12}\, c_2(t) + q_1(t) \qquad (6a)$$

$$\dot{c}_2(t) = f_{21}\, c_1(t) + f_{22}\, c_2(t) + q_2(t) \qquad (6b)$$

or in matrix notation

$$\dot{\underline{c}}(t) = \underline{\underline{f}}\ \underline{c}(t) + \underline{q}(t) \tag{7}$$

$$\underline{c}(t) = \begin{vmatrix} c_1(t) \\ c_2(t) \end{vmatrix}, \quad \dot{\underline{c}}(t) = \begin{vmatrix} \dot{c}_1(t) \\ \dot{c}_2(t) \end{vmatrix} \tag{8a,b}$$

$$\underline{\underline{f}} = \begin{vmatrix} f_{11} & f_{12} \\ f_{21} & f_{22} \end{vmatrix}, \quad \underline{q}(t) = \begin{vmatrix} q_1(t) \\ q_2(t) \end{vmatrix} \tag{8c,d}$$

The problem is to estimate the elements of the flow matrix f from measurements of the tracer gas concentration. However, Equation (7) is not suitable for this purpose, since it requires also the knowledge of the derivative of the tracer gas concentration. In principle, it could be obtained from the measurement values of the concentration by numerical differentiation, but the result would be very sensitive to measurement errors. Instead, the elements of the flow matrix can be determined by an eigenvalue analysis. Another possibility is to remove the derivative of the concentration by integrating (7) over the time interval of the measurement, say for $t_0 < t < t_1$. One obtains

$$\underline{c}_\Delta = \underline{\underline{f}}\ \underline{c}_I + \underline{q}_I \tag{9}$$

with

$$\underline{c}_\Delta = \begin{vmatrix} c_1(t_1) - c_1(t_o) \\ c_2(t_1) - c_2(t_o) \end{vmatrix} \tag{10a}$$

$$\underline{c}_I = \begin{vmatrix} \int_{t_o}^{t_1} c_1(t)\,dt \\ \int_{t_o}^{t_1} c_2(t)\,dt \end{vmatrix}, \quad \underline{q}_I = \begin{vmatrix} \int_{t_o}^{t_1} q_1(t)\,dt \\ \int_{t_o}^{t_1} q_2(t)\,dt \end{vmatrix} \tag{10b,c}$$

Equations (7) and (9) are called the differential and the integral form of the tracer gas conservation law. Although the integral form does not contain any derivatives of the measurement values, it cannot be readily solved for the elements of the flow matrix, since the set of linear equations is underdetermined. Additional information in form of a second set of equations is necessary in order to invert the integral conservation law. Two different methods will be discussed here: The second set of equations can be obtained by integrating the concentration data over a second time interval or by using a second tracer gas and applying the conservation law to two tracer gases.

The above mentioned methods for the determination of the flow matrix differ by the form of the conservation law and the number of tracer gasses:

form of conservation law	number of tracers	injection strategy	name of method
differential	one	initial	eigenvalue analysis
integral	one	repeated	pulse decay
integral	two	initial	two tracer decay

The second method is called the pulse decay method, because a new pulse of tracer gas is injected before each integration interval. The names of the other methods are obvious. These methods and their injection strategies will now be described.

2.2 Eigenvalue Analysis

This method has been outlined in detail by Sinden [10]. A concise description using matrix notation can be found in [15]. Here, we will explain only the general idea.

We assume that the tracer gas has been injected into one or two of the zones at the beginning of the measurement and no more tracer gas is injected during the measurement. Then the tracer gas concentration curves $c_1(t)$ and $c_2(t)$ in each room are the sum of the same two exponential functions, but with different weights. It is the objective of this method, to extract information on the eigenvalues and the eigenvectors of the flow matrix f from these concentration curves. We consider the weighted difference of the two concentrations $h(t,a) = c_1(t) - a \cdot c_2(t)$, with variable weighting factor a. There are two distinct values for a where either one of the two exponentials cancels out. These values can be determined by attempting to fit a straight line to the log of $h(t,a)$ for varying a. A minimum of the squared residuals signals that the straight line model of log $h(t,a)$ is true. This indicates cancellation of one exponential term. This method yields two values for a and two time constants of the exponential function (i.e. the slopes of the straight line model). An eigenvalue analysis reveals that the time constants are the eigenvalues of the flow matrix, while the distinguished values for a determine the eigenvectors of the flow matrix. Thus the flow matrix can be calculated from this information.

This method was found to work well for uncorrupted data. But even a small amount of noise (2% and more) produced large errors in the estimated flows. A thorough analysis of this effect showed, that the presence of noise inhibits the determination of the right values for a from a goodness-of-fit condition ([14,15]). We will therefore exclude this method from further discussion.

2.3 Pulse Decay Method

The pulse decay method starts from the integral form of the tracer gas conservation law (9). It requires a suitable injection and measurement strategy that determines the vectors c_Δ, c_I and q_I in such a way, that the flow matrix f can be calculated with high accuracy. This strategy will be developed here. For a more general treatment of pulse injection tracer techniques see [12].

As already noted, the system of equations (9) is underdetermined and cannot be readily solved for the flow matrix. Sufficient information can be obtained by conducting two concentration measurements over different time intervals ΔT_1 and ΔT_2 with

$$\Delta T_k = [t_{k0},\ t_{k1}] \qquad ,\quad k = 1,\ 2 \tag{11}$$

First, we have to make some remarks concerning the choice of the time intervals relative to each other and with respect to the times of tracer gas injection. The intervals ΔT_1 and ΔT_2 should not overlap, because then their information content would not differ very much. On the other hand, they should not be spaced too far apart, because then the assumption of time independent flows becomes questionable. Furthermore, if ΔT_1 and ΔT_2 are chosen such that tracer gas injection and concentration measurement happen at disjunct time intervals, we can omit the source term q_I in (9). Figure 2 shows a time schedule for injection and measurement, that meets these requirements. The space between the intervals is just large enough to allow a quick release of tracer gas (pulse).

From each set of measurement values, we obtain the vectors (compare (10))

$$\underline{c}_{\Delta k} = \begin{vmatrix} c_1(t_{k1}) - c_1(t_{k0}) \\ c_2(t_{k1}) - c_2(t_{k0}) \end{vmatrix} \tag{12}$$

$$\underline{c}_{I,k} = \begin{vmatrix} \int_{t_{k0}}^{t_{k1}} c_1(t)\ dt \\ \int_{t_{k0}}^{t_{k1}} c_2(t)\ dt \end{vmatrix} \tag{13}$$

For each interval holds the conservation law (9). If we assume, that the air flows do not change between the begin of the first and the end of the second time interval (i.e. between t_{10} and t_{21}), then the flow matrices in both intervals are the same. Thus the conservation laws for both intervals can be combined into one matrix equation

$$\underline{\underline{c}}_{\Delta} = \underline{\underline{f}}\ \underline{\underline{c}}_I \tag{14}$$

with

$$\underline{\underline{c}}_{\Delta} = [\ \underline{c}_{\Delta 1}\ \underline{c}_{\Delta 2}\ ] \tag{15a}$$

$$\underline{\underline{c}}_I = [\ \underline{c}_{I,1}\ \underline{c}_{I,2}\ ] \tag{15b}$$

This set of equations is fully determined and can be solved for the flow matrix

$$f = \underline{\underline{c}}_I^{-1} \cdot \underline{\underline{c}}_{\Delta} \tag{16}$$

Although the basic procedure is rather simple, two problems might arise in the practical evaluation of (16). The first one concerns the accuracy with which the matrices c_Δ and c_I can be determined from noisy measurement data. The second problem is the inversion of the matrix c_I in case of (near) singularity. Both problems are discussed in some detail in [15]. Here we mention only briefly how they can be overcome.

The accuracy of the elements of c_Δ and c_I depends on the amount of noise with which the concentration decay curves are corrupted. While the integration in c_I tends to cancel out noise induced fluctuations, the accuracy of the elements of c_Δ is directly affected by the measurement noise. A better approach to the calculation of c_Δ is to fit the concentration decay curves with a parameter estimation algorithm. c_Δ follows then from the start and end points of the fitted curves. The advantage of this procedure is that all measurement values of each interval are used for the determination of c_Δ and not just the first one and the last one. Thus the error bounds for the elements of c_Δ are significantly reduced. c_I can be obtained in the same way, however the error reduction will be less pronounced.

Ill conditioning of the matrix c_I can be avoided by a suitable injection strategy. A good choice is (s. [12,15]):

1. prior to time interval ΔT_1:
   inject tracer gas only into zone 1, such that $c_1(t_{10}) > 0$, $c_2(t_{10}) = 0$.

2. prior to time interval ΔT_2:
   inject tracer gas only into zone 2, such that $c_2(t_{20}) \gg c_1(t_{20})$.

Additional protection from error amplification through near singular matrix inversion can be obtained by the use of a singular value decomposition algorithm for the inversion of c_I.

Figure 3 shows a typical measurement. The measurement values are denoted by markers, while the solid lines indicate the result of the parameter estimation. At first, we note that the parameter estimation determines the values at the beginning and the end of each interval with higher accuracy than the measurement values at these points. An inspection of the area under the concentration curves shows, that the diagonal elements of c_I are greater then the off-diagonal elements, which shows a good condition of c_I.

2.4 Two Tracer Method

The two tracer method is closely related to the pulse decay method. It is also based on the integral form of the tracer gas conservation law (9). Again, a second measurement has to provide the missing set of equations. Rather than performing the second measurement with the same tracer gas during a different time interval, two tracer gasses are used during the same time interval $\Delta T = [t_0, t_1]$. Thus, we obtain four sets of tracer gas concentrations $c_{k,i}(t)$, i.e. the concentration of tracer gas k in zone i for k, i = 1, 2. From these concentration values, we obtain the vectors (compare (12), (13))

$$\underline{c}_{\Delta k} = \begin{vmatrix} c_{k,1}(t_1) - c_{k,1}(t_0) \\ c_{k,2}(t_1) - c_{k,2}(t_0) \end{vmatrix} \tag{17}$$

$$\underline{c}_{I,k} = \begin{vmatrix} \int_{t_0}^{t_1} c_{k,1}(t)\,dt \\ \int_{t_0}^{t_1} c_{k,2}(t)\,dt \end{vmatrix} \tag{18}$$

Since the decay of both tracer gases is governed by the same air flow pattern, we can combine the tracer gas conservation for both tracers into matrix form as in Equation (14). We have a similar system of linear equations as in the pulse method. The matrices c_Δ and c_I are constructed from the corresponding vectors as in Equation (15). However, these vectors have a different meaning here, as can be seen by comparison of Equations (17), (18) with (12), (13). The flow matrix follows through solution of the system of linear equations according to (16).

Again some remarks concerning the accuracy of the matrices c_Δ and c_I are appropriate. Basically, the considerations of the pulse decay method apply here also. Especially the elements of the matrix c_Δ are obtained in the same way as before. Singularity of c_I can be avoided by a similar injection strategy:

prior to time interval ΔT:
- inject tracer gas 1 only into zone 1,
- inject tracer gas 2 only into zone 2,

such that $c_{1,1}(t_0) > 0,\ c_{2,2}(t_0) > 0$
and $c_{1,2}(t_0) = 0,\ c_{2,1}(t_0) = 0$.

Figure 4 presents an illustrative example. Again, measurement points are denoted by markers and solid lines stand for concentration profiles which are calculated from parameter estimations. Diagonal elements of matrix c_I are large in comparison with off-diagonal elements, as coinciding numbers of zone and gas yield higher concentrations than mixed combinations of these numbers do.

Although the mathematical description and numerical evaluation for the two tracer gas method and the pulse decay method are rather similar, there are considerable differences in the practical application.

The use of two tracer gases usually doubles the experimental expense for gas handling and analyzing. On the other hand, it allows to gather sufficient data for the air flow analysis of a two zone building during only one measurement interval. Thus, if the assumption of time independent flows is questionable (as is always the case), we can expect the most accurate results from the two tracer method.

3. NUMERICAL SIMULATION

In this section, we will analyze the pulse decay method and the two tracer method by means of numerical simulation. To this end, we assume a set of given flows F_{ij}, i,j = 1,2, volumes V_i, and initial concentrations $c_i(0)$, i = 1,2 and calculate the resulting concentration curves of the forward problem (7). Synthetic data sets are obtained by corrupting these curves with additive noise. The performance of the various methods can be analyzed, if they are used to estimate the airflows from the synthetic data. The comparison of the estimated flow values with the original ones allows quantitative statements on the accuracy of each method. Since the eigenvalue analysis has already shown to be very sensitive to measurement errors it will not be included here.

3.1 Numerical Model

It was intended to compare the performance of the above mentioned methods for different magnitudes of the interzonal air flows as well as for different measurement durations. Two combinations of airflows were chosen, and for each one measurements over three different time periods were simulated.

In order to calculate the exact solution of the differential form of the homogeneous form of the tracer gas conservation law (7), the flow matrix f is expressed by its eigenvalues and eigenvectors:

$$\underline{\underline{f}} = \underline{\underline{M}}\ \underline{\underline{\Lambda}}\ \underline{\underline{M}}^{-1} \tag{19}$$

with

$$\underline{\underline{\Lambda}} = \begin{vmatrix} \lambda_1 & 0 \\ 0 & \lambda_2 \end{vmatrix}, \quad \underline{\underline{M}} = \begin{vmatrix} r_1 & r_2 \\ 1 & 1 \end{vmatrix}. \tag{20a,b}$$

λ_1 and λ_2 are the eigenvalues of f and the columns of M are the eigenvectors of f. The solution of (7) for q(t) =0 and a given initial concentration c(0) is then

$$\underline{c}(t) = \underline{\underline{M}}\ \exp(\underline{\underline{\Lambda}}t)\ \underline{\underline{M}}^{-1}\ \underline{c}(0) \tag{21}$$

with

$$\exp(\underline{\underline{\Lambda}}t) = \begin{vmatrix} e^{\lambda_1 t} & 0 \\ 0 & e^{\lambda_2 t} \end{vmatrix}. \tag{22}$$

The following numerical values were used for the simulation ($r = r_1 = -r_2$):

interzon. air exchange	F_{11} F_{22} F_{12} F_{12} in ℓ/h	f_{11} f_{22} f_{12} f_{12} in 1/h	λ_1 λ_2 in 1/h	r
low	-60 -60 20 45	-1/2 -1/2 1/6 3/8	-1/4 -3/4	2/3
high	-240 -240 80 180	-2 -2 2/3 3/2	-1 -3	2/3
	$V_1 = V_2 = 120$ ℓ			

The concentration decay is governed by the eigenvalue with the smallest magnitude (λ_1). The measurement time was therefore chosen in dependence on λ_1. Three different durations were simulated:

- short duration: $\tau_1 = 1/(2\lambda_1)$,
- medium duration: $\tau_2 = 1/\lambda_1$,
- long duration: $\tau_3 = 2/(\lambda_1)$.

The following measurement durations resulted for the two cases of low and high interzonal air exchange:

interzon. air exchange	duration of measurement in h		
	τ_1	τ_2	τ_3
low	2 h	4 h	
high	0.5 h	1 h	2 h

3.2 Generation of Synthetic Data Sets

This numerical model was used to simulate air exchange measurements for each method under investigation. Concentration values were calculated from these air flows every 20 s alternating for each zone. A second tracer gas injection in the middle of the measurement time was assumed for the case of the pulse decay method. Synthetic data sets were obtained from these concentration samples by adding Gaussian distributed white noise with a standard deviation of 10% of the initial concentration. About thousand data sets were generated

- for each measurement method (pulse decay and two tracer),
- for each system of interzonal airflows (low and high),
- for various measurement durations (τ_1, τ_2, τ_3).

3.3 Monte-Carlo-Simulation

The synthetic data sets were evaluated with the corresponding measurement methods in a Monte-Carlo fashion. Each run produced a slightly different result due to the different error signals. The frequency distribution of the estimated air flows was evaluated using histograms. The original values were determined correctly in most cases. From these histograms, we can calculate the relative standard deviation of each air flow value. Figure 5 shows the frequency distribution of F_{11}, F_{22}, F_{12}, F_{21} according to the system of high interzonal air flows obtained with the pulse decay method for a medium duration of the measurement (1 h). The relative standard deviations vary from 4.0% (F_{12}) to 10.6% (F_{21}). The influence of the measurement duration is shown in Figure 6 for F_{21} estimated with the pulse decay method for the measurement durations 0.5 h, 1 h and 2 h (high interzonal air exchange). The relative standard deviation drops from 20.3% to 4.8% with increasing duration.

3.4 Results

The results of the various simulation runs are compiled in Figures 7 and 8. Figure 7 compares the pulse decay method and the two tracer method for the system of high interzonal air flows.

The two tracer method performs well even for a short measurement duration of 0.5 h. An extended duration of 1 h decreases the relative standard deviation of the flows slightly to ca. 5 % and less. The pulse decay method achieves the same accuracy, if a measurement duration of 2 h is selected. Shorter durations produce unacceptable high errors.

Figure 8 shows the performance of the pulse decay method for high and for low air flows. (The curves for the high air flow case correspond to fig. 7.) The pulse decay method achieves an accuracy of 5 % and less for both cases, provided that the duration of the measurement is sufficiently long (2 h for the high, 4 h for the low air flow case).

4. EXPERIMENTAL EQUIPMENT AND MEASUREMENT RESULTS

Numerical simulation showed, that the pulse decay method and the two tracer method are both capable of delivering accurate results for the air flows in two zone buildings. It was therefore desirable to test these methods more thoroughly also under field like conditions.

To this end, a two zone test box and a flow generator were built. The test box consists of two air-tight chambers and a tubing system that provides air exchange paths between the chambers according to Figure 1. The flow generator consists of air pumps, flow meters and adjustable valves. It is connected to the tubing system of the test box and allows to establish arbitrary air flows between the chambers with high precision. The combination of the test box and the flow generator serves as a laboratory-scale two zone building model with well determined air flows.

These air flows were measured with the tracer gas system MULTI-CAT [16]. Beneath various types of single zone measurements it is also able to perform the above described three two-zone measurement methods.

This equipment was used to carry out measurements on the laboratory-scale model. The air flow systems produced by the flow generator were somewhat different than those reported here. However, the tracer gas measurements results were accompanied by the corresponding Monte-Carlo-Simulations. (See [14,15] for more details.) The results indicate, that in practical situations the total measurement time is critical. If it is chosen sufficiently long, then the pulse decay method delivers satisfactory results with one tracer gas only.

5. CONCLUSIONS

In conclusion, we can sum up with the following points:

- The eigenvalue analysis method is not suitable for field measurements with any sizeable scattering in the concentration profiles. It is of theoretical value only.

- For short-time measurements the two/multiple tracer method promises to yield better accuracy than the pulse decay method. This is confirmed by evaluation results of both simulations and measurements. In this context the term "short-time" means a time interval in which typically half of the chamber volume is exchanged by the air flows.

- If, however, the pulse decay technique is applied for a longer period of time (e.g. corresponding to a two times exchange of the volume) it performs equally well as the short-time two tracer method. Again, this follows from MC-simulations as well as from laboratory measurements.

Since smaller and short-term fluctuations of the air change rate during a longer measuring period result in added noise superposed to the concentration profiles, this possible effect is already included to some extent in our MC-simulations with 10% noise. From their results one can draw the conclusion that such fluctuations should not be critical.

Therefore, the pulse decay method has to be considered as a very interesting and competitive technique, with similar accuracy as the two tracer method when properly used. It avoids higher equipment cost -as it is required for the two tracer method due to multiple or flexible analysers - and needs only one tracer gas.

Further investigations are planned in real buildings, under conditions which are not as steady as in a laboratory, in order to attempt a verification of the predicted well performance of pulse decay methods.

6. REFERENCES

[1] American Standard Test Method ASTM E 741, Determining Air Leakage by Tracer Dilution, Annual Book of ASTM Standards, Vol. 04.07

[2] Swedish Standard SS 02 15 56, Buildings - Determination of the total outdoor air flow (in swedish), identical to INSTA 131

[3] M.H.Sherman, D.J.Dickerhoff: A Multigas Tracer System for Multizone Air Flow Measurements, April 1989, submitted to Therm. Perf. Ext. Env. IV, AIVC #3428

[4] R.N. Dietz, R.W. Goodrich, E.A. Cote, R.F. Wieser: Detailed Description and Performance of a Passive Perfluorocarbon Tracer System for Building Ventilation and Air Exchange Measurements, Measured Air Leakage of Buildings, ASTM STP 904, pp. 203-64, American Society for Testing and Materials, Philadalphia, 1986

[5] R. Compagnon, A. Kohler, C. Roecker, C.-A. Roulet: Development of an Efficient Control Algorithm for a Multizone Constant Concentration Tracer Gas Air Infiltration Measurement System, Proceedings of the 9th AIVC Conference, Gent, Belgium, 1988, pp. 103-121

[6] J.J. Prior, C.J. Martin, J.G.F. Littler: An Automatic Multi-Tracer-Gas Method for Following Interzonal Air Movement, ASHRAE Annual Meeting, 1985

[7] C. Irwin: A Method of Measuring Air Movements in Compartmentalized Buildings, Ph.D. Thesis, University of Manchester, Institute of Science and Technologie, Dept. of Building, 1985

[8] B. Kvisgaard, P.F. Collet: Constant Concentration Measurement with Two Tracers, Proceedings of the 9th AIVC Conference, Gent, Belgium, 1988, pp. 181 - 193

[9] R.C. Fortmann, H.E. Rector, N.L. Nagda: A Multiple Tracer System for Real-Time Measurement of Interzonal Airflows in Residences, Design and Protocol for Monitoring Air Quality, ASTM STP 1002, American Society for Testing and Materials, Philadelphia, 1989, pp. 287 - 289

[10] F.W. Sinden: Multi-Chamber Theory of Infiltration, Building and Environment, Vol. 13, 1978, pp. 21 - 28

[11] C.F.A. Afonso, E.A.B. Maldonado, E.Skaret: A Single Tracer-Gas Method to Characterize Mult-Room Air Exchanges, Energy and Buildings, Vol. 9, 1986, pp. 273 - 280

[12] J. Axley, A. Persily: Integral Mass Balances and Pulse Injection Tracer Techniques, Proc. of the 9th AIVC Conf., Gent, Belgium, 1988, pp. 125 - 157

[13] S.B. Riffat, M. Eid: Measurement of Air Flow Between the Floors of Houses using a portable SF_6 System, Energy and Building, Vol. 12, 1988, pp. 67 - 75

[14] G. Schepers: Aufbau und Untersuchung verschiedener Meßverfahren zur Bestimmung des Gasaustauschs in Zwei-Zonen-Modellen, Diploma-Thesis (in German), Dept. of Physics, University of Siegen, June 1990

[15] F.D. Heidt, R. Rabenstein, G.Schepers: Performance and Comparison of Tracer Gas Methods for Measuring Air Flows in Two Zone Buildings, submitted to ASHRAE symposium "Field Studies on Ventilation Efficiency", New York, USA, 1991

[16] F.D. Heidt, R. Rabenstein: MULTI-CAT (multichannel concentration analysis of tracers) Dokumentation, Internal Report (in German), Dept. of Physics, University of Siegen, Nov. 1988

FIGURE CAPTIONS

Fig. 1: Nomenclature and air flow scheme in a two zone building model.

Fig. 2: Time schedule for injection and measurement for pulse decay measurement method.

Fig. 3: Concentration curves for pulse decay method.

Markers: + measured concentration in zone 1,
Δ measured concentration in zone 2.

Solid lines: Calculated concentrations from parameter estimations.

Fig. 4: Concentration curves for two tracer method.

Markers: + measured concentration in zone 1,
Δ measured concentration in zone 2.

Solid lines: Calculated concentrations from parameter estimations.

Fig. 5: Frequency distributions of results from Monte-Carlo-simulations (pulse decay method, case of high interzonal air flows, medium measurement duration): flows F_{11}, F_{22}, F_{12}, F_{21} and corresponding relative standard deviation.

Fig. 6: Frequency distributions of results from Monte-Carlo-simulations (pulse decay method, case of high interzonal air flows, flow F_{21}): short, medium, long measurement duration (top down) and corresponding relative standard deviation.

Fig. 7: Comparison of the pulse decay method (solid lines) and the two tracer method (dashed lines): relative standard deviations for the case of high interzonal air flows and different measurement durations.

Fig. 8: Pulse decay method: comparison of the cases of high and low interzonal air flow. Relative standard deviations for different measurement durations.

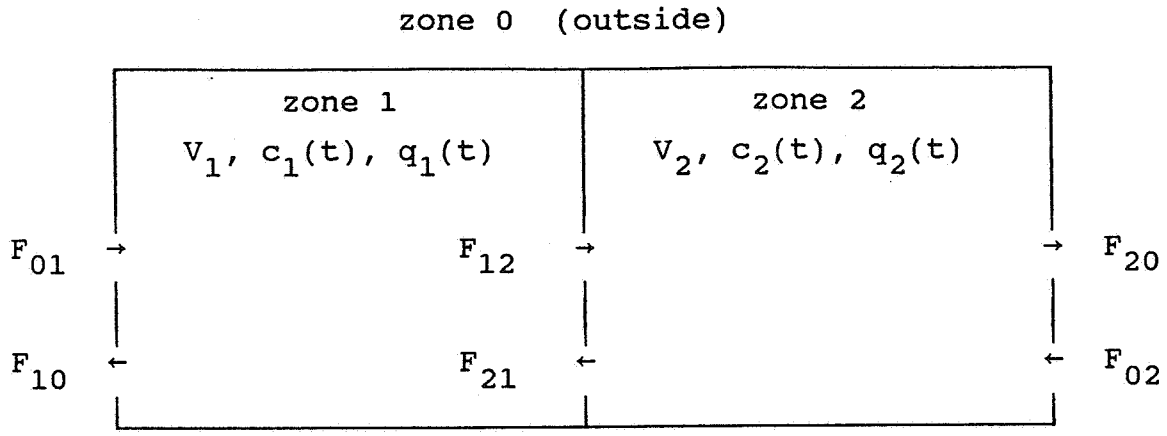

Figure 1

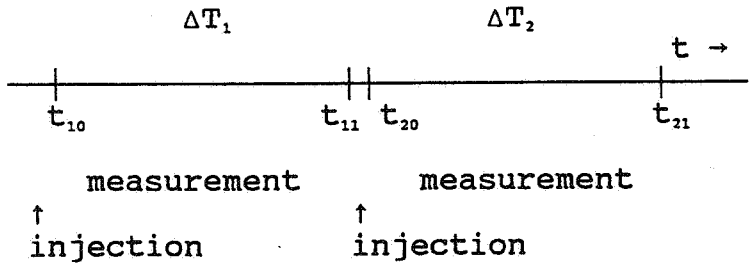

Figure 2

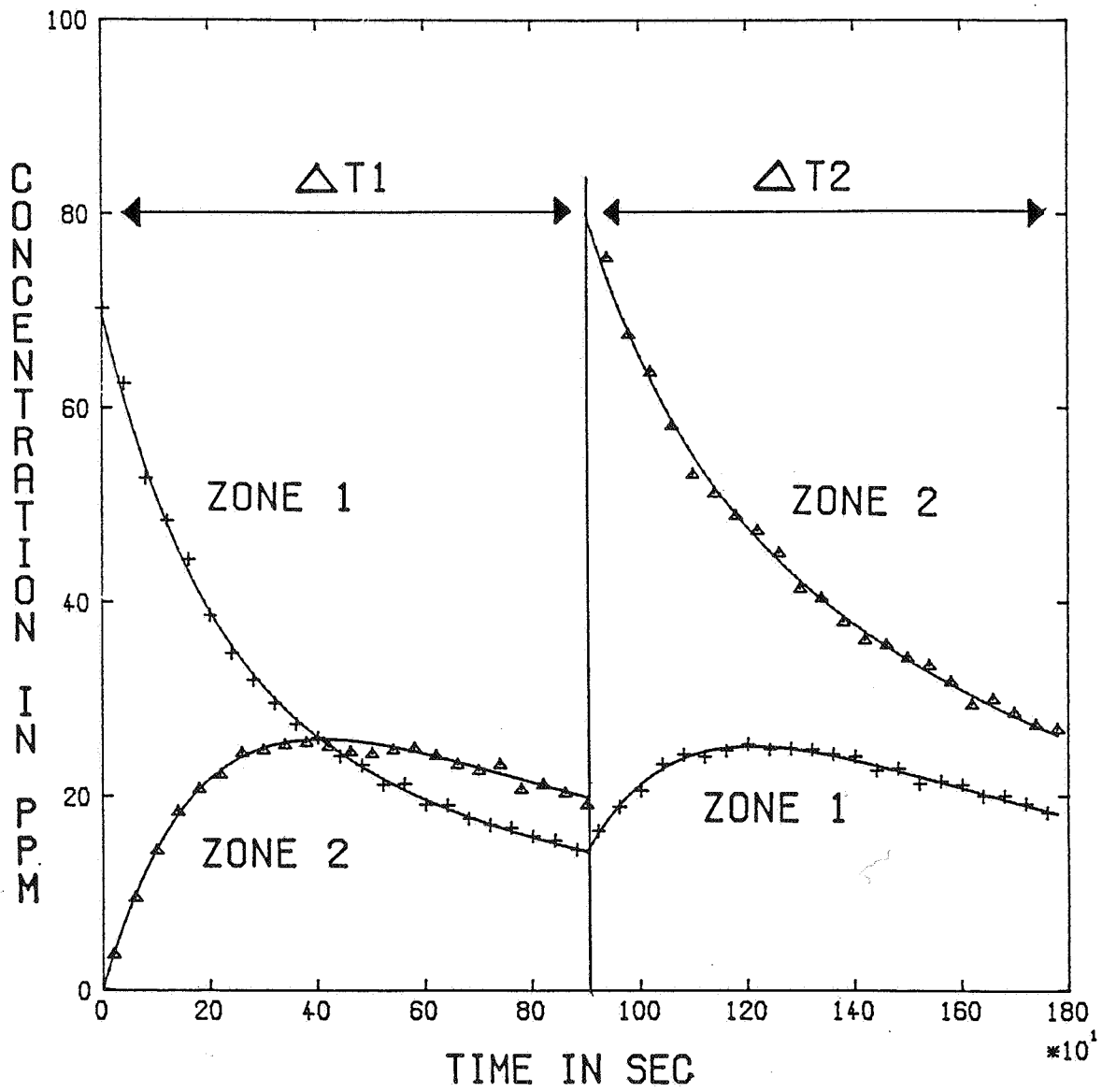
CONCENTRATION IN PPM
100
80
60
40
20
0
△T1
△T2
ZONE 1
ZONE 2
ZONE 2
ZONE 1
0
20
40
60
80
100
120
140
160
180
*10¹
TIME IN SEC

Figure 3

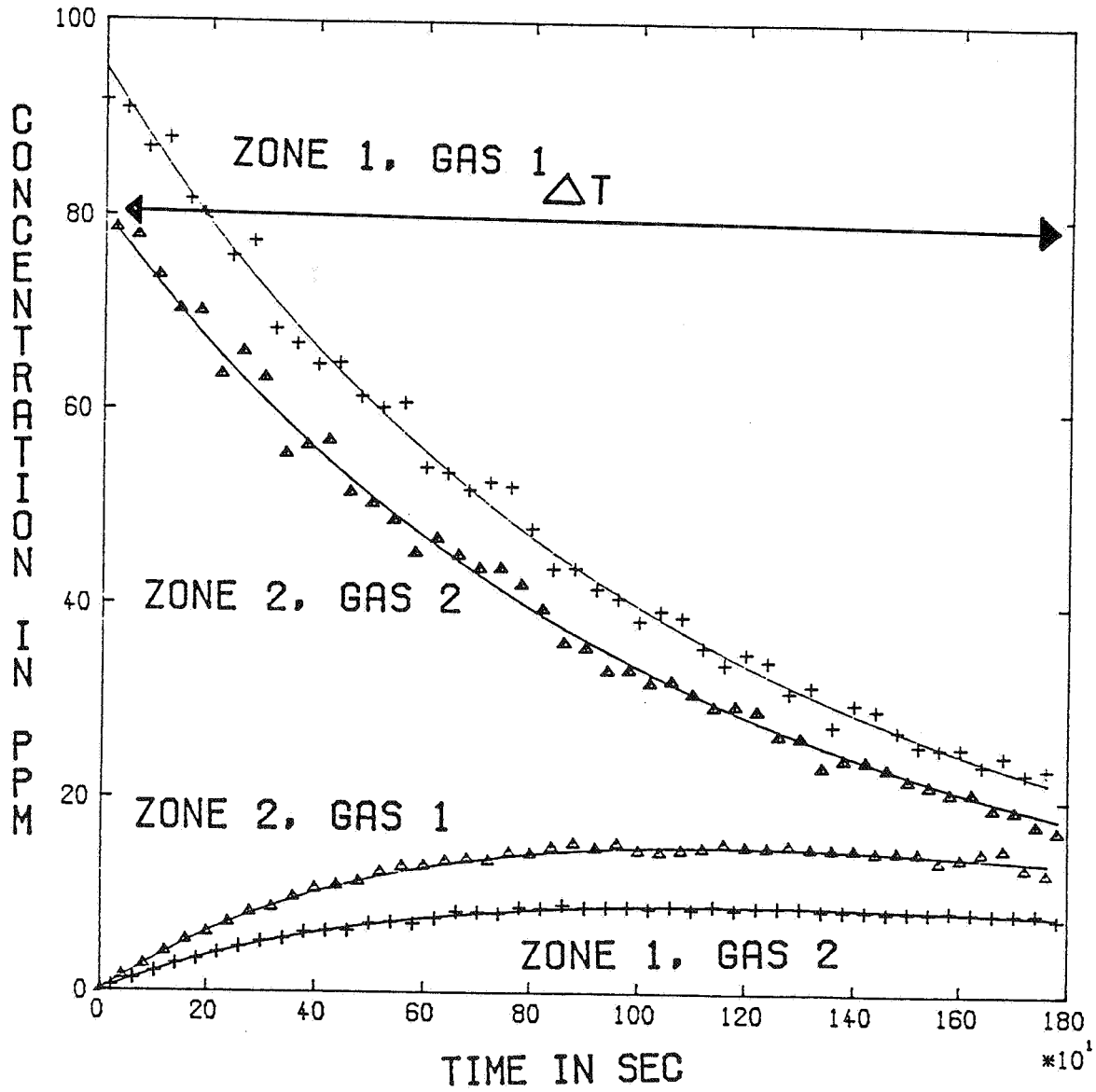
CONCENTRATION IN PPM
100
80
60
40
20
0
ZONE 1, GAS 1
ΔT
ZONE 2, GAS 2
ZONE 2, GAS 1
ZONE 1, GAS 2
0
20
40
60
80
100
120
140
160
180
TIME IN SEC
*10¹

Figure 4

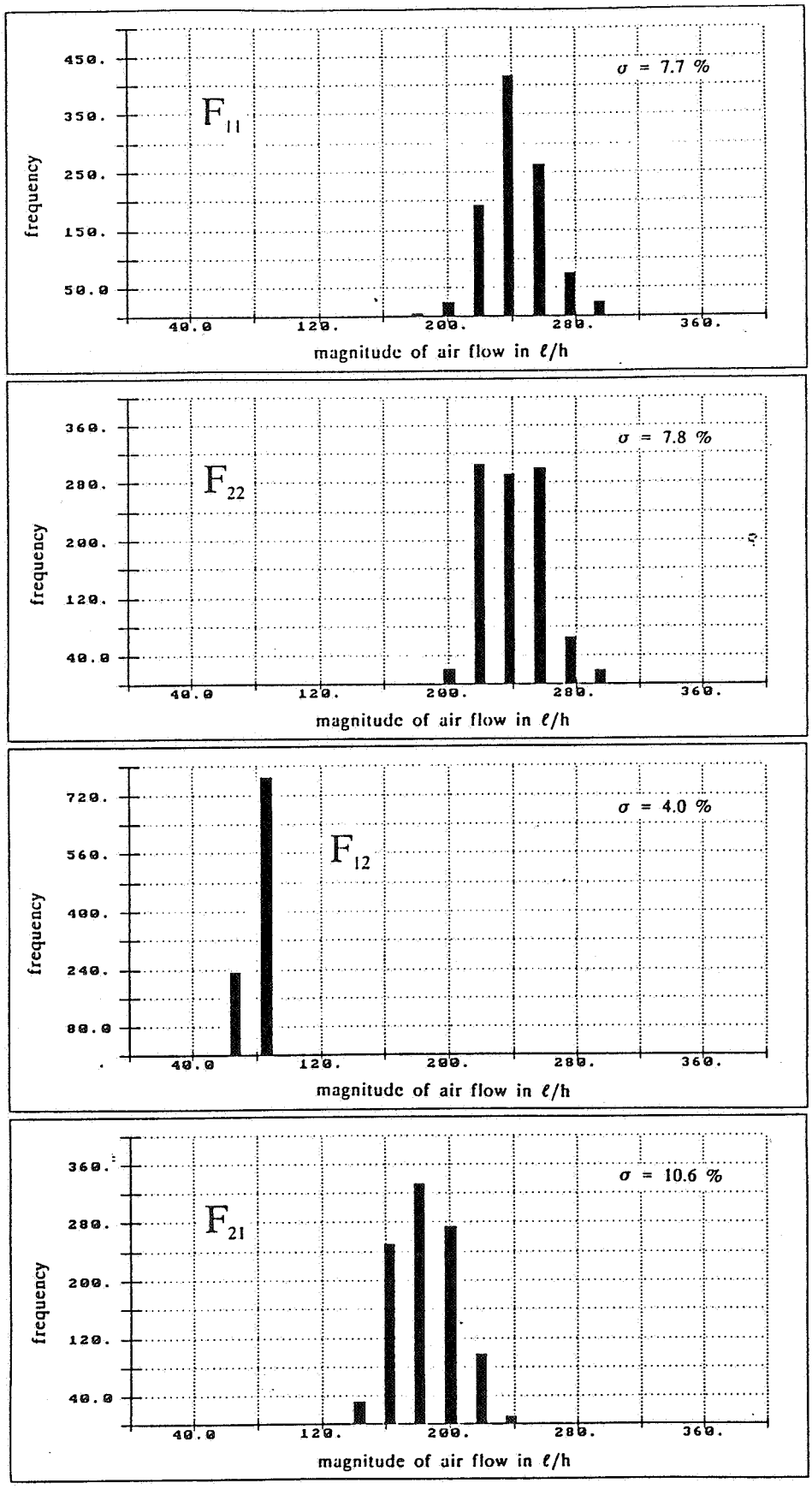
450.
350.
250.
150.
50.0
frequency
F_{11}
σ = 7.7 %
40.0
120.
200.
280.
360.
magnitude of air flow in ℓ/h
360.
280.
200.
120.
40.0
frequency
F_{22}
σ = 7.8 %
40.0
120.
200.
280.
360.
magnitude of air flow in ℓ/h
720.
560.
400.
240.
80.0
frequency
F_{12}
σ = 4.0 %
40.0
120.
200.
280.
360.
magnitude of air flow in ℓ/h
360.
280.
200.
120.
40.0
frequency
F_{21}
σ = 10.6 %
40.0
120.
200.
280.
360.
magnitude of air flow in ℓ/h

Figure 5

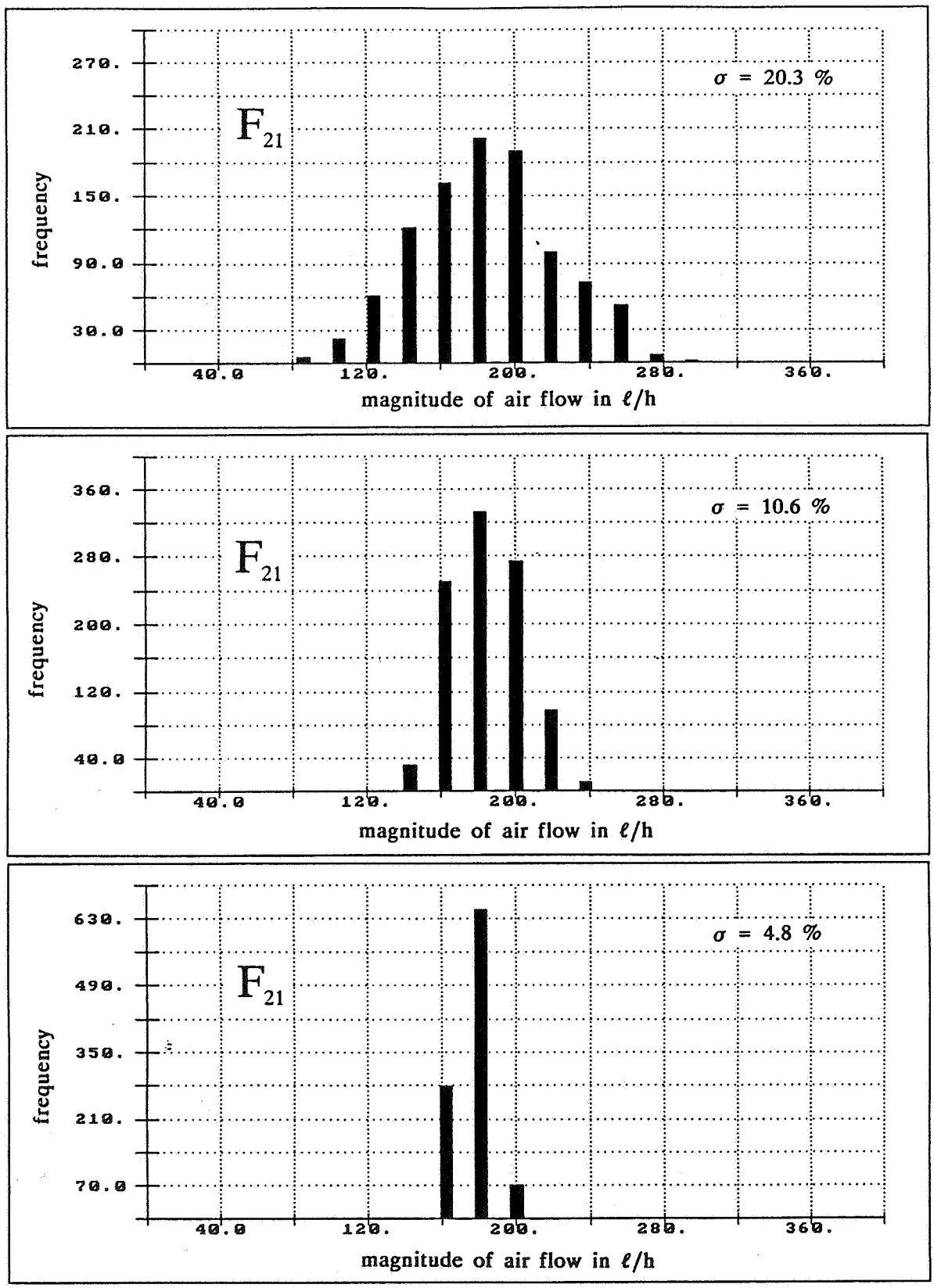
270.
210.
150.
90.0
30.0
frequency
F_{21}
σ = 20.3 %
40.0
120.
200.
280.
360.
magnitude of air flow in ℓ/h
360.
280.
200.
120.
40.0
frequency
F_{21}
σ = 10.6 %
40.0
120.
200.
280.
360.
magnitude of air flow in ℓ/h
630.
490.
350.
210.
70.0
frequency
F_{21}
σ = 4.8 %
40.0
120.
200.
280.
360.
magnitude of air flow in ℓ/h

Figure 6

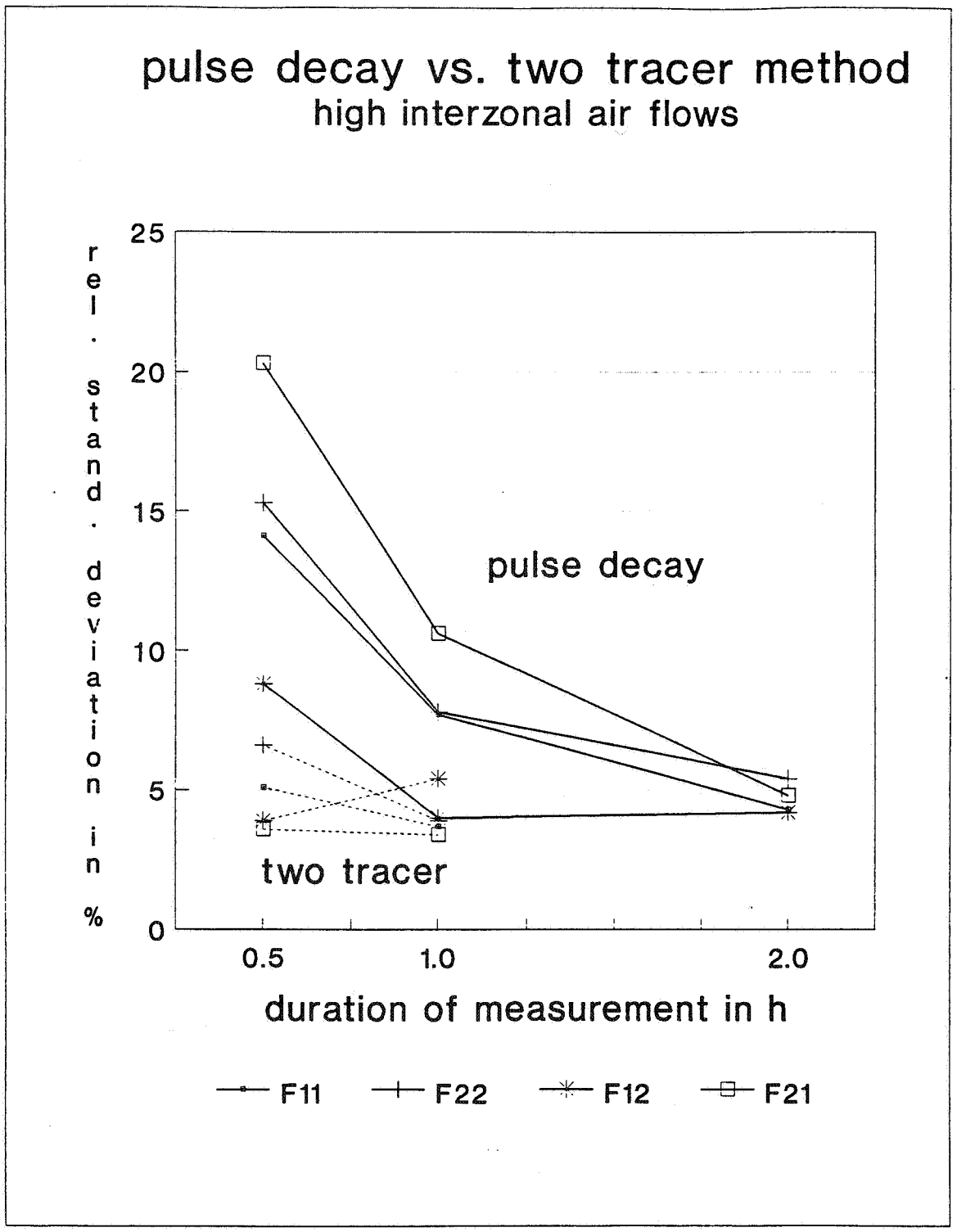
pulse decay vs. two tracer method
high interzonal air flows
rel. stand. deviation in %
25
20
15
10
5
0
pulse decay
two tracer
0.5
1.0
2.0
duration of measurement in h
F11
F22
F12
F21

Figure 7

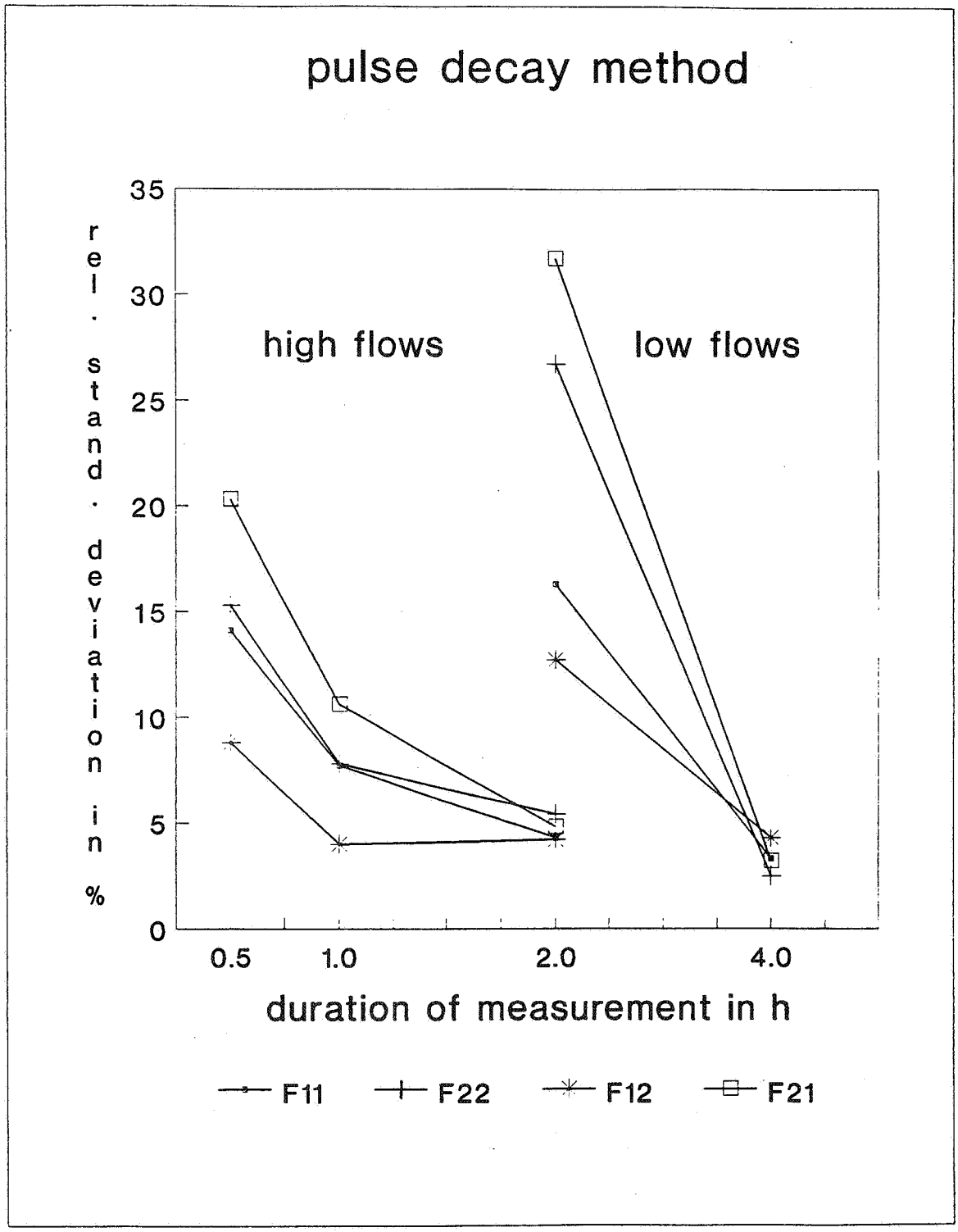
pulse decay method
rel. stand. deviation in %
35
30
25
20
15
10
5
0
high flows
low flows
0.5
1.0
2.0
4.0
duration of measurement in h
F11
F22
F12
F21

Figure 8

Discussion

Paper 10

M.Liddament (AIVC, UK)

Your comparison represents a special case of the general multizone tracer measurement problem which was presented by Sherman at the 10th AIVC conference. Could you compare your findings with those?

R.Rabenstein, F.D. Heidt (Univ.of Siegen, Germany)

I am sorry that I don't remember the results of the paper by Sherman last year. But I would like to emphasise that our special case of comparison comprises very detailed investigations with numerical simulations and laboratory scale measurements as well. And the interesting outcome so far is that the accuracy of the wo tracer method and the pulse decay method become comparably good provided that the measurement time is sufficiently long.

Earle Perera (BRE, UK)

Would it be realistic to use the pulse-technique in a real building given that sufficient tracer (for measuring purposes) may not have moved to all zones (other than the one in which it was initially distributed) within the measuring period.

R.Rabenstein, F.D. Heidt (Univ.of Siegen, Germany)

The answer to this question can come only from field experience. We mentioned that point at the end of our conclusions. It may be helpful for measuring under field conditions that we can select the integration borders according to the performance of measured concentration profiles. This could be a possibility to avoid the above-mentioned problem.

J.Axley (MIT, USA)

Several issues must be kept in mind: For multizone air flow determination we presently have; 1) Two injection strategies (constant and pulse injection); 2) Two mass balance formulations to form the inverse problems and; 3) The possibility of using single or multiple tracers. Pulse injection offers the advantages of requiring less gas and allowing relatively rapid completion of a test that both saves time and tends to avoid error induced by flow variation, but pulse injection must be more sensitive to imperfect mixing within the zone. Constant injection tests demand larger quantities of tracer gas and tend to take more time but constant injection tends to drive zones at more uniform concentrations (whether well-mixed or not) and thus tend to be less sensitive to imperfect mixing. Finally, if the resources are in hand one should prefer to use multiple tracers rather than single tracers, because the test procedure may be completed in less time and thus errors induced by unsteady flows will be avoided or minimized.

R. Rabenstein, F.D. Heidt (Univ.of Siegen, Germany)

This is a useful comment concerning the general classification of multizone air flow measuring techniques. But it reaches beyond the scope of our paper, in which we confined ourselves to two-zone-models with initial and or intermediate pulse decay and with one or two tracer gases.

VENTILATION SYSTEM PERFORMANCE

11th AIVC Conference, Belgirate, Italy
18-21 September, 1990

Paper 11

MEASUREMENT OF AIRFLOW IN HVAC SYSTEMS USING TRACER-GAS TECHNIQUES

S B RIFFAT[1] and M HOLMES[2]

1. Building Services Group,
Department of Civil Engineering,
Loughborough,
Leicestershire, LE11 3TU,
United Kingdom.

2. Arup Research and Development,
13 Fitzroy Street,
London, W1P 6BQ,
United Kingdom.

SYNOPSIS

This paper describes the use of tracer-gas techniques to measure airflow in a rectangular duct and a HVAC system. Experimental procedures are discussed for the application of the constant injection, pulse injection and decay techniques using N_2O and SF_6 as tracer gases. This paper also describes a new tracer-gas system with variable sampling speed which was used to measure the decay of tracer-gas concentration. A comparison is presented between tracer-gas measurements and those made with a pitot tube and a hot wire anemometer.

LIST OF SYMBOLS

C	tracer gas concentration (ppm)
C_0	concentration of tracer gas at t = 0 (ppm)
F	volumetric flow rate (m^3s^{-1})
V	effective volume of the duct (m^3)
q	injection flow rate of tracer gas (m^3s^{-1})
G	tracer volume generation rate (m^3s^{-1})
I	air exchange rate (h^{-1})
t	time (s)
X	distance from the duct inlet in the direction of flow (m)
D_h	hydraulic diameter of the duct (m)
W	duct width (m)
H	duct height (m)
α	an instant in time within a given interval (s)

1. INTRODUCTION

Indoor air quality, thermal comfort and energy use in buildings are largely dependent on the performance of HVAC systems. Incorrect ventilation rate is a common cause of poor indoor climate in office buildings and this can have detrimental effects on the occupants. If these problems are to be avoided, frequent checks on the performance of HVAC systems must be carried out. Measurement of air flow in HVAC systems is usually carried out using traditional instrumentation such as, hot-wire anemometers, vane anemometers and pitot tubes. This type of instrumentation is difficult to employ in practice as a long measuring duct is required for the establishment of fully developed flow profiles. In addition, traditional instrumentation fails to give an accurate picture of the performance of the HVAC system as a whole.

Tracer-gas techniques such as constant injection, constant concentration, concentration decay and pulse injection offer an alternative approach for measuring air flow in HVAC systems and unlike traditional instrumentation, are not limited by the complexity of duct configurations. Tracer-gas techniques can be used to measure flow rates over a wide range of values (i.e. laminar and turbulent flow) as very low concentrations of tracer gas can easily be detected using gas chromatographs. Moreover, tracer-gas techniques can be used to measure flow rates directly and do not require determination of the cross-sectional area of the duct or the flow profile at the duct wall. One further application, in which the use of tracer-gas techniques offers considerable advantages over the deployment of traditional instrumentation, is the determination of the air tightness of air ductwork. Control of air leakage is important if energy losses and leakage noise are to be minimised.

The literature contains only limited data on the use of tracer-gas techniques for measuring airflow in ducts[1-3]. The present study investigates the application of these techniques for the measurement of airflow in a duct and a HVAC system. Measurements of airflow made with tracer-gas techniques are compared with those made with a pitot tube and a hot wire anemometer.

2. FUNDAMENTALS OF TRACER-GAS TECHNIQUES

There are three fundamental ways to make use of tracer gases in air flow rate measurements:

Constant injection - The dilution of a tracer gas injected into the duct system at a fixed rate is used to infer the main flow rate.

Pulse injection - Uses the dilution of a short duration injection of a tracer gas.

Concentration decay - The rate of dilution of a known concentration is used to indicate the airflow rate.

The theoretical basis of each of these will now be discussed.

2.1 Constant Injection Technique

The constant injection tracer-gas technique can be used to measure air flow in ducts. Assuming that the air and tracer-gas are perfectly mixed within the duct and that the concentration of tracer gas in the outside air is zero, the mass balance equation is:

$$V\,dC_{(t)}/dt + F_{(t)}\,C_{(t)} = q_{(t)} \qquad (1)$$

The duct air exchange rate, I, is given by:

$$I_{(t)} = F_{(t)}/V \qquad (2)$$

Assuming that both the injection rate of tracer gas into the duct and the air exchange rate are constant during the measurement, the solution of equation (1) is:

$$C_{(t)} = q/F + (C - q/F)\exp(-It) \qquad (3)$$

If the system were close to equilibrium, the concentration of tracer gas would change slowly and the rate of change of concentration of tracer gas would be small. After a sufficiently long period, steady state conditions should be achieved. This means that the transient term in equation (3) would be close to zero and so the airflow can be calculated from:

$$C = q/F \qquad (4)$$

Hence, if measurements of tracer-gas flow rate and concentration can be made, F can be evaluated.

2.2 Pulse Injection Technique

This technique is based upon the injection into the duct inlet of a short-duration pulse of tracer-gas at a rate $G_{(t)}$. The variation of tracer concentration with time is measured at the duct exit. The amount of injected tracer gas is small, so it does not contribute significantly to the volume flow rate of air in the duct.

If we assume that the tracer gas is well mixed across the section of the duct, then the volume flow rate of tracer gas leaving the duct is equal to the product of the flow rate and the exit concentration, i.e. $F_{(t)}\,C_{(t)}$. If the tracer gas is assumed to be purged from the duct after some time interval, (t_1 to t_2) then the volume of tracer gas leaving the duct must equal to the amount injected. Applying the integral volume balance of tracer gas, we have:

$$\int_{t1}^{t2} F_{(t)}\,C_{(t)}\,dt = \int_{t1}^{t2} G_{(t)}\,dt \qquad (\text{for } F_{(t)} \geq 0) \qquad (5)$$

The integral mean value theorem can be applied to equation (5) as follows:

$$F_{(\alpha)} = \left[\int_{t1}^{t2} C_{(t)}\,dt\right]^{-1} \int_{t1}^{t2} G_{(t)}\,dt \qquad (\text{for } t_{t1} \leq \alpha \leq t_2) \qquad (6)$$

2.3 Concentration Decay Technique

This method involves an initial injection of tracer gas into the duct. The gas is allowed to mix with the internal air while the duct fan is switched off. The fan is then switched on and the concentration of tracer gas is monitored over a given time

interval. Assuming that the concentration of tracer gas in the outdoor air is negligible, and that there is no source of tracer gas within the duct (i.e. $q_{(t)} = 0$), equation (1) becomes:

$$V\, dC_{(t)}/dt = -F_{(t)}\, C_{(t)} \qquad (7)$$

This can be rearranged to give:

$$dC(t)/C_{(t)} = -(F_{(t)}/V)dt \qquad (8)$$

Equation (8) can be solved by integration (assuming F is constant) as follows:

$$\int_{C_{(0)}}^{C_{(t)}} dC_{(t)}/C_{(t)} = -(F/V)\int_{t=0}^{t=t} dt \qquad (9)$$

Hence:

$$1n\,(C_{(t)}/C_{(0)}) = -\,(F/V)\,t \qquad (10)$$

Equation (10) can be rewritten as follows:

$$C_{(t)} = C_{(0)}\ \exp(-It) \qquad (11)$$

This technique does not require the measurement of the absolute concentration of the tracer gas. If the logarithm of the tracer gas concentration is plotted against elapsed time, the slope of the line is equal to I. The volumetric flow rate, F, can be determined by multiplying the air change rate, I, by the effective volume of the duct.

3. MEASUREMENT OF AIRFLOW IN A DUCT

This section describes the equipment and techniques used to compare the methods outlined in section 2, and presents results obtained.

3.1 Experimental

The duct shown in Figure 1 was constructed from plywood 12 mm thick and had a bellmouth made from wooden bars. The duct was 2.43m long and had an internal cross-section of 250mm x 40mm. The downstream end of the duct was connected to the suction side of a centrifugal fan by means of a diffuser and the flow rate through the duct was varied using a slide gate located at the discharge end of the fan. The centrifugal fan was driven by an AC motor of 335W.

Static and velocity pressure tappings were positioned along the duct as shown in Figure 1. The velocity tappings allowed the insertion of a pitot tube which could be traversed across the duct cross-section in order to measure velocity at various distances from the wall. A single tube inclined manometer, made by Airflow Development Ltd, UK, was used to measure the static and velocity heads.

The following techniques were used to measure airflow rate in the duct:

i) Constant Injection Technique

Figure 2 shows the instrumentation used with the constant injection technique. Nitrous oxide tracer gas was injected at a constant rate into the duct inlet through a number of small injection tappings located around the perimeter of the duct inlet. These tappings were connected to a manifold by flexible tubing. Nitrous oxide was supplied to the manifold via a type, F-100/200, mass flow controller which had maximum flow capability of 1 Litre/min and was manufactured by Bronkhorst High-Tech B V, Holland. The measurement accuracy of the mass flow controller was ± 1%; the flow rate was controlled using a variable power supply and the rate of tracer gas injected was displayed on a digital unit. A steady flow rate was achieved by means of a reservoir between the N_20 cylinder and the mass flow controller. Initial tests of tracer-gas concentration (as measured by the gas analyser) showed fluctuations because of poor mixing of tracer gas and air. This difficulty was overcome using a honeycomb disperser at the inlet of the duct.

Samples of air and tracer gas were collected in a sampling tube that could be positioned at different points along the duct. The tube was mounted on a traversing mechanism that allowed samples to be taken at various distances from the duct wall. The concentration of N_20 tracer gas was measured by an IRGA 120 Infra-red Gas Analyser manufactured by J and S Sieger Ltd, UK.

ii) Pulse Injection Technique

Use of this technique involved the injection by syringe (Figure 3) of a known amount of tracer gas at the inlet of the duct. Multi-point injection was necessary for the approximation of a uniform concentration across the cross-section of the duct at the measurement point.

The concentration of tracer gas had to be measured at the downstream point to determine the the integral of the concentration. It was important to collect samples at different heights from the duct wall to obtain an average concentration of tracer gas across the duct. The concentration was determined by filling an air sample bag by means of a small pump. Sampling was begun one minute before the pulse was injected and continued until the pulse was completely purged from the duct. The concentration integral was determined by multiplying the average concentration by the time over which the sample bag was filled.

iii) Concentration Decay Technique

Air flow measurements were carried out using a microprocessor tracer gas system, Figure 4. This incorporated solenoid valves, tracer gas sample bags, a pulse pump, a microprocessor-based controller, a manifold and a by-pass valve. The sampling period of the tracer gas system could be adjusted over a wide range (seconds, minutes, hours, weeks or months). Sampling periods of minutes to months are normally used to measure averages of infiltration rate in buildings. As the decay of tracer gas in the duct was very rapid, short sampling periods (i.e. seconds) were required to measure concentration in these experiments.

The system was designed to take up to 40 samples at short or long intervals and its sampling period could be different during the transient and dominant periods of an experiment. In a typical experiment, a large number of samples were taken during the transient period and a small number during the dominant period. Use of a large number of data points for the transient period minimised the error in the term dC/dt

(see tracer gas equation 1) and hence allowed the air flow in the duct to be calculated more accurately.

Samples of air and tracer gas were collected from several points along the duct and injected automatically into a portable gas chromatograph/analyser. This allowed the concentration of tracer gas in each sample to be determined.

3.2 Results and Discussion

Measurements of airflow rate in the duct were carried out by means of the constant injection, the pulse injection and the decay tracer gas techniques. The first set of experiments was carried out using the constant injection technique. Tracer gas was injected into the duct inlet using the mass flow controller, as described in the experimental section. For small duct air flows, the rate of injection was approximately 0.35 Litre/min; for high air flows, it was approximately 0.75 Litre/min.

The concentration of tracer gas at different heights from the duct wall was measured at the fully developed region of the duct, i.e. $X/D_h = 100$; it was found to be smallest near the duct wall and reached a maximum value at the centre of the duct. The concentration profile across the duct cross-section was similar in shape to the velocity profile obtained using the pitot tube. Measurements of the centre-line concentration along the duct were carried out for various flow rates. The concentration of the tracer gas was found to decrease as X/D_h increased until it reached a constant value at the fully developed region of the duct.

The second set of experiments was performed using the pulse injection technique. A plastic bag and a small pump were used to collect air samples at the fully developed region of the duct. The pump was switched on one minute before the injection of tracer gas was begun and switched off several minutes after the injection was completed. The concentration of tracer gas was found to be slightly higher at measurement points furthest away from the duct wall.

The microprocessor-controlled tracer gas system was used in the third set of experiments which were conducted using the decay technique. With the sampling period set to one second, it was only with low air flows in the duct that we were able to determine the concentration of tracer gas. For flow rates greater than $0.05 m^3/s$ the decay of tracer gas was too rapid to allow measurements of tracer gas concentration.

Figure 5 shows a comparison between measurements of duct airflow rate made with the tracer gas techniques and those with a pitot tube. For small flow rates (i.e. below $0.02 m^3/s$) the results obtained from the tracer gas techniques were found to be in a good agreement with those obtained with the pitot-tube. For high flow rates (i.e. above $0.02 m^3/s$) the results obtained from the constant injection technique were found to be in closer agreement with the pitot-tube results than those obtained using the pulse injection technique and the decay method. Note, however that there are uncertainties in the measurements made with the pitot tube, which is sensitive to alignment with the flow and to turbulence level. Additional errors arise from the difficulty of measuring the velocity close to the duct wall and measuring the internal cross-sectional area of the duct.

Use of the pulse injection technique incorporates errors arising from the uncertainty in estimating the concentration integral. The error can be minimised if a large number of tracer gas samples are taken across the duct so that the concentration

obtained represents the real average value. The accuracy of using this technique can be further improved if the tests are repeated several times and an estimate of the repeatability of the experiments is thereby obtained.

Use of the decay technique produced the largest error as the decay of tracer gas concentration was very rapid and it was difficult to obtain a large number of data points at high flow rate. Modification of the present measuring equipment to allow a high sampling frequency (for example oils) would improve experimental accuracy. A further source of error arises from to the difficulty of measuring the effective volume of the duct.

4. MEASUREMENT OF AIRFLOW IN A HVAC SYSTEM

Comparison of measurements of duct airflow made with tracer gas techniques and a pitot tube showed that the constant injection technique was the most accurate. Further tests were carried out to establish the viability of this technique for measurement of airflow in a HVAC system. Experiments were performed in a room-sized environmental chamber connected to a HVAC system, see Figure 6; SF_6 rather than N_2O, was used as the tracer gas for safety reasons. An SF_6 gas analyser (type Binos 1) made by Leybold-Heraeus GMBH, was employed.

Measurements were carried out in the fresh-air supply and recirculated-air ducts of the HVAC system. Fresh air was drawn into the system from outside the building by means of a centrifugal fan which was driven by a variable speed DC motor and had maximum speed of 1400 rpm. The fresh-air supply was passed through a filter before being mixed with the recirculated-air at the Air-Conditioning Bench. The first set of measurements were carried out at various flow rates in the fresh-air supply duct. The equipment used to measure flow rates in the fresh-air supply duct is shown in Figure 7. SF_6 tracer gas was injected at a constant rate at a number of points in the inlet region of the duct and concentration of tracer gas was measured at positions upstream from the Air-Conditioning Bench.

Figure 7 shows a comparison of measurements of duct airflow made with the tracer gas technique and a hot-wire anemometer. A hot-wire anemometer was used in preference to a pitot tube as it allows more accurate measurement of flow rate at low air-velocity. The flow rate correlation between the tracer gas measurements and hot-wire measurements is given by:

$$F_{\text{tracer gas}} = 0.769\ F_{\text{hot-wire}} + 2.46 \times 10^{-3} \qquad (12)$$

General agreement was found between the tracer gas results and those obtained with the hot-wire anemometer; the average difference between the two sets of measurements was approximately 16%. Uncertainties arise in measurements made with the hot-wire anemometer as this instrument is sensitive to turbulence level. Additional errors arise as a result of the difficulty of measuring the velocity close to the duct wall and measuring the internal cross-sectional area of the duct.

The second set of measurements were carried out in the recirculated-air supply duct and the equipment used to make these measurements is shown in Figure 9. Tracer gas was injected at the merger point of the two return-ducts from the environmental chamber and the tracer concentration was monitored downstream from the bend in order to obtain good mixing, Figure 9. Measurements of the background concentration of tracer gas were also made as some tracer gas was contained in the recirculated flow from the environmental chamber.

Figure 10 shows a comparison of airflow measurements made in the recirculated-air supply duct with the constant injection technique and the hot-wire anemometer. The flow rate correlation between the tracer gas measurements and hot-wire measurements is:

$$F_{\text{tracer gas}} = 0.675\, F_{\text{hot-wire}} + 4.93 \times 10^{-2} \qquad (13)$$

The agreement between measurements made with the tracer-gas technique and those made with the hot-wire anemometer was not as good as was the case for measurements made in the fresh-air duct. This could be due to incomplete mixing of tracer gas and experimental error arising from the delay in measuring the background concentration of tracer gas. Use of a second gas analyser situated close to the sampling position would reduce this delay.

CONCLUSIONS

1. Tracer-gas techniques were found to be a simple and useful approach for measuring airflow in ducts.

2. Comparison of measurements made with a pitot tube and those made with different tracer-gas techniques showed that closest agreement was obtained for measurements made using the constant-injection technique.

3. The accuracy of airflow measurements in HVAC systems could be improved by sampling at a point immediately downstream of a filter, bend or heat exchanger coil to achieve good mixing of tracer gas.

4. The accuracy of measurements made with the decay and pulse injection techniques could be improved by more frequent sampling and better mixing of tracer gas.

ACKNOWLEDGEMENTS

We gratefully acknowledge the contribution of M. Goh and the financial support of the Science and Engineering Research Council.

REFERENCES

1. LUNDIN, L.
"Air leakage in industrial buildings-preliminary results".
Proceedings of the 4th AIVC Conference 'Air Infiltration Reduction in Existing Buildings' Elm, Switzerland, September 1983, pp.6, 1-6, 8.

2. AXLEY, J. and PERSILY, A.
"Integral mass balances and pulse injection tracer gas techniques".
Proceedings of the 9th AIVC Conference 'Effective Ventilation', Gent, Belgium, Paper No.7, September 1987.

3. RIFFAT, S.B. and LEE, S.F.
"Turbulent flow in a duct: Measurement by a tracer gas technique".
Building Services Engineering Research and Technology, 11(1), pp.21-26, 1990.

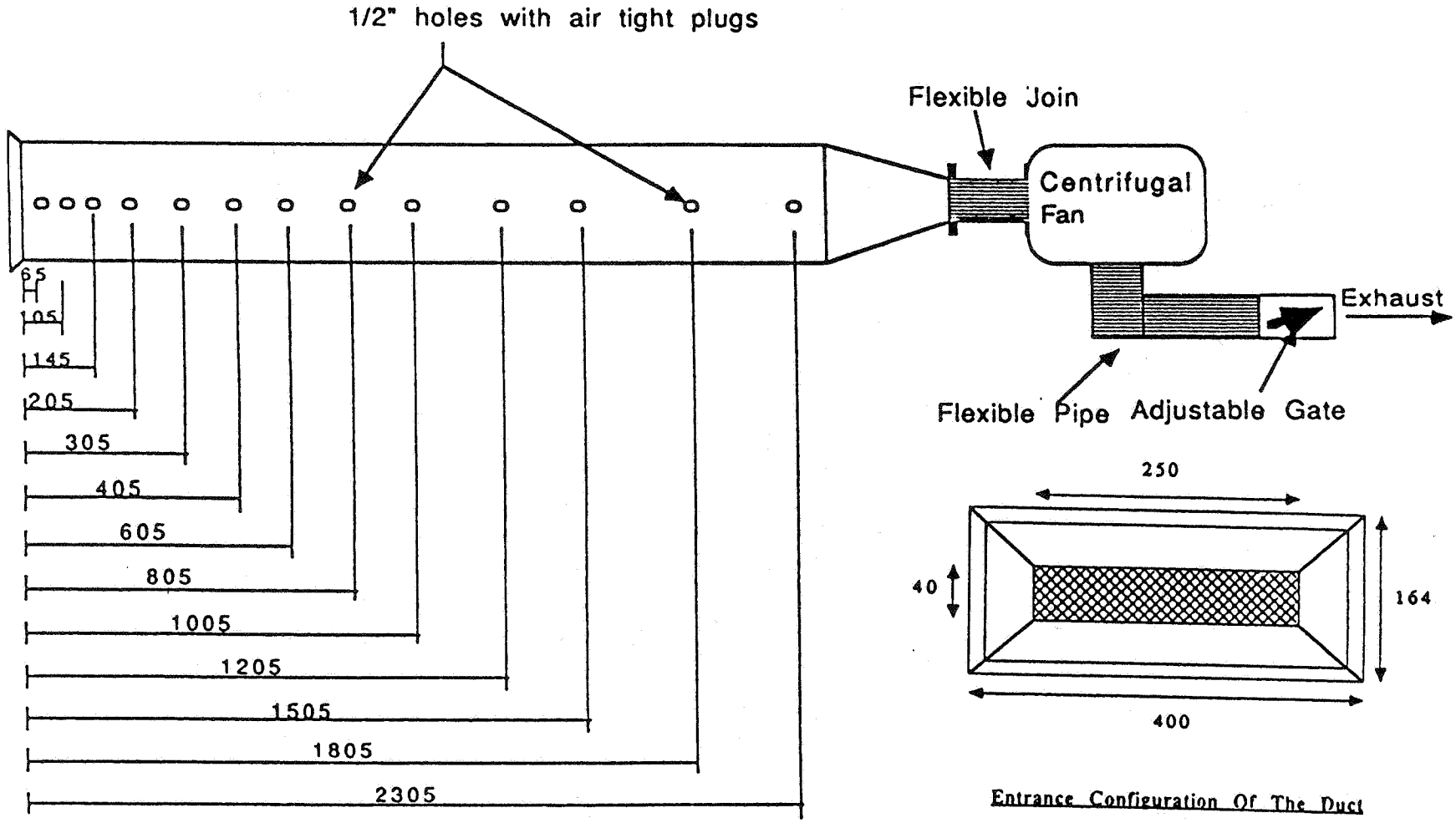

Figure 1 Schematic diagram of the duct system

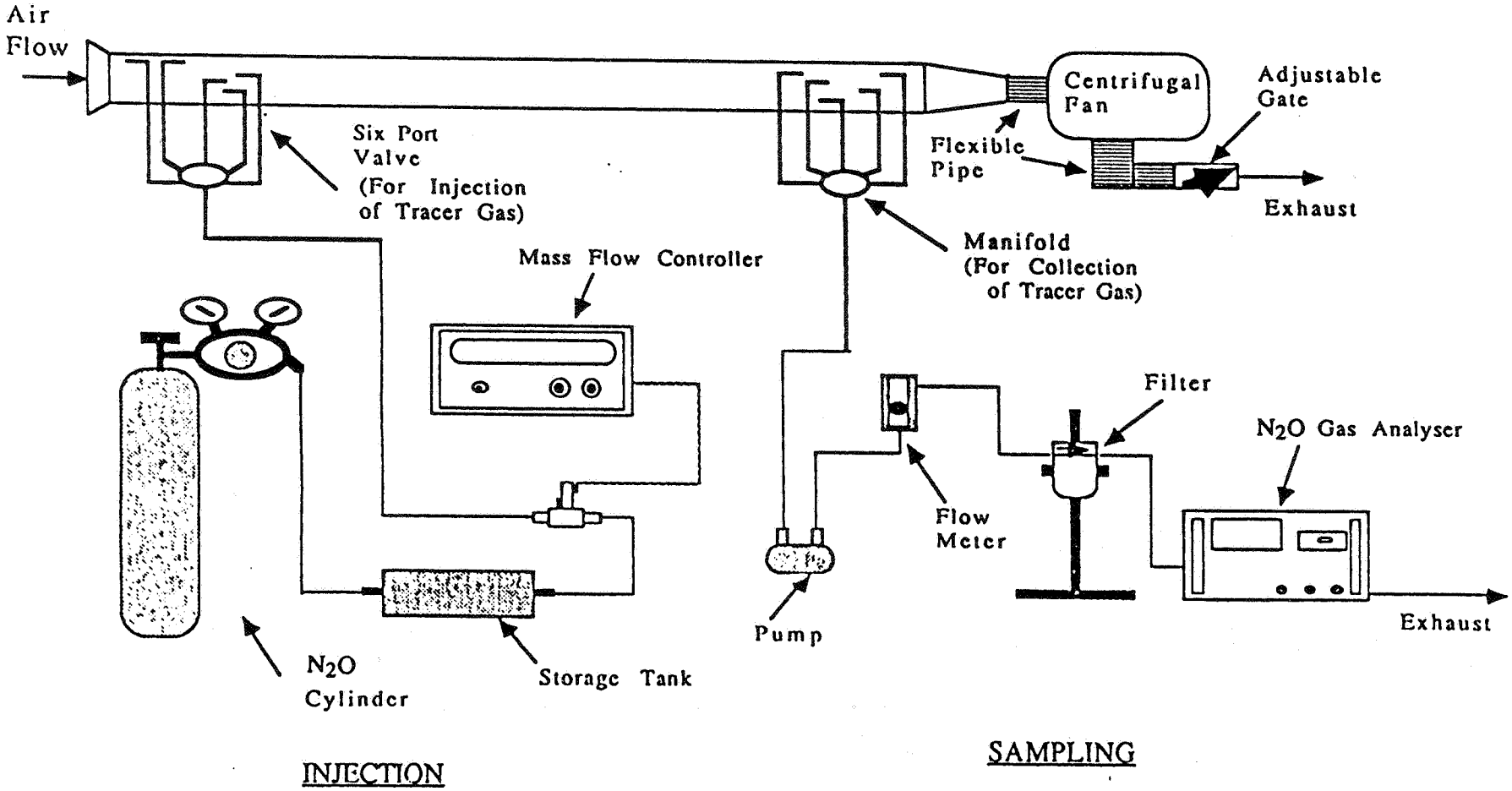

Figure 2 **Instrumentation for the constant injection technique**

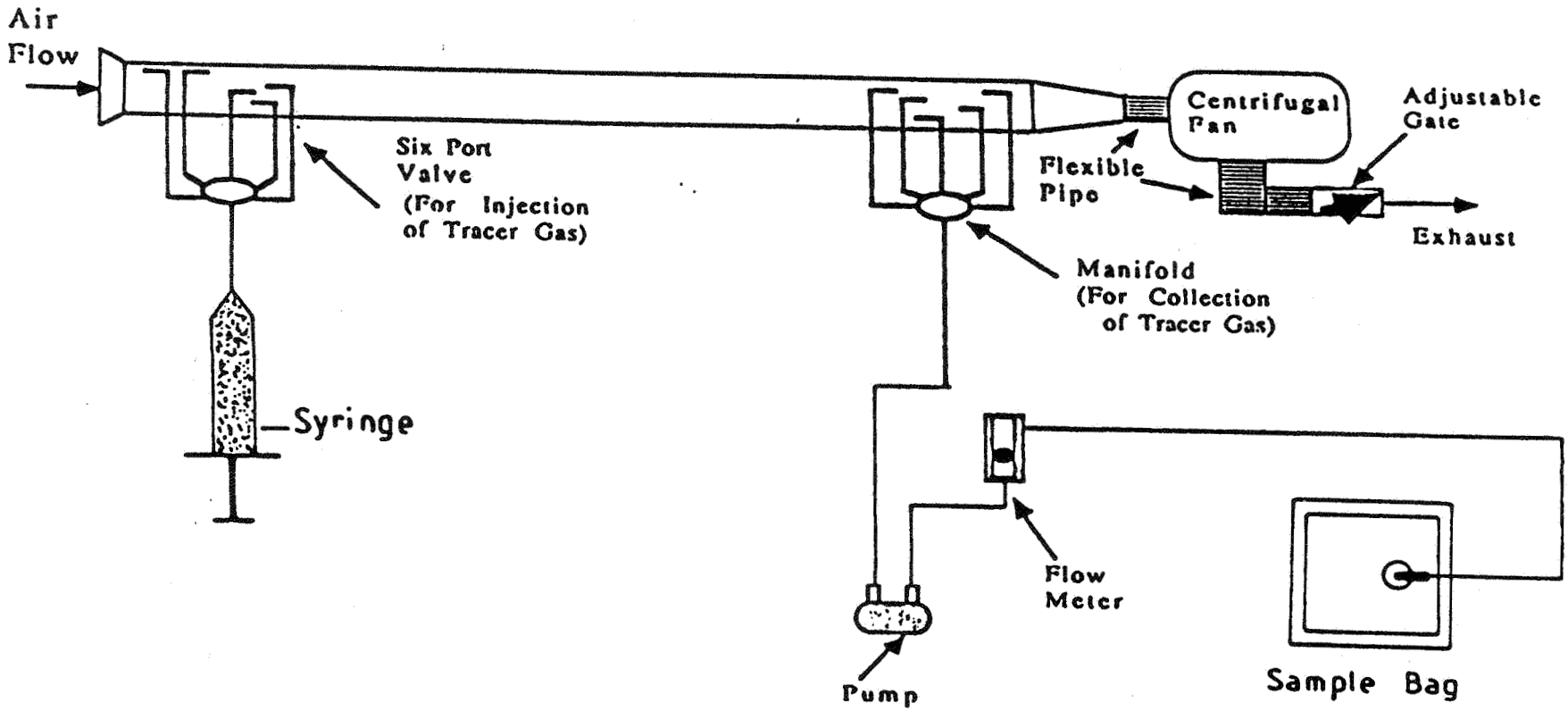

Figure 3 **Instrumentation for the pulse injection technique**

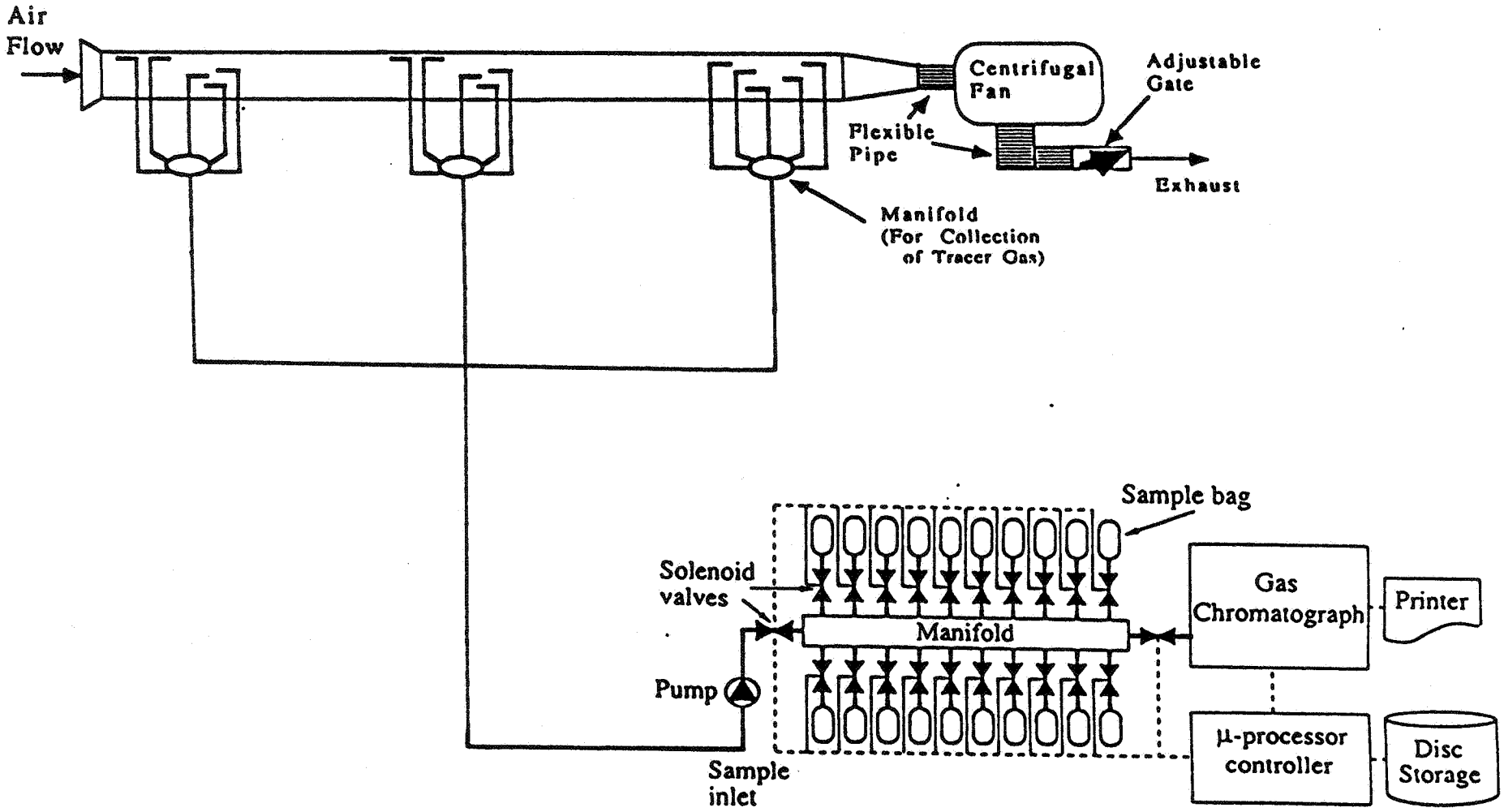

Figure 4 Instrumentation for the concentration decay technique

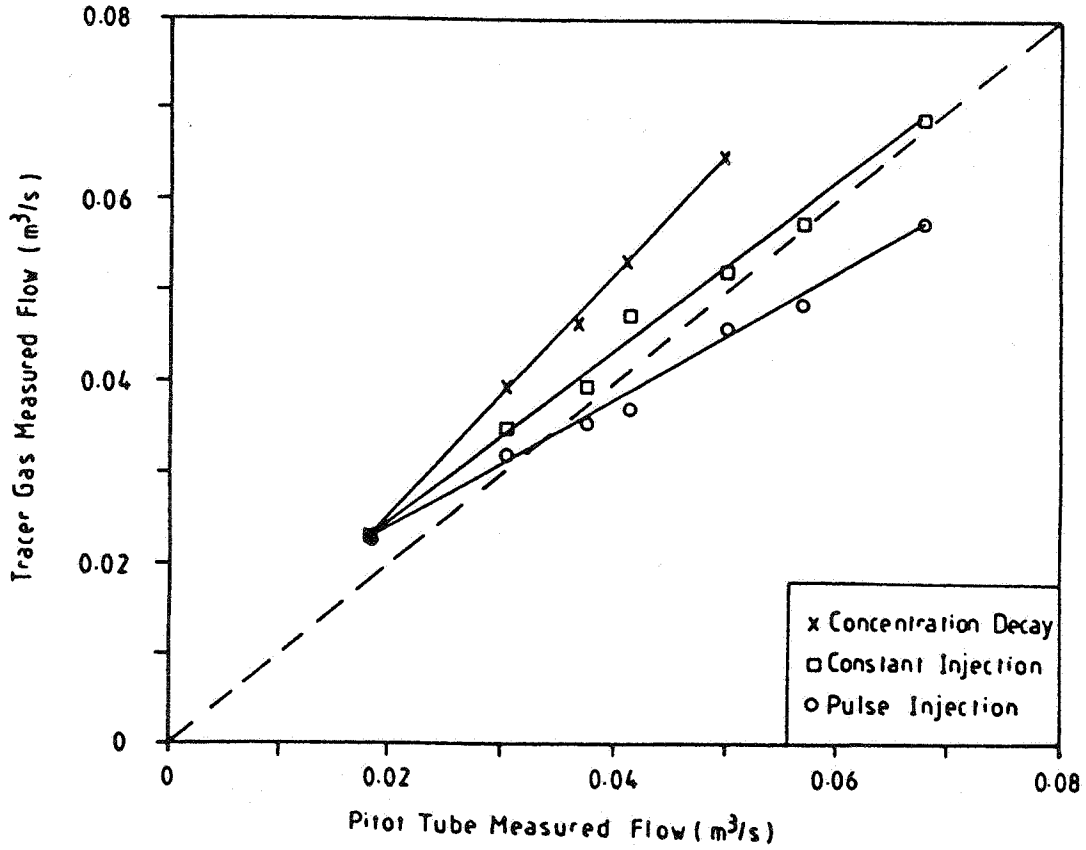

Figure 5 Comparison of tracer gas air flow measurements and measurements made with a pitot tube.

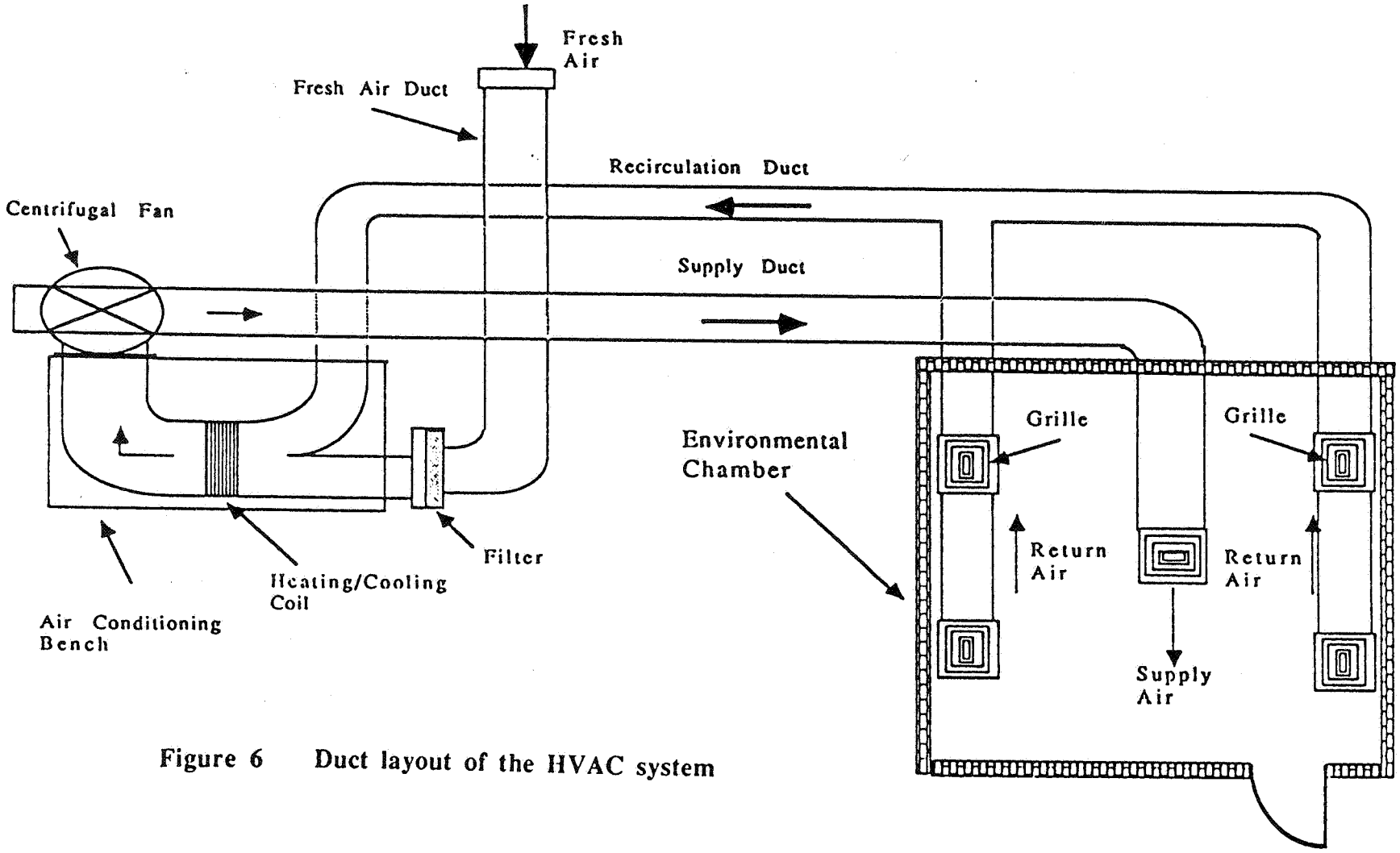

Figure 6 Duct layout of the HVAC system

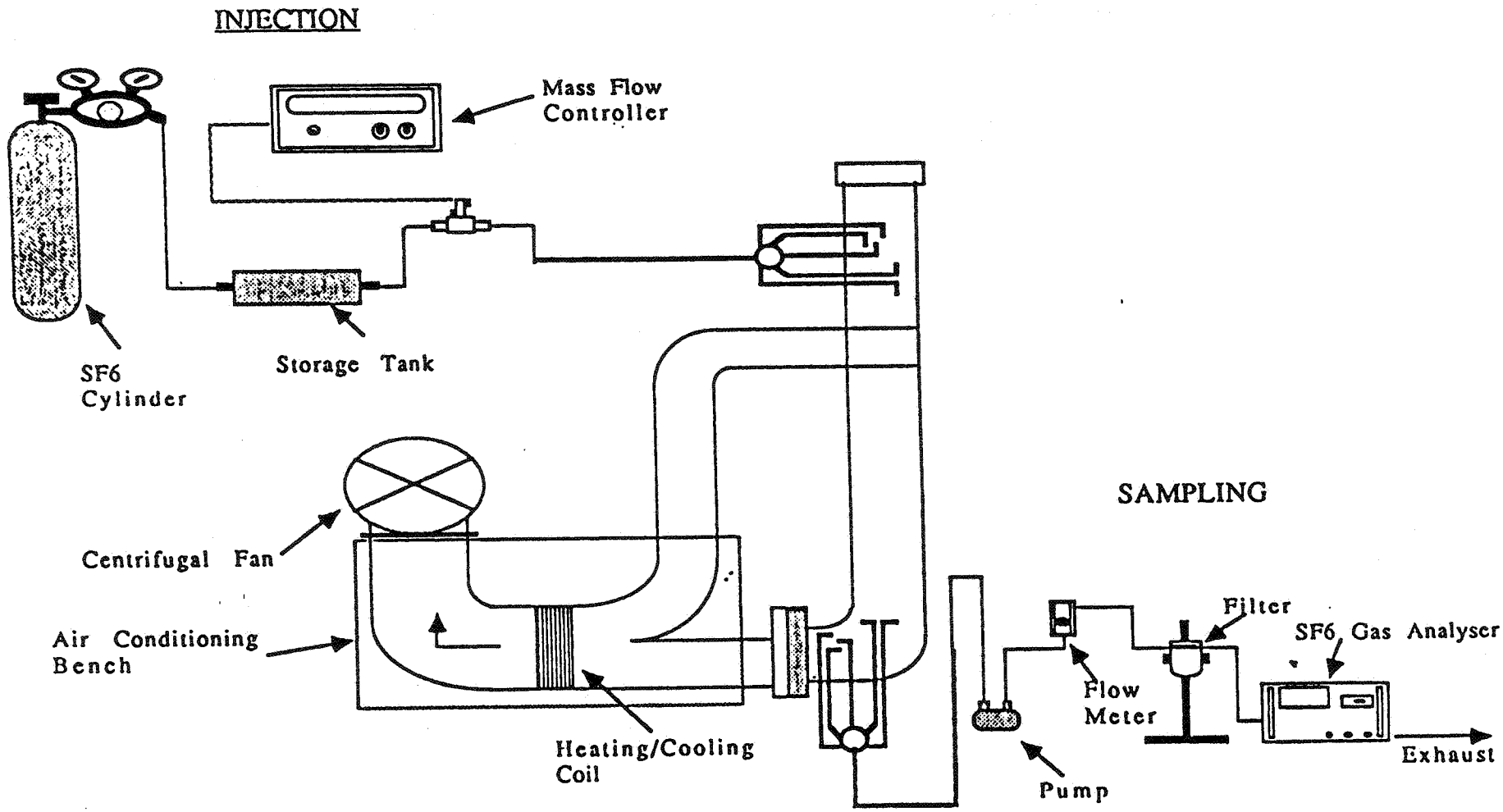

Figure 7 Equipment used to measure flow rate in the fresh-air supply duct

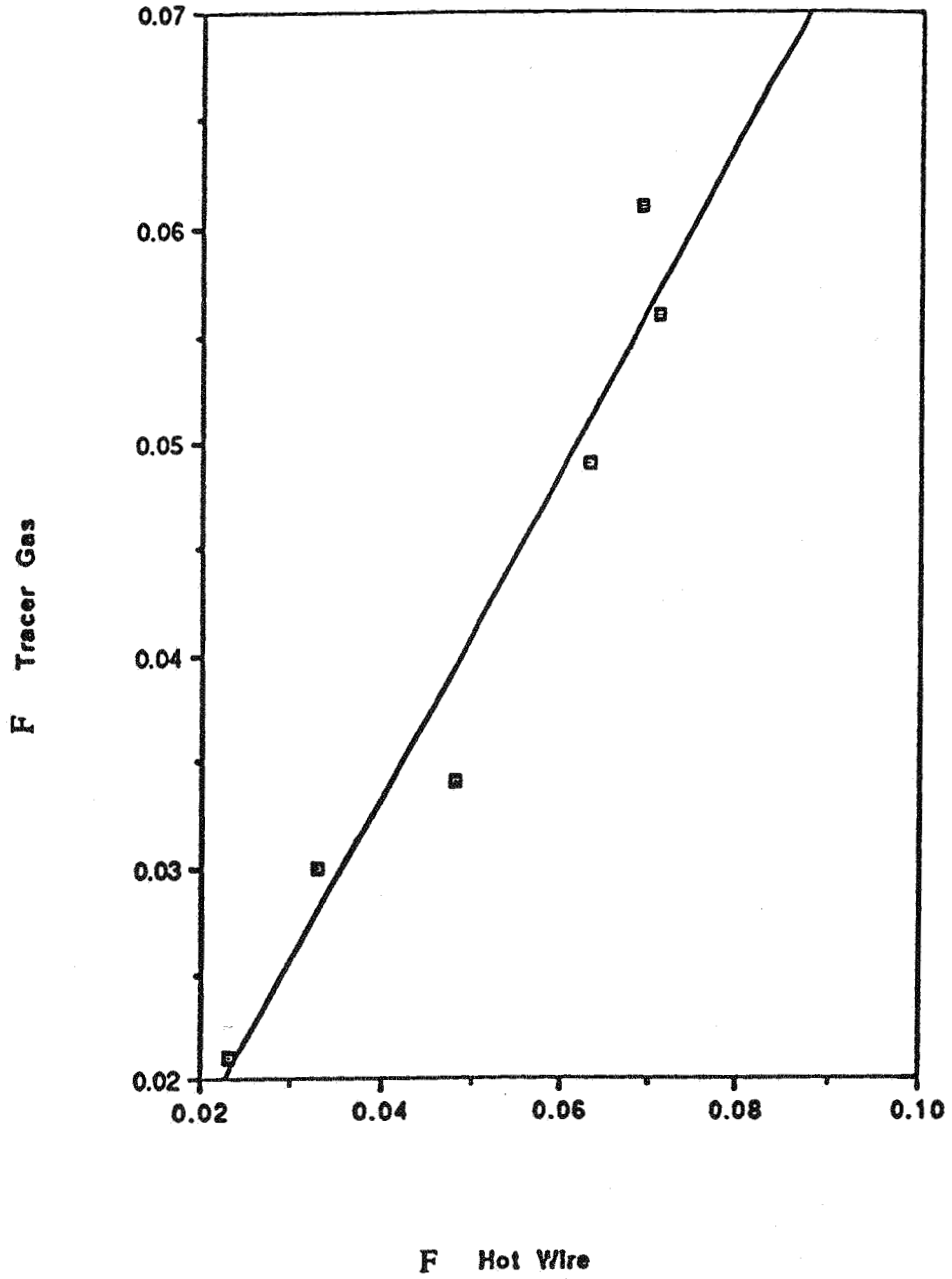

Figure 8 Comparison of airflow rate in the fresh-air supply duct measured with the constant injection technique and a hot-wire anemometer

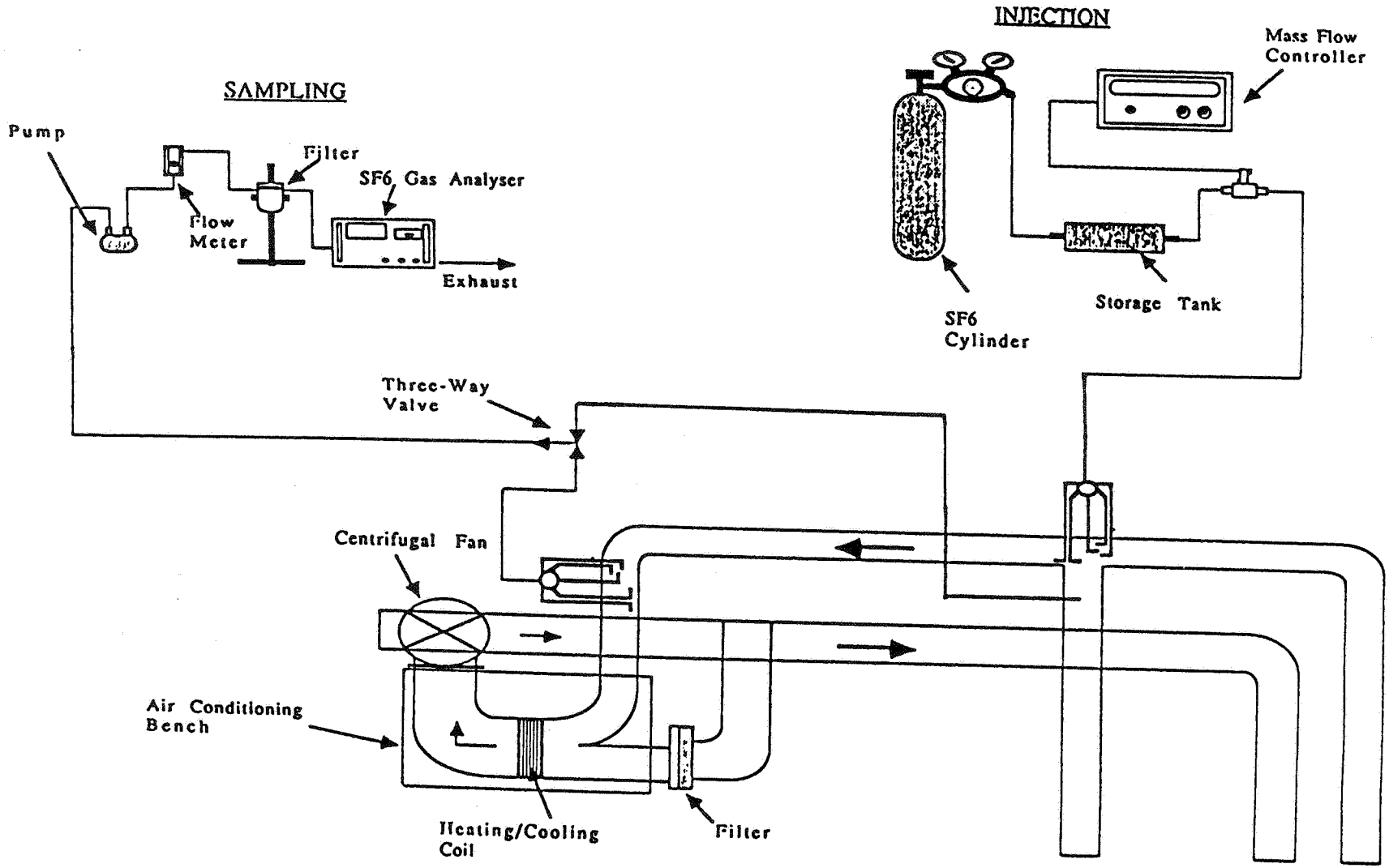

Figure 9 Equipment used to measure airflow in the recirculated-air supply duct

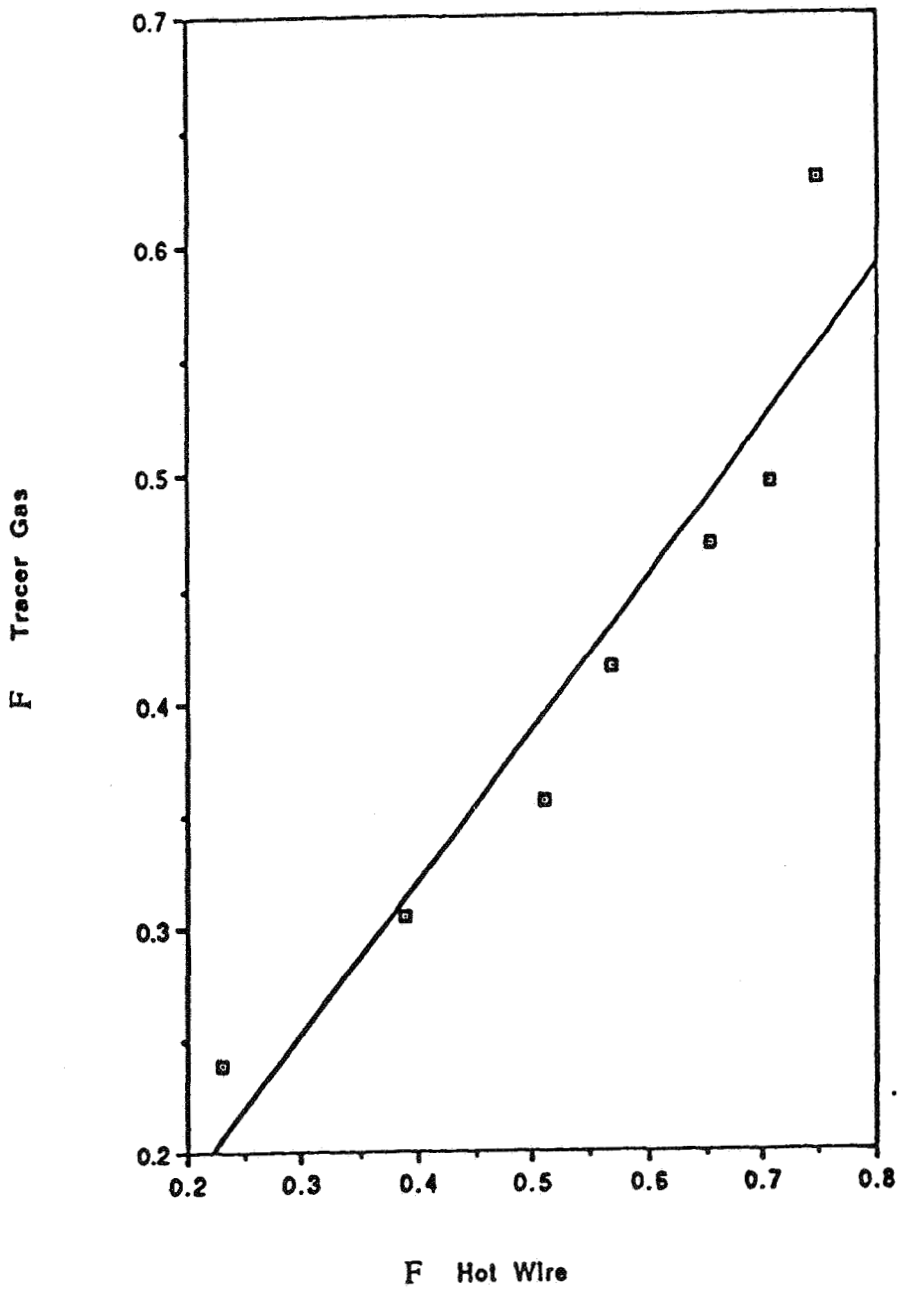

Figure 10 Comparison of flow rate in the recirculated-air supply duct measured with the constant injection technique and a hot-wire anemometer.

VENTILATION SYSTEM PERFORMANCE

11th AIVC Conference, Belgirate, Italy
18-21 September, 1990

Paper 12

VENTILATION EFFICIENCY ASSESSMENT IN RESIDENTIAL BUILDINGS

D. BIENFAIT

Centre Scientifique et Technique du Bâtiment
84 avenue Jean Jaurès, BP 02
77421 MARNE LA VALLEE CEDEX 2
FRANCE

FAX : (33-1) 64.68.83.50.

ABSTRACT

Ventilation efficiency may be defined as the capability of a given ventilation system to achieve the best balance between indoor air quality and energy conservation requirements :

- inside a room, ventilation efficiency is depending on air diffusion, which is mainly governed by air terminal devices and characteristics,

- in a partitionned building, ventilation efficiency is depending on air flowrates distribution, i.e. : air change values in each room as a function of time.

This second aspect is addressed in the present paper : a method based on a multizone computer model is derived ; this proposed method makes it possible to quantify the efficiency of the different ventilation systems in residential buildings.

LIST OF SYMBOLS

t	(h)	time
Pi(t)	(g/h)	pollutant emission rate at time t in room i
P(t)	(g/h)	pollutant emission rate at time t in the whole house
Ci(t)	(g/m^3)	pollutant concentration at time t in room i
ni(t)	(-)	number of occupants at time t in room i
n(t)	(-)	number of occupants at time t in the whole house
k	(m^3/h)	air amount breathed in one hour by an occupant
Q(t)	(m^3/h)	make up air flowrate at time t
Da	(W.h)	heat losses due to air change during heating season
Text(t)	(°C)	outdoor temperature assumed to be time constant
Ti	(°C)	indoor air temperature assumed to be time constant
Qb	(g)	quantity of pollutant breathed by the occupants alltogether during heating season
Qa	(m^3/h)	air quality flowrate
Qh	(m^3/h)	deperdition flowrate
NH	(h)	duration of heating season
e	(-)	ventilation efficiency.

1 – INTRODUCTION

Ventilation of residential buildings may be achieved according a wide range of different techniques, among them natural ventilation using vertical shafts, mechanical ventilation systems and many other techniques. These systems are designed to ensure both a sufficient level of air quality and good operating conditions, which include low energy consumption. Quality assessment of these various systems is an important issue because it may ease the development of more efficient systems.

The efficiency of a ventilation system may be defined as the capability of this system to ensure an acceptable air quality level (i.e. : mean pollutant concentration in the air, condensation hazards, ...) with as low energy consumption as possible.

It is well known that for some kinds of systems, for instance passive stack ventilation or humidity controlled systems, the air change is highly varying against time : in the case of passive stack ventilation, exhaust flowrates are more important in winter, which lead to poor over the year efficiency. Actually, the best efficiency would have been achieved with systems providing low exhaust flowrates when outdoor temperature is low, which is exactly the opposite of passive stack systems. An efficiency assessment method should therefore tend to take these phenomena into account.

2 - COMPUTER MODELS

Considering a ventilation system, the easiest way to assess the efficiency is to calculate over the heating season a mean value of pollutant concentration and condensation hazards. This may be done using a multizone computer code taking into account the phenomena which influence air movement and pollutant concentration (wind velocity, building shell air leakage, moisture transfer, ...) as well as the ventilation components (i.e. : fan, exhaust vent, ...) characteristics.

Although research work is still needed in order to improve the existing models, numerous codes have already been developped (see for instance fig. 1) and may be used in order to compute on a yearly basis the heat losses amount and the time dependent pollutants or moisture concentration in each room. The addressed problem is then, how to use these results in order to yield criteria for both air quality and heat losses level : we propose, here-after, definitions of criteria for air quality and heat losses (calculation details are in appendix).

3 - DEFINITION OF HEAT LOSSES CRITERION : Qh

Heat losses amount may be expressed by a so called "heat losses", Qh :

Qh (m^3/h) is the make-up air flowrate value which, assumed to be constant during the heating season, would lead to the same heat losses amount than the value calculated using the computer code.

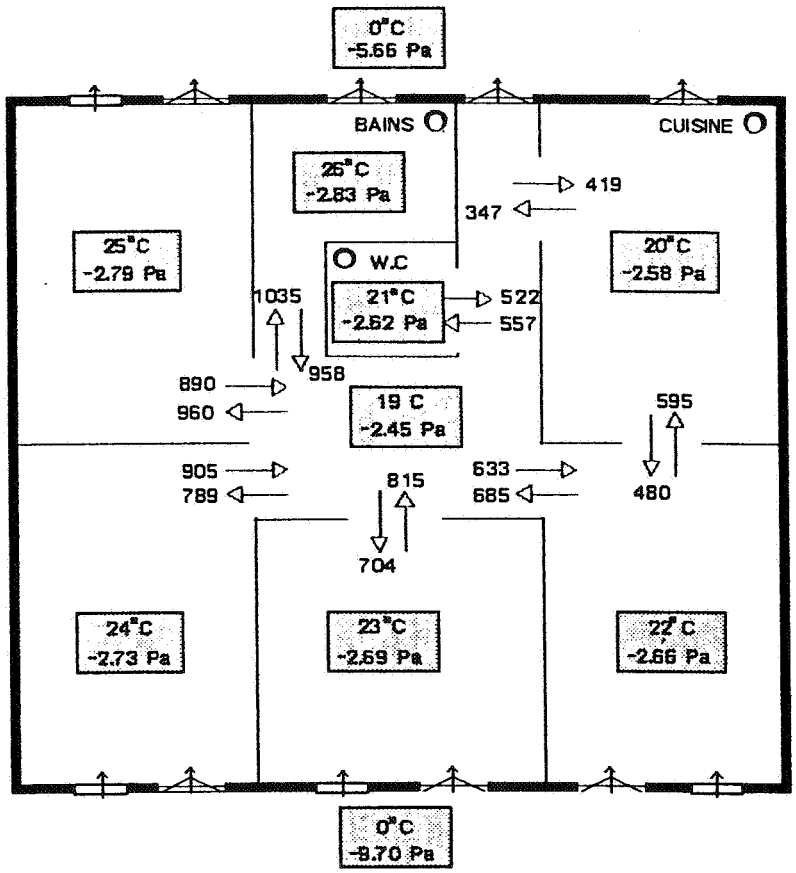

Figure 1 : Example of multicell computer codes result (code SIREN 2)

4 – DEFINITION OF AIR QUALITY CRITERION : Qa

General considerations

The health effect of indoor air pollutant exposure with regard to ventilation techniques assessment is almost impossible to evaluate on a deterministic basis for the following reasons :

- many pollutants are involved and there may exist some synergy between pollutants (i.e.: supposedly between radon and tobacco smoke)
- pollutant emission rates are considerably scattered according the house under consideration
- health effect of most pollutant is only known with a poor accuracy
- pollutants and furnishings may interact.

For these reasons, a practical way to account for pollutant concentration is to consider a single fictive pollutant called "virtual pollutant" which accounts for all the home air pollutants.

The criterion would then be the yearly amount of pollutant breathed by the occupants (it is consequently assumed that the relationship between exposure and health detriment is linear). This quantity may be calculated using multizone computer models, which requires some assumptions, relevant both to the occupancy schedule of each room and the "virtual pollutant" emission rate. In order to make things easier to handle it is proposed to express this in the following manner :

Air quality criterion, Qa

Qa (m^3/h) is the make-up air flowrate value which, assuming it to be constant all over the year and the air being perfectly mixed between rooms, would lead to the same amount of virtual pollutant breathed by the occupants than the value calculated using the computer code.

Ventilation efficiency, e

Usually the values of Qa and Qh are different. The ratio, e = Qa/Qh, is called the multizone ventilation efficiency.

5 - EXAMPLES

For real systems, calculations require detailed computer simulation, which allow to predict the pollutant concentration $C_i(t)$ in each room as a function of time t. The values of Qa, Qh and e can then be derived according to appendix 1.

However, for some very simple cases, the calculations may be readily hand made without any computer model. This is illustrated by the two simple following examples :

First example :

Let us consider a ventilation system (fig. 2). For a single zone house, whose exhaust flowrate is equal to Q1 during half of the heating season and Q2 during the other half. Assuming the pollutant emission, the outdoor temperature and the human occupancy to be time constant, and the pollutant concentration equal to C(t) = P(t)/Q(t) yields readily, using appendix 1, to :

$$Qa = \frac{2}{1/Q1 + 1/Q2} \qquad Qh = \frac{Q1 + Q2}{2} \qquad e = \frac{4.\,Q1\,.\,Q2}{(Q1 + Q2)^2}$$

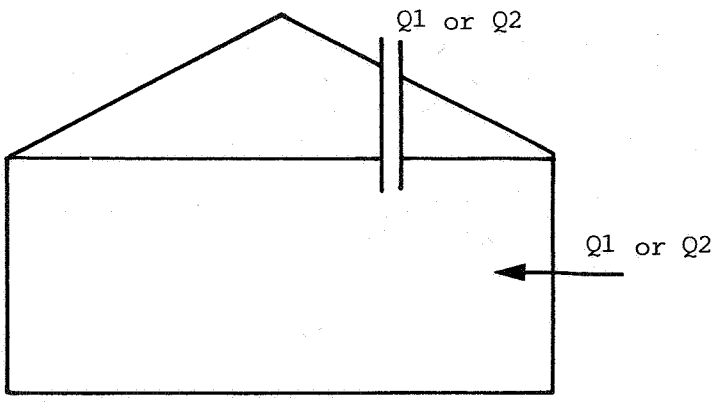

Figure 2 : Single room house with variable airflow

Second example :

Let us consider a ventilation system (fig. 3) whose flowrates Q1 and Q2 are time constant. Assuming : a/ the outdoor temperature to be time constant, b/ the human occupancy and the pollutant emission P to be equal in each room and time constant, yields using appendix 1 to :

$$C_1 = \frac{P}{Q1} \quad ; \quad C_2 = \frac{2P}{Q_1 + Q_2}$$

$$Qa = \frac{4}{\frac{1}{Q1} + \frac{2}{Q1 + Q2}} \qquad Qh = Q1 + Q2 \qquad e = \frac{4}{\frac{Q1 + Q2}{Q1} + 2}$$

The optimum (e = 1, 3) is obtained for Q2 equal to zero.

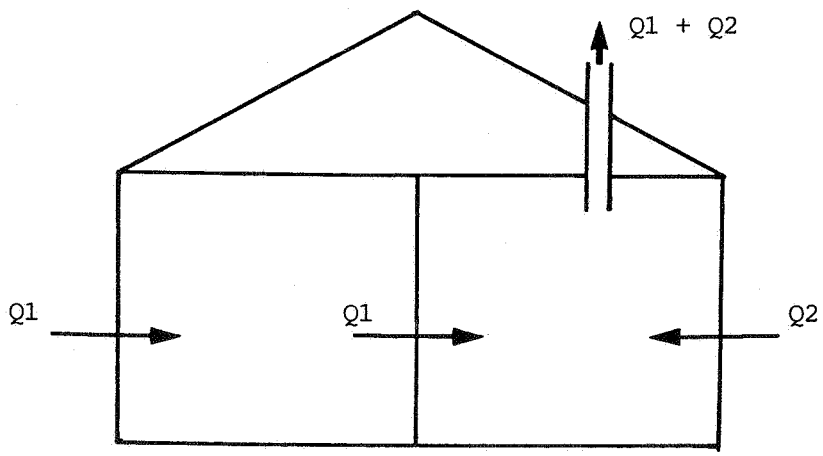

Figure 3 : Two rooms house with constant airflow

6 - CONCLUSIONS

The above method makes it possible using a computer code to assess the efficiency of the different ventilation systems in use in residential buildings. It may therefore be used to improve dimensioning and design of ventilation systems. However, more research work is required in order :

a/ to improve existing multizone computer models, particularly with regard to matters such as influence of wind turbulence, moisture transfer, ...

b/ to gather realistic data concerning :

- building air leakage value and distribution on each facade,
- moisture generation and pollutant emission in each room,
- meteorological data,
- moisture characteristics of furnishing.

c/ to evaluate the condensation hazards, which are not addressed here

d/ to assess the validity of the assumptions that had to be taken into account (linearity of the exposure-health effect relationship ; no physical reaction between pollutants, uniformity of pollutant concentration in a given room, ...).

APPENDIX 1

Formulas

$$Qb = k \cdot \sum_i \int Ci(t) \cdot ni(t) \cdot dt$$

$$Qa = \frac{\int P(t) \cdot n(t)\, dt}{\sum_i \int Ci(t) \cdot ni(t) \cdot dt}$$

$$Qh = \frac{\int Q(t) \cdot [Ti - Text(t)] \cdot dt}{\int [\, Ti - Tex(t) \,] \cdot dt}$$

$$Da = 0.34 \int Q(t) \cdot [Ti - Text(t)] \cdot dt$$

$$e = Qa / Qh$$

VENTILATION SYSTEM PERFORMANCE

11th AIVC Conference, Belgirate, Italy
18-21 September, 1990

Paper 13

STRUCTURE OF MODELS FOR THE PREDICTION OF AIR FLOW AND CONTAMINANT DISPERSAL IN BUILDINGS

Richard A. Grot[1], James A. Axley[2]

1
Lagus Applied Technology
Olney, MD 20832
USA

2
Building Technology Program
Massachusetts Institute of Technology
Cambridge, MA 01273
USA

Abstract

This paper treats the structure of models for predicting interzonal airflow and contaminant dispersal in buildings. It will discuss the mathematical structure of such models, the use of modern data structures, the application of structured program techniques and the use of object-oriented structures for the development of users interfaces and building description processes. Two computer models developed at National Institute of Standards and Technology (NIST) will be used as examples of how these techniques can be applied to air flow analysis and contaminant dispersal: **NBSAVIS** - a building description processor for multizone buildings, and **CONTAM88** - an interzonal airflow and contaminant dispersal analysis program. **NBSAVIS** treats the building as a collection of physical objects which have flow and leakage characteristics and creates a building idealization (flow paths, zones and contaminant source data) from the physical description of the building. It will be demonstrated that with the proper data structure, general interfaces which are both user-friendly and physically correct can be developed. **CONTAM88** combines previously developed interzonal airflow and contaminant dispersal analysis programs **AIRMOV**, **CONTAM86** and **CONTAM87** into one model which includes such features as contaminant reactions, pressure induced contaminant sources for modeling radon entry and plateout and disposition of contaminants onto surfaces. An example is presented on the use of these programs for airflow and contaminant dispersal analysis in a large apartment building.

1 Introduction

The National Institute of Standards and Technology (NIST) (formerly the National Bureau of Standards (NBS)) has over the past several years developed a series of computer models for calculating air flow and contaminant dispersal in multizone buildings.[1-5] Though these models have been developed with the purpose of providing state-of-the-art, documented, public domain algorithms for calculating interzonal air flows and contaminant levels in buildings, they have required a rather laborious preparation of input data and sophisticated building idealization in order to model realistic building configurations. In an attempt to facilitate the use of these models in the analysis of indoor air quality problems in buildings, a preprocessor program **NBSAVIS** (The National Bureau of Standards Air Infiltration, Ventilation and Indoor Air Quality Analysis Program in Multizone Buildings) has been developed which assists in the preparation of input files for air flow and indoor air quality analysis. The main features of the programs **AIRMOV** [1,2] and the programs **CONTAM86** and **CONTAM87** [4,5] have been combined into a program called **CONTAM88** which integrates multizone air flow analysis and contaminant dispersal analysis into one program.

The program **NBSAVIS** is a building description processor for multizone buildings. It is menu driven and has the capability of editing and creating a building description and calculating the required zone and opening data for a multizone air flow and contaminant dispersal analysis.

The steps in performing an air movement and indoor air quality analysis of a building using the above mentioned programs are:

Create and edit a building description using **NBSAVIS**

Perform and air movement analysis and contaminant dispersal analysis using **CONTAM88**

If a more detailed indoor air quality analysis is desired use **CONTAM86** or **CONTAM87**

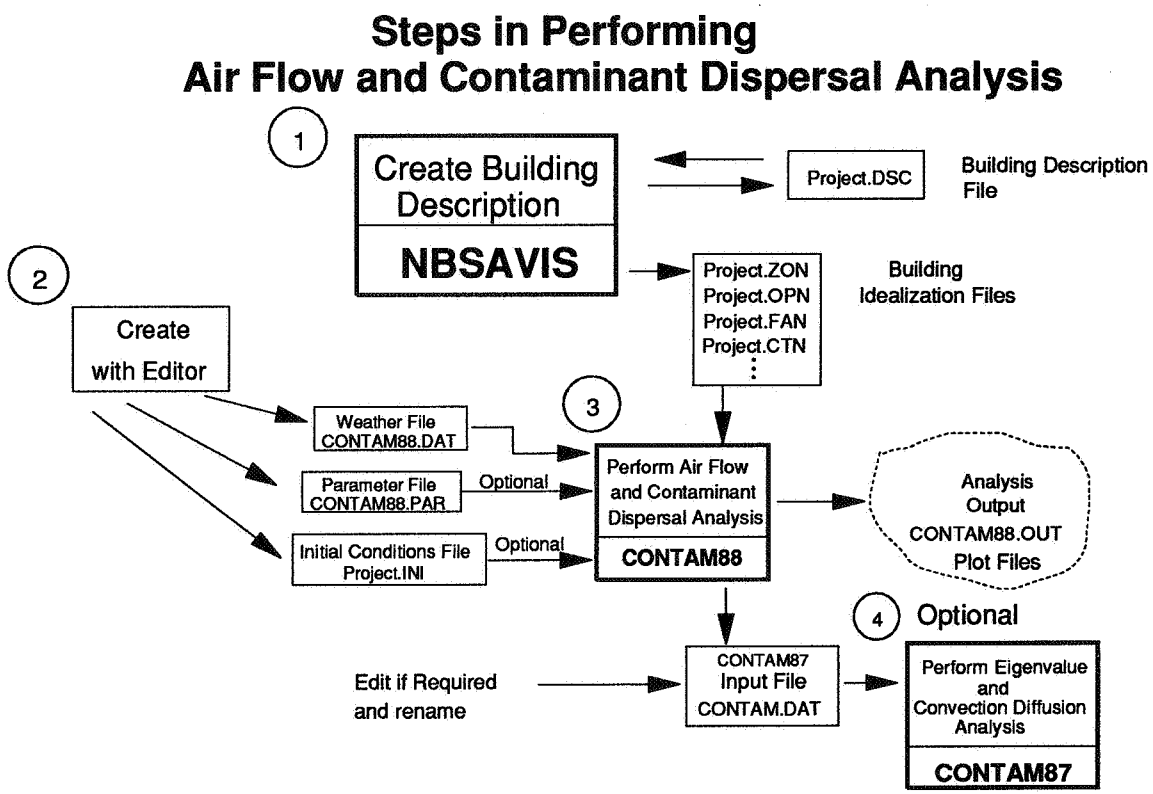

Figure 1. Steps in Performing Air Flow and Contaminant Analysis

2 Description of the Program NBSAVIS

The program **NBSAVIS** is designed to run as a preprocessor for the interzonal air movement and contaminant dispersal analysis program **CONTAM88** and the indoor air quality analysis program **CONTAM87**. It takes data on the building envelope construction, internal configuration, HVAC system and contaminant generation sources and prepares input files for **CONTAM88**. **NBSAVIS** is designed to create a building description which is modular in nature and the description of the building can be refined as more data are acquired or as a more detailed analysis of the air flows and contaminant dispersal into and within the building is desired. **NBSAVIS** supports the following basic functions:

1.) Creation of a new building description.

2.) Editing of an existing building description.

3.) Saving a created or edited building description to disk.

4.) Calculation of the opening, zone and fan data from the building description and preparation of the input files for **CONTAM88**.

In addition **NBSAVIS** has two program utility functions which allow:

5.) Changing certain program parameters such as the physical units used and how building leakages are described (either as leakage area or flow coefficients).

6.) Returning to DOS in an orderly manner.

The input of data for the program **NBSAVIS** is controlled by a series of screen originated sub-routines for the description of the building, the types of exterior walls, exterior doors, windows, interior walls, interior doors, open passageways, miscellaneous openings, filters and fans, descriptions of the rooms of the building and descriptions of the building HVAC systems.

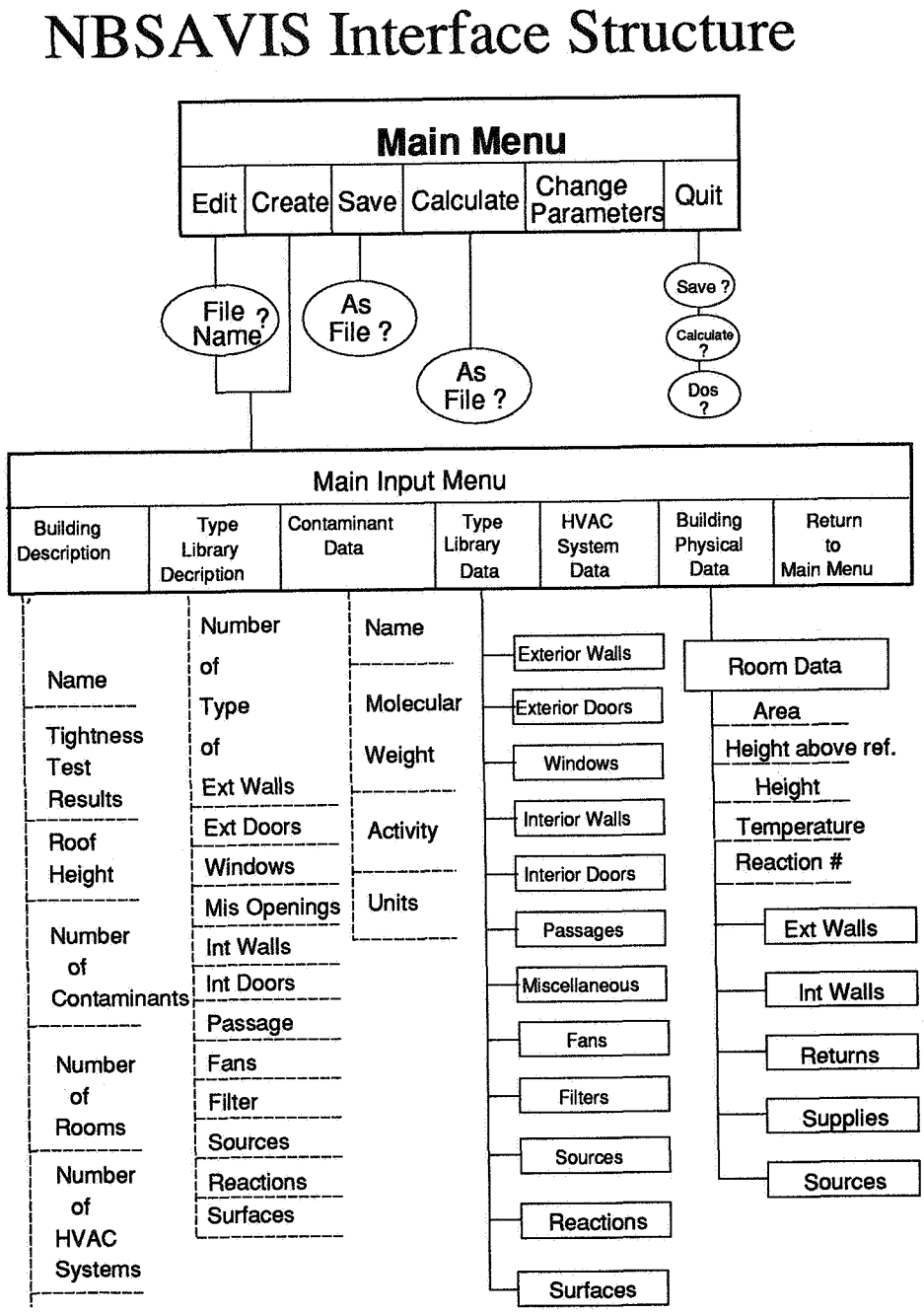

Figure 2. **NBSAVIS** Interface Structure

For **NBSAVIS** a building consists of rooms and HVAC systems. Rooms for **NBSAVIS** can be actual building rooms, hallways, basements, garages, porches, stairwells, elevator shafts, return air shafts, exhaust shafts, supply air shafts and in general any physical volume. Rooms have physical properties, contaminant sources, HVAC system connections, exterior walls and interior walls. Exterior walls, interior walls and HVAC connections contain the flow paths through which air and contaminants can move into, out of and throughout a building. Exterior walls consist of an opaque wall area, exterior doors, vents, windows, intake fans and exhaust fans. Interior walls consist of an opaque wall area, interior doors, open passages, vents, exhaust fans and intake fans. An exterior wall points to the outside, an interior wall points to a previously defined adjacent room.

There is no restriction as to the size of the building which **NBSAVIS** can handle. Features of large buildings such as stairwells, elevator shafts, exhaust shafts, return air shafts and supply shafts can be modeled using **NBSAVIS** and **CONTAM88** by considering such features as rooms. The author has successfully modeled a twelve story apartment building with two stairwells, a vent shaft, an elevator shaft as a 100 zone building using **NBSAVIS** and **CONTAM88** without taxing the resources of 640K PC.

The specific leakage data, contaminant source data and fan flow rates are specified in a library of building component types. The building component types that **NBSAVIS** support are exterior wall types, exterior door types, window types, interior wall types, interior door types, open passage types, miscellaneous or vent types, fan types, filter types and contaminant source types. The actual building part is described by specifying what types it consists of. For example the north exterior wall of the master bedroom is of exterior wall construction type # 1, has one exterior door of exterior door type # 3, two exterior windows of window type # 1, no vents, no exhaust fans and no intake fans. The master bedroom has two contaminant sources, one of type #2 which is a kerosene heater and another of type # 3 which is an air freshener. Given such information on the construction of the building and the location of contaminant sources, **NBSAVIS** can construct the idealization of the building in terms of flow paths, zones and contaminant generation rates required to perform airflow and contaminant dispersal analysis.

2.1 Type Component Library Data

The program **NBSAVIS** uses a building specific library of leakage types, filters and fans which exist in the building. The purpose of this library is to allow the same building component to be used in various parts of the building without repeatedly inputting the data which describes the component. The type library contains the physical and leakage data for exterior walls, exterior doors, windows, interior walls, interior doors, open passages (large openings), miscellaneous leakages (vents), fans, contaminant filters, contaminant sources, kinetic reactions, and exterior surfaces. The description of the buidling layout is speicified in terms of the types contamined in the type library. One only needs to specify the type number of the component and number of components which exist in the building part for which one is preparing a description. For example the family room of the building has an exterior north facing wall with a floor height of 2.5 meters, a width of 4 meters of exterior wall type # 2, this wall has 2 exterior windows of type 4 and 1 exterior door of type 4.

2.2 Physical Building Data

The physical building data are the data required to describe a building in terms of its physical components. For a small building the building is considered to be composed of rooms and HVAC systems. The rooms and HVAC systems are the well-mixed zones of the flow and contaminant dispersal analysis idealization which **NBSAVIS** creates. Attics, basements,

halls, stairways, garages, porches etc are considered to be rooms. Rooms are connected to the HVAC systems through room supplies and returns, to other rooms through interior walls and to the exterior through exterior walls. These connections are the flow paths through which contaminants and air move throughout, into and out of the building. Rooms also have contaminant sources and sinks which generate or remove contaminants.

2.3 General Data Structure

In general, data for **NBSAVIS** are organized as either global variables or as a field of a record in a linked list. Global variables are usually properties of the whole building (such as building height, building leakage area) or govern the way one wishes to input data (metric or English units, use leakage area or flow coefficient for leakage properties, use mass flow rates or volumetric flow rates). Global variables always exist and a value must be always specified or the default value is assumed.

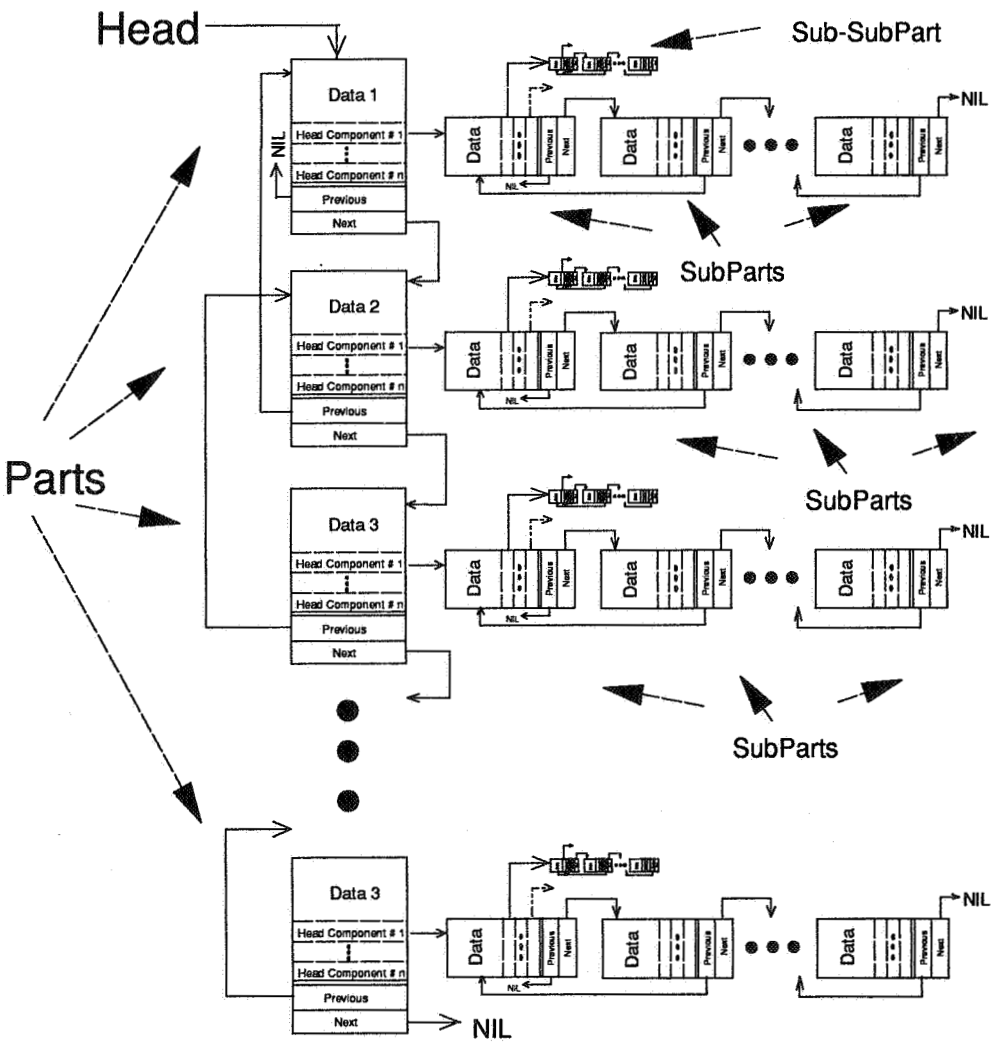

Figure 3. Schematic of Data Structure of NBSAVIS.

Linked lists (**NBSAVIS** uses double linked lists) contain a series of related records (see figure 3). Records in general contain physical properties of item described by the record (for example, a exterior wall type, a room, etc), pointers to the next and previous record in the list and pointers to the beginning of a list or records describing subparts of the physical item described (for example, the exterior walls of a room, the doors and windows of an exterior wall).

This data structure has been found to be efficient in describing a building in terms of its parts and the relationship between various components and the parts of the building. It allows for easy insertion or deletion of parts and components and permits a description of the interdependencies among the parts and components. This data structure also corresponds much to the way one physically views a building. The division of the data for a building into the data required to specify the physical description of the buidling and its HVAC systems and the data required to describe the flow and contaminant emission characteristics of building conmponents allows the modification of one class of data without altering the other class of data. The data for the physical description of the buidling requires only geometrical data and a specification of the components making up the part of the buildings being described. It does not depend on the physical properties of the componet which specifies the components air leakage, air flow or contaminant emission characteristics. Those properties are specified in the component library.

3 Description of CONTAM88

The program **CONTAM88** implements the airflow and contaminant dispersal theory described in the reports and papers of Walton and Axley in one software package. The structure of the program **CONTAM88** is shown in figure 30. **CONTAM88** starts by initializing the global variables and pointers to arrays and link lists. It then checks for the existence of the parameter file. If the parameter file is found in the current directory, the file is open and the parameters are read. If the file does not exist, the default set of parameters is used. **CONTAM88** then opens the weather data file CONTAM88.DTA and reads the starting time/data and the name of the initial building description. It then proceeds to open the corresponding data files for the zone data, contaminant data, opening data, fan data, surface data and kinetic reaction data. In reading these files the corresponding linked lists and arrays are created and the data is storage in these data structures. If an error occurs in reading these files or in allocating the required data storage, an error flag is set and upon exit from the corresponding input routine, the program is terminated with an error message. **CONTAM88** then reads the weather data, advances to the next data record and reads the next time/date. If an end of file is encountered in advancing the data record, the program terminates. The flow system of equations is then formed and solved. If an error occurs in the solution of the flow system, the program terminates with an error message. The logic for solving the flow system of equations is presented in the next subsection. **CONTAM88** then forms and solves the contaminant dispersal system of equations if the number of contaminants is greater than zero. If an error occurs in the solution of the contaminant dispersal system, an error message is given, however the program does not terminate. **CONTAM88** then read the next building description name. If it is different from the previous building description name, the zone data, contaminant data, opening data, fan data, surface data and kinetic data are read for the new description. Some basic checks of the new building description are made to determine if it is consistent with the previous description: that is that the number of zones has not changed and that the number of contaminants are the same. The next weather data are then read and **CONTAM88** proceeds to solve the new flow and contaminant dispersal systems. This process continues till an end of file is encountered on the weather data file. Note that the weather data on

the last record is not processed; therefore if one wishes to analysis the flows and contaminant dispersal for these weather conditions, a dummy record must be added. Note also that if the next time/data is less then the previous time/date, the program will also terminate.

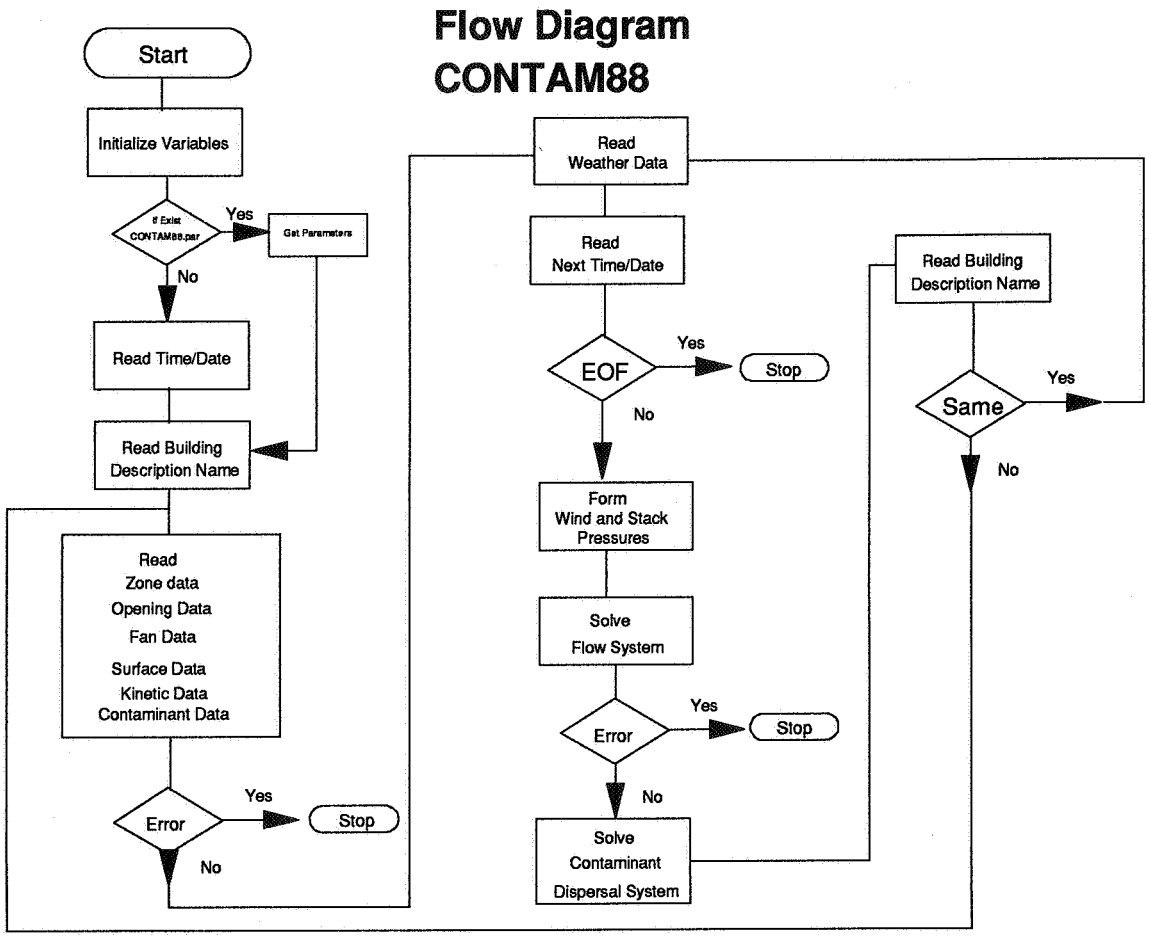

Figure 4. Schematic of Airflow and Contaminant Dispersal Program **CONTAM88.**

The solutions scheme for the air flows in the building is depicted in figure 5. The subroutine solvzp allocates arrays eqn_number and zone_number. If i is an index of a zone, the eqn_number[i] is the equation number of the flow equation for the zone; if n is an equation number, then zone_number[n] is the zone number corresponding to the equation. The system of flow equations is then reordered in such a way that zones which are not coupled by openings (such zones would have a zero diagonal in the Jacobian matrix) to other zones are excluded from the system. The logic used to reorder the flow system equations is shown in figure 6. The diagonal of the Jacobian of the unordered flow system is formed. The equations are renumbered so that all zones with non zero diagonal elements occur first, the zone with zero diagonals in the Jacobians appear last. Examples of zones which would have zero diagonal elements in the Jacobian are HVAC systems or zones coupled by only specified flows. The reorder subroutine returns the number of equations which are to be solved. If this number is zero (as would happen if all flows were specified), the solution algorithm is terminated. One then calculates and stores the square of the air densities in each zone and allocates storage for the bandwidth vector used to determine the storage requirements of the Jacobian matrix. The flow elements are then transversed, deter-

mining their connectivity and their influence on the bandwidth vector. One then determines the sums of all fixed flows into each zone and stores these results in each zone memory structure. Storage is then allocated the element Jacobian matrix, the four vectors need for the solution technique (**B** - the vector of sum of the flows into a zone, **C** - the vector of corrections to the zone pressures, **D** - the previous pressure correction vector, **F** - the vector of the sum of the absolute values of the flows into or out of the zone) and **A** - the Jacobian matrix for the flow system The solution of the flow system is then solved using a Newton-Raphson technique which is described in more detail later.

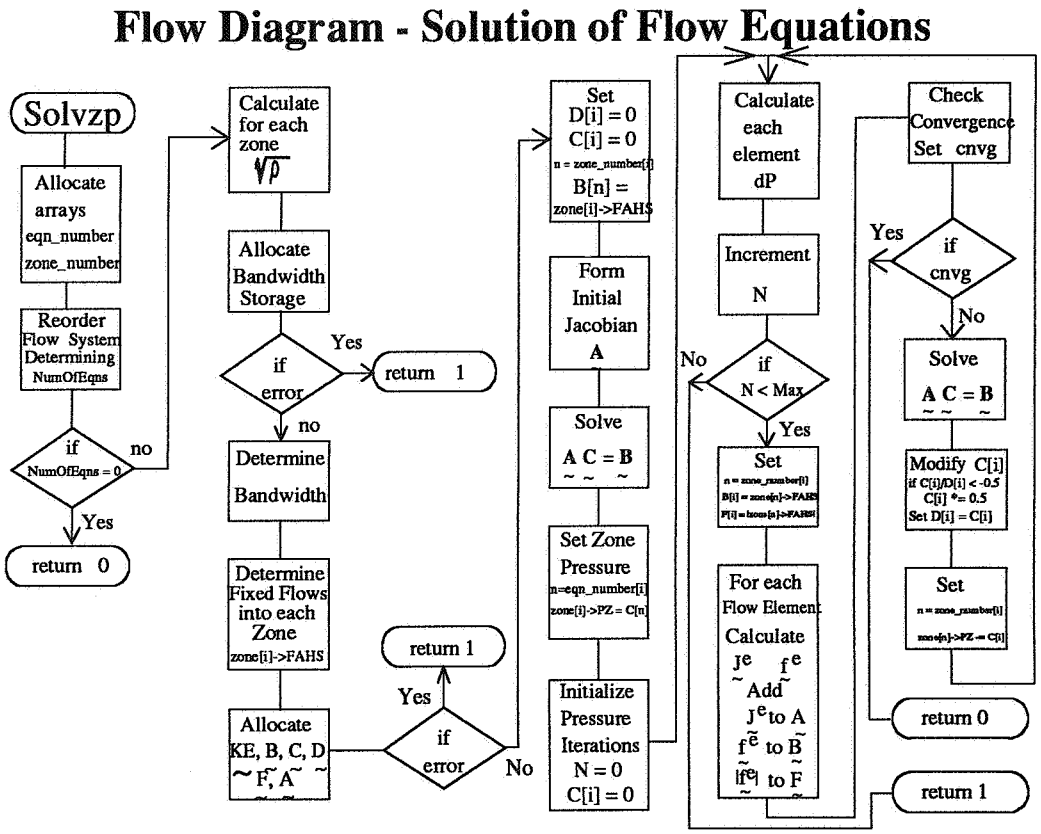

Figure 5. Schematic of Solution Method for Airflow Analysis Used by **CONTAM88.**

After solving for the air flows between zone, CONTAM88 formulates and solves both the steady state and transient contaminant dispersal problem. The general method for solving the contaminant dispersal problem is shown in figure 7.

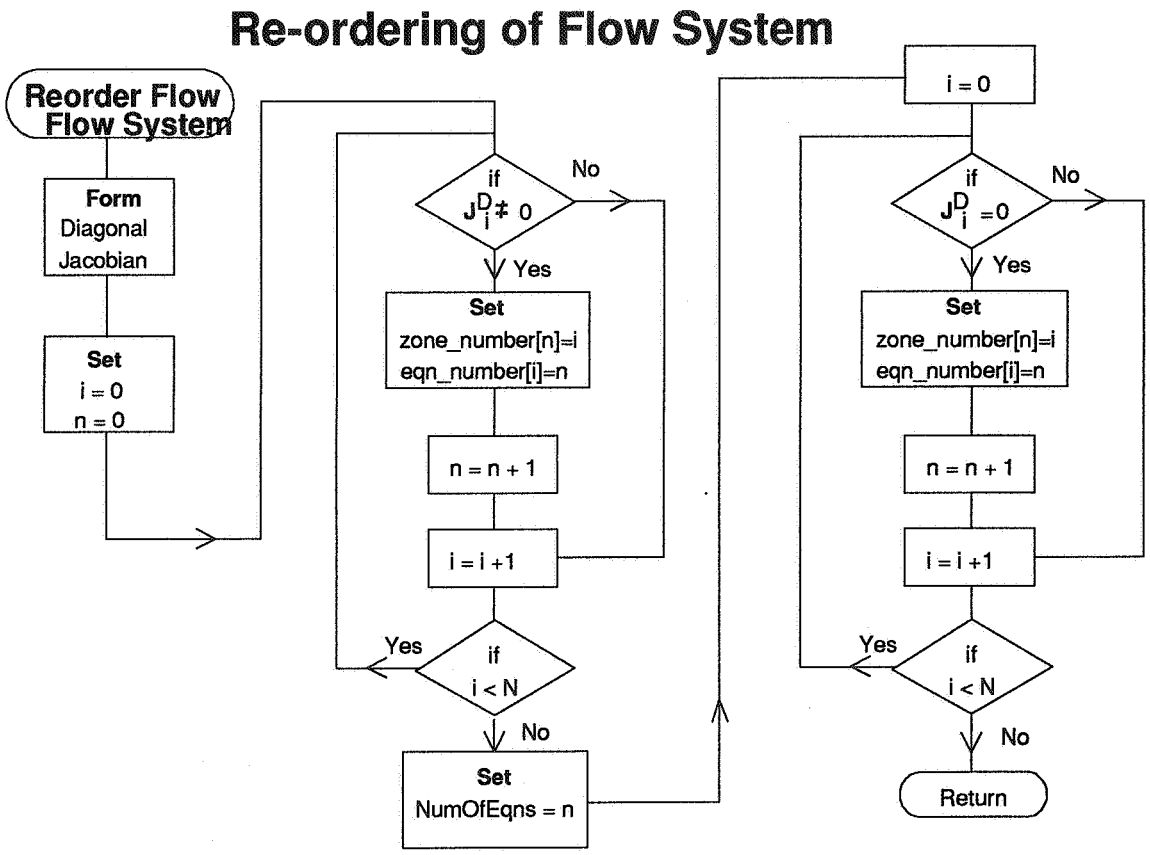

Figure 6. Schematic of Method for Re-ordering Flow System of Equations

The solution of the dynamic response of the transient contaminant dispersal system of equations uses the predictor-corrector model explained in the reports of Axley[4,5]. Three vector work arrays, **dE**, **dC** and **ddC** are allocated along with the storage for the modified dispersal matrix $\mathbf{K}_M$. The initial rate of change of the contaminant concentrations is estimated from the dispersal equations and used to estimate the time step dt to guarantee at least an accuracy of 5 percent in the solution. The time is incremented and the modified dispersal matrix is calculated. For each time step dt, an initial estimate of the increment **dC** is determined and then a correction is calculated and the concentration is updated. If the print interval is reached, the concentrations of the massless nodes are calculated and the concentrations for each zone are printed both to the screen and the output file. This process continues till the end of the time interval is reached.

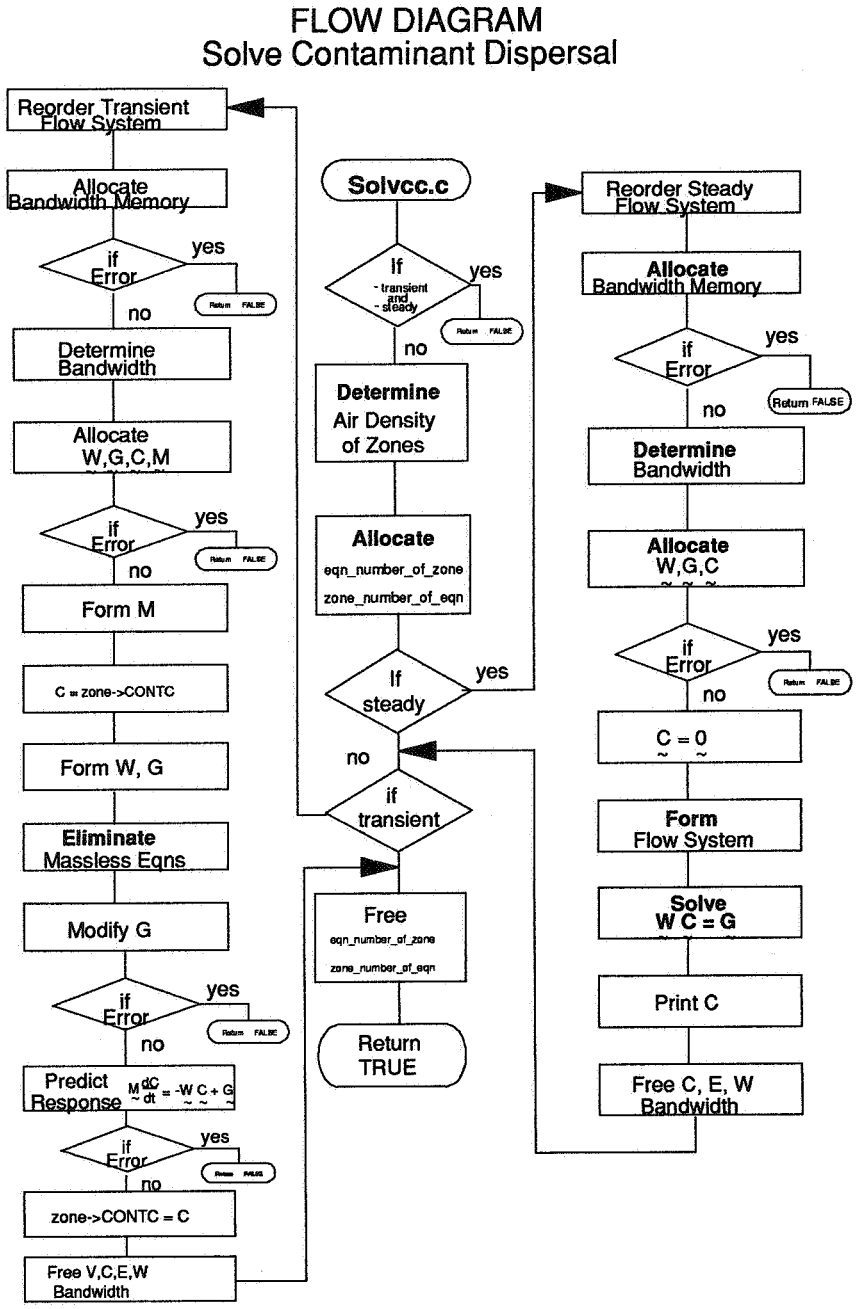

Figure 7. Schematic of Solution Method for Contaminant Dispersal Analysis Used by **CONTAM88.**

If the number of contaminants is greater then zero, **CONTAM88** checks to see if either a transient or steady state analysis of the contaminant dispersal problem is desired. **CONTAM88** can do either one or both for each set of weather conditions. If none is wanted, it returns to the main program, otherwise it determines the air density of each zone and allocates memory for two integer arrays eqn_number_of_zone which will later give the contaminant equation number of the

zone and zone_number_of_eqn which will give the zone of the corresponding to the contaminant equation. **CONTAM88** will reorder the contaminant dispersal equations to eliminate isolated zones and for the transient analysis eliminate zones with zero volume. If a steady state analysis is desired, **CONTAM88** formulates and solves this problem. It first reorders the flow system such that zones with non-zero airflows on the diagonal of the dispersal matrix appear as the first $N_f \cdot M$ unknown contaminant concentrations and the remaining $(N-N_f) \cdot M$ are contaminant concentrations for isolated zones where N is the number of zones in the building and M is the number of contaminants. The number N_f is the number of non-isolated zones and is determined by the reordering algorithm.

The bandwidth of the dispersal matrix is then determined and the memory storage required for the dispersal matrix W, the contaminant generation vector E and the unknown contaminant concentrations C is allocated. If an error occurs in the allocation of memory, the solution is aborted. The contaminant dispersal system is then formulated and solved. The results are then written to both a file and the screen. The memory required to solve the steady state dispersal problem is then freed. **CONTAM88** then checks to see if a transient contaminant dispersal solution is wanted. If so, it reorders the dispersal system zones which both are isolated and have zero volume are eliminated from the solution. It then partitions the remaining equations so the non-zero volume zones are first and the remaining zones are those with zero volume. The bandwidth of the renumbered dispersal system is then determined, memory allocated for the dispersal matrix **W**, the contaminant generation vector **E**, the reordered zone mass vector **V** and the transient concentrations **C** of the reordered system. If an error occurs in the allocation of memory, the solution is aborted. The dispersal mass vector **V** is then formed, the initial concentrations are retrieved from the zone data structures and the dispersal matrix **W** and the generation vector **E** are formed. If there are equations with zero volumes (massless equations), they are eliminated from the transient system of dispersal equations [1]. The dynamic response of the system

$$\overleftrightarrow{\mathbf{M}}\frac{d\vec{\mathbf{C}}}{dt} = \overleftrightarrow{\mathbf{W}}\vec{\mathbf{C}} + \vec{\mathbf{E}}$$

is solved. Figure 3 gives the schematic of the logic for solving the transient system of equations. After the transient solution is finished for the time interval for which the weather conditions are valid, the results of are storage in the zone data structures and the memory required for the transient solution is freed. **CONTAM88** then frees the memory for the arrays eqn_number_of_eqn and zone_number_of_eqn and returns to the main routine.

---

1 The massless equations are in essence a steady state subsystem which needs only to be solved when the results of the transient solution are written to either the screen or a file.

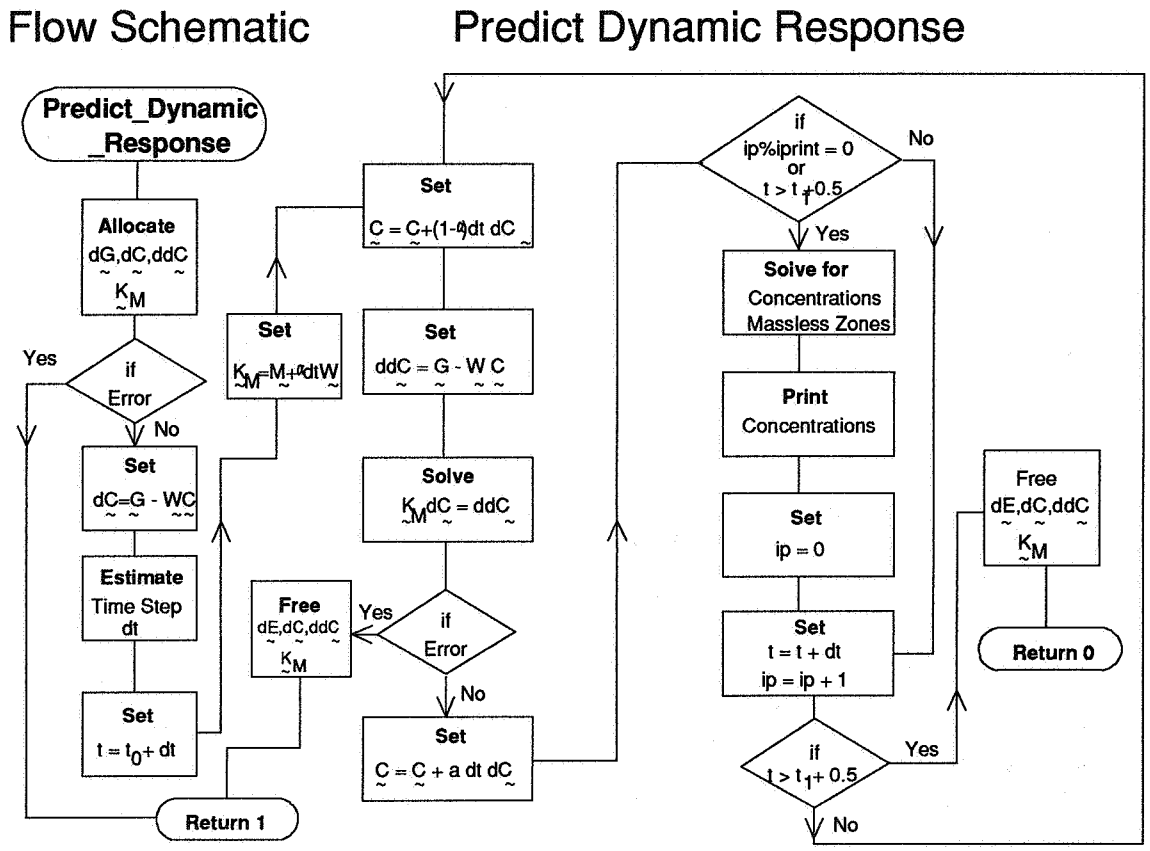

Figure 8. Schematic of Solution of Transient Contaminant Dispersal Equations

4 Theory of Airflow and Contaminant Dispersal Analysis Used by CONTAM88

The basic theory of airflow analysis used by **CONTAM88** is based on the idealization that a building can be treated as a series of pressure nodes connected by a group of flow paths and that the flow through each flow path is a function of the pressures at the nodes connected by the flow paths. In buildings, the pressure nodes are usually called zones and the flow paths will be called flow elements. A zone requires three parameters to specify its state for flow analysis, its pressure, its temperature and its volume. In **CONTAM88** the pressure is considered an unknown to be solved for by the system of equations formulated by **CONTAM88** and the zone's temperature and volume are considered specified, though not necessarily constant. A flow element is specified by giving the numbers of the pressure nodes it connects and the functional form of the relation between the flow through the element and the element node pressures.

CONTAM88 used two types of flow elements: openings and fans. Each of these elements are two node elements. If we consider the index i, i = 1,2 than the element can be defined by determining the quantities (${}^{e}f_i, {}^{e}p_i, {}^{e}T_i$,) where ${}^{e}f_i$ is the flow into i^{th} node from the element and ${}^{e}p_i$ and ${}^{e}T_i$ are the nodes pressure and temperature respectively. All of these quantities are not independent. Conservation of mass on the element requirements requires that

$$ {}^{e}f_1 = -{}^{e}f_2 \equiv {}^{e}f(\delta p^{e}) \qquad (1) $$

where $\delta p^{e} = {}^{e}p_2 - {}^{e}p_1 + {}^{e}p_w + {}^{e}p_s$

and $ {}^{e}p_s = g(\rho_2 h_2 - \rho_1 h_1)$,stack pressure

and $ {}^{e}p_s = \frac{1}{2} pc[m_s]\rho_0 V(H_s)^2 (\delta_{0n_2} - \delta_{0n_1})$,wind pressure

In the above ${}^{e}p_w$ is the wind pressure on the element, ${}^{e}p_s$ is the stack pressure across the element. h_1 and h_2 are the heights of the element above the reference height of the zones n_1 and n_2, where n_1 is the zone number of the zone from which the flow comes (if ${}^{e}f$ is positive) and n_2 is the zone number of the zone to which the flow goes. ρ_1 and ρ_2 are the density of air in the zone n_1 and n_2 respectively. A convention that **CONTAM88** uses is that the number of the exterior zone is 0. In the expression for the wind pressure p_w, $V(H_s)$ is the wind speed at the height of the surface containing the opening.

$$ V(H_s) = V_m \left(\frac{H_s}{10} \right)^{0.143} \qquad (2) $$

where V_m is the measured meteorological wind speed at a height of 10 meters.

$pc[m_s]$ is the m_s^{th} pressure coefficient of the surface. The integer m_s is determined from the wind direction a_w and the azimuth angle a_z of the surface which contains the opening by determining the sector relative to the surface from which the wind comes:

$$ m_s = n_s \cdot \frac{\phi}{360} + \frac{1}{2} \qquad (4) $$

where $\phi = a_w - a_z$ if $a_w \geq a_z$

$= 360 - (a_z - a_w)$ if $a_w < a_d$

if $m_s > n_s$ then $m_s = 1$;

In the above expression, n_s is the number of surface coefficients of the surface containing the opening.

Flow-Pressure Equation for an Opening.

In **CONTAM88** the mass flow air through the opening is related to the pressure drop across the opening by a power-law equation in the turbulent flow regime and by a quadratic equation in the laminar flow regime.

$$^{e}f = \sqrt{\rho_i} C \delta p |\delta p|^{x-1} \quad \text{if} \quad |\delta p| \geq \Delta p_t \tag{5}$$

$$= \sqrt{\rho_i}\, \delta p (\alpha + \beta |\delta p|) \quad \text{if} \quad |\delta p| < \Delta p_t$$

where

$$\alpha = (2-x) C \Delta p_t^{x-1}$$

$$\beta = (n-1) C \Delta p_t^{x-2}$$

$$\Delta p_t = \frac{0.0034}{C} \tag{6}$$

and ρ_i is the inlet air density: $i = 2$ if $\delta p \geq 0$,$i = 1$ if $\delta p < 0$

In the above equation Δp_t is the transient pressure at which the flow through the element changes from laminar to turbulent. Though this form of a relationship between the flow is physically correct, its real purpose in the theory is to assure convergence of the mathematical method used to solve the flow system of equations. Note that if a linear region is not assumed about 0, the derivative of the flow equation with respect to pressure is infinite. In contrast to AIRNET[9], **CONTAM88** requires that both the f and its derivative are continuous at the transient pressure. The expression for α and β are derived from these conditions.

One can justify the expression for the transition pressure by the following reasoning: Let U be the velocity of air passing through the opening.

$$U = \frac{f}{\rho A_l} \tag{7}$$

$$A_l = \frac{C}{k} \tag{8}$$

$$k \equiv \frac{\delta P_{ref}^{0.5-x}}{\sqrt{2}} \tag{9}$$

where A_l is the leakage area of the opening and k is the discharge coefficient. The reference pressure δP_{ref} is usually chosen to be 4 Pa in the United States. Then the Reynolds number of the flow through the opening can be expressed as

$$Re \equiv U \frac{L}{\nu} \tag{10}$$

ν is the viscosity of air $= 1.5 \cdot 10^{-5}$

L is a representative length $\equiv \sqrt{A_l}$

In the turbulent flow region, the Reynolds number can be related to the pressure drop across the flow path by

$$Re = \sqrt{\frac{2A_l}{\rho}\frac{k}{\nu}}\delta p^x \tag{11}$$

The transition pressure Δp_t can thus be estimated by the expression

$$\Delta p_t = \left(\sqrt{\frac{\rho}{2A_l}\frac{Re_t}{k}}\nu\right)^{\frac{1}{x}} \tag{12}$$

$$= \left(\sqrt{\frac{\rho}{2Ck}}Re_t\nu\right)^{\frac{1}{x}}$$

$$\cong \frac{\rho}{2Ck}(Re_t\nu)^2$$

where Re_t is the Reynolds number at which the flow becomes turbulent.

If one assumes that the transition to turbulence occurs for a Reynolds number of about 5000, one obtains the previous given expression for Δp_t.

Fan Flow Element

The fan flow element used by **CONTAM88** is a simple fixed flow element whose flow pressure relation is given by

$$f(\delta p^e) = F_0 \tag{13}$$

If F_0 is positive , flow is from node 2 to node 1 of the element; if F_0 is negative, the flow is from node 1 to node 2 of the element. There is no mathematical difficulty in introducing fan curves in the theory; however the present version of **CONTAM88** treats fans as constant flow elements.

Formation of the Flow System

The system of flow equations which are to be solved for the pressures in each zone can be formulated by defining the flow and pressure vectors for each element as

$$\vec{\mathbf{p}}_e \equiv \begin{bmatrix} {}^e p_1 \\ {}^e p_2 \end{bmatrix} \tag{14}$$

$$\vec{\mathbf{f}}_e \equiv \begin{bmatrix} {}^e f_1 \\ {}^e f_2 \end{bmatrix} \tag{15}$$

If one defines the system pressure vector $\vec{\mathbf{p}}$ and zone flow vector $\vec{\mathbf{f}}$ such that

$$\vec{\mathbf{p}} \equiv \begin{bmatrix} p_1 \\ p_2 \\ \cdots \\ p_N \end{bmatrix} \quad \vec{\mathbf{f}} \equiv \begin{bmatrix} f_1 \\ f_2 \\ \cdots \\ f_N \end{bmatrix} \tag{16}$$

where p_i is the pressure of the ith zone and f_i is the system of the mass flows into the ith zone minus the sum of the flows out of the ith zone from all elements and N is the number of independent pressures nodes for the system.

One can then consider the mapping of the element node pressures into the zone pressures given by the equation:

$$\vec{\mathbf{p}}_e = \overleftrightarrow{\mathbf{B}}_e \vec{\mathbf{p}} \tag{17}$$

where

$$\overleftrightarrow{\mathbf{B}}_e \equiv [B_{ij}^e] = \begin{bmatrix} B_{11} & B_{12} & \cdots & B_{1N} \\ B_{21} & B_{22} & \cdots & B_{2N} \end{bmatrix} \tag{18}$$

where $B_{ij}^e = \delta_{il}\delta_{jn_1} + \delta_{i2}\delta_{jn_2}$

In equation (18), n_1 is the zone number of element node 1 and n_2 is the zone number of element node 2. The zone numbers n_1 and n_2 are determined by the building description processor **NBSAVIS** and stored by **CONTAM88** in the data structure for each element.

The system flow vector $\vec{\mathbf{f}}$ can then be formed from the element flow vectors by the operation:

$$\vec{\mathbf{f}}(\vec{\mathbf{p}}) = \sum_{\forall e} \overleftrightarrow{\mathbf{B}}_e^{\,T} \vec{\mathbf{f}}_e(\overleftrightarrow{\mathbf{B}}_e \vec{\mathbf{p}}) \tag{18}$$

where the summation is over all flow elements.

The conservation of mass at each zone requires that

$$\vec{\mathbf{f}}(\vec{\mathbf{p}}) = \frac{d\vec{\mathbf{m}}}{dt} \tag{19}$$

where $\vec{\mathbf{m}}$ is the vector of zone masses.

$$\vec{\mathbf{m}} \equiv \begin{bmatrix} \rho_1 V_1 \\ \rho_2 V_2 \\ \cdots \\ \rho_N V_N \end{bmatrix} \tag{20}$$

where ρ_i is the air density of the ith zone and V_i is the zone volume.

The above set of equations constitutes as nonlinear system of N equations for the N zone pressures.

In most cases, the right hand side of the flow equations is zero (that is, there is no rate of change of mass inside the zone). However there instances in which these terms cannot be neglected. For example, in the case of change zone temperature or varying barometric pressure, the zone air densities will change with time. If one is modelling two sections of an elevator shaft with a moving elevator, the volumes of the two zones will change with time. **CONTAM88** does however consider the right hand side of the flow equations to be negectible.

Solution Technique for Solving the Flow System

The system of flow equations is solved using a Newton-Raphson technique. If one defines the Jacobian matrix

$$\overleftrightarrow{J}(\vec{p}) \equiv -\frac{\partial \vec{f}}{\partial \vec{p}} \tag{21}$$

then the flow system can be solved iteratively by the procedure

$$\overleftrightarrow{J}(\vec{0})\Delta\vec{p}^{0} = \vec{f}(\vec{0}) - \frac{d\vec{m}}{dt} \tag{22}$$

$${}^{1}\vec{p} = \Delta\vec{p}^{0}$$

then for $\alpha = 1\ldots$

$$\overleftrightarrow{J}({}^{\alpha}\vec{p})\Delta\vec{p}^{\alpha} = \vec{f}({}^{\alpha}\vec{p}) - \frac{d\vec{m}}{dt} \tag{23}$$

$${}^{\alpha+1}\vec{p} = {}^{\alpha}\vec{p} + \overleftrightarrow{\omega}\Delta\vec{p}^{\alpha}$$

until the convergence criteria satisfied or $\alpha > \max$

In the above scheme, ω_i are relaxation factors used to prevent oscillations in the convergence of the solution.

It can be shown that the Jacobian matrix of the flow system can be formed from the Jacobian matrices of the flow elements:

$$\overleftrightarrow{J}(\vec{p}) = \sum_{\forall e} \overleftrightarrow{B}_e^{T} \overleftrightarrow{J}_e \overleftrightarrow{B}_e \tag{24}$$

where $\overleftrightarrow{J}_e \equiv -\frac{\partial \vec{f}_e}{\partial \vec{p}_e}$

For two node flow elements in which the flow depends on the difference of the nodal pressures if can be shown that the element Jacobian has the form:

$$\vec{\mathbf{J}}_e = d^e f \begin{bmatrix} 1 & -1 \\ -1 & 1 \end{bmatrix} \quad \text{if } n_1 \neq 0 \text{ and } n_2 \neq 0 \tag{25}$$

$$= d^e f \begin{bmatrix} 1 & 0 \\ 0 & 0 \end{bmatrix} \quad \text{if } n_2 = 0$$

$$= d^e f \begin{bmatrix} 0 & 0 \\ 0 & 1 \end{bmatrix} \quad \text{if } n_1 = 0$$

where $d^e f \equiv \dfrac{d^e f}{d\delta p}$

Note that since the element Jacobian matrices are symmetric, the flow system Jacobian is symmetric. Also, since $d^e f > 0$, the diagonal elements are positive and the off-diagonal elements are negative or zero and the sum of the absolute value of off-diagonal elements is equal to or less than the diagonal elements for each element matrix, the same holds true for the system Jacobian. Therefore, the system Jacobian is a symmetric M-matrix and if the a diagonal element of the system flow matrix is zero, then all elements in the row and column which contain the diagonal element are zero. That the Jacobian is a M-matrix has two important consequences for the theory: First, the solution of the system of equations (23) for $\Delta \mathbf{p}$ can be accomplished by LU decomposition without pivoting. That pivoting is not required allows the use of compact and skyline matrix storage techniques which could be destroyed by pivoting. Second, that a zone is isolated can be determined by checking if the diagonal element of the Jacobian is zero. Note also from the form of the element pressure-flow relation, a zero diagonal element at any pressure implies that the flow coefficients of all elements connected to the zone are zero and therefore diagonal element is identically zero ate all pressures.

Convergence Criteria

CONTAM88 uses a combination of an absolute and relative convergence criteria on the components of the zone flow vector.

if $|f_i| > \varepsilon_1$ and $|f_i| / \sum_{\forall e} |^e f_i| > \varepsilon_2$ for any i, then cnvg = false otherwise convg = true

The default values for ε_1 and ε_2 are 0.000001 and 0.0001 respectively.

Contaminant Dispersal

The contaminant dispersal theory implemented by **CONTAM88** is a slightly modified version of the well-mixed zone theory presented by Axley[4,5]. The theory of **CONTAM87** has been expended to include the phenomena of plateout without resorting to the use of dummy kinetic reaction elements. The convection diffusion element of **CONTAM87** has not been included in **CONTAM88**. The contaminant dispersal theory of **CONTAM88** is a multi-contaminant theory which includes the physical effects of the transport of contaminants by air movement, the removal of contaminants by plateout and the kinetic reaction of contaminants within a zone. The theory also includes contaminants sources which can depend on the exterior-interior pressure differences across the building (for example, pressure driven radon sources). The basic equations for the contaminant dispersal in a building can be derived from the conservation of mass for contaminant specie in each zone of the building:

$$\frac{d}{dt}(m_i C^{\alpha}{}_i) = -(f_i^{(out)} + R_i^{\alpha})C^{\alpha}{}_i + \sum_{\forall e}\sum_{j=0}^{N}(1-{}^{e}\eta^{\alpha})\,{}^{e}f_{ij}^{(in)}C^{\alpha}{}_j + m_i\sum_{\beta=1}^{M}\kappa^{i}_{\alpha\beta}C^{\beta}{}_i + g^{\alpha}{}_i \quad , \text{i=1...N} \tag{26}$$

where $m_i \equiv \rho_i V_i$

In equation 26, $C^{\alpha}{}_i$ is the concentration of the αth contaminant specie in the ith zone, m_i is the mass of air in the ith zone, $f^{(out)}{}_i$ is the sum of all air flows out of the ith zone, $f^{(in)}{}_{ij}$ is the sum of all air flows into the ith zone for the jth zone, $R^{\alpha}{}_i$ is the removal rate by plateout or deposition of the αth specie in the ith zone, ${}^{e}\eta^{\alpha}$ is the filter efficiency for the eth flow element and the αth specie, $\kappa^{i}_{\alpha\beta}$ is the kinetic reaction coefficient in the ith zone between α^{th} and β^{th} species and $g^{\alpha}{}_i$ is the generation rate of the αth specie in the ith zone. In equation 26, j = 0 denotes the exterior zone; that is $f^{(in)}{}_{i0}$ is the flow into the ith zone form the exterior and ${}^{\alpha}C_0$ is the concentration of the αth specie in the exterior zone. **CONTAM88** uses mass flow rates for air flows and mass concentration units per unit mass of air for the concentration of pollutant species in its contaminant dispersal calculations. Note also the definition of the kinetic rate matrix is such that a positive coefficient produces an increase in contaminant mass (**CONTAM87** uses the oppositive sign convention).

If for each flow element we define ${}^{e}f^{(out)}{}_i$ as the flow out of the zone through the flow element and ${}^{e}f^{(in)}{}_{ij}$ as the flow into the ith zone from the jth zone then

$${}^{e}f_i^{(out)} = \delta_{in_2}\,{}^{e}f \quad \text{if} \quad {}^{e}f \geq 0 \tag{27}$$

$$= -\delta_{in_1}\,{}^{e}f \quad \text{if} \quad {}^{e}f < 0$$

$${}^{e}f_{ij}^{(in)} = \delta_{in_1}\delta_{jn_2}\,{}^{e}f \quad \text{if} \quad {}^{e}f \geq 0 \tag{28}$$

$$= -\delta_{in_2}\delta_{jn_1}\,{}^{e}f \quad \text{if} \quad {}^{e}f < 0$$

then $f^{(out)}{}_i$ and $f^{(in)}{}_i$, the total flows out of and into the ith zone respectively, are given by:

$$f_i^{(out)} = \sum_{\forall e}{}^{e}f_i^{(out)} \tag{29}$$

$$f_i^{(in)} = \sum_{j=0}^{N}\sum_{\forall e}{}^{e}f_{ij}^{(in)} \tag{30}$$

From the conservation of mass for the air in the ith zone (eqn 19), it can be shown that $f^{(out)}{}_i$ and $f^{(in)}{}_i$ are related by

$$\frac{dm_i}{dt} = -f_i^{(out)} + f_i^{(in)} \tag{31}$$

Therefore, equation 26 can be written as

$$m_i\frac{d^{\alpha}C_i}{dt} = -{}^{\alpha}R_i\,{}^{\alpha}C_i - \sum_{j=0}^{N}\sum_{\forall e}\{{}^{e}f_{ij}^{(in)\alpha}C_i - (1-{}^{e}\eta^{\alpha})\,{}^{e}f_{ij}^{(in)\alpha}C_j\} + m_i\sum_{\beta=1}^{M}\kappa^{i}_{\alpha\beta}\,{}^{\beta}C_i + g_i^{\alpha} \tag{32}$$

Note that equation (32) is the correct form of the conservation of species equation for the case where m_i are not constant but time varying functions (the coefficient of ${}^{\alpha}C_i$ in the equation for ${}^{\alpha}C_i$ is the sum of the flows into the ith zone, not necessarily the flow out of the zone).

If one defines for each zone, the specie's vector $\vec{C}_i$

$$\text{where} \quad \vec{C}_i = \begin{bmatrix} {}^1C_i \\ {}^2C_i \\ \cdots \\ {}^MC_i \end{bmatrix} \tag{33}$$

and for each element the specie element vector ${}^e\vec{C}^{\alpha}$

$$\text{where} \quad {}^e\vec{C}^{\alpha} \equiv \begin{bmatrix} {}^{\alpha}C_1^e \\ {}^{\alpha}C_2^e \end{bmatrix} \tag{34}$$

and forms the system contaminant vector $\vec{C}$

$$\vec{C} \equiv \vec{C}_1 \oplus \vec{C}_2 \oplus \ldots \oplus \vec{C}_N = \begin{bmatrix} \vec{C}_1 \\ \vec{C}_2 \\ \cdots \\ \vec{C}_N \end{bmatrix} \tag{35}$$

the contaminant dispersal equations can be written in the form

$$\vec{\vec{m}} \frac{d\vec{C}}{dt} = -\vec{\vec{W}} \cdot \vec{C} + \vec{g}' \tag{36}$$

where $\vec{\vec{m}}$ is the system mass matrix, $\vec{\vec{W}}$ is the total system dispersal matrix and $\vec{g}'$ is the total system contaminant generation vector.

The system mass matrix is

$$\vec{\vec{m}} \equiv \vec{\vec{m}}_1 \oplus \vec{\vec{m}}_2 \ldots \oplus \vec{\vec{m}}_N = \begin{bmatrix} \vec{\vec{m}}_1 & \vec{\vec{0}} & \vec{\vec{0}} & \cdots & \vec{\vec{0}} \\ \vec{\vec{0}} & \vec{\vec{m}}_2 & \vec{\vec{0}} & \cdots & \vec{\vec{0}} \\ \vec{\vec{0}} & \vec{\vec{0}} & \cdots & \cdots & \vec{\vec{0}} \\ \vec{\vec{0}} & \vec{\vec{0}} & \cdots & \vec{\vec{0}} & \vec{\vec{m}}_N \end{bmatrix} \tag{37}$$

where $\vec{\vec{m}}_i$ is the mass matrix of the ith zone

$$\vec{\vec{m}}_i \equiv m_i \vec{\vec{I}}_M \tag{38}$$

where $\vec{\vec{I}}_M$ is the $M \times M$ unit matrix

and the system dispersal matrix $\overleftrightarrow{\mathbf{W}}$ is given by

$$\overleftrightarrow{\mathbf{W}} \equiv \overleftrightarrow{\mathbf{R}} + \overleftrightarrow{\mathbf{F}} - \overleftrightarrow{\mathbf{K}} \tag{39}$$

where $\overleftrightarrow{\mathbf{R}}$ is the removal rate matrix given by

$$\overleftrightarrow{\mathbf{R}} \equiv \overleftrightarrow{\mathbf{R}}_1 \oplus \overleftrightarrow{\mathbf{R}}_2 \oplus \ldots \oplus \overleftrightarrow{\mathbf{R}}_N = \begin{bmatrix} \overleftrightarrow{\mathbf{R}}_1 & \overleftrightarrow{\mathbf{0}} & \overleftrightarrow{\mathbf{0}} & \cdots & \overleftrightarrow{\mathbf{0}} \\ \overleftrightarrow{\mathbf{0}} & \overleftrightarrow{\mathbf{R}}_2 & \overleftrightarrow{\mathbf{0}} & \cdots & \overleftrightarrow{\mathbf{0}} \\ \overleftrightarrow{\mathbf{0}} & \overleftrightarrow{\mathbf{0}} & \cdots & \cdots & \overleftrightarrow{\mathbf{0}} \\ \overleftrightarrow{\mathbf{0}} & \overleftrightarrow{\mathbf{0}} & \cdots & \overleftrightarrow{\mathbf{0}} & \overleftrightarrow{\mathbf{R}}_N \end{bmatrix} \tag{40}$$

with

$$\overleftrightarrow{\mathbf{R}}_i \equiv \begin{bmatrix} {}^1R_i & 0 & 0 & \cdots & 0 \\ 0 & {}^2R_i & 0 & \cdots & 0 \\ 0 & 0 & \cdots & \cdots & \\ 0 & 0 & \cdots & \cdots & {}^MR_i \end{bmatrix} \tag{41}$$

and $\overleftrightarrow{\mathbf{F}}$ is the flow matrix

$$\overleftrightarrow{\mathbf{F}} \equiv \sum_{\forall e} \sum_{\alpha=1}^{M} {}^{\alpha}\overleftrightarrow{\mathbf{B}}^{eT} \cdot {}^{e}\overleftrightarrow{\mathbf{f}}^{\alpha} \cdot {}^{\alpha}\overleftrightarrow{\mathbf{B}}^{e} \tag{42}$$

where ${}^{e}\overleftrightarrow{\mathbf{B}}^{\alpha}$ is the mapping of the element species onto the system contaminant species

$${}^{e}\overleftrightarrow{\mathbf{B}}^{\alpha} \equiv [{}^{e}B^{\alpha}_{ij}] = \begin{bmatrix} {}^{e}B^{\alpha}_{11} & {}^{e}B^{\alpha}_{12} & \cdots & {}^{e}B^{\alpha}_{1N_c} \\ {}^{e}B^{\alpha}_{21} & {}^{e}B^{\alpha}_{22} & \cdots & {}^{e}B^{\alpha}_{2N_c} \end{bmatrix} \tag{43}$$

where ${}^{e}B^{\alpha}_{ij} = \delta_{in_{1\alpha}} + \delta_{jn_{2\alpha}} \quad i,j = 1 \ldots N_c$

and $n_{\alpha l} = M(n_l - 1) + \alpha \quad \text{if} \quad n_l \neq 0$

$= 0 \quad \text{if} \quad n_l = 0 \quad \text{for l=1,2}$

and ${}^{e}\overleftrightarrow{\mathbf{f}}^{\alpha}$ is the element flow matrix for α^{th} specie

$${}^{e}\overleftrightarrow{\mathbf{f}}^{\alpha} = {}^{e}f \begin{bmatrix} 1 & 0 \\ -(1-{}^{e}\eta^{\alpha}) & 0 \end{bmatrix} \quad \text{if} \quad {}^{e}f \geq 0 \tag{44}$$

$$= -{}^{e}f \begin{bmatrix} 0 & -(1-{}^{e}\eta^{\alpha}) \\ 0 & 1 \end{bmatrix} \quad \text{if} \quad {}^{e}f < 0$$

and $\vec{\mathbf{g}}'$ is the system generation vector

$$\vec{\mathbf{g}}' \equiv \vec{\mathbf{g}}'_1 \oplus \vec{\mathbf{g}}'_2 \oplus \ldots \oplus \vec{\mathbf{g}}'_N = \begin{bmatrix} \vec{\mathbf{g}}'_1 \\ \vec{\mathbf{g}}'_2 \\ \cdots \\ \vec{\mathbf{g}}'_N \end{bmatrix} \tag{45}$$

where $\vec{\mathbf{g}}'_i \equiv \begin{bmatrix} {}^1g'_i \\ {}^2g'_i \\ \cdots \\ {}^Mg'_i \end{bmatrix}$

with ${}^\alpha g'_i = g^\alpha{}_i + \sum_{\forall e} {}^e f_{i0}^{(\text{in})} (1 - {}^e\eta^\alpha)^\alpha C_0 \quad \text{for } \alpha = 1 \ldots M$

and $\overleftrightarrow{\mathbf{K}}$ is the system reaction matrix:

$$\overleftrightarrow{\mathbf{K}} \equiv \overleftrightarrow{\mathbf{K}}_1 \oplus \overleftrightarrow{\mathbf{K}}_2 \oplus \ldots \oplus \overleftrightarrow{\mathbf{K}}_N = \begin{bmatrix} \overleftrightarrow{\mathbf{K}}_1 & \overleftrightarrow{\mathbf{0}} & \overleftrightarrow{\mathbf{0}} & \cdots & \overleftrightarrow{\mathbf{0}} \\ \overleftrightarrow{\mathbf{0}} & \overleftrightarrow{\mathbf{K}}_2 & \overleftrightarrow{\mathbf{0}} & \cdots & \overleftrightarrow{\mathbf{0}} \\ \overleftrightarrow{\mathbf{0}} & \overleftrightarrow{\mathbf{0}} & \cdots & \cdots & \overleftrightarrow{\mathbf{0}} \\ \overleftrightarrow{\mathbf{0}} & \overleftrightarrow{\mathbf{0}} & \cdots & \overleftrightarrow{\mathbf{0}} & \overleftrightarrow{\mathbf{K}}_N \end{bmatrix} \tag{46}$$

where $\overleftrightarrow{\mathbf{K}}_i = [\kappa^i_{\alpha\beta}]$

$$= \begin{bmatrix} \kappa^i_{11} & \kappa^i_{12} & \cdots & \kappa^i_{1M} \\ \kappa^i_{21} & \kappa^i_{22} & \cdots & \kappa^i_{2M} \\ \cdots & \cdots & \cdots & \cdots \\ \kappa^i_{M1} & \kappa^i_{M2} & \cdots & \kappa^i_{MM} \end{bmatrix}$$

The method used in **CONTAM88** for forming and solving the system of equations for the building contaminant dispersal are discussed in the next sections.

Data Structure

CONTAM88 uses a link list data structure for storing the data for the zones, openings, fans, kinetic reaction data and surface data. These link lists are allocated dynamically when the corresponding data is read. The contaminant physical data is stored in a series of dynamically allocated arrays.

The zone data structure is shown in figure 9. The zone data is stored in the structures of a linked list. The zone data structure contains physical data which describes the zone (its volume, temperature, height above the reference), variables which are the results of the calculations (zone air density, total mass of air in the zone, the zone pressure and a pointer to the results of the last transient contaminant dispersal analysis) and pointers to arrays which describe the contaminant sources (generations rates, removal rates, coefficients and exponents of pressure driven sources) in the zone and the kinetic reaction occurring in the zone. Each zone data structure contains a

point to the data structure of the next zone. The pointer, FirstZone, to the head of the list is a global variable. The last data structure is the list is contains a NULL pointer. In **CONTAM88**, the first zone data structure (pointed to by FirstZone) contains the outside ambient conditions. The first building zone is the second zone data structure (pointed to by FirstZone->NextZonePtr). The data contained in the file PROJECT.ZON are stored in the link list of zone data structures.

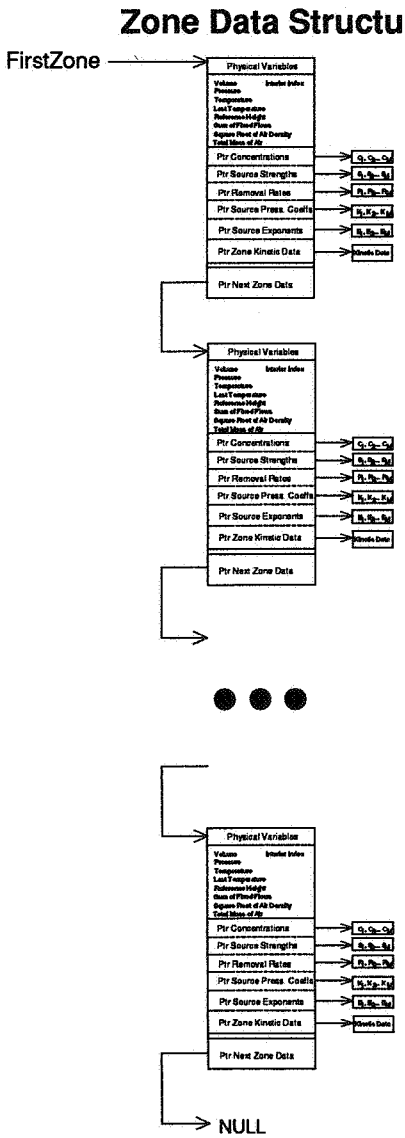

Figure 9. Zone Data Structure

The opening and fan data structures are shown in figure 9. The data for openings and fans are also stored in linked lists. The data structure of an opening contains the physical description of the opening contained in the data file PROJECT.OPN, the zones connected by the opening ,(LM[2] - where LM[0] = n_1, LM[1] = n_2 ,the zones numbers of the first and second node of the element), the flow coefficient, the flow exponent, the opening stack height, the height of the sur-

face containing the opening, the azimuth angle and tilt of the wall containing the opening and the number of the surface containing the opening. The opening data structure also contains results derived from these quantities: the transient pressure and the laminar region coefficients. During the airflow calculations the wind pressure, stack pressure, the flow through the opening and the pressure drop across the opening are storage in the zone data structure. Thus these quantities do not have to be recalculation very time they are needed. The fan data structure consist of the number of the zones connect by the fan (LM[2] has the same meaning as for an opening), the fan flow rate and a pointer to the efficiencies of any contaminant removal filters the fan may have. The head of each of these linked lists is determined by the global variables FirstOpening and FirstFan, respectively. Each list is NULL terminated.

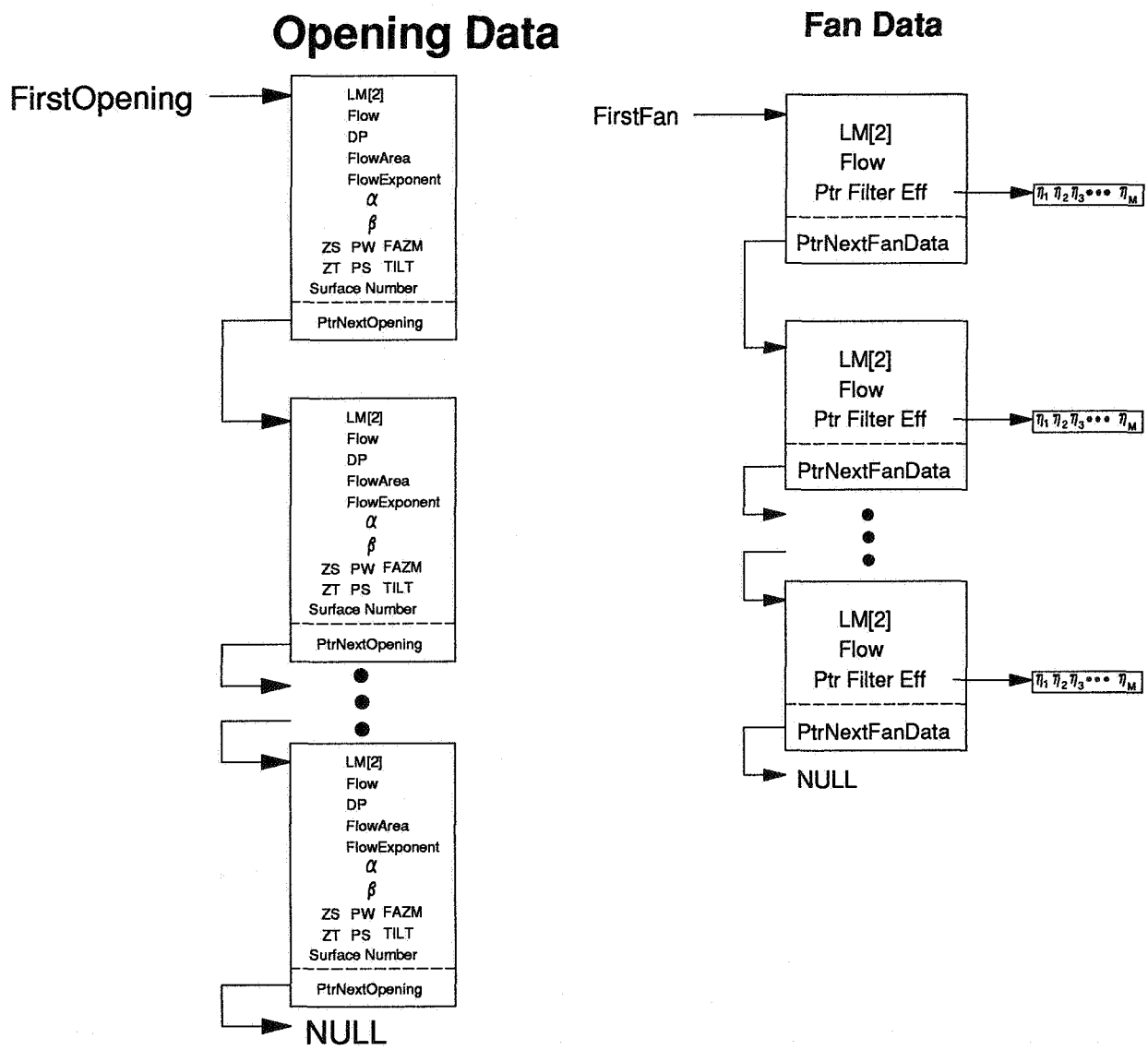

Opening Data Structure Fan Data Structure

Figure 10. Data Structure of Flow Elements

The data structure for the kinetic reaction data and the surface data are shown in figure 10. Each of these data are stored in simple linked lists which contain only the physical data which describes the kinetic reactions and the surfaces pressure coefficients respectively. The kinetic data structures contains a pointer to a dynamically allocated matrix (see the following section on matrix storage techniques) of the reaction coefficients. The surface data structures contains an integer indicating the number of pressure coefficients of the surface (this can vary from surface to surface) and a pointer to a dynamically allocated array containing the pressure coefficients. The global variables which point the headers of these linked lists are FirstKineticData and First-Surface.

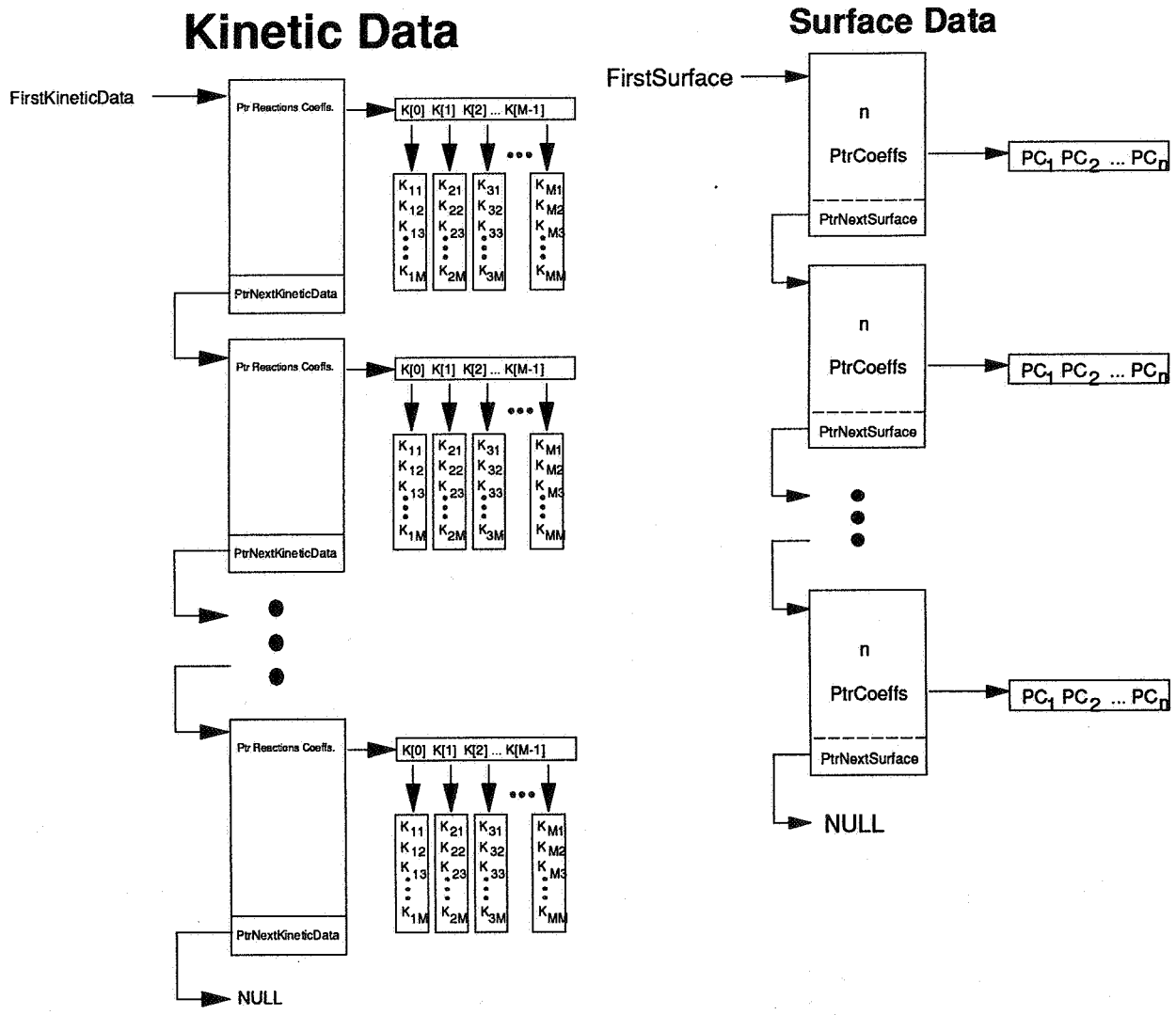

Figure 11. Kinetic Data Structure

Surface Data Structure

The data describing the properties of the contaminants are stored in dynamically allocated arrays: an array of string variable containing the contaminant name, an array of doubles containing the radioactivity of the contaminant, an array of doubles containing specific density of the contaminant, a boolean array indicating where the results are to be expressed in mass of air or volume of air and an array of integers indicating the units to be used in outputting the concentrations results for the contaminant. There is also an array of string variables which contain the name of the zones.

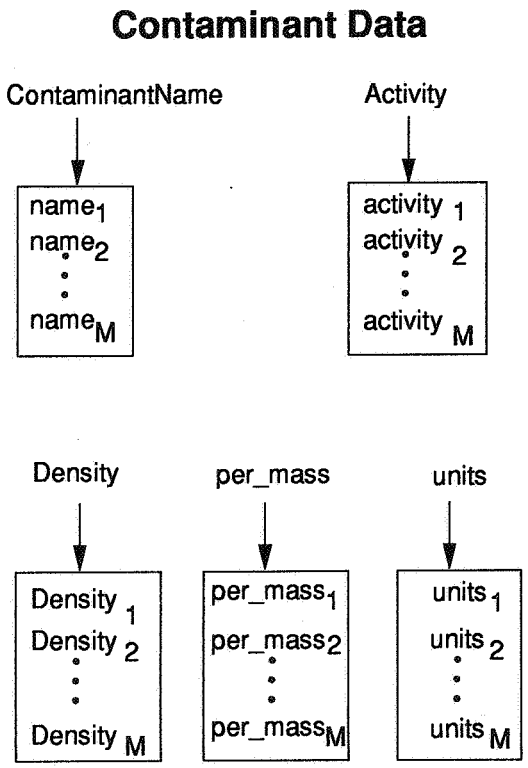

Figure 12. Contaminant Data Structure

The Use of CONTAM88 Data Structure to Form the Air Flow and Contaminant Dispersal Equations

The above data structure permits a simple and compact method for forming the air flow and contaminant dispersal systems of equations. The equations describing to the forming of the system Jacobian $\overleftrightarrow{\mathbf{J}}$ (eqn 24) and the system contaminant dispersal matrix $\overleftrightarrow{\mathbf{W}}$ contains theoretical matrices $\overleftrightarrow{\mathbf{B}}_e$, ${}^e\overleftrightarrow{\mathbf{B}}^\alpha$ etc. These matrices are never really form in the assembly of the system equations. The lists of elements (for the air flow analysis, the opening and fan linked lists; for the contaminant dispersal matrix, the opening, fan, and zone link lists) are transversed, the element matrices are construction and added to the system matrix using the integer array which contains the equations number of nodes of the element. The following indicates this process for the air flow Jacobian

"C" Code Forming Air Flow Equations

```
/* Form Flow Jacobian and Zone Flows */
  LastOpening = FirstOpening;
  i = 0;
  while(LastOpening != NULL)
  {
    i++;
    n = LastOpening->AFSPTR[0];
    m = LastOpening->AFSPTR[1];
    LastZone = ZonePointer(n);
    NearZone = ZonePointer(m);
/* Calculate pressure drop across opening */
    LastOpening->DP = ZonePointer(m)->PZ - ZonePointer(n)-
>PZ
                      +LastOpening->PS + LastOpening->PW;
/* Calculate flow through openig */
    LastOpening->Flow = 0.0;
    DPL = LastOpening->pl;
    if(fabs(LastOpening->DP) > DPL) /*Turbulence flow */
    {
      if(LastOpening->DP < 0.0)
        LastOpening->Flow = - LastOpening->FlowArea *
LastZone->SQRTDZ
                    *pow(-LastOpening->DP,LastOpening-
>FlowExponent);
      else
        LastOpening->Flow = LastOpening->FlowArea *
NearZone->SQRTDZ
                     *pow(LastOpening->DP,LastOpening-
>FlowExponent);
    }
    else  /* Laminar Flow */
    {
      LastOpening->Flow = LastOpening->DP * (LastOpening-
>ALaminar +
      fabs(LastOpening->DP) * LastOpening->BLaminar);
      if (LastOpening->DP < 0.0)
        LastOpening->Flow *= LastZone->SQRTDZ;
      else
        LastOpening->Flow *= NearZone->SQRTDZ;
    }
/* Calculte Derivative of Flow with respepect to DP */
    if(fabs(LastOpening->DP) > DPL)
    {
      DF = LastOpening->Flow * LastOpening-
>FlowExponent/LastOpening->DP;
    }
    else
    {
      DF = LastOpening->ALaminar
           + 2.0 * LastOpening->BLaminar *
fabs(LastOpening->DP);
      if(LastOpening->DP < 0.0)
        DF *= LastZone->SQRTDZ;
      else
        DF *= NearZone->SQRTDZ;
    }
/* Add Element Flow into first node to Zone Flows */
    BB[eqn_number[n-1]] += LastOpening->Flow;
    SUMAF[eqn_number[n-1]] += fabs(LastOpening->Flow);
/* Form Element Jacobina */
    nelem = 1;
    LM[0] = eqn_number[n-1];
    LM[1] = 0;
    KE[0][0] = -DF;
    KE[1][1] = 0.0;
    KE[0][1] = 0.0;
    KE[1][0] = 0.0;
    if(m > 0) /* m = 0 indicates exterior */
    {
/* Node 2 of element is building zone */
      nelem = 2;
      LM[1] = eqn_number[m-1];
      KE[1][1] = -DF;
      KE[0][1] = DF;
      KE[1][0] = DF;
/* Add element node 2 to Zone Flows */
      BB[eqn_number[m-1]] -= LastOpening->Flow;
      SUMAF[eqn_number[m-1]] += fabs(LastOpening->Flow);
    }
/* Add Element Jacobian to System Jacobian A */
    add_element_matrix(AA,PressureMatrixType,NZON,BandWidt
h,KE,LM,nelem);
  LastOpening = LastOpening->NextOpeningPtr;
  }
  if(LIST > 4) dump_matrix(AA,PressureMatrixType,NZON,Ban-
dWidth);
  if(LIST > 4) dump_vector(BB,NZON);
  factored = FALSE;
/* Solve for Pressure Correction */
  solve_linear_system(AA,BB,CC,&factored,Pressure-
MatrixType,
NumOfEqns,BandWidth);
/* Update Zone Pressures */  n = 0;
  if(LIST > 3) printf("\n    Initial ZonePressures \n");
  if(LIST > 3) fprintf(dataoutfile,"\n    Initial Zone-
Pressures \n");
  LastZone = FirstZone->NextZonePtr;
  while((LastZone != NULL) && (n < NZON))
  {
    LastZone->PZ -= CC[eqn_number[n]];
    if(LIST > 3 )
    {
      printf(" PZ: %4d %15.3e\n",n+1,LastZone->PZ);
      fprintf(dataoutfile," PZ: %4d
%15.3e\n",n+1,LastZone->PZ);
    }
    LastZone = LastZone->NextZonePtr;
    n++;
  }
/* Calculate Pressure Across Openings */
  LastOpening = FirstOpening;
  while(LastOpening != NULL)
  {
    n = LastOpening->AFSPTR[0];
    m = LastOpening->AFSPTR[1];
    LastOpening->DP = ZonePointer(m)->PZ - ZonePointer(n)-
>PZ
                      +LastOpening->PS + LastOpening->PW;
    LastOpening = LastOpening->NextOpeningPtr;
  }
/* Check Convergence */
```

Matrix Storage

CONTAM88 uses seven types of matrix storage techniques: three of symmetric matrices and for asymmetric matrices. The asymmetric matrix storage types are : storage for the full N by N matrix (asymmetric_full), storage for a diagonally banded matrix by rows (asymmetric_compact) and storage for a diagonally banded matrix by arrays parallel to the diagonal (asymmetric_compact2) and a skyline storage technique. The symmetric matrix storage techniques are: storage for the N·(N-1)/2 diagonal and upper diagonal elements (symmetric_full), storage by arrays parallel to the diagonal by a diagonally banded symmetric matrix (symmetric_compact) and a skyline technique for symmetric matrices (skyline_symmetric). The above matrix storage techniques are used dynamically in **CONTAM88**.

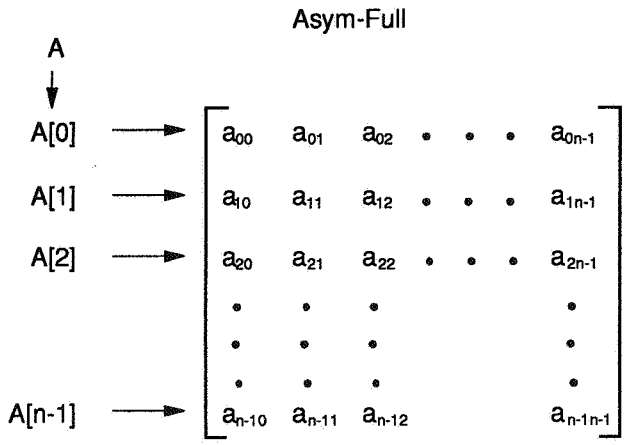

Asymmetric Full Matrix Storage Technique

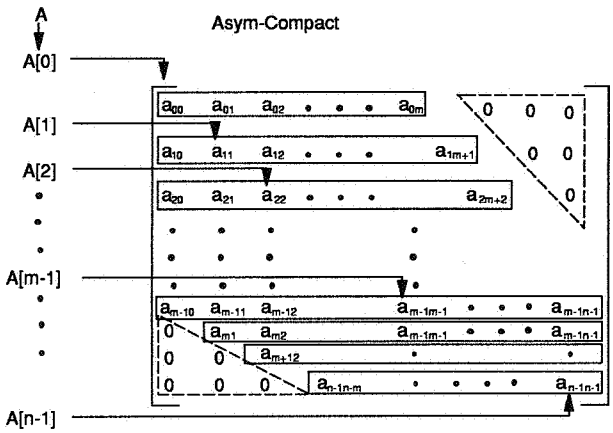

Storage Technique Asymmetric Compact Matrix - Row

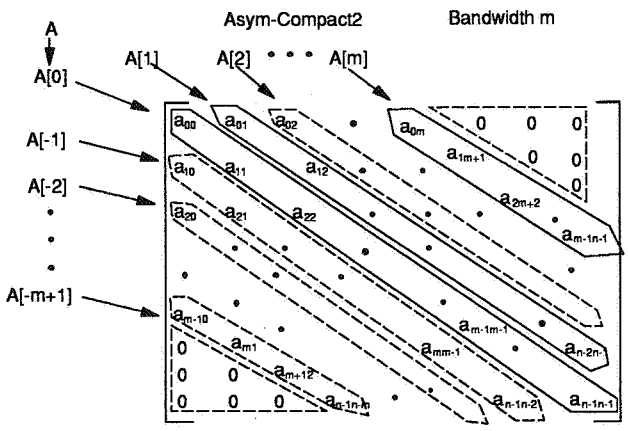

Asymmetric Compact Matrix - Diagonal Storage Technique

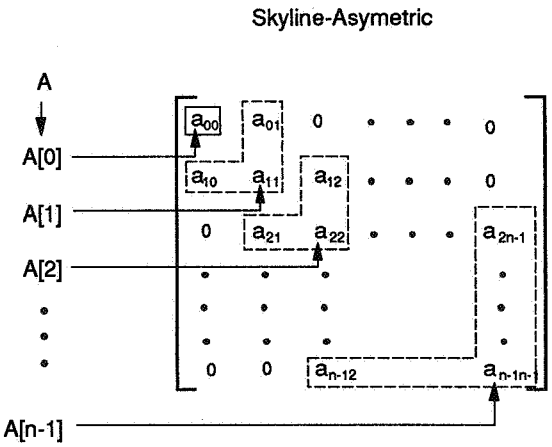

Asymmetric Skyline Matrix Storage Technique

Figure 13. Schematics of Asymmetric Matrix Storage Techniques

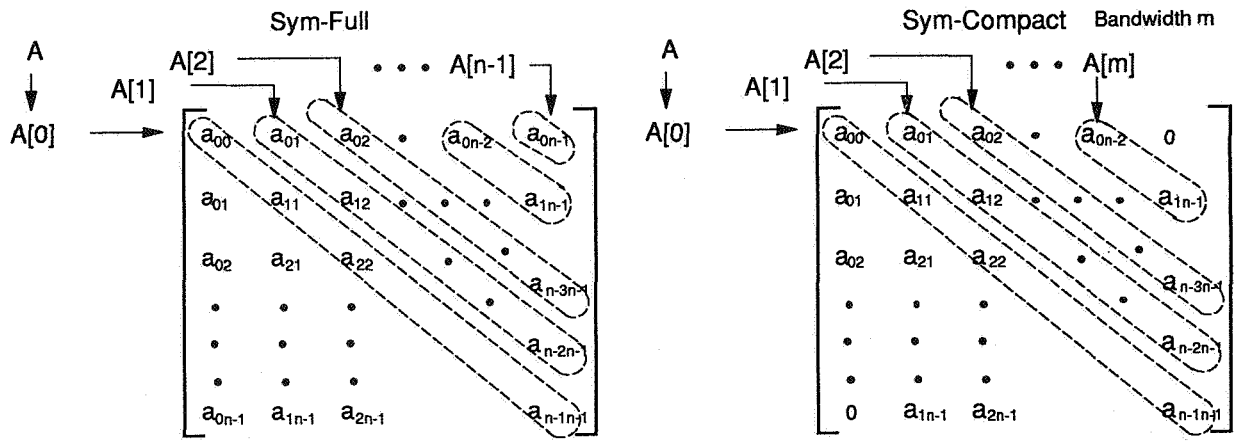

Symmetric Full Matrix Storage Techniques Symmetric Compact Matrix Storage Technique

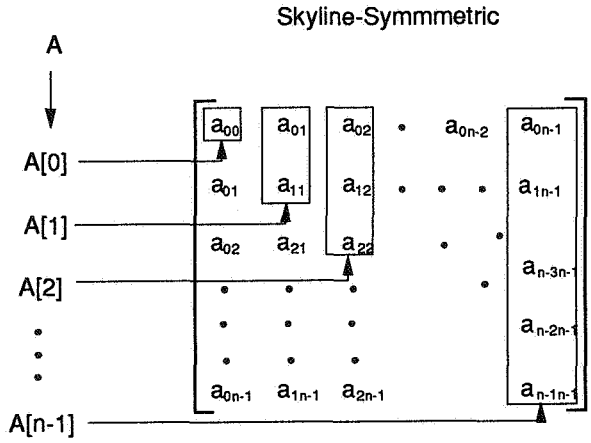

Skyline Symmetric Matrix Storage Techniques

Figure 14. Schematics of Symmetric Matrix Storage Technique

The basic method for dynamically allocating for a matrix is a structured language such a "C" which has pointers as a data type is to allocate storage for an array of pointers which point to the storage for the one-dimensional arrays which make up the matrix and then allocate the storage for each of these one-dimensional arrays. To illustrate this technique consider defining the two data types vector and matrix for the storage of "double" variables.

```
typedef  double *vector
typedef  vector *matrix
```

where * in the pointer operator in "C". Then to allocate memory for a N⊗N matrix, first allocate storage for an array A of N "vectors" {A[0] ... A[N-1]} and then for each A[l] ,l=0...N-1 allocate storage for a linear array of N doubles. This can be accomplished with the "C" code (where error checking has been omitted);

```
int l;
matrix A;

A = (matrix) calloc(N,sizeof(vector));
for(l=0;l<N;l++) A[l] = (vector) calloc(N,si-
zeof(double));
```

Then either the notation *A[k][l]* or **(*(A+k)+l)* can be used to storage or retrieve the double variable stored in the kth row and l[th] column of the matrix. Figure 13 illustrates the meaning of these variables.

In many physical problems, the matrix describing the system contains many zeros and the non-zero elements exist near the diagonal. Such matrices are called banded (see figure 13). **CONTAM88** allows two types storage schemes for compact asymmetric matrices as illustrated in figure 14. The first stores data by rows, the second by one-dimensional arrays parallel to the diagonal. If m is the half bandwidth of the matrix

$$m = \max |i-j| \quad \ni A_{ij} \neq 0$$

then the code

```
int l,n1,n2,N,m; /* N = dimension, m = half bandwidth */
matrix A;

A = (matrix) calloc(N,sizeof(vector);
for(l=0;l<N;l++)
{
  n1 = (l-m > 0) ? l-m : 0;  /* max(l-m,0) */
  n2 = (l+m > N-1) ? N-1 : l+m ; /* min(l+m,N-1) */
  A[l] = (vector) calloc(n2-n1+1,sizeof(double));
  A[l] += n1; /* shift pointer to diagonal */
}
```

allocates the storage for the banded matrix and leaves the pointer A[l] pointing to the diagonal element. Leaving the pointer A[l] pointing to the diagonal element, in the author's opinion, produces cleaner code. Beware that in freeing the allocated memory, the pointer must be restored to its value when memory was allocated.

The value stored in A[i][i-j] is the non-zero value of the element in the ith row and j[th] column.

$$A_{ij} = A[i][i-j] \quad \text{if} \quad |i-j| \leq m$$

$$= 0 \quad \text{if} \quad |i-j| > m$$

The storage of a band asymmetric matrix by one-dimension arrays parallel to th diagonal can be accomplished by the code

```
int l,N,m; /* N = dimension, m = half bandwidth */
matrix A;

A = (matrix) calloc(2m+1,sizeof(vector);
A *= m; /* shift A to point to diagonal *
for(l=-m;l<m+1;l++)
```

```
{
  A[l] = (vector) calloc(N-abs(l),sizeof(double));
}
```

The value stored in A[j-i][min(i,j)] is the non-zero value of the element in the ith row and j^{th} column.

$$A_{ij} = A[j-i][\min(i,j)] \quad \text{if} \quad |i-j| \le m$$

$$= 0 \quad \text{if} \quad |i-j| > m$$

Probably the most efficient storage scheme is the last one illustrated in figure 13. This is the skyline scheme. In this scheme one stores the non-zero elements in arrays A[l] which include the diagonal, the column of value to the last non-zero element above the diagonal and the row to right till the last non-zero element. If m[l] is the half bandwidth of this row/column

$$m[l] = \max_{\forall i < l}(l-i) \quad \ni \quad A_{kl} = 0 \quad \text{and} \quad A_{lk} = 0 \quad \forall k > i$$

The code for allocating memory for a skyline matrix is

```
int l,N,*m; /* N = dimension, m -> half bandwidth */
matrix A;

A = (matrix) calloc(N,sizeof(vector);
for(l=0;l<N;l++)
{
  A[l] = (vector) calloc(2*m[l]+1,sizeof(double));
  A[l] += m[l]; /* shift pointer to diagonal */
}
```

The value stored in A[max(i,j)][j-i] is the non-zero value of the element in the ith row and j^{th} column.

$$A_{ij} = A[\max(i,j)][j-i] \quad \text{if} \quad |i-j| \le m[\max(i,j)]$$

$$= 0 \quad \text{if} \quad |i-j| > m[\max(i,j)]$$

Figure 14 illustrates the three storage schemes for symmetric matrices.

The scheme for the full symmetric matrix and the banded compact symmetric matrix both storage the upper triangular part of the matrix by one-dimensional arrays parallel to the diagonal. Both these methods can be allocate by the code:

```
int l,m,N; /* for a full symmetric matrix m = N-1 */
matrix A;

A = (matrix) calloc(m+1,sizeof(vector);
for(l=0;l<m+1;l++)
{
  A[l] = (vector) calloc(N-l,sizeof(double));
}
```

In these cases A[|i-j|][min(i,j)] is the value of the non-zero element in the ith row and j^{th} column.

$A_{ij} = A[|\, j-i \,|][\min(i,j)]$ for a full symmetric matrix

and

$A_{ij} = A[|\, j-i \,|][\min(i,j)]$ if $|\, i-j \,| \le m$

$= 0$ if $|\, i-j \,| > m$ for a banded symmetric matrix

The code for allocating memory for a symmetric skyline matrix is

```
int l,N,*m; /* N = dimension, m -> half bandwidth */
matrix A;

A = (matrix) calloc(N,sizeof(vector);
for(l=0;l<N;l++)
{
  A[l] = (vector) calloc(m[l]+1,sizeof(double));
}
```

The value stored in A[max(i,j)][|j-i|] is the non-zero value of the element in the ith row and j^{th} column.

$A_{ij} = A[\max(i,j)][|\, j-i \,|]$ if $|\, i-j \,| \le m[\max(i,j)]$

$= 0$ if $|\, i-j \,| > m[\max(i,j)]$

As it will be shown in the following sections, the bandwidths can be determined without forming the matrices by using the indices of the element nodes and the matrix solution and manipulation techniques of CONTAM88 preserves the structure of the matrices (that is, they do not destroy the bandwidth).

Solution of Linear System of Equations

The linear systems of equations formed by **CONTAM88** are solved using a LU decomposition following by forward and backward substitution of the factored matrix. This method preserves the matrix structures treated above: that is the solution technique requires only the values stored in the banded and skyline storage schemes. If one considers the linear set of equations

$$\overleftrightarrow{\mathbf{A}}\vec{\mathbf{X}} = \vec{\mathbf{F}}$$

then it is possible to factor the matrix $\overleftrightarrow{\mathbf{A}}$ into the product of a lower triangular matrix $\overleftrightarrow{\mathbf{L}}$ and an upper triangular matrix $\overleftrightarrow{\mathbf{U}}$

$$\overleftrightarrow{\mathbf{A}} = \overleftrightarrow{\mathbf{L}} \cdot \overleftrightarrow{\mathbf{U}}$$

where $\overleftrightarrow{\mathbf{L}} = \begin{bmatrix} 1 & 0 & 0 & 0 & \cdots & 0 \\ L_{21} & 1 & 0 & 0 & \cdots & 0 \\ L_{31} & L_{32} & 1 & 0 & \cdots & 0 \\ \cdots & \cdots & \cdots & \cdots & \cdots & \cdots \\ L_{N-11} & L_{N-12} & \cdots & \cdots & 1 & 0 \\ L_{N1} & L_{N2} & \cdots & \cdots & L_{NN-1} & 1 \end{bmatrix}$

and $\overleftrightarrow{\mathbf{U}} = \begin{bmatrix} U_{11} & U_{12} & U_{13} & U_{14} & \cdots & U_{1N} \\ 0 & U_{22} & U_{23} & U_{34} & \cdots & U_{2N} \\ 0 & 0 & U_{33} & U_{34} & \cdots & U_{3N} \\ \cdots & \cdots & \cdots & \cdots & \cdots & \cdots \\ 0 & 0 & 0 & 0 & \cdots & U_{NN} \end{bmatrix}$

The decomposition can be accomplished by the algorithm

$$U_{11} = A_{11}$$

for $s = 2, \ldots, N$

$$L_{si} = \left(A_{si} - \sum_{m=1}^{i-1} L_{sm} U_{mi} \right) \frac{1}{U_{ii}} \quad i = 1, \ldots, s-1 \tag{47}$$

$$U_{is} = A_{is} - \sum_{m=1}^{i-1} L_{im} U_{ms} \quad i = 1, \ldots, s \tag{48}$$

Note that in performing the LU decomposition of a matrix A, the results can be stored in the same storage locations as the original matrix $\overleftrightarrow{\mathbf{A}}$ if the 1's on the diagonal of lower triangular matrix $\overleftrightarrow{\mathbf{L}}$ are not stored.

$$\overleftrightarrow{\mathbf{A}} = \begin{bmatrix} U_{11} & U_{12} & U_{13} & U_{14} & \cdots & U_{1N} \\ L_{12} & U_{22} & U_{23} & U_{24} & \cdots & U_{2N} \\ L_{31} & L_{32} & U_{33} & U_{34} & \cdots & U_{2N} \\ \cdots & \cdots & \cdots & \cdots & \cdots & \cdots \\ L_{N1} & L_{N2} & L_{N3} & \cdots & L_{NN-1} & U_{NN} \end{bmatrix}$$

using the algorithm

for $s = 2, \ldots, N$

$$A_{si} = \left(A_{si} - \sum_{m=1}^{i-1} A_{sm} A_{mi} \right) \frac{1}{U_{ii}} \quad i = 1, \ldots, s-1 \tag{49}$$

$$A_{is} = A_{is} - \sum_{m=1}^{i-1} A_{im} A_{ms} \quad i = 1, \ldots, s \tag{50}$$

The LU decomposition preserves the banded and symmetric structure of the matrices formed in **CONTAM88**[10].

5 Adsorption Modeling

Adsorption-desorption mass transport processes introduce complexities in contaminant dispersal analysis that demand thoughtful structuring of both the data describing the building system to be analyzed and the associated systems of equations that describe the dispersal of contaminants in the building. To set the stage for consideration of these complexities, the underlying theory of one of two families of adsorption elements, that have been recently developed to augment the existing library of contaminant dispersal elements[11], will be reviewed here.

Adsorption involves the separation of a substance _ the adsorbate _ from one phase, indoor air in the present context, and the accumulation of that substance on the surface of another phase _ the adsorbent _ building materials and furnishings, here. Limiting consideration to those adsorbate-adsorbent systems that exhibit reversible sorption (i.e., both adsorption and desorption transport processes are possible) the adsorption process may be thought to be a reversible exchange between alternative phases of the adsorbate _ the free phase and the adsorbed phase. In the building context such a reversible adsorption process may be idealized as illustrated below in Figure 15.

Air flows into a given building zone carrying, perhaps, an adsorbate species _ identified here with the Greek leading superscript α. Within the core of the building zone the adsorbate species exists at a bulk mean concentration of ${}^{\alpha}C$ (mass-a/mass-air) and is transported via diffusion transport processes to a near-surface location where its free phase concentration is ${}^{\alpha}C^{*}$. At this near-surface location adsorption processes come into play to bind the species to the surface establishing the adsorbed surface-phase concentration ${}^{\alpha}C_{s}$ (mass-a/mass-adsorbent). The rate of species transport to and from the adsorbent surface is, thus, determined by both diffusion and adsorption mechanisms.

Diffusion: Diffusion transport to and within effective adsorbents invariably involves a complex variety of transport mechanisms including boundary layer molecular and turbulent diffusion from the bulk phase and molecular, Knudsen, Poiseuille, and surface diffusion within macroporous and microporous interstices[12]. For our present purposes it will be sufficient to limited consideration to boundary layer diffusion which may be modeled as a spatially discrete process using boundary layer

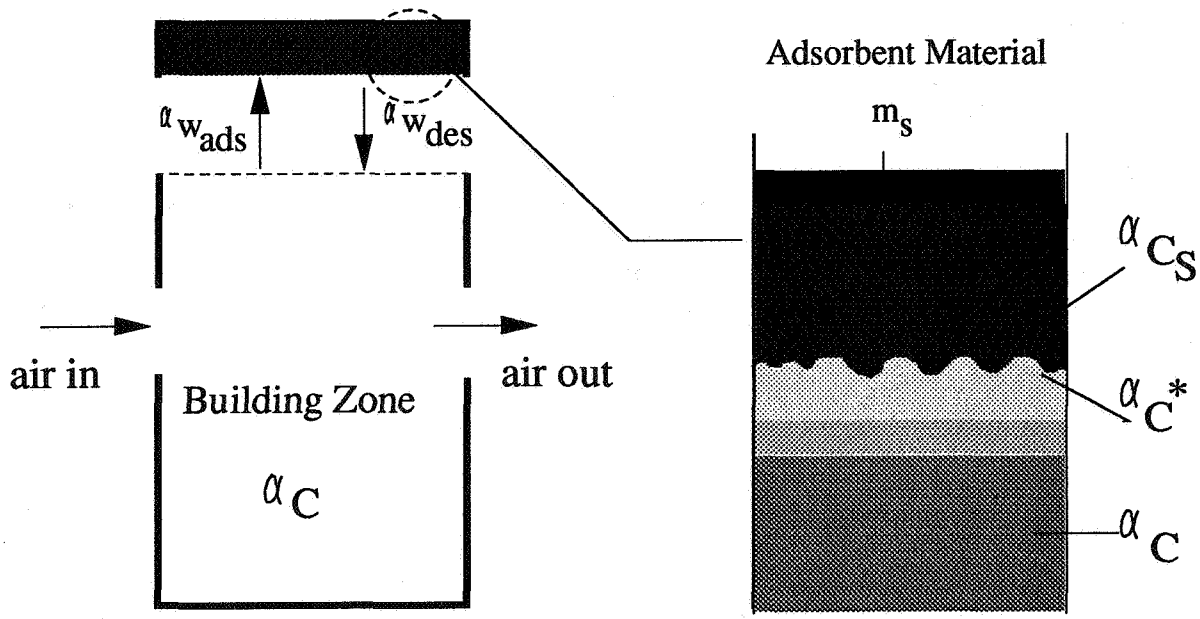

Figure 15. Adsorption Element Variables

theory[13]; macro and microporous diffusion processes which are, by their nature, spatially continuous may, conceivably, be modeled using discrete finite element approximations. From boundary layer theory, the net mass transport of the adsorbate species, $^{\alpha}w_S$ (mass-a/time), from the bulk phase to the near-surface location is directly related to free-phase concentration difference between the bulk and near-surface locations as:

$$\alpha_{ws} = (^{\alpha}w_{ads} - ^{\alpha}w_{des}) = h_m \rho A_S (^{\alpha}C - ^{\alpha}C^*) \tag{51}$$

where h_m (length/time) is the average film mass transfer coefficient acting over the adsorbent surface, r is the film density of air, the average of the bulk and near-surface densities, and A_S is the projected surface area of the adsorbent. The film transport coefficient is correlated to fundamental characteristics of the airflow over the adsorbent; the surface flow Reynolds number and the free phase Schmidt number.

Adsorption: In typical circumstances the rate of the adsorption step may be expected to be practically instantaneous relative to the diffusion transport processes and/or the rate of mass transport by advection into a given building zone, thus, it is not normally necessary to explicitly model the adsorption kinetics. Although practically instantaneous, adsorption is limited by its equilibrium state. That is to say, for closed systems under steady conditions the rate at which adsorbate molecules bind to the adsorbent surface will eventually equal the rate at which they are released from the surface and the concentration in the free and adsorbed phases will remain constant at their respective

equilibrium values, ${}^{\alpha}C^{*}_{e}$ and ${}^{\alpha}C_{Se}$. In functional notation, we may say that the adsorbed phase equilibrium concentration is related to the free phase equilibrium concentration and the thermodynamic state of the system defined by temperature, T, and pressure, P, as:

$$ {}^{\alpha}C_{Se} = f({}^{\alpha}C^{*}_{e}, T, P) \tag{52} $$

These equilibrium relations are, generally, unique to the adsorbate-adsorbent system being considered and, when reported for isothermal conditions at atmospheric pressure, are identified as adsorption isotherms. Although a large variety of models have been proposed for adsorption isotherms three physically-based models, the Linear, Langmuir and BET models, have become fundamental to the field. The Linear model may be expected to useful in those situations where adsorbate free-phase concentrations are low (i.e., relative to saturation levels) and it is especially straightforward:

$$ {}^{\alpha}C_{Se} = K_P {}^{\alpha}C^{*}_{e} \tag{53} $$

where K_P is the so-called partition coefficient that exhibits an Arrhenius type dependency on temperature for ideal reversible systems.

Adsorption Element Equations: Two families of adsorption element equations may be formulated by: a) demanding instantaneous conservation of species mass in the adsorbent phase; b) demanding equilibrium conditions prevail at the surface of the adsorbent (i.e., as described by one of the several equillibrium relations available); and c) modeling the diffusion transport step as either instantaneous _ equillibrium adsorption _ or as described by the boundary layer theory presented above _ boundary layer diffusion controlled adsorption. These element equations have the general form:

$$ [{}^{\alpha}\mathbf{w}^{e}]\{{}^{\alpha}\mathbf{C}^{e}\} + [{}^{\alpha}\mathbf{m}^{e}]\frac{d\{{}^{\alpha}\mathbf{C}^{e}\}}{dt} = \{{}^{\alpha}\mathbf{g}^{e}\} \tag{54} $$

where $\{{}^{\alpha}\mathbf{C}^{e}\}$ is a vector of contaminant species a discrete concentration variables associated with the element "e" and $\{{}^{\alpha}\mathbf{g}^{e}\}$ is a vector of element derived contaminant species generation rates. The element matrices $[{}^{\alpha}\mathbf{w}^{e}]$ and $[{}^{\alpha}\mathbf{m}^{e}]$ are square transformation matrices known as the element species transport matrix and species mass matrices respectively.

For the combination of the linear equillibrium adsorption model and the boundary layer diffusion model, a two-node element results with:

$$ \{{}^{\alpha}\mathbf{C}^{e}\} = \begin{Bmatrix} {}^{\alpha}C_{i} \\ {}^{\alpha}C_{j} \end{Bmatrix} \quad ;\text{i = well-mixed zone node, j = adsorbent node} \tag{54} $$

$$ [{}^{\alpha}\mathbf{m}^{e}] = \begin{bmatrix} 0 & 0 \\ 0 & m_S \end{bmatrix} \tag{54} $$

$$ [{}^{\alpha}\mathbf{w}^{e}] = (h_m \rho A_S) \begin{bmatrix} 1 & -\dfrac{1}{K_P} \\ -1 & \dfrac{1}{K_P} \end{bmatrix} \tag{55} $$

where m_s is the total adsorbent mass available.

In conclusion then, when diffusion transport is accounted for, adsorption modeling will demand the introduction of additional degrees of freedom (i.e., nodes), beyond those corresponding to each well-mixed zone, to be included in the system model. In multi-contaminant dispersal analysis contaminants may be selectively adsorbed, thus, in general, the number of additional adsorbent nodes associated with each building zone may be expected to vary in number and type from zone to zone A data structure to include material absorption in a general contaminant dispersal analysi is shwon in the following figure. One adds to the data structure of the zone data of CONTAM88 a pointer to a list of data structures which contain the absorption characteristics of the materials contained in each zone. The contaminant dispersal assembly process then adds the corresponding material nodes and coupling to the zone contaminant dispersal equations. This theory and assembly process has been implemented in CONTAM89, a prototype of the next version of CONTAM88.

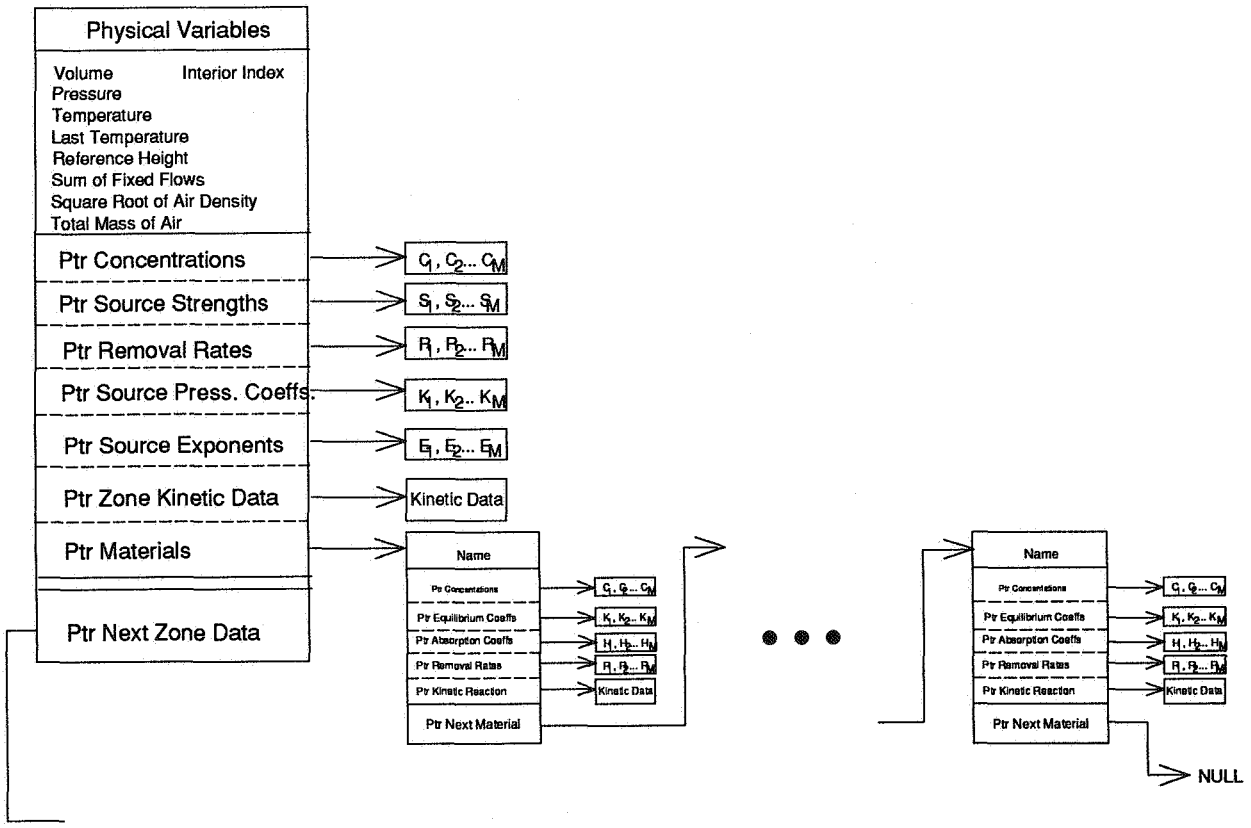

Figure 16. Schematic of Zone data Structure to Include Material Absorption

6 Modeling of a 12 Storey Apartment Building

NBSAVIS and **CONTAM88** has been used to model the air flows and contaminant dispersal in a 12 storey apartment building shown schematically in figures 17 and 18.

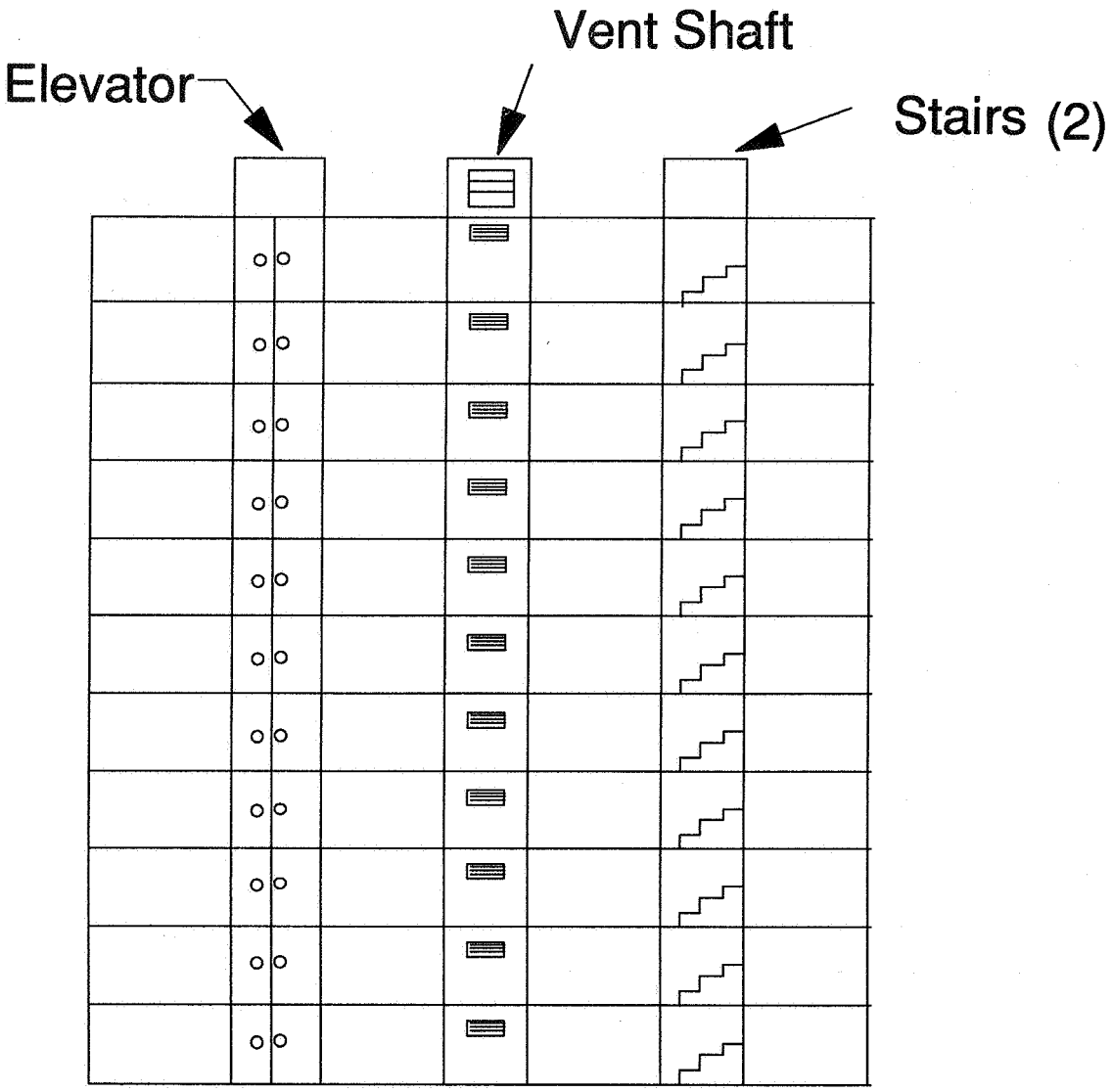

Figure 17. Schematic of the Elevation of a 11 Storey Apartment Building

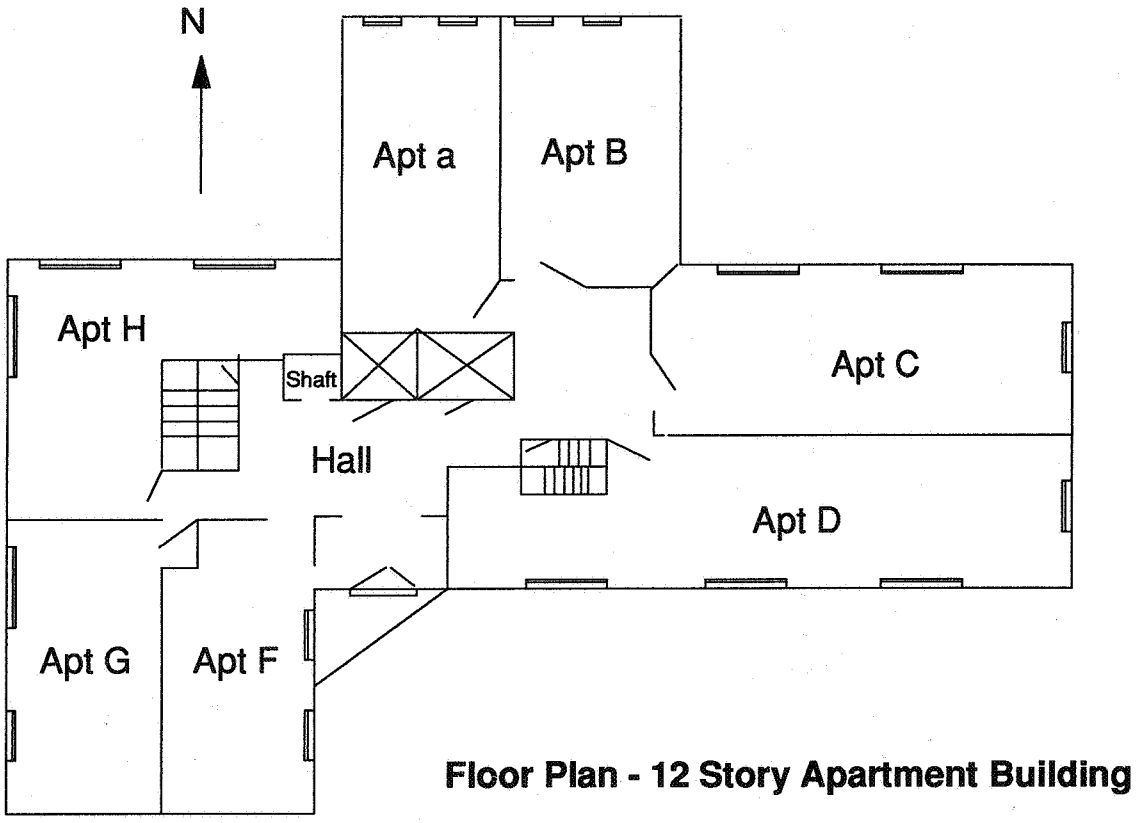

Figure 18. Typical Floor Plan of the Apartment Building

The apartment building has two stairwells running from the main floor to the roof. It also has an elevator shaft and a passive ventilation shaft. There is a large grill in the entrance way of the first floor to provide air for the ventilation shaft. Each floor has a hallway and 7 apartments. The building was described by NBSAVIS as a 100 room building: the two stairwells, elevator shaft and the ventilation shaft plus for each floor, the hall and each apartment. The description produced by **NBSAVIS** had over 1000 flow paths. The results of simulating a pressure driven radon source in the apartments on the first floor are shown in figure 19. It took approximate 20 seconds and 5 iterations to solve the flow-pressure system of equations on a 386/33 IBM clone without a math coprocessor and 2 seconds to solve the steady state contaminant dispersal system of equations. The problem required about 40K of memory by **NBSAVIS** for the building description and 180K (leaving 190K of the 640K of memory not used) by **CONTAM88** for solving the flow and contaminant dispersal systems.

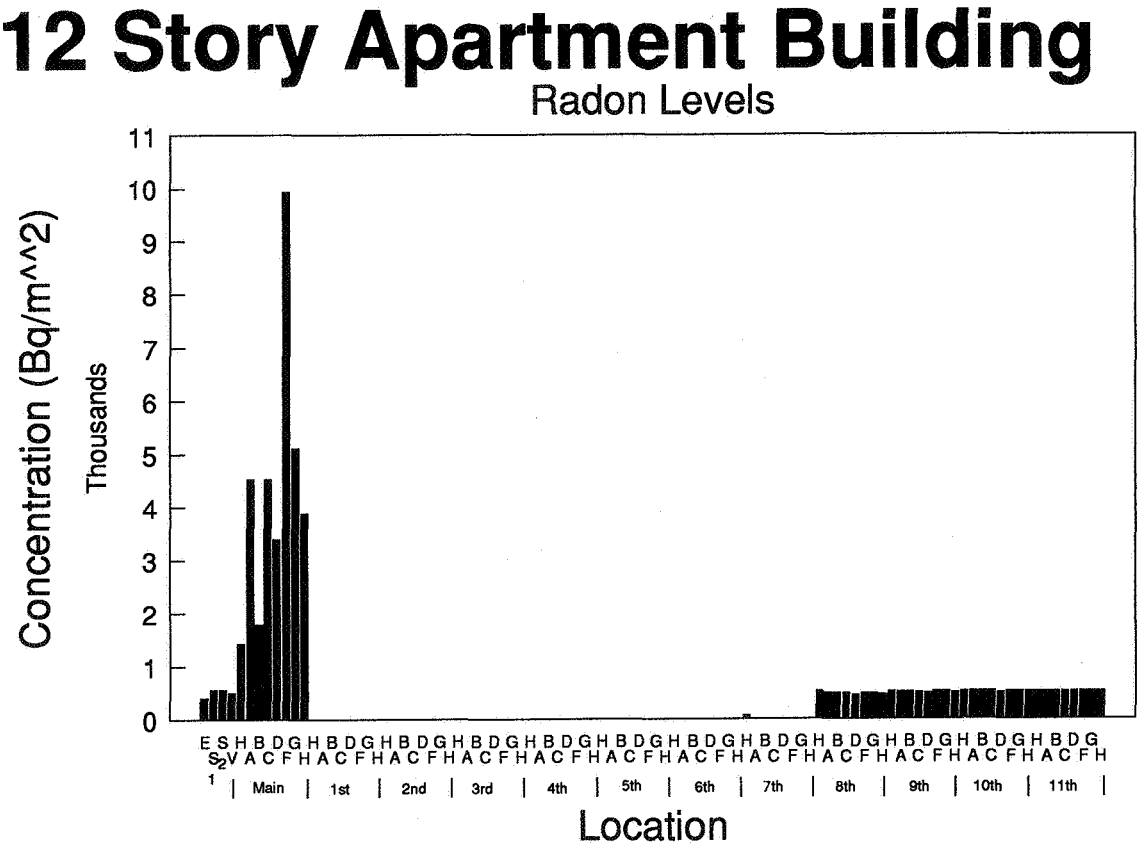

Figure 19. Results of Simulating Radon Migration in a 12 Storey Building

Figure 19 shows the high radon levels on the first floor in the apartments where the radon sources are. However it also shows that radon will migrate up the shafts of the building and exit through the apartments on the upper levels due to the stack effect. Note that there is no radon on floors 1 through 7 since there is no source of radon on the upper floors and the air flow enters the apartments on these floors form the exterior and exists through the shafts. On floors 8 through 11, the air flow is from the shafts through the apartments to the exterior. Level of radon in the apartments on floor 8 through 11 is basically the level of radon in the vertical shafts of the building.

References

1. Walton, G.N. "A Computer Algorithm for Estimating Infiltration and Inter-Room Air Flows", February 1983, NBSIR 83-2635
2. Walton, G.N. "A computer algorithm for predicting infiltration and interroom airflows", 1984, ASHRAE Transactions, vol 90,Part 1
3. Persily, A.K. & Grot, R.A., "The Airtightness of Office Building Envelopes", ASHRAE SP49, Thermal Performance of Exterior Envelopes of Buildings III, 1986
4. Axley, J., "Indoor Air Quality Modeling Phase II Report", 1987, NBSIR 87-3661

5. Axley, J., "Progress Toward A General Analytical Method for Predicting Indoor Air Pollution in Buildings - Indoor Air Quality Modeling Phase II Report", 1988, NBSIR 88-3814

6. Liddament, M.W, "Air Infiltration Calculation Techniques - An Applications Guide", Air Infiltration and Ventilation Centre, Coventry, UK, 1986

7. Nazaroff, W. W & Nero, A.V. (Editors), Radon and Its Decay Products in Indoor Air, John Wiley & Sons, NY,NY, 1988.

8. ASHRAE Handbook of Fundamentals, ASHRAE, Atlanta, GA, 1988.

9. Walton, G.N., "AIRNET - A Computer Program for Building Airflow Network Modelling", NISTIR 89-4072. 1989

10 Grot, R.A., User's Manual for NBSAVIS and CONTAM88, NISTIR 90-XXXX (in review)

11 Axley, J. W. Adsorption Modeling for Macroscopic Contaminant Dispersal Analysis. NIST/GCR 90/573. National Institute of Standards and Technology. 1990.

12. Ruthven, D. M. "Adsorption Kinetics." Adsorption Science and Technology. Rodrigues ed. 1989 Kulwer Academic Publishers. Dordrecht.

13. White, F. M. "Heat and Mass Transfer." 1988 Addison-Wesley Pub. Co. New York.

Discussion

Paper 13

Earle Perera (BRE, UK)

Has your air movement model been validated against a known bench-mark case? If not, then how can all those who have similar multizone programs get together to set-up such a validation?

R.Grot (Lagus Applied Technology, USA)

These models have not been completely validated. The numerical procedures have been checked quite extensively by George Wilton. Andy Persily and I wrote a paper for ASHRAE comparing the results of AIRMOV on earlier version with two large building Air Infiltration results; however the accuracy of the multizone flows has not been checked. The last part of your question is more political and depends on the ability of many of us to convince our countries to fund validation research.

C-A Roulet (LESO, Switzerland)

Evaluation of computer codes is a huge task which consists not only in comparing computation results with measurements but also in evaluating the effects of small changes in input data on the results and this is all the possible range of the input parameters. I hope that Annex 23 can make some progress in this quite unexplored domain.

R.Grot (Lagus Applied Technology, USA)

I also hope that Annex 23 can provide answers to this very important issue.

VENTILATION SYSTEM PERFORMANCE

11th AIVC Conference, Belgirate, Italy
18-21 September, 1990

Paper 14

EFFECT OF WIND PRESSURE FLUCTUATIONS ON AIR MOVEMENTS INSIDE BUILDINGS

J. Riberon, D. Bienfait, G. Barnaud, J. Villain

Centre Scientifique et Technique du Batiment
84 avenue Jean-Jaures, BP 2
77421 MARNE LA VALLEE Cedex 2
France

ABSTRACT

An appropriate way to identify the most efficient ventilation systems and improve their design is to use design codes for ventilation rates.

These rates are strongly influenced by spatial and temporal fluctuations in wind pressure on the façade and roof. The influence of the effects of wind on ventilation was studied using a model which includes air compressibility, together with the pressure field measured on a model in a boundary layer wind tunnel.

The simulation results obtained are analyzed using a design code. The effect of wind fluctuations on the quality of ventilation is evaluated using the concentration of a polluting agent as an indicator.

Flow rates measurements have been undertaken in an experimental house near Nantes, in order to allow comparison with computer results. The measurement methodology is described and first experimental results are given in this paper.

1 - INTRODUCTION

One of the mainsprings of ventilation in buildings is the pressure due to wind. Because of its fluctuating character, wind produces a pressure field around a building which is also fluctuating [1] [2]. However, most multi-zone numerical models for air transfer disregard this phenomenon by using a certain number of simplifying hypotheses including that of air incompressibility and that of the steadiness of wind pressure during the same period of time.

These simplifications lead to erroneous conclusions in certain cases. For example, when the pressure inside a room is equal to the wind pressure on the façade, taking temporal wind fluctuations into account produces an air flow rate which is not equal to zero. Similarly, when a room only communicates with the outside via a single opening, the air transfers are not zero, if both the air compressibility and temporal wind fluctuations are considered.

Research works have been conducted at the C.S.T.B. in order to assess the effect of wind pressure fluctuations on air movements inside buildings.

The influence of wind fluctuations was studied at the C.S.T.B. using a numerical model which includes air compressibility, together with the pressure field measured on a model in a boundary layer wind tunnel. The simulation results obtained are analysed. The effect of wind fluctuations on the quality of ventilation is evaluated using the concentration of a pollutant as an indicator.

The experimental validation of the computer code is under way using flow rates measurements in an experimental rotating house at Bouin (near Nantes). The measurement methodology is described and first experimental results are given.

2 - NUMERICAL STUDY

2.1 - Modelling

The SIREN 2 code was used (see figure 1) to evaluate the air movement between zones within the same building under given temperature and wind pressure conditions and for ventilation installations and buildings with given characteristics [3]. The pressure fields are determined (see figure 2) by measurements in a boundary layer wind tunnel on a 1/150 scale model [4].

For each zone i, the mass balance, assuming isentropic transformation yields:

$$\frac{Vi}{\gamma\, rTi} \cdot \frac{dPi}{dt} = Qi$$

Vi : volume of the zone i
Ti : temperature in zone i
Pi : pressure in zone i
γ : ratio of specific heat at constant pressure to that at constant volume (for air, $\gamma = 1.4$)
r : gas constant (for air, r = 287 J/kg K)
Qi : mass flow rate exchanged between zone i and other zones. It can be expressed as follows :

$$Qi = \sum_{j} (qij - qji)$$

The index j runs from 0 (outside air) to the number N of zones, but is different of i.

qij : mass flow rate from zone i to zone j. It depends on pressure difference between zones i and j (qij = f(Pi,Pj)).

The differential equations system is solved using Levenberg-Marquardt algorithm (minimimum of the sum of the squares of functions).

2.2 - Effect of wind turbulence on single-family houses

Air transfers are calculated according to different hypotheses depending on whether spatial and temporal fluctuations in the wind pressure and air compressibility are taken into account. In order to ascertain the effect of these hypotheses on the results, a pollution indicator i.e. the carbon dioxide concentration was used. Two cases were considered [5] :

First case : study of a two-room house

The CO_2 concentrations were calculated in each of the two rooms for different wind angles and with the communication door closed and open. Figure 3, for example, shows the result of a simulation where the wind is parallel to the façades, the communication door is open and there is a constant flow of pollutant in room n° 1.

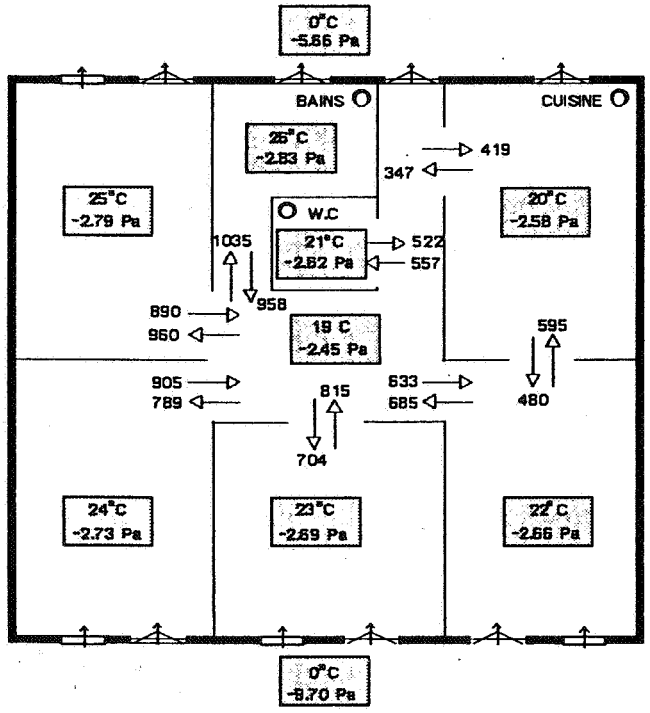

Figure 1 :
Computed flow rates (in kg/h) in a dwelling with mechanical ventilation

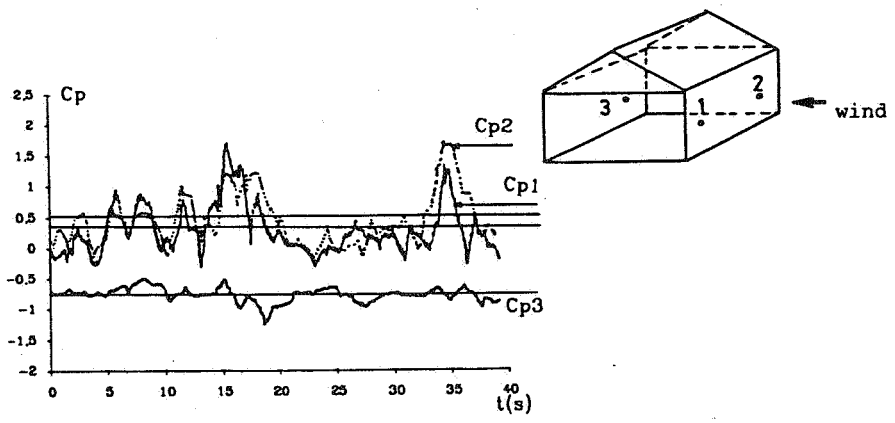

Figure 2 : Examples of wind pressure spatial and temporal fluctuations

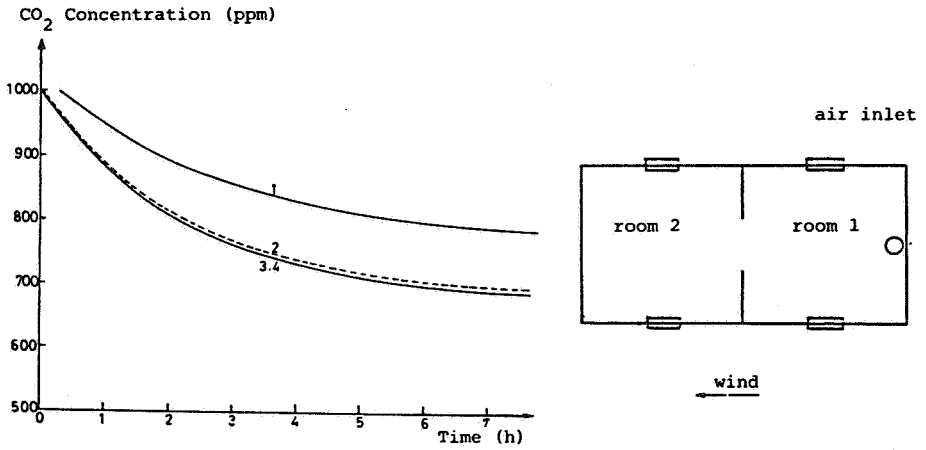

1 : incompressible air, constant wind pressure
2 : incompressible air, temporal wind fluctuations
3 : incompressible air, spatial and temporal wind fluctuations
4 : compressible air, spatial and temporal wind fluctuations

Figure 3 :
Changes in the carbon dioxide concentration in room n° 2 as a function of time. Wind is parallel to the façades and communication door open

The results show that, unlike the air compressibility, the effect of temporal wind fluctuations cannot be ignored. This effect on the ventilation is particularly important when the wind is parallel to the main façades (see figure 3) ; ignoring this can produce errors of up to 35 % in the CO_2 concentration. The effect of wind pressure spatial fluctuations was also investigated and proved to be lower (10 % instead 35 %) than the temporal fluctuations effect.

Second case : study of a single room house

The case of a house with single exposure and no special ventilating system was considered. The air from the façade passes through a free section of 200 cm^2, while the opening in the opposite façade, corresponding to defective airtightness, is only 10 cm^2. It is assumed that no carbon dioxide is emitted inside the house and that the initial concentration is 1 000 ppm.

Figure 4 shows the changes in the carbon dioxide concentration as a function of time for various hypotheses. It can be observed that, unlike the previous example, the hypothesis of air compressibility is a relevant factor. This is explained by the large difference between the sections of the two openings (ratio of 1 to 20).

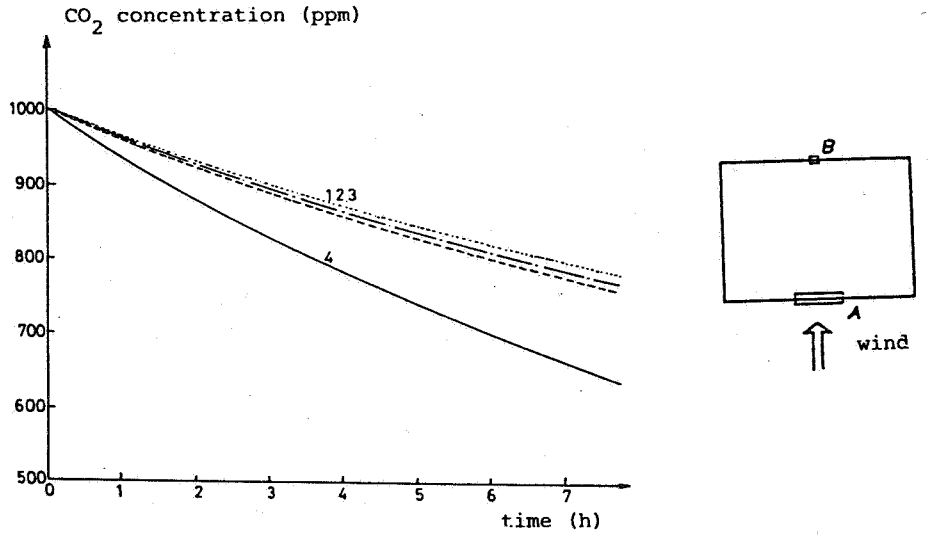

Figure 4 : Carbon dioxide concentration versus time
(refer to figure 3 for meaning of hypotheses 1, 2, 3 and 4)

2.3 – Effect of wind turbulence on a whole-house ventilation system

The effect of wind fluctuations on a seven floor building ventilated by collective passive stack ventilation ducts [6] was also investigated. Emissions of carbon dioxide with constant flow rates equal to 1 200 g/hr and 60 g/hr respectively on the fourth and top floors of the building were considered. The air transfers were analyzed for various hypotheses depending on whether or not spatial and temporal fluctuations in wind pressure were taken into account. The results show that taking the wind fluctuations into account considerably modifies the instant flow rates and may explain the reverse air flow on the top floor for high values of the network head loss (figure 5).

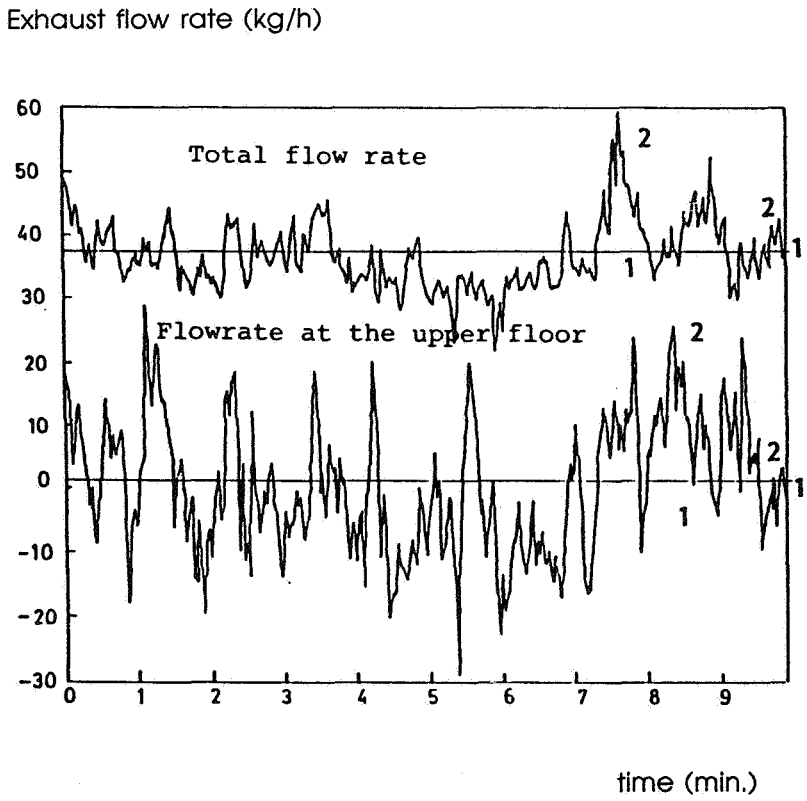

Figure 5 : Computed flow rates in a shunt duct

1 : flow rates are calculated using time averaged wind pressure
2 : flow rates are calculated using actual wind pressure records

3 - EXPERIMENTAL STUDY

An experimental house was designed to globally validate the design codes by dealing with problems which it is impossible to simulate on a scale model in a boundary layer wind tunnel due to the lack of similitude. This is the case when determining the effective ventilation rates in a house, because the head loss is not a linear function of the flow rate.

3.1 - Experimental house

The experimental house is located at BOUIN, on the atlantic coast, in a windy area. It is a single-storey house (9m x 5m x 4m) ; the roof is pitched at 30 degrees (see figure 6). The BOUIN experimental house is a rotating house which can be turned toward a given direction of wind.

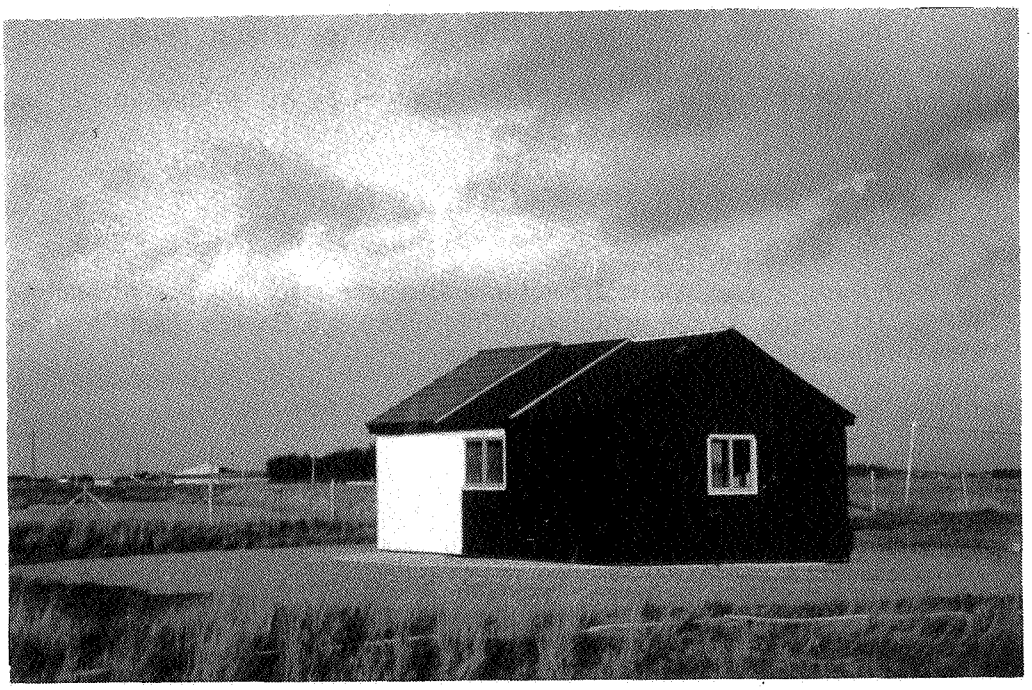

Figure 6 : View of the BOUIN experimental house

Particular attention was paid to improve the building envelope airtightness. The measured air leakage value proved to be equivalent to 5 cm^2.

3.2 - Instrumentation

Pressure tapping points are distributed along the outside surface of the walls, and close to the air inlet and outlet orifices. The speed and direction of the wind are recorded together with other measurements. The ventilation rate is measured using the tracer gas method. This instrumentation is completed by a fast response (40 Hz) measuring equipment [7], designed to instantaneously record the air flow entering or leaving the external openings.

3.3 - Tests

Single sided ventilation through one external opening of the house has been studied [8]. Two openings were tested : sharp-edged slots with dimensions of 40cm x 2.5cm or 40cm x 5cm. The opening was located either windward or leeward, at 2m above the ground level.

Tests were carried out in order to measure air change inside the house. The test procedure is as follows :

- orientation of the experimental house
- sealing of the opening
- tracer gas injection
- mixing of gas inside the volume during 10 minutes period, using fans
- data logging : the acquisition frequency is 5 Hz, the decay test period (opening unsealed) is 20 minutes.

3.4 - Results

Tests results for differents configurations are given in following table.

test	opening		wind		air change rate
	area (cm^2)	location	mean (m/s)	standard deviation (m/s)	(ach)
1	100	windward	7.7	1.2	0.25
2	100	leeward	10.2	1.5	0.69
3	200	windward	5.8	1.15	0.44
4	200	leeward	5.8	1.1	0.24

Air compressibility and wind fluctuations assumptions are required to explain the measured air change values.

Dynamic pressure at the opening and wind velocity and direction are shown, for example, in figures 7, 8 and 9. The data refer to the test 1.

Figure 10 depicts for the test 1 the variation of the measured inside pressure (relative to outside static pressure) and the inside pressure calculated using SIREN2 computer code.

For this same test, the variation of the tracer gas concentration as a function of time is shown in figure 11 : measured and calculated values are plotted in the same graph. In this case, predicted and measured results are in close agreement.

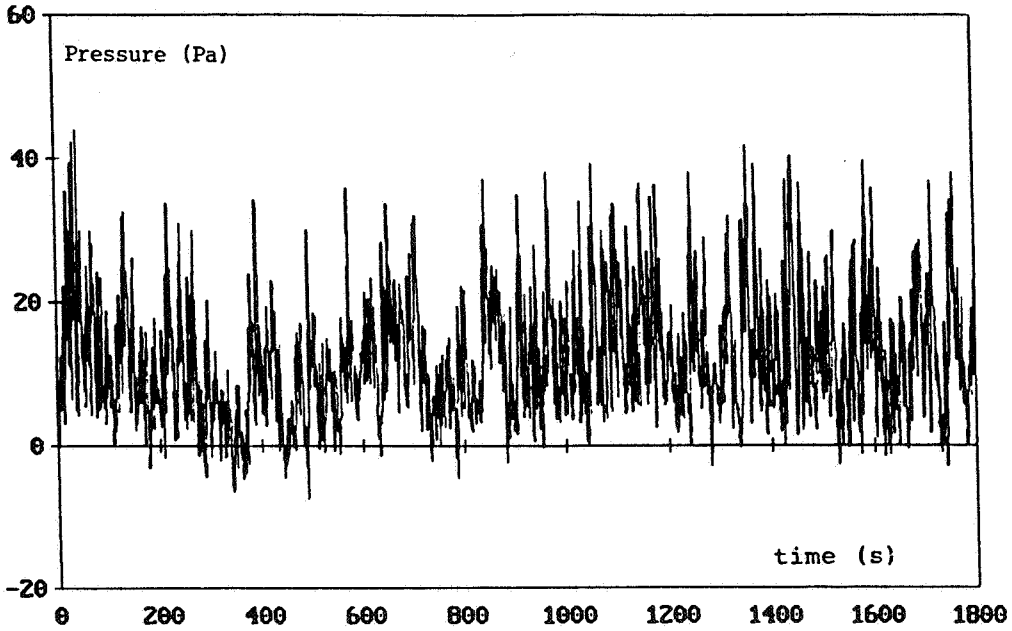

Figure 7 : Dynamic pressure at the opening

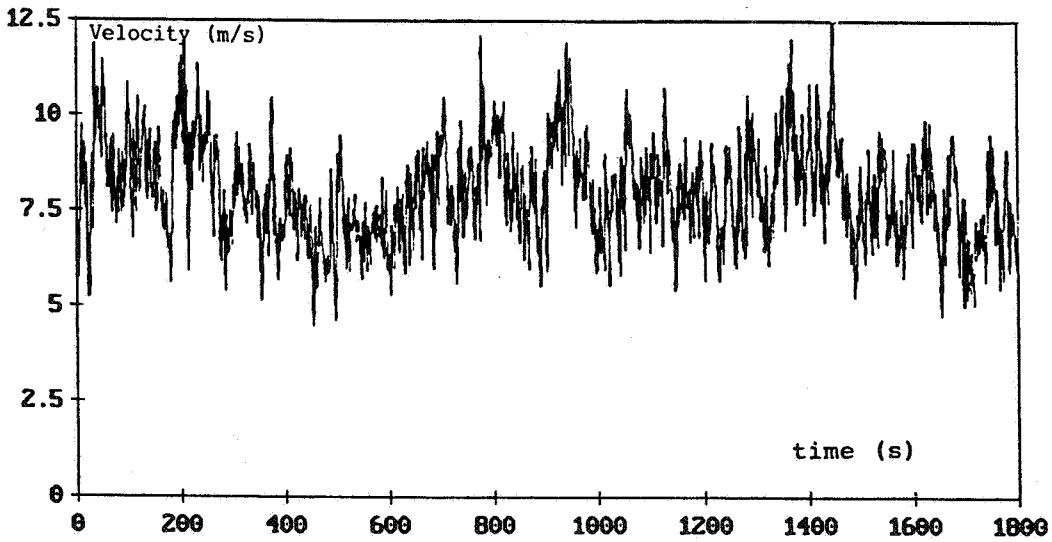

Figure 8 : Wind velocity at the top of the house

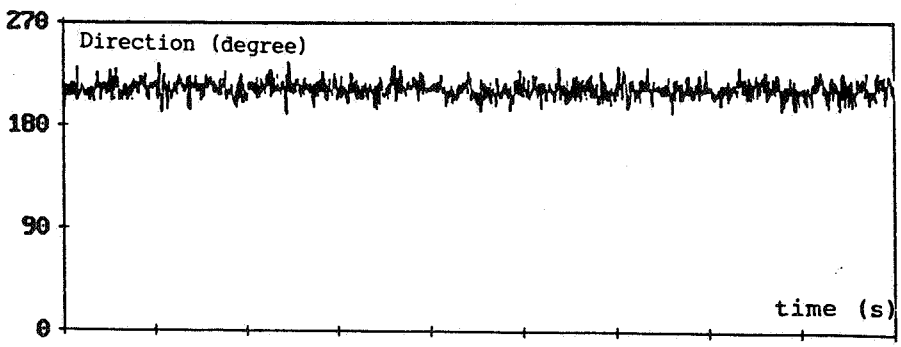

Figure 9 : Wind direction at the top of the house

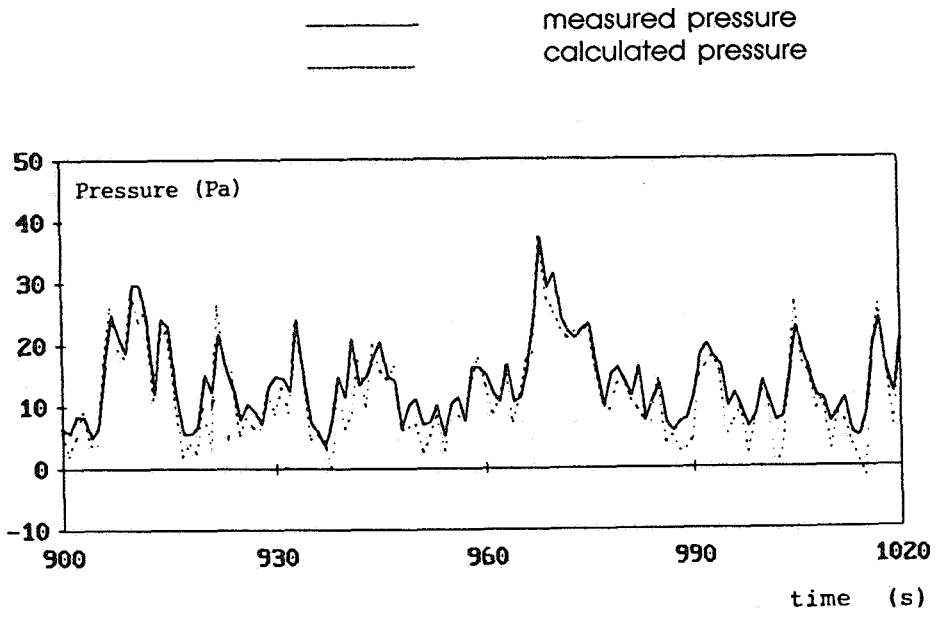

Figure 10 : Inside pressure versus time

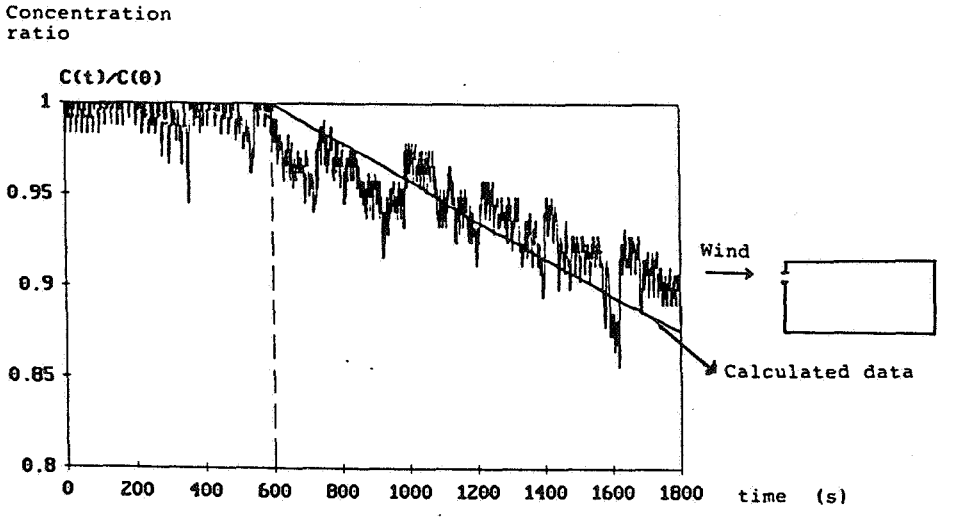

Figure 11 : Tracer gas concentration versus time
(measured and calculated data)

For the other tests, the agreement between measured concentrations and those derived from calculated flow rates is not as well. The predicted decrease in concentration is generally greater than the measured decrease. The discrepancy might be explain because at the same time air flows go through the opening into opposite directions ("inlet-outlet openings"), assuming wind pressure spatial fluctuations distributed along the opening. This flow pattern is not taken into account in the model.

4 - CONCLUSIONS

Due to non linearity of phenomena governing the air transfers in a building, the assumption of wind fluctuations results in discrepancies with respect to calculations made using an average wind pressure value.

Calculations show the necessity to take temporal wind fluctuations into account as well as air compressibility for evaluating the air change in a flat with air passages mainly located on one façade.

The wind turbulence can also result in reverse flow occuring in ventilation ducts linked to different floors. Further research will be devoted to studying this problem by incorporating the influence of the mechanical inertia of the air mass present in the pipe.

The first experimental results refer to single sided ventilation when the external opening is windward or leeward : the renewall rates are about 0.2 to 0.4 ach. These values are not, in all the cases, in agreement with values predicted by the model : the differences might be due to pressure and concentration measurement method or computer model which does not take bi-directional flow through the opening into account or different behaviour of the air inlet according to its location is either windward or leeward.

However, very few tests have been analysed and more research work is still needed in order to ascertain results. The experimental research programme is carried out to study another cases of wind-induced ventilation.

ACKNOWLEDGEMENTS

The authors whish to express theirs thanks to R. MOUNAJED who developed computer model.

Participation of A.F.M.E. (Agence Française pour la Maîtrise de l'Energie), to research support is gratefully acknowledged.

REFERENCES

1. SACRE, C. BIETRY, J. and DUCHENE-MARULLAZ, P.
   "Climatologie"
   REEF, Vol. II, Sciences du Bâtiment, CSTB, Décembre 1979

2. GANDEMER, J. BIETRY, J. and BARNAUD, G.
   "Aérodynamique"
   REEF, Vol. II, Sciences du Bâtiment, CSTB, Avril 1980

3. MOUNAJED, R.
   "Fascicule de documentation du code de calcul SIREN 2"
   CSTB, GEC n° 89.4824, Champs sur Marne, Juin 1989

4. LEMOULT, B.
   "Etude préliminaire en soufflerie atmosphérique des pressions induites par le vent sur pavillon individuel. Contribution à la ventilation naturelle"
   CSTB, EN.ADYN 87-1, Nantes, 1987

5. RIBERON, J. MOUNAJED, R. BARNAUD, G. and VILLAIN, J.
   "Turbulence du vent et ventilation."
   Séminaire Ventilation et Renouvellement de l'air. AFME, Sophia-Antipolis, 19-20 Septembre 1989

6. MOUNAJED, R.
   "La modélisation des transferts d'air dans les bâtiments. Application à l'étude de la ventilation"
   Thèse de Doctorat, ENPC, Paris, 1989

7. VILLAGINES, R.
   "Réalisation d'une nouvelle chaîne de mesures de concentration gazeuse instantanée"
   Thèse de Doctorat de l'Université de Nantes, 1988

8. RIBERON, J. and VILLAIN, J.
   "Etude en vraie grandeur des débits effectifs de renouvellement d'air"
   CSTB, GEC/DAC-90.101R, Champs-sur-Marne, Juillet 1990

Discussion

Paper 14

Earle Perera (BRE, UK)

Is compressibility the real factor which influences ventilation in an enclosure with a single opening? Would not effects like two-way flow or turbulence effects (similar to the work of N.Potter, as reported in ASHRAE Transactions) be the factor?

D.Bienfait (CSTC, France)

2 way flow over openings has much more effect than the air compressibility. Our research work is only concerned with small apertures (less than 100 cm^2) for which two-way flow is likely to be less important. At the moment there is rather good agreement between measurements and the air compressibility explanation, but it is obviously necessary to investigate more thoroughly the question you have raised.

W.F.De Gids (TNO, Netherlands)

The air leakage of the dwellings were expressed as L_{50} value. What are the n_{50} values. So the air change rates measured at 50 Pa during pressurisation test.

$L_{50} \approx 1200 m^3/h \hat{=} n_{50} of ? ACH$

D.Bienfait (CSTC, France)

Mean values are: multifamily buildings: n_{50} # 5 ach, single family buildings: n_{50} # 2 ach. It should be stressed that these values were measured some years ago. Since that time new building codes of practice have been issued and hopefully in the future the n_{50} values will be less important.

VENTILATION SYSTEM PERFORMANCE

11th AIVC Conference, Belgirate, Italy
18-21 September, 1990

Paper 15

INTERACTION BETWEEN AIR INFILTRATION AND COMBUSTION APPLIANCES - VALIDATION OF A NUMERICAL MODEL

G.V. Fracastoro[2], M. Masoero[1], E. Mazza [1]

1
Dipartimento di Energetica
Politecnico di Torino
Corso Duca degli Abruzzi 24, 1-10129 Torino, Italy

2
Instituto di Fisica
Universita della Basilicata, Via Nazario Sauro 85
1-85100 Potenza, Italy

SYNOPSIS

This paper presents some of the early theoretical work conducted within the framework of a research program aimed at analysing the interaction between gas-fired domestic appliances and the indoor environment in terms of energy consumption, indoor air quality and operational safety.

A simplified multizone mathematical model has been developed, which is capable of analysing the thermo-fluid dynamics behaviour of the building + appliance + chimney system. A parametric study has been completed which points out the influence of factors such as outdoor temperature, wind speed, spatial distribution of building envelope permeability on the overall system performance.

LIST OF SYMBOLS

C = permeability coefficient of envelope element ($m^3/s\ Pa^n$)
C_d = flow coefficient
ΔP_{loss} = pressure losses in the heat exchanger (Pa)
ΔP_r = reference pressure difference (Pa)
K = proportionality constant $(m/kg)^2$
L = equivalent air leakage area $(m)^2$
LF = load factor of boiler
M = gas mass flow rate (kg/s)
M_{off} = gas flow in the stack in the OFF phase (kg/s)
M_{on} = gas flow in the stack in the ON phase (kg/s)
M_s = average gas flow in the stack (kg/s)
OS = boiler oversizing factor
ρ = air density (kg/m^3)
S_r = ratio of stack flow and boiler flow
T_i = indoor temperature (°C)
T_o = outdoor temperature (°C)
T_{od} = outdoor design temperature (°C)
τ_{off} = boiler OFF-time in a typical operation cycle (s)
τ_{on} = boiler ON-time in a typical operation cycle (s)

1. INTRODUCTION

Individual heating with gas-fired boilers has grown to become the most popular heating system in residential buildings in Italy. New installations are usually designed in such a way that risks of accidents due to defective exhaust of combustion products (CO poisoning) are minimised; this is normally accomplished by installing the boiler outside the living space (e.g. in a small outdoor ventilated cabinet), or adopting balanced-draft units.

Nevertheless, a significant number of existing installations, as well as new installations in refurbished dwellings where outdoor installation is not feasible, are characterised by the presence of the boiler within the living space. Fairly detailed regulations exist in Italy, which specify how a safe system should be installed. However, due to a lack of technical culture among many building contractors and insufficient information of the occupants, and because of the objective difficulty in controlling such an enormous number of existing installations, lethal accidents during the heating season are unfortunately not unusual.

The concern for safety issues, and more generally for indoor air quality problems which may arise from combustion systems, has suggested the Politecnico di Torino and the national gas utility Italgas to promote a joint research effort on these subjects. The research program, which has started in the Spring 1990, will consist both of thoretical/numerical and of experimental work. To this aim, Italgas has constructed in the vicinity of Torino two identical single-family houses, which are fully instrumented for experimental analyses concerning the performance of combustion units for space heating and cooling, the thermal behaviour of the building, the quality of indoor air, etc.

This paper presents some of the early theoretical work produced by the research program. A mathematical model has been developed and tested, which is capable of analysing the thermo-fluid dynamics interaction between a building and the boiler + chimney installed within the building itself, taking into account the geometric and air permeability properties of the building envelope, the climatic conditions at the building site, and the characteristics of the heating system. A number of analyses were conducted with the model and the most significant results are presented in the paper.

2. FEATURES OF THE MATHEMATICAL MODEL

The numerical model which is the object of this paper is an enhancement of the model developed by Fracastoro and Masoero, described in a previous AIVC conference paper /1/. Improvements with respect to the original model only are described herein; reference can be made to the previous paper for background information on the assumptions and algorithms adopted by the model.

The model can be defined as an enhanced single-zone model, since it permits a simplified multizone representation. In practice, it is possible to describe the building as constituted by vertically stacked individual zones, each corresponding to one storey; the resistance to air flow between stories is taken into account in the calculation, and ambient temperatures at various storeys can be assumed different. Furthermore, the influence of combustion appliances located within the building on airchanges can be evaluated through the analysis of the behaviour of the gas exhaust system (or "chimney"), including the flue, the draft diverter, and the stack.

2.1 Air flow through the envelope

The permeability function which characterises each element of the external envelope is determined using the equivalent air leakage area concept; the latter values are determined as a function of type, number, and extension of the openings located in the element, based on literature values of air leakage area at 4 Pa, assuming a unitary airflow coefficient /2,3,4,5/. For each envelope element, the permeability equation is determined assuming the flow exponent value and calculating the permeability coefficient with the following equation:

$$C = L\,C_d\,(2/\rho)^{1/2}(\Delta P_r)^{1/2-n} \qquad (1)$$

where:

L	=	equivalent air leakage area
C_d	=	flow coefficient
ΔP_r	=	reference pressure difference
ρ	=	air density

Assuming $\Delta P_r = 4$ Pa, $\rho = 1.29$ kg/m^3, $C_d = 1$, $n = 0.65$, eqn. 1 yields:

$$C = 1.0114\,L$$

Wind pressure is calculated using the equations for wind speed and pressure coefficients given in the AIVC Calculation Guide /3/. It is also possible to consider zero wind speed on any of the building sides.

2.2 Boiler and gas exhaust analysis

The model is capable of analysing the part-load behaviour of the boiler. Assumption is made that the boiler operates at full load when outdoor temperature reaches the winter design temperature. At partial loads, the boiler operates according to ON-OFF regulation. In order to analyse the system behaviour in the OFF phase, it is essential to calculate the load factor LF, which is defined as:

$$LF = \frac{(T_i - T_o)}{(T_i - T_{od})}\,(1 + OS) = \frac{\tau_{on}}{\tau_{on} + \tau_{off}} \qquad (3)$$

where:

T_i	=	indoor temperature
T_o	=	outdoor temperature
T_{od}	=	outdoor design temperature
OS	=	boiler oversizing factor
τ_{on}	=	boiler ON-time in a typical operation cycle
τ_{off}	=	boiler OFF-time in a typical operation cycle

It is assumed that flue gas temperature downstream the heat exchanger in the OFF phase is T_{off} = 90°C. Such assumption can be justified as follows: in small size boilers, which are typically considered in our analyses, the temperature of the metal walls delimiting the combustion chamber is virtually equal to the water temperature. Therefore, it can be assumed that, when the burner is OFF, the air temperature in the combustion chamber drops rapidly to a value which is slightly above the water temperature (typically 70 to 80°C) /6/. Pressure losses in the heat exchanger are calculated with the equation:

$$\Delta P_{loss} = K \rho M^2 \qquad (4)$$

where:

K = proportionality constant
M = gas mass flow rate

under the assumption that K assumes the same value both in the ON- and OFF-phases.

The algorithm calculating the global mass balance of the system (building + boiler + gas exhaust) is basically the same in the ON and OFF phase, the major difference being that in the ON phase the gas flow through the boiler is given and constant (being a function of the constant power delivered by the boiler), while in the OFF phase the gas flow is no longer known "a priori", but must be calculated within the overall iterative procedure. Indicating with M_{on} and M_{off} the gas flow in the stack in the ON and OFF phase respectively, the average stack flow can be estimated as:

$$M_s = M_{on}\, LF + M_{off}\, (1 - LF) \qquad (5)$$

This approach permits to take into account the influence on gas flow of the time variations of gas temperature due to intermittent operation. Obviously, in real operation the gas temperature varies continuously rather than assuming two distinct values, as assumed above; however, the inaccuracies introduced by such approximation are negligible and no significant improvements would be obtained by assuming a continuous temperature trend.

2.3 Limits of the model

Compared to a standard single-zone model, this model permits to analyse multi-storey buildings, albeit in a simplified manner. Strictly speaking, each zone (viz. storey) should include a single dwelling with rooms connected by large openings, so that no significant flow resistance exists between rooms; nevertheless, useful results can be obtained even with relatively complex buildings, particularly if the main goal of the analysis is to evaluate the interaction between envelope permeability and boiler operation.

A noteworthy limitation concerns the assumptions for wind pressure calculation: such assumptions only apply if the building height does not exceed about 10 to 12 m.

3. RESULTS OF THE MODEL

The results presented in Table 1 and in Figures 1 through 4 are based on the following assumptions:

- the floor plan of the building is square, 15 x 15 m;
- the building consists of three storeys, respectively 2.5 m, 3.0 m and 3.0 m high;
- the temperature of the lower storey (unheated) is 5°C, while for the two upper storeys (heated) is 20°C;
- there are no obstructions around the building;
- each size of the building has the same permeability, the average value being 0.63 $m^3/h\ m^2\ Pa^n$;
- each of the two upper storeys is heated by an individual boiler;
- wind speed is 2 m/s;
- outdoor temperature is -5°C;
- internal air flow resistance between storeys is 0.5.
- in the graphs showing temperature differences, 1 indicates the upwind wall (orthogonal to wind direction), 2 the leeward wall, and 3 and 4 the two walls parallel to wind direction.

The model was been employed to investigate parametrically the interaction between the building structure and the boiler plus chimney system. In particular the following aspects were analysed: i) the influence of the presence of one or more boilers on the overall value of natural airchanges; and ii) the influence of envelope permeability on boiler operation under various meteorological conditions, aiming at identifying the potentially dangerous situations when gas exhaust becomes critical.

The type of building considered in the parametric analysis is the same as in the above example; four different cases for the distribution of envelope permeability were considered:

1 - high-leakage building with equal permeability of all sides (0.63 $m^3/h\ m^2Pa^n$ - ASHRAE class G);
2 - low-leakage building with equal permeability of all sides (0.20 $m^3/h\ m^2Pa^n$ - ASHRAE class D);
3 - perfectly airtight (ASHRAE class F) upwind side, the other three sides as in case 1);
4 - perfectly airtight (ASHRAE class F) leeward side, the other three sides as in case 1).

As a result of the parametric analysis, the following quantities were calculated:

- overall buiding airchanges;
- total gas flow through the stacks;
- ratio of stack flow and boiler flow (the difference between the two being the flow through the flow diverter), indicated in the following as S_r.

The variable parameters in the analysis were:

- wind speed;
- outdoor temperature;
- useful height of the stack;
- boiler operation (ON-OFF vs. steady-state).

In the previously presented paper /1/, it was shown that the gas flow through the stack decreases as both wind speed and outdoor temperature increase. Figures 5 and 6 give the

gas flow values in the case of ON-OFF and steady-state operation. The graphs indicate that the gas flow decreases as outdoor temperature increases more markedly in the case of intermittent operation than in steady-state. This result can be explained by the fact that in ON-OFF operation both the boiler load and the stack draft are reduced.

The graphs of Figures 7 and 8 allows the comparison of overall airchanges in the cases of intermittent (50% load factor) and steady-state boiler operation. The ACH variation shown in Fig. 7 between operations is minimal, and can be detected only for very low wind speeds and high internal flow resistance. The variation of gas flow through the stack, given in Fig. 8, is on the order of 10% and is only marginally influenced by wind speed and internal flow resistance.

It has been observed that the reduction of natural airchange due to the increase of outdoor temperature may be offset, in some cases, by the reduction of the overpressure created by the stack at the boiler level: in such case, the gas flow through the stack turns out to be virtually constant with varying outdoor temperatures. This situation may occur when the boiler is located well below the neutral plane of the building, in the case that a single boiler is installed for heating the two upper storeys.

Figures 9 and 10 permit to evaluate the influence of envelope permeability on the airchanges and boiler operation. The graph of Fig. 9 shows how the variations in envelope permeability affect the building overall airchanges with respect to the reference high leakage envelope (building 1). As expected, a reduction of permeability greatly reduces the building airchanges: with wind speed equal zero, the airchanges with a low permeability envelope (building 2) are about a half the airchanges of building 1. If wind speed equals zero, the presence of a perfectly airtight wall determines a reduction of overall airchanges on the order of 20% (buildings 3 and 4). For high wind speed (e.g. 4 m/s), the position of the airtight wall becomes important: in the upwind case (building 3), the reduction of airchanges is significant (about 50%), while in the leeward case (building 4), only a 10% reduction is found with respect to building 1. The graph of Fig. 10 shows the effect of envelope permeability on the stack flow ratio S_r (stack flow / boiler flow). From this graph it can be noticed that the variation in stack flow due to wind effect is negligible in all cases, except if the upwind wall is perfectly airtight and the wind speed is high (building 3). A reduction of gas flow in the stack is a symptom that critical conditions may be reached with respect to combustion products exhaust: in the limit case, gases may be discharged indoors through the flow diverter.

In Figures 11, 12 and 13 the ratio S_r is given as a function of stack height and wind speed. The results were calculated assuming that the overall length of the gas exhaust system is constant and equal to 3 m, for varying stack height. A potentially dangerous situation is encountered when the ratio S_r decreases and approaches the unit value: in such case, the pressure difference across the flow diverter becomes zero and flow reversal can therefore occurr. The stack height value for which S_r reaches one may therefore be defined as the "critical height" of the stack. The graphs show that the critical height increases as the envelope permeability decreases, when the wind speed is zero. For intermediate wind speeds, the critical height is the same for the permeability cases 2) and 3), even if in case 3) the average permeability is much higher; this is due to the fact that in case 3) the presence of an airtight upwind wall induces a significant reduction of indoor pressure. Finally, for very high wind speeds, the critical height is first reached in the case of upwind airtight wall.

4. CONCLUSIONS

The results presented in this paper indicate that mathematical modeling of the interaction between building structure, boiler and chimney may provide useful guidelines concerning the proper installation of combustion equipment within inhabited spaces. The overall behaviour of the system was analysed under varying conditions with respect to climate, envelope construction and boiler operation. It is particularly interesting to notice that, with respect to safety, it is not only important to provide an adequate envelope leakage, but also to properly locate the ventilation openings with respect to dominant wind directions.

REFERENCES

/1/ Fracastoro G.V., Masoero M. "*Air infiltration induced by heating appliances*" Proc. 9th AIVC Conference, Gent, 1988.

/2/ ASHRAE Handbook of Fundamentals, Ch. 23 "*Infiltration and Ventilation*", 1989.

/3/ Liddament M.W. *Air infiltration calculation techniques - An application guide*, AIVC, 1986.

/4/ Baker P.H., Sharples S., Ward I.C. "*Air flow through cracks*" Building and Environment, Vol. 22, No. 4, 1987.

/5/ ASHRAE Standard 119 - *Air leakage performance for detached single family residential buildings*, 1989.

/6/ Anglesio P. et al. "*Prestazioni termofluidodinamiche dei camini*" (Thermal and fluid dynamics performance of chimneys - in Italian), Politecnico di Torino, Research Report CNR 85.00898.59, 1987 (unpublished).

Table 1 - Sample of model output

Normalised equivalent leakage area =	0.6249
Airtighteness class (according to ASHRAE Standard) =	G
Internal flow resistance coefficient =	0.50
Outdoor temperature =	-5°C
Local wind speed at 10 m height =	2.01 m/s
Overall building airchange =	0.156 ach
Air flow out through building envelope =	182.9 m^3/h

BOILER # 1	
Stack cross section =	0.0079 m^2
Useful stack height =	3.0 m
Boiler output =	23.6 kW
Boiler load factor =	89.3 %
Flow through draft diverter, ON phase =	15.0 m^3/h
Flow through boiler, ON phase =	36.5 m^3/h
Flow through draft diverter, OFF phase =	1.4 m^3/h
Flow through boiler, OFF phase =	4.1 m^3/h
Stack/Boiler flow ratio, ON phase Sr =	1.41
Stack/Boiler flow ratio, OFF phase Sr =	1.25
Gas temperature at boiler exit, ON phase =	271.1°C
Gas temperature in the stack, ON phase =	198.7°C
Gas temperature at boiler exit, OFF phase =	90.0°C
Gas temperature in the stack, OFF phase =	77.2°C
Gas speed at boiler exit, ON phase =	2.69 m/s
Gas speed in the stack, ON phase =	3.29 m/s
Gas speed at boiler exit, OFF phase =	1.66 m/s
Gas speed in the stack, OFF phase =	2.01 m/s

BOILER # 2	
Stack cross section =	0.0079 m^2
Useful stack height =	3.0 m
Boiler output =	23.6 kW
Boiler load factor =	89.3 %
Flow through draft diverter, ON phase =	17.6 m^3/h
Flow through boiler, ON phase =	36.5 m^3/h
Flow through draft diverter, OFF phase =	1.7 m^3/h
Flow through boiler, OFF phase =	4.3 m^3/h
Stack/Boiler flow ratio, ON phase Sr =	1.48
Stack/Boiler flow ratio, OFF phase Sr =	1.30
Gas temperature at boiler exit, ON phase =	272.1°C
Gas temperature in the stack, ON phase =	190.2°C
Gas temperature at boiler exit, OFF phase =	90.0°C
Gas temperature in the stack, OFF phase =	75.6°C
Gas speed at boiler exit, ON phase =	2.69 m/s
Gas speed in the stack, ON phase =	3.39 m/s
Gas speed at boiler exit, OFF phase =	1.76 m/s
Gas speed in the stack, OFF phase =	2.19 m/s

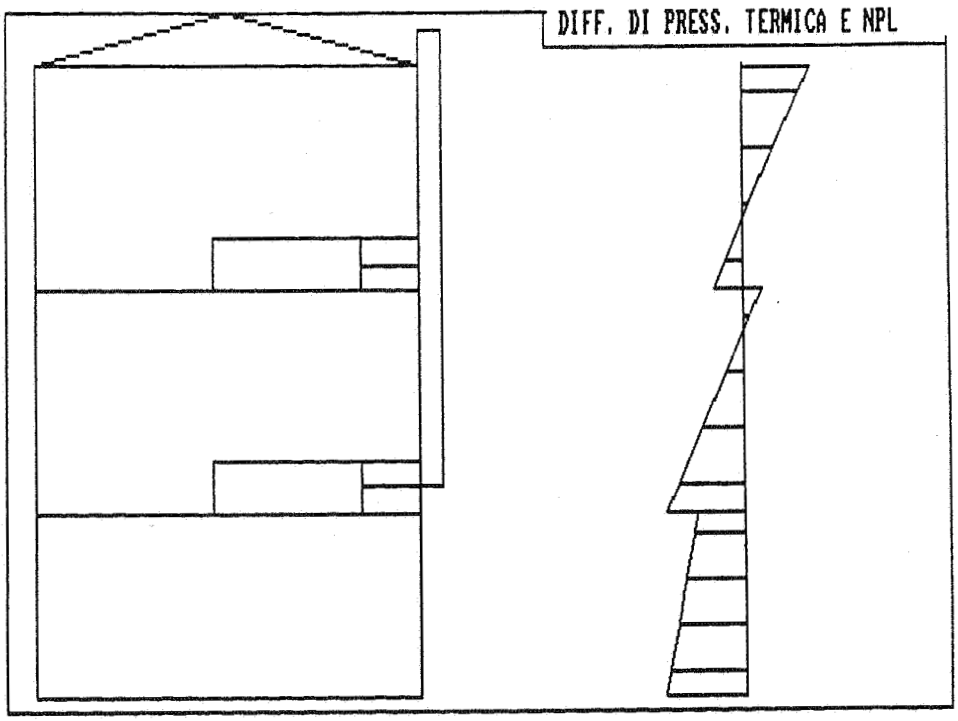

Fig.1 - Total pressure difference and neutral plane level

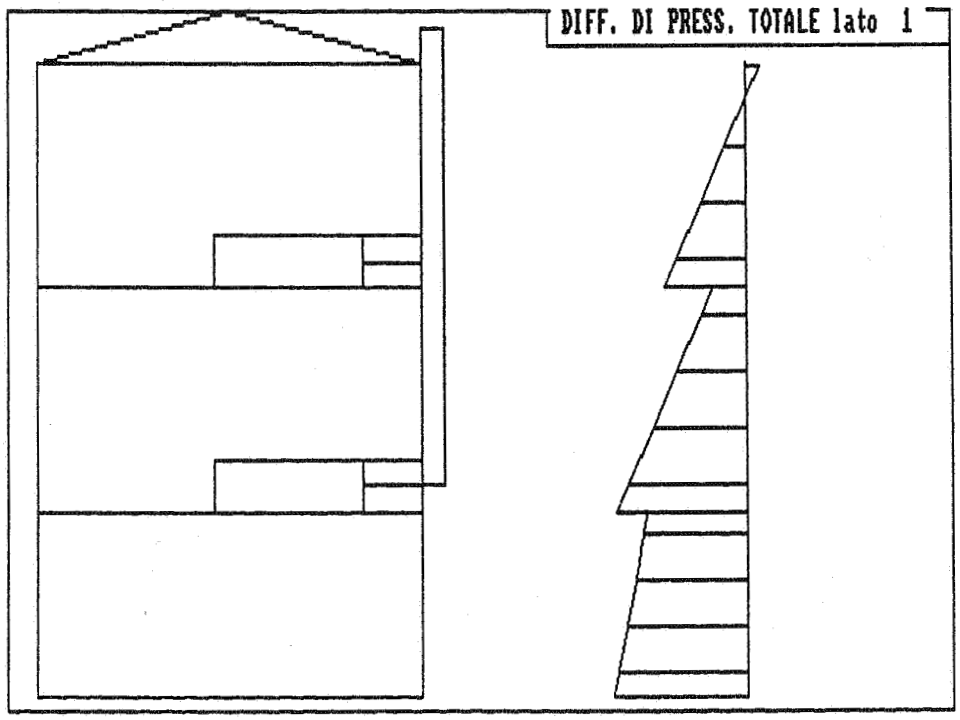

Fig.2 - Total pressure difference, wall 1 (upwind)

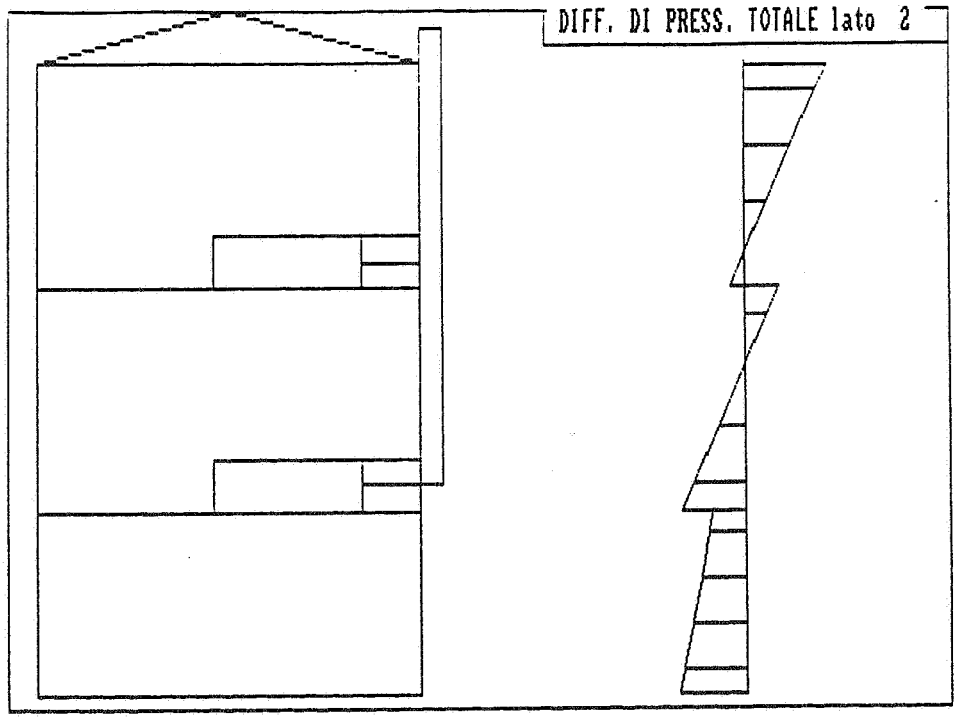

Fig.3 - Total pressure difference, wall 2 (downwind)

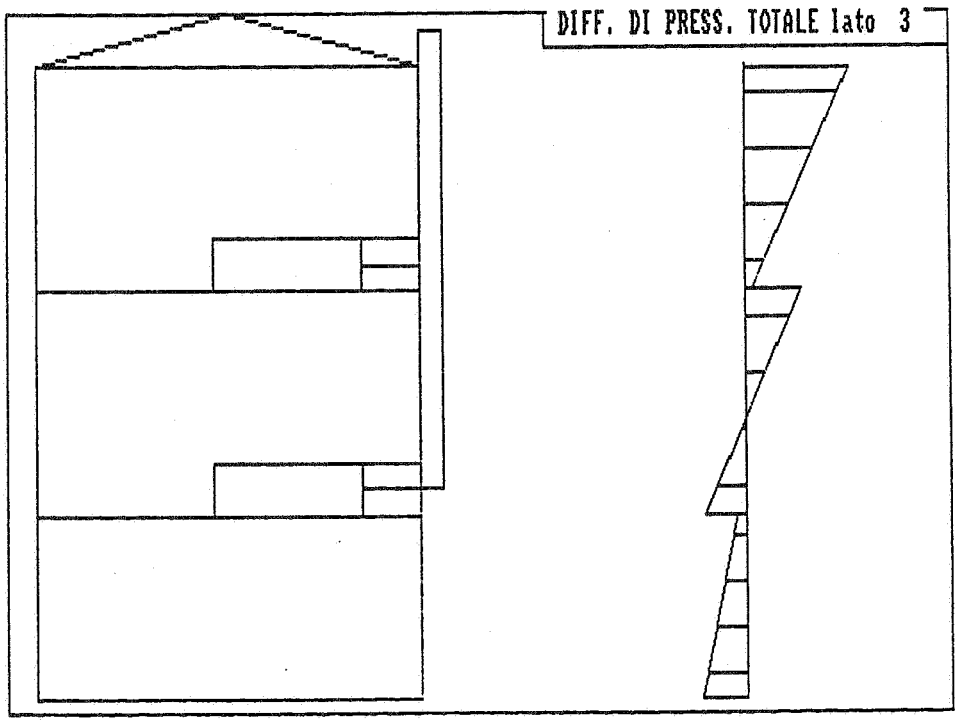

Fig.4 - Total pressure difference, wall 3 (lateral)

Fig. 5 – Flow rate through stack

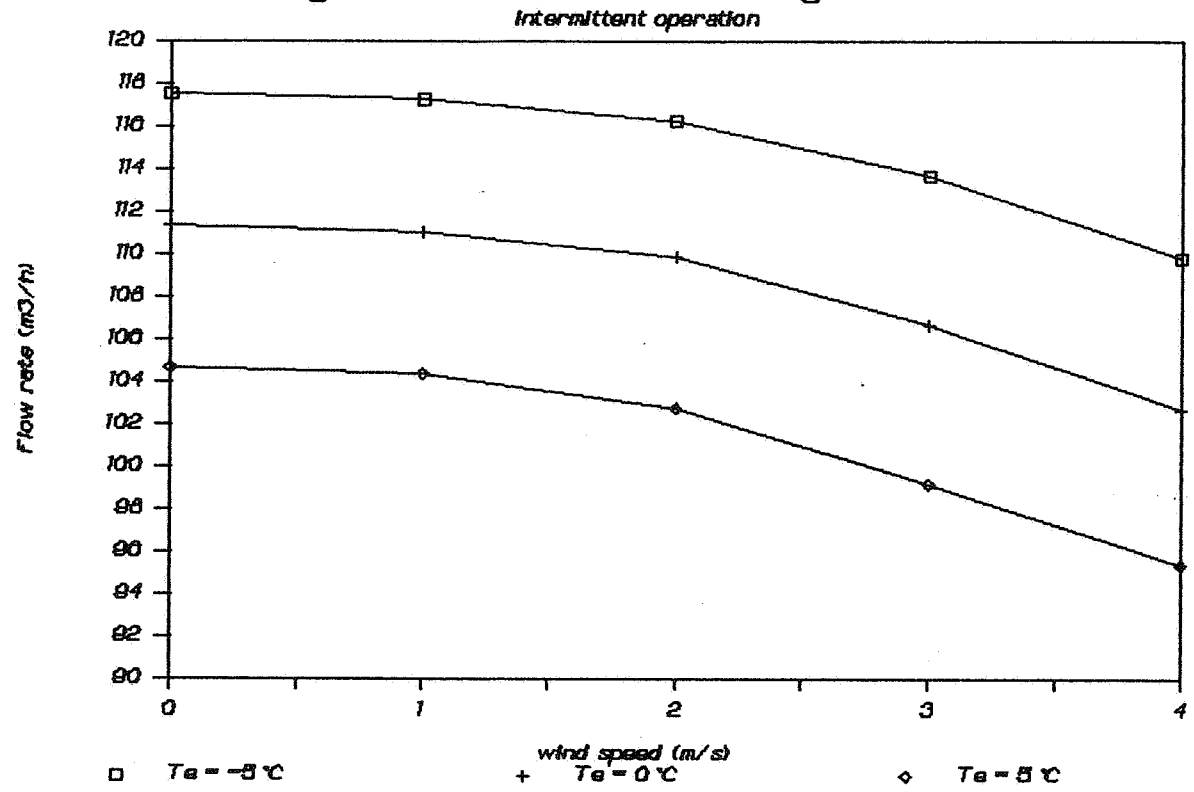

Fig. 6 – Flow rate through stack

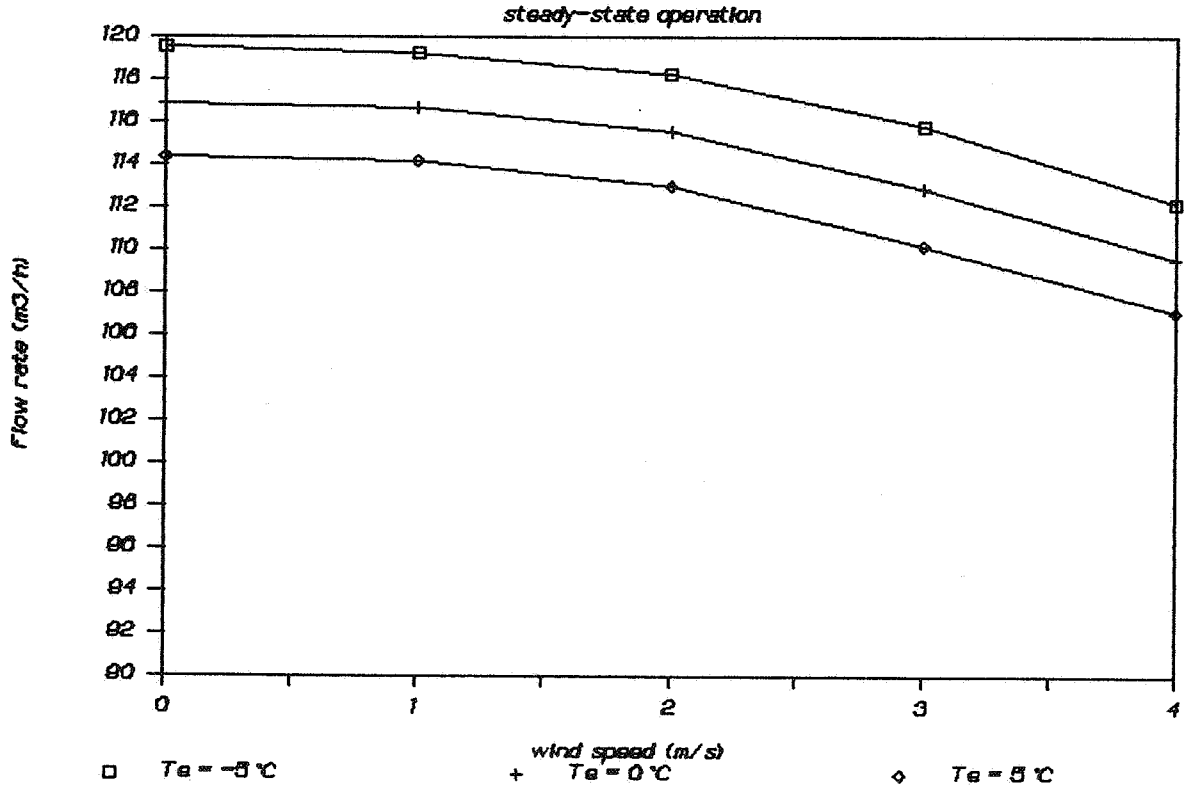

Fig.7 – ACH Ratio on-off/steady-state

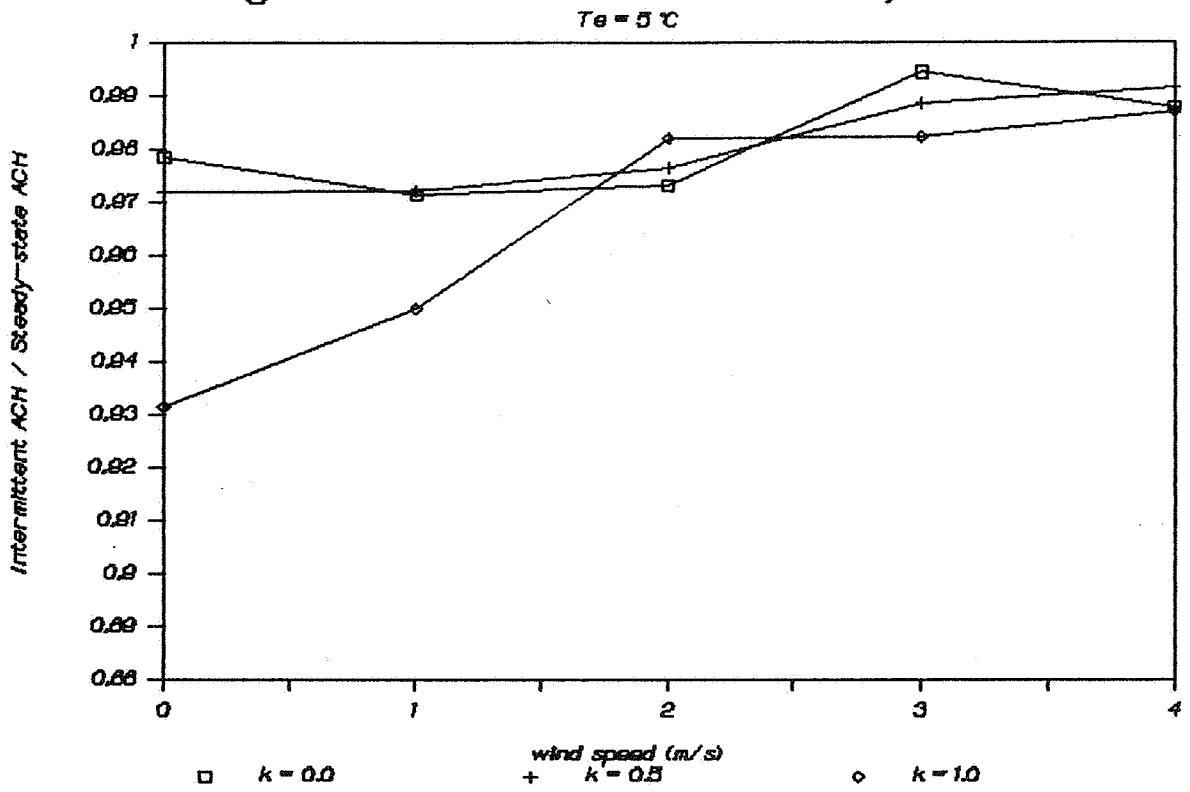

Fig. 8 – Stack flow ratio

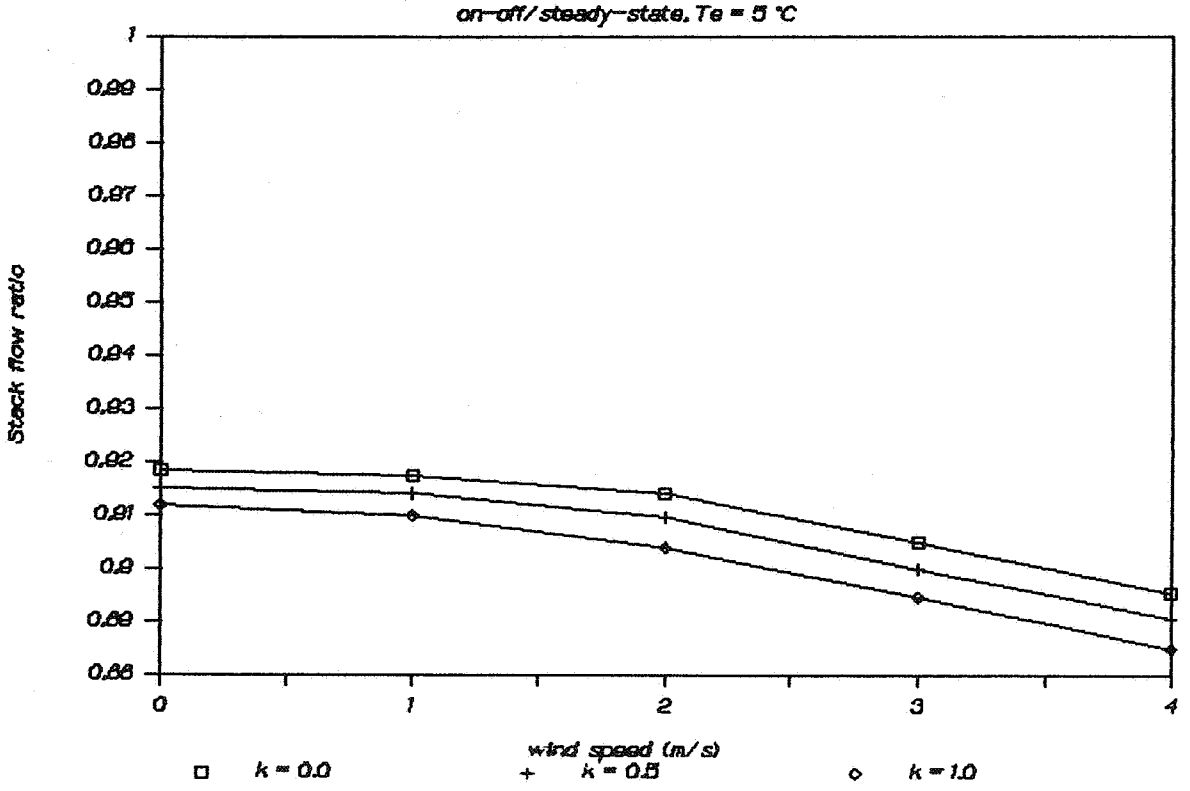

Fig. 9 – ACH ratio to building #1

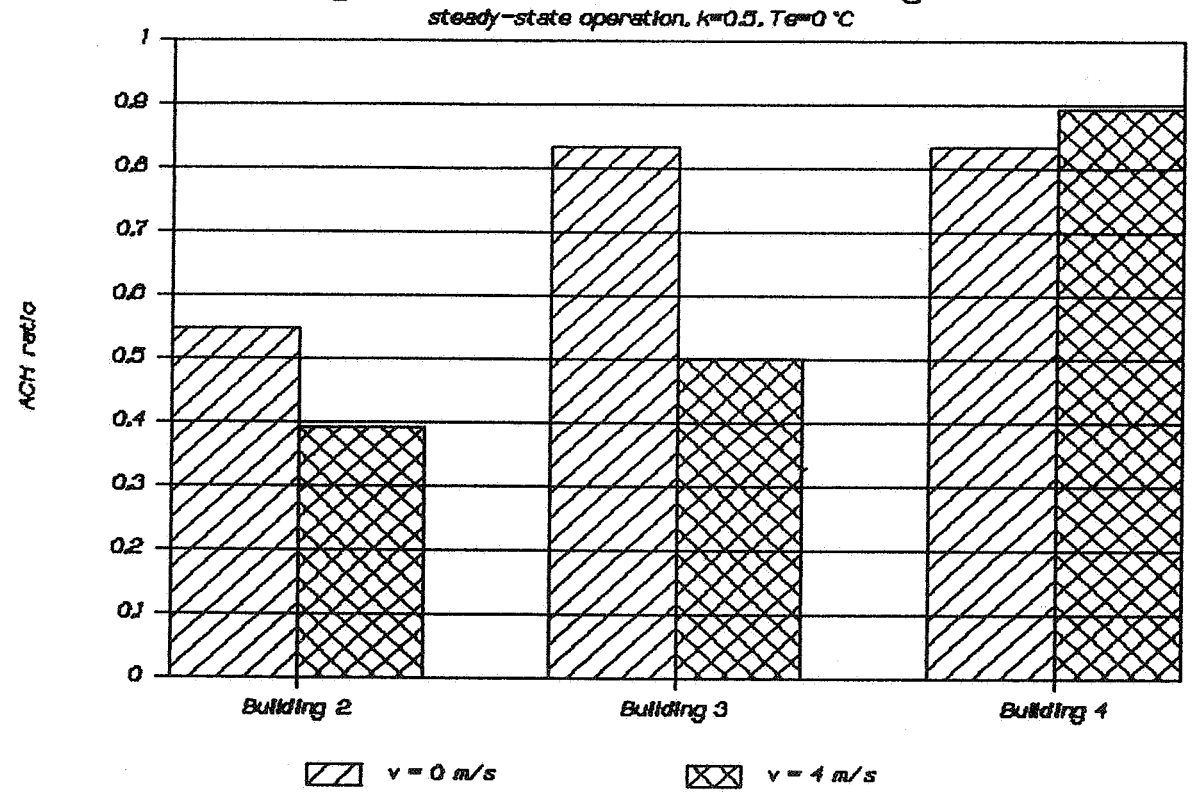

Fig. 10 – Stack flow ratio to bldng. #1

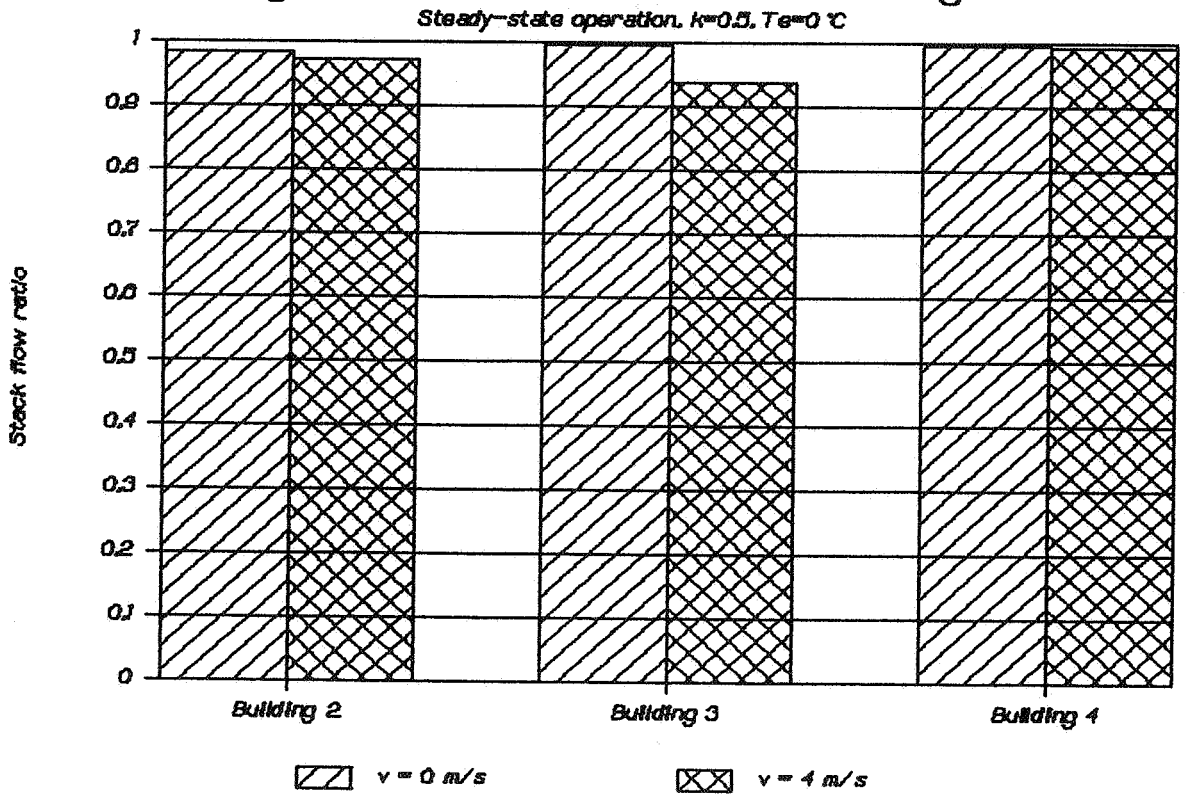

Fig. 11 – Sr vs. useful stack height

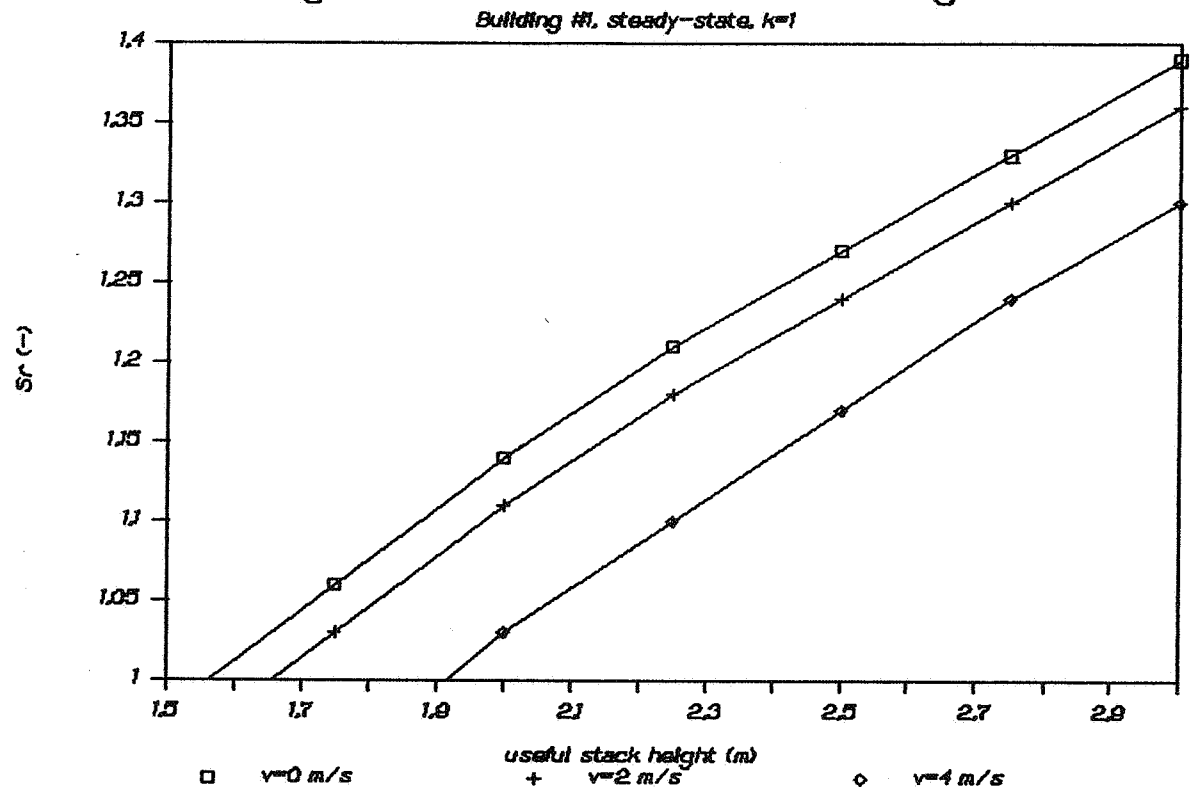

Fig. 12 – Sr vs. useful stack height

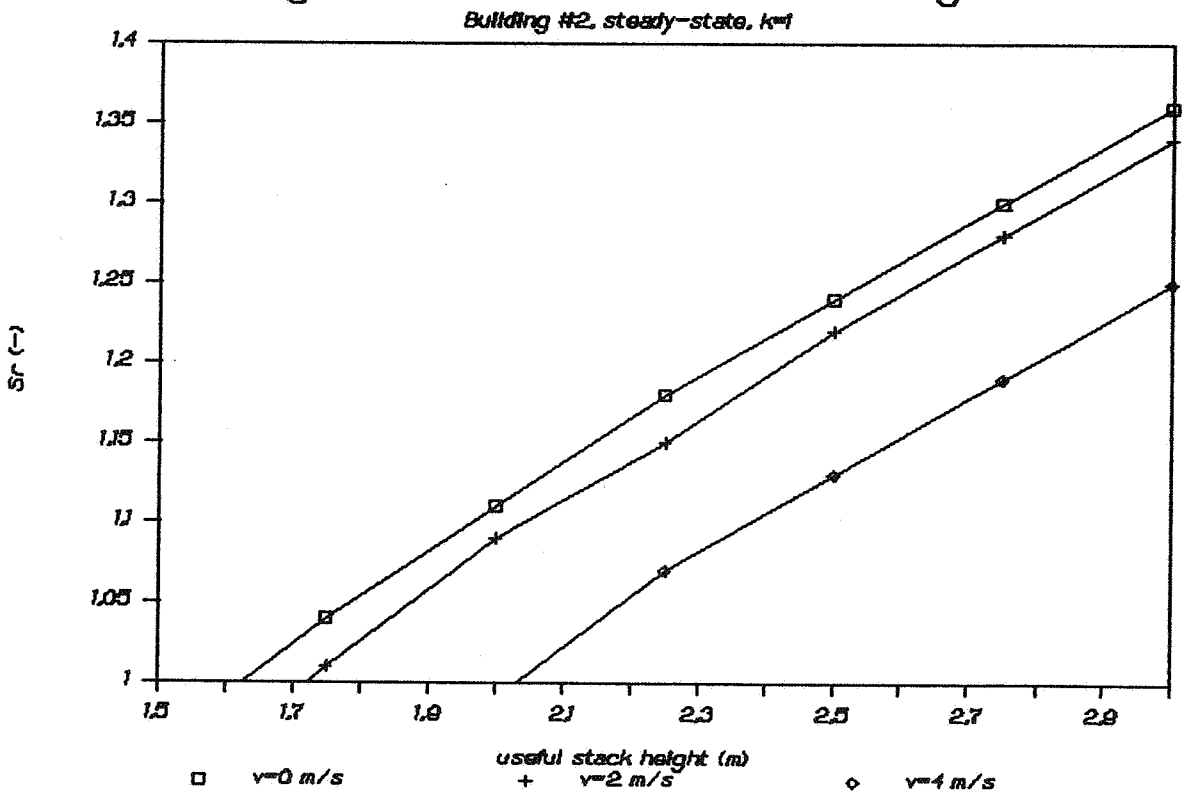

Fig. 13 – Sr vs. useful stack height

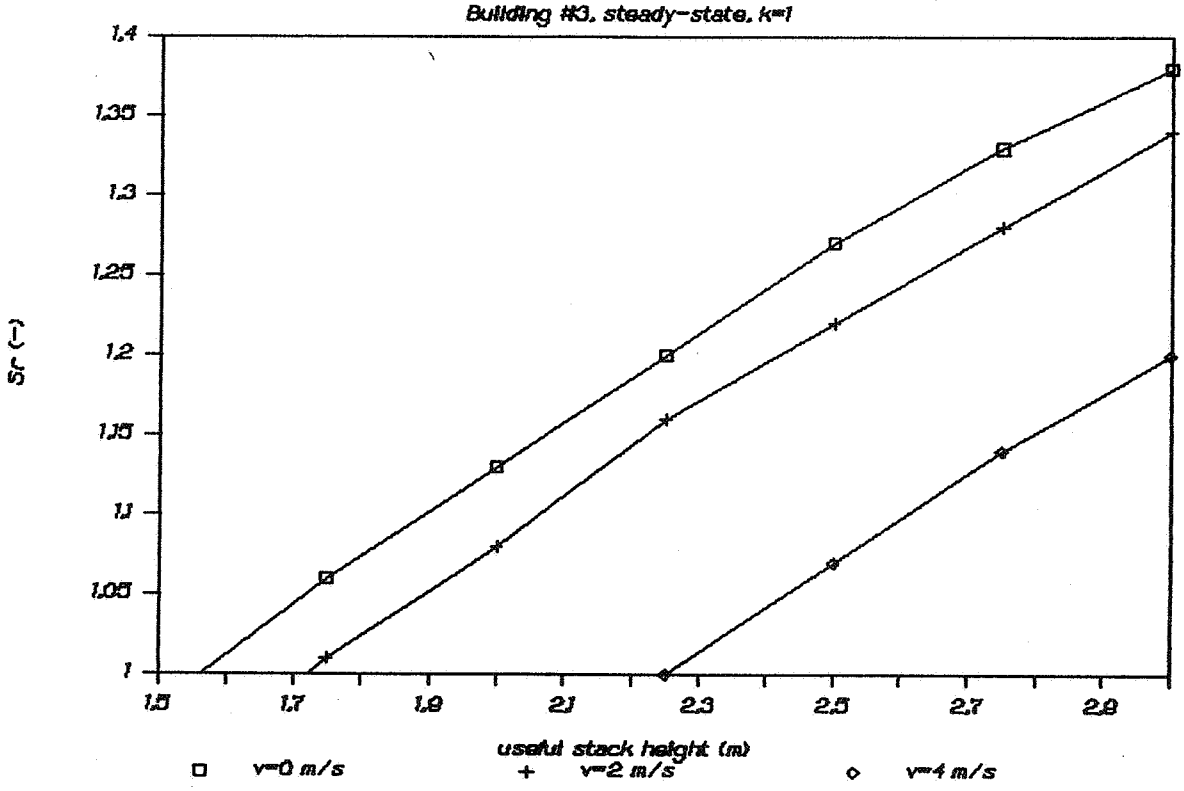

Discussion

Paper 15

D. Bienfait (CSTB, France)

We found that air flow in the stack increases with increasing wind speed due to the negative Dp induced by the wind on the top of the stack. Your results show an opposite trend. Why?

G Fracastoro & M Masoero (Politecnico Torino, Italy)

Because we adopted, as a conservative assumption, Dp = 0, due to the absence of reliable experimental data on the pressure coefficient at the top of the chimney, which can vary from 0 to 0.7.

J Van Der Maas (LESO, Switzerland)

Comment: The effect of turbulence on ventilation should be studied in the presence of temperature differences, because else there is a tendency of no-mixing (the incoming air goes immediately out).

VENTILATION SYSTEM PERFORMANCE

11th AIVC Conference, Belgirate, Italy
18-21 September, 1990

Paper 16

AIR CURTAINS FOR INFILTRATION CONTROL - A COMPUTATIONAL FLUID DYNAMICS ANALYSIS

J K-W Lam, K G Ruddick and G E Whittle

Arup Research and Development

13 Fitzroy Street
London W1P 6BQ
UK.

SYNOPSIS

An investigation has been carried out using computational fluid dynamics methods to study the performance of an air curtain at the door of a heated building. A number of operating conditions have been studied and observations are made on the effectiveness of infiltration control and energy use. Comparisons are also made with previously published design data and results from an accepted infiltration analysis.

It is shown that the calculation method generates plausible and very detailed results which conform well to physical interpretation.

It was found that at too low a supply velocity the air curtain was deflected to outdoors and the energy supply was wasted. Similarly, too high a supply temperature also prevented the air curtain operating correctly.

With the air curtain operating successfully the predicted heat transfer characteristics indicated an efficient use of energy and acceptable indoor temperatures, but with air speeds of up to 2.5 m/s at low level within the building.

1. INTRODUCTION

Air curtains are used to reduce unwanted infiltration through open doors whilst maintaining easy access for people and vehicles. They provide the potential for improved comfort, contaminant and moisture control, and energy efficiency. Their performance depends on a wide range of factors which include: the geometry of the door opening and configuration of curtain, the temperature difference across the opening, wind effects, the ventilation provision in the building, and the momentum and temperature of the discharge air.

In most cases design engineers and suppliers specify and install system which operate successfully as measured against subjective criteria. However, the increasing requirements for higher standards of environmental control and quality and a need to minimise energy use demands a greater attention be focussed on understanding the physical mechanisms involved in order that performance can be optimised.

In this paper a computational investigation is

carried out using fluid dynamics to study the performance of an air curtain at a number of operating conditions. Observations are made on the effectiveness of infiltration control and energy use, and comparisons are made with previously published design data.

2. BACKGROUND AND LITERATURE REVIEW

Mott[1] has discussed the principles behind the operation of air curtains and has outlined the basic information required for design. The equations used are those derived from momentum conservation. The curtain is initially discharged at an angle causing the jet to prescribe a parabolic trajectory when subjected to the pressure gradient generated across the opening. It is the change in horizontal component of momentum which offsets the flow which would otherwise occur through the opening. A typical discharge angle is 15°, though this can increase substantially for certain applications.

For a given angle of discharge optimum performance is obtained by taking the return air from opposite the position of discharge, for example through a floor grille in the case of a downward vertical air curtain. However, it is pointed out that this optimum configuration is not always the most practical. Where a return duct is not used then the curtain will part into two streams at floor level. It is stated that it is for the designer to decide in what proportion the curtain should be divided.

Wolfberg[2] describes an air curtain installation in a department store in Minnesota, USA. The doorway is 2.3m height and it is claimed that the door remains open in any weather conditions between the design outdoor temperatures of -28°C and +35°C.

In Hayes and Stoecker[3] the heat transfer characteristics of air curtains are identified. An analysis of performance was carried out based on the fundamental momentum and energy conservation equations, and findings were compared to laboratory experiments.

An important factor in the design of the curtain was found to be the level of turbulence at the discharge. Heat transfer across the air curtain is very dependent on turbulent exchange, a relatively

high turbulence level (8%) indicated an inferior performance to that of a lower level (2%).

The trajectory of the jet forming the curtain was identified using smoke as a tracer and by measurements using hot-wire anemometers. For isothermal tests good agreement was found between the measurements and the theoretical analysis. Again for isothermal tests, the pressure differences across the curtain were measured for discharge velocities between 3.0m/s and 15.2m/s and for discharge angles of 15° and 30°, and were found to agree with the theory within an 8% tolerance.

For non-isothermal tests the agreement between experiment and theory was slightly less satisfactory showing that jet deflection, for example, was over-predicted. This was believed to be due partly to the variation of temperature difference across the curtain, with height, caused by internal stratification. Errors were broadly in the range 5 to 15%.

Regarding heat transfer, which was expressed in dimensionless form by the ratio of Nusselt no. to the product of Reynolds no. and Prandtl no., the parameter H/b_o was found to be the most influential (where H is the door height and b_o the slot width). The dimensionless heat transfer relates heat transfer across the curtain to the energy supplied by the curtain. At high values of deflection modulus (essentially based on the ratio of jet inertia to buoyancy) both the discharge angle and the deflection modulus were found to have little effect on dimensionless heat transfer. At this condition the heat transfer coefficient is directly proportional to the discharge velocity. As expected, where jet buoyancy became important (low values of deflection modulus) the dimensionless heat transfer increases substantially. This corresponds to increasing deflection of the curtain leading eventually to the curtain breaking down and being swept aside by flow through the open door. In most cases the minimum value of dimensionless heat transfer occurs at a discharge angle of 15° towards the warm side, although the discharge angle may be increased to 30° without significant increase in dimensionless heat transfer.

In a further paper, which addresses design needs, Hayes and Stoecker[4] describe relationships which allow the discharge velocity and the resulting heat transfer coefficient to be identified for the ratio

of H/b°, and an equation is presented to correct for door height and temperature difference. Specific design recommendations are also made regarding the need to minimise turbulence at the discharge of the curtain, and that thick curtains reduce heat transfer rate by approximately 10%. Also because of susceptibility to wind pressures, air curtains should not be installed on opposite sides of the same building. The recommendation is that they should serve a space which is otherwise well sealed. In real operation, a change in wind pressure will cause the curtain to deflect allowing air to pass until the pressure gradient across the curtain adjusts. Thus under dynamically-varying wind conditions the heat transfer rate is expected to be greater than that predicted.

The economics of air curtains are considered by Asker[5]. Curtain efficiency is defined as the ratio of the thermal load imposed by an unprotected doorway compared to that of the air curtained doorway. A number of design points are listed which should be considered to ensure satisfactory control:

- air curtained doors should be located in one wall only;
- whilst ensuring safe passage the area of doorway should be minimised;
- air curtains do not perform well in buildings where a substantial excess of supply or extract air is provided;
- air flow in a room protected by a curtain should be directed to be parallel to the wall in which the curtain is located.

It is claimed that the use of air curtains to prevent access to food and pharmaceutical plants by most flying insects can be very successful provided the velocity is at least 4.0m/s.

The US National Sanitation Foundation Standard No. 37[6] specifies requirements for air curtains for entranceways in food establishments. Curtain thicknesses and velocities are specified for different types of openings. For example, at a service entrance the minimum curtain discharge thickness should be at least 75mm and the velocity should not be less than 8m/s at a height of 0.9m above the floor.

Learmonth[7] discusses a number of installations and states that for comfort the jetted velocity should

not exceed about 6.0m/s, although in industrial applications this could be higher. A sketch is shown claiming to show a representation of the earliest patent application (dated 1904) related to an air curtain.

Some design guidance on the installation of both vertical and horizontal air curtains is provided by Creek[8]. Operating benefits are claimed by allowing on-site flexibility:

- in setting the flow rate and discharge angle of the curtain;
- by providing automatic control of supply temperature;
- by providing on-off fan operation in conjunction with an automatic door.

Baturin[9] describes a practical and theoretical analysis of the air curtain. The effectiveness of the curtain depends on the ratio of the momentum of the curtain discharge and that of the potential air flow through the door. A substantial amount of practical information is given supplemented by examples of the design process. Results of measurements on floor- and side-discharge air curtains including one at a coach depot on the Moscow underground are shown. The door heights are 2.2m to 4.0m.

The flow of outside air through the unprotected doorway, which was at velocities of 2.6 to 3.9m/s, was approximately halved by the curtains. The curtains used typically 11% of the flow rate which would otherwise pass through the unprotected door. Examples are also shown of temperatures within a workshop both with and without an air curtain operating. Substantial improvements in temperatures are indicated by the operation of the curtain.

Developments in air curtains in the USSR and in Sweden are described where the emphasis is on utilising unheated (outside or inside) air[10]. An example of air speed and temperature profiles in the area of a door is shown, indicating the benefits of air curtains.

Simper[11] discusses novel uses for air curtains for, for example, control of dust in quarrying and foundry applications and deflection of raindrops from open-roofed areas. For the latter, power ratings of 0.8 to 1.2kW/m^2 of roof opening are

indicated.

Air curtains are claimed to have an energy efficiency of 40 to 95% compared to a closed door[12]. An example is shown of measured temperatures 4m and 20m inside a building in which a 4m x 4m door is protected by an air curtain. With an outside temperature of 0°C and 4Pa under-pressure in the building the temperature at both locations were 6 to 11°C without the curtain operating and 15 to 16°C with the curtain.

Ligtenberg[13,14] reports a combined laboratory and computational approach to investigating air curtain performance, with the emphasis on product development. Wind tunnel tests and computational fluid dynamics analyses were undertaken. A main finding, confirming previous work, was the importance of minimising turbulence intensity at the discharge. A halving of energy losses by operation of a well-engineered air curtain is claimed.

3. ANALYSIS - THE COMPUTATIONAL METHOD

The computational fluid dynamics code, AIRFLO, has been used for these simulations. The code is an implicit-integration, finite-volume Navier-Stokes solver, which has been developed within Arup R&D. It is configured particularly for application to natural and forced convection air flow problems in buildings[15].

The code uses a pressure-coupled formulation involving the simultaneous solution of the momentum equations for velocity components, and the mass continuity equation for pressure. The equation for pressure is derived by substituting the momentum equations (for velocity components) into the statement of mass continuity[16]. A re-arrangement of terms results in a diagonally-dominant equation for pressure. The mass continuity equation is, therefore, exact thus obviating the need for a pressure-correction algorithm such as SIMPLE or its derivatives[17].

The velocity components are calculated at cell faces using a staggered grid. A standard linearization of the equations is used, where the linearized coefficients comprise the convection and diffusion fluxes over the staggered momentum cells and scalar temperature cells, as appropriate.

In the work reported here the energy equation is solved in a segregated form where the act of linearization de-couples it from the momentum and mass continuity equations. Although very simple to implement, this can result in the need for substantial under-relaxation to retain stability, and hence the well-known difficulties of delayed convergence in high Rayleigh number buoyant flows. Although not implemented here, a Newton-Raphson linearization of the energy equation would be expected to significantly enhance the convergence rate for buoyant flow[18]. Buoyancy force is modelled using the Boussinesq approximation.

The 'hybrid' differencing scheme[17] is used, giving central differences at low cell Peclet number and upwind differences, with diffusion suppressed, for high Peclet number. A point Gauss-Seidel solver with multi-directional sweep is implemented for all equations. Appendix A shows the finite-volume form of the equations. The code allows the equations to be solved in either steady-state or transient form, where in the latter a simple Euler integration with forward-differencing in time is used.

4. DESCRIPTION OF SIMULATIONS

The test problem was chosen to represent a shopping mall in winter with an opening to outside protected by a warm air curtain projected downwards from above the opening - a typical application of air curtains encountered by design engineers.

The mall is 15m long, 4m high and 4m wide with an opening of height 2.5m extending across the full width of the mall (see Fig. 1). There is assumed to be negligible leakage of air from the mall except through the door opening. The case of zero wind pressure was chosen. Strong or gusting winds or high leakage would be expected to degrade the performance of the air curtain.

The air curtain unit draws air in at the top, which is then heated and projected downwards and towards the warm mall at an angle of 15° to the vertical. The discharge slot width is 100mm.

Air in the mall is heated by contact with the floor, ceiling, end wall and the shops on either side. This was modelled by assuming a constant surface temperature for these surrounding surfaces (extending from 1m from the opening to the end wall) and a convective heat transfer coefficient of

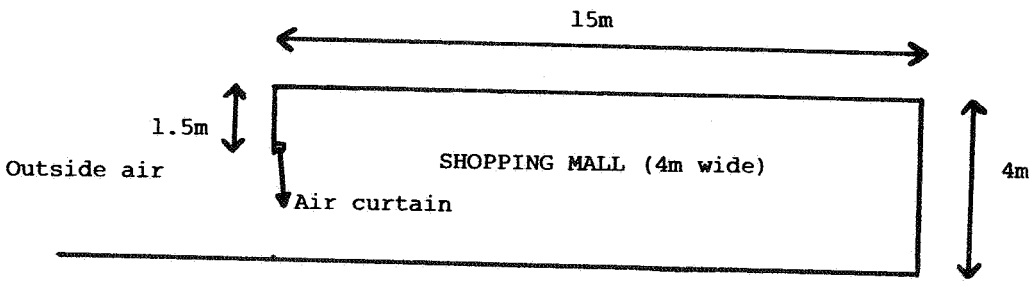

Figure 1. Geometry of test problem (side elevation)

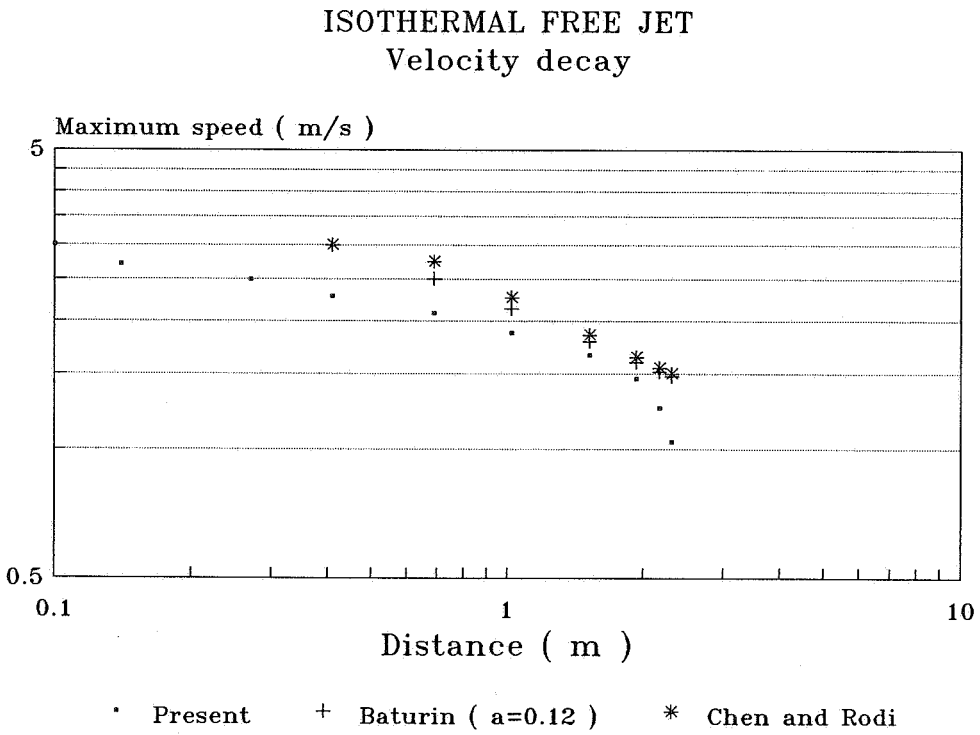

Figure 2. Projection of isothermal jet

$3W/m^2/°C$. The outdoor air temperature is -1°C and the 'outdoor' boundary is taken 5m from the opening. A fixed external pressure boundary condition is applied here where the mass flow rate across the boundary is based on a constant (equal to the product of density and flow area) multiplied by the linear pressure difference.

The mall was modelled two-dimensionally with attention concentrated on the projection of the air curtain. Three-dimensional edge effects were neglected except for the heat flux from the sides of the mall. The mesh comprised 100 cells horizontally and 56 cells vertically with a maximum cell aspect ratio of twelve at the far end of the mall remote from the door. In the horizontal direction, two cells were used to represent the air curtain discharge. A constant and uniform eddy-viscosity of $1.8x10^{-3}Ns/m^2$ has been used.

From initial conditions of zero velocity and uniform temperature, approximately 1,500 steady-state iterations were necessary to reduce mass and energy flux errors through the doorway down to 2 to 5%. The simulations were carried out on an 8 Mbyte SUN SPARCstation which achieved a throughput of approximately 600 iterations per hour.

5. RESULTS AND DISCUSSION

Six simulations were performed including one (A) to assess the isothermal performance of the air curtain and one (B) to simulate conditions if the opening were not 'protected' by an air curtain. The temperature (Tsupp) and velocity (Vsupp) of the supply air were varied to determine the effect on the performance of the air curtain.

For each simulation the heat lost by convection and diffusion at the opening (Qlost), heat supplied by the air curtain (Qsupp) and heat lost by the surrounding shops (Qload) to the mall by convection were recorded. For an energy balance,

$$Qlost = Qload + Qsupp$$

The thermal comfort conditions for people inside the mall are, for the purpose of these simulations, quantified by the maximum air speed (Umax) and the maximum (Tmax) and minimum (Tmin) temperatures at a vertical plane 5m from the opening up to a height of 1.8m.

The conditions and results of each simulation are shown in Table 1.

	CONDITIONS		HEAT FLUXES			WALL CONDITIONS		
	Vsupp (m/s)	Tsupp (°C)	Qlost (kW/m)	Qload (kW/m)	Qsupp (kW/m)	Umax (m/s)	Tmin (°C)	Tmax (°C)
A	3.0	-	-	-	-	1.8	-	-
B	No supply		1.96	1.94	0.0	0.37	-0.6	2.3
C	3.0	20	7.47	2.15	5.65	0.33	-0.7	2.3
D	3.5	20	8.69	2.37	6.65	0.40	-0.6	2.1
E	4.0	20	2.20	0.50	1.58	2.50	15.6	17.0
F	4.0	30	14.50	2.39	12.60	0.41	-0.6	2.1

Table 1. Summary of test conditions and results

The isothermal simulation was performed to allow comparison with established data for the velocity decay of free plane jets. Figure 2 shows the projection of the isothermal jet for this geometry with discharge angle of 15°. The velocity decay from Baturin[9] is found from:

$$U_x = U_o \, 1.2 \, [(2aX/b) + 0.41]^{-0.5}$$

where U_x = velocity at distance X (m/s)
U_o = initial jet velocity (m/s)
a = a constant for the type of outlet (0.12)
b = slot width (m)

and that from Chen and Rodi[19] from:

$$U_x = U_o \, 2.4 \, (X/b)^{-0.5}$$

It can be seen that in the proximity of the discharge the predicted velocity is lower than expected. This indicates an enhanced and unrealistic diffusion which is believed to be due to the relatively poor mesh resolution and to associated factors related to turbulence modelling and differencing scheme. At a large distance, velocity is seen to fall off rapidly as the jet becomes influenced by the proximity of the floor such that it can no longer be considered as 'free'.

For an unprotected opening (B) cold air penetrates

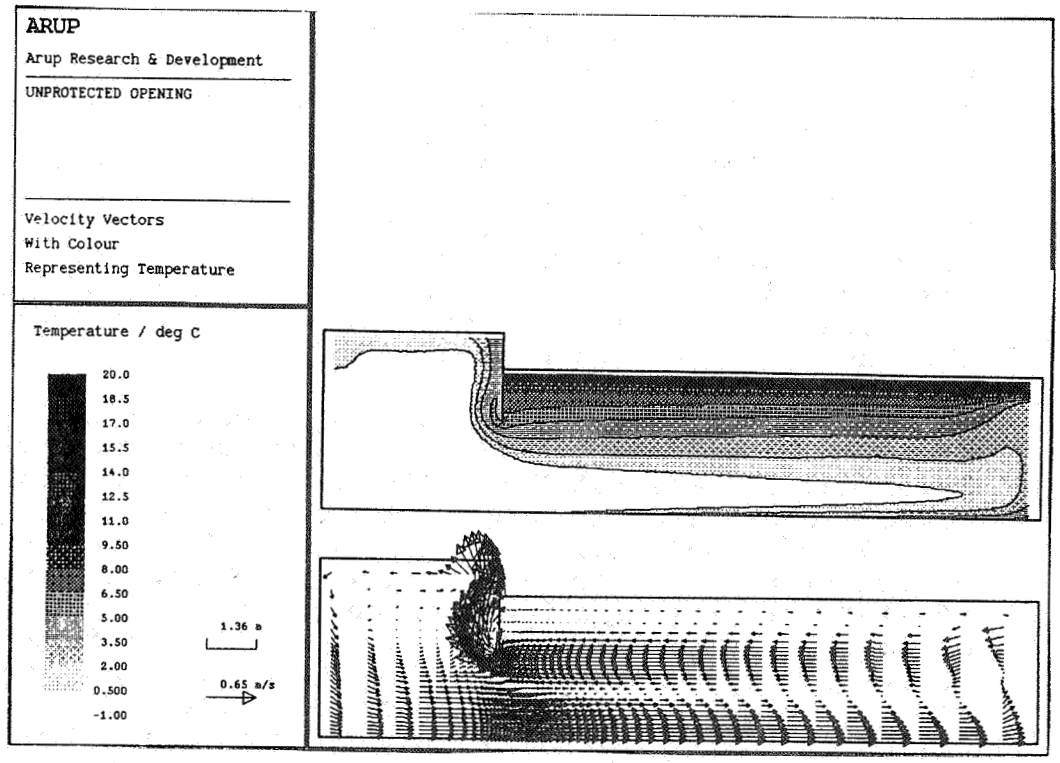

Figure 3. Unprotected opening (simulation B)

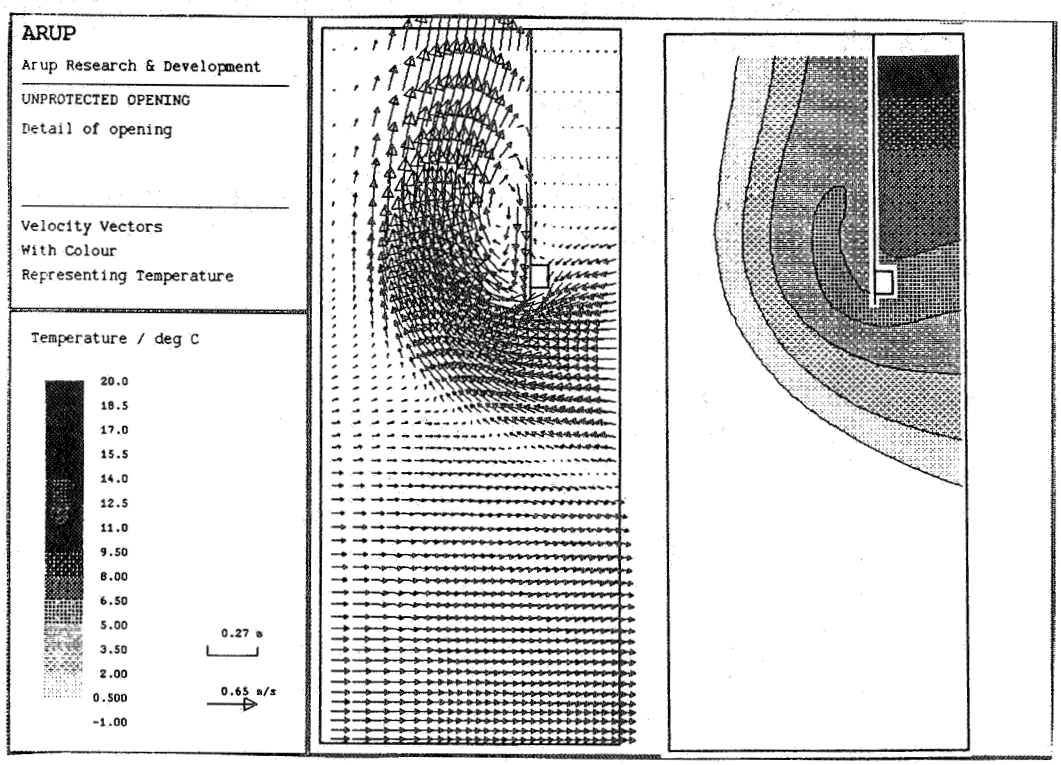

Figure 4. Unprotected opening (simulation B) - detail

at low level far into the mall causing unacceptable conditions for occupants. An equal quantity of air warmed by the surroundings of the mall escapes from the upper part of the opening. Figures 3. and 4. show the velocity and temperature fields (with only one-in-four velocity vectors plotted in Figure 3. to simplify presentation). There is a tendency for stratification of warmer air above the level of the opening and it can be seen that in the plane of the door the neutral-plane is approximately two-thirds the way up the height of the door.

The maximum velocities through the open door are found to be 0.3 m/s (at -1°C) into the mall at low level and 0.7 m/s (at 5 to 6°C) to outdoors at high level. These figures compare to a maximum velocity of 0.38 m/s indicated by a numerical infiltration calculation which assumes an external temperature of -1°C and a uniform internal temperature of 5°C. Using the latter model, the assumption of uniform internal temperature locates the neutral plane at the mid-height of the door hence generating a symmetric inflow / outflow velocity profile. The total flow rate and energy flux through the door indicated by the CFD code was 0.35 m^3/sm and 1.96 kW/m, and by the infiltration model was 0.32 m^3/sm and 2.31 kW/m, respectively. A simpler calculation from the CIBSE Guide[21] indicates a flow rate of 0.43 m^3/sm. The comparison is encouraging and gives confidence in the modelling approach.

The infiltration model, which uses ten vertical segments through which the flow is calculated, is based on that described by Liddament[20], where the flow equation is:

$$Q = 1.29\ C_D\ A\ \Delta P^{0.6}$$

where Q = volume flow rate (m^3/s)
C_D = discharge coefficient (0.6)
A = area (m^2)
ΔP = pressure drop (N/m^2)

Figures 5. and 6. show the velocity and temperature fields for simulation C with Vsupp= 3m/s, which corresponds to the initial design estimate for the outlet velocity. It can be seen though that the air curtain is swept aside by the pressure gradient generated by 'stack' effect. Cold air penetrates the mall virtually unimpeded and conditions are similar to those for an unprotected opening. The energy provided to heat air and drive the fan in the air curtain unit is entirely wasted as the warm

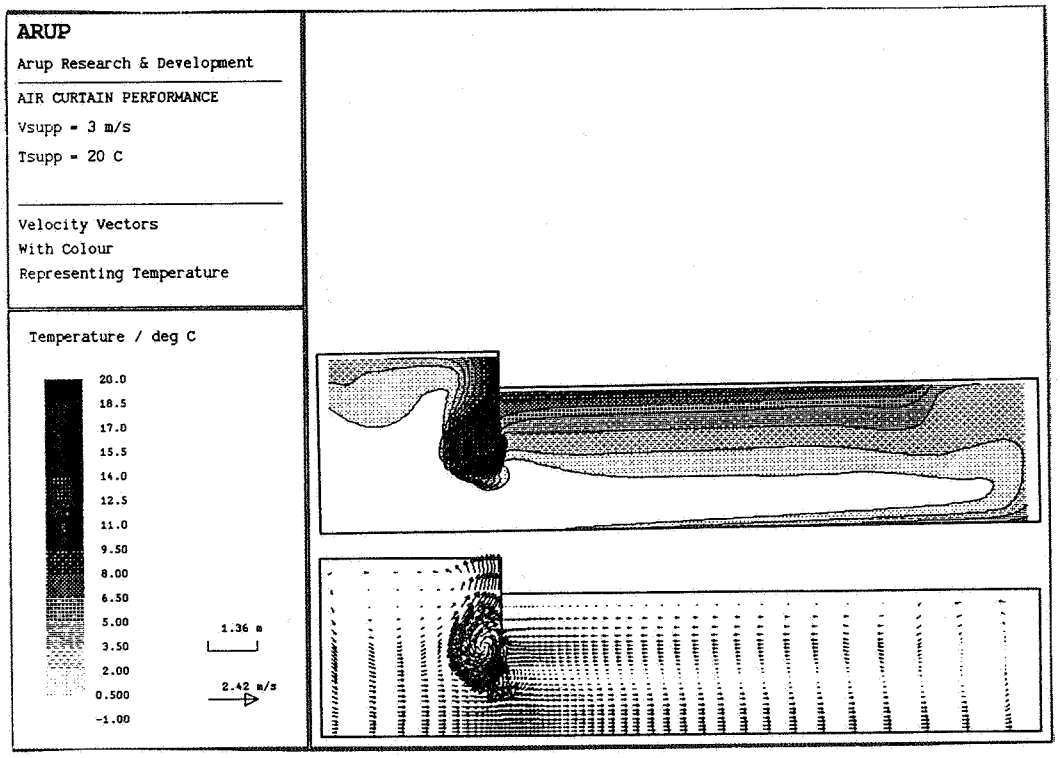

Figure 5. Air curtain with Vsupp=3m/s, Tsupp=20°C (simulation C)

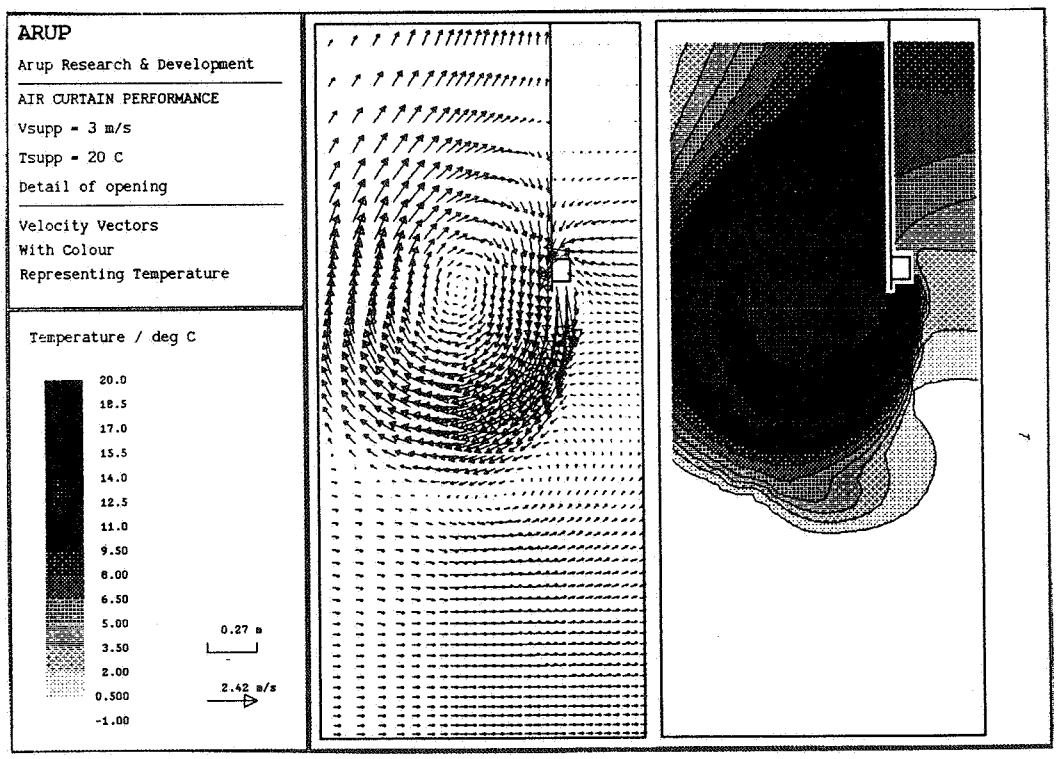

Figure 6. Air curtain with Vsupp=3m/s, Tsupp=20°C (simulation C) - detail

air jet is deflected and lost outside the mall.

Simulation D with a slightly higher supply velocity of 3.5m/s gives a similarly poor behaviour to simulation C.

Figures 7. and 8. show the velocity and temperature fields for simulation E with a higher supply velocity of 4m/s. Here the air curtain is seen to behave as desired. The curtain extends to the floor preventing the large infiltration found in simulations B and C. Incoming air is warmed by mixing with the curtain to give an acceptable and fairly uniform mall temperature of 16°C. The air curtain does, however, produce high air speeds (2.5m/s) within the mall which may cause some discomfort. The efficiency is good since the energy expended in heating the supply air is not wasted but serves to keep air within the mall at a reasonable temperature.

Simulations D and E indicate that the critical supply velocity for correct operation of the air curtain is somewhere between 3.5m/s and 4m/s and that heat transfer across the curtain for a supply velocity of 4 m/s is about 2.2 kW/m. This compares with a critical supply velocity of 2.1 m/s from Hayes and Stoecker[4]. For the higher supply velocity of 4.0 m/s, Hayes and Stoecker indicate a heat transfer rate of 3.6 kW/m (see Appendix B). Not surprisingly the agreement is not perfect, but it is encouraging considering the complexity of the flow and the difficulty of the theoretical analysis on which these predictions of critical supply velocity and heat transfer are based.

Simulation F was performed with a supply velocity of 4m/s, but with a raised supply temperature of 30°C. The additional buoyancy forces caused the jet to break away from the floor and to be swept aside and exhibit similar performance to simulation C.

Clearly care should be taken when sizing and selecting air curtains since the implications, on both performance and energy use, of incorrect selection are dramatic. However, further work is needed to identify the extent to which the present results may be contaminated with numerical discretisation errors.

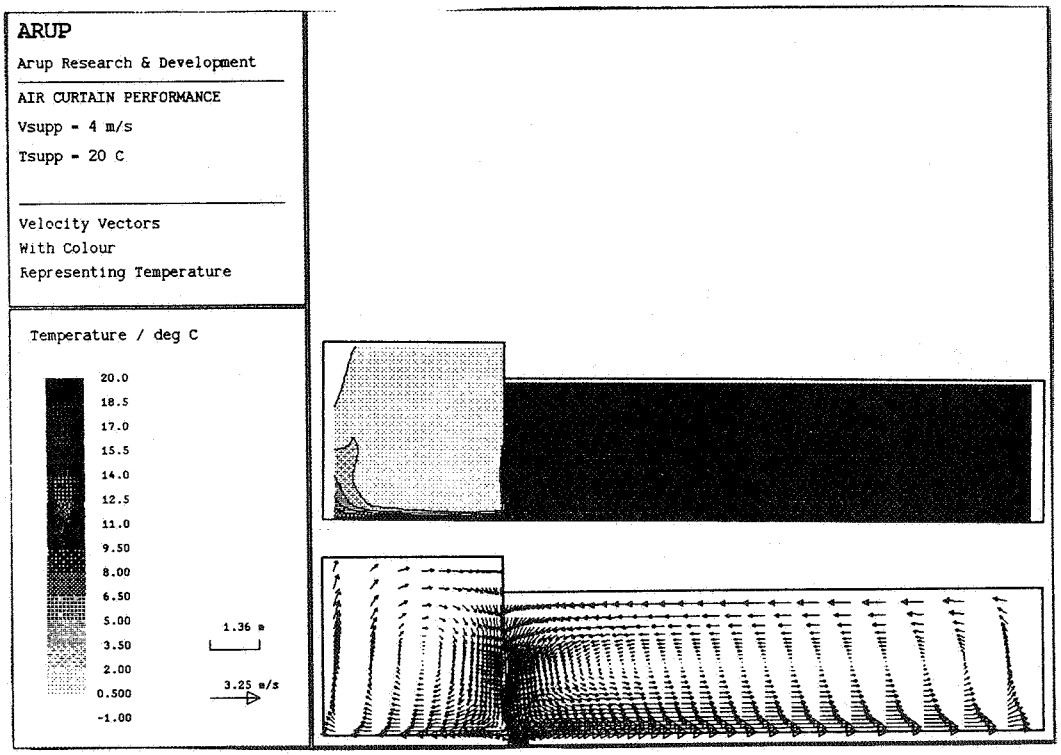

Figure 7. Air curtain with Vsupp=4m/s, Tsupp=20°C (simulation E)

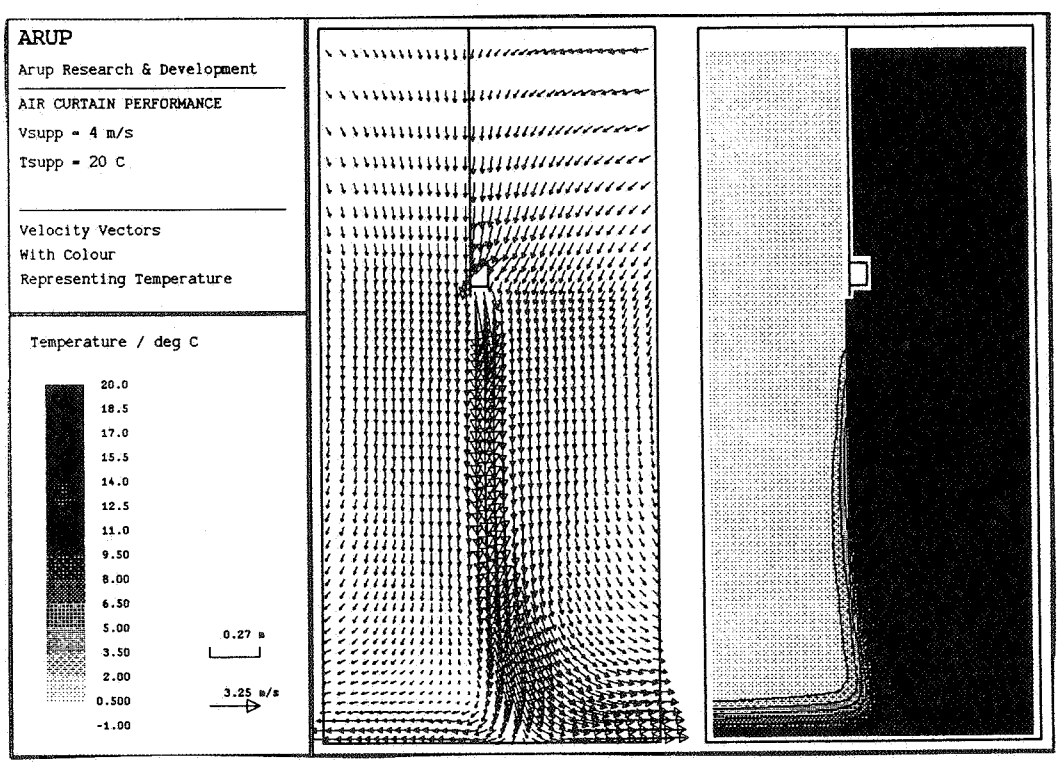

Figure 8. Air curtain with Vsupp=4m/s, Tsupp=20°C (simulation E) - detail

6. CONCLUSIONS

An investigation has been undertaken of air curtain performance using computational fluid dynamics methods, and findings have been compared to previously published design data.

Initial predictions of flow through an open door and the comparison with an accepted infiltration analysis show the calculation method generates plausible and very detailed results which conform well to physical interpretation.

For an external temperature of -1°C the heat loss through the unprotected open door was found to be 1.96 kW/m giving a mean internal temperature in the occupied zone 5 m distant from the door of 0.9°C. With the air curtain operating, but not successfully (since the air curtain was deflected to outdoors), the heat loss increased to between 7 and 9 kW/m without any improvement in internal conditions. With the momentum in the discharge from the unit increased such that the air curtain operated correctly the heat loss was 2.20 kW/m and an internal temperature of 16.3°C was achieved.

The corresponding heat transfer coefficients are 0.85 $kW/m^{2o}C$ without a curtain, 3.6 $kW/m^{2o}C$ with the curtain operating incorrectly, and 0.051 $kW/m^{2o}C$ with the curtain operating successfully. Clearly, when the air curtain is operating incorrectly the energy supplied via the curtain is totally wasted.

With the air curtain operating successfully, an increase in the temperature of the supply air from 20°C to 30°C caused the curtain to be deflected to outdoors resulting in a very high energy use and no improvement of temperature conditions beyond those generated without a curtain present. This behaviour was due to the increased buoyancy force.

It should be noted that when the air curtain was operating successfully high air speeds (2.5 m/s) were generated at low level within the building.

It was found that for the configuration studied, the critical momentum flow at the discharge of the air curtain should be significantly higher than that indicated by the design method, although further work is needed to establish mesh independence and freedom from contamination by numerical discretisation errors.

7. APPENDIX A - Discretized CFD equations

7.1 Discretized momentum equation in X direction

$$a_P U_P = a_N U_N + a_S U_S + a_E U_E + a_W U_W + a_H U_H + a_L U_L + b_U$$

where a = convection / diffusion fluxes - a function of (C, D)
C = convection (mass) flux
D = diffusion flux
$a_P = a_N + a_S + a_E + a_W + a_H + a_L + V \rho_P / dt$
b_U = momentum source + $V \rho_P^{\circ} U_P^{\circ} / dt$
V = cell volume
ρ = density
U = computed velocity
U° = velocity at previous time step
dt = time step

Subscript P refers to the in-cell variable value, and subscripts N, S, E, W, H and L refer to surrounding north, south, east, west, high and low variable values. Superscript 'o' refers to the variable value at the previous time step.

The form of the function defining a_N, etc, follows from the selection of the discretization scheme, eg. upwind, central, hybrid differencing.

7.2 Discretized mass continuity equation

$$(\rho_P - \rho_P^{\circ}) V / dt + C_N + C_S + C_E + C_W + C_H + C_L + b_c = 0$$

where b_c = mass source

7.3 Discretized energy equation

$$a_P h_P = a_N h_N + a_S h_S + a_E h_E + a_W h_W + a_H h_H + a_L h_L + b_h$$

where h = enthalpy (Cp T)
Cp = specific heat
T = temperature
b_h = energy source + $V \rho_P^{\circ} h_P^{\circ} / dt$

8. APPENDIX B - Air curtain design procedure

When selecting an air curtain the design engineer must consider a number of parameters affecting performance:

- discharge configuration - overhead, side or

floor;
- warm- and cold-side temperatures;
- slot width, supply velocity and, hence, flow rate;
- supply temperature;
- discharge angle.

Overhead discharge is usually preferred over floor discharge for reasons of comfort and for both ease of installation and contamination control.

In the case of overhead discharge, Hayes and Stoecker[4] suggest a procedure for estimating the supply momentum required for a given slot width, b_o, door height, H, and design inside, Tw, and outside, Tc, temperatures. From their theoretical and experimental work the critical supply velocity, U_o'', to ensure that the air curtain reaches the floor is estimated as:

$$U_o'' = 3.4 \text{ m/s}$$

and the coefficient for the rate of transfer of sensible heat across the curtain, h_o'', as:

$$h_o'' = 0.071 \text{ kW/m}^2\text{°C}$$

under the conditions H= 2.13m, H/b_o= 25, Tw= 23.9°C, Tc= -23.3°C, with discharge downwards and towards the warm mall at an angle of 15° to the vertical.

Applying a correction factor, K_B, to extrapolate to an air curtain designed for H= 2.5m, b_o= 0.1m, Tw= 16°C, Tc= -1°C, where,

$$K_B^2 = (H/2.13\text{m})*(Tw_{(abs)}/Tc_{(abs)} - 1) /(297\text{K}/250\text{K} -1)$$

$$Tw_{(abs)} = Tw + 273$$

$$Tc_{(abs)} = Tc + 273, \text{ and}$$

$$U_o' = K_B * U_o'',$$

gives $K_B = 0.62$, and

$$U_o' = 2.1 \text{ m/s}$$

To ensure that the air curtain establishes itself properly after any disruption and to allow a margin for error a "velocity factor", $F= 2^{0.5} = 1.4$, is employed, giving,

$U_o = F * U_o' = 1.4 * 2.1$ m/s

$= 2.9$ m/s

The rate of sensible heat transfer across the curtain, Q, is then :

$Q_{2.9m/s} = (F * K_B * h_o'') * H * (Tw - Tc)$

$= 1.4 * 0.62 * 0.071$ kW/m^{2o}C * 2.5 m * (16°C + 1°C)

$= 2.6$ kW/m

For the higher supply velocity of 4m/s,

$Q_{4m/s} = 2.6$ kW/m * (4m/s / 2.9m/s)

$= 3.6$ kW/m

9. REFERENCES

1. MOTT, L.F.
"Design of the air curtain. Refrigeration, Air Conditioning and Heating", pp.1-23, September 1961.

2. WOLFBERG, H.A.
"Get 1350 tons of cooling from 875hp in shopping-parking facility". Heating, Piping and Air Conditioning, May 1964.

3. HAYES, F.C. AND STOECKER, W.F.
"Heat transfer characteristics of the air curtain". ASHRAE Trans. vol.75, pt2, pp.153-167, 1969.

4. HAYES, F.C. AND STOECKER, W.F.
"Design data for air curtains". ASHRAE Trans. vol.75, pt2, pp.168-180, 1969.

5. ASKER, G.C.F.
"What, where and how of air curtains". Heating, Piping and Air Conditioning, June 1970.

6. NATIONAL SANITATION FOUNDATION, Standard No. 37, "Air curtains for entranceways in food establishments", 1970, 1980, 1985.

7. LEARMONTH, R.A.

"The use of air curtains". H & V E, September 1970

8. CREEK, H.P.
"Warm air curtains". H & V E, October 1971.

9. BATURIN, V.V.
"Fundamentals of industrial ventilation", Chapter 15 - Air curtains, Pergamon Press, Oxford, 1972.

10. "Doorway protection with an unheated air curtain", Building Services Engineer, vol.43, April 1975.

11. SIMPER, J.I.
"New uses for air curtains". Building Services Engineer, vol.43, November 1975.

12. "Air curtains - Energy savings for industry". HAC December 1986 / January 1987.

13. LIGTENBERG, P.J.J.H.
"Economical air curtains". Biddle Air Curtains Ltd, Enfield, Middlesex, UK.

14. LIGTENBERG, P.J.J.H.
"It's curtains for cold air". HAC pp.30-32, October 1989.

15. HOLMES, M.J., LAM, J.K-W., RUDDICK, K.G. AND WHITTLE, G.E.
"Computation of convection, conduction and radiation in the perimeter zone of an office space". Proc. Int. Conf. Roomvent 90, Oslo, June 1990.

16. ZEDAN, M., AND SCHNEIDER, G.E.
"A coupled strongly implicit procedure for velocity and pressure computation in fluid flow problems". Numerical Heat Transfer, vol.8, pp.537-557, 1985.

17. PATANKAR, S.V.
"Numerical heat transfer and fluid flow". Hemisphere Publishing Corporation, New York, 1980.

18. GALPIN, P.F., AND RAITHBY, G.D.
"Treatment of non-linearities in the numerical solution of the incompressible Navier-Stokes equations". International

Journal for Numerical Methods in Fluids, vol.6, pp.409-426, 1986.

19. CHEN, C.J. and RODI, W.
"Vertical turbulent buoyant jets - A review of experimental data". Pergamon Press, Oxford, 1980.

20. LIDDAMENT, M.W.
"Air infiltration calculation techniques - An application guide". Air Infiltration and Ventilation Centre, International Energy Agency, 1986.

21. CIBSE Guide. Air Infiltration, Table A4.5. London, 1986.

Discussion
Paper 16

C-A Roulet (LESO, Switzerland)

Since water is between 200 and 400 times more efficient than air to transport heat (the figure depending on the considered phenomenon), why insist on using air for that purpose? Water temperature conditioning may solve many problems encountered in air conditioning.

M J Holmes (Arup R & D, UK)

There is no general solution to cooling problems, the structural form may influence the air conditioning system, that is a concrete or steel frame. For example, the type of voids generated could mean a ceiling or floor systems are more appropriate - concrete favours floor supply. An obvious comment on water cooled equipment at desks could cause problems with flexibility.

VENTILATION SYSTEM PERFORMANCE

11th AIVC Conference, Belgirate, Italy
18-21 September 1990

Paper 17

CALCULATION OF THE AIR FLOW PATTERN IN A PROPOSED NEW EUROPEAN TEST CHAMBER FOR RADIATORS

A. Huber, A. Moser, Q. Chen

ETH Zürich
Institut für Energietechnik - LES
CH-8092 Zürich, Switzerland

Calculation of the air flow pattern in a proposed new European test chamber for radiators

A. Huber, A.Moser and Q. Chen
Swiss Federal Institute of Technology, Zürich
Energy Systems Laboratory

A new European norm for measuring the heat transfer rate of radiators is under discussion [CEN TC 130]. This testing can be done either in a closed chamber with cooled walls or in a open chamber with a controlled air supply.

The air flow pattern around a typical radiator is calculated for both types of chambers.

The calculation is done with the program PHOENICS, a finite volume program that solves the conservation equations for mass, momentum and energy. For turbulence, the k-ε model is used with the Lam-Bremhorst correction for low Reynolds numbers.

It has been found that the flow field around the radiator looks the same for both types of chamber. In the closed chamber there is a recirculating zone at the ceiling. This can be avoided in the open chamber when the air change rate exceeds some minimum value. This minimum value for the air change rate is dependent only on the heat output of the radiator.

BERECHNUNG DER STRÖMUNGSFELDER AM GEPLANTEN NEUEN HEIZKÖRPERPRÜFSTAND DER EMPA

Zusammenfassung

Im Rahmen der EG-92-Normbestrebungen soll für die Heizkörperprüfung in Europa eine einheitliche Lösung gefunden werden. (CEN TC 130). Heute in gebrauch sind einerseits die geschlossenen Prüfkammern, bei denen die Wärmeabfuhr durch die gekühlten Wände erfolgt und andererseits die offenen Prüfkammern (DIN 4704 und ISO TC 116).
Als Entscheidungsgrundlage für die Typenwahl des neuen Prüfstandes sollten folgende Fragen beantwortet werde:

- Inwiefern beeinflusst bei einer offenen Prüfkammer ein Lufteinlass das Strömungsbild um den Heizkörper?
- Wie sieht bei einem typischen Heizkörper die Temperaturverteilung in einer geschlossenen und wie in einer offenen Kammer aus?
- Welche Temperaturen und Massenströme sind bei einem offenen Kammertyp am Lufteinlass zu wählen, und wie verändert eine Variation dieser Werte das Strömungsbild im Raum?

Zur Klärung dieser Fragen wurde am Laboratorium für Energiesysteme an der ETH Zürich eine rechnerische Variantenstudie sowohl am geschlossenen als auch am offenen Prüfkammertyp durchgeführt. Ausgeführt sind die Berech-nungen mit PHOENICS, einem finite Volumen Programm, das die Impuls-, Kontinuitäts- und Energiegleichungen löst. Die Turbulenz wird mit dem k-ε - Turbulenzmodell mit den Low-Reynolds-Erweiterungen nach Lam - Bremhorst bestimmt. (cf [2] - [18])
Als Resultat der Untersuchungen können folgende Punkte festgehalten werde:

- Das Strömungsbild beim Heizkörper ist praktisch unabhängig vom Prüfkammertyp und Volumenstrom am Lufteinlass.
- In einer geschlossenen Prüfkammer gibt es an der Decke eine Rezirkulationszone.
- In einer offenen Prüfkammer tritt die Rezirkulation nur dann auf, wenn der Volumenstrom beim Heizkörper grösser ist als der Volumenstrom des Einlasses. Der minimale Volumenstrom am Einlass wird also durch die konvektive Wärmeleistung des Heizkörpers bestimmt.
- Rezirkulation ändert schlagartig das Strömungs- und Temperaturbild und kann die Regelung erschweren.

Die Aenderung der konvektiven Wärmeleistung eines Heizkörpers bei verschiedenen Kammertypen kann wegen der getroffenen vereinfachenden Annahmen nicht beziffert werden.

1. Today's measurement of the heat transfer rate of radiators

The measurement of the heat transfer rate is described in the norms DIN 4704 and ISO TC 116. Open test chambers are allowed as well as closed ones. The test results of these two types of chamber are in any case not comparable. In Switzerland the closed type of test chamber is used (**Fig. 1**). The walls are cooled with water (Hartmann [1]). In other countries, as for example in Italy, the closed type with air cooled walls is in use. The open type of test chamber can be found in Stuttgart at the laboratory of Prof. Bach (**Fig. 2**).

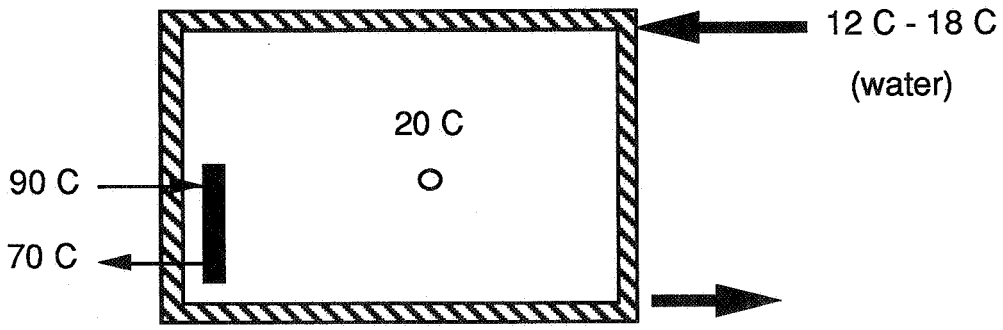

Fig. 1 : The closed type of test chamber at the EMPA, Switzerland

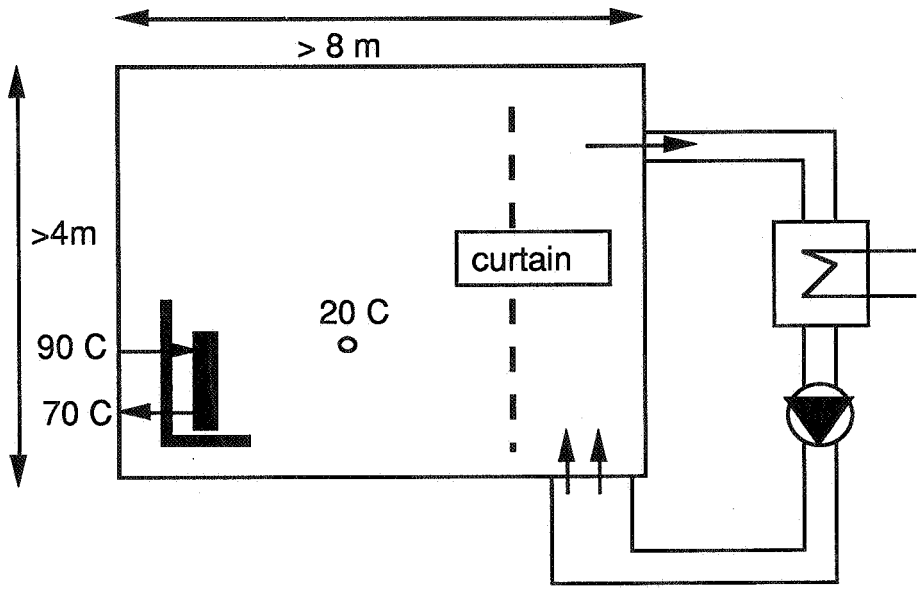

Fig. 2 : The open type of test chamber (DIN - norm)

An important disadvantage of a closed test chamber is the large time that is needed for measuring the heat transfer rate at different water temperatures in the radiator, since the chamber must be in equilibrium for each measurement. Another point is, that the walls of the different types of test chamber are at different temperatures and this leads to a different radiative heat transfer rate. This is one reason why the measurement of the same radiator in different test chambers can lead to different results. Another reason can be found in the different air flow patterns caused by these different wall temperatures.

2. Proposal of a new test chamber (CEN TC 130)

In the future in all European countries there will be only one type of radiator test chamber. This type will be described in a CEN norm (CEN TC 130). For this norm there is now an open as well as a closed type under discussion. For the closed type there is a water cooling system possible, or a system with air cooled walls (**Fig. 1**). The open system would have water cooled walls that keep the walls at a constant temperature and an inlet with controlled air temperature and mass flow rate (**Fig. 3**).

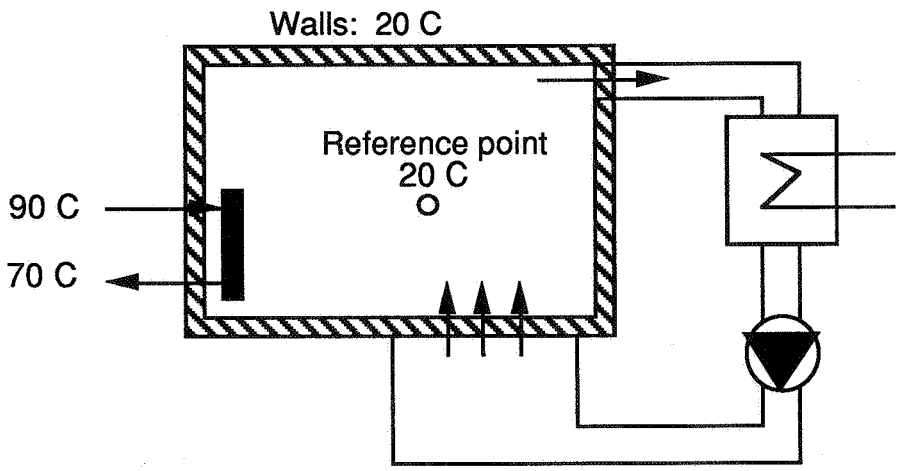

Fig. 3: Proposal of the new open type of test chamber

3. Geometry of the calculated two types of test chamber

The following pictures show the geometry of the two rooms for which calculations have been performed (**Fig. 4 - 5**). They do not have to correspond in every detail to the rooms that are discussed in TC 130. They only need to show us the principal differences in the air flow pattern and the temperature gradient in the two types of test chamber.

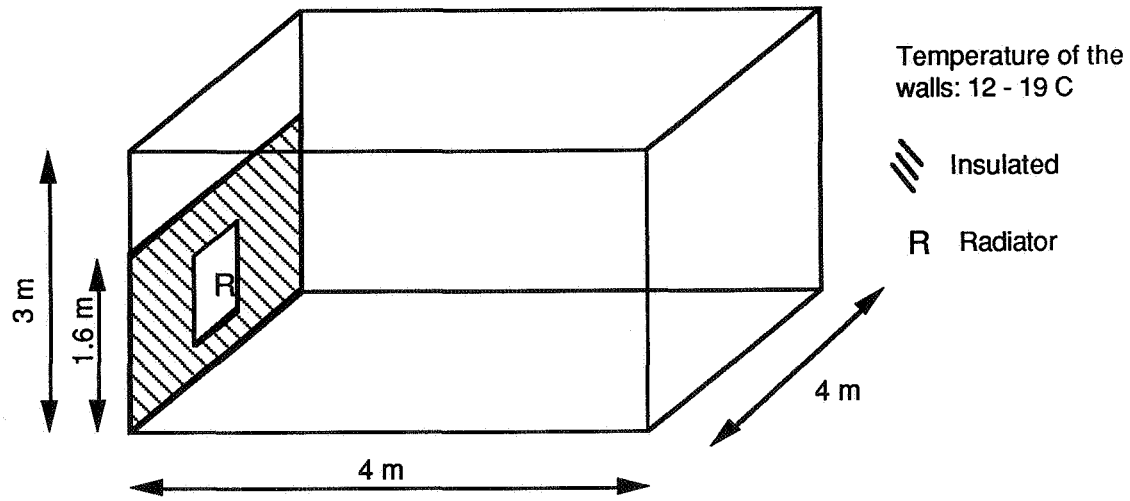

Fig. 4: Geometry of the closed test chamber

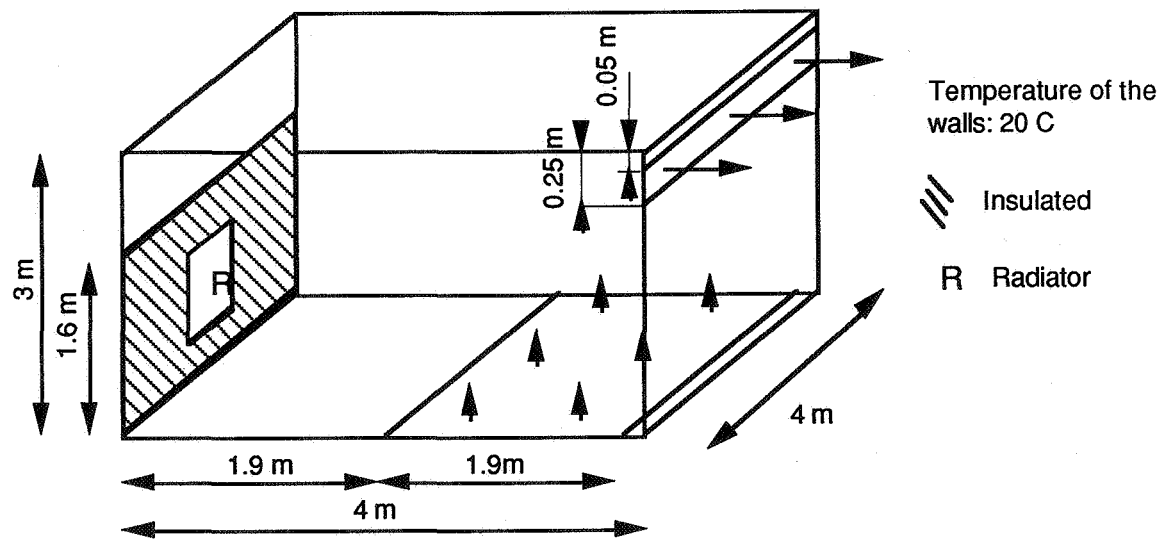

Fig. 5: Geometry of the open test chamber

4. The Radiator

The calculation is based on a flat type of radiator as can be seen in Fig. 6:

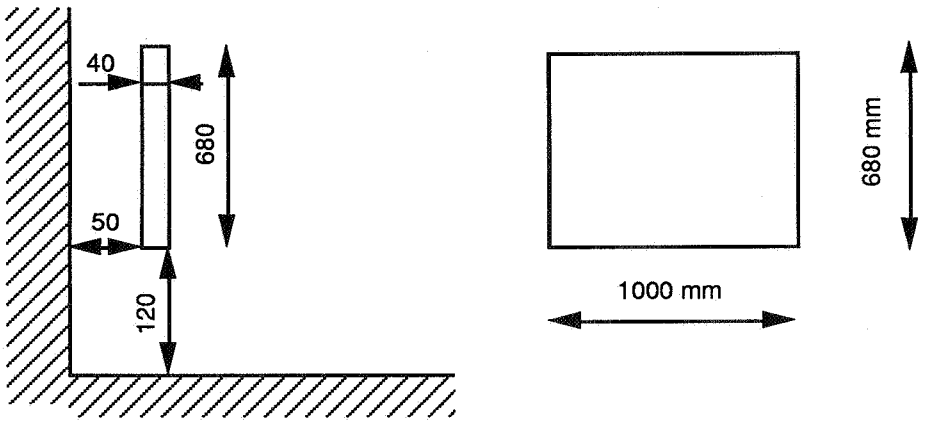

Fig. 6: Geometry of the radiator

From measurments of a similar type of radiator (Prolux, Typ S60) the following data have been found at the EMPA:

- heat transfer rate due to convection: 630 Watt
- heat transfer rate due to radiation 420 Watt

In the calculation radiation can be neglected since the wall temperature is used as boundary condition and there is hardly any direct radiative heat transfer between the walls and the air.
There are two ways to model the radiator. The first is to model the temperature on the surface of the radiator. This can not be done without considering the mass flow in the radiator and the radiative heat transfer between the walls and the radiator. Neither of these is known at the start of the calculation, so the result can only be found in a iterative process. Once the surface temperature is known, the convective heat transfer can be calculated from the temperature gradient at the radiator, as is done at the other walls. Since it is not our goal to calculate the heat transfer rate of the radiator, and thus replace the measurement by a calculation, this method will no longer be looked at. What we actually want to know is the changing of the air flow pattern in different test chambers for a given convective heat transfer rate. Therefore the second possibility is chosen. Here a constant convective heat transfer rate is given as a source term. In our case it is 315 W on both sides of the radiator, so that we have a total convective heat transfer rate of 630 W.

5. Boundary conditions at the inlet for the open test chamber

Two different air change rates have been considered:

- 0.01 m/s inlet velocity, corresponding to a air change rate of 5.7 per hour
- 0.05 m/s inlet velocity, corresponding to a air change rate of 28.5 per hour.

When there is no recirculation from the ceiling an inlet temperature of 20 C is necessary to get a fixed temperature of 20 C at the reference point (**Fig. 3**). When there is recirculation, the inlet temperature must be lower since in this case the fresh air is mixed with the warm air from the ceiling. In the calculation the inlet temperature is always 20 C, so the temperature at the reference point is variable.

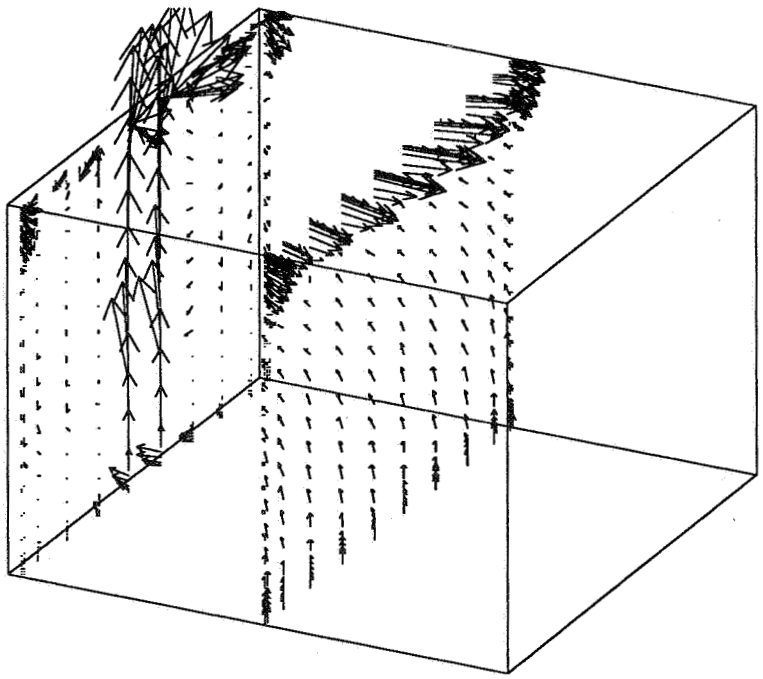

Fig. 7: Air flow pattern in the open test chamber, Run 88C: Velocity of the air at the inlet is 0.05 m/s

6. Wall temperatures in the closed test chamber

In the closed test chamber all energy must leave the room through the walls. Therefore the walls must be cooled to a temperature between 12C and 18C, depending on the heat transfer rate of the radiator.

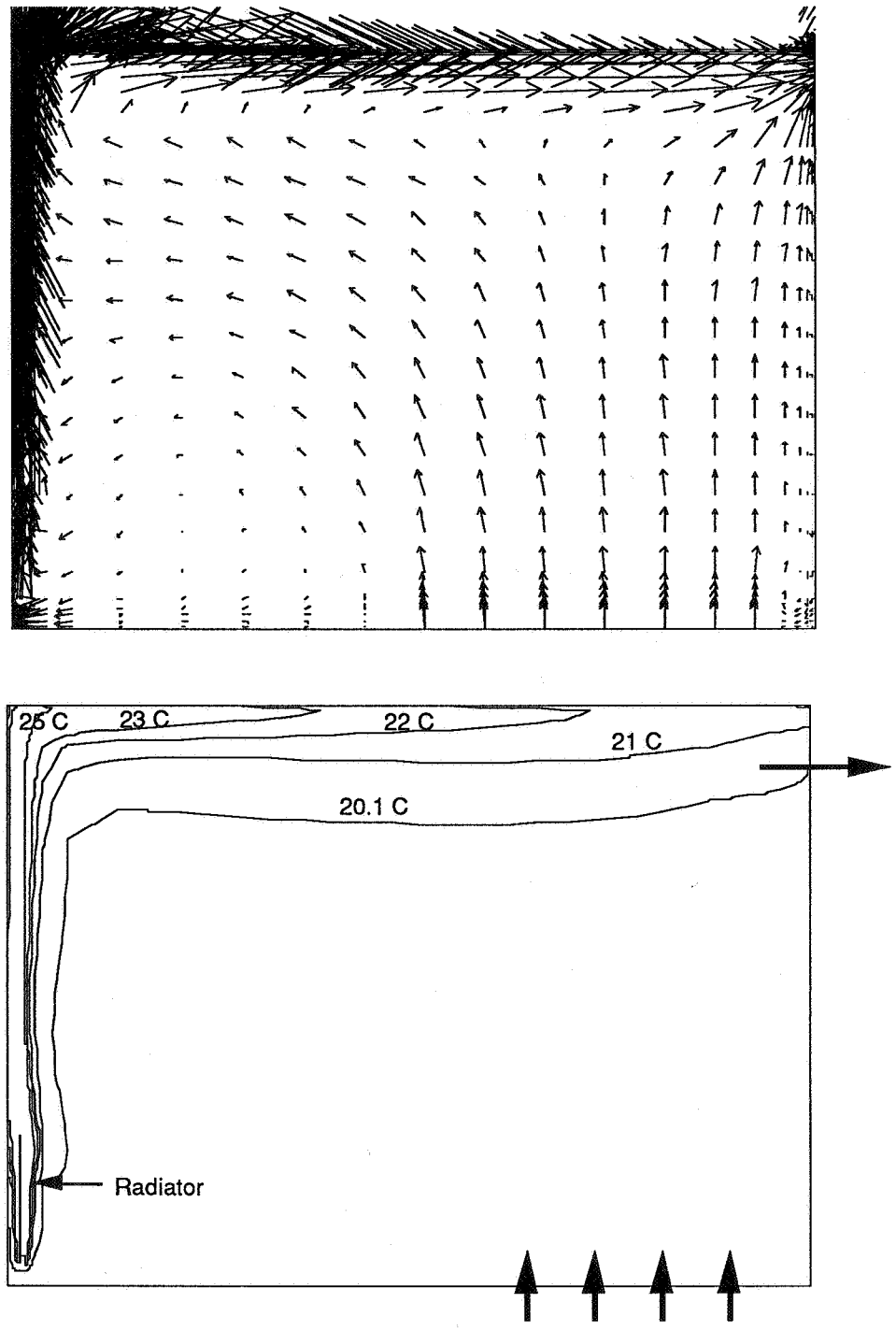

Fig. 8 - 9: **Run 88C, open test chamber, air flow pattern and distribution of the temperature, inlet velocity: 0.05 m/s**

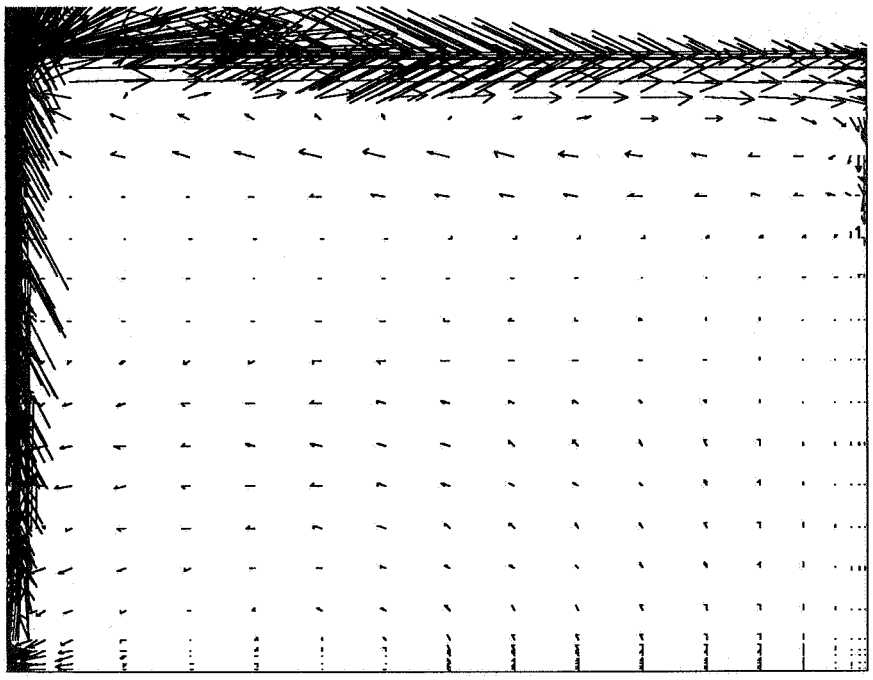

0.2 m/s

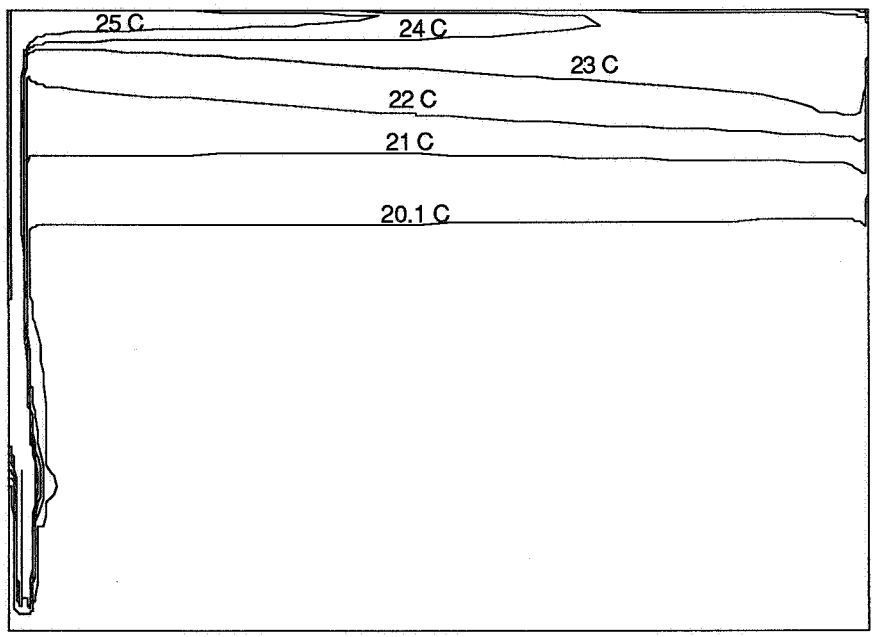

Fig. 10 - 11: **Run 88E, open test chamber air flow pattern and distribution of the temperature, inlet velocity: 0.01 m/s**

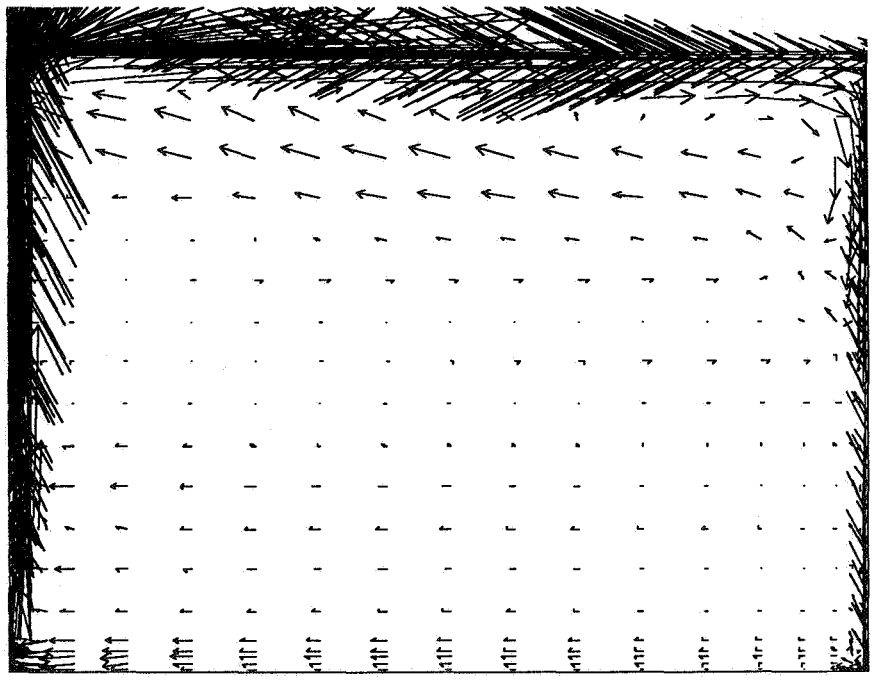

0.2 m/s

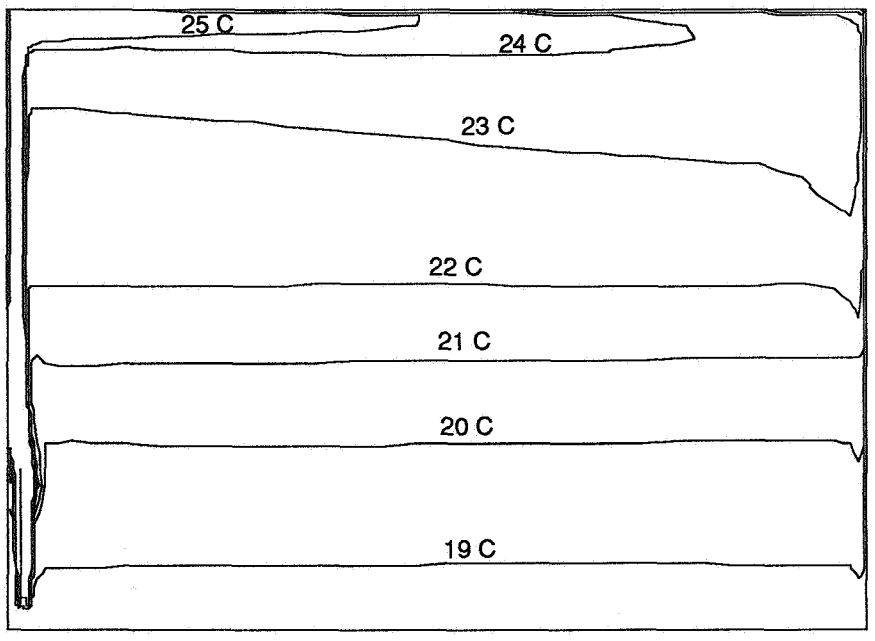

Fig. 12 - 13: **Run 89C, closed test chamber air flow pattern and distribution of the temperature, wall temperature: 18 C**

7. The grid

Fig. 14 shows the grid for the calculation around the radiator. The first grid point is 0.5 mm away from the wall, the second 1.5 mm. The reason for this very fine grid can be found in the way the heat transfer at the walls is calculated. It is not calculated by any empirical Nusselt number formula but by calculating the temperature profile near the wall.This is possible because a low Reynolds number turbulence model is used.
In total there are 42 x 31 x 20 grid points used in the calculation.

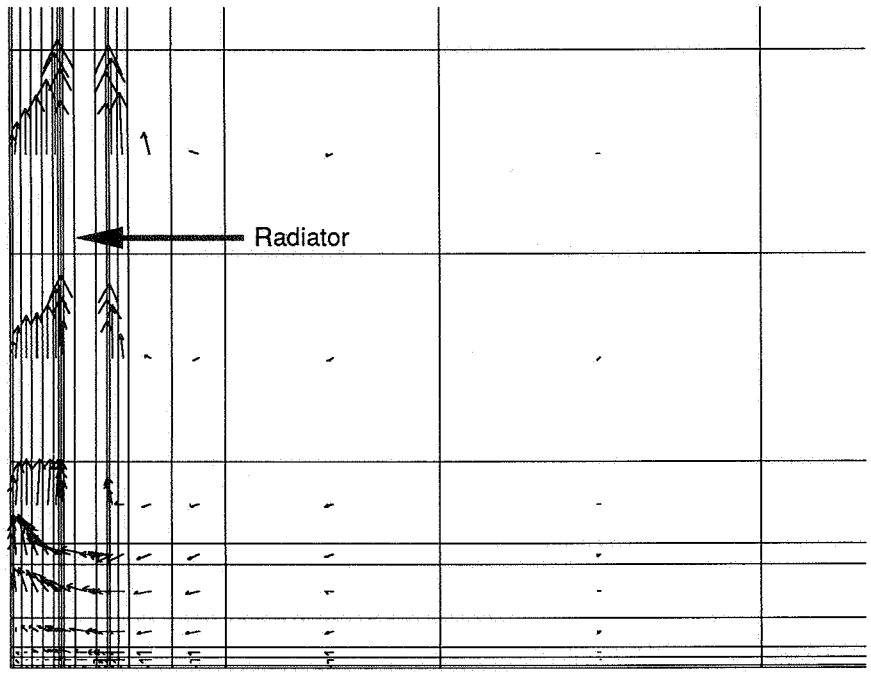

Fig 14: Grid around the radiator

8. The influence of the inlet velocity in the open test chamber

In order to investigate the influence of the inlet velocity on the air flow pattern and the temperature profile, the inlet velocity was reduced from 0.05 m/s (**Fig. 8 - 9**) to 0.01 m/s (**Fig. 10 - 11**) and a principal change in the air flow pattern can be seen. The mass flow of air at the radiator is about the same for both cases. The mass flow at the outlet must be the same as at the inlet. This means that when the mass flow of air at the radiator is greater than the mass flow at the inlet a recirculation is observed. To avoid this recirculation there is a minimum air change rate necessery that depends only on the convective heat transfer rate of the radiator.
Recirculation means that the hot air from the ceiling is mixed with the fresh air from the inlet. This could cause problems in controlling the temperature at the reference point and prolongs the measurement.

9. Outline of the mathematical models

Recent developments of numerical techniques to solve the basic equations of fluid mechanics and the advent of supercomputers have led to the opportunity to compute space air diffusion as reviewed by Nielsen [17] and Ceschi [18]. With these techniques, it is possible to study the field distributions of air velocity, temperature and turbulence intensity.
In the present study, the airflow program developed by Rosten and Spalding [14] has been employed to calculate air distribution. The computations involve the solution of three-dimensional equations for the conservation of mass, momentum (u, v, w), energy (H), turbulence energy (k), and the dissipation rate of turbulence energy (ε). The turbulence model used is the low Reynolds number k-ε model of Lam and Bremhorst [11] that has been implemented in the airflow program. This model has been verified to be more suitable for indoor airflow simulations, and a better agreement between computation and experiment has been found with respect to velocity and turbulence energy distributions and heat exchange through solid walls (Chen et al. [6]). The governing equations of the model can be expressed in a standard form:

$$\mathrm{div}\,(\rho \vec{V} \Phi - \Gamma_\Phi \,\mathrm{grad}\Phi) = S_\phi \qquad (1)$$

where ρ is the air density (kg/m^3), $\vec{V}$ is the air velocity vector (m/s), Γ_Φ is the diffusive coefficient (kg/sm), S_Φ is the source term of the general fluid property, and Φ can be any one of 1, u, v, w, k, ε or H. When $\Phi = 1$ the equation changes into the continuity equation.

10. Conclusions

- It is possible to calculate the air flow pattern around a radiator with a known convective heat flux, and numerical simulation allows prediction of parameter sensitivity.
- The amount of computing time is huge (cf. appendix A).
- The air flow pattern around the radiator is independent of the type of test chamber (open or closed) and of the inlet velocity (0.01 m/s or 0.05 m/s).
- In a closed test chamber there is always a recirculation zone at the ceiling.
- In the closed test chamber a recirculation can be observed, when the inlet mass flow is smaller than the mass flow at the radiator. The mass flow at the radiator is only dependent on its convective heat output.
- Recirculation changes the air flow pattern and the temperatur distribution in the room entirely.

References

1) **P. Hartmann (1973):**
Der Heizkörperprüfstand der EMPA.
Schweizerische Blätter für Heizung und Lüftung, Heft Nr. 4/73

2) **D. Aiulfi (1986):**
Numerische Berechnung eines Luftstrahls mit dem k - ε - Turbulenzmodell, und Vergleich mit Messungen; Interner Bericht ETHZ-LES

3) **D. Aiulfi (1990):**
Simplified Combustion Models for Turbulent Gas Diffusion Flames
Diss. ETH Zürich

4) **J. Borth, K. Eisele (1988):**
Vergleich von LDA - Messungen mit Ergebnissen der numerischen Simulation am Beispiel eines klimatisierten Raumes. Teil II : Numerik ; Interner Bericht Nr. 1704, Gebr.SULZER AG.

5) **Q. Chen (1988):**
Indoor Airflow, Air Quality and Energy Consumption of Buildings.
Ph.D. thesis, Delft University of Technology.

6) **Q. Chen, A. Moser, A. Huber (1990):**
Prediction of Buoyant, Turbulent Flow by a Low-Reynolds-Number k-ε Model.
ASHRAE Transactions 1990, V.96, Pt.1.

7) **L. Davidson (1989):**
Numerical Simulation of Turbulent Flow in Ventilated Rooms
Ph.D. thesis, Chalmers Univeristy of Technology, Göteborg, Sweden

8) **H. Durrer (1988):**
Numerische Ermittlung von Luftströmungen im Einzelraum. 2.Status-Seminar ERL Seite 43.

9) **A. Heiss (1987):**
Numerische und experimentelle Untersuchungen der laminaren und turbulenten Konvektion in einem geschlossenen Behälter
Diss. TU München

10) **A. Huber , A. Moser (1989):**
Numerische Ermittlung von Luftströmungen im Einzelraum. 3.Status-Seminar ERL Seite 17.

11) **C. Lam, B. Bremhorst (1981):**
A Modified Form of the k - ε - Model for Predicting Wall Turbulence; Transactions of the ASME, Vol. 103

12) **P. Nielsen (1979):**
Buoyancy-Affected Flows in Ventilated Rooms; Numerical Heat Transfer, Vol.2

13) **S. Patankar (1980):**
Numerical Heat Transfer and Fluid Flow
Hemisphere Publishing Corporation

14) **H. Rosten, B. Spalding (1987):**
The Phoenics Reference Manual.
Software Version 1.4, CHAM Report number TR200

15) **A. Schachenmann, D.Wiss, G.Metzen (1990):**
Numerische Berechnung von Raumluftströmungen und Vergeich mit LDA-Messungen im Fall freier und erzwungener Konvektion
Technische Rundschau SULZER, 1/1990, Seite 30.

16) **Chr. Schönenberger (1988):**
Low Reynolds Number Turbulence Model; Interner Bericht ETHZ-LES

17) **P. Nielsen (1989):**
Progress and trends in air infiltration and ventilation research,
Proceedings of the 10th AIVC Converence

18) **P.A. Ceschi (1990):**
Numerische Berechnung eines turbulenten ebenen Strahls.; Interner Bericht ETHZ-LES

Short description of run 88C

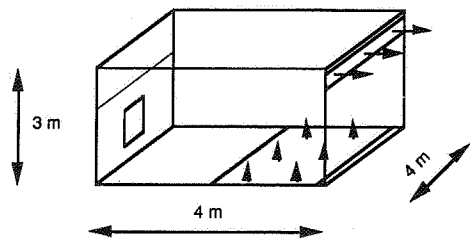

Computing program:-		PHOENICS of CHAM Ltd, London
Algorithm:	-	Finite volume
	-	SIMPLEST - algorithm
	-	Upwind - interpolation
	-	steady calculation
grid:	-	42 x 31 x 20
	-	Staggered grid
Turbulence model:	-	Low-Reynolds k - ε model of Lam-Bremhorst [11]
	-	Turbulent Prandtl number: 0.9
Buoyancy:	-	With Boussinesq approximations
Boundary conditions:-		Convective heat transfer rate at the radiator: 630 W
	-	Velocity at the walls 0 m/s
	-	Linear / logarithmic wall formulae
	-	Wall temperature: 20 C
	-	k and ε at the 1st grid point:

$$k = \frac{\tau_w}{\rho \sqrt{0.09}}$$

$$\varepsilon = \frac{0.1643}{0.435} k^{1.5} \frac{1}{d}$$

Inlet conditions	-	Velocity	0.05 m/s
	-	Area	1.9 m x 4 m
	-	Temperature	20 C
	-	k	0 m2/s2
	-	ε	0 m2/s3
CPU time:	-	2500 sweeps, 10h CPU-time Cray-XMP	

Short description of run 89C

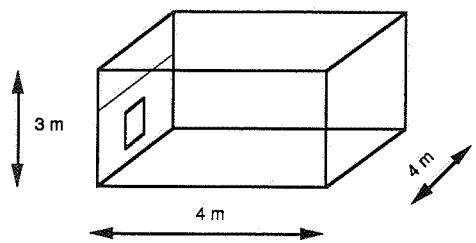

Computing program:-		PHOENICS of CHAM Ltd, London
Algorithm:	-	Finite volume
	-	SIMPLEST - algorithm
	-	Upwind - interpolation
	-	steady calculation
grid:	-	42 x 31 x 20
	-	Staggered grid
Turbulence model:	-	Low-Reynolds k - ε model of Lam-Bremhorst [11]
	-	Turbulent Prandtl number: 0.9
Buoyancy:	-	With Boussinesq approximations
Boundary conditions:-		Convective heat transfer rate at the radiator: 630 W
	-	Velocity at the walls 0 m/s
	-	Linear / logarithmic wall formulae
	-	Wall temperature: 18 C
	-	k and ε at the 1st grid point:

$$k = \frac{\tau_w}{\rho \sqrt{0.09}}$$

$$\varepsilon = \frac{0.1643}{0.435} k^{1.5} \frac{1}{d}$$

CPU time:	-	2500 sweeps, 10h CPU-time Cray-XMP

Discussion
Paper 17

M J Holmes (Arup R & D, UK)

How did you handle radiant heat transfer in your simulation?

A. Huber & A Moser (ETH, Zurich, Switzerland)

Earlier measurements have shown that the radiator heat output is about 60% convection and 40% radiation. In a typical case the 60% convection amounts to 630W. These 630W have been used as heat source at the radiator for the air flow simulation. Radiative exchanges between walls were not computed because the walls had a prescribed temperature of 20 degrees C.

VENTILATION SYSTEM PERFORMANCE

11th AIVC Conference, Belgirate, Italy
18-21 September, 1990

Paper 18

THE VENTILATION CHAMBER OF THE UNIVERSITY OF BASILICATA

G.V. Fracastoro, E. Nino, G. Coretti

Instituto di Fisica
Universita della Basilicata
Via Nazario Sauro
85 - 85100 Potenza
Italy

THE VENTILATION CHAMBER OF THE UNIVERSITY OF BASILICATA

G.V. Fracastoro, E. Nino, and G. Coretti
Istituto di Fisica - Università della Basilicata
Via Nazario Sauro, 85 - 85100 Potenza (Italy)

Synopsis

*A new facility for the study of ventilation in buildings has been recently developed at the University of Basilicata (Potenza, Italy). This facility consists in a Controlled Ventilation Chamber (CVC), with an overall size of 2.4*2.4*3.0 m (the length may be extended to 4.2 m). The CVC is divisible in two parts with a connecting door and is equipped with four grilles from which air can be immitted or extracted. A variable speed fan can adjust a flow rate of 0 to 10 ach. Instrumentation includes a flow rate transducer in the ducts, six low speed hot film anemometers in the room, a two-cell infrared gas analyzer for SF_6 and N_2O concentration, and a differential pressure manual meter. Air sampling at different locations is controlled through a pneumatic scanner by a PC which also serves for data collection and elaboration. The CVC will be used both for ventilation frequency and ventilation efficiency measurements. Black-box identification will be adopted as a novel technique to determine the ventilation frequency (under perfect mixing hypothesis) with varying air change rates and tracer gas immission rates.*

List of symbols

$C(t)$	= concentration of tracer gas at time t
n	= ventilation frequency (number of air changes)
t	= time
V	= volume of the room
$\dot{V}(t)$	= air flow rate across the confined space
τ	= 1/n, time constant of the system
ϵ_j	= ventilation efficiency at point j

Subscripts

b	= background
e	= extraction
g	= tracer gas

1. Introduction

The study of air infiltration, mechanical ventilation, and related hygienic problems has recently raised an increasing interest within the research community (see, e g, Sandberg, 1983, Skåret, 1986), and also the public opinion and mass media. In fact, the concern about environmental problems, both outdoors and indoors, has at the moment drawn much of the attention from energy savings problems.

The initiative to build a Controlled Ventilation Chamber (CVC) at the University of Basilicata responds to the need to improve our knowledge about the phenomena of pollutant diffusion and removal by means of forced ventilation devices.

Financing of the project started in november 1988, and the

experimental apparatus was fully operating already in spring 1990, after less than 18 months.

The CVC will be used to evaluate, under different testing procedures and ventilation strategies, ventilation efficiency and pollutant removal in the rooms. It will be employed to validate 2-D or 3-D computer models describing the fluid dynamics in a confined space. Moreover, this facility will be used to determine the ventilation frequency using non-conventional data elaboration procedures.

2. The Controlled Ventilation Chamber (CVC)

The Controlled Ventilation Chamber (see Fig. 1) is a small but full size room of 2.4 (height) x 2.4 x 3.0 m. The frame of the chamber is made of steel shapes. Its length (3.0 m) can be increased up to 4.2 m, and a moveable wall can divide the room in two communicating parts, in order to simulate contaminant diffusion from one room to another. One of the 3.2 x 2.4 m wall is made of acrylics, better known with its commercial name "plexiglass", in order to allow visualization of the air flow.

2.1 The ductwork

The ventilation system of the CVC includes a variable speed fan with flow rates ranging from 0 to 160 m^3/h (corresponding to about 10 ach), a ductwork connecting the fan to the CVC, equipped with ball valves, and four grilles for air inlet or outlet.

These grilles are located on the two smaller opposite walls, one close to the ceiling, the other to the ground. On each of them a grille is mounted on which individually orientable vertical fins are located. Width of the grilles is 2.0 m, slightly less than that of the wall, and their height is 0.25 m. Air can be introduced and extracted into or out of the CVC from each of the grilles, realizing different ventilation strategies. At the moment no thermal treatment of the air is provided for.

2.2 Instrumentation

Instrumentation (see Fig. 2) includes:
- an air flow meter
- six hot film anemometers
- a two-cell infrared gas analyzer for simultaneous measurement of N_2O and SF_6 concentrations
- a "home-made" automatic pneumatic scanner
- an automatic acquisition system
- a barometer
- a thermometer
- a differential pressure meter

The air flow meter is mounted on the intake duct, upstream of the fan when the CVC is overpressurized, downstream of the fan in the other case. It is based on the hot film anemometry principle, and has an accuracy of 2% of the reading + 0.2% of full scale.

Air velocity measurements are realized by means of six high precision, low-velocity hot film anemometers, providing the modulus of air speed. They are mounted on a moveable structure whose position may be changed from the outside. This structure is also used to carry the tubes for air sampling to the gas analyzer. Their accuracy is 1 % of full scale.

The two-cell infrared gas analyzer can provide simultaneous reading of the concentration of two tracer gases (SF_6 and N_2O) from 0 to 200 ppm with an accuracy of 2 % full scale. The analyzer is equipped with special filters to avoid the influence of water vapour variations on the measured value. The outfit of the ventilation laboratory includes pure oxygen protoxide, sulphur hexafluoride, pure nitrogen to test the zero of the instrument and two mixtures of N_2O-nitrogen and SF_6-nitrogen to be used as references.

Three supplementary manual instruments are also part of the CVC experimental apparatus: a barometer and a thermometer, needed to correct for air pressure and temperature variations in measuring the air volume flow rate, and a differential pressure meter, with an accuracy of 1 Pa.

2.3 Control and acquisition

Automatic scanning of channels through which air is sampled and introduced into the infrared analyzer has been built in the lab using a PC both for the control of the pneumatic scanner and for the data acquisition and elaboration. The schematic of the Data Acquisition and Control System is provided in fig. 3.

The control section and the acquisition section are connected to the PC filling the eight-line capacity of the BUS. The control section consists in an I/O interface, a high voltage decoupling device, a power section, and by six electrovalves. The acquisition section consists in an I/O interface, and A/D converters of the signal from the transducers (flow rate, velocities and concentrations).

The schematic of the pneumatic scanner is shown in Fig. 4.

An OUT instruction from the PC opens valve 1 and 2, while the two-way valve 7 lets the air stream sampled through channel 1 to reach the analyser, and the three-way valve 8 "prepares" channel 2 filling it with air sucked by pump 2. As soon as the measurement in channel 1 is completed, valve 1 is closed and valve 3 is opened, and the two three-way valves 7 and 8 reverse their operation. In this way the air stream through channel 2 is admitted to the analyser, while channel 3 is prepared. And so on.

3. Potential uses of the CVC

The CVC will be used to test experimental techniques for the measurement of ventilation rates in buildings, and for the determination of ventilation efficiency and pollutant removal efficiency under different ventilation strategies. It will also be employed to study contaminant diffusion between rooms and within a single room, and to validate 2-D and 3-D fluid dynamics codes. Another possibility will be the test of Demand Controlled Ventilation Systems, i e, those ventilation systems in which the air flow rate is adjusted according to the level of a suitable contaminant chosen as an indicator of indoor air quality (e g, carbon dioxide, water vapour, etc.).

3.1 Measurement of ventilation frequency with novel experimental techniques

The equation of continuity, written for a tracer gas within a confined space of volume V, under perfect mixing hypothesis (i e, uniform concentration), yields:

$$V \cdot dC(t)/dt = \dot{V}(t) \cdot [C_b(t) - C(t)] + \dot{V}_g(t) \qquad (1)$$

Solution of Eq. 1 when both volume air flow V(t) and V_g are a function of time may be difficult. Therefore, usual experimental techniques adopt procedures aiming at the simplification of Eq. 1. First of all, they all adopt tracer gases whowe concentration in the outdoor air may be assumed equal to zero ($C_b = 0$). Moreover, special modes of injection of the tracer gas are adopted to further simplify the solution of Eq. 1. According to such modes, these methods belong to one of the three following categories:

1. Decay method ($\dot{V}_g = 0$)
2. Constant concentration method ($dC/dt = 0$)
3. Constant flow method ($\dot{V}_g$ = constant)

The first method, although requiring a very simple apparatus, does not allow accurate evaluations of air exchange rates when this varies with time. The second method is the most accurate, but requires a very expensive apparatus in order to adjust the tracer gas flow rate in such a way that the concentration keeps constant. Finally, the third method has the same limitations of the first one, while requiring large amounts of tracer gas.

For the aforementioned reasons, there may be some interest in developing simple experimental techniques which yet allow the accurate determination of variable frequency of air change. The idea is to adopt sophisticated numerical techniques to solve Eq. 1, while reducing the complexity of the experimental procedure. A numerical technique which can be conveniently adopted to solve Eq. 1 is the so-called "black-box identification" technique. In fact, Eq. 1 may be rewritten in a time discrete form (δ = time step) by means of an ARMA model as follows:

$$C(t) = \sum_{1}^{m} a_i \cdot C(t - i\cdot\delta) + \sum_{0}^{m} b_i \cdot \dot{V}_g(t - i\cdot\delta) \qquad (2)$$

Eq. 2 represents the diffusion of a contaminant within a confined space. The model order m is representative of the complexity of the real system (i e, the tracer gas in the air). A model order equal to 1 corresponds to a lumped parameters system, i e, in our case, to a uniform concentration situation. Whether the real system exhibits a strong zonization, the model order will correspond to the number of interconnected zones.

For a first order model (m = 1) and no tracer gas injection (V_g = 0), Eq. 2 reduces to:

$$C(t) = a_1 \cdot C(t - \delta) \qquad (3)$$

where coefficient a_1 is named the "direct link".

In this case, Eq. 1 allows a simple analytical solution, i e:

$$C(t) = C(0) \cdot \exp(-t/\tau) \qquad (4)$$

or

$$C(t) = C(0) \cdot \exp(-t \cdot n) \qquad (4')$$

Equalizing Eqs. 3 and 4 at time $t = \delta$ one gets:

$$a_1 = \exp(-\delta/\tau)$$

and

$$\tau = -\delta/\ln(a_1) \qquad (5)$$

or

$$n = 1/\tau = -\ln(a_1)/\delta \qquad (6)$$

It can be shown that Eq. 6 stands also for more complex situations ($m > 1$, and $V_g \neq 0$), provided that the main time constant of the system is much larger than the other ones. Therefore, under the hypothesis of quasi-perfect mixing (i e, quasi-uniform concentration), knowledge of direct link a_1 may lead to determine the number of air changes.

Coefficients $a_1 \ldots a_m$ and $b_0 \ldots b_m$ of Eq. 2 may be determined using a black-box identification approach, e g, by means of SIMIDE, an extended least squares method which has already been used for the identification and simulation of dynamic thermal systems with very satisfactory results (Calì et al., 1983).

The procedure which has just been described will enable to determine in a discrete form the time series of the ventilation frequency, provided the time series of tracer gas flow rate is known and concentrations are measured.

3.2 Air quality measurements

Measurements described in the previous paragraph refer to a situation where quasi-perfect mixing of a tracer gas occurs.

However, there are many situations when the main interest is focused on the pollutant removal efficiency of a ventilation system. In these cases, the hypothesis of uniform mixing are often no longer valid, and, on the opposite, the pollutant concentration distribution within the space and from room-to-room has to be investigated.

Therefore, the CVC has been equipped with the six-channel pneumatic scanner, which drives the sampled air from six different levels to the gas analyzer. The vertical rod on which the air sampling ducts are mounted may be moved around the room using appropriate displacement systems. An automatically driven mechanism is provided for and will be soon completed for the purpose.

In order to complete the information derived from pollutant concentrations, the CVC has been equipped with six hot film anemometers, located on the same vertical rod used for the air sampling ducts.

4. Preliminary results

A calibration campaign of the CVC has started a few weeks ago. The intent is to verify the reliability of the experimental apparatus under different conditions. At first, the conventional decay method has been tested with overpressurized CVC.

Results are summarized in Fig. 5 and 6. Fig. 5 shows a comparison between the theoretical (perfect mixing) decay of concentration calculated from the values of volume flow rate measured by the flow meter placed on the inlet duct (solid lines) and the actual concentration data (symbols). Fig. 6 shows the time outline of the percent error, i e, the difference between the theoretical and measured values referred to the theoretical value.

From both figures it appears clear that the quality of results is rather good for $n = 1.0$ and $n = 2.0\ h^{-1}$, while the initial estimate of airchanges is rather poor for $n = 0.5\ h^{-1}$. In all cases, the error reduces with time. It ranges from -33 % (at t = 15') to -2 % (at t = 105') for $n = 0.5\ h^{-1}$, from -8% (at t = 15') to almost zero (at t = 120'), from -3 % (at t = 15') to + 3% (at t = 60').

A second campaign was performed in order to test the CVC as regards the measurement of ventilation efficiency, defined as:

$$\epsilon_j = C_e/C_j \qquad (7)$$

Three balanced ventilation strategies, illustrated in Fig. 7, have been tested.

In all cases the nominal ventilation frequency was 3 ach, the starting concentration of the tracer gas was uniform and equal to 200 ppm, and no tracer gas was injected during the measurement ($\dot{V}_g = 0$). Figures 8 to 10 show the time trend of ventilation efficiency at different heights above the floor in the middle of the room for the three cases.

Strategy A (Fig. 8) shows a good ventilation efficiency ($\epsilon > 1$) from 0 to 80 cm above the floor, but at higher levels ϵ is always less than 1. There is also a clear indication of a "diverging" air quality situation.

In strategy B (Fig. 9) the situation is generally better, with $\epsilon > 1$ at all levels, but with a marked improvement below 1.2 m. After half an hour (1.5 times the nominal time constant) perfect mixing conditions are achieved again.

Strategy C (Fig. 10) shows an interesting and unexpected finding: concentration remains uniform (perfect mixing) all over the CVC, and equals the value at extraction.

Figure 11 allows a good summing up of the three strategies, providing the log concentration decay together with the theoretical curve (straight line). While case C is very close to the theoretical curve, case A shows a marked upward concavity, an evidence of poor performance of the system, and case B shows a marked downward concavity, an evidence of good performance of the system.

A clear indication of the performance of the three systems is the volume of tracer gas extracted by the system during time t:

$$V_g = \int_0^t \dot{V}_g \cdot C_e \, dt$$

The higher the value of V_g, the better is the performance of the system. The measurements confirm the above conclusions, yielding:

strategy	V_g (m^3)
A	0.001917
B	0.002700
C	0.002375

5. Acknowledgements

This research was fully sponsored by the Italian National Research Council (CNR) under a grant provided by the Progetto Finalizzato Energetica (Finalized Energy Project). The authors wish to thank A. Carcuro for his skillful assembling of the CVC, D. Di Bello for realizing the automatic scanner, V. Tramutoli for assistance in preparing the interface software, and G.B. Vaccaro for the execution of part of the measurements.

6. References

Calì, M., Fracastoro, G.V., Greco, C., Marchis, V., Masoero, M., Vannelli, G., *Identification methods applied to building thermal behaviour*, Int. Journal of Modelling & Simulation, Vol. 3, n. 4, 1983.

Sandberg, M., *Ventilation efficiency as a guide to design*, ASHRAE Transactions 1983, Vol. 89.

Skåret, E., *Ventilation by displacement - characterization and design implications*, Ventilation '85, Goodfellow, H.D. (Ed.). Amsterdam, Elsevier, 1986.

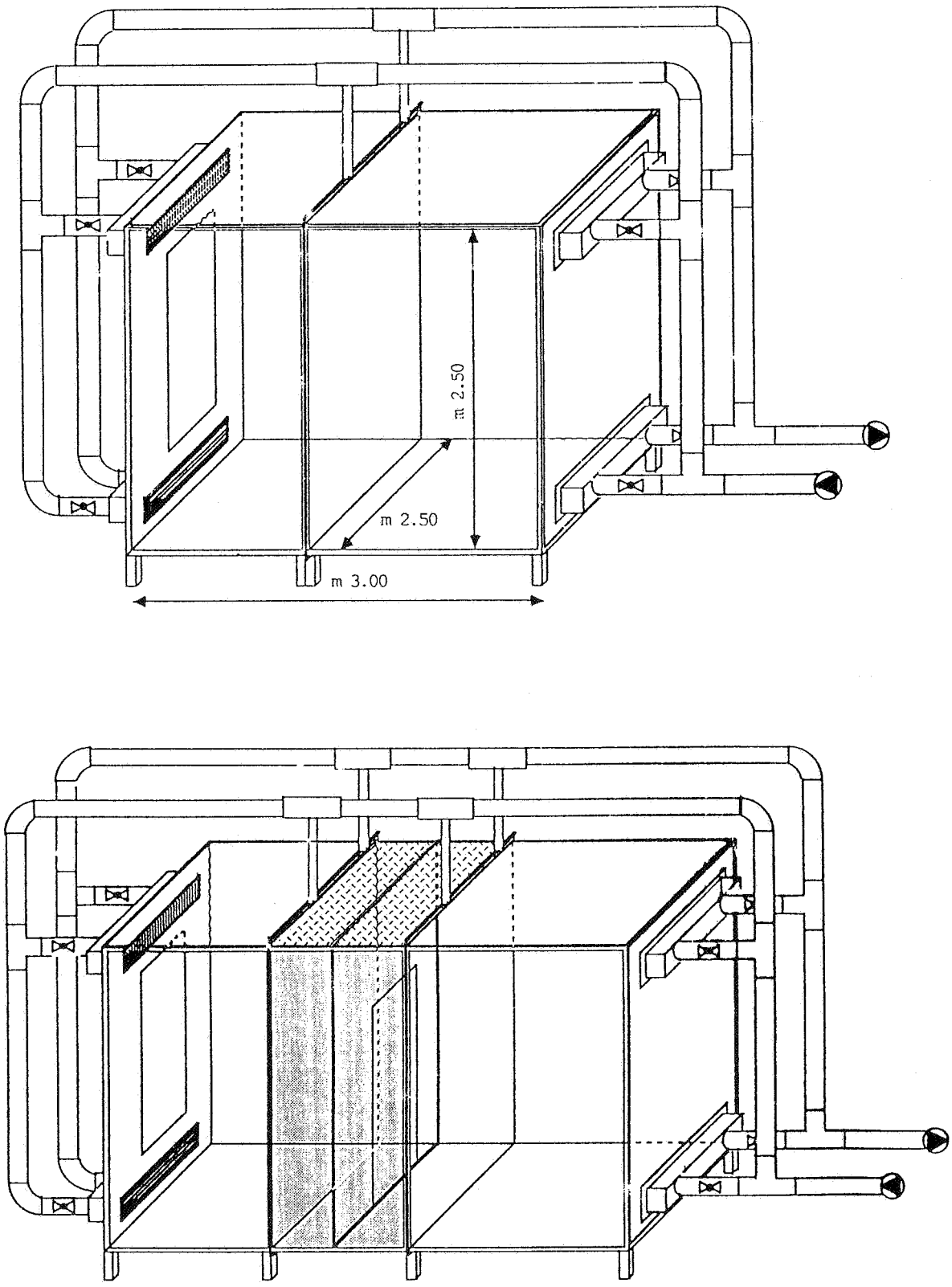

Fig. 1 - The Controlled Ventilation Chamber (CVC)

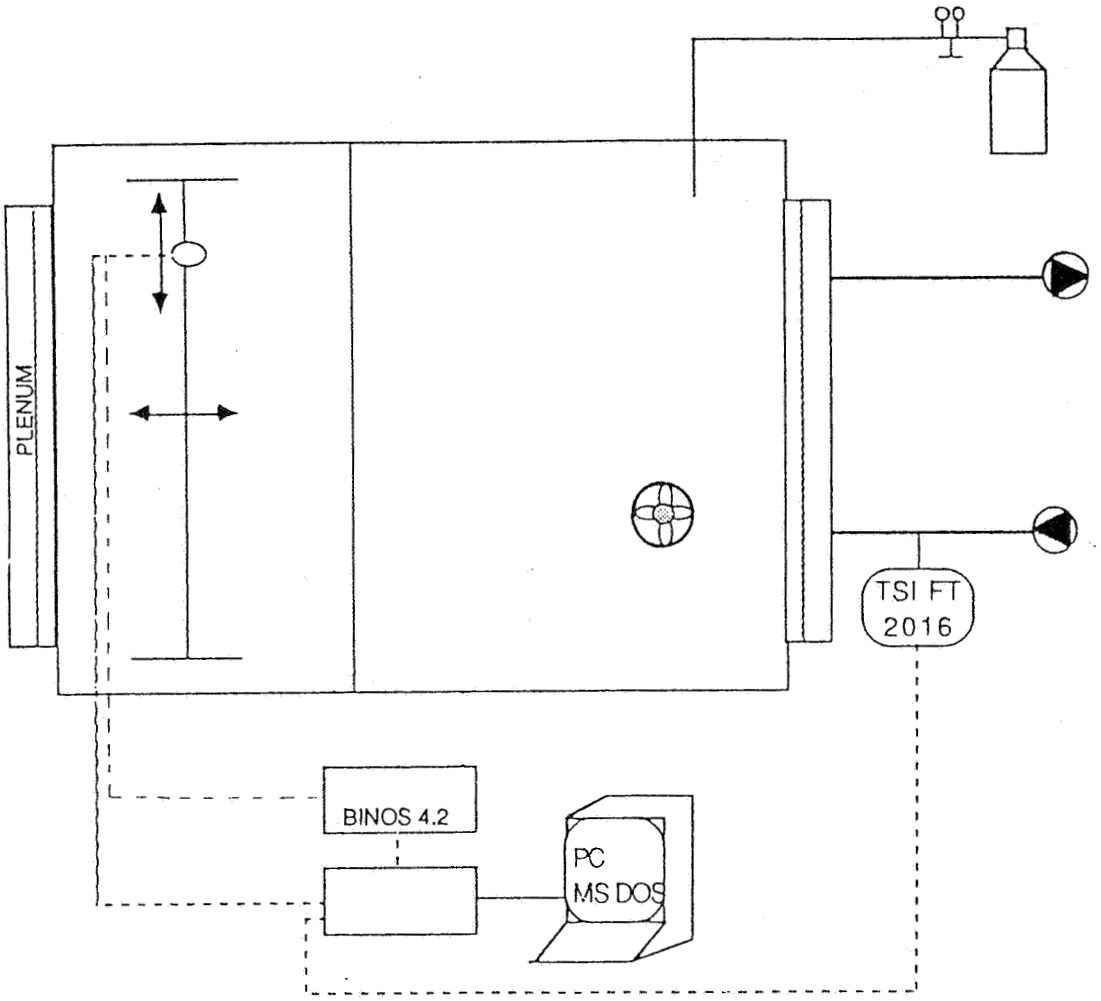

Fig. 2 - Layout of the instrumentation of the CVC

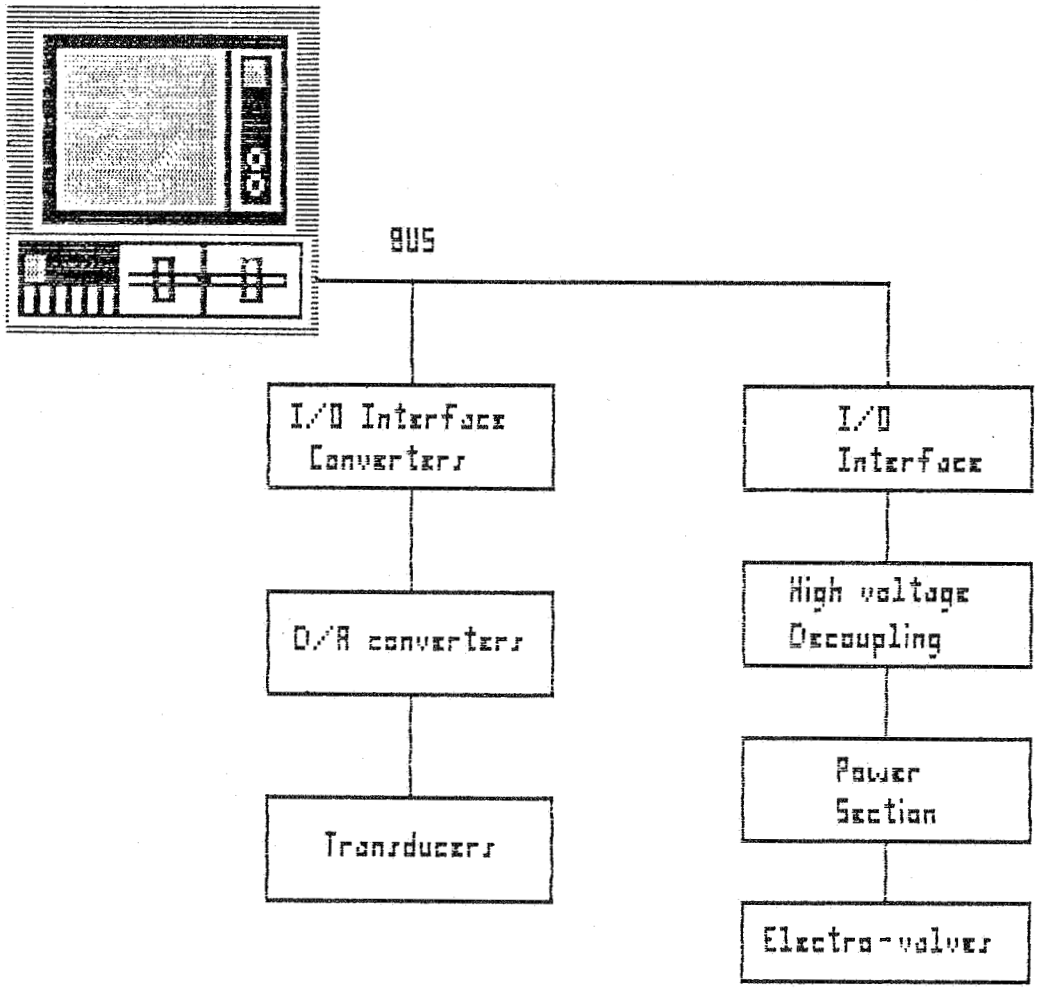

Fig. 3 - The Data Acquisition and Scanner Control System

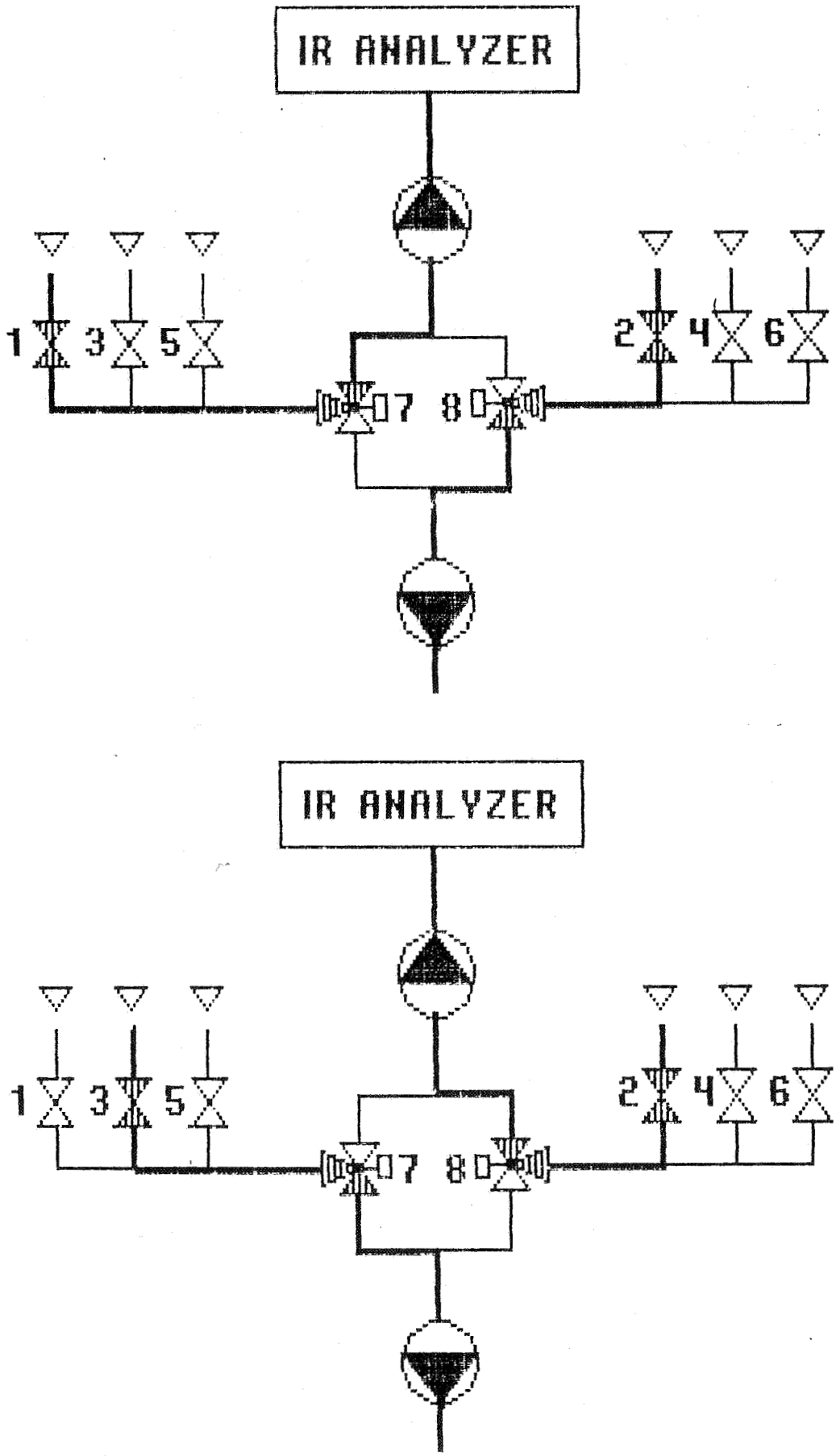

Fig. 4 - The Automatic Pneumatic Scanner

Fig. 5 Measured and estimated N20 concentration decay

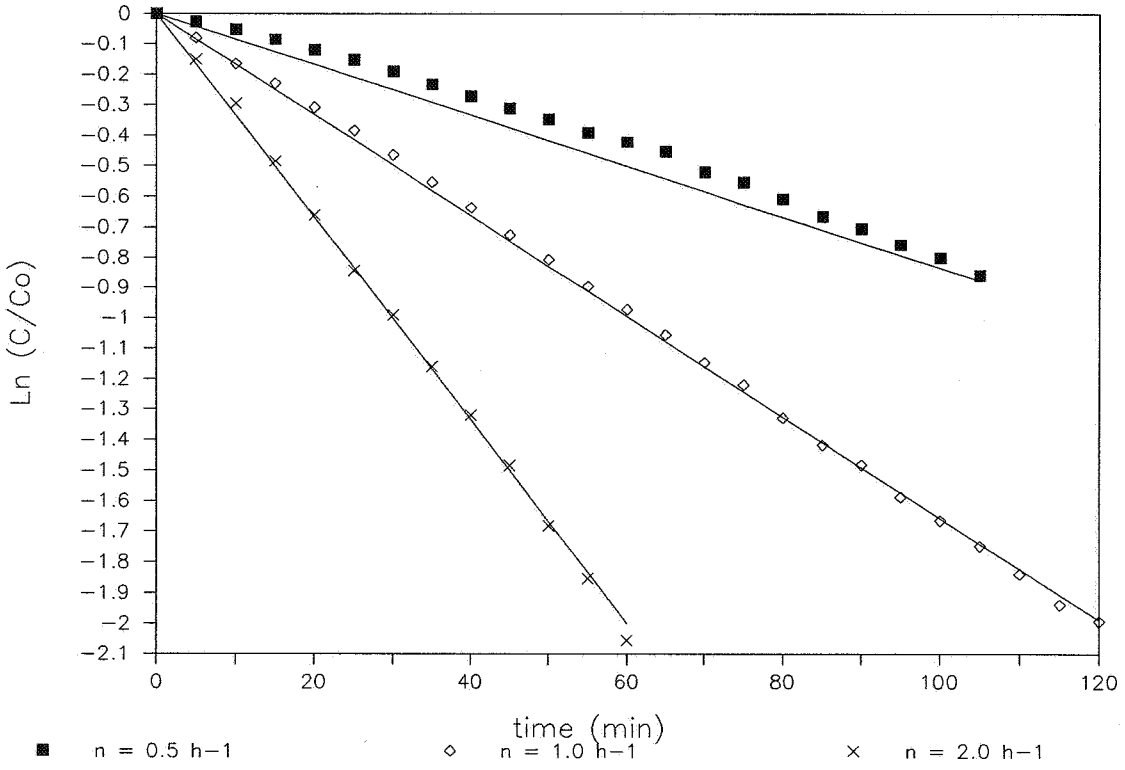

Fig. 6 Percent error vs. time

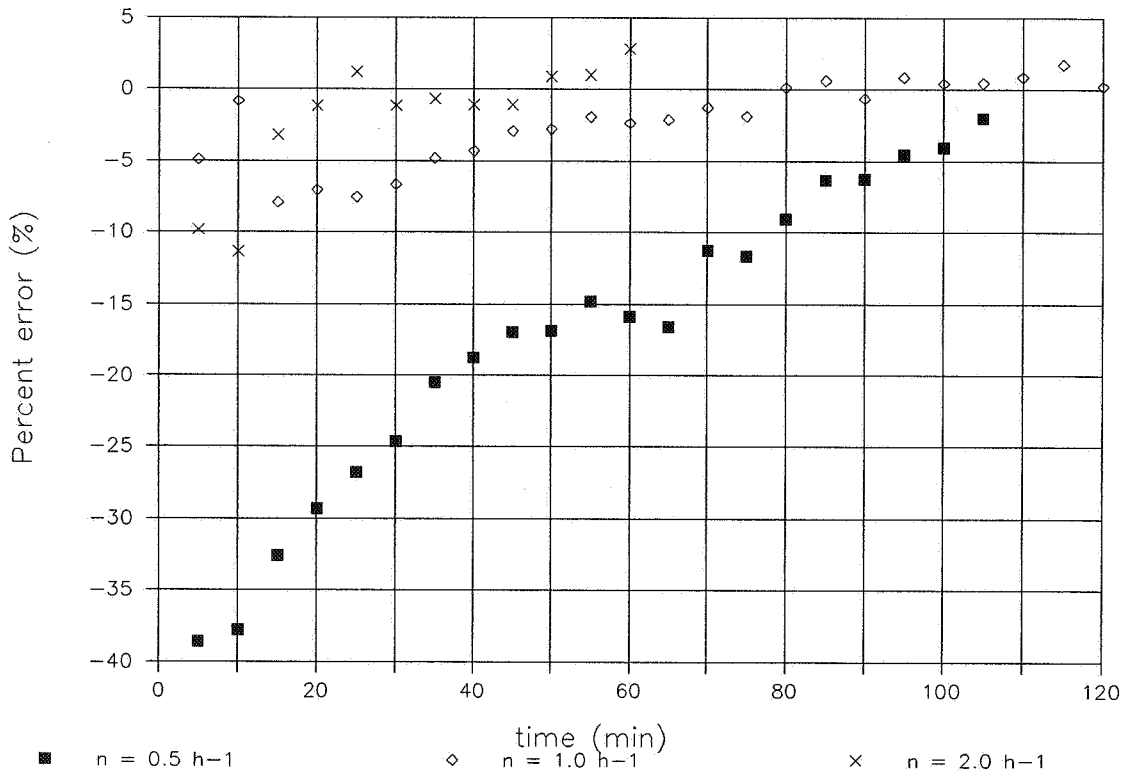

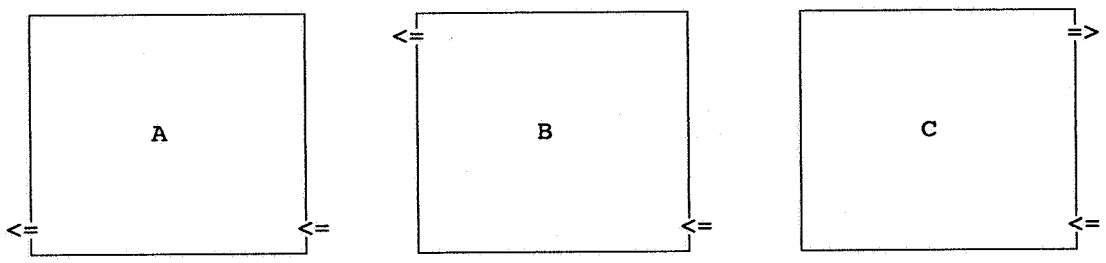

Fig. 7 - Ventilation strategies.

Fig. 8 Ventilation efficiency vs. time

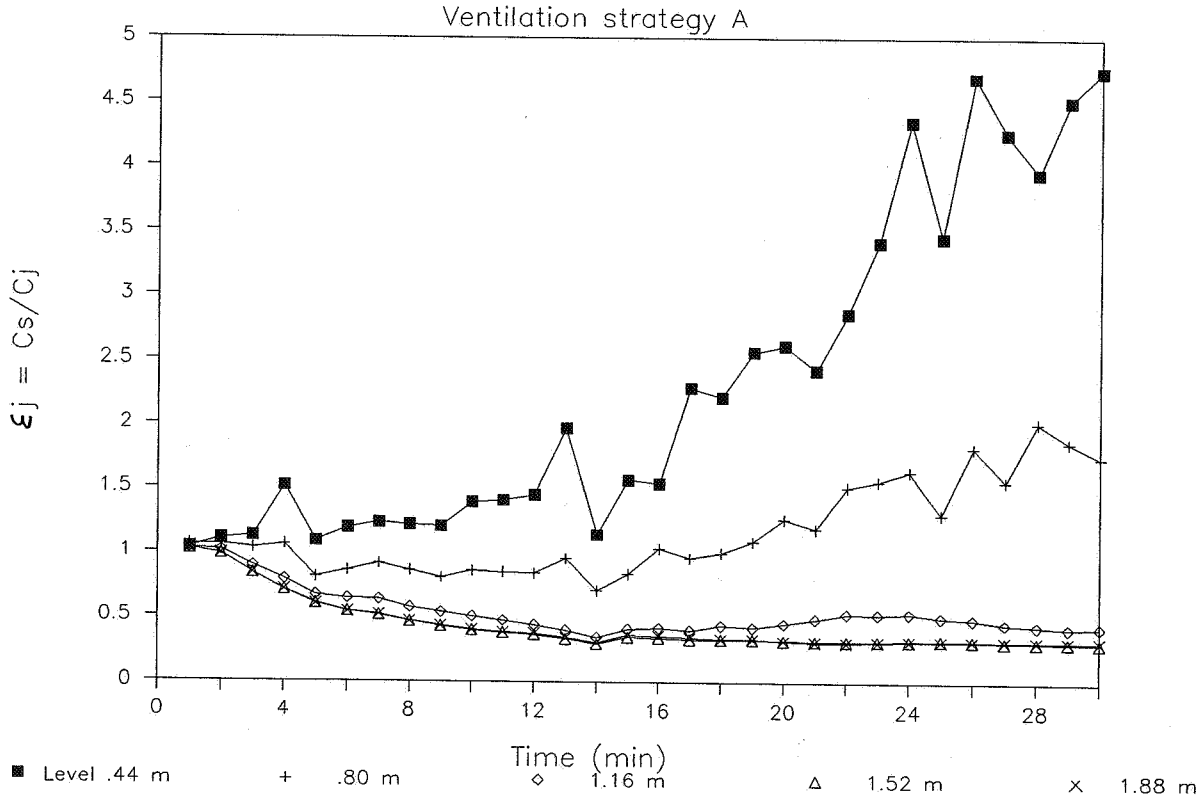

Fig. 9 Ventilation efficiency vs. time

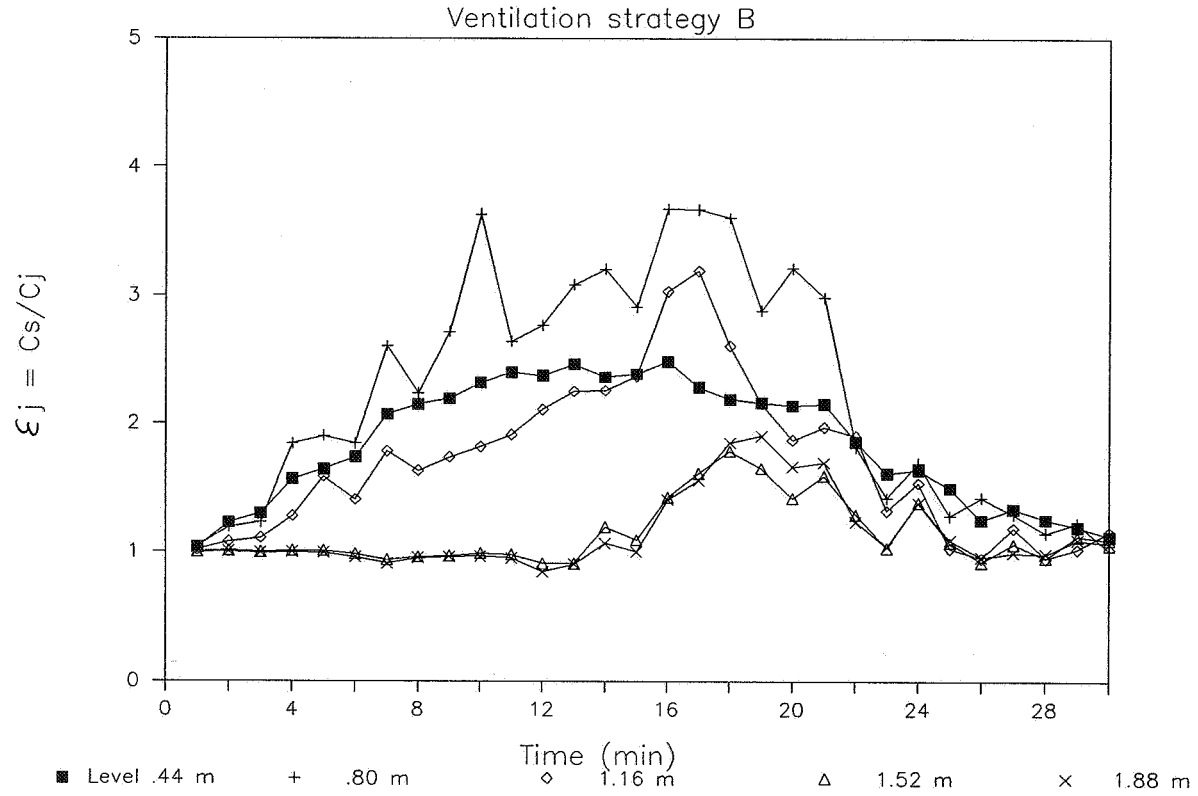

Fig. 10 Ventilation efficiency vs. time

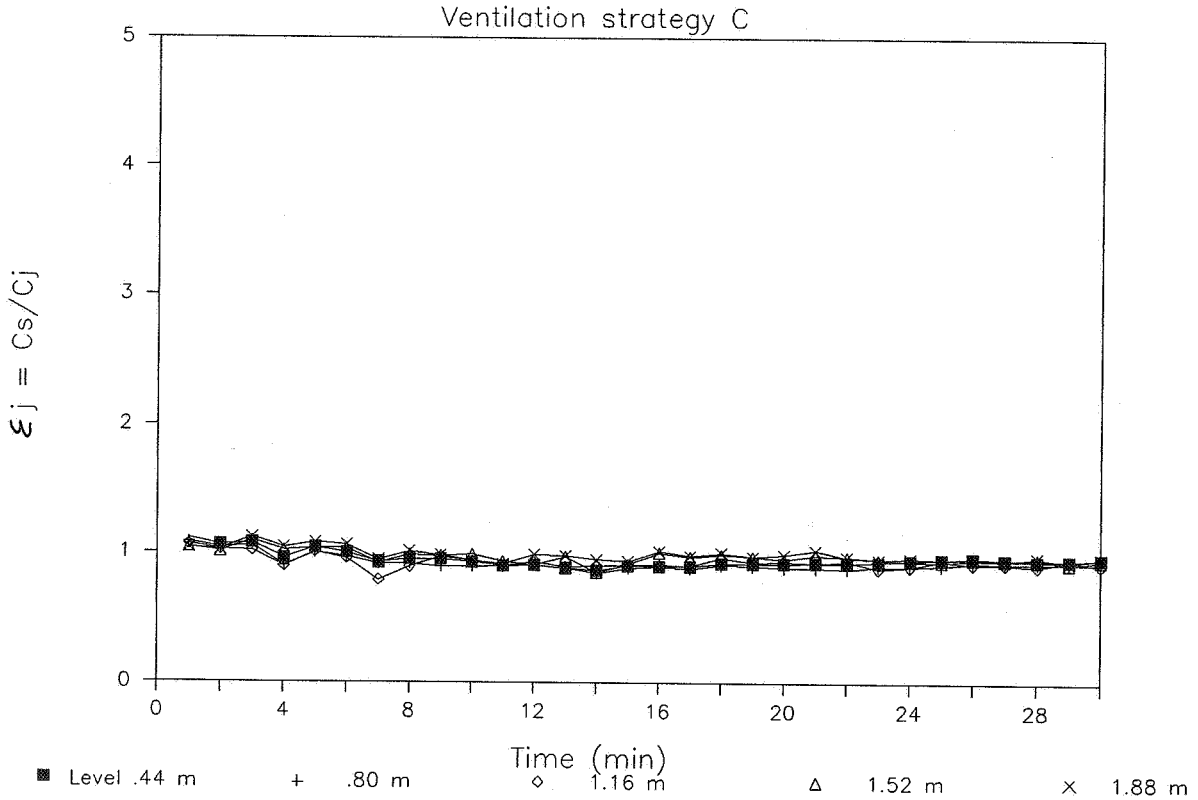

Fig. 11 Concentration in exhaust air terminal

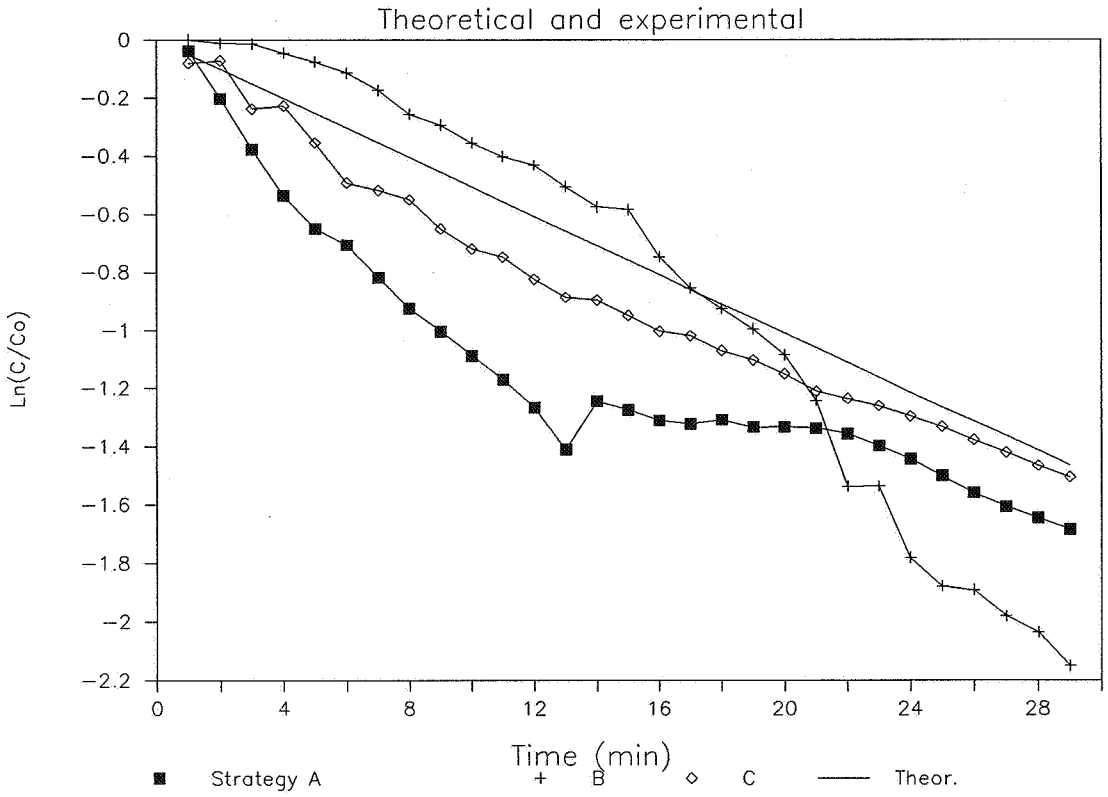

VENTILATION SYSTEM PERFORMANCE

11th AIVC Conference, Belgirate, Italy
18 - 21 September 1990

Paper 19

Ventilation Systems and Removal of Particles

R. Schwab; E. Mayer

Fraunhofer-Institut für Bauphysik
(Leiter: Prof. Dr. Dr. h.c. Karl A. Gertis)
Postfach 1180
8150 Holzkirchen
Germany

1. Introduction

As part of the IEA Research Program Annex 18 "Demand Controlled Ventilation Systems" various ventilation systems were examined in a test room. During research, in addition to thermal comfort issues, removal of particles was of importance. In order to assess ventilation systems, besides using pressure - volume current graphs, the air exchange rate was frequently applied as a criterion. The air exchange rate is, however, defined only for gaseous components. The question arose as to how far the air exchange rate is suitable for assessment of transport of particles or whether a more suitable identification factor can be found.

2. Measurements and Results

To solve the problem different ventilation systems were subsequently installed in the wall of a testing room. Cigarette smoke was produced and distributed homogeneously throughout the room. After switching on the ventilation system to be tested a measurement of the concentration of particles of the size 1µm followed using a particle counter for a period of two hours. The result was an exponential reduction of concentration of particles similar to the tracer gas decay method for assertaining the air exchange rate. A typical measurement of particle concentration is shown in figure 1.

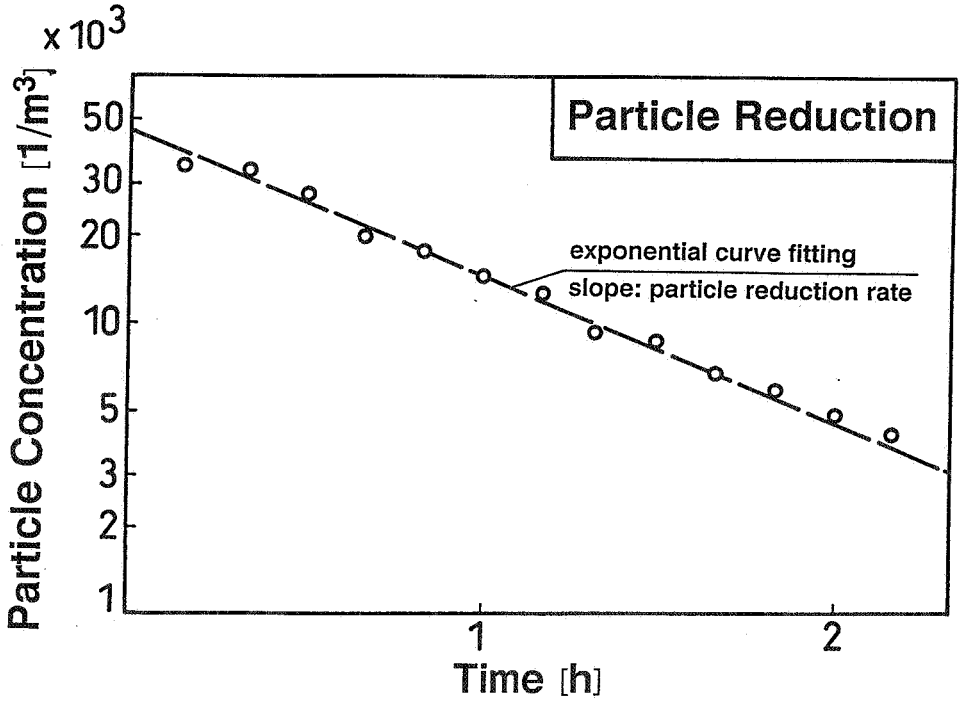

Fig. 1: Typical decay of concentration of particles (size 1µm) after switching on the ventilation system. Semi-logarithmic presentation.

The concentration decay is plotted logarithmically against the time axis. A straight line graph is the result, which depicts the reduction of particles in the room. A particle reduction rate analogous to the

air exchange rate of the tracer gas decay method was defined.

$$P_i(t) = P_0 \cdot e^{-p_i \cdot t} \quad (1)$$

or $$\ln(P_i(t)) = \ln(P_0) - p_i \cdot t \quad (2)$$

respectively $$p_i = \frac{\ln(P_0) - \ln(P_i(t))}{t} \quad (3)$$

P_i Concentration of particles of the size i [$1/m^3$]

P_0 Concentration of particles at the time t = 0 [$1/m^3$]

p_i Particle reduction rate for particles of the size i [h^{-1}]

This definition of a particle reduction rate p_i enabled us to work out a simple method of comparing the removal of particles by ventilation systems.

Comparison of the particle reduction rate with the air exchange rate showed differences between air exchange (gas) and removal of particles. The results for each ventilation system are presented in table 1.

Ventilation System	Particle Reduction Rate p_1 [h^{-1}]	Air Exchange Rate n [h^{-1}]	Differences [%]
VS 1	1.7	1.3	+30
VS 2	1.3	1.4	-10
VS 3	1.8	1.9	-10
VS 4	3.6	2.9	+20
VS 5	2.4	2.1	+10
VS 6	4.0	2.8	+40
VS 7	3.3	2.6	+30

Tab. 1: Comparison of particle reduction rate against air exchange rate for seven tested ventilation systems.

It is shown that the ventilation systems numbers 1, 4, 5, 6 and 7 removed particles more effectively than gaseous components. The ventilation systems 2 and 3 showed the opposite, giving a better exchange of gaseous components.

3. Conclusions

Test results lead to the following conclusions. The air exchange rate alone does not suffice to describe the removal of particles by ventilation systems. The definition of a particle reduction rate provides a feasible method for comparing ventilation systems with regard to the removal of particles. When using this method it is necessary to take into account that the particle reduction rates are defined for particles of a certain size and depend on the type of the particles. Particles in the air intake are either to be avoided or suitably taken into consideration.

4. References

[1] Schwab, R.; Mayer, E.: Fortschrittliche Systeme für die Wohnungslüftung. Teil A: Raumklimatische Laboruntersuchungen. Bericht RB-10/1989 des Fraunhofer-Instituts für Bauphysik, Holzkirchen (1989).

VENTILATION SYSTEM PERFORMANCE

11th AIVC Conference, Belgirate, Italy
18-21 September, 1990

Paper 20

BUILDING PERFORMANCE AND VENTILATION SYSTEM

Walter Braun

Geilinger Ltd
CH-8401 Winterthur
Switzerland

Summary

With a dynamical model, the thermal behavior of a single office room is simulated. The model includes among other things the behavior of occupants, the heat production of machines and lights, the heat flux into masses, real weather data (hourly observations) and different HVAC and control systems. The computer program calculates monthly and yearly energy consumption and a statistical distribution of the room air temperature. It can also be used to investigate the time evolution of physical processes for short periods.

A parametric study shows how the U-value of the facade and the building performance influence the energy consumption. Climatic conditions and types of HVAC-systems are also varied.

For office buildings with an envelope of a good quality, the total energy consumption is predominantly determined by the electrical supply power of the machines (computers, copying machines, etc). Other factors may be important, as for example the type and the control strategy of the HVAC-system. The building performance and the ventilation system are strongly related to the comfort of the occupants.

1. Introduction

The performance of a building is governed by the user behavior and by the features of the building. *Comfort and energy consumption* are important characteristics of the building performance. Their interdependence may be investigated by parametric simulation studies.

In this paper results are presented which apply to modern office buildings.

2. A Dynamical Model for Room Simulations

The dynamical model used in this study is named HIT-KOMFORT [1]. HIT is the acronym of High Insulation Technology, which means a building concept [2] based on low-U-value windows and a comfort ventilation system [3]. The model has been developped on behalf of the experience, that the *performance* of such a building is *totally different* compared to a conventional type.

HIT-KOMFORT is a model for the dynamical simulation of the thermal and energetical performance of a single office room. The behavior of the occupants, all the relevant heat sources and sinks and the thermal masses are included. Different HVAC-systems can be used.

The computer program produces three types of results:

- **energy consumption**
  Included are among other things the energy consumption for lights, machines, ventilators, etc. Heat recuperation is also simulated.
  The energy consumption is directly related to the operation costs and to questions about environmental protection.
- **energy balance**
  Energy balance of the room, e.g.: transmission losses, losses due to crack flow, sun gain, heat gain of lights and machines and the effects of the HVAC-system.
  These are the primary parameters in the course of the computations. They can also be a help to understand the physical and technical processes.
- **temperatures**
  Temperature statistics (period: one year) and evolution in time (some days).

The physical processes (visual and infrared radiation, convection at the surfaces, heat conduction into the thermal masses, heat sources and sinks) were transformed into an electrical network with 18 resistances and 14 capacities. A time step of 6 Minutes is used in order to simulate also the thermal discharge of the room air.

Different sets of hourly weather data, each for the period of one year, can be used. The program needs the outdoor temperature and the solar radiation. The outdoor temperature influences the transmission through the fassade und the energy amount for the pre-conditioning of the supply air. The transmitted solar radiation effects as heat load and controls the operation of the sun protection and the lights.

In the context of modern HVAC-systems, the terms "cooling" and "heating" must carefully be defined: it has to be distinguished between the pre-conditioning of the air (affects the energy consumption) and the energy input/output of the air to/from the room (energy balance). E.g.: In many office rooms excess heat is produced even in winter. The room may then be cooled (passiv cooling) by the ventilation system although the outdoor air has to be heated up.

The standard version of the computer program offers five different types of HVAC-systems, each of them with a realistically modelled control concept:

1. Natural ventilation
   - window opening at office time
   - radiator heating

2. Mechanical ventilation
   - all-air system
   - cold outdoor air is heated up to the prescribed supply air temperature
   - supply air can additionally be heated, if needed (controled by room air temperature)
   - two different air change rates controlled by the room air temperature
   - free cooling at night
   - system off, if $t_a > 22^{\circ}C$

3. Air condition
   as "mechanical ventilation", except:
   - outdoor air can be cooled to have the prescribed supply air temperature

4. Combined air-water-system
   - air system for room air quality, similar to "air condition", except: fixed air change rate
   - water system for energy transport, mainly cooling by ceiling-mounted radiators

5. Traditional HVAC-system
   as "air condition", but:
   - supply of heat energy by wall-mounted radiators

The model has been *validated* with measurements of real buildings. It is a tool for parametric studies (research and consulting) and for the interpretation of observations (research).

The results, which are presented in this paper, apply to an office room with the following features:

- floor surface: 23.2 m^2
- air volume: 64.9 m^3
- panel height: 0.9 m
- area of glazing: 4.4 m^2
- U-value panel: 0.3 W/m^2K
- U-value frame: 1.3 W/m^2K for HIT-windows
  2.0 W/m^2K for other types
- glazing: varied
- crack flow: varied
- no heat transfer to other rooms
- lights: 15 W/m^2 (below 500 lux)
- sun protection: exterior (above 10000 lux)
- occupants: 2, 70% of office time
- machines: varied, up to 50 W/m^2

- maximum heat load: 15 W/m^2 lights or sun
  5 W/m^2 occupants
  x W/m^2 machines
  total: up to 70 W/m^2
- HVAC-system: types 2 or 4
- efficiency of heat recovery: 0.6

3. Range of Energy Consumption

The energy consumption of buildings varies over a very large range. This is even true, if one concentrates on one specific type. In figure 1, the yearly total energy consumption for four different cases are given, demonstrating this fact. It leads to the urgent question about the reasons of the extreme variability and the possibilities to avoid excessive energy consumption. Therefore, the *relevance* of the different parameters and their *interdependence* has to be investigated.

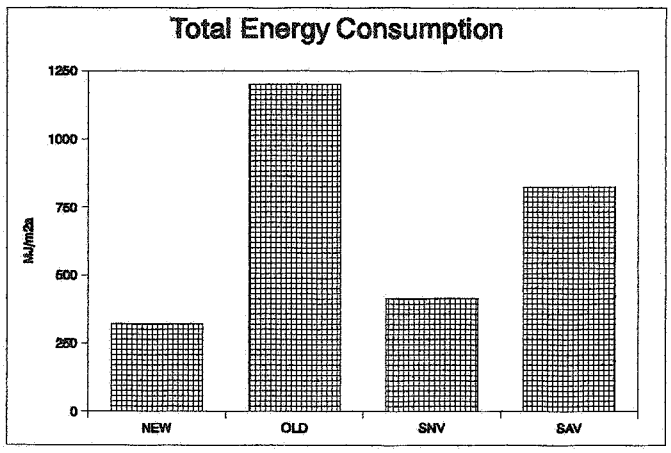

Figure 1. Yearly total energy consumption
NEW = HIT-part of an old office building in Winterthur, Switzerland, which was extended in 1988. (Conditions for the extension were not optimum.)
OLD = conventional part of this building. (Leaking window frames)
SNV = swiss nominal value, recommended by the Swiss Society of Engineers and Architects (SIA)
SAV = swiss average in 1988 (buildings with heavy deficiencies have been excluded)

A strongly dominating factor, which can not be influenced by the building designer, is the **energy consumption for machines**. If one assumes the electrical supply power of the computers, copying machines, etc, to be 50 W/m^2, they would already consume around 500 MJ/m^2a ! In figure 2 the total yearly energy consumption for four different situations is given as a function of the supply power. They arise from the

variation of two further parameters:

1. climate/weather data
   - Kloten 1983
     swiss midlands climate
     av. temp. = 9.4°C
     solar radiation = 4066 MJ/m^{2}a
   - Samedan 1985
     alpine climate
     av. temp. = 0.8°C
     solar radiation = 5245 MJ/m^{2}a
2. type of glazing
   - IV3 (tripple insulated glazing)
     U-value = 2.1 W/m^{2}K
     visual transmission rate = 74%
     crack flow = 0.37 ac/h
   - HIT window with film type 88
     U-value = 0.76 W/m^{2}K
     visual transmission rate = 65%
     crack flow: none

In all cases, the same HVAC-system and control strategy is adapted: it is the combined water-air-system (type 4) with a water temperature (ceiling radiators) of 19°C beeing active for room air temperatures above 23°C. The ventilation operates during office times at 1.5 air changes per hour.

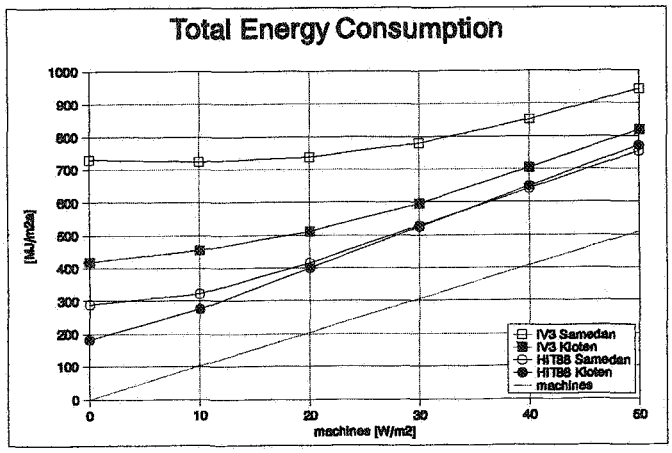

Figure 2. Yearly total energy consumption as a function of the electrical supply power of machines.

The results show the clear *predominance of the supply power* as a parameter in most of the cases. For well insulated fassades in a moderate climate, the functional relation is linear, whereas in the alpine climate some additional heat energy is needed, if the internal heat loads are low. But nevertheless, the climatic influence is nearly negligible. In the case of a conventional fassade, the internal heat loads loose of their dominance, but other factors become more relevant: these are the climate, but equally important the U-value of the fassade.

The air change rate of the mechanical ventilation is an other relevant factor. Assumed are an overall U-value

of 0.6 W/m^2K, absence of crack flow, electrical machine power of 10 W/m^2 and a mechanical ventilation system (type 2). The air change rates are kept constant within one case, but varied as a parameter in the range of 0.5 up to 6.5 ac/h. The energy consumption for the ventilation system is presented in figure 3, again for the climates of Samedan and Kloten. It is obvious that, depending on the maximum air change rate and climate, this *can be the dominating part* of the total energy consumption. With the above mentioned assumptions, the climate gains its importance by the temperature of the outdoor air, which has to be brought up to the supply air temperature. But if one considers a conventional fassade, the transmission losses would also have to be covered by the mechanical ventilation.

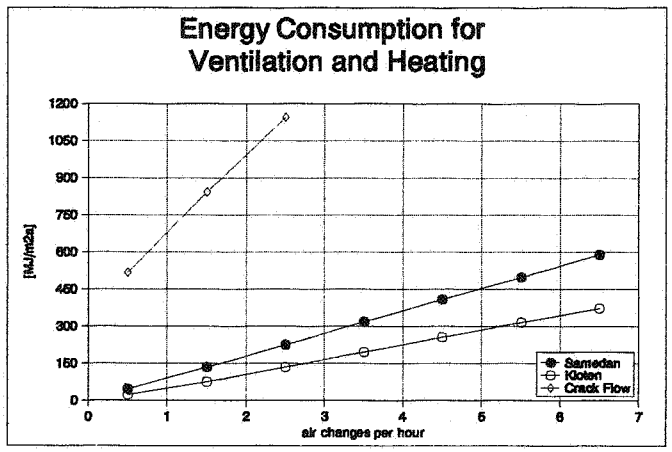

Figure 3.
Yearly energy consumption for ventilation and heating.

In buildings of poor quality, losses due to **crack flow** can accumulate to a considerable amount. As an example, a naturally ventilated room with double insulated glazing and leaking window frames is considered. The intensity of crack flow, measured in air changes of room volume per hour, is taken as parameter. In figure 3 (upper left part), one can see the energy consumption of the radiator heater for the swiss midland climate. Obviously, excessive heat amounts can be lost, if the fassade is not tight enough.

The gain of natural **light** depends on the area of the glazing and the visual transmission rate. For an office room without windows (interior space), the consumption of electricity for the lights amounts approximately 150 MJ/m^2a, whereas with normal double glazing (size as defined above), this is around 30 MJ/m^2a. Consequently, for low-energy office buildings, the lighting (natural and artificial) has also to be optimized with respect to the total energy consumption.

4. Fields of Operation of a Mechanical Ventilation System

With displacement ventilation a high comfort (good air quality, no draft) can be achieved. Nevertheless, there are operational limitations [5]: the supply air temperature must be some where between 18 and 20°C, the vertical temperature difference in the zone of occupancy should not exeed 3 K and the velocities should be kept as low as possible. Consequently, the energy transport capacity of this type of ventilation is limited. The field of operation of **all-air ventilation systems with displacement flow** in office rooms is therefore restricted to offices with moderate internal heat loads.

Here, a case is presented with HIT-windows and a mechanical ventilation (type 2) operating at 1.0 and 5.0 ac/h, respectively, controled by the room air temperature. Again, the electrical supply power of the machines is the independent parameter. The results are the annual mean room air temperature (figure 4, left scale) and the number of hours with $t_i > 27.5°C$ (figure 5, right scale). All the statistical numbers were sampled at office times only. The figure indicates, that the number of hours with "high temperatures" should be used as a criterion to limit the field of operation for the all-air mechanical ventilation. From this, an upper limit for the maximum heat load seems to be some where around 40 W/m^2, which, in this case, corresponds to an electrical supply power of the machines of 20 W/m^2.

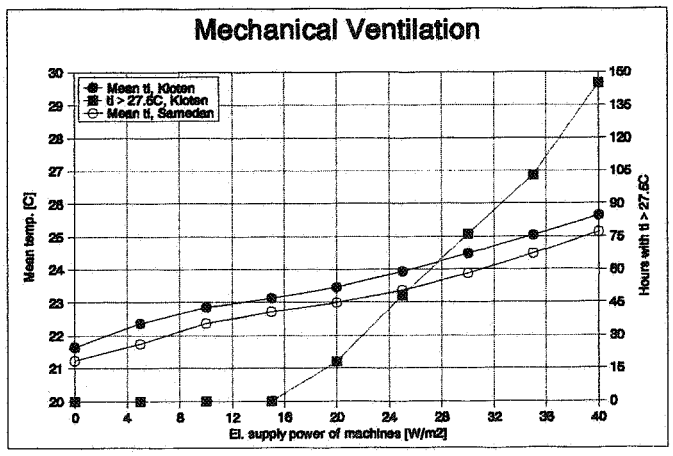

Figure 4. Annual mean room air temperature (left scale) and number of hours with "high" room air temperatures (right scale) as a function of the supply power of the machines.

5. Thermal Comfort and Energy Consumption

Many laboratory tests, field studies and numerical calculations (flow models) have already been carried out to investigate the comfort conditions of different ventilation systems, and further research will have to be done in future. The total of these investigations is rather comprehensive with respect to the observed parameters, but restricted to a very limited number of climatic conditions (winter case, summer case). Quite often, it is only possible to look at stationary situations.

The modell, which is presented in this paper, offers the opportunity to overcome these deficiencies, though at the expense of the variety of the parameters. In the following, the room air temperature is used as a simple indicator of the thermal comfort.

The **thermal performance** of a room lies some where between the two extremes:

- The temperature must remain constant during operation time. This means, that all heat gains or losses (due to internal heat loads, transmission, etc) must immediately be balanced out by the HVAC-system. The implication on the size and power of the system are well known!
- The temperature may vary over a wide range during a day or over the seasons. Disregarding the air quality, a simple heater may be sufficent.

Whereas in production processes, the first strategy might have to be applied, the temperature in an office roome normaly may vary to a certain degree. (Quite often, the customer defines to what extent variations will be accepted.)

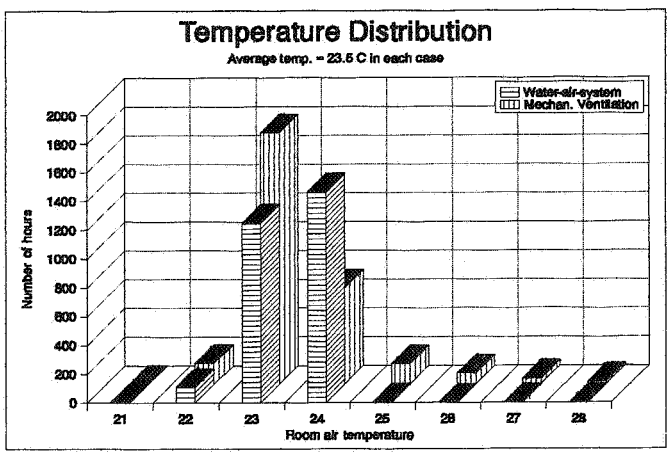

In figure 5, the temperature distributions of two cases can be compared for the above defined office room and a supply power of 20 W/m^2 (40 W/m^2 max. heat load). The HVAC-types 2 and 4, respectively, were given. The target values were chosen in such a way, that the average room air temperature over the

year (office times only) were 23.5°C in each case. The figure shows, that the temperature distribution for the all-air system extends over a wider range than for the combined water-air-system. This can also be expressed with the number of hours, when the temperature exceeds 24.5°C:

Type	Hours	Energy
2	274	426
4	4	405

The table reveals, that in the less comfortable case, more energy is consumed (total energy consumption in [MJ/m^{2}a]). This is due to the fact, that with heat loads as assumed here, the mechanical ventilation operates at its maximum air change rate nearly all the time. This causes comparatively high energy consumptions for ventilators and pre-conditioning of the outdoor air.

Finally, it is looked at a control parameter of the combined water-air-system (same room as above). The target cooling temperatue, at which the water system comes into operation, is varied from 22°C up to 26°C. (The model incorporates a linear valve-function with a spreading of 2 K).

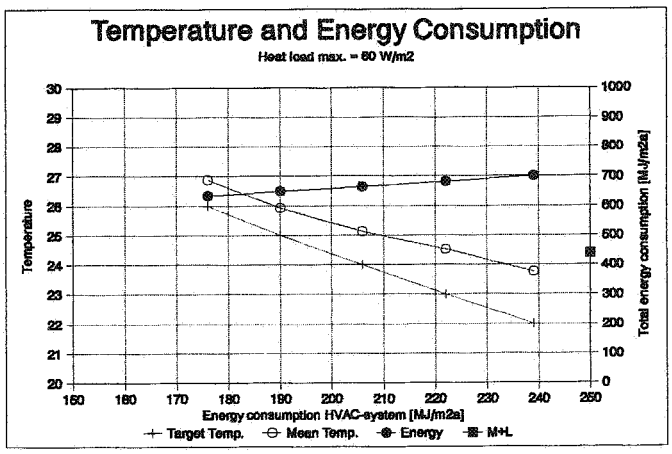

Figure 6.
Mean room air temperature and energy consumption as a function of the target cooling temperature.

The results are presented in figure 6, where four parameters are related to each other:

1. Target cooling temperature (left axis)
2. Energy consumption for HVAC-system (horizontal axis)
3. Mean room air temperature (left axis)
4. Total energy consumption (right axis)

With a target cooling temperature of 22°C, the HVAC-system consumes approximately 240 MJ/m^{2}a, the mean temperature is 23.8°C and the total energy consumption

is 700 MJ/m^2a. In all cases, the lights and machines consumed 440 MJ/m^2a. The essential insight is, that raising the target cooling temperature up to 26°C, the total energy amount is reduced by about 10%, though at the expence of an acceptable thermal comfort.

References

[1] BRAUN, W. et al.
Dynamische Gebäudesimulation in der Vorprojektphase
Koordinationsstelle für Wärmeschutz im Hochbau,
6. Seminar, ETH Zürich, Switzerland, 1990

[2] BRAUN, W.
A modern concept for office buildings: energy saving and good indoor climate are no longer contradictory.
10 th AIVC conference, Espoo, Finland, 1989

[3] MATHISEN, H.M.
Analysis and evaluation of displacement ventilation
Thesis NTH Trondheim, Norway, 1989

[4] Swiss Society of Engineers and Architects (SIA)
SIA-Empfehlung 380/1, Energie im Hochbau, 1988

[5] SANDBERG, M. and BLOMQVIST, C.
Displacement ventilation systems in office rooms
ASHREAE Transactions, vol 95, pt 2, 1989

VENTILATION SYSTEM PERFORMANCE

11th AIVC Conference, Belgirate, Italy
18-21 September, 1990

Paper 21

TWO-DIRECTIONAL AIR MOVEMENTS IN STAIRWELLS

R. Edwards,[1] C. Irwin[2]

1.
Dept of Building Engineering
UMIST
P O Box 88
Manchester M60 1QD, UK

2.
Willan Building Services
2 Brooklands Road
Sale, Cheshire M 33 3SS UK

Abstract

The predominant route for air movements between the floors of two-storey dwellings is via the stairwell. Such air movements are of significance in the assessment of building performance: for instance, it is possible that moisture could be transferred from ground floor areas to rooms on the first floor, resulting in an increase in condensation risk in such rooms. Several domestic heating schemes have been designed such that heating appliances are provided on the ground floor only; the upper floor relying on convective airflows for heating. If the ground floor to first floor airflow induce by such a system is too small, then the upstairs room will not attain the desired temperature, which in turn could lead to condensation problems, quite apart from the issue of occupant discomfort.

This paper summarises two case studies of air movement measurements performed by means of the UMIST PCS system, and analyses the data in terms of moisture migration and heat transfer.

Introduction

Condensation in dwellings has proved to be one of the biggest technical problems confronting the building professions during the 1980s. The three principle causes of condensation can be reasonably said to be inadequate heating, inadequate ventilation and occupant behaviour, and much research in the field has been concerned with the influence of these variables. Ventilation research in relation to condensation has generally been confined to measurements of whole house ventilation rates: air movements within dwellings have received comparatively little attention, mostly, it suspected by the authors, as a result of a lack of widespread access to suitable interzonal airflow measurement apparatus. Air movement within a building envelope can be a significant factor in the occurrence of condensation risk: for instance, it could be envisaged that water vapour could be transferred by air movement from areas of high moisture production within a dwelling (such as kitchens and bathrooms) to other rooms if insufficient consideration is given to building layout and distribution of ventilation.

This paper briefly describes two studies of airflows between the two floors of domestic properties. The first study centres upon an assessment of the efficiency of a partial heating scheme within a local authority property, in terms of the provision of sufficient heating to the first floor. The second study is concerned with the influence of a kitchen extract fan upon upstairs/downstairs airflows.

Experimental

i) Partially-heated house.

The test house is shown in figure 1. It is a local authority-owned house, and is a mid-terraced property. The design U-values of the walls and roof (0.27 and 0.35 $W/m^2/degC$ respectively) are significantly lower than those laid down by the Building Regulations in force at the time of construction (1984). All windows are single glazed. The house is heated by two balanced-flue gas heaters. The first is located in the lounge, and is rated at 0.76 to 2.35 kW output. The second heater is located in the hall. It is fitted with a heat exchanger for space heating, and is rated at 0.83 to 2.5 kW output. In order to supply background heating to the ground floor stores and WC, permanent grilles are provided give free passage of air from the lounge to the WC via the two stores. A wall fan, switched with room lighting, is installed in the WC so as to ensure a background level of air movement from the lounge to these spaces. The purpose of the house design is to heat the first floor by means of natural convection. To encourage air movement on the first floor, fanlights are positioned above all first floor doors, and, in addition, gaps have been deliberately left under the doors themselves. A fan pressurization test of the property revealed an air leakage rate of $1787m^3/hr$ at 50 Pascals positive pressure difference, which represents an air change rate of approximately 9.7ach.

During the tracer gas study, the following parameters were measured and recorded:

a) ventilation rates on the ground floor and first floor;

b) two-directional air movements between the two floors;

c) dry and wet bulb temperatures on both floors;

d) external dry and wet bulb temperatures;

e) wind speed and wind direction at a height of 10 metres.

ii) Low energy house

In this study, the test house is a three-bedroomed, end-terraced local authority property of low energy design: ground and first floor plans are shown in figure 2. The house was built in the early 1980s, and is of brick and block construction with a filled cavity. The design U-values of walls and roof are 0.24 and 0.27 $W/m^2/degC$ respectively .The windows are double glazed. The house is heated by means of a solid fuel heater, which supplies ducted warm air to both

floors. Careful consideration was given to the issues of air leakage and ventilation provision at the design stage. The design ventilation rate is set at 1.0ach: this has been achieved by paying careful attention to the quality of joints in the construction, by the use of draught stripping, and by the provision of draught lobbies. The kitchen is fitted with extract fan, whilst all windows are fitted with window head trickle ventilators. For this particular study, the trickle ventilators an internal doors were left open.

The parameters measured during the tracer gas study were to all intents and purposes the same as those measured during the partially heated house study.

iii) Details of tracer gas technique

Ventilation rates and inter-zonal air movement measurements were performed using the PCS equipment developed at UMIST.[1] Briefly, the equipment consists of an Analytical Instruments Model 505 portable electron capture gas chromatograph, modified for parallel column operation. The purpose of the modification is to increase the rate of data acquisition by utilising the "dead time" associated with the passage of air/tracer gas samples through a chromatographic separation columns.

In both studies, two tracer gases were used, namely Freon 12 and Freon 114. Prior to tracer gas injection, the two floors of the test house in question were isolated by means of a PVC sheet and adhesive tape. The tracer gases were injected, (Freon 12 into the ground floor, Freon 114 into the first floor: good mixing was achieved by means of oscillating fans. At the commencement of each test, the PVC sheet was removed.

Results and Discussion

i) Partial heating study.

The results are given in table 1. For this house, whole house ventilation rates, taken as the mean of the ground floor and first floor ventilation rates, varied between 0.38-0.91 air changes per hour for a range of windspeeds between 1.0 and 5.5 m/s. Variation in wind direction during the test period was very limited, but despite this, it is apparent that whole house ventilation rates are rather sensitive to changes in wind direction. As might reasonably be expected, wind directions perpendicular to the ridge axis are associated with the highest whole house ventilation rates for a given windspeed.

Air movements between ground and first floor with the heaters on lie in the range of 100 to 250 m^3/hr, whilst air movements in the opposite direction lie in the range of 60 to 100m^3/hr,

airflows lie in the range 130 to 178m³/hr: airflows in the opposite direction are of a similar order of magnitude. When the kitchen fan is switched on, however, the ground floor to first floor airflows are reduced to the range 10-30m³/hr. At windspeeds less than 2m/s, the use of the kitchen fan does not appear to have a pronounced effect upon first floor to ground floor airflows: above this value, however, increasing windspeed has the effect of reducing the airflow from first floor to ground floor. This is due to the increased cross-flow ventilation on the first floor.

The value of extract fans in the removal of water vapour at or close to the area of production is well established. Quite apart from reducing the vapour pressure in the zone in which the fan is located, the concomitant reduction in airflow to the first floor is of the order of 85%, which would result in a significant reduction in the amount of water vapour being allowed to migrate to rooms on the first floor such as bedrooms which are susceptible to condensation problems. It should be mentioned in passing that there is another benefit to the use of the ground floor extract fan namely that airflow (and hence migration of water vapour) into the roofspace is also significantly reduced.[3]

CONCLUSIONS

The two studies briefly described in this paper demonstrate the usefulness of multiple tracer gas techniques in the measurement of airflows between two floors of a dwelling. It should be acknowledged, however, that the division of a typical two floor house in two zones represents an approach to the measurement of airflows which may in many cases not be sufficiently sophisticated to yield data with sufficient detail. In such circumstances, the degree of subdivision, and hence the number of tracer gases used, should be increased.

REFERENCES

(1) C Irwin, R E Edwards, A T Howarth :
BSE&RT, vol 6, No 4, pp 146-152, 1985.

(2) I Brewerton:
"Low-cost full house heating in low energy housing":
Final report to BRECSU, 1987.

(3) R E Edwards, C Irwin :
Proceedings of the 6th AIVC Conference, Netherlands, 1985.

Test No.	Temp(Up) db °C	wb	Temp(Dn) db °C	wb	Temp(out) db °C	wb	Downstairs Vent Rate (ACH)	Upstairs Vent Rate (ACH)	Whole House Vent Rate (ACH)	Airflow Dn to Up (m^3/hr)	Airflow Up to Dn (m^3/hr)	Wind Speed (m/s)	Wind Direction	Comments
1	19	15	18	14	12	11	0.84	0.74	0.79	140	75	4	NW	All windows shut Htg on
2	19.5	15	19	15	12	10	0.80	0.98	0.89	130	100	3.5	W	W facing bed. window open
3	"	"	"	"	"	"	0.55	0.42	0.49	100	100	1	NW	All windows shut heating off
4	20	16	20	16	12	10	1.25	0.55	0.90	120	60	5	NW	-Ditto-
5	12	8	12	8	14	11	0.4	0.4	0.4	30	10	<1	SW	-Ditto- heating off
6	14	9	15	10	10	8	0.62	0.38	0.5	125	110	1	NW	-Ditto- heating on
7	15	10	17	12	10	8	0.71	0.51	0.61	100	95	2	NW	-Ditto-
8	17	10	17	10	11	9	1.00	0.75	0.88	150	100	4	NW	-Ditto-
9	19	16	21	18	10	8	0.48	0.32	0.40	95	70	1.5	W	-Ditto-
10	19	16	21	18	11	8	0.55	0.29	0.42	100	100	2	NW	-Ditto-
11	16	10	18	12	8	6	0.78	0.52	0.65	55	100	3	NW	Gr.floor window open,htg on
12	16	10	18	12	8	6	0.85	0.45	0.65	40	90	2.5	W	-Ditto-
13	17	10	16	10	8	6	0.99	0.58	0.79	70	115	5	NW	-Ditto-
14	18	11	14	9	8	6	0.65	0.49	0.57	80	100	4	W	-Ditto-
15	19	15	19	15	9	7	0.55	1.00	0.78	110	49	3.5	NW	1st floor window open
16	17	13	19	15	9	7	0.45	1.25	0.85	120	55	5	W	-Ditto-
17	16	12	19	15	9	7	0.81	1.01	0.91	100	50	5.5	NW	-Ditto-
18	14	10	20	15	10	6	1.01	0.75	0.88	50	40	4	W	Gr & 1st floor windows open
19	14	10	17	13	10	6	0.86	0.78	0.82	78	81	3	NW	-Ditto-
20	12	9	16	13	9	7	0.65	0.65	0.65	85	58	4	NW	-Ditto-
21	12	9	16	13	9	7	0.72	0.49	0.61	120	80	2.5	W	-Ditto-
22	21	17	21	17	9	9	0.45	0.31	0.38	150	150	1	NW	All doors shut
23	22	17	22	17	10	8	0.51	0.29	0.40	125	110	2	NW	-Ditto-
24	10	7	10	7	12	8	0.65	0.45	0.55	100	100	1.5	W	-Ditto-
25	10	7	11	7	13	7	0.71	0.58	0.65	85	75	2.5	SW	-Ditto-

Table 1.

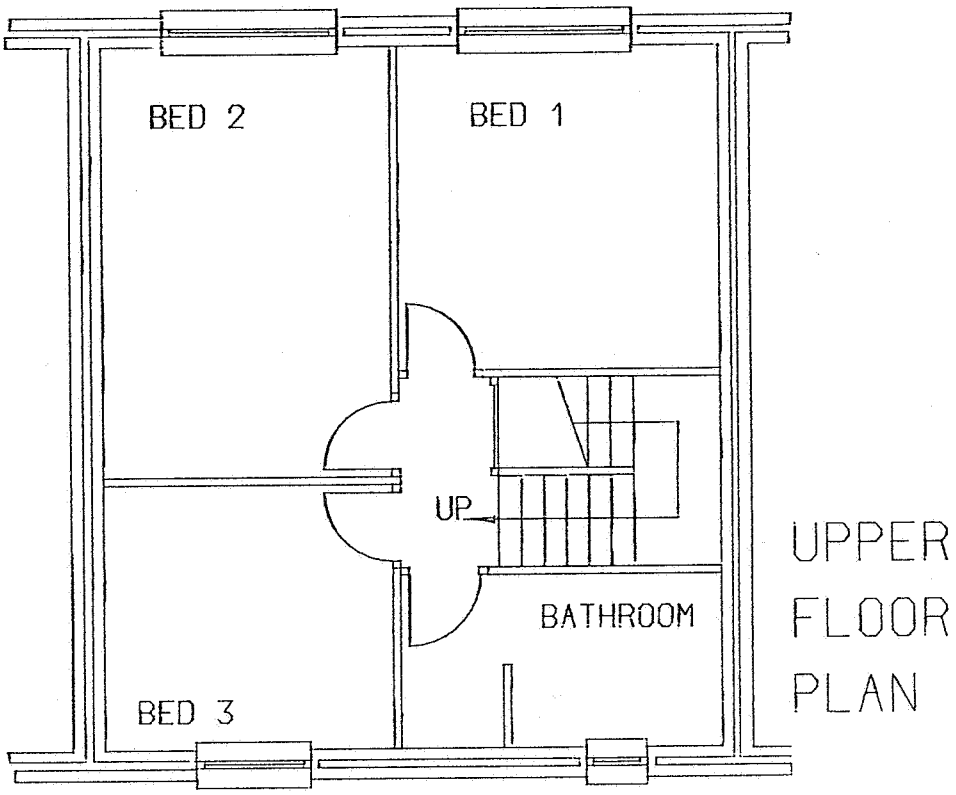
BED 2
BED 1
UP
BATHROOM
BED 3
UPPER
FLOOR
PLAN

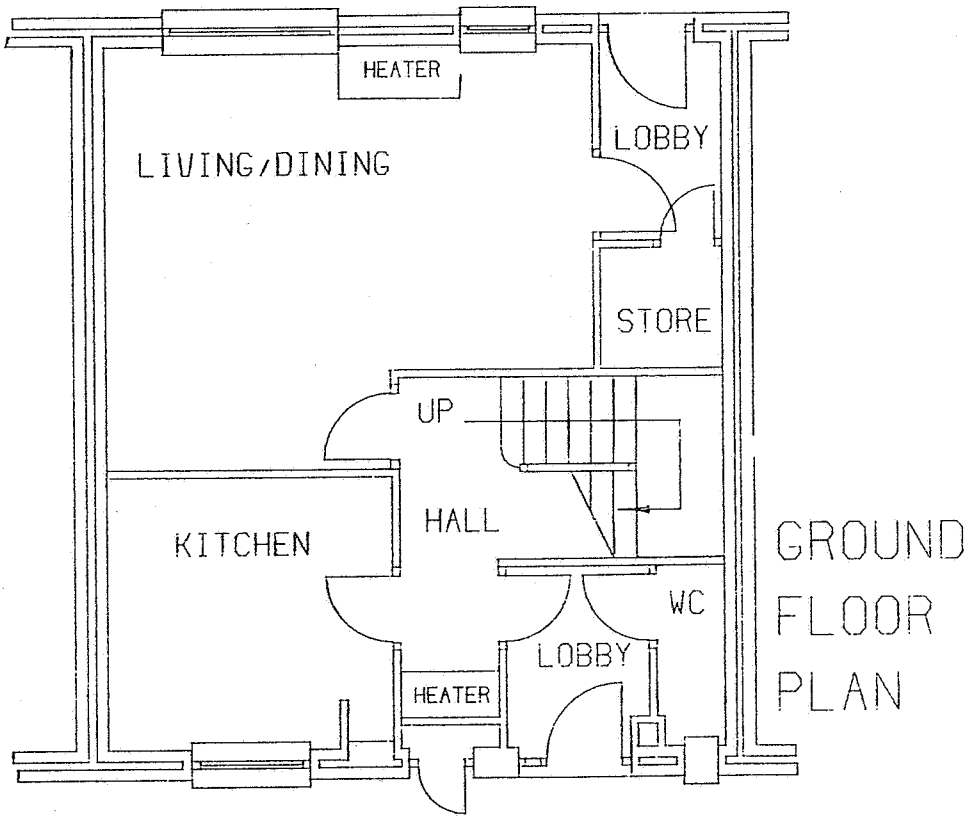
HEATER
LOBBY
LIVING/DINING
STORE
UP
KITCHEN
HALL
WC
LOBBY
HEATER
GROUND
FLOOR
PLAN

Figure 1.

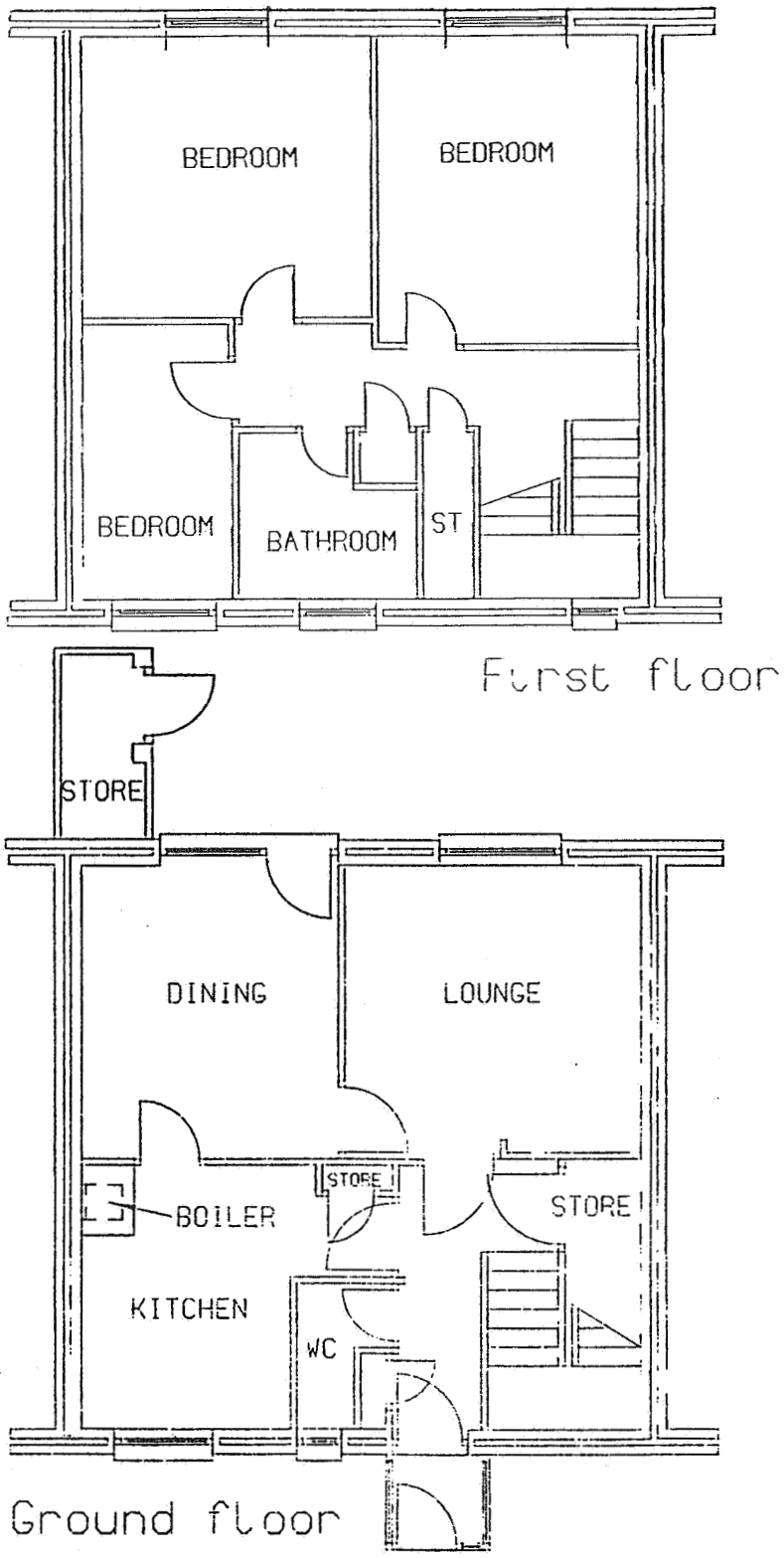
BEDROOM
BEDROOM
BEDROOM
BATHROOM
ST
First floor
STORE
DINING
LOUNGE
STORE
BOILER
STORE
KITCHEN
WC
Ground floor

Figure 2.

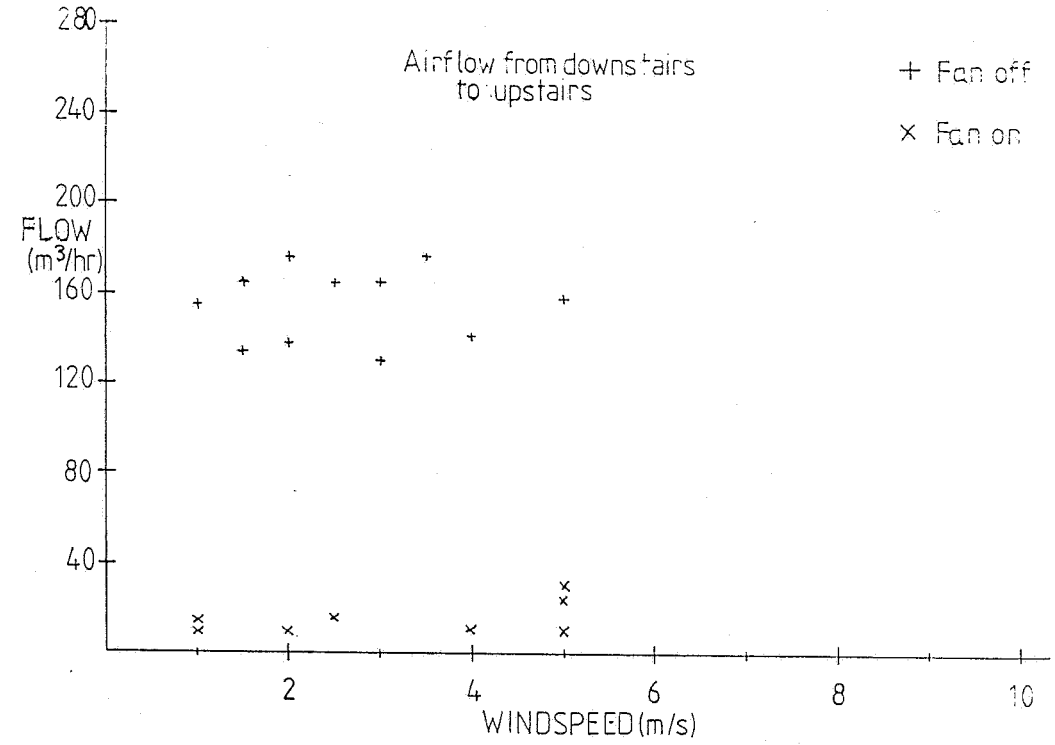

Figure 3.

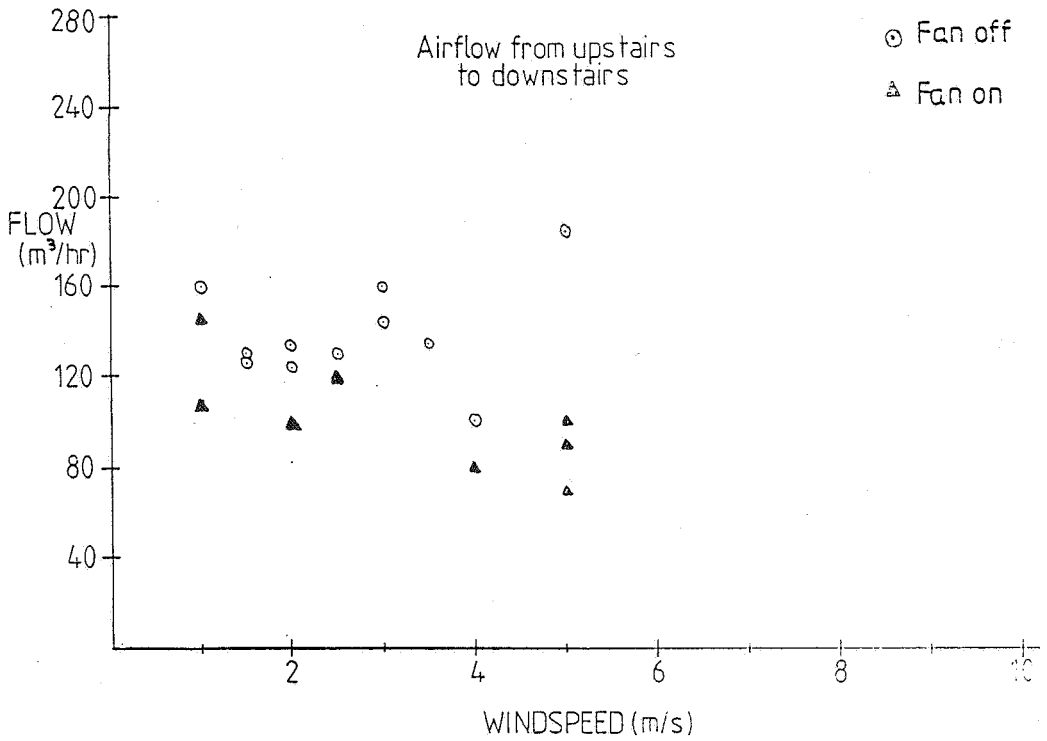

Figure 4.

VENTILATION SYSTEM PERFORMANCE

11th AIVC Conference, Belgirate, Italy
18-21 September, 1990

Paper 22

AIR FLOW THROUGH BUILDING SLITS AND COMPONENTS

B.A. FLEURY & A.Y. GADILHE
E.N.T.P.E. - L.A.S.H.
Rue Maurice AUDIN
69518 Vaulx en Velin Cedex, FRANCE

P. NIARD
E.D.F. - D.E.R./A.D.E.
Centre des Renardières - BP 1
77250 Moret-sur-Loing, FRANCE

J.L. CHAZELAS
L.R.P.C.
8-10 Rue B. Palissy - Z.I. du Brézet - BP 11
63014 CLERMONT-FERRAND, FRANCE

Abstract

Pressure models require a good knowledge of the pressure distribution around the building and a precise description of air paths. The hydrodynamic behavior of these connections is usually reduced to an empirical power law $Q = K\Delta P^n$ with n equal to 0.5 for a turbulent flow and 1.0 for a laminar one. We present three levels of approach to improve our knowledge of the flow behavior of building components. First, we propose a new light experimental tool to determine the on site flow behavior of building elements. Second, we present the flow behavior of innovative air inlets developed in France and from on-site feedback, we suggest design improvments. Finally, we expose an extensive set of experiments on calibrated slits in the 0-100 Pa range and compare our results with other experiments. We point out that the fixed power law is not well suited in the low ΔP (0-20) Pa range which is the range of interest for building ventilation.

LIST OF SYMBOLS

Ca	discharge coefficient
Dh	hydraulic diameter
e	height
K	permeability
l	width
L	depth
n	exponent of the power law
Q	flow rate
Re	Reynolds number
S	section
V	air velocity
ΔP	pressure difference
λ	friction loss
ρ	density
ν	cinematic viscosity
ξ	minor friction loss

1 INTRODUCTION

The knowledge of the flow behavior of building components is important from many points of view :

- the results of pressure model simulation is conditioned by the relevance of the coefficients (K,n) given in input data [1].
- the efficiency of the ventilation system could be dangered by a poor component. Experiences has demonstrated that a high leakage area in a kitchen with a mechanical exhaust system induces a short-circuiting within this room [2].
- the energy losses through leakages may significantly increase the energy bill.
- the leakage comparaison between two building elements is based on their flow equation.
- the quality of the building construction can be evaluated from these data.
- the improvement of ventilation components and the development of innovative ones should integrate the hydrodynamic behavior in the design approach.

Unfortunately, the flow behavior through building elements is not well apprehended and documented. In most of the numerical pressure models, the flow equation for the parasitic openings is supposed to be a fixed power law $Q = K \Delta P^n$ where K is the component permeability and n is an exponent depending on the flow type. n is equal to 0.5 for a turbulent flow like through large openings, or 1 for a laminar flow like through thin cracks. Otherwise, n can vary between these limits and is usually set to a fixed value issued from practice or building regulation, because of a lack of more precise information. However, parametric studies have demonstrated the sensibility of the ventilation analysis with the parameters (K,n). We propose three levels of approach to improve our knowledge on the hydrodynamic behavior of building components. They correspond to a hierarchy in the understanding of the leakage physics : on-site components, innovative products, calibrated slits.

2 MEASUREMENT OF THE BUILDING COMPONENT AIRTIGHTNESS

DC pressurization techniques has been used for many years for the evaluation of the on site building envelope leakage [3]. This method has been refined and extended to identify the behavior of a specific component in various directions : reductive sealing of the element with a plastic foil and tape in two consecutive DC pressurisation tests allows the deduction of the flow behavior of the component. Baker and Valotaire (1987), Furbringer (1988) use a secondary fan to isolate hydrodynamically the component or the zone. Phaff (1987) develops a pressure compensating flow meter to place in an interior door to measure the relative contribution of the room façade. However, these tests are lengthly, require heavy equipements and are not really appropriate during the contruction phase. However, for important building complexs, we note that if a component (window, shutter,...) is not well set, fixed or installed, the probability of the others to be as poorly set is high. Therefore, we wanted to develop a prototype in order to evaluate the quality of construction from an airtighness issue at the construction phase and as well to identify the flow characterics of any building component. To answer these two objectives, the equipment had to be light and robust and the experimental procedure rapid and illustrative.

The prototype (protected by patent) is composed of three main elements :

- a light ajustable frame, (0.8mx1.1m to 1.6mx2.3m). Its weight never exceeds 20 kg.
- A measurement equipement including a flow meter, a flow controller, a pressure device
- a smoke generator

The various stage of positioning the frame are illustrated in figure 1. Before starting the recording phase, we do some pressure overshootings in order to simulate the position of our element after various wind loadings. We record the measures (Q, ΔP) in an ascending then descending ΔP and finally for a few random ΔP. The curve (Q, ΔP) is instantaneously drawn.

In the design process, we looked at various perturbations and found the following conclusions [4] :

- the test should be conducted in an opened space (ie the interior door is opened)
- the position of the base (ie the injection or extraction point), do not influence the result

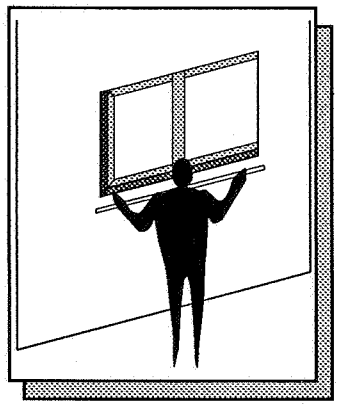

1 Measurement of the element size

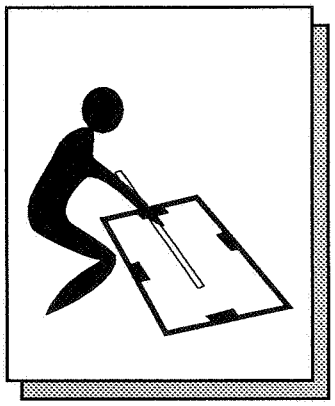

2 Rough adjustment of the frame to the element size

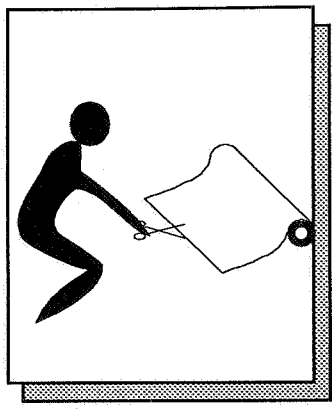

3 Cutting up of plastic foil

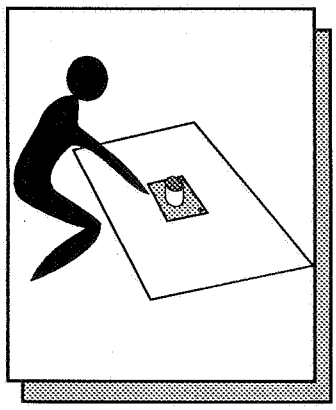

4 Fixing of the base on the plastic sheet

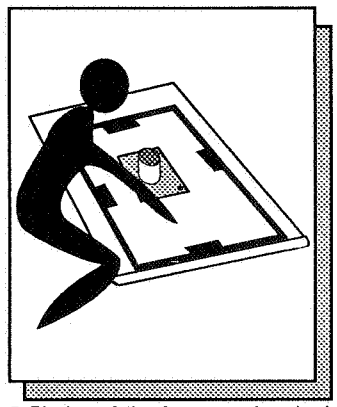

5 Placing of the frame on the plastic sheet and folding loosely the edges

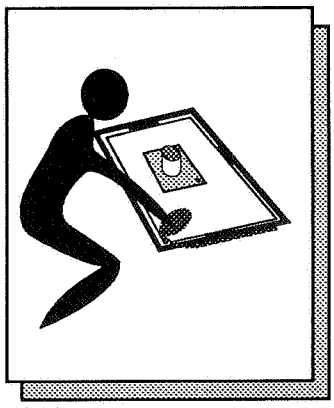

6 Sticking a 5 centimeter wide rubber joint around the frame

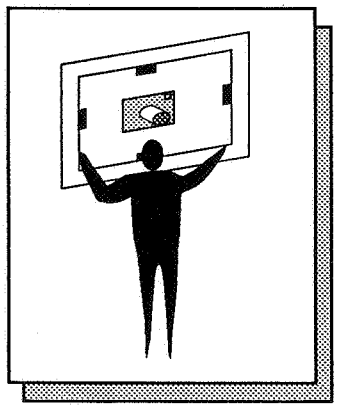

7 Lifting and placing of the frame

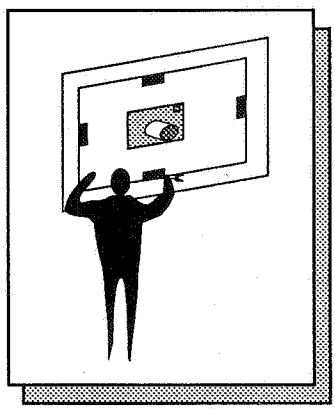

8 Adjustment of the frame

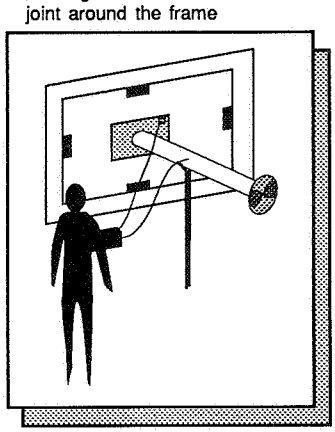

9 Connecting the fan and the measurement device

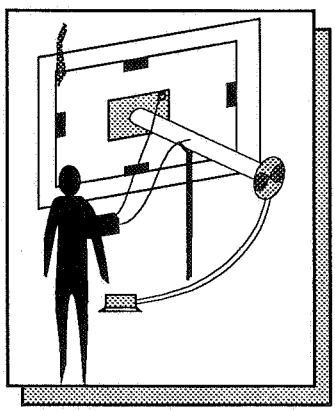

10 Injection of smoke

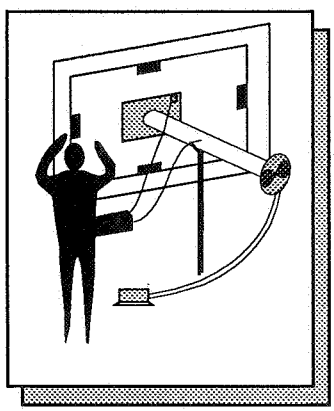

11 Sealing of potential leakage under high pressure conditions

Figure 1 : The various stage of positioning the frame

- the frame should be placed as far as possible of the tested element. However, the zone between the frame and the element is at an homogeneous pressure even with a few centimeters gap.

The overall test requires one hour and a single technician if the frame is placed in the interior side and two technicians otherwise.

From the curve characteristics, we control if the initial performance of the element are preserved. With the release of smoke, we identify the location of the poor mounting. This visualization allows the building workers to correct their installation procedure in the early stage of the project. This equipment appears to be an attractive tool for building quality. After the preliminary succesful tests, we are presently refining the prototype for ease of use by unqualified technicians. This equipment allows us to characterize on-site components and to better apprehend the leakages in the buiding stock but is not appropriate in the design phase of building components.The next two approaches are devoted to answer this issue.

3 IDENTIFICATION OF THE FLOW BEHAVIOR OF INNOVATIVE COMPONENTS

The French market of ventilation has been active and successful in developing new devices to control the flow rate through inlets or outlets according to the humidity, the temperature, the pressure difference and so on. Unfortunatey, the flow behavior of these innovative products is not really available in the range of interest for the pressure differences -20 to 100 Pascals. The characterics of these components can not be simulated by a power law. Let us present some results.

The flow rate is not limited to a maximum value when the pressure difference increased. The regulating device is not efficient and draft problems may occur with this product. This product acts as a hole in the façade.

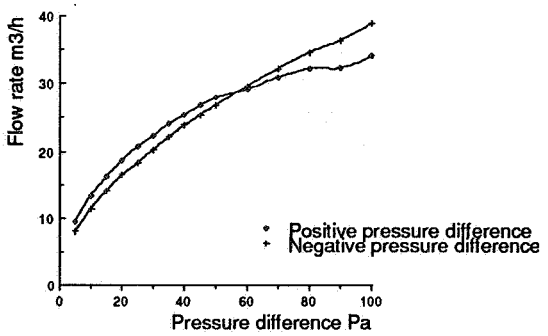

When the pressure increase on the building façade, the flow rate is limited to a maximum value of 50 m^3/h. When the pressure difference is opposite (ie the facade is on the leeward side of the building), the inlet acts as a hole and some air exist through an inlet !

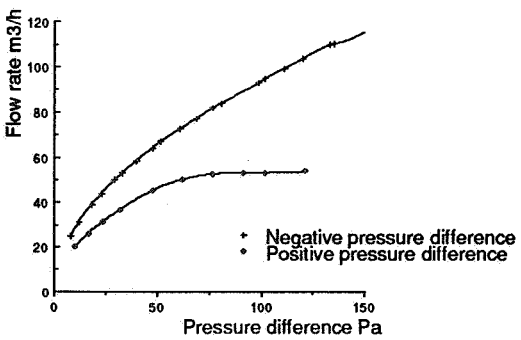

This inlet which limits the flow rate presents a large hysteresis and evaluating the flow rate with a fluctuating wind is tricky because of the dependance of the flow rate and the previous stage of the controlling device. This hysteresis can be simply explained by the sudden blockage of the regulating blade on the inlet frame. Above a high pressure limit (100Pa), the controller blade reaches its maximum deformation and can no longer reduce the inlet area.

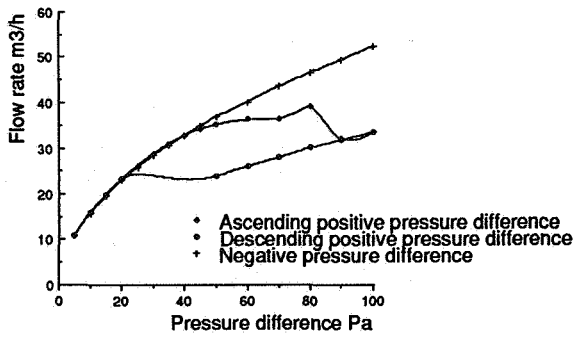

This inlet was manufactured for a maximum flow rate of 30 m^3/h but in fact we notice this overshoot around 30 Pascals. Under 30 Pascals, this product acts as a hole and the regulating device plays its role only above this limit. Backward flow is restricted to 5 m^3/h by a special device.

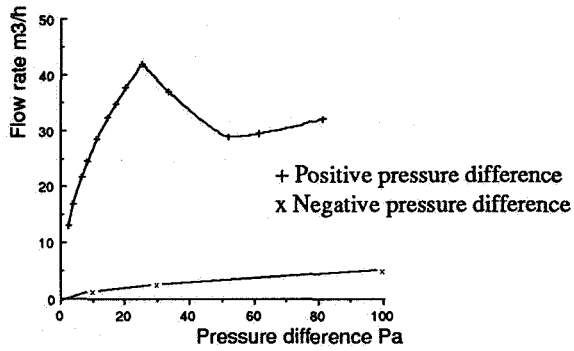

Air inlets represents the major source of fresh air and conditions the efficiency of the ventilation system. The improvement of their performance has resulted in a complex flow behavior which can not be apprehended by a power law.

Limitation the flow rate under high pressure differences is essential if we want to avoid draft problems and excess of incoming air. Because of the conditions of the certification, we notice that no care has been taken to avoid the air to exist when the pressure difference is opposite. This configuration is frequent, especially with the limited extraction rate we encounter in the new French houses. Moreover, in the presence of high wind, infiltrations in existing buildings are high and satisfy the requirement of fresh air. The air transiting through the inlet is not necessary. Therefore, we could imagine to shut down the air inlet above a ΔP limit. Unfortunately, the French regulations do not allow this opportunity. Knowing that a building will never be perfectly tigth, Figure 2 represents the ideal behavior of an air inlet. The limits are given as examples.

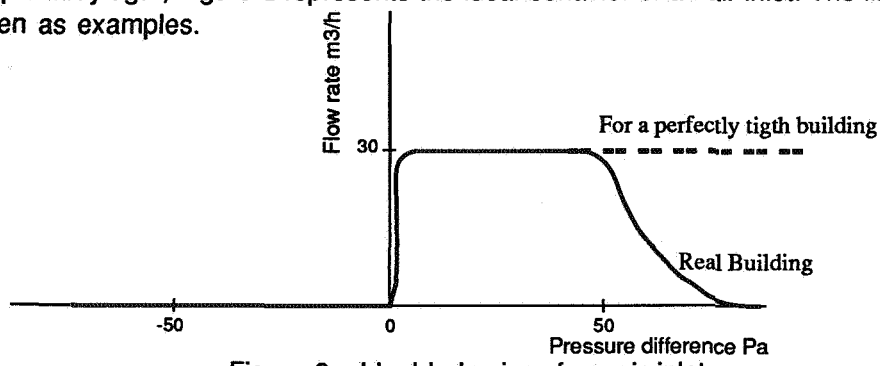

Figure 2 : Ideal behavior of an air inlet

4 AIR FLOW THROUGH BUILDING SLITS

4.1 Introduction

In the first approach, we supposed that the flow behavior follows the empirical power law. This assumption is valid above a 20 Pa pressure difference [5] and appropriate for on-site experiments where the control at low pression is tricky. However, building elements encounter more often pressure differences under this limit. Therefore, we develop an experimental laboratory equipement to test calibrated slots and evaluate the most appropriate law to suit the data. Figure 3 illustrates the test facility.

4.2 Fluid mechanics approach

The equilibium between the body, inertia, viscosity and pressure forces on a moving fluid in a duct is represented by the Navier-Stockes equations,which can not be solved analytically except in very simple configurations. So in fluid mechanics, the pressure difference between two points in a duct is supposed to be correlated with the fluid average velocity :

$$\Delta P = \frac{\lambda \rho L V^2}{2\,Dh}$$

The friction loss coefficient has to be evaluated according to multiple parameters of the flow configuration including the Reynolds number. For a building crack of height e and of width l, the pressure difference between the two sides is less than 100 Pa, the aspect ratio is low and the flow can be considered between parallel plates. So

$$\lambda = \frac{96}{Re}$$

Some particular accidents such as entrance, exit... increase the flow resistance :

$$\Delta P = \frac{\xi \rho V^2}{2} + \frac{96 \rho L V^2}{2\,Re\,Dh}$$

Using $Re = \frac{VDh}{\nu}$ and Q = VS, we get the two following equations :

$$\Delta P = AQ + BQ^2 \qquad (1)$$

with

$$A = \frac{K_1 L \nu \rho}{2\,S\,Dh^2}$$

$$B = \frac{K_1 \rho}{S^2}$$

or

$$Q = Ca\ S \left(\frac{2\,\Delta P}{\rho}\right)^{0.5} \qquad (2)$$

with

$$\frac{1}{Ca^2} = K_1 \frac{L}{Re\,Dh} + K_2$$

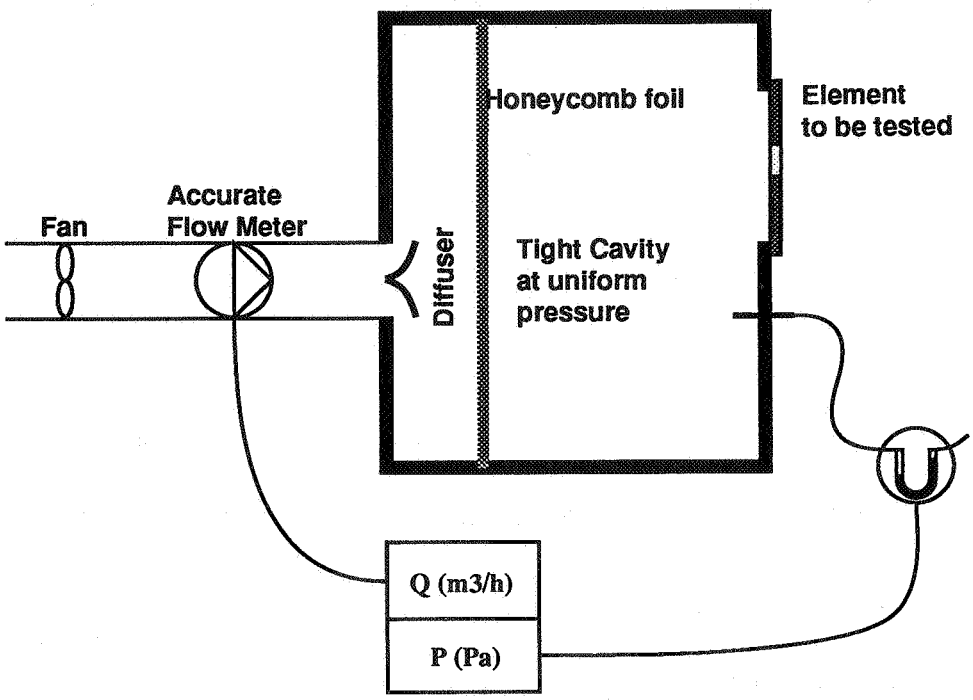

Figure 3 : View of the test facilities

4.3 Experiments

Different cracks of various sizes have been tested in order to evaluate the coefficient Ca. From our set of experiments (Figure 4), we get : $\frac{1}{Ca^2} = 114 \frac{L}{Re\ Dh} + 2.0$

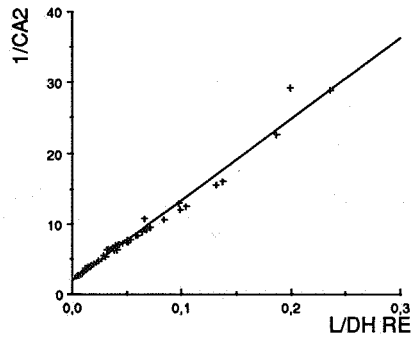

Figure 5 : Evolution of the discharge coefficient

The equation (2) is therefore well appropriate for our experimens and the correlation is closed to Etheridge and Baker's analysis.

Etheridge [6] proposed for a planear opening $\frac{1}{Ca^2} = 95.7 \frac{L}{Re\ Dh} + 1.5$

and Baker [5] $\frac{1}{Ca^2} = 103 \frac{L}{Re\ Dh} + 1.4$

Pressure models require an analytical expression of the flow rate as a funtion of the pressure difference. Unfortunately, equation (1) or (2) do not satisfy this condition. In order to overcome this problem, Etheridge expressed (1) in an other way :

$$Q = K\,\Delta P^{n(\Delta P)}$$

with $$n = \frac{1}{2}\left(1 + \frac{1}{\left(1 + 4\left(\frac{B}{A^2}\Delta P\right)^{0.5}\right)}\right)$$

Homna [7] also found that n should vary with ΔP and proposed :

$$n = \frac{1}{2 - \exp(-\beta k\,\Delta P)}$$

In building situations, typical pressure differences range from 0 to 20 Pa inducing that the power law with constant exponent is not well adequate.

From this preliminary investigation, it seems than a quadratic law or a power law with a variable exponent is more appropriate in the low ΔP range but extensive experiments have to be conducted to propose a general law. Therefore, it is preferable to characterize a component by the couples (Q,ΔP) in the entiere ΔP range including below 20 Pascals instead of fitting the data with a power law.

6 CONCLUSION

The need for improved knowledge of the hydrodynamic behavior of building components has been pointed out in this paper. Three levels of approaches are exposed to answer specific objectives. Their use will help to better understand the flow behavior through building elements and will increase the databasis used in numerical simulations.

REFERENCES

[1] A. GADILHE
Comportement aeraulique des enveloppes de bâtiment : Détermination numérique des pressions en façade - Mdélisation de la perméabilité à l'air.`
Thèse de doctorat : INSA de LYON, 1990

[2] B. FLEURY, A. GADILHE
Etude des transferts d'air dans un appartement
Rapport final à la convention A.F.M.E. n° 9.04.0036, MAI 1990

[3] IEA-ECB Annex 20
Air leakage measurements methods - Air flow rate and air tightness measurement techniques - An application guide.

[4] B. FLEURY, A. GADILHE, A. BENAYACHI
Mesure de perméabilité à l'air : Mise au point d'un banc de mesure in situ pour les équipements du bâtiment.
Rapport d'avancement à la convention n° 9.04.0071, JUILLET 1990

[5] P.H. BAKER, S. SHARPLES, I.C. WARD
Crack flow equations and scale effet.
Building and environnement, 1977, Vol. 12, p.181-189

[6] D.W. ETHERIDGE
Air leakage characteristics of house - a new approach.
Building services engineering research and technology, Technical Note, 1984, Vol. 5, n°1, p. 32-36

[7] H. HONMA
Ventilation of dwellings and its disturbances.
Stockholm : Institut for UPPVARMNINGS och Ventilationsteknik KTH, 1975, Tekniska meddelanden 63, Vol. 3

VENTILATION SYSTEM PERFORMANCE

11th AIVC Conference, Belgirate, Italy
18-21 September, 1990

Paper 23

SENSOR FOR CONTINUOUS VENTILATING RATE MEASUREMENT IN LIVESTOCK BUILDINGS

D.Berckmans, Ph.Vandenbroeck, V.Goedseels

Laboratory for Agricultural Building Research
Katholieke Universiteit Leuven
Kardinaal Mercerlaan 92
3030 Heverlee
Belgium

SENSOR FOR CONTINUOUS VENTILATING RATE MEASUREMENT IN LIVESTOCK BUILDINGS

by

D. Berckmans, Lecturer Res. Assoc.
National Fund of Scientific Research Belgium,
Laboratory for Agricultural Buildings Research
Katholieke Universiteit Leuven
Kardinaal Mercierlaan 92
3030 Heverlee Belgium

Ph. Vandenbroeck, Project Engineer
V. Goedseels, Professor
Laboratory for Agricultural Buildings Research
Katholieke Universiteit Leuven
Kardinaal Mercierlaan 92
3030 Heverlee Belgium

Written for presentation at the 1990
AIVC Conference

Villa Carlotta
Belgirate
September 18-21, 1990

Summary : A new turbinemeter is developed to be used as a ventilating rate sensor in livestock buildings. Starting from a previous sensor, which we introduced in 1983, several improvements were done to become a low cost air flow rate sensor with an acceptable accuracy of 60 m^3/h in a range from 200 to 5000 m^3/h and this for pressure differences from 0 to 120 Pa. This sensor can be integrated in the climate control equipment of livestock buildings to improve process control.

1 PROBLEM

1.1 The importance of the ventilation rate and the airflow pattern in livestock buildings.

In literature for some time already the ventilating rate trough a livestock building is considered to be one of the most important parameters in inside climate control in livestock buildings. The recognition of barn ventilation problems and early investigations of these provided a milestone in environmental control of animal production structures (King, 1908; Bond, 1976). The influence of air flow rate on the values of physical micro-environmental parameters such as inside temperature, humidity and gasconcentration has been treated (Guss and Grout, 1973; Bruce, 1975; Clark and Cena, 1981). Carpenter (1974) explains the importance of the ventilation rate by its relationship with air temperature and with the air velocity around the animal. He explains the complexity of the role of the ventilation system by the interactions between the inside climate and on the other hand variables such as structure of the building, risk for disease, number of pigs in one pen, etc. The objective of the ventilation system is described as control of gasconcentration, of air humidity and of inside temperature (Bruce, 1981). Consequently the three quantitative criteria are known to determine the ventilation rate through the building and to provide the optimum conditions for the livestock by controlling the physical micro-environment. To achieve this, the two basic funtions of a ventilation system are to provide effective control over the ventilation rate and efficient control over the airflow pattern within the ventilated structure. These should be attained simultaneously (Randall, 1981).
The air flow pattern in the livestock building forms the physical link between the control inputs (ventilating rate and heat supply) and the physical micro-environment around the animal. An adequate control of the ventilating rate through the building indeed has been proven to be decisive in establishing a suitable air flow pattern as well (Randall, 1975; Randall and Battams, 1979; Barber et al., 1982).
The influence of the ventilating rate and its control on energy use in modern livestock buildings also has been described in literature (Buffington and Skinner, 1976; Surbrook et al.,1979; Berckmans et al., 1989).
From literature it can be concluded that the ventilating rate trough a livestock building is one of the most important variables to be conrolled.

1.2 Control of the ventilating rate in commercial livestock buildings

Based on the effect of inside climate control on productivity in modern livestock buildings and on the knowledge about the importance of the ventilating rate, research has been done on the efficiency of normal proportional air flow rate control. By statistical analysis of field data, analysis of control equipment in laboratory test installations and a theoretical approach it has been analysed why normal mechanical ventilating systems (proportional control) do not perform adequately in the field (Berckmans and Goedseels, 1986; Berckmans et al., 1988). Consequently a new controller has been developed, in an attempt to achieve improved control of air flow and hence more effective environmental control in livestock buildings . The principle of this improved air flow rate controller,introduced in 1983, is that the signal of a low cost air flow rate sensor (price of about 130 U.S. dollar) is used to realise a feedback control (Berckmans and Goedseels, 1983; Berckmans and Goedseels, 1986; Berckmans et al., 1986).

2 OBJECTIVES

It is clear that the efficiency of this higher mentioned principle, as it is used today by different European producers of control equipment, depends on the accuracy of the air flow rate sensor that is integrated in the control system. The previous sensor which we developed for the introduction of this controller in 1983 had a limited accuracy of about 600 m^3/h over a measuring range of 500 to 5000 m^3/h.

The objective of this paper is to present a new low cost air flow rate sensor with improved accuracy to be used in modern livestock buildings. This means more specifically that the resulting air flow rate sensor :

- must be usable in the hard environment of a livestock building with high temperature differences (from -10 °C to 55 °C in the exhaust chimney), with a lot of moisture and corrosive gases in the exhaust air and in a very dusty environment,
- must operate for a period of 10 years without any major maintenance,
- must permit to measure the ventilating rate in an exhaust chimney with a diameter of 0.5 m and a short tube length of 1 m and with turbulent air flow in it,
- has a small time constant to be usable as a control sensor,
- has a little weight for a mounting in the chimney,
- has a measuring range from 200 to 5000 m^3/h with an acceptable accuracy and low pressure influence,
- creates a minor pressure drop for the fan.
- must have a low price since it is the objective to integrate this sensor in the control equipment of livestock buildings..

3 METHOD

3.1 Position of the sensor

In most of the modern livestock buildings in Europe the underpressure system is used. In spite of the fact that the building envelope has been improved the last years and is carefully tight up against air infiltration, it still is hardly to realize a leakage-free construction in the field. An exhaust chimney with a diameter of about 0.5 m is a standard in Belgium and the Netherlands. To be sure of measuring the global ventilating rate through the building the air flow rate sensor is placed in the exhaust chimney (Figure 1).

3.2 Principle of the sensor

From the measurements of the characteristics of axial fans, it is known that a back flow effect can appear if the underpressure in the ventilated building is increasing. Because of the high pressure difference to overcome, the fan still keeps his rotational speed but takes the air back through its own impeller. The resulting total ventilating rate is decreasing while the fan still is using a high voltage (Figure 2). In these conditions the air flow in the exhaust chimney is subject to important changes of air flow direction within the considered outlet section. Because of these effects on the turbulent flow in the outlet chimney it is concluded that the sensor should cover the whole outlet section. Consequently a sensor that permits to measure in one point of the section is useless. Taken into account the acquired working conditions of the sensor (see Objectives) and the condition of a low price (to become a sensor for control purposes) the choice was made for the principle of a free running turbine covering the whole outlet section. In literature it is shown that a pressure correcting measurement can be realised with turbinemeters of smaller diameters (Lee et al., 1981, 1982).

3.3 Test rig

In the higher mentioned position a flow rate sensor of the considered principle will be subject to changes in air flow rate and variations in pressure difference over the test chimney as well. Because of the principle of a free running turbine the measurements are focused on the relationship between rotational speed of the turbine, the measured air flow rate and the pressure difference over the test section. Consequently the procedures for fan testing with variation of pressure difference should be applied for testing this air flow rate sensor.
To measure the characteristics of the air flow rate sensor a test chimney is used with a diameter of 0.5 m and a length of 1 m which are the dimensions of the standard chimney as used in the field (Figure 3). In this test chimney it is possible to realise an air flow rate from 0 to 5000 m^3/h and this for pressure differences (underpressures in the testroom) from 0 to 120 Pa. The test installation has been built accordingly to the German Standards DIN 1952, the Belgian Standard NBN 688 and the British Standard BS 848. The principle of this test rig is that the air flow rate can be controlled using the fan of the test rig (nr. 30 in figure 3) while an orifice is used (with compensation for air temperature and air humidity) to measure the flow rate (nr. 27 in figure 3). As long as the second fan (nr. 23 in figure 3) is producing the same air flow rate as fan nr. 30, there is no pressure difference between the test room and the environment. In these conditions fan nr. 30 is taking care for the pressure losses through the system. From the moment where fan nr. 23 is producing a higher air flow rate than the one that is

supplied by fan nr. 30, the underpressure in the test room is increasing. This makes it possible to change the pressure difference over the test section from 0 to 120 Pa and this for every air flow rate from 200 to 5000 m^3/h. Since it takes a lot of time to realize constant steady state conditions in the installation and to do reliable measurements (fluctuations of pressure etc.) the global test installation has been computerized (Figure 3) with the necessary statistical procedures in it. The orifice allows to measure the flow rate with an accuray of 10 m^3/h in the range of 200 to 1500 m^3/h and an accuracy of 30 m^3/h in the range of 1500 to 5000 m^3/h. The rotational speed of the turbine is measured by using a fixed approximity switch with 4 indication points on the turbine. The system allows to measure the rotational speed with an accuracy of +- 0.5 rev/min. The repeatability as calculated from 4 experiments to measure the characteristics of a fan was better than 3 %.

4 RESULTS

To realize the objectives, a number of improvements were carried through on the previous type of turbine. Each of these is described.

4.1 Reduction of the number of blades of the turbinemeter.

At the time of the introduction of the previous type of turbinemeter as a ventilating rate sensor for livestock buildings an identical impeller as the one from the fan was used for practical reasons. This still is done by most of the European producers of this type of equipment and consequently most of the existing turbinemeters for livestock buildings still do have 6 or 8 blades on their impeller (Stylianos, 1989).
Since it can be assumed that a high number of blades does increase the resistance to the fluid flow, experiments were done to measure the air flow rate at 4 different levels of voltage to the fan and this for turbines with 8, 4 and 2 blades.
From Table 1 it can be seen that the resulting air flow rates are higher (up to 900 m^3/h) when turbines with 2 blades are used instead of 8 blades. The pressure losses are minimized by using 2 blades. This is in agreement with the equation for the so called specific number of revolutions :

$$n_s = n \cdot Q / (\Delta P)^{3/4} \qquad (7)$$

Minimum pressure drop is achieved by maximizing n_s and high values of the specific number are characteristic for axial designs (largest flowsection for a given diameter). Moreover, the number of blades reduces as n_s increases. It can be concluded that, as opposed to current practices, it is desirable to use a turbine with only 2 blades on its impeller.

4.2 Position of the turbinemeter.

It has already been explained that the ventilating rate sensor should be positioned in the exhaust chimney (see Method 3.1).
For maintenance reasons the first sensor, as we introduced it in 1983, was positioned after the fan in the outlet-chimney. Since it can be expected that the fluid will have a more uniformly flow pattern before passing through the fan, it is tested whether the turbine should be positioned upstream or downstream with regard to the fan in the fluid flow. For both these positions of the turbine the air flow rate and the corresponding rotational speed of the turbine for different pressure differences over the test section have been measured. From Figure 5 it

can be concluded that the upstream position of the turbine with regard to the position of the fan does have an important positive influence on the characteristics of the turbinemeter. Notwithstanding the great pressure influence and symptoms of back flow below an air flow rate of 2000 m^3/h, there is a good linearity for an air flow rate higher than 2000 m^3/h (Figure 5).

4.4 Design of the turbine impeller.

The impeller of the turbine has different components : the **boss**, the **bearings** and the **blade**.

- The **boss** normally should be as small as possible since a bigger boss decreases the usable area for fluid flow and increases the air velocity. It is known that the pressure losses in ducted flows are proportional to the square of this fluid velocity. But the minimization of the dimensions of the boss are limited by the fact that the positioning of the blades becomes impossible on a too small boss. Moreover the use of too long blades should introduce turbulences. The boss used in this development has a diameter of 0.1 m.
- The **bearing** is a standard SKF enclosed bearing with low temperature Natrium-grease.
- The **length of the blade** is determinated by the difference between the tubediameter and the bossdiameter. When using an inside tubediameter (chimney with an outer diameter of 0.50 m) of 0.45 m and with a so called tip clearance of 0.05 m, the length of the blade is 0.17 m.
  The **chord of the blade** is not commonly calculated in design procedures. Mostly the design is evaluated and improved by windtunnel experiments. Following considerations should be taken in account : the force exerted by the air on the turbine is proportional to the area of the blade. This prompts the use of a large chord. On the other hand a large blade creates more disturbances in the fluid flow. As a compromise, the chord was taken equal to 0.1 m in this development.
  Calculation of the **blade angle** involves determination of the inlet angle β_1. The blade outlet angle β_2 can be determined on the basis of this inlet angle and the curvature of the blade (which is defined as β_2-β_1). Use has been made of the concept of velocity triangles. These vectordiagrams, drawn for a random point of the streampath through the machine, make a study of the different velocity components possible :
- absolute flow velocity V (stationary frame of reference).
- relative flow velocity W (rotating frame of reference)
- peripheral velocity of the rotor blades U , being equal to the product of radius and angular velocity of the rotor.

  The absolute velocity equals the sum of relative and peripheral velocity vectors.
  The calculation of the **blade angle** has to be preceded by the determination of a 'design point', which is to be chosen with the specific application of the turbinemeter in mind. In livestock buildings, the lower values of the ventilating rate are the most critical to control. A high rotational speed is necessary to minimize unstabilities at these low air flow rates. A blade geometry was calculated for a 500 m3/h-250 rev/min design point.
  Table 2 shows the variation of blade inlet angle with radius for this prototype.
  The **curvature of the blade** was expected to be small, since in this application, the turbine has to surmount merely friction losses (as it is not used for the transformation of kinetical to mechanical energy). This can be verified by calculation (Vandenbroeck, 1988) : the maximum curvature amounted to no more than 1°, and was in the actual design assumed to be zero.

4.5 Linearity of the relationship between flow rate and rotational speed of the turbine at different pressure differences.

To determine the steady state characteristics of the turbinemeter its rotational speed was measured at different flow rates and at various pressure differences. Flow rates varied between 200 and 5000 m^3/h. For low flow rates up to 1600 m^3/h, the measuring interval was held on 200 m^3/h. For larger rates, the interval was expanded to 500 m^3/h.Pressure differences varied from 0 to 120 Pa, with a step of 20 Pa. The axial fan in use during these tests was a Woods-2100 fan. The complete range of flow rate from 0 to 5000 m^3/h was measured three times in identical circumstances. A linear regression analysis was carried out on the data. The R^2 was calculated as a measure for the goodness of fit. A good fit implicates independence of pressure variations to a large extent. Calculation of the mean (MΔ) and maximum (MaxΔ) deviation from the regression-based predicted value enables to establish a criterion of accuracy.
Figure 6 shows the corresponding linear regression covering the complete flow rate interval from 0 to 5000 m^3/h. In figure 7 the result of a comparable analysis is shown for a turbinesensor of the previous type (diameter 0.45 m, pressure differences 0-120 Pa). Table 3 shows the comparison of the regression analyses on these results.
It is clear that there is an improvement in the linearity of the steady state characteristics of the turbinemeter used as an air flow rate sensor. The corresponding improvement in accuracy is important since the mean deviation has been reduced from 488 m^3/h to 91 m^3/h which value is 1.8% of the full scale (5000 m^3/h). Since the maximum deviation is occuring for the very low air flow rates (see Figures 6 and 7), the reducement of this value might be of importance for automation of the setpoints of minimum ventilating rate.

4.6 Pressure drop caused by the freely rotating impeller of the turbine flowmeter.

The air flow rate produced by an axial fan at a certain voltage supply is very sensitive to the static pressure to overcome by the fan as seen from the steady state characteristics of the fan. Consequently it is important to minimize the pressure drop caused by the air flow rate sensor positioned in front of the fan. Therefore the influence of a turbinemeter, used as an air flow rate sensor, on the fan characteristics was measured. More specifically, since feedback control of the air flow rate will be used, it is important to know what maximum air flow rate can be produced by the fan.
As already indicated, the testrig can be used to determine fan characteristics. This implicates the measurement, at various flow rates, of the power required to establish a certain pressure difference. The same pressure and flow rate intervals as in the foregoing were covered to realize a determination of the saturation values (the flow rates at maximum voltage supply of 220 V to the fan). The results are given in Table 4. Following observation can be made : the introduction of the turbinemeter in the measurement system has but a small effect on the realised maximum flow-rates. Maximum reduction of saturation values amounts to no more than 150 m^3/h.

4.7 Influence of the type of axial fan on the characteristics of the freely rotating turbine.

Since the efficiency of a turbinemeter is influenced by the flow pattern as the air reaches the blades, it can be expected that the type of fan (different blades, etc.) does influence the characteristics of the turbinemeter. Therefore the turbinemeter was subjected to an identical series of tests, the only modification being the type of axial fan used. Instead of the Woods-2100, a Siemens 2CC2 fan, one of the more competitive types on the market, was chosen.These results will be compared with the corresponding measurement data under 4.5 for the Woods-fan. Figure 8 and Table 5 give the result of a linear regression analysis. The whole flow rate range has been taken in consideration, pressure differences varying between 0 and 120 Pa. Compared to the Woods-2100, the mean deviation has been further reduced from 91 to 60 m^3/h which is 1.2% (instead of 1.8 % see 4.5) of the full scale (5000 m^3/h). In addition, it can be noticed from Table 6 that the reduction of saturation values for the Siemens-fan if combined with the turbinesensor is of an equally small measure as for the Woods. Maximum reduction amounts to 250 m^3/h.

5. CONCLUSIONS

5.1 The relationship between the rotational speed and the flow rate for the new developed turbinemeter is highly linear (R^2 = 0.995). This implies a flow rate measurement of satisfying accuracy, nearly independent of prevailing pressure differences (Mean deviation from regression-predicted values = 91 m3/h or 60 m3/h, depending on the type of axial fan in use). The comparable accuracy of the previous turbinesensors had the poor value of about 600 m^3/h.
It must be noted that this turbinemeter can be used as a ventilating rate sensor in a chimney with a diameter of 0.5 m and a length of 1 m and that this sensor then permits to measure the ventilating rate with an accuracy of 60 m^3/h in a range from 200 to 5000 m^3/h and this for pressure differences from 0 to 120 Pa. The price of each prototype was around 220 U.S. dollar and should decrease for bigger series.

5.2 The free running impeller of the flow rate sensor causes only limited pressure losses. Saturation values of the fan suffer a reduction of maximum 250 m^3/h.

5.3 The behaviour of the flow rate sensor is dependent of the type of axial fan in use. This is demonstrated by comparing the linearity of the relationship of rotational speed versus flow rate and this for the flow rate sensor in combination with two different axial fans (Woods-2100 and Siemens 2CC2, diameter 0.45 m). The flow rate sensor will only operate satisfyingly when combined with an appropriate fan. In that case the improved turbine will not give the higher mentioned problem of changing its direction of rotation.

NOTATION

g	accelaration due to gravity = 9.81	m/s^2
n	number of revolutions	1/s
n_s	specific number of revolutions	
p	pressure	Pa
ΔP	pressure difference	Pa
r	root mean square of inner and outer radius of flow passages at turbine blading	m
Q	volume flow rate	m^3/s
v	absolute velocity of fluid flow	m/s
w	relative velocity of fluid flow	m/s
u	peripheral velocity of rotor blade	m/s

greek symbols

β	blade angle	grad.

subscripts

a	axial component
θ	rotational component
1	inlet section
2	outlet section
in	outside
out	inside

Table 1: Air flow rates (m^3/h) as measured by a 2-, 4- and 8-blade turbine with a same fan at different voltages to the fan and for different pressure differences (ΔP) to overcome.

ΔP (Pa)	0	19.6	39.2	58.9	78.5	98.1	117.7
(Volt)	turbine with 2-blade impeller						
100	1600 m^3/h						
140	3800	2700	1500				
180	5500	5200	4800	4200	3600	2000	
220	5500	5500	5500	4500	4000	3000	1500
(Volt)	turbine with 4-blade impeller						
100	1900						
140	3500	2500	2100				
180	5100	5000	4500	4000	3500	2100	2000
220	5500	5000	5000	4500	3900	2000	2000
(Volt)	turbine with 8-blade impeller						
100	1600						
140	3100	2300	1700				
180	4600	4500	4100	3600	3200	2000	1600
220	5000	4500	4500	4000	3500	2000	2000

Table 2 : Variation of inlet blade angle β_1 with radius for the prototype; design/point : 500 m2/h - 250 rev/min.

V (m)	Va (m/s)	V (m/s)	β_1 (°)
0,01	0,87	0,202	17°
0,02		0,524	31°
0,03		0,785	42°
0,04		1,047	50°
0,05		1,309	56°
0,06		1,571	61°
0,07		1,833	64°
0,08		2,094	67°
0,09		2,358	69°
0,010		2,620	71°
0,011		2,880	73°
0,012		3,142	74°
0,013		3,403	75°
0,014		3,665	76°
0,015		3,927	77°
0,016		4,184	78°
0,017		4,451	78°

Table 3 : Results of the regression analyses of rotational speed of (the previous and the new) turbinemeters as a function of the air flow rate (from 0 to 5000 m^3/h) and for pressure differences from 0 to 120 Pa.

	Previous Sensor	Prototype
R^2	0.672	0.992
Mean (m^3/h)	488	91
Max (m^3/h)	1267	346

Table 4 : Effect of the turbinemeter to the maximum air flow rates produced by a Woods 2100 fan at a voltage of 220V.

ΔP (Pa)	with turbinemeter (m^3/h)	fan without meter (m^3/h)
0	5550	5550
19.6	5300	5300
39.2	4950	5050
58.9	4550	4650
78.5	4050	4200
98.1	2450	2600
117.7	1950	2000

Table 5 : comparison of the R^2 and the mean deviation of the turbinemeter characteristics if combined with two different types of fans for a flow rate range of 200 to 5000 m^3/h and pressure differences from 0 to 120 Pa.

	Woods-2100	Siemens-2CC2
R^2	0.992	0.995
Mean	91	60

Table 6 : Effect of the turbinemeter to the maximum air flow rates produced by a Siemens 2CC fan at a voltage of 220V.

ΔP (Pa)	with turbinemeter (m^3/h)	fan without meter (m^3/h)
0	5025	5225
19.6	4625	4800
39.2	4125	4350
58.9	3500	3700
78.5	2125	2300
98.1	1250	1575
117.7	750	1000

REFERENCES

Barber, E.M., S. Sokhansanj , W.P. Lampman and J.R. Ogilvie, 1982. Stability of airflow patterns in ventilated airspaces. ASAE-paper no. 82-4551, 10 pp.

Berckmans, D. and V. Goedseels, 1983. Principles of the Enecom-R controller for livestock buildings. Internal Report in industrial contract, Katholieke Universiteit Leuven, 30 pp.

Berckmans, D. and V. Goedseels, 1986. Development of new control techniques for the ventilation and heating of livestock buildings. J. Agric. Engng. Res., 33, 1-12.

Berckmans, D. , V. Goedseels and R. Geers, 1986. Development of a controller for livestock buildings based on an air flow rate measurement device. Proc. first European symposium on air condition and refrigeration, Brussels, 5-6 Nov., 61-68.

Berckmans, D., E. Vranken, R. Geers and V. Goedseels, 1988. Efficiency of climate control equipment in pig houses. Farm Building Progress, 93, 15-22.

Berckmans, D.and V. Goedseels and E. Van der Stuyft, 1989. Influence of the climate controller on inside climate and on energy use in livestock buildings. Proc. eleventh int. congress on agric. engng., Dublin, 4-8 Sept.,1305-1311.

Bond, T.E. 1976. Milestones in environmental control of animal production structures - and future outlook. ASAE paper No. 76-4046

Bruce, J.M. 1975. The open ridge as a ventilator in livestock buildings. Farm Buildings, R-D studies no. 7 and 8, November 1975, 8 pp.

Bruce, J.M. 1981. Ventilation and temperature control criteria for pigs. In : Environmental aspects of housing for animal production by Clark, J.A., Butterworths, London, 197-216.

BS 848 Part 1, 1980. Britisch Standards Institution. Fans for general purposes. Part 1 : Methods of testing performance, 80 pp.

Buffington D.E. and T.C. Skinner, 1976. Energy analyses of buildings based on seasonal vs. design day weather data. ASAE-paper no. 82-4553, 14 pp.

Carpenter , G.A. 1974. Ventilation of buildings for intensively housed livestock. In : Heat loss from animals and man by Monteith, J.L. and L.E. Mount, Butterworths, London, 389-403.

Clark, J.A. and K. Cena, 1981. Monitoring the house environment. In: Environmental aspects of housing for animal production. Clark, J.A., Butterworths, London, 309-330.

DIN 1952, 1952. Deutsche Normen. Durchfluszmessung mit genomen Düsen, Blenden und Venturidüsen, 13 pp.

Guss, S.B. and A.R. Grout, 1973. Effects of housing on the health of dairy cows. National Dairy Conf. ASME Publication SP-01-73, Febr. 1973, 120-127.

King, F.H. 1908. Ventilation for dwelling, rural school and stables. Madison WI Published by the author.

Lee, W.F.Z., H.W. Fisher and D.R. Montag, 1981. Development of a self-checking gas turbinemeter. In : Flow, its measurement and control in science and industry Vol. 2 by W.W. Durgin. Instrument. Society of America, pp. 453-469.

Lee, W.F.Z., D.C. Blakeshee and R.V. White, 1982. A self-correcting and self-checking gas turbine meter. Journal of Fluids Engng., Vol. 104, 143-149.

NBN 688 NI, 1966. Belgische Norm. Debietmeting van fluïda door drukvalapparaten - Algemeen, 32 pp.

Randall, J.M., 1975. The prediction of airflow pattern in livestock buildings. J. Agric. Engng. Res., 20, 199-215.

Randall, J.M., 1981. Ventilation system design. In : Environmental aspects of housing for animal production by Clark, J.A., Butterworths, London, 351-369.

Randall, J.M. and V.A. Battams, 1979. Stability criteria for airflow patterns in livestock buildings. J. Agric. Engng. Res., 24, 361-374.

Stylianos, L., 1989. Onderlinge vergelijking van luchtdebietmeetsystemen voor agrarische toepassingen. Eindverhandeling voorgedragen tot het behalen van de graad van landbouwkundig ingenieur, Unpublished Thesis, Katholieke Universiteit Leuven, 133 pp.

Surbrook, T.C., M.L. Esmay and W.G. Bickert, 1979. Control effectiveness and energy comparison for animal housing ventilation and heating systems. ASAE-paper no. 70-4526, 12 pp.

Turton, R.K., 1984. Principles of Turbomachinery, E & F.N. Spon. London, 199 pp.

Vandenbroeck, Ph., 1988. Optimalisatie van het luchtdebietmeetsysteem in dierlijke productie-eenheden. Eindwerk voorgedragen tot het behalen van de graad van Landbouwkundig Ingenieur, Unpublished Thesis, Katholieke Universiteit Leuven, 109 pp.

Wislicenus, G., 1965. Fluid mechanics of turbomachinery, Vol.I, Dover Publications, New York, 416 pp.

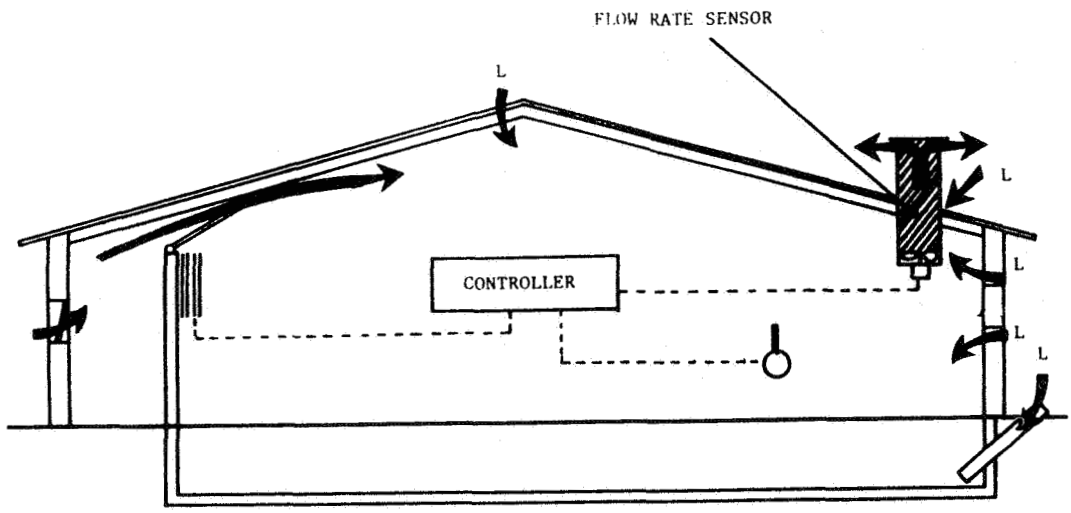

Figure 1. Place where the flow rate sensor should be mounted because of possible leakages in the building envelope (L: Leakage).

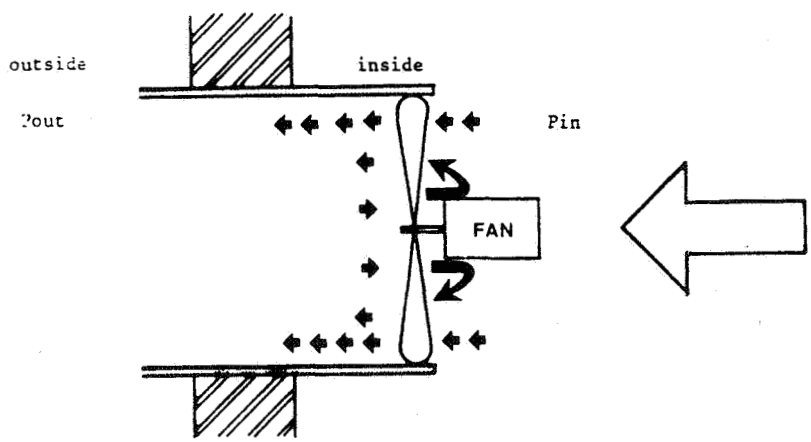

Figure 2. Back flow effect of an axial fan ($P_{in} << P_{out}$).

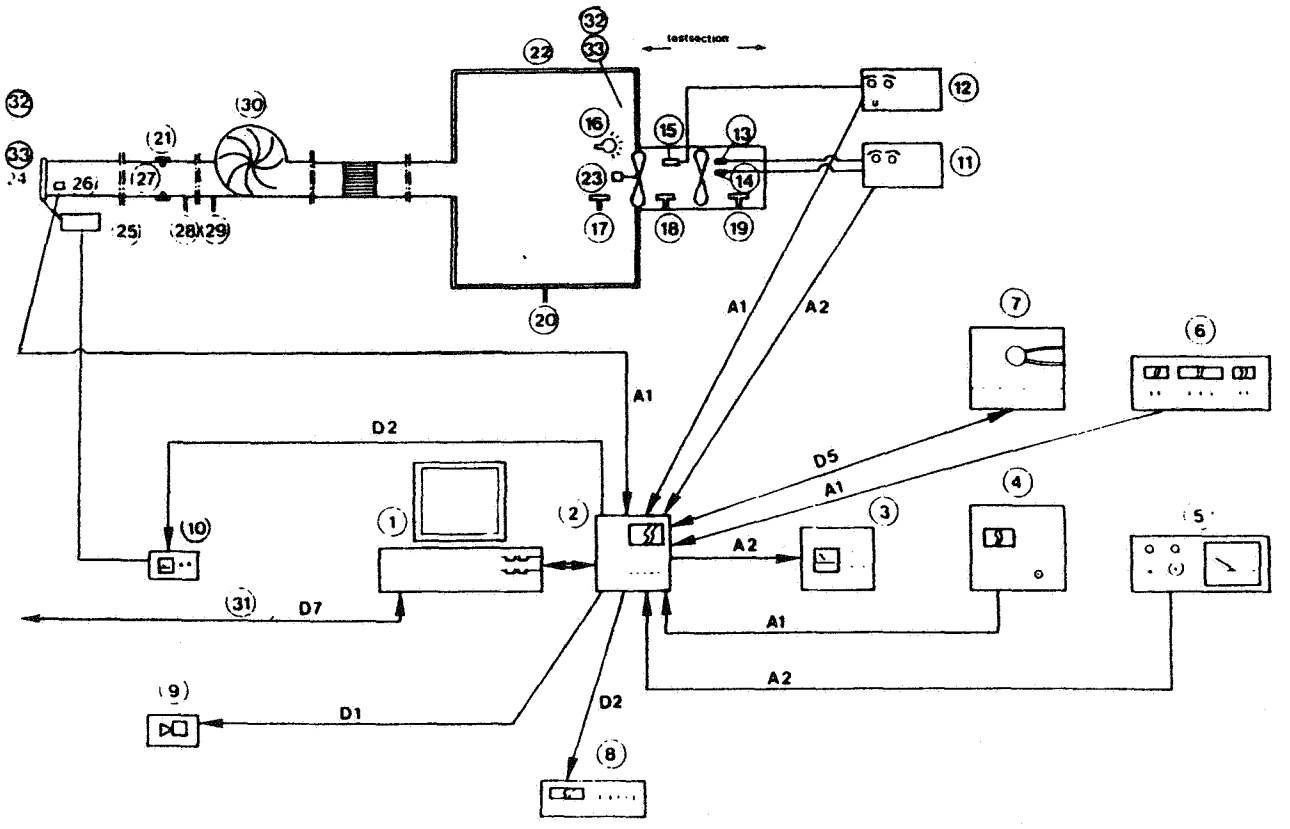

1. Minicomputer for controlling the test rig and storing results.
2. Parallel-coupled measure and control interface for digital and analogue signals.
3. Linearised and filtered transmitter 0-10 V_{DC} to 0-220 V_{AC}.
4. Pressure-sensor 0 to 26 Pa with digital display and analogue output (Furness control). (Furness Control 040 ; Accuracy 1 Pa)
5. Reference pressure-sensor for calibration 0 to 200 Pa with analogue output (Furness control).
6. Power-meter 0-200 kW, analogue output.
7. Controller for scanning 10 pressure-channels.
8. 3-channel digital voltmeter.
9. Digital controlled acoustic signal.
10. Unit for flow rate control.
11. Transducer for fan speed and direction measurements of turbinemeter
12. Transducer for fan speed measurements of fan
13 and 14: proximity switches.
15. Photocell. (Sprague ULN 333 Y)
16. Light resource.
17, 18, 19, 20: Location of measuring points for pressure-measurements.
21. Tubes to produce pseudo-laminar air flow.
22. Testchamber.
23. Testfan
24. Diaphragm for air flow rate control.
25. Motor for diaphragm control.
26. Sensor to measure the position of the diaphragm.
27. Shaped orifice.
28, 29 Pressure-measurement over the orifice. Furness Control FC040 (range 0-2500 Pa, Accuracy 10 Pa)
30. Auxiliary fan.
31. Serial data-transmission to Tektronix 4052 A graphic workstation.
32. Humidity sensors (Vaisala HMP 23U; Accuracy <3% RH)
33. Temperature sensors (Analog Device AD 590 ; Accuracy 0.5°C)

Figure 3. Schedule of the testrig.

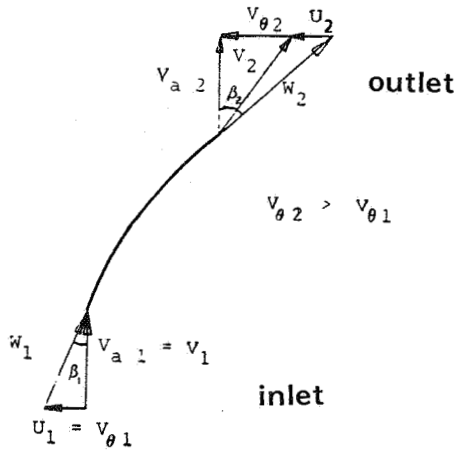

Figure 4. Velocity triangles at inlet and outlet of a turbine blade

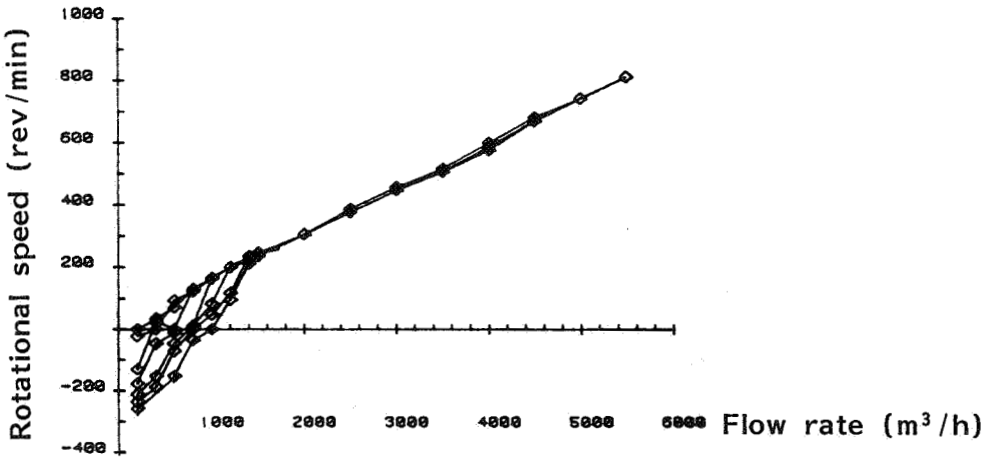

Figure 5a. Rotational speed vs. flow rate for a 2-blade impeller, downstream position.

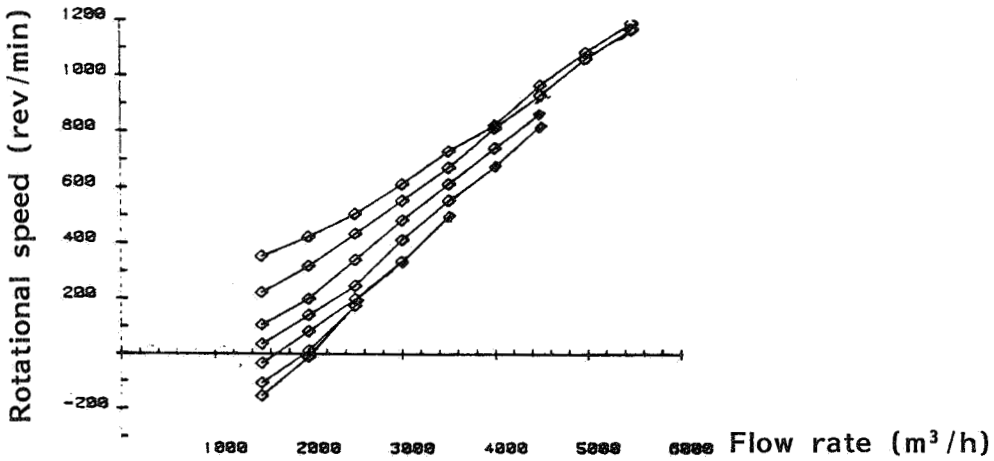

Figure 5b. Rotational speed vs. flow rate for a 2-blade impeller, upstream position.

Figure 5. Comparison of turbinemeter performance (old design) for upstream and downstream positioning (flow rate : 1500-5000 m^3/h; Δp = 0-120 Pa).

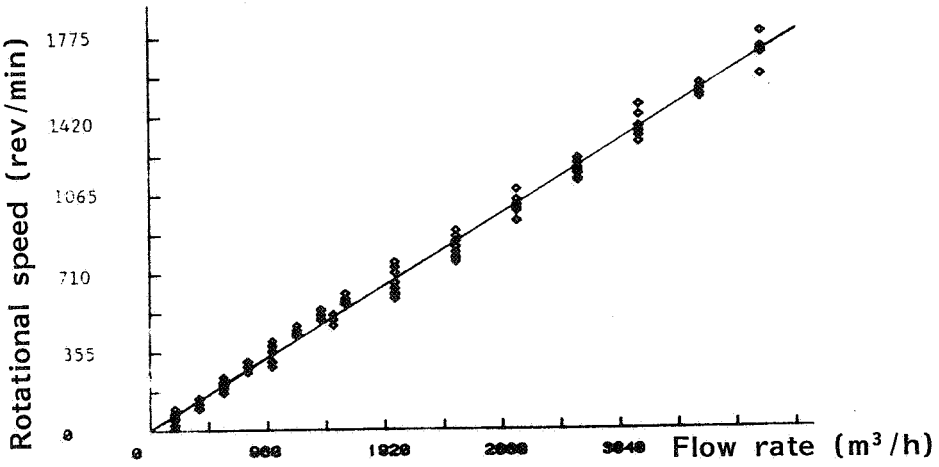

Figure 6. Linear regression analysis. 2-blade impeller prototype (flow rate : 200-5000 m^3/h, Δp : 0-120Pa), upstream position, combined with Woods 2100-fan.

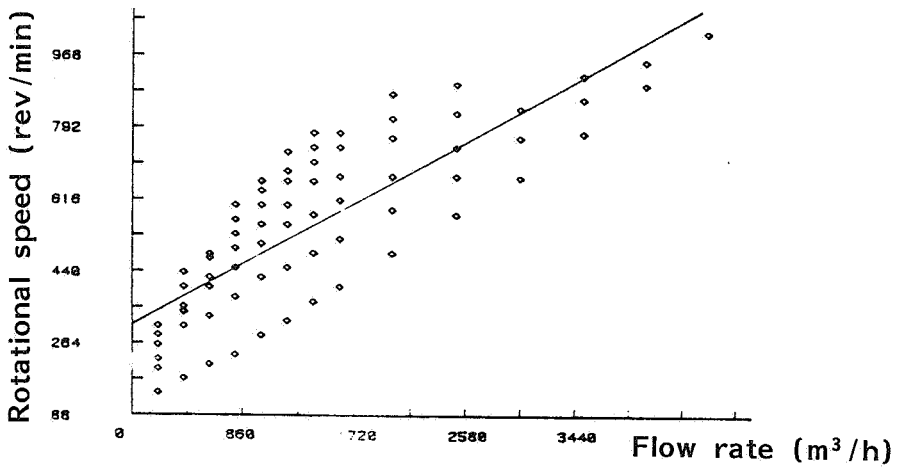

Figure 7. Linear regression analysis. Turbinemeter old design (flow rate : 200-5000 m^3/h, Δp-120 Pa), downstream position, combined with Woods 2100 - fan.

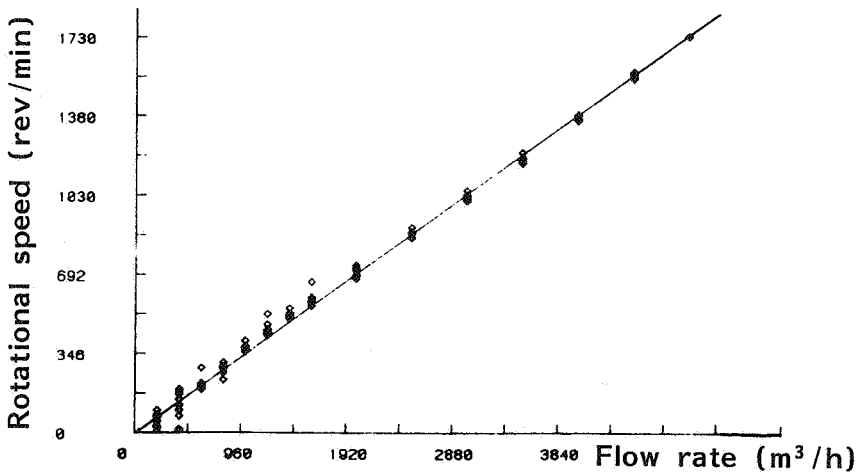

Figure 8. Linear regression analysis. 2-blade impeller prototype (flow rate : 200-5000 m^3/h, Δp : 0-120Pa), upstream position, combined with Siemens 2CC2 - fan.

VENTILATION SYSTEM PERFORMANCE

11th AIVC Conference, Belgirate, Italy
18-21 September, 1990

Paper 24

VENTILATION SYSTEM PERFORMANCE OF VERTICAL EXHAUST COMMON-DUCT IN A MULTI-STORY HOUSE

SHUZO MURAKAMI
KUNIO MIZUTANI*

Institute of Industrial Science
University of Tokyo
5-7-1 Roppongi, Minato-ku
Tokyo 106
Japan

HIROSHI YOSHINO

Department of Architecture
Faculty of Engineering
Tohoku University
Sendai 980
Japan

SHIN-ICHI AKABAYASHI

Department of Architecture
Faculty of Engineering
Niigata University
8050 Igarashi-Ninomachi
Niigata 950-21
Japan

KOU HASEGAWA

Technical Research Laboratory
Mitsui Construction Co., Ltd.
518-1 Komaki, Nagareyama-shi
Chiba 270-01
Japan

*Contract researcher from Sanken Setsubi Kogyo Co., Ltd.

SYNOPSIS

Ventilation performance of a vertical exhaust common-duct installed in a multi-story house was analysed using model experiment and computer simulation. Pressure losses at the flow junctions in the vertical common-duct were investigated using the model experiment. The pressure distributions along the vertical common-duct in three different multi-story houses of 5, 15 and 25 stories, respectively, were calculated by the computer simulation. The results are as follows:

(1) The pressure losses in the converging flow at the junctions in the vertical common-duct were expressed by approximate equations with two ratios, namely, the ratios of the velocity of airflow and the sectional area of the vertical common-duct to those values of the branch duct.

(2) The pressure loss in the converging flow at the junction through the vertical common-duct was positive in the case of the T-type junction. But the pressure loss in the case of the elbow-type junction was negative, which means that the elbow-type junction increases the pressure in the common-duct and may cause a reverse flow from the vertical common-duct to the apartments, especially those in the upper stories. Therefore, the T-type junction should be used in order to prevent such reverse flow.

(3) It is possible to keep the difference between the static pressure in the common-duct and the outside pressure small by controlling the rotational speed of the exhaust fan mounted at the top of the vertical common-duct.

List of symbols

A_1	:Sectional area of a vertical exhaust common-duct	[m^2]
A_2	:Sectional area of a branch duct	[m^2]
d_e	:Equivalent diameter of a rectangular duct	[m]
V_1	:Velocity of airflow through a common-duct before a junction	[m/s]
V_2	:Velocity of airflow through a branch duct	[m/s]
V_3	:Velocity of airflow through a common-duct after a junction	[m/s]
Q_1	:Volume of airflow through a common-duct before a junction	[m^3/h]
Q_2	:Volume of airflow through a branch duct	[m^3/h]
Q_3	:Volume of airflow through a common-duct after a junction	[m^3/h]
ζ_{13}	:Pressure loss coefficient in converging flow through a common-duct with a single junction	
ζ_{23}	:Pressure loss coefficient in converging flow from a branch duct to a common-duct with a single junction	
ζ_{13}'	:Pressure loss coefficient in converging flow through a common-duct with double junctions	
ζ_{23}'	:Pressure loss coefficient in converging flow from a branch duct to a common-duct with double junctions	
λ_s	:Friction loss coefficient through a common-duct	
ζ_e	:Pressure loss coefficient due to a elbow-type junction	
ζ_f	:Pressure loss coefficient due to a leg of the angle appeared inside of a common-duct	
ζ_{ex}	:Pressure loss coefficient of the outlet at the top of the common-duct	
ζ_{in}	:Pressure loss coefficient of the inlet at the bottom of the common-duct	
ΔP_r	:Pressure loss from the outside to the inside of an apartment through the envelop	[Pa]
ΔP_{df}	:Pressure loss from the inside of an apartment to the end of the branch duct connecting with a common-duct	[Pa]
R_e	:Reynolds number of a common-duct	
P_s	:Static pressure (A difference from the atmospheric pressure)	[Pa]
P_1	:Total pressure in a common-duct before a junction	[Pa]
P_2	:Total pressure in a branch duct before a junction	[Pa]
P_3	:Total pressure in the common-duct after a junction	[Pa]
ΔP_{13}	:Total pressure loss in converging flow through a common-duct	[Pa]
ΔP_{23}	:Total pressure loss in converging flow from a branch duct to a common-duct	[Pa]
ν	:Coefficient of kinematic viscosity	[m^2/sec]
ρ	:Air density	[kg/m^3]

1. INTRODUCTION

The center-core-type apartment, which has a kitchen, a bath, a lavatory, and a laundry in the center area of the floor plan, is a popular type of multi-story apartment house in Japan from the viewpoints of daylighting and natural ventilation for the living room and bedrooms. Many types of mechanical systems have been employed for ventilation of this center-core area. Presently, a mechanical ventilation system with a horizontal duct installed in each apartment (individual ventilation system) is used in many multi-story houses. Prior to the use of this type of system, a mechanical ventilation system with a vertical exhaust common-duct connected with the branch ducts from apartments was popular. The reasons why this latter ventilation system became unpopular are as follows:

1) Unstability of exhausted air volume, which leads to the possibility of a reverse flow of odors from the vertical common-duct to individual apartments.

2) Disadvantages in building construction, including time needed for construction, and maintenance of the vertical common-duct.

3) Difficulty in dealing with occupants' complaints of noise from other apartments and reverse flow from the vertical common-duct.

4) Problems from the viewpoint of fire protection.

However, the ventilation system with this vertical exhaust common-duct has some advantages as follows:

1) Horizontal ducts are not needed, which eliminates the necessity of installing such ducts through beams.

2) Low ceilings necessary for concealing such horizontal ducts, are not needed in the case of the individual ventilation system.

3) The ventilation system with the vertical exhaust common-duct is relatively uninfluenced by outdoor wind pressure. On the hand, the individual ventilation system with a horizontal duct is easily influenced by outdoor wind pressure, because the exhaust air outlet of the horizontal duct is installed on the outer wall.

High-rise apartment houses with more than 25 stories are now common in the center of large cities. When the individual ventilation system with a horizontal duct is installed, some of the following problems are encountered;

1) A large capacity fan should be installed to overcome strong wind pressure on exhaust from the air outlet of the horizontal duct.

2) If such a large capacity fan is installed, there is a possibility of negative high indoor pressure, which leads to troubles such as difficulty in opening doors and noise due to air infiltration.

3) The height of beams can not be reduced because the horizontal ducts pass through these beams.

On the other hand, high performance household equipment and control systems have been rapidly developed in recent years. Nowadays, there is a possibility that the defects of the ventilation system with the vertical common-duct can be overcome by means of such kind of household equipment and control systems.

The most important point for design of the ventilation system with the vertical common-duct is how to prevent reverse flow. The reverse flow from the common-duct to apartments may occur when the static pressure in the common-duct rises to a level higher than that of an apartment due to the stack effect and the converging flow effect. There is a possibility that the rise of static pressure may be prevented by taking into consideration the type of flow junction, the sectional area of the common-duct, the performance of the exhaust fan mounted at the top of the common-duct and the performance of the individual exhaust fan (kitchen fan) in an apartment. However, there is little data available on pressure loss in converging flow at the junction.

In this study, firstly, the pressure loss coefficient of converging flow at the junction is investigated by use of an experimental model. Secondly, a computer program for calculating the pressure distribution along the vertical common-duct and airflow volume through the vertical common-duct and the branch duct is developed by use of a network model. Thirdly, the pressure distribution and airflow volume is calculated in many cases with different combinations of parameters: the type of junction, the number of stories, the roof fan performance, the internal heat gain from cooking stoves, the sectional area of the vertical common-duct, and the pressure loss coefficient of the inlet installed at the bottom of the vertical common-duct. Lastly, ways of designing a ventilation system employing with a vertical exhaust common-duct are recommended.

2. MODEL EXPERIMENT FOR PRESSURE LOSS IN CONVERGING FLOW

2.1 Description of the Experiment

(1) Model used for the experiment

Figures 1 and 2 show the experimental model used. The model incorporated a vertical exhaust common-duct of four stories, assumed to be part of such a duct of a high-rise apartment house with 14 stories. The sectional area of the vertical common-duct was 0.5 meter by 0.5 meter. The model of vertical common-duct was horizontally situated for the experiment. No experiment regarding the stack effect was conducted. Figure 3 shows the two types of

junctions employed. The elbow-type junction was popular for the common-duct from the viewpoints of fire protection and making upward airflow. The branch duct connected to the common-duct from each apartment had three different sectional areas. Types of roof fans and kitchen fans commonly used for actual high-rise apartment houses were employed. The chambers were connected with the top and the bottom of the common-duct. In some cases of actual common-ducts, the legs of angles for connecting the parts of the common-ducts are inside the common-duct. But such legs were not employed in our model. The pressure loss coefficient of such legs, which was used for computer calculation, was measured in other experiments.

(2) Measurement methods

The points at which static pressure on the inside surface of the common-duct were selected every 75 mm along the center line of each side of the common-duct. The volume of intake airflow from the bottom of the common-duct was estimated by measuring the velocity of airflow at the center of the intake air duct, which was connected to the intake air chamber. The relation between the velocity of airflow and the airflow volume was investigated by measuring the profile of airflow velocity in the intake air duct.

The volume of exhaust airflow from a branch duct was estimated by measuring the velocity of airflow at the center of a branch duct connected with a kitchen fan. The relation between the velocity of airflow and the airflow volume measured by an orifice plate was also investigated.

The rotational speed of the roof fan could be changed by an inverter. The airflow volume of the kitchen fan was changed by a damper installed in the branch duct.

The pressure difference between each point on the inner surface of the common-duct and reference point A in the common-duct was measured by a capacitance manometer. The pressure difference between reference point A and the atmosphere was also measured. For the expression of measurement results, the static pressure on the inner surface of the common-duct was indicated as the difference between such pressure and the atmospheric pressure.

2.2 Friction Loss Coefficient

(1) Friction loss of the common-duct

The friction loss of the common-duct was estimated by measuring the pressure loss between point A and point B as shown in Fig. 1 under the condition without branch ducts. It was estimated that the friction loss factor varied from 0.017 to 0.032, depending on the Reynolds number.

(2) Pressure loss due to an elbow-type junction

The pressure loss due to an elbow-type junction was estimated by

subtracting the friction loss of the common-duct from the pressure loss between point A and point B as shown in Fig. 1 under the condition with elbow-type junctions. It was estimated that the pressure loss coefficient due to the elbow-type junction was 0.135 - 0.200, which depended on the diameter of the branch duct.

2.3 Pressure loss of flow junctions

There were six types of flow junctions employed as shown in Fig. 3. The point at which pressure was measured in the branch duct was 40 cm from the connection of the branch duct with the common-duct.

The total pressure loss in the converging flow at the junction through the vertical common-duct (ΔP_{13}) was estimated by subtracting the pressure loss due to the elbow-type junction and the friction loss of the common-duct, from the total pressure loss between point A and point B. The total pressure loss in the converging flow at the junction from the branch duct to the common-duct (ΔP_{23}) was estimated by subtracting the total pressure loss from point C to the end of the branch duct and the friction loss from the end of the branch duct to point B, from the total pressure loss between point C and point B.

(1) Static pressure distribution along the common-duct

Figures 4 and 5 show the static pressure distribution along the vertical common-duct with T-type junctions and elbow-type junctions, respectively, which were installed at the first to third floor levels. For T-type junctions, in all three cases with different rotational speeds of the roof fan, the static pressure decreases around the flow junctions and becomes lower in upper floor levels.

In the case of the elbow-type junction, the static pressure decreases just before flow convergence and increases after flow convergence. The static pressure in upper floor levels is greater than that in lower floor levels in the case of low airflow volume of a roof fan. On the contrary, in the case of high air volume of a roof fan, the static pressure in upper floor levels is smaller.

This difference corresponds with which is larger, the total of the friction loss in the common-duct and the pressure loss due to the elbow-type junctions, or the static pressure rise due to flow convergence.

(2) Pressure loss coefficient in converging flow in the case in which only one branch duct is connected

Figure 6 shows the pressure loss coefficient in the converging flow at the junction from the branch duct to the common-duct (ζ_{23}), which is expressed by the function of only the velocity ratio of airflow, V_2/V_3.

Figure 7 shows the pressure loss coefficient in the converging flow at the junction through the common-duct (ζ_{13}). The ζ_{13} of the

T-type junction is roughly proportional to the velocity ratio of airflow, V_2/V_3, and the slope of the line depends on the sectional area of the branch duct. The ζ_{13} of the elbow-type junction is negative in the range of the velocity ratio of airflow, V_2/V_3, being more than 2.0, and depends on the cross-sectional area of the branch duct.

(3) Pressure loss coefficient of converging flow in the case of two adjacent branch ducts connected with the common duct

The converging flow may influence the pressure loss in the converging flow at the adjacent downward junction. Figure 8 shows the measurement results of the pressure loss coefficient in converging flow at the downward junction through the common-duct (ζ_{13}'). In the case of the T-type junction, the marks plotted can be divided into three groups. The pressure loss in converging flow from the branch duct to the common-duct was not influenced by the adjacent upward junction and is equal to the case in which there is only one branch duct.

2.4 Approximate Equations of the Pressure Loss Coefficient in Converging Flow

In order to calculate the pressure losses at the junctions for the network model, the approximate equations of the pressure loss coefficient depending on the velocity ratio of airflow were formulated based on the relationships as shown in Figs. 6 - 8 using the least square method. The results are shown in Table 1. The ζ_{13} is expressed as the function of both the velocity ratio of airflow and the cross-sectional area ratio.

3. VALIDATION OF CALCULATION MODEL

3.1 Calculation Method

Input data for the calculation are as follows:

1) Type of a flow junction
2) Fan performance curve
3) Indoor and outdoor temperatures
4) Internal heat gain from a cooking stove

The airflow volume through each branch duct from the kitchen fan and that from outdoors taken in to the bottom of the common-duct are initially given. Secondly, the static pressure is calculated for each junction along the common-duct from the bottom to the top. If the relation between the pressure difference in front of and behind the roof fan mounted on the top of the common-duct and the exhaust airflow volume through the roof fan dose not fall on the performance curve of the roof fan employed, the airflow volume taken in from the bottom of the common-duct is revised and the same calculation is repeated. If the relation between the two values falls just on the fan curve, then the pressure difference in front of and behind the kitchen fan is calculated for each apartment. If the relation between the pressure difference and the

airflow volume through the branch duct initially assumed dose not fall on the performance curve of the kitchen fan, the airflow volume is revised and the calculation is repeated from the first stage. If the relation between the two values falls just on the fan curve, the iterative calculation finally yields the static pressures at all the nodes and the airflow volumes through all the branches between nodes.

3.2 Comparison Between Measurements and Calculations

Figures 4 and 5 include the calculation results of pressure distribution, which are shown by solid lines. The pressure distribution around the flow junctions as shown by calculation and that based on measurement were different, because, in the case of calculation, the pressure change due to flow convergence occurs just at the flow junction. The calculation showed that the static pressure along the common-duct decreases in upper floor levels in the case of the T-type junction and increases in upper floor levels in the case of the elbow-type junction. It can be said that the characteristics of the calculated pressure distribution totally correspond to the measurement results.

4. CALCULATION OF PRESSURE DISTRIBUTION AND AIRFLOW VOLUME

4.1 Parameters for Calculation

Three different multi-story houses, which had 5, 15 and 25 stories, respectively, were used for calculation models. The vertical exhaust common-duct was of two different sizes as shown in Table 2. The pressure loss coefficients of flow junctions and duct fittings are also included in Table 2. The seven combinations for operating conditions of the kitchen fans installed in apartments were assumed on the basis of the data in Ref. 1. The type of junctions, internal heat gain from the cooking stove, kitchen fan performance and pressure loss coefficient of the air inlet at the bottom of the common-duct had two different values for parameters. As to the roof fan type, calculations were performed for fans with and without rotational speed control. The performance curves of the roof fan are shown in Figure 9. Figure 10 shows the performance curve of the kitchen fan. There was 1344 combinations of calculation conditions.

4.2 Calculation Results

In this paper, calculation results are reported for two cases: one is that in which kitchen fans are used in some lower level apartments, and the other is that in which such fans are not used.

(1) Cases without rotational speed control of the roof fan

Figures 11 and 12 show the pressure distribution along the vertical common-duct calculated for three different multi-story apartment buildings with 5, 15 and 25 stories, which have the common-duct sizes of 600 mm by 600 mm and 600 mm by 1000 mm.

In the cases without operation of kitchen fans, the static pressure strongly depends on both the pressure loss coefficient of the air inlets at the bottom of the common-duct and the size of the common-duct. When the pressure loss coefficient changes from 1.0 to 10.0, the static pressure at the bottom of the common-duct decreases from around 0 Pa to -20 ∿ -40 Pa, depending on the number of stories. The static pressure at the top of the common-duct is -70 ∿-80 Pa in the case of the duct size of 600 mm by 600 mm and -45 ∿-55 Pa in the case of the duct size of 600 mm by 1000 mm.

The pressure distribution is clearly different between the T-type junction and the elbow-type junction in the case of the 25 story apartment house. In the case of the T-type junction, the increase of the static pressure in upper floor levels is small, because the pressure loss at the junction offsets the pressure rise due to the stack effect. On the other hand, in the case of the elbow-type junction, the pressure loss at the junction is negative, which means that the static pressure increases at the junction. Therefore, the static pressure at the seventh floor level reaches 30 Pa due to both the pressure rise in converging flow and the stack effect. In these case, the effect of the ζ_{in} on the pressure distribution was small.

Figure 15(a) shows the airflow volumes at the top and the bottom of the common-duct and the airflow volumes from the branch ducts calculated for eight cases. The airflow volumes from the branch ducts are 520 m^3/h and 500 m^3/h in the cases of the elbow-type junction and the T-type junction, respectively. The reverse flow from the bottom of the common-duct to outdoors occurs in some cases with the duct size of 600 mm by 600 mm. But in cases with the duct size of 600 mm by 1000 mm, there is no such reverse flow.

(2) Cases with rotational speed control of the roof fan

In order to keep the static pressure in the common-duct small for any combinations of operating conditions of kitchen fans, it is assumed that the rotation speed of the roof fan can be controlled to maintain the static pressure at the top of the common-duct at a constant. Figures 13 and 14 show the pressure distribution calculated for the two cases with duct sizes of 600 mm by 600 mm and 600 mm by 1000 mm, respectively, under the condition that the static pressure at the top of the common-duct is constant at -30 Pa. Figure 15(b) shows the airflow volumes calculated for the same conditions. When an apartment house had 25 stories, the duct size was 600 mm by 1000 mm, and the flow junction was the T-type, the static pressure in the common-duct is 0 ∿-30 Pa, regardless of any combinations of operating conditions of kitchen fans with and without heat gain. But in the case with the duct size of 600 mm by 600 mm and the elbow-type junction, the static pressure is 30 Pa at the maximum near the ninth floor, which leads to the possibility of reverse flow from the exhaust vertical common-duct to the apartment through the branch duct.

5. CONCLUSIONS

5.1 Pressure Loss Coefficient for Converging flow

1) The pressure loss coefficients for converging flow, which depended on the velocity ratio of airflow, could be expressed by several approximate equations.

2) In the case with the elbow-type junction, the value of pressure loss at the flow junction in the common-duct was negative where the velocity ratio of airflow was more than 2, which means that the static pressure rises at the flow junction.

3) Computer calculation using the network model with approximate equations of pressure loss coefficients for converging flow gave reasonable results of pressure distribution in the common-duct and of airflow volumes, which totally corresponded to the results of measurement.

5.2 Recommendations for the Vertical Exhaust Common-Duct Design

1) The T-type junction is desirable for the connection of individual ducts to the vertical common-duct. If the elbow-type junction is used, the static pressure in the common-duct increases in upper floor levels leading to the possibility of reverse flow from the common-duct to the apartment through the branch duct.

2) When the T-junction is employed, if the optimum combination of duct size and performance of the roof fan is selected, it is possible to keep the static pressure at a relatively low level by controlling the static pressure at the top of the common-duct using a inverter for the roof fan control.

REFERENCE

1. Shuzo Murakami, Nobuo Yamada
"A study on a rate of simultaneous use of town gas in a kitchen of high-rise apartment house in town area (based on a load survey of town gas used in the kitchen)"
Summaries of Technical Papers of Annual Meeting, Architectural Institute of Japan, 1987, pp1089-90

2. Shuzo Murakami, Hiroshi Yoshino, Kunio Mizutani, Shin-ichi Akabayashi, Kou Hasegawa
"Ventilating Performance of Vertical Exhaust Duct in a Multi-story House :Model Experiment and Computer Simulation for Pressure Distribution through the Duct"
Transaction of the Society of Heating, Air-Conditioning and Sanitary Engineers of Japan, No.32, 1986, pp37-47

Table 1 Approximate equations for pressure loss coefficient in converging flow

	Equations	
Elbows ζ_{13}	$\zeta_{13}=C_1R^3+C_2R^2+C_3R+C_4$ $R=\{6.93\,(A_2/A_1)+0.510\}\,(V_2/V_3)$	
	Single elbow	$C_1=1.56\times10^{-3}$ $C_2=-1.50\times10^{-2}$ $C_3=1.67\times10^{-1}$ $C_4=5.90\times10^{-3}$
	Double elbows	$C_1=-3.25\times10^{-3}$ $C_2=-1.34\times10^{-2}$ $C_3=2.54\times10^{-2}$ $C_4=1.05\times10^{-2}$
Tees ζ_{13}	$\zeta_{13}=C_1\{C_2\,(V_2/V_3)+C_3$ $C_1=1.48\log(A_2/A_1)+2.70$	
	Single tee	$C_2=1.40\times10^{-1}$ $C_3=0.0$
	Double tees	$C_2=8.16\times10^{-2}$ $C_3=0.0$ $(V_2/V_3\leqq1.77)$
		$C_2=2.34\times10^{-1}$ $C_3=-2.69\times10^{-1}$ $(1.77<V_2/V_3\leqq3.82)$
		$C_2=3.24\times10^{-2}$ $C_3=5.00\times10^{-1}$ $(3.82<V_2/V_3)$
ζ_{23}	$\zeta_{23}=0.967\,(V_2/V_3)^2-0.195\,(V_2/V_3)-1.20$	

Note: $\zeta_{13}=\Delta P_{13}/\{\rho/2\}\cdot V_3^2$
$\zeta_{23}=\Delta P_{23}/\{\rho/2\}\cdot V_3^2$

Table 2 Values assumed for calculation

λ_s	$\lambda_s=10^{-0.232\log Re-0.463}$	
Duct size[mm]	600×600	600×100
D_e [m]	0.60	0.75
ζ_e	0.127	0.016
ζ_r	1.09	0.73
ζ_{13}, ζ_{23}, ζ_{13}', ζ_{23}'	See Table 1	
ζ_{ex}	$\zeta_{ex}=1.24$	
ΔP_r	$\Delta P_r=2.18\times10^{-3}Q_2^{1.54}$	
ΔP_{dT}	$\Delta P_{dT}=5.94\times10^{-4}Q_2^{1.9}$	

Note: $R_e=V_1 d_e/\nu$

Table 3 Parameters for calculation

Number of stories	5 , 10 , 15						
Common duct size	600 × 600 600 × 1000[mm]						
Number of floor levels of kitchen fans operated	0	1 lower level	1 middl level	1 highest level	N lower level	N-1, for higher levels and 1 for lower level	N randomly situated
Type of junction	Tee(150 ϕ) Elbow(150 ϕ)						
Internal heat gain from a cooking stove	0kw(0 kcal/h) 1.744kw(1500kcal/h)						
Roof fan	With or without rotational speed control(Fig.9)						
Kitchen fan	High speed operated or Low sped operated(Fig.10)						
ζ_{in}	$\zeta_{in}=1.0$ $\zeta_{in}=10.0$						
Total number of the combination : 1344							

Note: N=3,6,and 8 when the number of story is 5,15,and 25 respectively

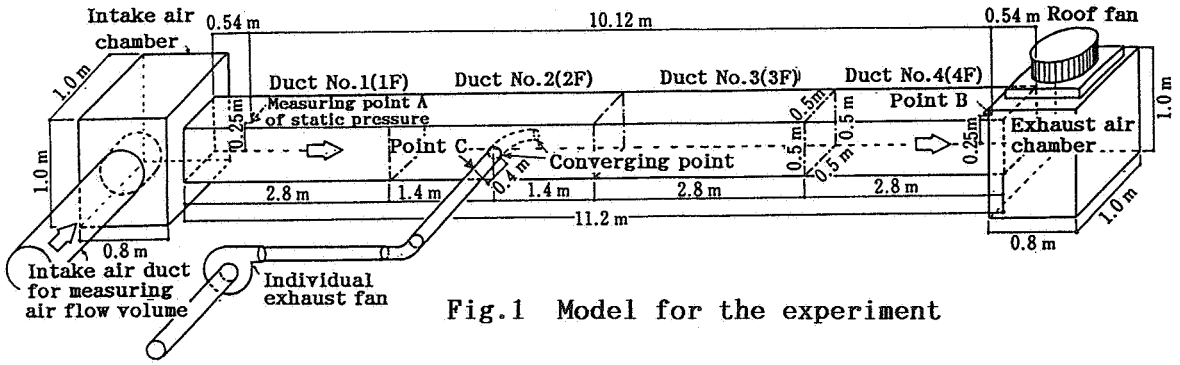

Fig.1 Model for the experiment

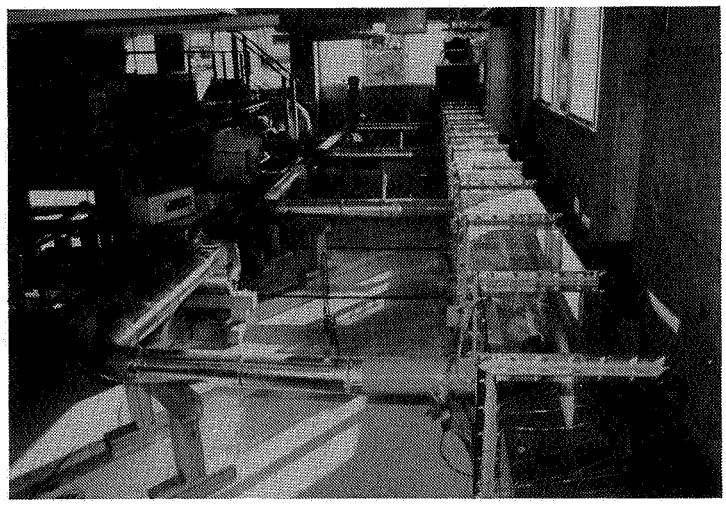

Fig.2 View of test facility

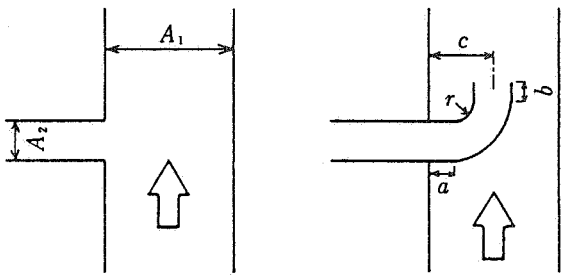

Branch duct size mm	Sectional area ratio (A_1/A_2)
ϕ100	0.03
ϕ150	0.07
ϕ250	0.20

(a) T-type junction

Branch duct size mm	Dimension (mm) r	a	b	c	Sectional area ratio (A_1/A_2)
ϕ100	50	150	50	250	0.03
ϕ150	75	100	75	250	0.07
ϕ250	125	0	0	250	0.20

(b) Elbow-type junction

Fig.3 Details of flow junctions

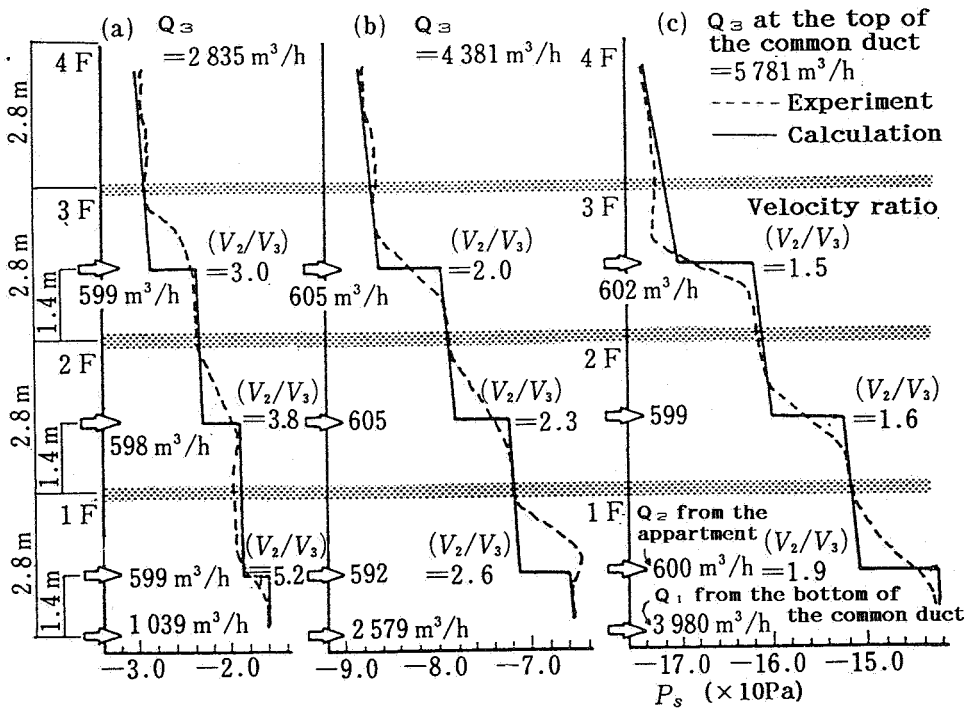

Fig.4 Pressure distribution along the common duct in the case of T-type junction with the duct diameter of 150mm

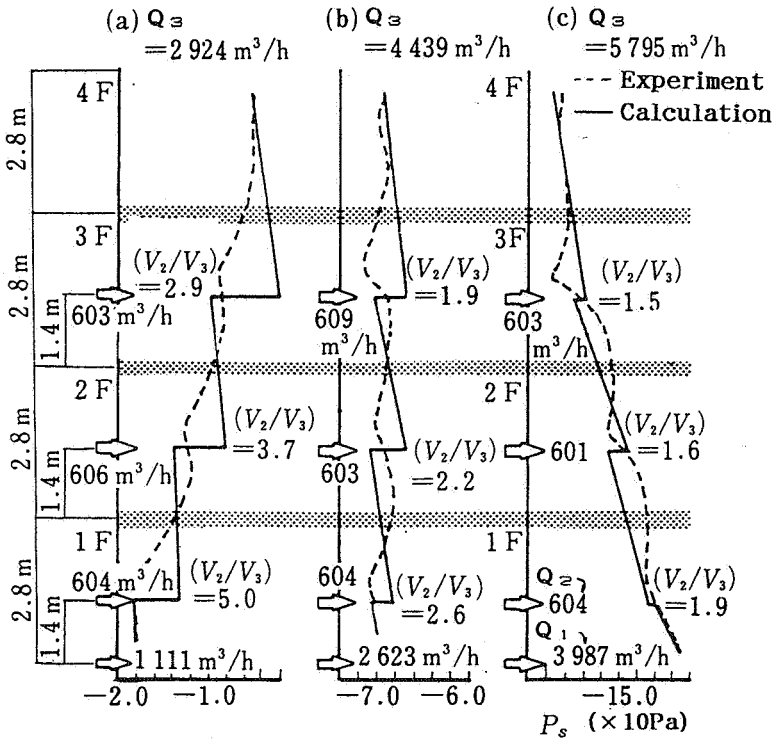

Fig.5 Pressure distribution along the common-duct in the case of elbow-type junctions with the duct diameter of 150mm

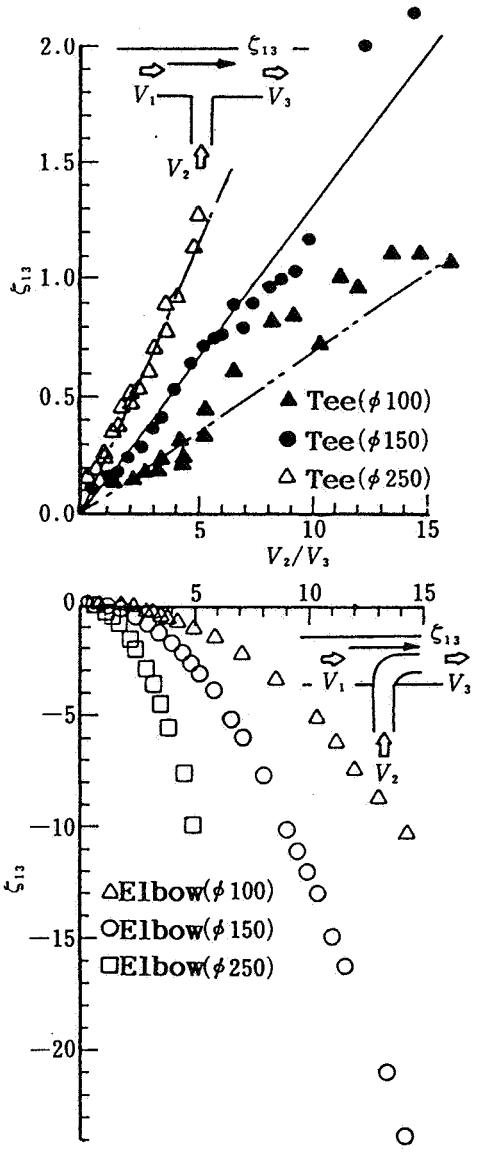

Fig.7 Pressure loss coefficient in converging flow through a common-duct

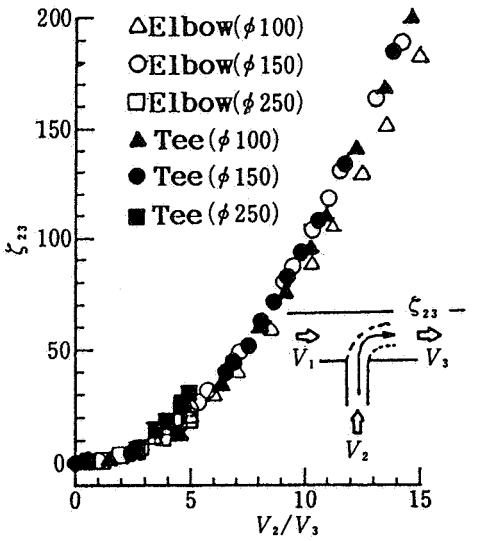

Fig.6 Pressure loss coefficient in converging flow from a branch duct to a common-duct

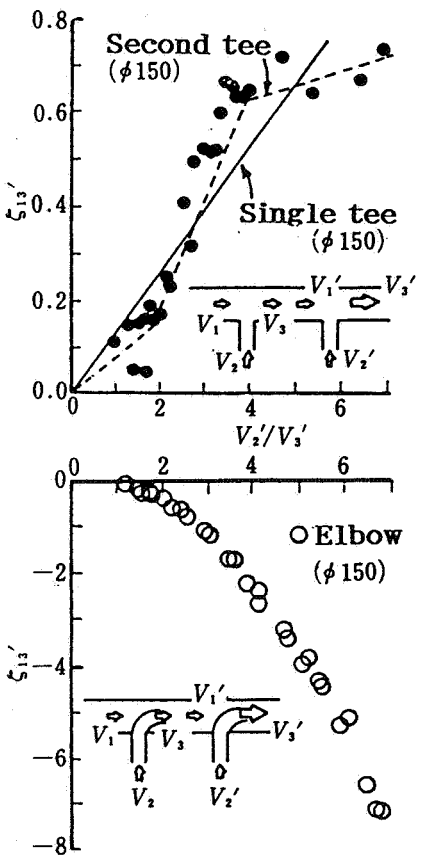

Fig.8 Pressure loss coefficient in converging flow at the second junction through the common-duct with double junctions

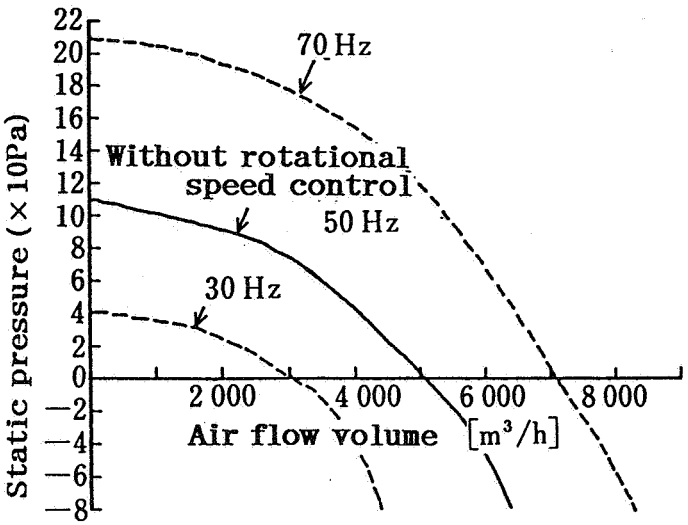

Fig.9 Performance curve of a roof fan

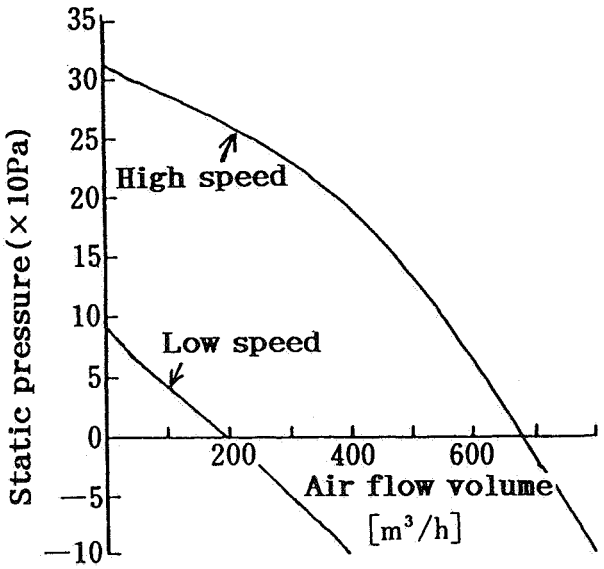

Fig.10 Performance curve of a kitchen fan

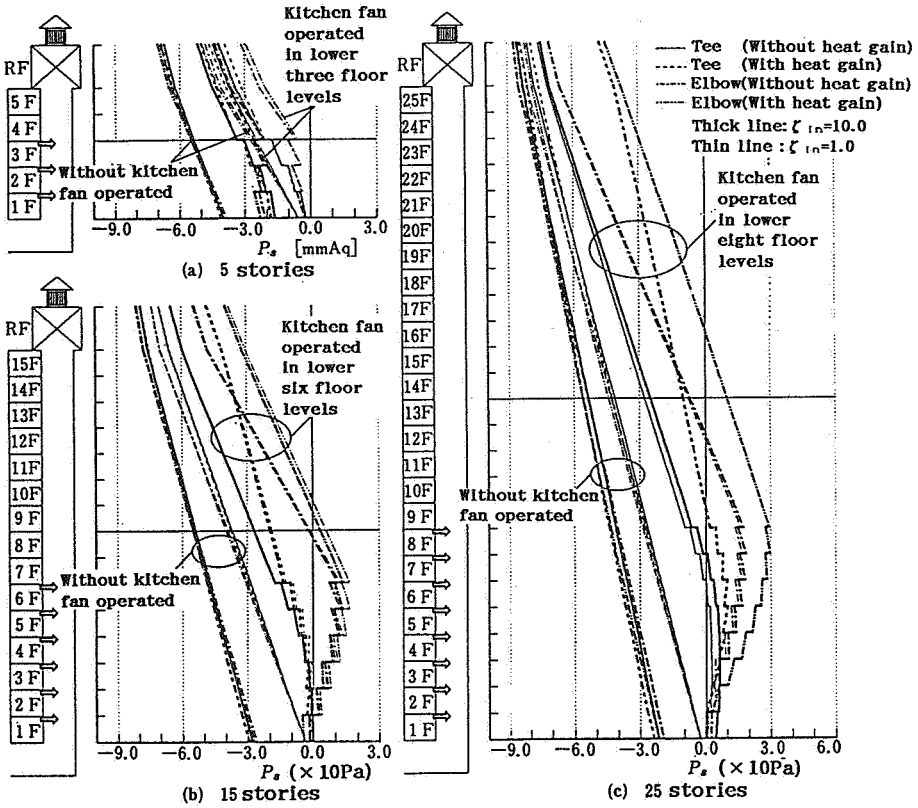

Fig.11 Static pressure distribution (Duct size:600 ×600, without rotational speed control)

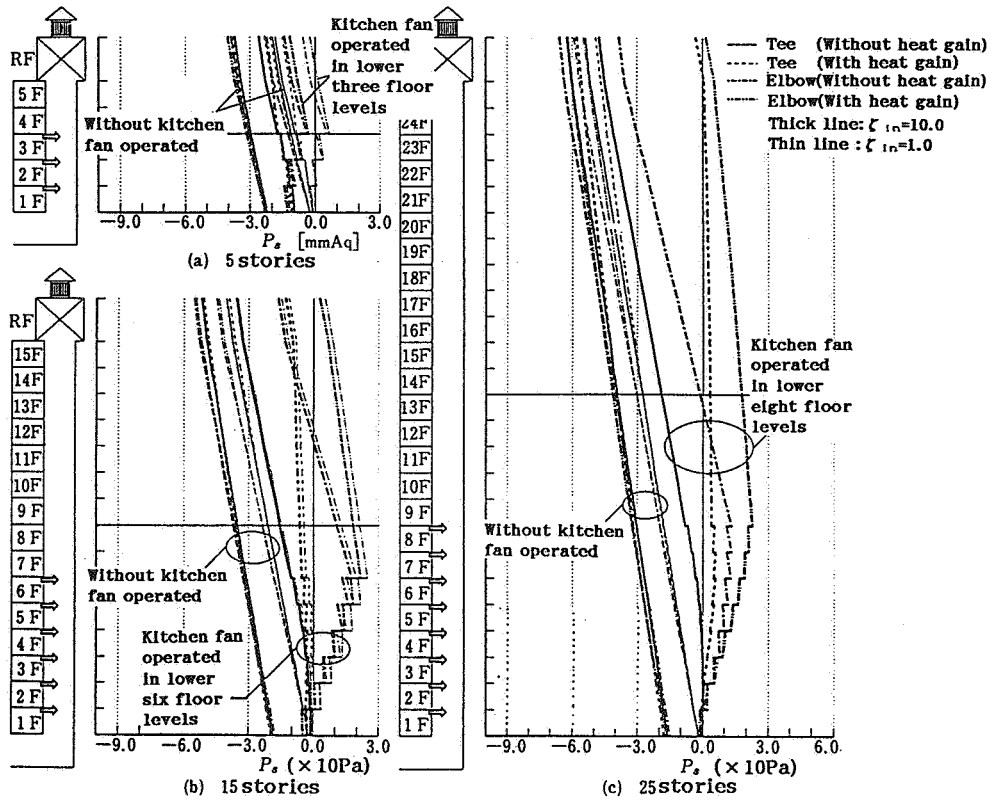

Fig.12 Static pressure distribution (Duct size:600 ×1000, without rotational speed control)

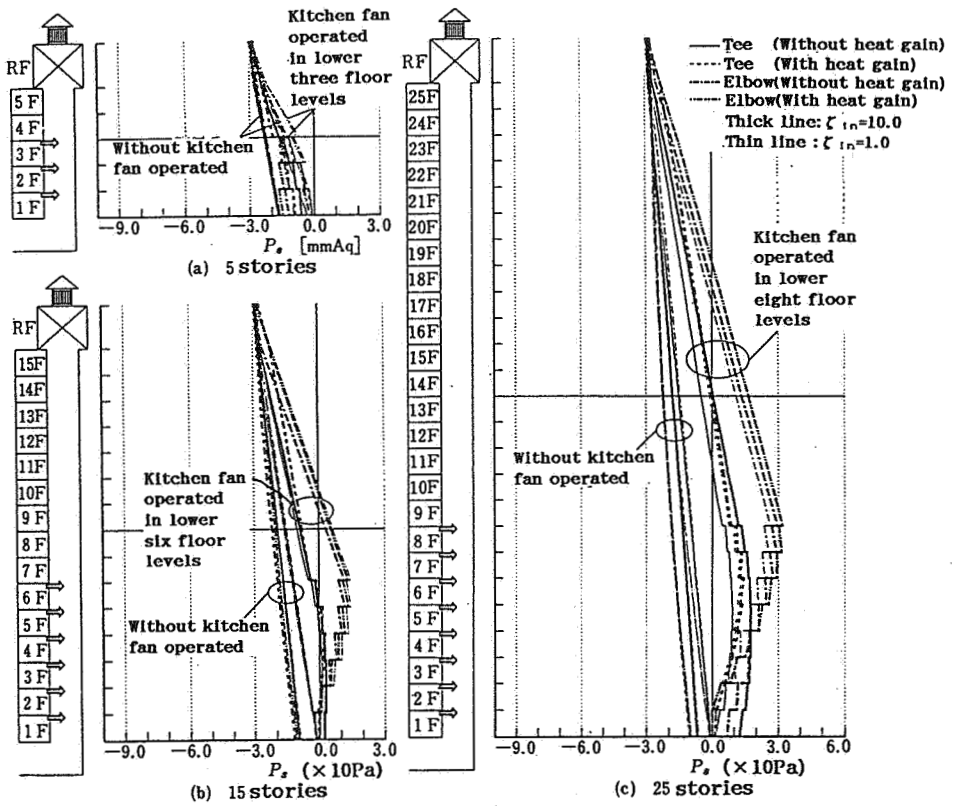

Fig.13 Static pressure distribution (Duct size:600 × 600, with rotational speed control)

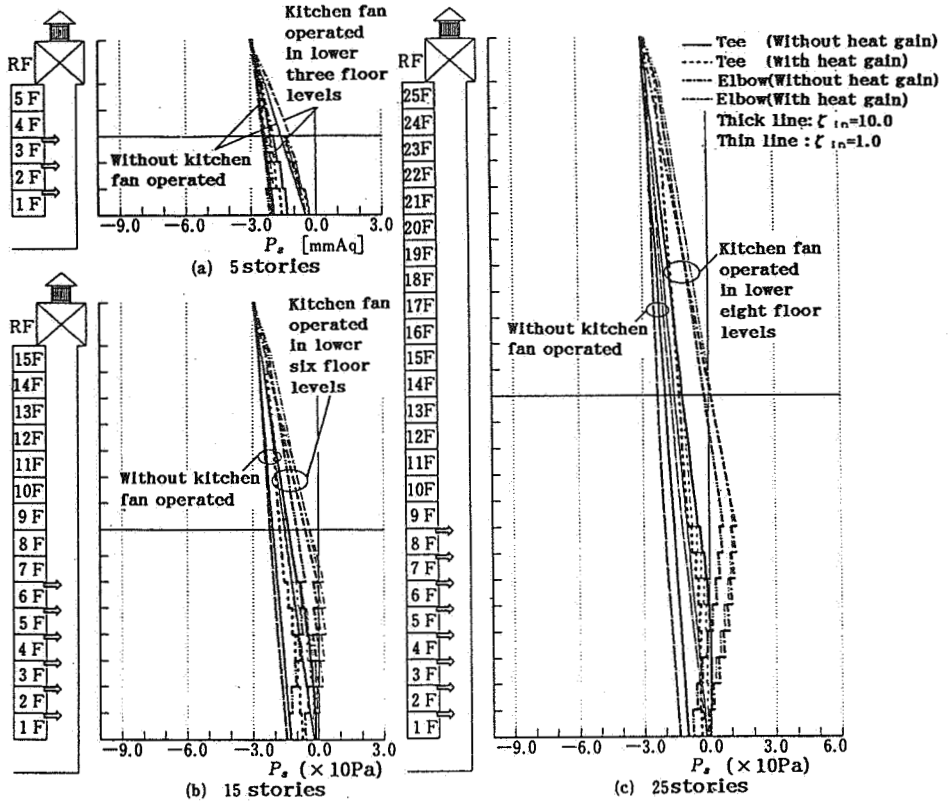

Fig.14 Static pressure distribution (duct size:600 × 1000, with rotational speed control)

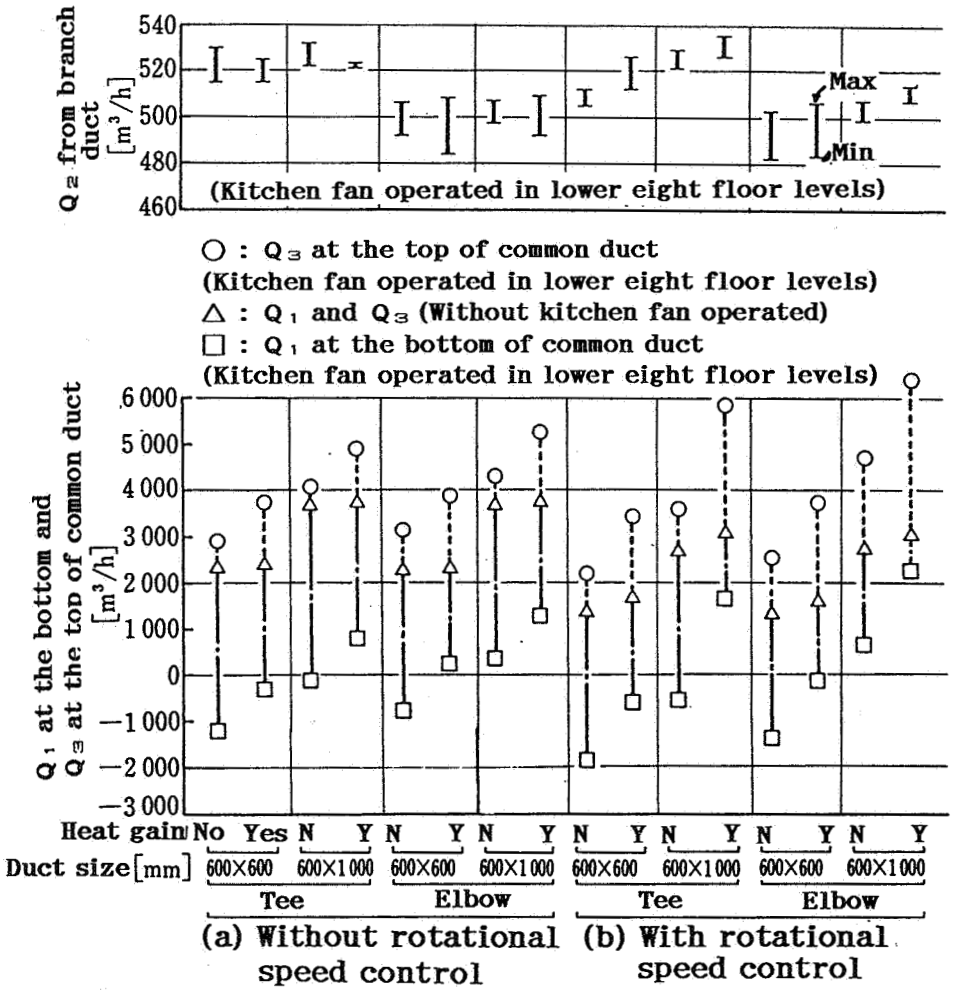

Fig.15 Exhaust air volumes in case of the apartment house with 25 stories